GEOTECHNICS ON THE VOLCANIC EDGE

TAURANGA, MARCH 2003
NEW ZEALAND GEOTECHNICAL SOCIETY SYMPOSIUM

Engineers New Zealand

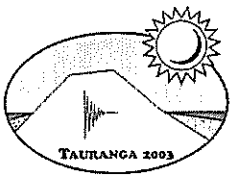

ORGANISING COMMITTEE

Stephen Crawford, Tonkin & Taylor Ltd
Paul Baunton, Tauranga District Council
Dr Sally Hargraves, Tonkin & Taylor Ltd

Administered by the Centre for Continuing Education,
The University of Auckland

Engineers New Zealand

This Symposium is endorsed by IPENZ.

The Institution of Professional Engineers New Zealand
PO Box 12241
Wellington
New Zealand

Proceedings of Technical Groups Vol. 30
Issue 1 (GM) 2003
ISSN 0111-9532

Cover photograph: View along Tauranga Port to Mt Maunganui, Bay of Plenty, NZ (courtesy of Sally Hargraves)

SYMPOSIUM SPONSERS

The Committee gratefully acknowledges the assistance provided by the following:

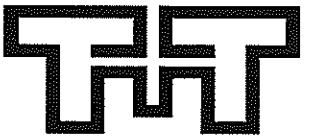

Tonkin & Taylor

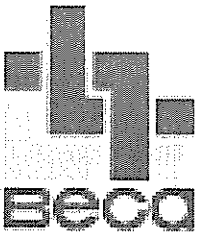

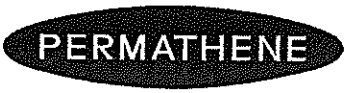

Maccaferri NZ Ltd **Connell Wagner Ltd**

Tauranga District Council

FOREWORD

This is the fourteenth Symposium held by the New Zealand Geotechnical Society. The Symposium was an opportunity to focus on the geotechnics of a wide range of engineering, materials and landforms set within an active volcanic seismic zone. It was held at the Baycourt Conference Centre, Tauranga, 27-30 March 2003. This Symposium followed a series of symposia held on a two to three year cycle.

2001	Engineering & Development in Hazardous Terrain	Christchurch
1998	Roading Geotechnics 98	Auckland
1996	Geotechnical Issues in Land Development	Hamilton
1994	Geotechnical Aspects of Waste Management	Wellington
1990	Groundwater and Seepage	Auckland
1986	Pile Foundations for Engineering Structure	Hamilton
1983	Engineering for Dams and Canals	Alexandra
1981	Geomechanics in Urban Planning	Palmerston Nth
1977	Tunnelling in New Zealand	Hamilton
1974	Stability of Slopes in Natural Ground	Nelson
1974	Lateral Earth Pressures & Retaining Wall Design (workshop)	Wellington
1972	Using Geomechanics in Foundation Engineering	Wanganui
1969	NZ Practices in Site Investigation for Building Foundations	Christchurch

The subject of this Symposium was selected by the Management Committee as a forum for practitioners to meet and exchange ideas on geotechnical and engineering geological issues. In particular, the Symposium was designed to specifically address soil/material behaviour and properties and risk in seismic volcanic settings and to present related technical issues and case studies.

The keynote address was given by Kenji Ishihara, Professor of Chuo University, Professor of University of the Tokyo University of Science, and Immediate Past President of the International Society for Soil Mechanics & Geotechnical Engineering (ISSMGE). This address outlined the observed liquefaction effects of the 1995 Kobe earthquake in Japan and presented the results of backanalysis and assessment of foundations subject to high seismic load in a coastal environment.

The support of all Symposium sponsors is gratefully acknowledged.

Stephen Crawford
Chairman, Organising Committee
Chairman, NZ Geotechnical Society
March 2003

GEOTECHNICS ON THE VOLCANIC EDGE

TAURANGA, MARCH 2003
NEW ZEALAND GEOTECHNICAL SOCIETY SYMPOSIUM

PROCEEDINGS

Edited by

Stephen Crawford
Dr Sally Hargraves

Technical Reviewers

Chris Bauld
Dr John Berrill
David Burns
Tony Cowbourne
Stephen Crawford
Glyn East
Geoffrey Farquhar
Bernard Hegan
Douglas Johnson
Dr John Marsh
Dr Kevin McManus
Peter Millar
Kelvin Moody
Grant Murray
Dr Marianne O'Halloran
Stuart Palmer
Prof. Michael Pender
Dr Warwick Prebble
Nick Rogers
Greg Saul
John Scott
Tim Sinclair
Sergei Terzaghi
Ann Williams

TABLE OF CONTENTS

SESSION 4: SEISMIC RISK & EMBANKMENT ENGINEERING
Sponsored by Riley Consultants Ltd

SESSION 5: PROPERTIES AND BEHAVIOUR OF VOLCANIC SOILS
Sponsored by Permathene Ltd

THEME SPEAKER:

SESSION 6: VOLCANIC FOUNDATION MATERIALS & ENVIRONMENTS
Sponsored by Meritec Ltd

SESSION 7: ROADING GEOTECHNICS & CASE STUDIES
Sponsored by Fulton Hogan Ltd

SESSION 8: GEOSYNTHETICS, ANCHORS & CASE STUDIES
Sponsored by Geotech Systems Ltd

LIQUEFACTION-INDUCED LATERAL FLOW AND ITS EFFECTS ON FOUNDATION PILES

Professor Kenji Ishihara
PhD
Professor, Chuo University, Tokyo, Japan

Keynote Address for Geotechnics on the Volcanic Edge
NZ Geotechnical Society Symposium

Friday 28 March, 2003

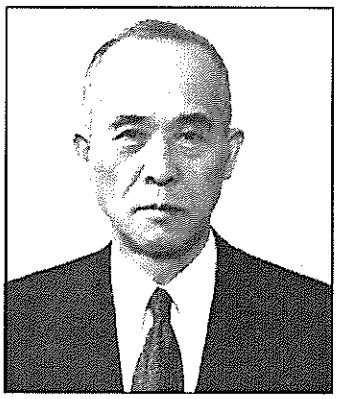

Professor Kenji Ishihara was born in Tokyo, Japan on 16th April 1934. Having graduat from the University of Tokyo in 1957, he went on to complete his PhD there in 1963. After period of research at the University of Illinois under the advice of Professor R.B. Peck, I returned to the post of Associate Professor at the University of Tokyo at the age of 32. 1977 he took up the position of Professor of Civil Engineering and remained at the Univers of Tokyo for 40 years. During this time he was active in the International Society for S Mechanics and Foundation Engineering (ISSMFE). He was particularly effective advancing the work of Technical Committee TC4 – Earthquake Geotechnical Engineerin His work with ISSMFE culminated in his appointment as President of the Society for the ter 1997-2001.

Professor Ishihara is currently a Board member as the immediate Past President of tl International Society of Soil Mechanics and Geotechnical Engineering. Professor Ishiha was the 1993 Rankine Lecturer delivering "Liquefaction and Flow Failures Duri Earthquakes". He was the recipient of H.B. Seed Medal in 1998 from A.S.C.E. In 1996, I published his textbook "Soil Behaviour in Earthquake Geotechnics" (published by Oxfo University Press), which summarises his life's work. This book is a testimony to a mc productive research and engineering life.

Professor Ishihara has published over 180 technical papers and three books and he h travelled as a consultant and lectured widely throughout the world. His work has focused modelling of cohesionless soils, dynamic pore pressure and liquefaction, and earthqual stability of foundations and dams. Much of his work is based on field evidence and tl assessment of real problems of soil behaviour during earthquakes. His keynote lecture this New Zealand Geotechnical Society Symposium is a notable example of this. He w instrumental in the research into the geotechnical effects of the Kobe earthquake and h been involved in revision of the earthquake-resistant design codes in Japan.

On his retirement from the University of Tokyo in 1995 he took up the post of Professor Geotechnical Engineering at the Tokyo University of Science and then at Chuo University 2001. We are indeed deeply honoured to have such a prestigious leader in geotechnic engineering present the keynote address at this 2003 New Zealand Geotechnical Socie Symposium.

LIQUEFACTION-INDUCED LATERAL FLOW AND ITS EFFECTS ON FOUNDATION PILES

Professor Kenji Ishihara
PhD
Professor, Chuo University, Tokyo, Japan

Abstract

Characteristic features of lateral spreading in liquefied deposits of sandy soils are addressed with reference to the damage during the Kobe Earthquake in 1995. The cases of injury to foundation piles due to the lateral spreading are then introduced along with the results of in-situ soil investigations. The back analysis was made by modelling the pile-soil interaction by way of the beam connected with several springs. The spring constants were reduced at varying levels so as to yield the observed difference in horizontal displacements between the ground surface and pile top at the time of the earthquake. The degree of stiffness degradation which is compatible with the observed difference in displacements was obtained with the result that the stiffness of liquefied soil deposits is drastically reduced by a factor of 10^{-2} to 10^{-3}.

Liquefaction-Induced Lateral Flow and its Effects on Foundation Piles

K Ishihara
PhD
Professor, Chuo University, Tokyo, Japan

Abstract: Characteristic features of lateral spreading in liquefied deposits of sandy soils are addressed with reference to the damage during the Kobe Earthquake in 1995. The cases of injury to foundation piles due to the lateral spreading are then introduced along with the results of in-situ soil investigations. The back analysis was made by modelling the pile-soil interaction by way of the beam connected with several springs. The spring constants were reduced at varying levels so as to yield the observed difference in horizontal displacements between the ground surface and pile top at the time of the earthquake. The degree of stiffness degradation which is compatible with the observed difference in displacements was obtained with the result that the stiffness of liquefied soil deposits is drastically reduced by a factor of 10^{-2} to 10^{-3}.

INTRODUCTION

The design of piles for the effects of seismic motions is generally performed by using a soil-pile interaction model in which a vertically placed beam is supported by a series of springs. The beam represents performance of the pile, and soil properties are represented by the spring constants. In the design of foundations it has been a common practice to take into account effects of horizontal seismic motions by incorporating a horizontal force at the top of the pile, which is equal to the inertia force from the superstructure. In this type of analysis, the series of the springs are fixed to a wall not moving and soil deformation is represented by the movement of the springs. For the condition of no softening of soils due to liquefaction, the spring constants are determined based on empirical formulas stipulated in the design code or by means of appropriate in-situ tests. When liquefaction is of concern, the stiffness of liquefied soils would be reduced, and these effects need to be considered. The Japanese Code of Highway Bridge Design stipulates, for example, that, for the back and force cyclic phase of loading, the spring constants be reduced by a factor of 1/6 to 2/3 reflecting upon the degree of safety factor against liquefaction.

When it comes to the effects of lateral spreading it would be necessary to replace the above-mentioned non-moving wall by a laterally deforming wall in compliance with the displacement of the liquefied soil. However, there had been no requirement stipulated in the code to allow for these effects in the phase of lateral flow following the main shaking of earthquakes. Thus, concerns have been kindled on this issue since the Kobe earthquake in 1995 because of the extensive occurrence of damage to foundation piles that occurred apparently due to the lateral spreading. Thus, somewhat detailed considerations is now the target of major studies among geotechnical engineers regarding the effects of lateral spreading on embedded foundations such as piles. In what follows, this aspect will be addressed more thoroughly by first referring to the enormous disaster at the 1995 Kobe earthquake.

GENERAL FEATURES OF THE KOBE EARTHQUAKE

The Hyogoken-Nambu earthquake, registering a magnitude of 7.2 (JMA), occurred before dawn at 5:47a.m. on January 17, 1995 and delivered a very high level of devastating shock to densely populated area of Kobe-Osaka corridor which forms a major industrial heartland in the western part of Japan main island. The total death toll was over 6,500 and more than 300,000 people were left homeless. The very strong shaking collapsed approximately 150,000 houses and buildings, ignited fires, wrecked elevated highways and railways, and destroyed ports and harbour facilities.

An overall feature of the geological setting in the region of Osaka Bay is depicted in Fig.1. A cross section A-A' in the west to east is shown in Fig.2 where it may be seen that sedimentary deposits of different geological eras exist in a bowl-shaped basin with a maximum depth of about 2km. It can also be seen that there exist several offsets in the underlying rock formation indicating presence of fault rupture zones. They are considered to be sources of historical earthquakes in the long geological past. Kobe and its neighbouring cities such as Ashiya and Nishinomiya lie on the north-western side of Osaka Bay.

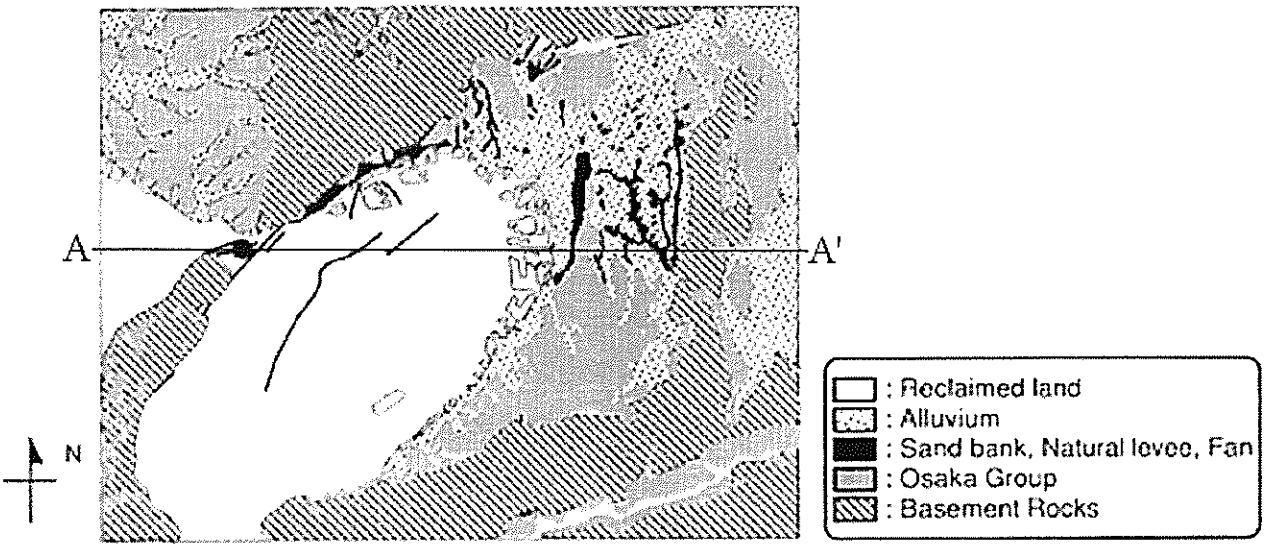

Figure 1. Geological Map in the Area Surrounding the Osaka Bay.

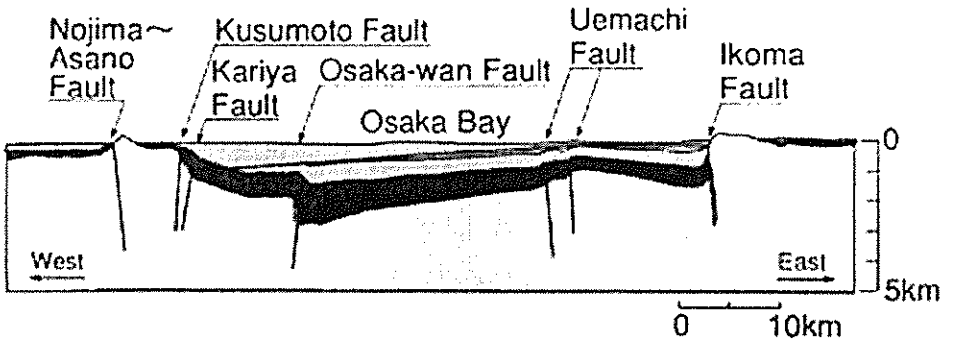

Figure 2. Cross Sectional View of the Geological Regime in the Osaka Bay.

As shown in Fig.3, they are located in the lowlands extending southwards from the foot of the Rokko Mountain Chain which consists of several fault blocks with steep escarpments dipping towards the sea. The mountain areas with an elevation in excess of 300m are essentially composed of base rock such as granite and granodiorite. The formation of the lowland extending from the mountain to the coast is a consequence of water run-off, which created a narrow flood belt and zones of numerous inter-connecting alluvial fans as illustrated in Fig.3. Terrace deposits of Pleistocene origin are shown to exist in the area south of the Rokko Mountain. The Pleistocene deposits are overlain by Holocene alluvium composed of sand, gravel and clay, which forms a relatively flat and narrow corridor of land on which the city of Kobe developed. A cross sectional view in the cross section A-A' in Fig.3 is shown in Fig.4. It may be seen that several southward dipping layers of sand, gravel and clay do exist with overlying reclaimed fills near the surface. The clay-rich deposit under the man-made fills is the seabed sediment before the reclamation was conducted.

The fills beneath several islands in the port area of Kobe were constructed using residual soil formed by weathering of granite rocks. The soil dubbed Masado was obtained from borrow sites in the Rokko Mountain and brought to the site through a combination of conveyor belts and push-barges.

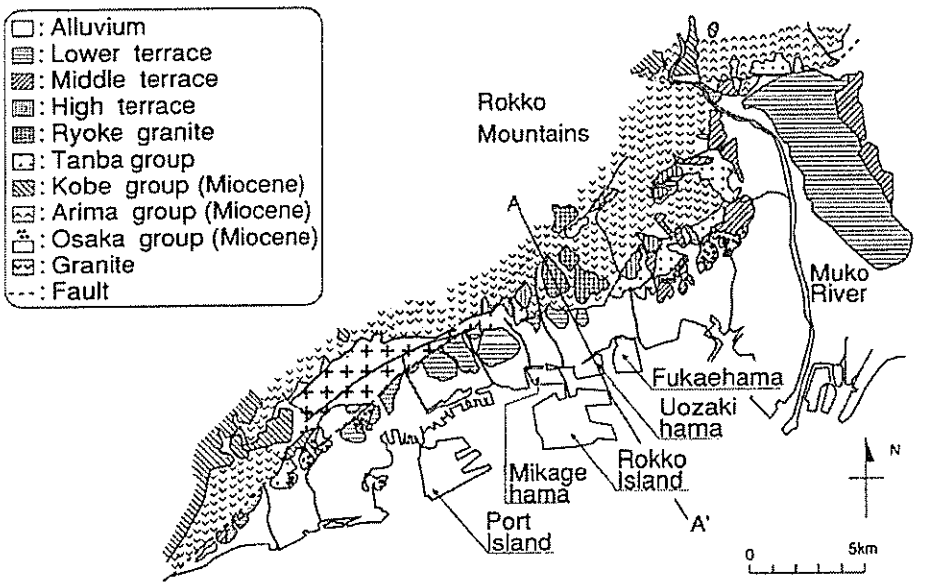

Figure 3. Geology and Geomorphology in Kobe Bay Area.

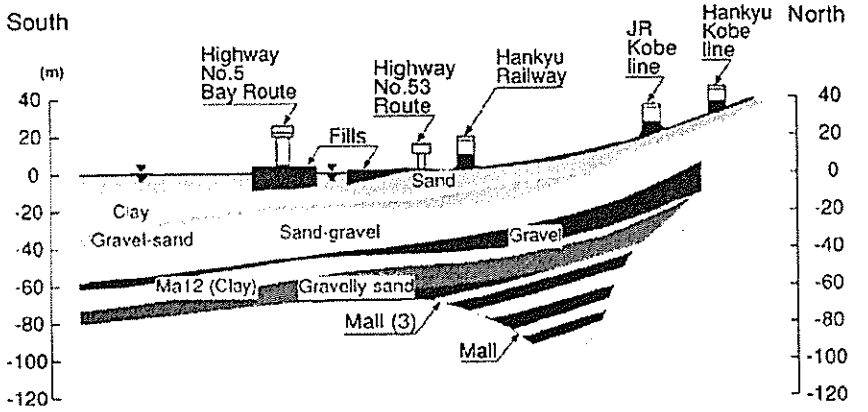

Figure 4. Subsurface Soil Profile in the Kobe Area (Cross Section A-A' in Fig.3).

The general range of grain size for the decomposed granite fills are shown in Fig.5. The characteristic feature of the grain composition is that the material is generally well-graded and contains a significant fraction of gravel. Superimposed in Fig.5 are the ranges of gradation for soils which are highly likely or likely to develop liquefaction if the soils are deposited in-situ under sufficiently loose conditions.

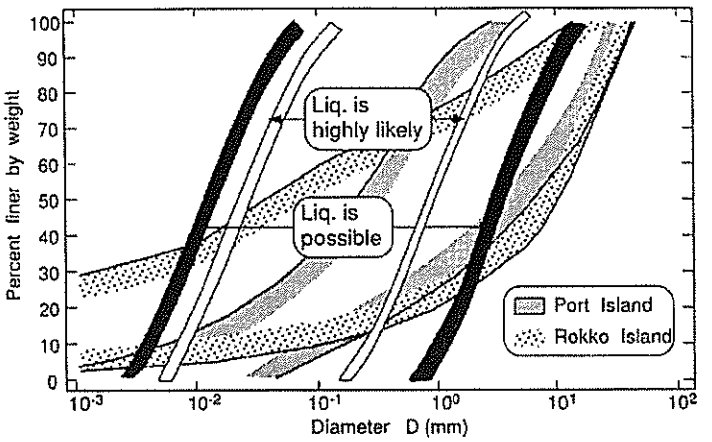

Figure 5. Grain Size Distribution Curves of Soils Used for Landing Port Island and Rokko Island.

These ranges were established by examining the grading curves of the vast majority of soils which were known to have developed liquefaction in past earthquakes. In comparison with these boundary curves, the soils in Kobe area were known to have grain composition outside the boundaries and hence had been considered not to be highly susceptible to liquefaction. It was ironically an unexpected incident that the liquefaction had indeed occurred in soils with such grading characteristics.

LIQUEFACTION INDUCED LATERAL SPREADING

During the earthquake, liquefaction developed extensively over the areas of reclaimed lands in the port and harbour district of Kobe City. In the terrain behind the quaywalls, the liquefaction gave rise to an increase in lateral force, and led to excessive movements of the caisson-type wall as much as 3 to 4m towards the sea.

The horizontal movement of the wall was accompanied by an equally large amount of lateral spreading of ground soils which propagated rearwards inland. The ground rupture as it propagated backwards is to be considered as a phenomenon of engineering significance as it defines the spatial extent of the ground distress to which due consideration may need to be given in relation to the design of foundations. In view of this, attempts were made to investigate features of ground displacements and settlements caused by the lateral spreading of liquefied soil during the earthquake in the wharf areas along the peripheries of Port Islands, Rokko Island and Fukae Island in Kobe district.

In-Situ Survey of Lateral Spreading

At a number of locations, measurements were made on the width of open cracks and vertical offsets across the cracks on the ground surface along an alignment in the direction perpendicular to the revetment line (Ishihara et al. 1997). This method will be referred to as the ground surveying. The scheme of survey on the ground surface is illustrated in Fig.6.

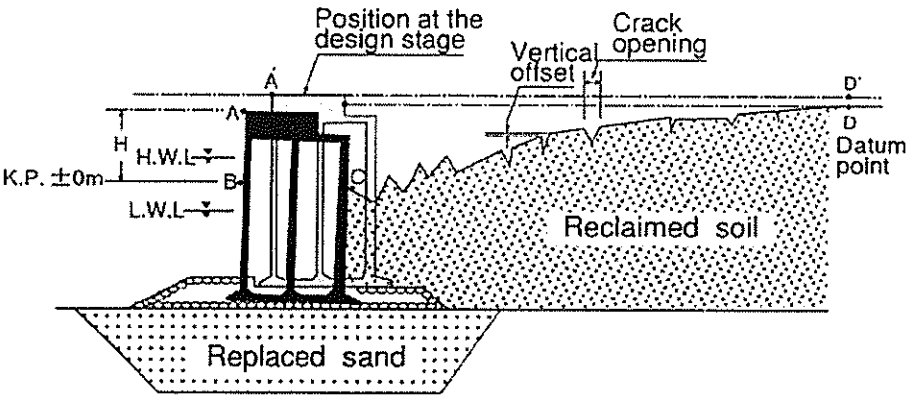

Figure 6. Illustration of Key Points to be Defined in the Method of Ground Surveying.

The in-situ measurements started from a point C behind a quaywall until a datum point D is reached where there is no crack visible on the ground surface. By summing up the width of the crack openings successively from the datum point towards the waterfront, the lateral displacement at any point on the alignment was determined. It became thus possible to depict the distribution of the lateral displacement as a function of distance inland from the waterfront where caisson-type quaywalls moved towards the sea.

The locations where measurements were made in the area of Kobe are shown in Fig.7.

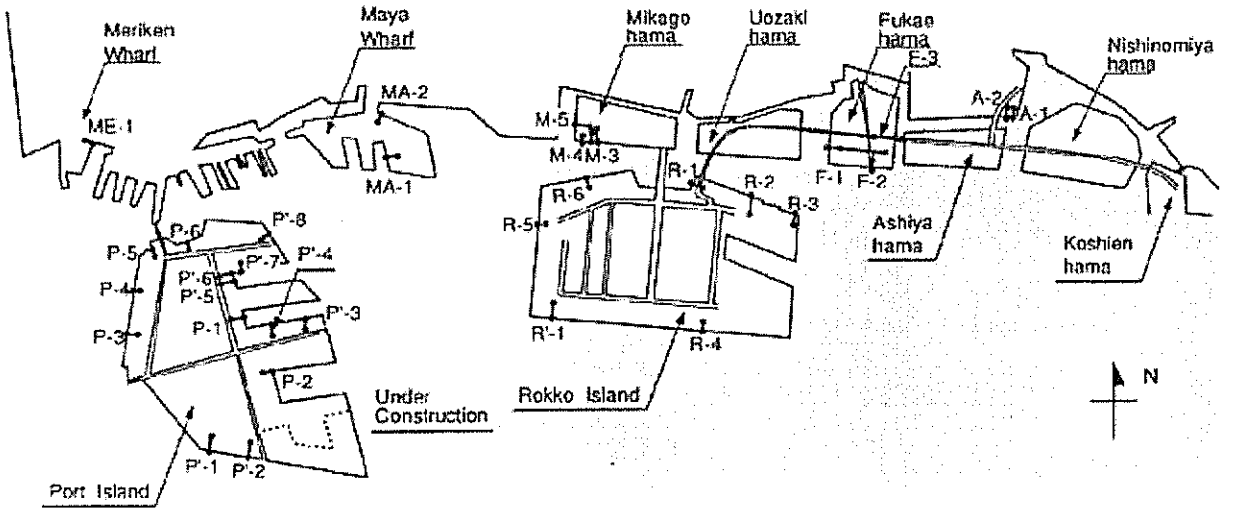

Figure 7. Location of Cross Sections Where Measurements Were Made Using the Ground Survey.

They are all located in the peripheries of man-made reclaimed islands in which the soil consists practically of the same materials, i.e., Masado derived from weathering of granite rocks. The revetments or quaywalls in this area were all constructed of gravity-type caisson walls with their inner compartments filled with sand. A vast majority of the caisson boxes were placed on the stone mounds resting on the Masado beds, which were artificially placed after the soft clay in the original seabed had been removed. The material behind the caisson walls was also the Masado, the same soil as that used for the foundation bed.

A typical result of displacement measurements is displayed in Fig.8 for the cross section R-2 in Rokko Island where it can be seen that the caisson body did stoop, accompanied by a lateral movement of 1.56m and settlement of 0.96m. The displacement is shown to have extended inland as far backwards as 183.7m. A soil profile near the point R-2 is shown in Fig.9. It may be seen that the man-made fills composed of Masado soil existed to a depth of about 20m. Liquefaction is considered to have occurred in this reclaimed fill.

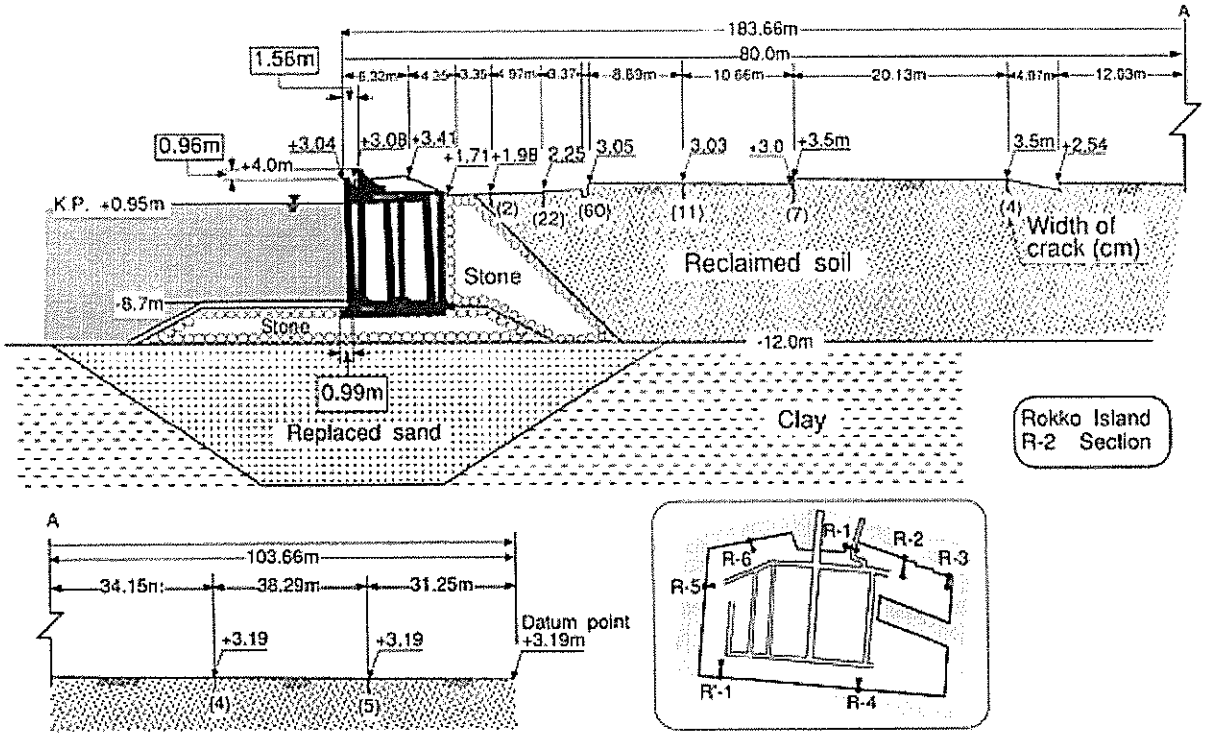

Figure 8. Detailed Profile of the Ground Deformation at R-2 Section in Rokko Island.

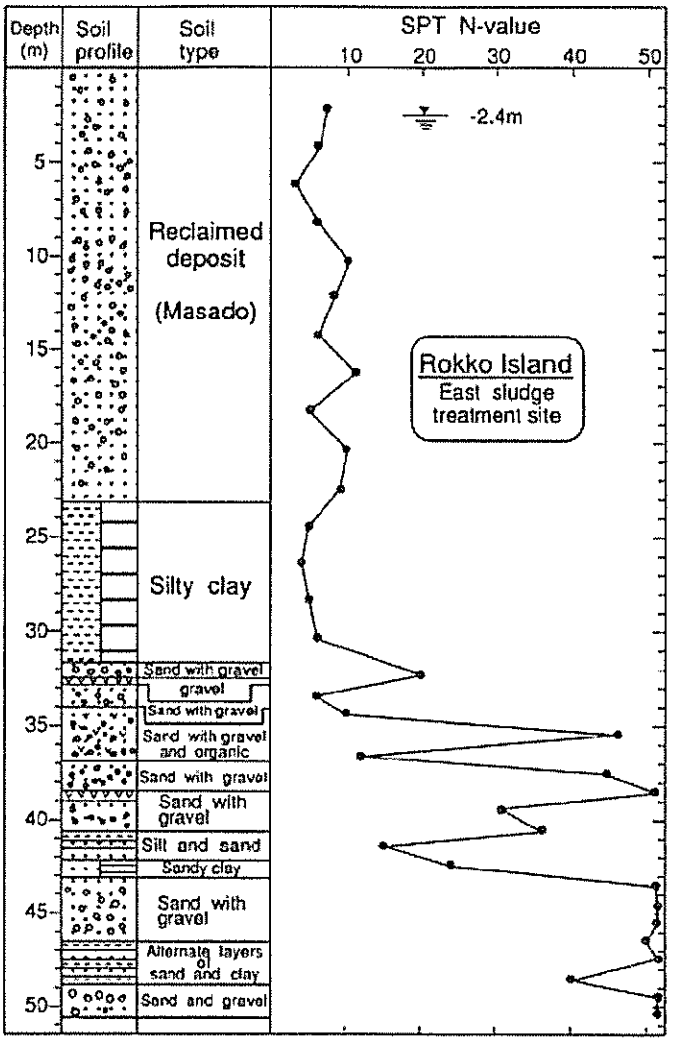

Figure 9. Soil Profile at a Site Near Sections R-2 and R-3 (Hanshin Highway Authority, 1993).

It is conceivable that there were dual factors which might have acted to produce the lateral displacement of the caisson walls. These are:

- inertia force due to the intense shaking, and
- softening of soils surrounding the caisson caused by buildup of pore water pressure.

It may be roughly assumed that the effects of pore water pressure buildup including liquefaction were, by and large, the same all over the waterfront areas in Kobe port that were affected by the earthquake.

However, the effects of inertia force are deemed different depending upon the direction to which the revetment line is oriented. As a matter of fact, the records of accelerations secured during the earthquake showed motion characteristics which are largely biased to the northwest-southeast direction.

Based on the records obtained nearby, the acceleration inferred to have acted on the quaywalls oriented in two directions were established by Inagaki et al. (1996) as indicated in Fig.10. It may be seen that the horizontal acceleration against the north- or south-facing walls was of order of 500gal whereas acceleration of the order of 250-300gal is inferred to have acted against the east- and west-facing walls.

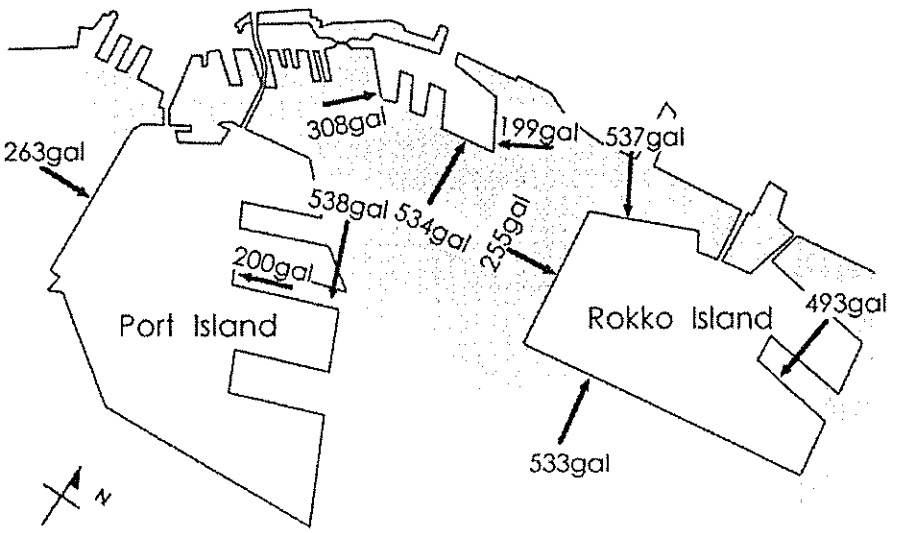

Figure 10. Magnitude of Acceleration Inferred to Have Acted on the Quaywall Facing Different Directions (Inagaki et al., 1996).

In view of this, all the data on the ground displacements measured by the method of the ground surveying at Port Island, Rokko Island and Fukaehama were divided into two groups; one pertaining to the north- or south-facing walls and the others to the east- and west-facing walls. Fig.11 shows all the lateral displacements from the north- or south-facing caisson walls plotted together, versus the distance from the line of revetment. It is noteworthy that there is an acute drop in the displacement in the vicinity of the walls, which is indicative of pronounced influence of inertia force in producing the large displacement near the walls.

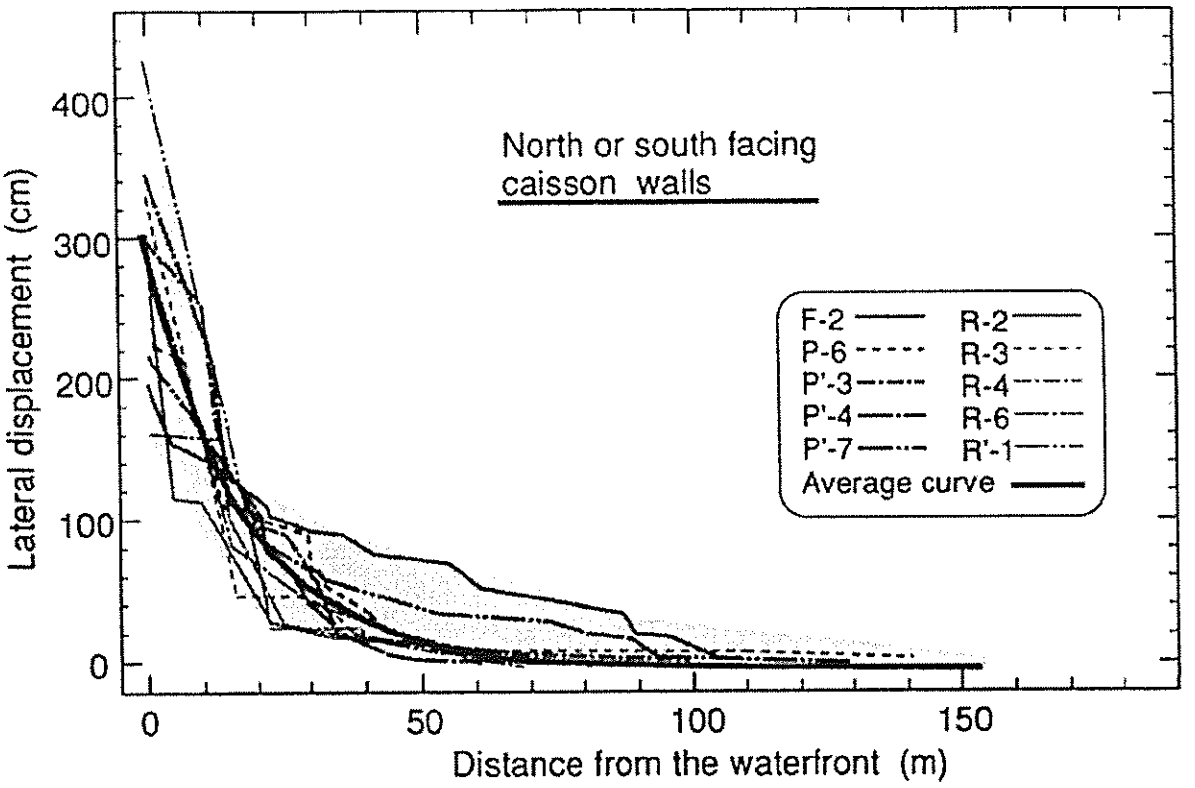

Figure 11. Lateral Displacements Versus the Distance from the Waterfront (North-or South-Facing Quaywalls).

Fig.12 shows all the data of the ground displacements obtained at the sites where the quaywalls are oriented towards the east or west. As compared to similar data arrangements shown in Fig.11, the attenuation of lateral displacements is seen in Fig.12 being more gradual even in the area in proximity to the walls.

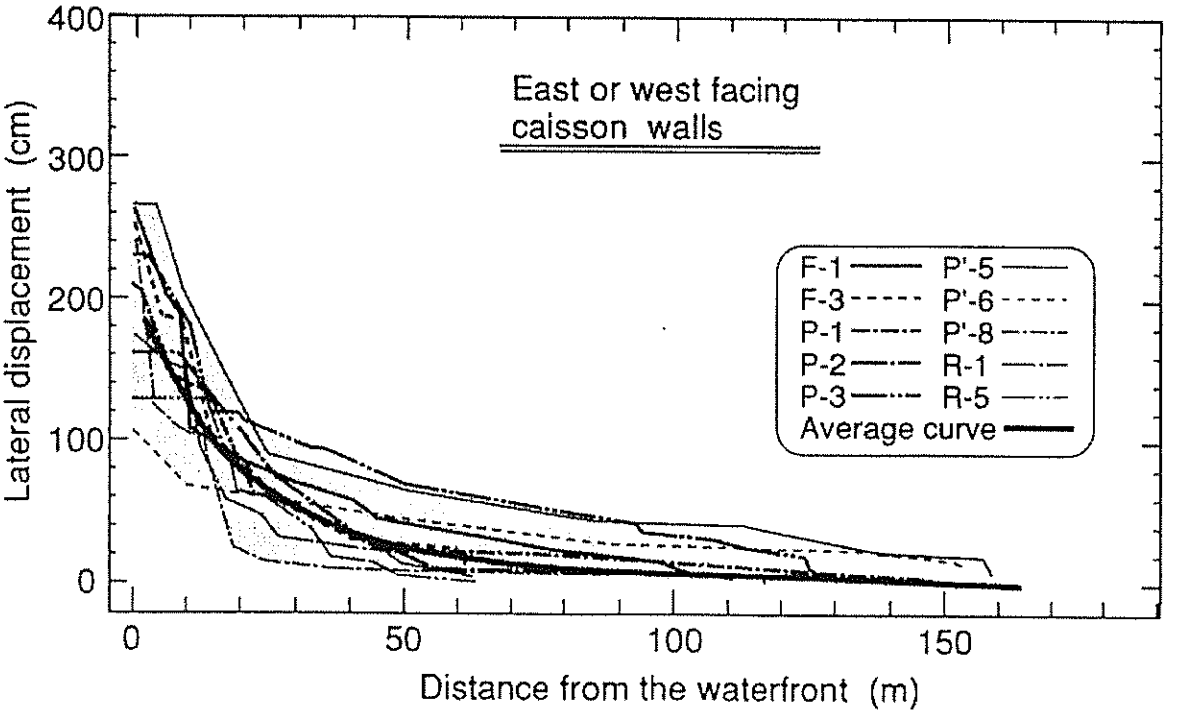

Figure 12. Lateral Displacements Versus the Distance from the Waterfront (East-or West-Facing Quaywalls).

Taking the average curves of attenuation shown in Fig.11 and 12, the lateral displacement at any point normalised to that at the waterfront is shown in Fig.13. It can be seen in Fig.13 that the attenuation is more pronounced for the soil deposit retained by the north- or south-facing caisson walls as compared to the ground behind the walls facing the east or west direction.

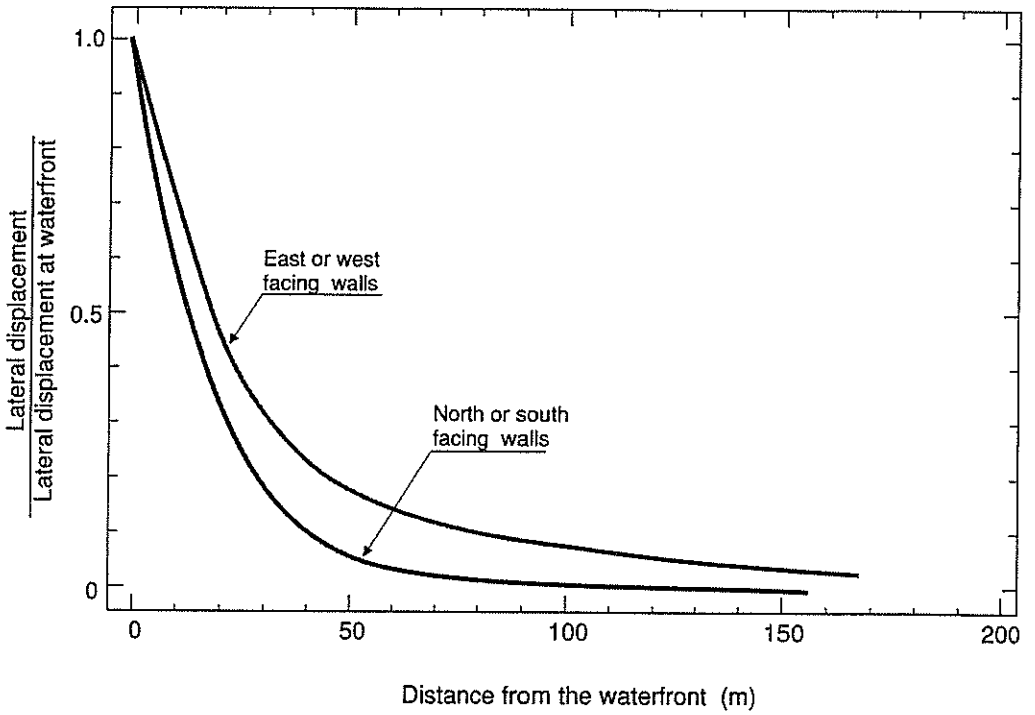

Figure 13. Comparison of Normalized Displacement Patterns in Liquefied Deposits Retained by the Quaywalls Facing Different Directions.

The reason for the rapid attenuation in the former case is simply the larger movements of the quaywalls which were caused by a greater acceleration in the north-south direction during the Kobe earthquake. As discussed above, the ground movements in the backland retained by the east- or west-facing walls appear to have been caused primarily by the liquefaction of the soil deposit. For this reason, it would be legitimate to choose the attenuation curve pertaining to the east- or west-facing walls for practical purposes where estimate of lateral displacements is needed given the quaywall movements less than 2.0m with a ground shaking of the order of 200-300gal.

DAMAGE TO BRIDGE FOUNDATIONS

Extensive damage was incurred to water-crossing bridges and elevated structures of the Hanshin Expressway along the bay area between Kobe and Osaka. This is a network of major toll highways and interlining feeder routes constituting one of the primary arterial highways within this region. Fig.14 shows the network of the expressway in the heavily damaged area of the Hanshin (Osaka-Kobe) district.

In the case of the No.5 Bay Route (Figs. 4, 14), located along the bay shore, the damage to piers or superstructures was more than severe in the terrain close to the waterfront. No less destructive was the damage to foundation system such as piers or footings. The Bay Route is located in the area of manmade deposits composed of the Masado soil in Kobe.

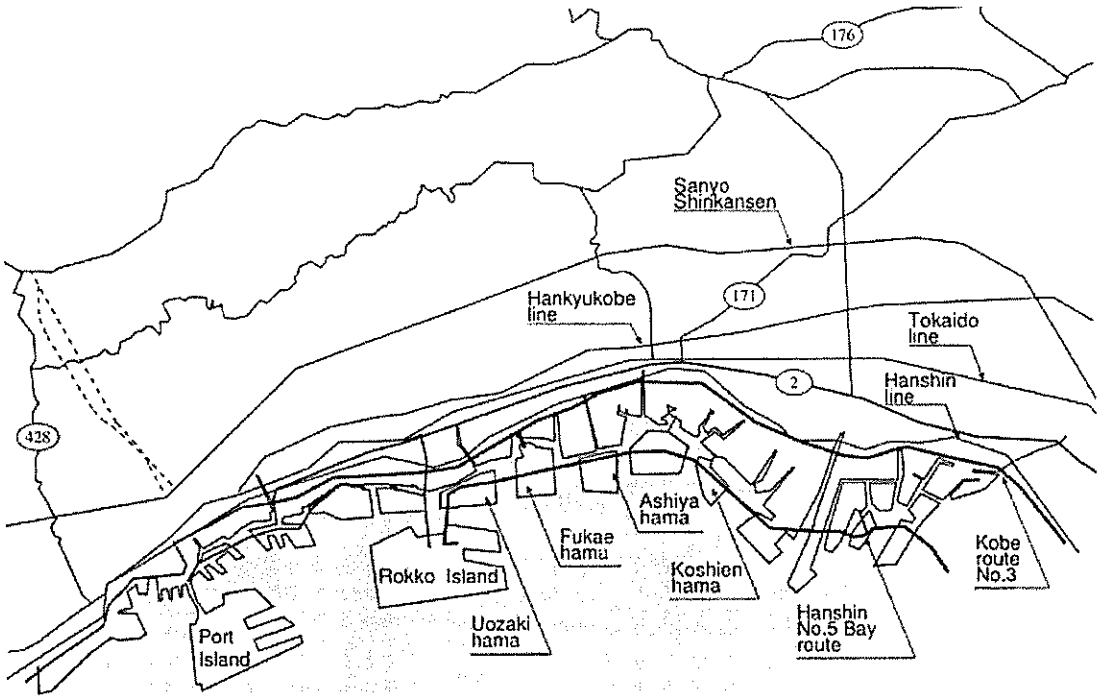

Figure 14. Highway System in the Osaka-Kobe District.

The ground displacements in some sections along the Bay Route No.5 were estimated by Hamada et al. (1996) over the widespread area by means of air-photograph interpretation. In this method, some target objects on the ground such as manholes or corners of drainage channels were pinpointed and designated on pairs of air-photographs taken before and after the earthquake and the displacements were obtained by taking the deference between the post-and pre-earthquake locations of these objects. The lateral displacements obtained in this way at specified points were used to obtain a picture of distribution of the horizontal displacements, based on a linear interpolation method using a finite element mesh. The picture of lateral displacements thus obtained for the southern part of Uozakihama is displayed in Fig.15, where it may be seen that in the area near the revetment line the lateral displacement is directed southwards to the waterfront with its maximum of 186cm. Note that the

lateral displacement of the bridge pier, P211, closest to the revetment was 62cm, a value which is significantly smaller than that of the surrounding ground.

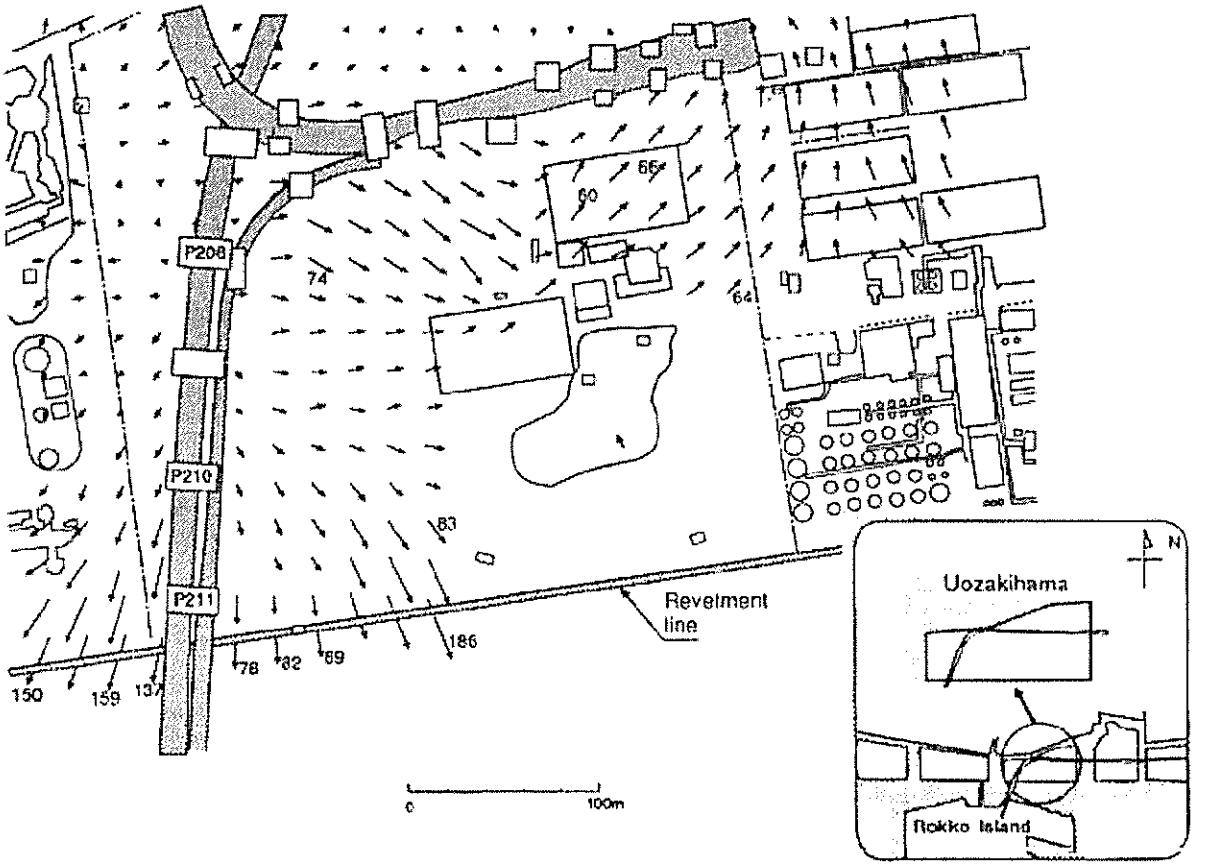

Figure 15. Ground Displacements in the South Part of Uozakihama Island (Hanshin Highway Authority. 1996).

Deleterious effects of lateral spreading were notably observed in performances of piers or bents of elevated highway structures standing in proximity to revetment lines. A typical example of such damage was seen in the Pier 211 of the Hanshin Expressway No.5 Bay Route which is located in the southernmost part of Uozakihama Island as shown in Fig.15. Features of the ground damage in the vicinity of Pier 211 are displayed in Fig.16 together with a plan view of the pier.

Several lines of fissures are visible on the ground surface near the revetment. A somewhat enlarged plan view of the foundation is shown in Fig.17 where it can be seen that two-column bents sit on a 22.5m long and 14.5m wide footing which is supported by 22 piles 1.5m in diameter. The piles were constructed of cast-in-place reinforced concrete. Side views of the Pier 211 are shown in Fig.17 where it is noted that the body of the footing is embedded to a depth of 4.18m.

A cross sectional view of the foundation and the quaywall across the section A-A' in Fig.16 is displayed in Fig.18, together with a soil profile. Exact location of the soil profile investigated (RP4-1) behind the quaywall is shown in Fig.16. As a result of measurements by GPS, it was discovered that the Pier 211 had moved towards the sea by 62cm, as accordingly indicated in Fig.18.

It is highly likely that liquefaction developed in the reclaimed fills in the back land leading to widespread occurrence of lateral spreading as demonstrated in Fig.15. The lateral displacement of the ground in close proximity to the Pier 211, but free from its influence, may be read off from Fig.15 as being in the order of 100cm.

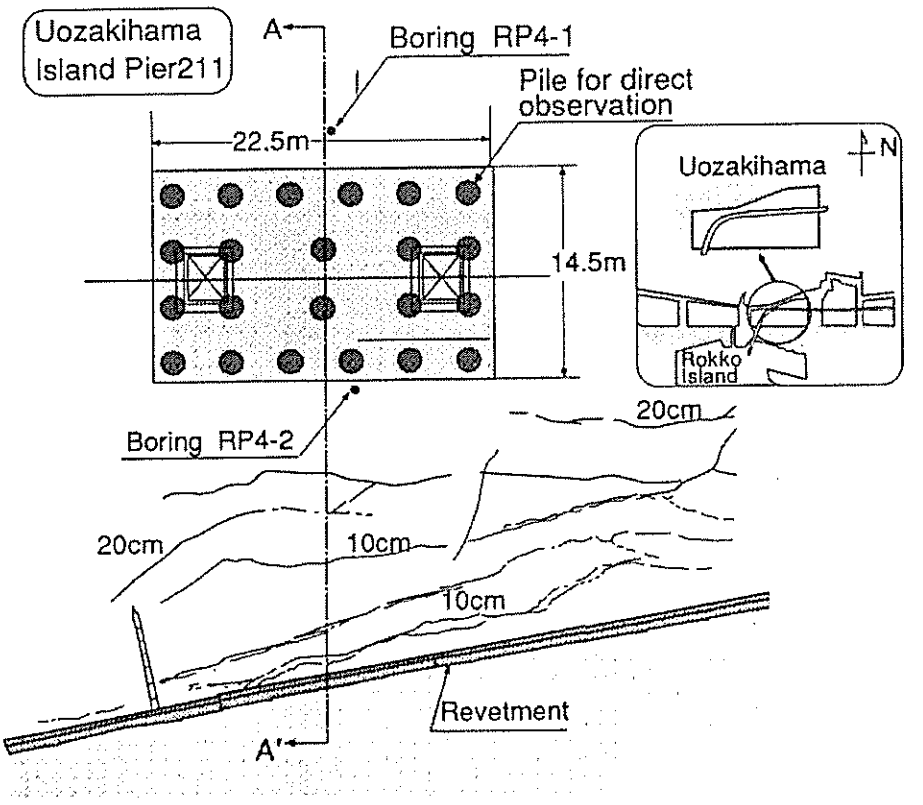

Figure 16. Ground Distortion and Location of Pier 211 (Hanshin Highway Authority, 1996).

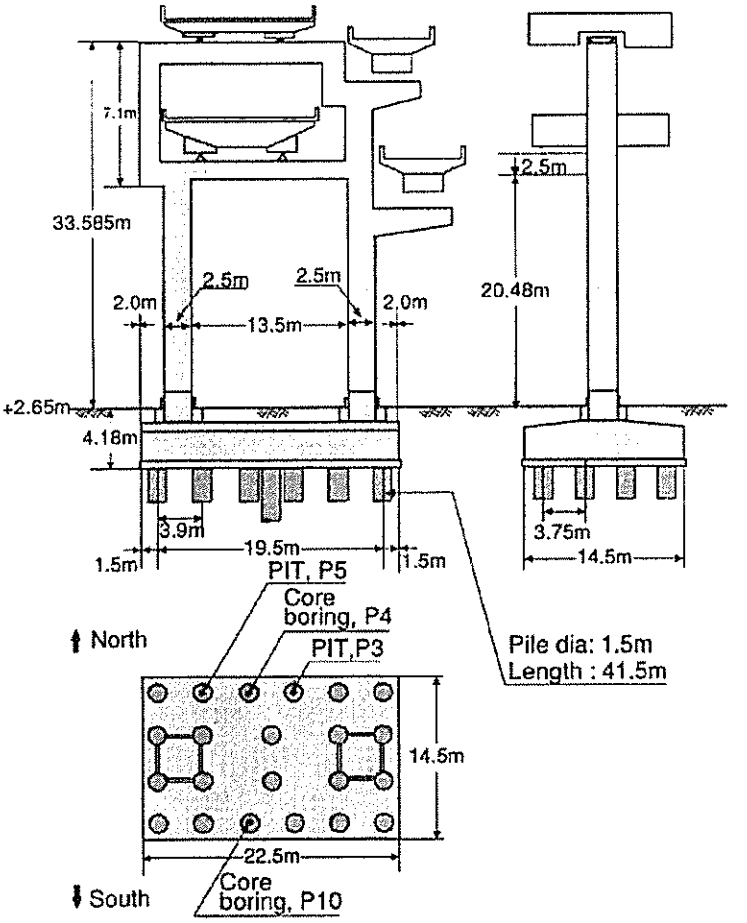

Figure 17. Plan and Side Views of Pier 211 (Hanshin Highway Authority, 1996).

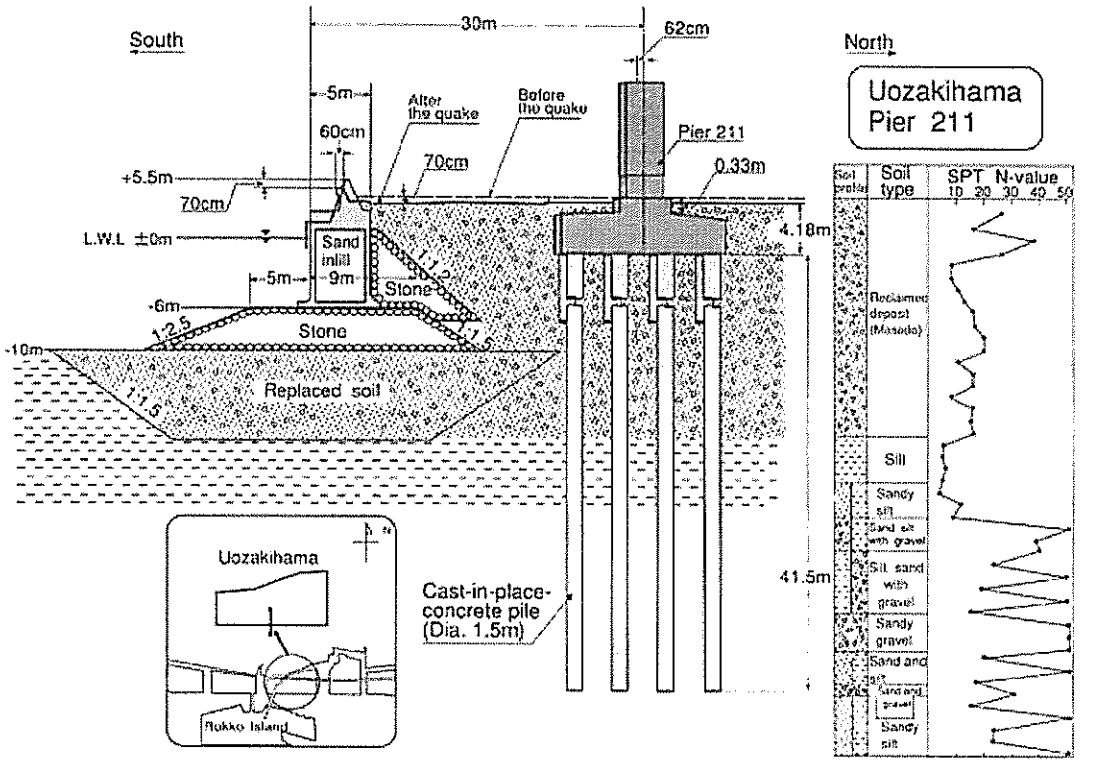

Figure 18. Quaywall, Foundation and Soil Conditions at Pier 211 (Hanshin Highway Authority, 1996).

To investigate the damage feature incurred to the foundations, three methods were employed for the bridge piers along the No.5 Bay Route line:

(1) excavation to the level of the pile head below the bottom of footings;
(2) picture-taking by means of video camera lowered to bored holes; and
(3) non-destructive method called "pile integrity test" using transmission of reflected waves.

For the investigation of piles supporting Pier 211, excavation was executed to a depth of 6m at the northeast corner of the footing, as shown in Fig.19, by enclosing a 3.2m by 4.5m section using sheet piles. Visual observation at the pile head disclosed several vertical and horizontal cracks a few millimetres wide.

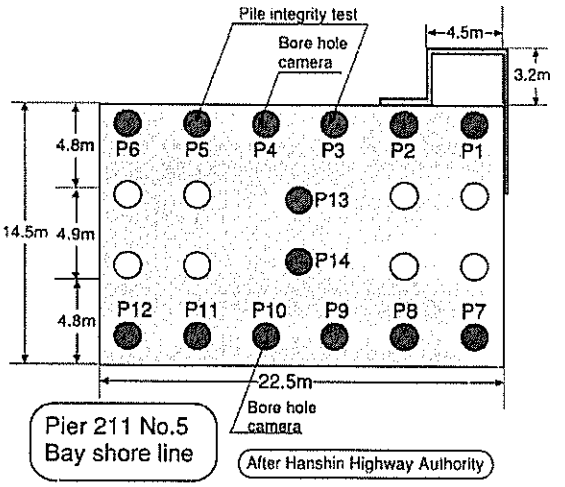

Figure 19. Plan View of the Foundation of Pier 211 (Hanshin Highway Authority, 1996).

In the second method of in-situ investigation, a borehole 7cm in diameter was drilled by the method of coring from the top surface through the footing slab down into the pile. If it happened to hit the reinforcement midway, another hole was drilled to reach a desired depth of 34m. A total of 2 holes were drilled to a depth of 34m for inspection of the damage in the foundation of Pier 211. Exact locations of the holes are shown in Fig.19. A video camera was lowered into the holes to examine feature of cracking around the walls. By and large, cracks were predominantly observed at depths corresponding to the boundary in soil deposits where liquefaction did and did not develop.

The outcome of the in-situ investigations as above revealed the fact that, generally speaking, the pile damage had taken place around the three depths illustrated in Fig.20. In practically all the piles investigated, cracks were detected at depths 0 - 3m below the bottom of the footing slab. The damage at the pile head was supposedly caused by a great magnitude of bending moment resulting from the inertia force from the superstructure during intense shaking at the time of the earthquake. The cracks near the interface between liquefied and unliquefied deposits were observed mainly in the piers located near the waterfront. The cracks were also observed at the depths of discontinuity where the cross sectional area or reinforcement was changed. This type of damage was identified, by and large, in the case of the piles located in proximity to the waterfront. Thus, it may be considered highly likely that the cracks at some depths were caused by the lateral spreading of the surrounding soils that had liquefied during the main shaking of the earthquake.

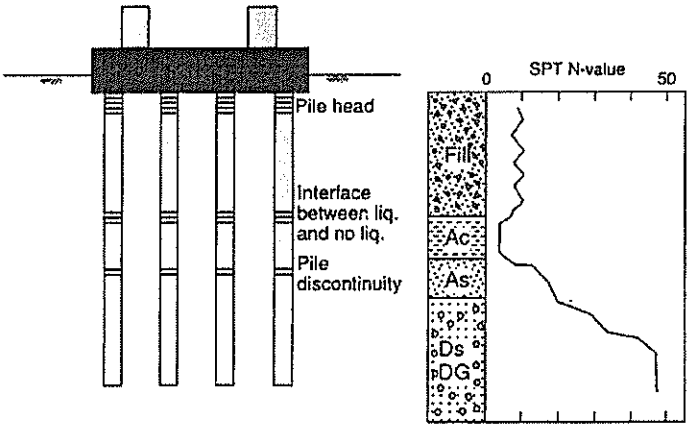

Figure 20. Three Locations in the Pile Body Where Cracks Were Predominantly Observed.

DAMAGE TO FOUNDATIONS OF STORAGE TANKS

There are several tank farms for storage of oil and liquefied propane gas (LPG) in the man-made islands in the port area of Kobe. Storage tanks with various capacities were shaken very severely and affected more or less by the ground damage due to liquefaction. Among several farms, the storage tanks and facilities in Mikagehama Island are those investigated in detail as to the effects emerging from the liquefaction of the ground.

The location of the tank farm is shown in Fig.7. Detailed layout of tanks and other related facilities are shown in Fig.21. As indicated, the triangular section in the southeast part is occupied by tanks and other related facilities for storage of LPG. The rest of the area in the northwest part is used for oil storage tanks. The LPG unshipping berth is located in front of the southern revetment and the berth for oil loading and unloading is located at the western revetment.

As a result of extensive liquefaction, lateral spreading took place over the island causing sand boiling, cracking in the premise of the LPG yard and settlements of the ground. The overall features of the ground cracking are demonstrated in terms of a sketch in Fig.22. It may be seen that there are depressions just behind the quaywalls accompanied by the large ground movements. Fissures or cracks are seen in the figure having developed farther inland from the waterfront.

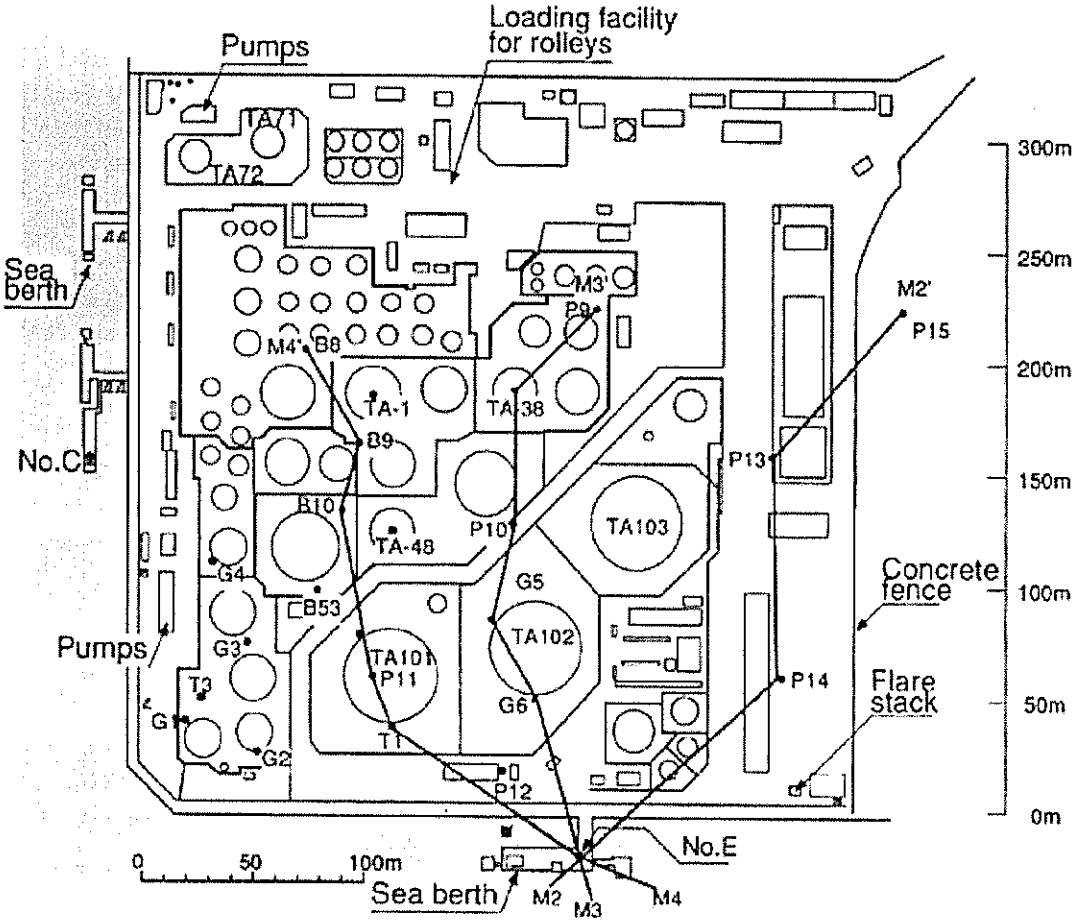

Figure 21. Map of the LPG Tank Location.

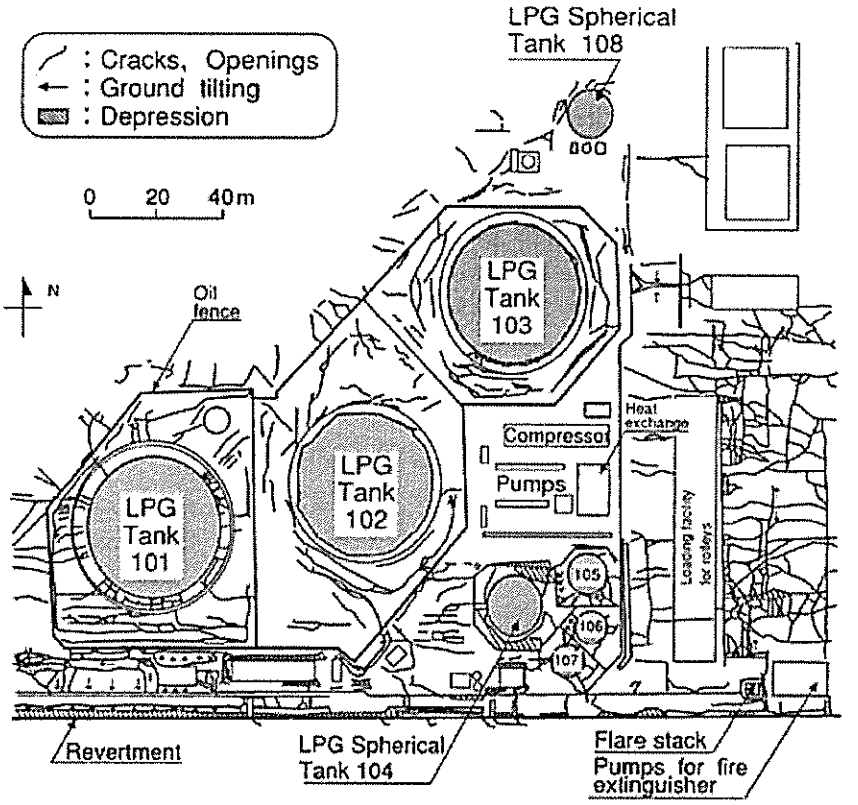

Figure 22. Ground Disruption in the Tank Farm (High Pressure Gas Institute, 1995).

Site investigations including SPT and tube sampling were conducted before and after the earthquake at various locations in the premise. Fig.21 shows the places where boring were performed to identify soil profiles. One of the soil profiles at a place in the centre of the LPG Tank 101 is shown in Fig.23 where it may be seen that the man-made Masado deposit consisting of sand with silt and gravel exists down to a depth of about 15m. The soil materials were taken from the weathered granite deposits at the foothill of the Rokko Mountain behind the Kobe City area. Underneath the reclaimed deposit, a layer of silty clay exists which is the seabed deposit before the reclamation was made in 1960's. It appears likely that the gravel containing silty sand had developed liquefaction due to the intense shaking during the earthquake.

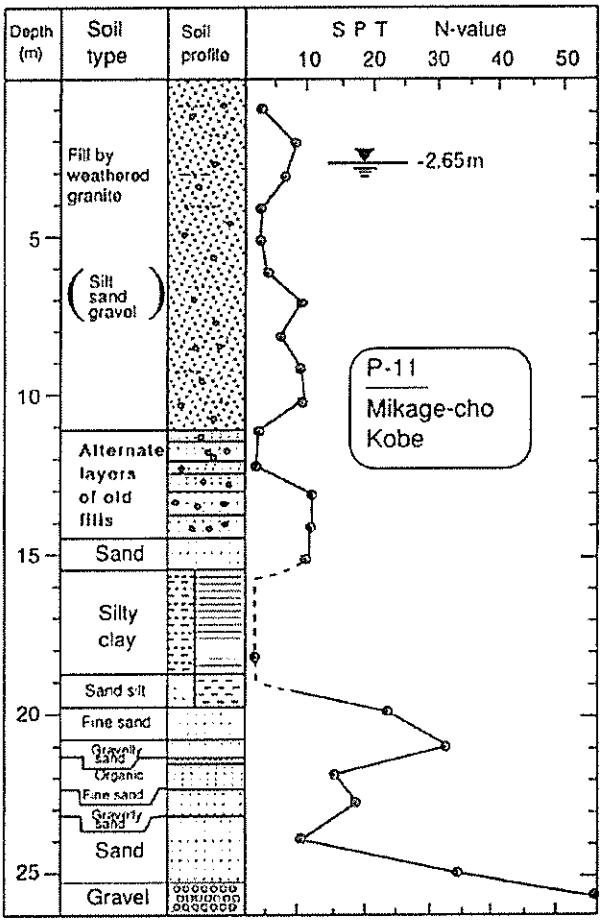

Figure 23. Soil Profile in the Centre of Tank 101.

In order to visualize overall features of soil profile, pictures of soil stratification through some cross sections were drawn based on individual soil profile data at several points. A cross sectional view through the sections M2-M2' and M3-M3' are shown in Fig.24 where it may be seen that, while the depth is variable to some extent, the reclaimed fill composed of Masado prevails to a depth of approximately 15-20m all over the island. The SPT N-values are low on the order of 10 to 15 and as such the reclaimed soils were under conditions susceptible to liquefaction. Underneath the reclaimed fills there exist a silty clay deposit in original seabed.

One of the LPG tanks (No.101 in Fig.22) with a storage capacity of 20,000kl sustained damage at the outlet-inlet nozzle (exit of liquefied gas) installed at the flank, leading to leakage of liquefied natural gas. At the time of the earthquake, this tank contained about 6,700kl of LPG and about half of the gas leaked in the premises enclosed by a protection fence. The remaining half was transferred to another uninjured tank after the quake. Luckily enough, the inflammable content did not catch fire, and therefore, a disastrous scenario was avoided. Some of the evaporated gas is purported to have dispersed in the air due to wind blowing towards south and the rest of the gas seems to have seeped into the ground through fissures of the ground created by the liquefaction.

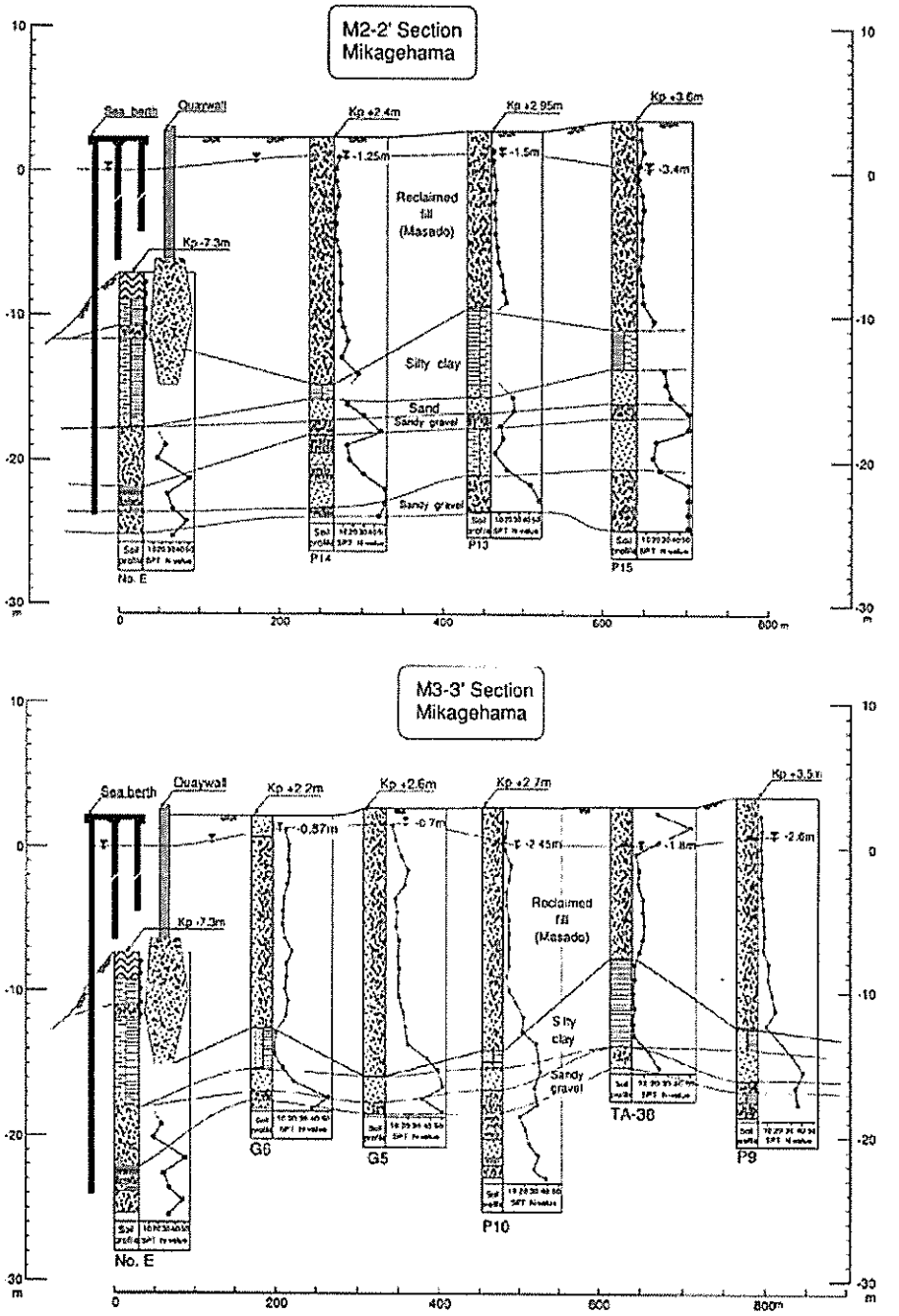

Figure 24. Soil Profile in the Cross Section M2-2' and M3-3'.

The cause of the leakage was explained as follows (High Pressure Gas Institute, 1995). A tall steel trestle had been installed outside the tank to hang up the emergency shut-off valve which was connected to the outlet nozzle pipe, as illustrated in Fig.25. This new installation was carried out some years after the start of the tank operation to ensure further safety. The steel trestle was resting on a simple concrete block embedded in the ground to a depth of about 1.5m.

Owing to the liquefaction, the ground moved seawards about 70cm. The concrete block also settled about 70cm accompanied by sinking of the trestle. As a result, all the weight of the trestle and its attachments were then applied as external loads to the emergency shut-off valve. This vertical load was transmitted to the inlet-outlet pipe rigidly connected with bolts to the flange of the LPG tank. Because of the excessive weight vertically applied, the bolt-fastened flange of the rigid inlet-outlet pipe was forced open slightly and this led to the leakage of LPG following the earthquake. It is apparent that this incident was caused by the large settlement of the concrete block supporting the trestle. As the pile-supported tank body remained unsettled, the relative settlement as much as 70cm occurred between the tank and trestle. This incident left an important lesson that the foundation of

auxiliary facilities should have been supported by a common foundation with the tank body. In spite of the leakage, no serious damage was incurred to the structure of Tank 101.

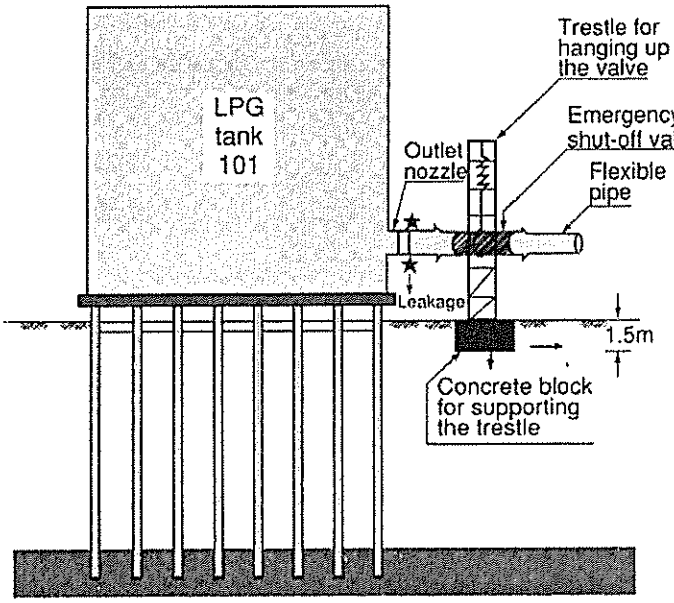

Figure 25. Illustration for the Gas Leakage due to Differential Settlement of Trestle and LPG Tank.

The foundation of the Tank 101 consists of 97 cast-in-place reinforced concrete piles installed using the Benoto excavation machine. The arrangements of the piles in plan and side views are shown in Fig.26. Each pile had a diameter of 1.1m and was embedded to a depth of 27m where a stiff deposit of gravel was encountered as shown in the soil profile of Fig.26. Note that the soil profile shown was obtained at the centre of tank before the construction.

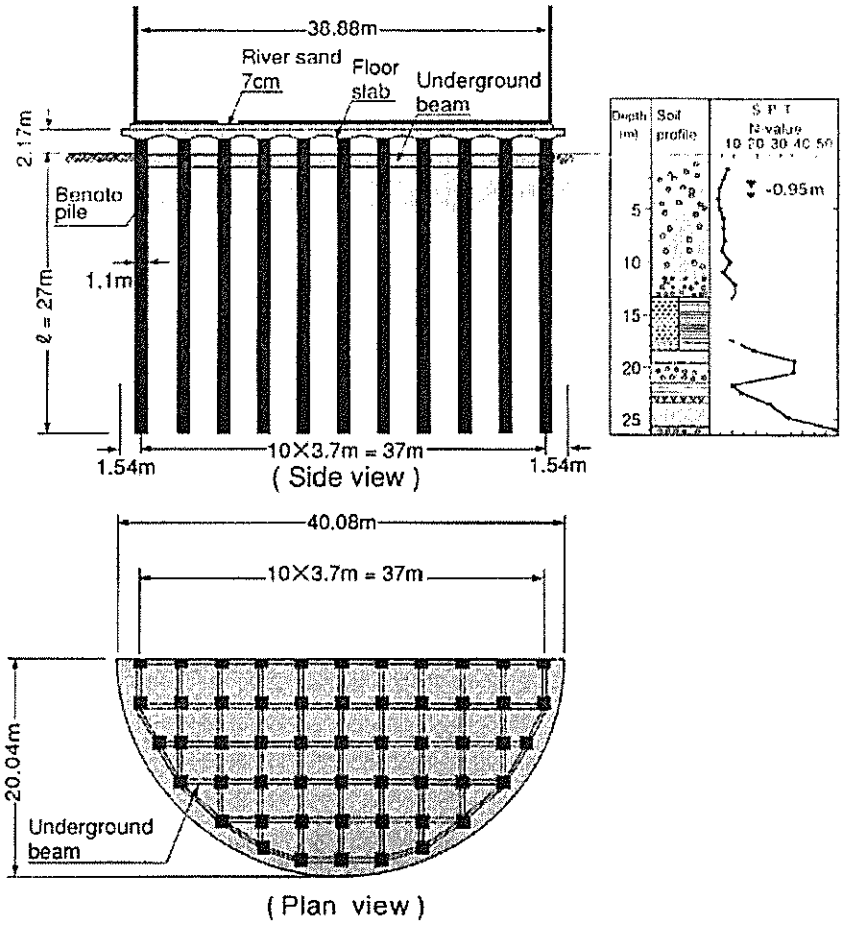

Figure 26. Side and Plan Views of the Foundation Pile Layout for the Cylindrical Tank 101.

To inspect soundness of the foundations, excavation was made after the earthquake underneath the Tank 101 all over the plan area to a depth of 2m where the ground water table was encountered. No damage whatsoever was discovered in the underground horizontal beams. The only small injury was horizontal cracks a few millimetres wide, which had developed on the side surface of some outside piles about 50cm below the tank slab. The surface concrete was scraped off to expose reinforcement, but no injury was identified at further depth.

BACK ANALYSES OF DAMAGED PILES

General Background

When piles are subjected to the lateral flow of once liquefied soils, lateral forces would be applied directly to the pile body throughout the depth of liquefaction. In assessing this force in the design, there would be two approaches:

- The first method consists of assessing directly the lateral force on the pile body either based on empiricism or by means of the concept of viscous flow (Chaudhuri et al., 1995; Hamada and Wakamatsu, 1998). This may be called the "Force-based approach". In either way, it would be difficult to introduce a parameter which reflects the degree of destructiveness in terms of the ground displacement. Thus, the specification of the lateral force would have to be made irrespective of whether the ground displacement is destructively large or small.
- In the second method, the lateral displacement of the ground is specified through the depth of the deposit. This prescribed displacement is applied to the spring-beam system thereby inducing lateral forces acting on the pile body. This procedure may be called the "Displacement-based approach".

One of the advantages of this latter method is that it allows the magnitude of ground displacement to be considered and specified, which is indicative of the degree of destructiveness or severity of the lateral spreading. In this method however, the choice of the spring constants has a profound influence on the magnitude of the lateral force induced, and as such, difficulty is encountered in correctly evaluating this value for design purposes. It is expected that the spring constant for the case of the laterally spreading soils is much smaller than that in the case of the back and forth movement of soils as stipulated in the Japanese Code of Highway Bridge Design mentioned above.

Thus, it becomes necessary to know the order of magnitude by which the conventionally used coefficient of subgrade reaction should be degraded to allow for the interaction taking place in the course of lateral spreading of liquefied soils. It is the objective of the following back analyses to clarify the degree of the stiffness degradation.

Characteristics of Piled Foundations

The majority of the piles damaged by the lateral flow of liquefied deposits at the time of the Kobe earthquake in 1995 may be divided into two groups, that is, the precast reinforced concrete piles and the cast-in-place reinforced concrete bored piles.

The precast concrete pile is hollow-cylindrical and has a diameter of 30-40cm. The length is generally in the range of 10-20m. The piles are arranged generally in a group of 4-6 piles which are capped at their top by a common footing about 0.5-1.0 m thick. The top of the piles are connected to the footing in different ways, and therefore it is difficult to identify whether the top was rigidly connected or not, especially because these piled foundations were constructed more than 20 years ago, and construction details are not known. The footing slab is generally embedded into the surface soil layer above the groundwater table which is therefore free from liquefaction. In many cases, the footings are connected to each other by horizontal beams forming a fairly rigid trestle placed near the ground surface. Therefore, it is likely that the large footing system near the ground surface does not move significantly together with the liquefied soils underneath. This implied the fact that the footing tends to restrict the movement of the pile body which is caused by the lateral flow of the underlying liquefied soil.

In contrast to the above, cast-in-place reinforced concrete bored piles are commonly used for supporting a large body of footings of piers for highway bridges. These piles have a diameter of 1.0-2.0m, and are constructed by the Benoto method. In this type of structures, the footing is constructed of massive reinforced concrete and has a thickness of 3 to 4m. The whole body is embedded in the ground to a depth of 3-4m where the ground water table is encountered. Thus, the lateral force in the non-liquefied surface layer acting on the sidewall of this embedded footing may not be ignored when making the back analyses for the behaviour of the underlying piles subjected to lateral flow.

Basic Assumptions and Rules of Load Partitioning

When making the back-analyses for the large-diameter group piles with a massive footing, it is necessary to assume, in one way or another, the magnitude and direction of the lateral force applied to the footing slab from the non-liquefied surface layer. It is also necessary to set up hypotheses as to how the total load on the footing is apportioned among the individual piles to which the analysis is to be conducted.

If the ground surrounding the footing moves by an amount larger than the footing slab itself, it is apparent that the lateral force applied to the footing is oriented in the direction of the ground flow as illustrated in Fig.27.

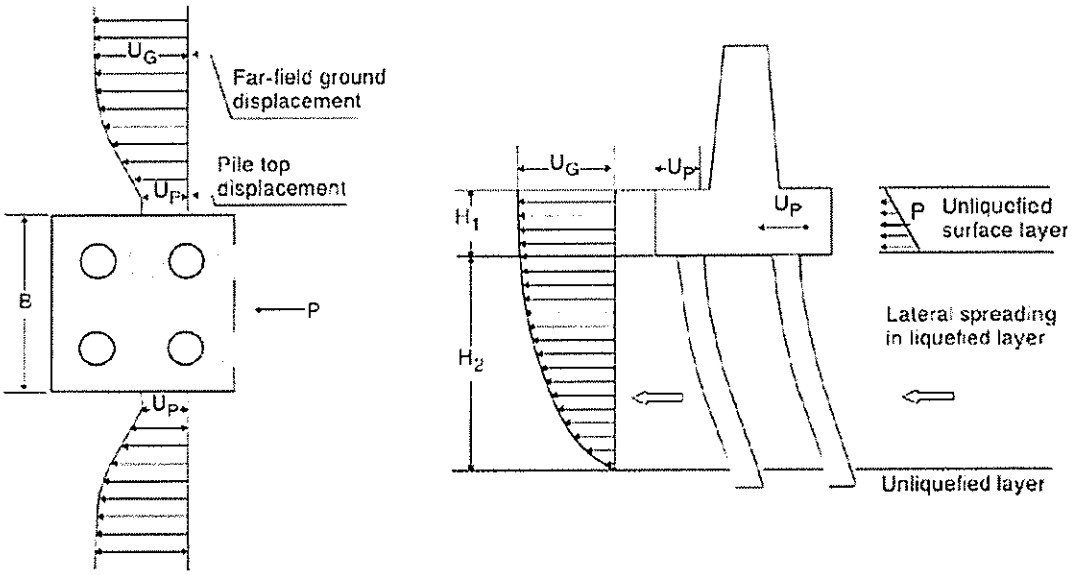

Figure 27. Pattern of Lateral Displacements of the Ground and Pile During Lateral Spreading of Liquefied Soil.

It may be assumed that the lateral force would be equal to or smaller than the passive earth pressure. The total lateral force, P, due to this earth pressure which is deemed as the maximum possible value is given by

$$P = 1/2\gamma_t K_P H_1^2 B \qquad (1)$$

where $K_P = \tan^2(45° + \phi/2)$, ϕ is the angle of internal friction, H_1 is the thickness of the unliquefied surface layer, and B is the width of the footing. It is to be noticed that the lateral force given by Eq. (1) is applied only when the relative magnitude of the displacement of the pile and surrounding soil is sufficiently large to mobilize the passive earth pressure. The total force P given by Eq. (1) is transmitted through the footing to the top of individual pile in the group.

In apportioning this total force to the individual pile, several assumptions may be made. While the exact rule has yet to be decided, the simplest concept would be to assume that the total lateral force is

carried equally by each pile. Thus, the back-analysis will be made in the present study for a single pile with a given flexural stiffness as illustrated in the side view of Fig.28.

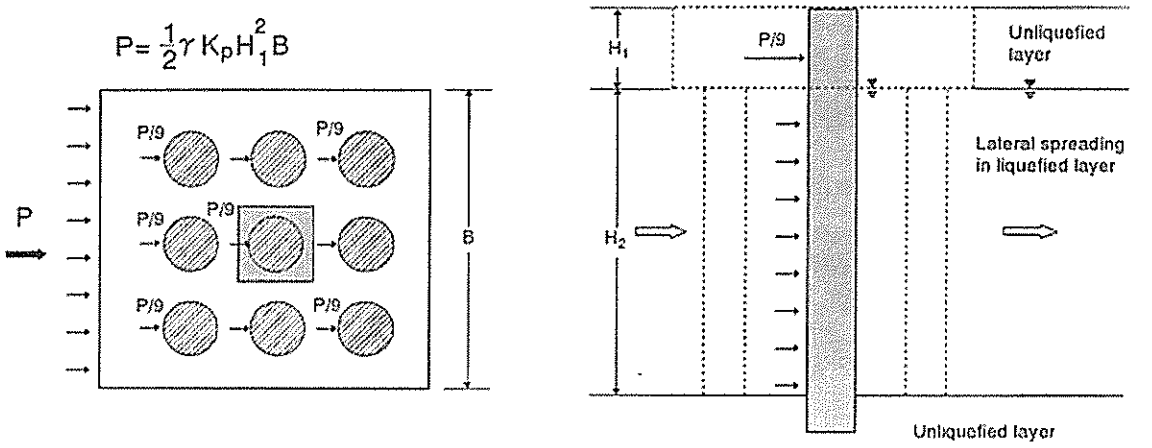

Figure 28. Hypothesis for Partitioning a Load from the Footing to Piles.

Scheme of Back-Analysis

The behaviour of piles is assumed to be represented by the model in which the lateral force, F, acting on the piles is proportional to the relative displacement between the pile and the surrounding soil in far-field condition. This may be written as

$$F = \beta k D (U_G - U_P) \qquad (2)$$

where U_G and U_P are lateral displacements of the ground and pile respectively, D is the diameter of the pile, and k is the coefficient of subgrade reaction. The model is schematically illustrated in Fig.29.

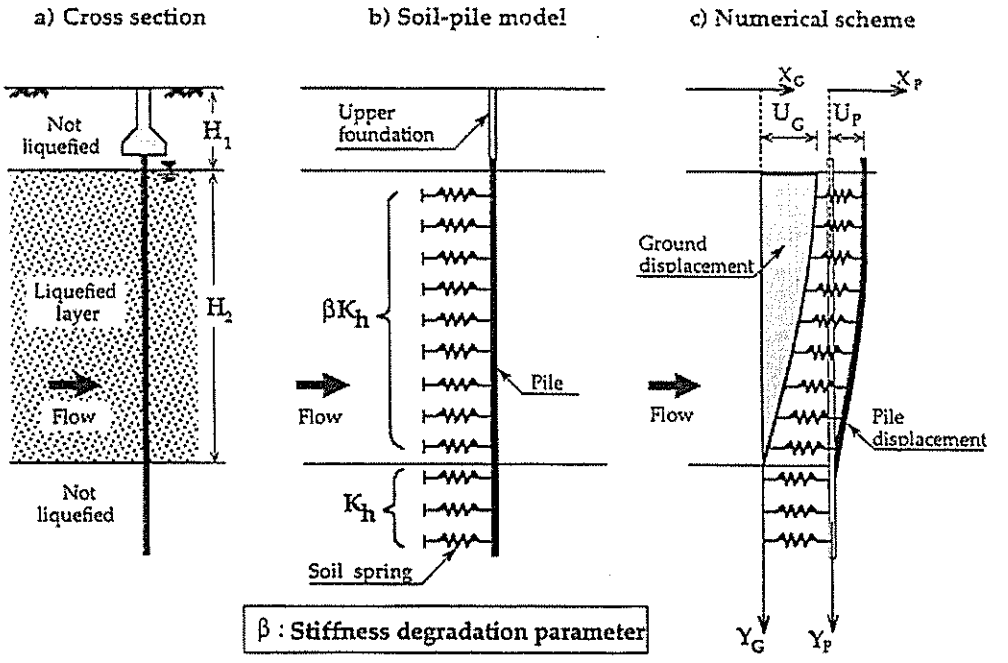

Figure 29. Soil-Pile Model and Numerical Scheme.

If the soil were brought to a state of liquefaction and consequent lateral flow, the stiffness of the soil would be reduced drastically leading to a reduction in the k-value. The degree of this stiffness reduction is expressed by β in Eq. (2), which will be referred to as the "stiffness degradation parameter". The main aim of the present back-analyses is to pursue the range of this degradation parameter. The steps of the analysis to be followed are described below.

(1) The stiffness of the spring is assumed to decrease by a factor β upon liquefaction and lateral spreading of the soil through the depth of liquefaction, H_2. The spring constant in the underlying non-liquefied zone is assumed not to be degraded. It is further assumed that the stiffness degradation occurs uniformly throughout the depth H_2 where lateral spreading is taking place.

(2) Generally, there is a non-liquefied layer to a certain depth H_1 near the surface. This depth may be roughly defined to be equal to the depth to the ground water table. The movement of this non-liquefied soil mass may be modelled in different ways:
   - One is to assume the surface layer moves in unison with the underlying liquefied stratum. This could be the case where the large diameter piles such as the cast-in-place piles are installed with a massive footing. In this case, it may be assumed that the passive earth pressure is applied to the side wall of the footing on the upstream side in the same direction as the flow of the underlying liquefied soil layer, as illustrated in Fig.27. In this type of surface soil movement, the displacement of the pile head is always considered smaller than the overall movement of the surrounding soil.
   - Another assumption would be there is only little movement of the surface non-liquefied layer due to the strong constraint imposed by a large frame of the footing system connected in lattice by a number of horizontal beams. This could be the case for the small-diameter piles such as the pre-cast reinforced piles frequently used for 5-10 storey buildings.

(3) The ground displacement due to lateral spreading is specified, and given to the springs in the liquefied portion of the soil deposit; displacements, bending moments and lateral forces acting on the pile body are calculated. The pile is assumed to deform in an elasto-plastic manner where the moment-curvature relation is represented by a trilinear relationship.

(4) The analysis as above is repeated several times with varying β-values. The stiffness degradation parameter, β, giving the pile head displacement which is equal to the observed value would be taken as the β-value actually encountered during the lateral flow at the time of the earthquake.

Analysis for Highway Bridge Pier

The piled foundation supporting the Pier 211 of the elevated structure of the Hanshin Expressway Bay route No.5 in Kobe will be considered in this back-analysis. The foundation consists of bored piles 1.5m in diameter and 41.5m in length as shown in Figs.17 and 18, where it can be seen that the footing embedded to a depth of 4.18m is supported by 22 cast-in-place reinforced concrete piles constructed by the bored-hole method. The cross sectional view of the piled footing and soil profile in its vicinity is shown in Fig.18. Here it may be seen that the reclaimed deposit composed of gravel, sand and silt exists to a depth of about 20m where liquefaction and consequent lateral spreading are assumed to have occurred.

As one of the investigations for examining the damage of the piles, two holes 7cm in diameter were drilled from the top surface through the footing slab down into the piles P4 and P10 shown in Fig.19. A video camera was lowered into the holes to inspect features of the crack development and the outcome is shown in Fig.30. It may be seen that the cracks are concentrated near the pile head and also in the vicinity of the interface between the liquefied deposit and underlying non-liquefied layer. In the analysis, the flexural stiffness characteristics of a single pile were assumed to be those shown in Fig.31 which were obtained from the cross sectional characteristics of the bored pile.

Characteristics of the soil model used for the piled foundation of Pier 211 are illustrated in Fig.32. In this figure the depth-wise distribution of the K_h-value ($K_h = k\,D$), as estimated from *SPT N*-value by way of empirical formulae in the Japanese Code of Highway Bridge Design, is given together with the depth of liquefaction which was evaluated from an independent analysis. As a result, liquefaction was considered to have developed to a depth of 20m.

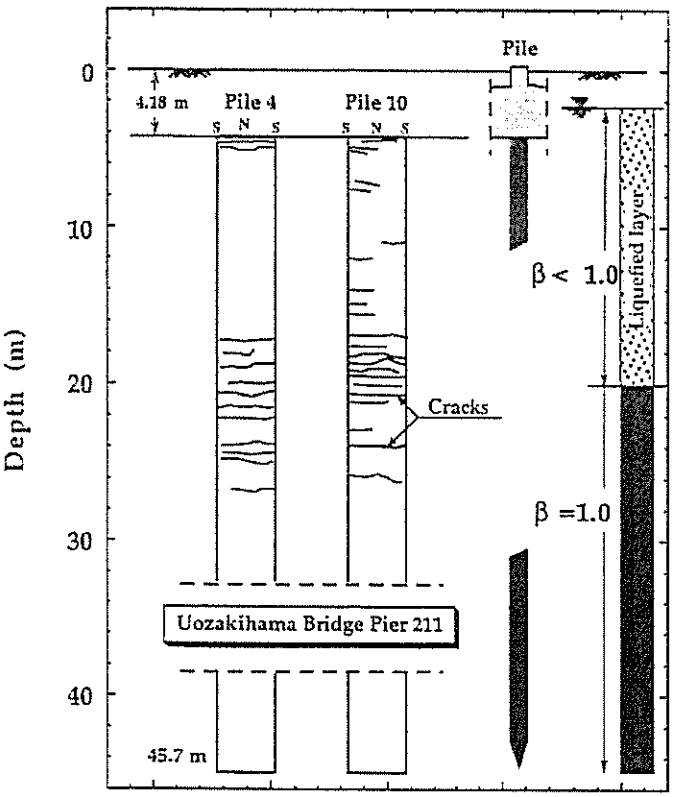

Figure 30. Crack Distribution in the Bored Piles at Bridge Pier 211 in Uozakihama Island.

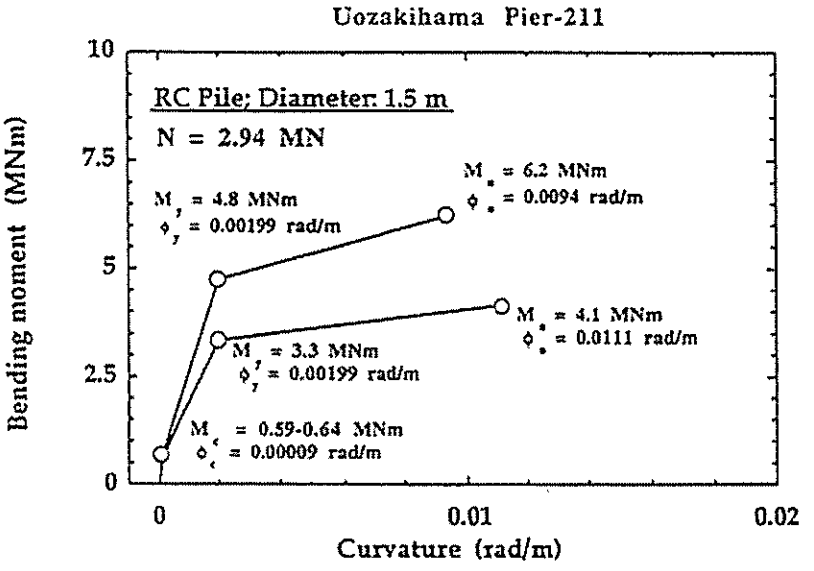

Figure 31. Bending Moment Versus Curvature Relation for the Large Diameter Piles at Bridge Pier 211.

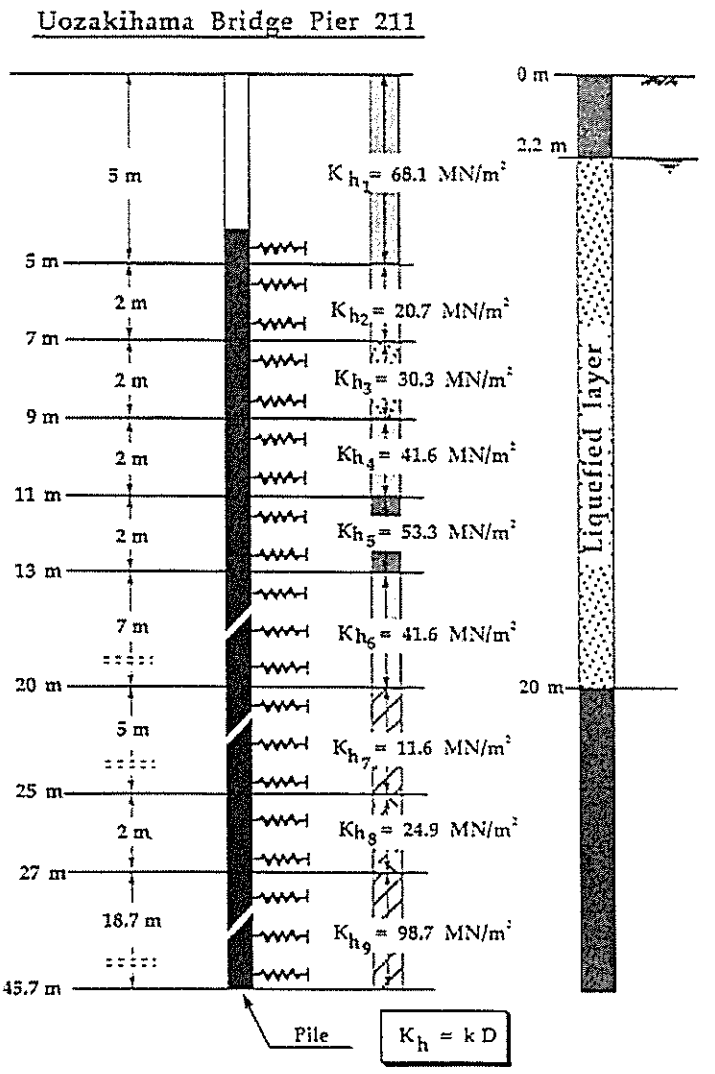

Figure 32. Soil Stiffness Properties for the Cast-In-Place RC Pile at the Bridge Pier 211 in Uozakihama Island.

Based on the data shown in Fig.15, the lateral displacement at the Pier 211 was assumed to be 1.0 m on the ground surface in the free-field condition and distributed in a form of cosine function through the liquefied layer down to a depth of 20m as displayed in Fig.33. In the actual computation, the presence of the footing was represented by an equivalent rigid beam and a single pile was postulated to extend and stand to the ground surface with the lateral force applied at the bottom of the footing (pile top) in the direction of flow, as indicated in Fig.33. The magnitude of the lateral force applied at the pile head was equal to the total passive earth pressure on the side of the footing divided by the number of piles.

Computation was made for varying values of the stiffness degradation parameter in the range between $\beta = 1\times10^{-3} - 1\times10^{-2}$. The deformation of the pile obtained from the analysis with different β-values is also shown in Fig.33.

Pier 211 is reported to have displaced about 60 cm as a result of the ground movement towards the sea. In the light of this value, the degradation parameter of $\beta = 5\times10^{-3}$ seems to yield the best fit to the observed performance of Pier 211. The bending moment distribution down the pile resulting from the computation is shown in Fig.34. For the case of $\beta = 5\times10^{-3}$, the computed bending moment is in excess of the yield moment, *My*, near the pile head and also around the depth of 20 m where discontinuity is encountered from the liquefied to the unliquefied layers. This observation is consistent with the location of the cracks as demonstrated in Fig.30. The result of the above analysis is plotted in

Fig.38 in terms of the stiffness degradation parameter β versus the relative displacement between the ground surface U_G and the pile top U_P divided by the depth H_2 of the liquefied deposit.

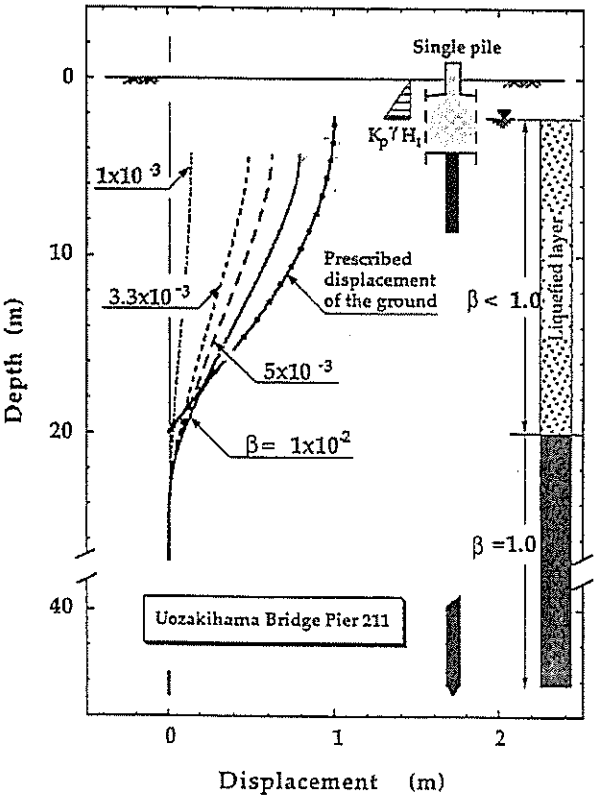

Figure 33. Lateral Displacement of the Pile at Pier 211: Analysis with the Single-pile Hypothesis.

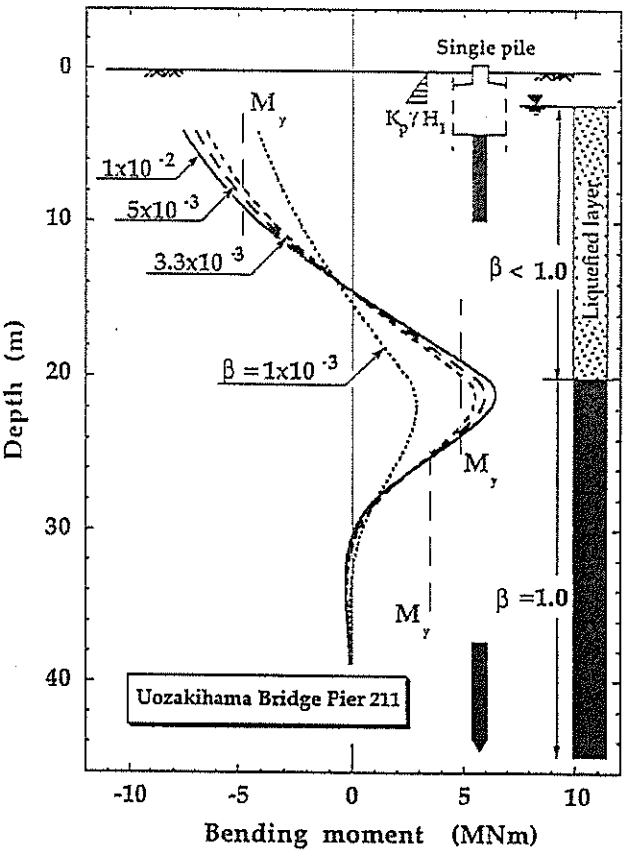

Figure 34. Bending Moment of the Pile at Pier 211: Analysis with the Single-pile Hypothesis.

Analysis for Foundation of Storage Tank

A cylindrical tank with a capacity of 20,000kl for storage of LPG (Liquid Propane Gas) located in Mikagehama was back-analysed. The details of the performance of this tank are described in the preceding section. This tank 39m in diameter was supported by a total of 97 cast-in-place bored piles 1.1m in diameter and 27m in length. Each of the piles spaced at 3.7m is connected by underground horizontal beams arranged in a lattice as displayed in Fig.26.

The horizontal beam 2.0m in height was embedded into the ground. It was assumed in the back-analysis that this 2.0m thick horizontal beam-lattice system constitutes a large footing which is considered rigid enough to be regarded as a massive footing. On this basis, the assumptions described above were incorporated for estimating the lateral force acting on a pile from the unliquefied surface layer.

At the centre of the Tank 101, located at a distance of 50m from the quay wall, the lateral displacement which would have occurred had the tank not been there is estimated to be 1.8m, based on the field measurements nearby. The exact amount of the lateral movement of the Tank 101 itself is not known, but in view of there having been practically no damage to the tank body, the lateral displacement is inferred to have been in the order of 20cm. The flexural stiffness characteristics of the bored pile are shown in Fig.35 in terms of trilinear relation between the bending moment and curvature of the pile.

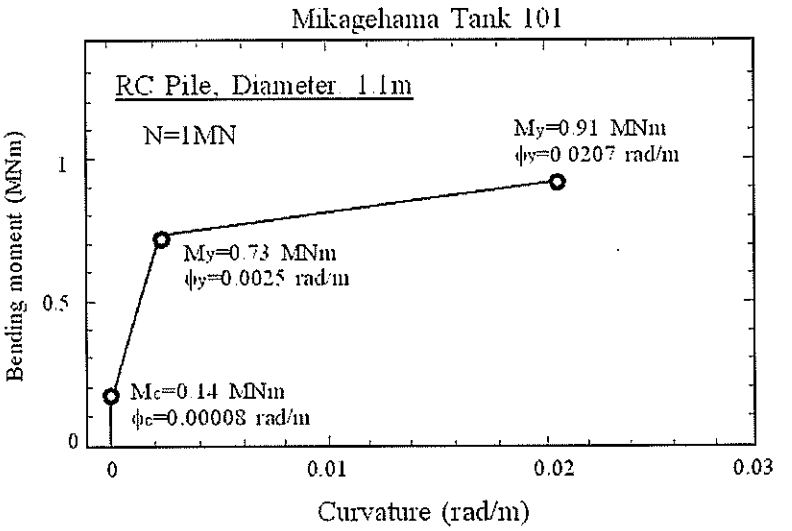

Figure 35. Bending Moment versus Curvature Relation for the Bored Piles at Tank 101.

The scheme of the back analysis, based on the single pile hypothesis, is schematically shown in Fig.36. The free field ground displacement was given in a form of the cosine function with its maximum of 1.8m on the ground surface. The resulting displacements of the pile are also shown in Fig.36 for varying values of the stiffness degradation parameter postulated in the analysis. It may be seen that the best fit for the pile deformation of 20cm is achieved with the parameter $\beta = 2 \times 10^{-4}$.

The bending moment induced in the pile is computed as displayed in Fig.37 where it may be seen that the parameter $\beta = 2 \times 10^{-4}$ gives a bending moment at the pile head which is about the yield value *My*, whereas the bending moment is less than the yield value at the interface.

In the case of Tank 101, no detailed investigation was conducted after the earthquake to examine features of damage to the pile body throughout the depth of 16m. Excavation was, however, performed after the quake to a depth of 2.0m to expose the horizontal beam as well as the pile head. Visual observation disclosed that only few horizontal hair-cracks had developed near the pile head but upon scraping the concrete surface, the cracks were found to not penetrate deep into the pile body. Thus, the pile head is conjectured to have been narrowly on the verge of minor injury.

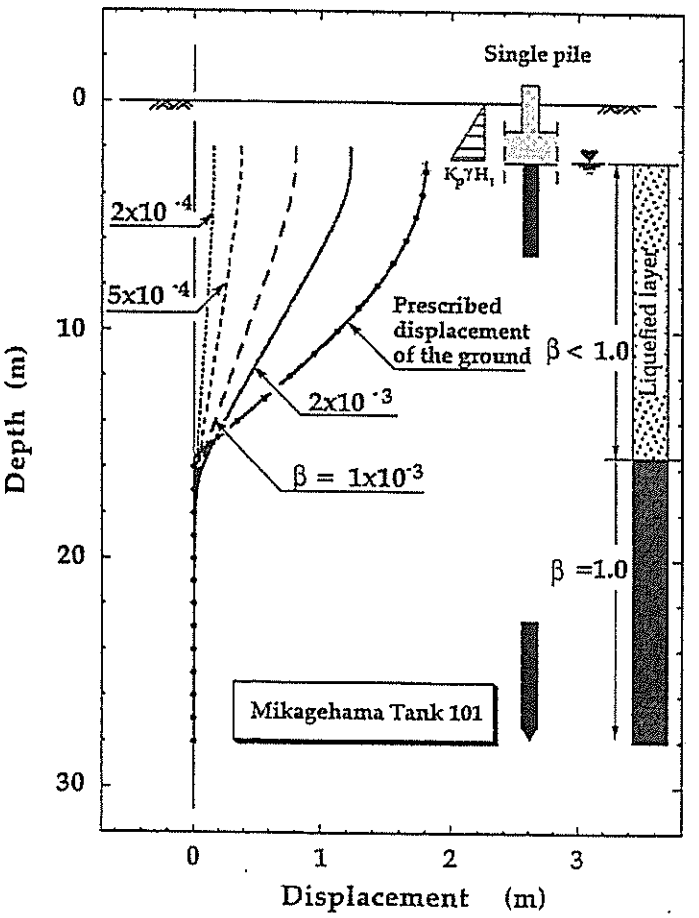

Figure 36. Lateral Displacement of the Bored Pile at Tank 101: Analysis with the Single-pile Hypothesis.

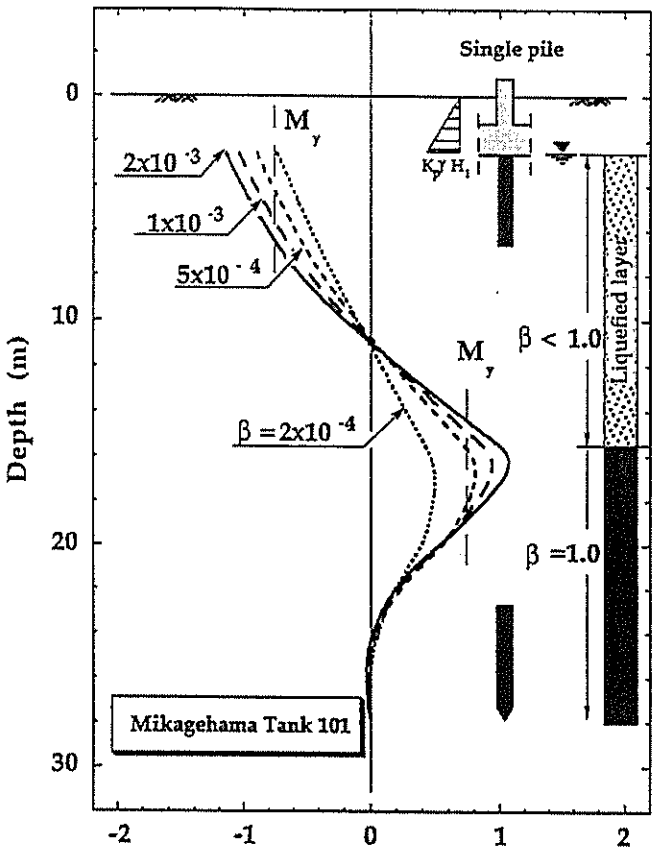

Figure 37. Bending Moment of the Bored Pile at Tank 101: Analysis with the Single-pile Hypothesis.

Reflecting upon the above observation, it may be mentioned that the value of $\beta = 2\times10^{-4}$ would be taken reasonable for the stiffness of the soil degraded as a result of liquefaction and consequent lateral spreading. The result of the above analysis is plotted in Fig.38 in a manner similar to the case of the Pier211 at Uozakihama.

Analyses of Small Diameter Precast Concrete Piles

The back-analyses for small-diameter precast concrete piles have also been done in similar manner for four cases of injury incurred at the time of the Kobe earthquake as well as at the time of the Niigata earthquake in 1961 (Ishihara, 1997; Ishihara and Cubrinovski, 1998). The results of the back-analysis are summarized in Fig.38 where the stiffness degradation parameter, β, is plotted versus the relative displacement $U_G - U_P$ divided by the thickness of the liquefied layer H_2. As illustrated in the inset of Fig.38, U_P and U_G denote the displacements of the pile top and the ground surface, respectively.

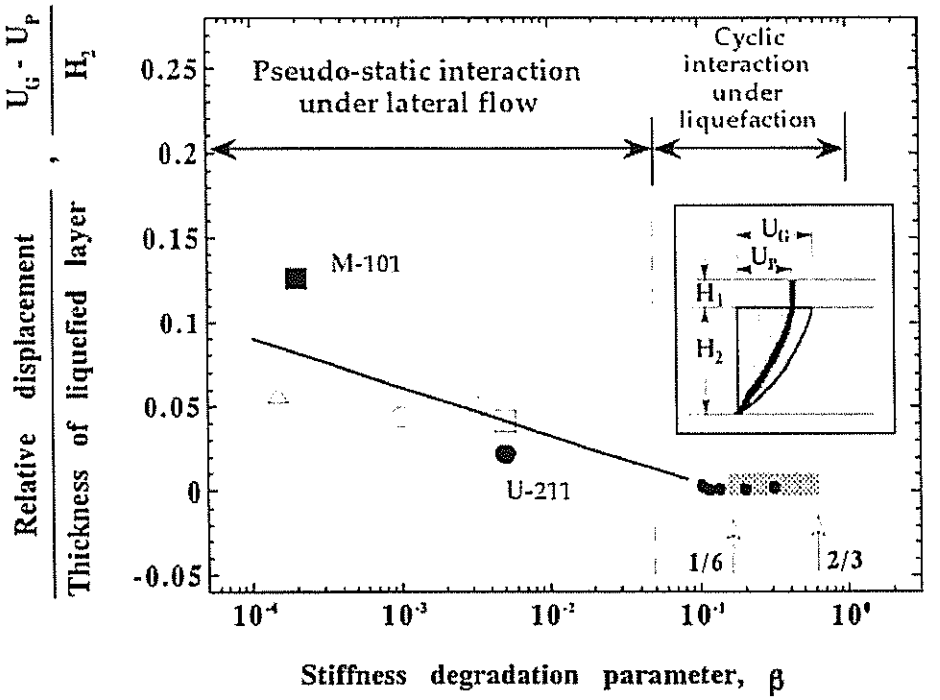

Figure 38. Summarized Relations Between the Normalized Relative Displacement and Stiffness Degradation Parameter.

In performing the analysis the soil-pile interaction was represented by the spring-beam model. It was also assumed that the pile extended upwards to the ground surface and characteristics of the footing slab were taken into consideration. In the analysis, the ground displacement with a given value U_G on the surface and with cosine distribution versus depth was given to the spring system, and the deformation of the pile body was calculated for various values of the stiffness degradation parameter.

Among several pile top displacements computed, the stiffness degradation parameter matching the observed or estimated displacement on the surface was chosen as the most likely value representing the realistic scenario of the pile-soil interaction during the lateral spreading. The results of the analyses shown in Fig.38 indicate that the stiffness degradation lies in the range as small as $2\times10^{-4} - 1\times10^{-2}$ for the pile-soil interaction under the condition of lateral spreading.

GENERAL CONSIDERATIONS

The majority of reinforced concrete pile foundations used hitherto in Japan may be classified roughly into two groups, that is, the precast reinforced concrete piles and the cast-in-place reinforced concrete bored piles. The precast concrete piles have an annular cross section with a diameter of 30-40cm and their length is 10-30m. They are used to support medium-weight structures such as buildings and warehouses. Four to six piles are connected in a group at their top to a small-size footing slab about 2×2 m in plan. The footing slabs embedded in the ground to a depth of 1.0-1.5m are connected to the neighbouring slabs through underground horizontal beams.

The cast-in-place reinforced concrete piles have a large diameter of 1.0-2.0m and their length is 30-40m. These piles are constructed by what is called the Benoto excavation method. They are used to support large structures such as piers of highway bridges and heavyweight buildings. A massive reinforced concrete footing is placed on top of the pile group consisting of 20-30 bored piles. The thickness of the footing is 2-4m and the whole body is embedded into the ground.

When foundation piles are subjected to strong motions during earthquakes the pile would be deformed back and forth in unison with the movement of the surrounding ground. This facet of the seismic event may be termed vibratory or cyclic loading phase. If the ground moves largely, the pile may move concurrently and this may lead to some degree of injury due to excessive cyclic deformation. If soils in the neighbourhood develop liquefaction during the main shaking, the stiffness of the soils will be degraded further leading to much larger deformation of the ground which may be sufficient to bring about injury to the piles embedded in such ground.

According to the Japanese code of bridge design, the stiffness degradation due to liquefaction is to be taken into consideration by reducing this coefficient by a factor of 1/6 to 2/3. It has been known that the deformation of the pile in the cyclic loading phase is dominated by the movement of the surrounding ground, and there is practically little difference in the lateral displacements between the pile and the surrounding ground. This implies that even by the degraded stiffness of the above order of magnitude. the pile moves almost in unison with the surrounding soils.

Thus, it may be postulated with good reasons that the value of the global strain as defined by $(U_G - U_P)/H_2$ would be small and likely to be in the order of less than about 1%. If this value is plotted versus $\beta = 1/6 - 2/3$ in Fig.38, the data would be located within the range indicated by the shaded area. There are some unpublished data in the above context obtained from effective stress analyses of pile behaviour in liquefied deposits in Port Island using the finite element technique. The results of these analyses are also shown in Fig.38 by small bold circles where it can be seen that the data from the effective stress analyses also lie well within the zone established for the values from the design code.

Thus, no matter whichever it is the vibratory or laterally moving phase, the relation between the relative displacement and the stiffness degradation parameter may be defined almost uniquely and expressed by a single curve for a given type of the pile, as indicated in Fig.38.

CONCLUDING REMARKS

As a result of back-analyses for cast-in-place and precast reinforced concrete piles damaged at the time of the Kobe earthquake, it was disclosed that when the piled are subjected to lateral spreading, the coefficient of subgrade reaction in the soil pile interaction model needs to be reduced by a factor of $2 \times 10^{-4} - 2 \times 10^{-2}$ from the values established for non-liquefaction conditions. It was also shown that, whichever the type of piles, the reduction of the coefficient of subgrade reaction should become more pronounced as the displacement of the pile increases in comparison to that of the surrounding ground.

ACKNOWLEDGEMENTS

The contents described in this paper are an excerpt of those published previously. The author wishes to acknowledge the efforts by his colleagues in Japan. The author also wishes to express his deep thanks to the New Zealand Geotechnical Society for extending an invitation to the author as a keynote speaker on the occasion of the Symposium in 2003.

REFERENCES

Berrill, J. and Yasuda, S. (2002). "Liquefaction and Piled Foundations: Some Issues", *Journal of Earthquake Engineering, Vol.6, Special Issue 1,* pp. 1-42.

Chaudhuri, D. Toprak, S, and O'Rourke, T.D. (1995). "Pile Response to Lateral Spread: A Benchmark Case", *Lifeline Earthquake Engineering, Proceedings 4th U.S. Conference, San Francisco, California*: pp. 1-8.

Hamada. M. and Wakamatsu, K. (1998). "A Study on Ground Displacement Caused by Soil Liquefaction", *JSCE Journal of Geotechnical Engineering, No. 596/III-43*, pp. 189-208.

Hamada, M., Isoyama. R., and Wakamatsu. K. (1996), "Liquefaction-Induced Ground Displacement and its Related Damage to Lifeline Facilities", *Soils and Foundations, Special Issue on Geotechnical Aspects of the January 17, 1995 Hyogo-ken Nambu Earthquake*, pp. 81-97.

Hanshin Highway Authority (1996), "Investigation on the Seismic Damages of Bridge Foundations in the Reclaimed Land (in Japanese)".

Hatanaka, M., Uchida. A. and Ohara, J. (1997), "Liquefaction Characteristics of a Gravelly Fill Liquefied During the 1995 Hyogo-ken Nambu Earthquake", *Soils and Foundations, Vol. 37, N0.3*, pp. 107-115.

High Pressure Gas Safety Institute of Japan (1995), "Interim Report of Investigation Committee on the LP-Gas Leakage from a Storage Tank Caused by the Kobe Earthquake".

Inagaki, H., Iai, S., Sugano, T., Yamazaki, H., and Inatori, T., (1996), "Performance of Caisson Type Quaywalls at Kobe Port", *Soils and Foundations, Special Issue on Geotechnical Aspects of the January 17, 1995 Hyogo-ken Nambu Earthquake*, pp. 119-136.

Ishihara. K. (1997). "Geotechnical Aspects of the 1995 Kobe Earthquake", *Terzaghi Oration Proceedings, 14th International Conference on Soil Mechanics and Foundation Engineering, Hamburg, Vol.4*, pp. 2047-2073.

Ishihara, K., Yoshida K., and Kato, M., (1997), "Characteristics of Lateral Spreading in Liquefied Deposits During the 1995 Hanshin-Awaji Earthquake", *Journal of Earthquake Engineering, Vol. 1, No. 1*, pp. 23-55, Imperial College Press.

Ishihara K., and Cubrinovski M. (1998). "Soil-Pile Interaction in Liquefied Deposits Undergoing Lateral Spreading", *Proc. 11th Danube-European Conference on Soil Mechanics and Geotechnical Engineering*, Porec, Croatia.

Ishihara K. (2001). "Lateral Flow-Affected Pile Behaviour as Interpreted by a Simple Model", *Proceeding, 11th Asian Regional Conference on Soil Mechanics and Geotechnical Engineering, Vol. 2,* pp.615-623.

Matsui, T. and Oda, K. (1996), "Foundation Damage of Structures", *Soils and Foundations, Special Issue on Geotechnical Aspects of the January 17, 1995 Hyogo-ken Nambu Earthquake*, pp. 189-200.

Earthquake Resistant Foundation Design

K J McManus
BE (Hons), ME, PhD, Regd Engr
Dept. Civil Engineering, University of Canterbury

Abstract: Recent experimental research at the University of Canterbury concerned with the load-displacement behaviour of both shallow and deep foundations is outlined. Issues addressed include base sliding friction and passive resistance mechanisms of shallow foundations, capacity of deep foundations with cyclic axial and lateral loading, and interactions between shallow and deep foundations. Practical considerations are discussed including two design examples.

Several full-scale shallow foundations were tested by shoving back-and-forth by using a powerful hydraulic actuator with several cycles of quasi-static lateral loading. These tests were supplemented with several, simpler interface sliding tests performed on concrete slabs constructed "on-grade" using one or two layers of polymer damp-proof membranes. A simple method of analysis was developed and found to give good predictions for the experimental results while accounting for all of the main parameters.

Many load tests have been made on large model piles with cyclic axial loading, combined cyclic axial and lateral loading, and monotonic and cyclic axial loading in a shaking soil deposit. Several full-scale load tests on driven and bored concrete piles were made to confirm applicability of the model test results to prototype foundation designs.

Application of the test results to practical design situations is discussed and illustrated by two design examples. The need for close interaction between the geotechnical designer and the structural designer in order to obtain optimum design solutions is stressed.

INTRODUCTION

Foundations are key elements in determining the overall performance of structural systems subjected to earthquake shaking, yet their behaviour is largely taken for granted by structural designers. Especially overlooked is the fact that during earthquakes the foundations actually apply the loads to the structure rather than the usual situation where the foundations receive gravity and environmental loads from the structure. Structural designers often make elaborate calculations assuming high levels of shear being applied to the base of a structure without a clear understanding of the load path necessary to transfer the shear force from the moving ground into the superstructure.

Some foundations are simply not capable of transferring large shear forces and act somewhat as a fusible link, limiting the base shear applied to the structure, structural accelerations, and resulting damage. Such foundations, however, frequently are severely damaged and unable to carry the gravity loads after the earthquake. During the 1999 Turkey earthquake for example, a very large number of buildings suffered brittle failure in shear, causing a huge loss of life. A smaller number of buildings were protected from significant damage when their foundations tipped, limiting the shear forces in the structure and structural damage, as shown in Figure 1. While these buildings were protected from shear failure, collapse, and resulting loss of life, they were no longer serviceable because of permanent rotations of their foundations.

Figure 1. Overturned Building in Adapazzari

Clearly, a better understanding of the behaviour of foundation systems during earthquakes is required, particularly the load-displacement response of the various foundation elements when taken to their ultimate limit state, including the effects of cyclic actions.

This paper summarises recent research carried out at the University of Canterbury where the load-displacement behaviour of all elements of foundation systems including base friction, passive soil resistance against shallow elements, and cyclic behaviour of deep foundations have been investigated. This summary is necessarily brief in details and the reader is referred to sources of additional information in some places. It is a snapshot of work in progress, with many aspects of foundation performance requiring further study. In particular, the interaction of foundation systems with liquefying soil strata is not directly addressed here. However, an attempt is made to introduce an integrated, systems view of foundation design by using simple examples.

SHALLOW FOUNDATIONS

Base Sliding

The simplest shallow foundation is a concrete slab poured on grade, usually with either one or two layers of polymer damp course (DPC). The sliding characteristics of such systems have been investigated experimentally.

Concrete slabs 2 m wide x 3 m long x 135 mm thick were constructed without edge beams but otherwise using standard construction details and materials. One and two layers of DPC were used and some slabs were weighted with ballast. Each test slab was forced to slide back and forth parallel to its long axis while measurements of force and displacement were taken.

A diagram of the test set-up is given in Figure 2. A wooden frame 3 m wide by 4 m long by 100 mm deep was constructed first. This was filled with pit-run granular material topped with a 25 mm thick sand blinding. The sand surface was levelled by screeding and then the DPC was rolled out and stapled to the wooden frame. The concrete slab then was constructed by pouring concrete into a steel form lying on top of the DPC. The concrete was cured for several days and then a hydraulic actuator was bolted to the slab and anchored to an adjacent pile head. A 100 KN load cell was used to measure the force required to cause sliding while a displacement transducer monitored slab movement. Data was recorded electronically.

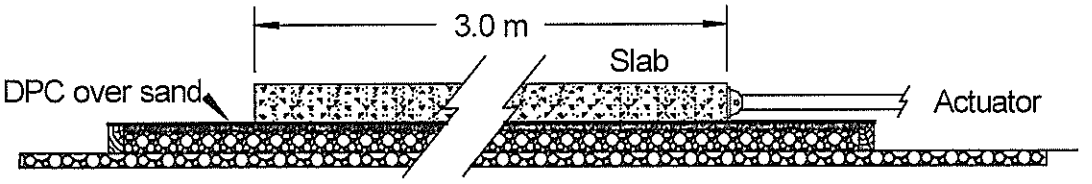

Figure 2. Section Showing Details of Base Sliding Tests

A simple test procedure was used as follows: each slab was pushed slowly, driven by a hand operated hydraulic pump, for 25 mm in one direction. Then the pump direction was reversed and the slab was dragged back to its starting position. Three or four cycles of load were applied in similar fashion until a steady load-displacement response was achieved. The results are summarised in Table 1.

Foundation Type	Contact Pressure (KPa)	Peak Friction Angle (degrees)	Mean Friction Angle (degrees)
Single Layer DPC	3.0	23	21
	6.6	28	26
Two Layers DPC	3.1	12	10
	6.2	24	22

Table 1. Base Sliding Friction for "Slab-on-Grade" Foundations

For some tests, the slab was ballasted by laying a previously tested slab on top supported on timbers laid at quarter points, effectively doubling the interface contact pressure. All tests were conducted on freshly made slabs.

For a single layer of DPC, there was a slight increase in friction with increased surcharge, probably caused by indentation of the sand grains into the soft material of the membrane. Some scuffing of the DPC was evident after testing. Placing two layers of DPC resulted in halving of the interface friction angle for the single slab without ballasting. However, ballasting of the slab to 6.2 KPa caused the interface friction to increase significantly and to be nearly the same as for a single layer of DPC. This result is surprising and no explanation is immediately obvious. A small amount of "bulldozing" of sand occurred in front of each slab as it was pushed back and forth, more for the ballasted slabs than the un-ballasted slabs. However, the effect of such "bulldozing" should be the same whether one or two layers of DPC were used. Further testing of interface friction using increased weights of ballast are recommended to investigate this phenomenon.

Combination Slab and Beam Experiments

Few foundations are ever made that consist only of "slab-on-grade" with no down-turned foundation beams of some type. Most shallow foundations have foundation beams of some description together with floor slabs that are either suspended or built "on-grade". Even when slabs are built "on-grade" they usually are structurally connected to the foundation beams, or should be. Isolated pad foundations supporting individual columns may also be part of a foundation design and sometimes these will not be inter-connected using beams. However, most foundations will have perimeter beams at least and it is beams that offer most potential for generating passive resistance to lateral movements.

A main objective of this study was to investigate the interaction between the passive resistance to lateral movement generated against vertical embedded surfaces such as beams and attached horizontal surfaces such as floor slabs. Therefore, a simplified structure consisting of two parallel foundation beams connected by a floor slab constructed "on-grade" was designed to incorporate the essential features of interest. Details of the structural design are given in Figure 3.

The structures were built as large as practicable given the limitations of available hydraulic actuators and field reaction points, the intention being to simulate behaviour at full-scale. Loads were applied by using a 500 KN MTS servo-hydraulic actuator under computer control.

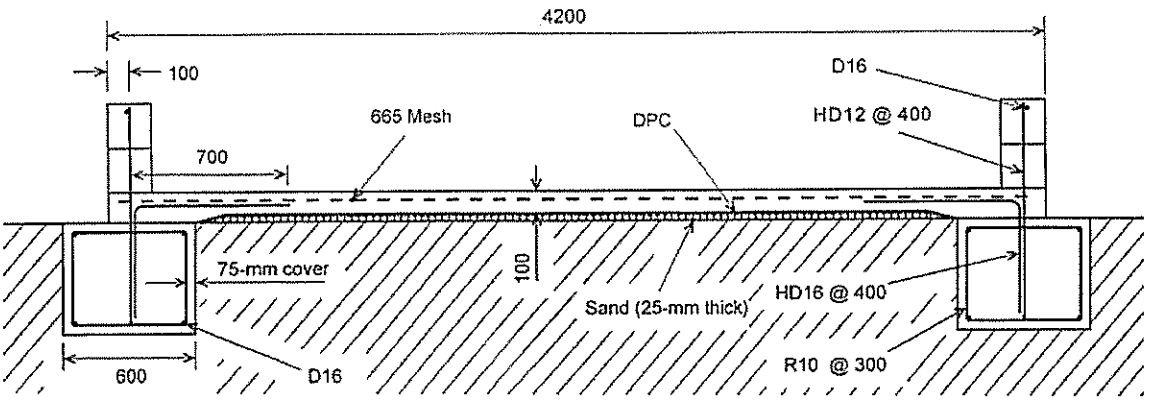

Figure 3. Section Showing Construction Details of Combination Slab and Beam Tests

Three similar structures were built. The first acted somewhat as a shakedown test. Significant rotations of the structure occurred unexpectedly during loading and these caused the hydraulic loading system to apply undesirable moments that may have upset the results. For the second test, the loading system was re-designed to better accommodate rotation of the structure. The third test was ballasted by laying the first structure on top, effectively simulating a two-storey structure.

The test procedure was essentially quasi-static. Each test proceeded as a series of shoves at a constant rate of displacement of 37.5 mm/min. At the end of each shove the test was stopped briefly so that observations of soil cracking, soil movements, structural rotation, and structural distress could be made. Then the direction of movement was reversed and the slab shoved to the opposite extreme of movement. For the first cycle of loading, the shove was terminated once a steady state load had been reached. For subsequent cycles the structure was shoved to the full range of the actuator (+/- 76 mm). Figure 4 shows a typical test in progress.

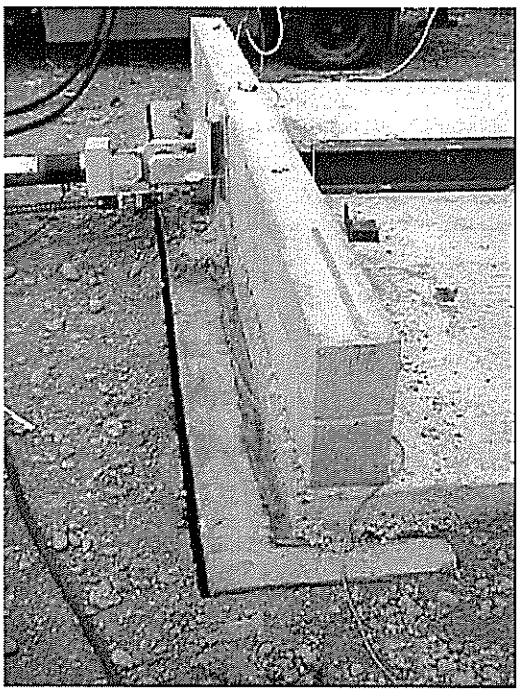

Figure 4. Test Set-Up for Test 3 (Burdon, 2000)

Load-displacement curves for Test 2 are shown in Figure 5. The curves for Test 3, the ballasted "two-storey" structure, were similar in shape although much higher peak loads were reached.

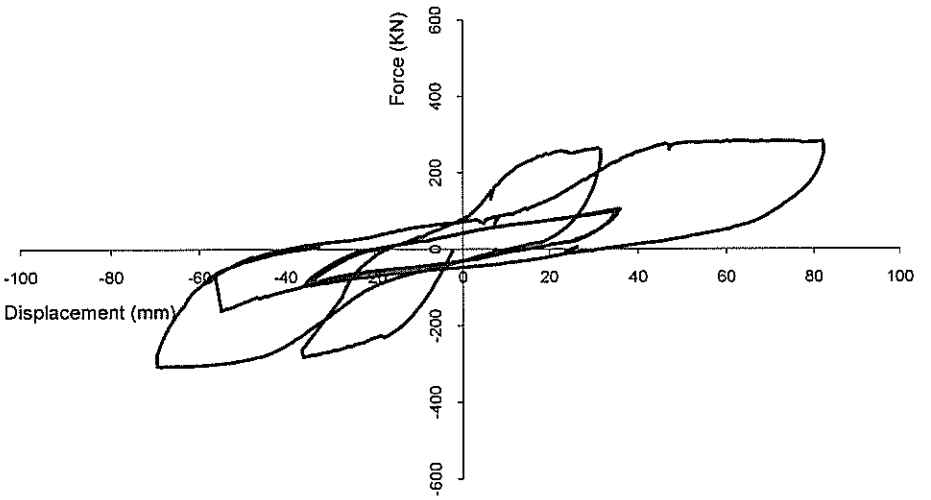

Figure 5. Load Versus Displacement for Test 2

A cartoon in Figure 6 indicates the general failure mechanism for the structures under lateral loading. A clearly defined passive wedge developed under the slab in the direction of loading that "jacked" the structure up off the ground leaving a void under the slab. Only one side was "jacked" off the ground because each foundation beam had slab attached to one side only. A large gap opened up behind each foundation beam as the foundation moved away from the soil. This gap proved to be significant because when the direction of loading was reversed the gap had to close before passive soil resistance could be mobilised in the opposite direction, causing substantial "pinching" of the load-displacement curves as seen in Figure 5.

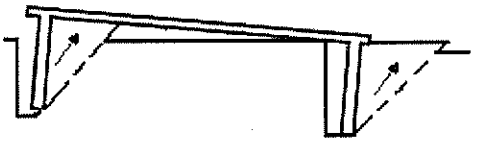

Figure 6. Observed Failure Mechanism

From the observed general failure mechanism, the forces acting on the structure may be summarised as shown in Figure 7. R1 and R3 represent the passive earth pressure acting against the faces of the foundation beams. R2 represents the additional lateral earth pressure from the force R5 acting on the passive wedge as it lifts one side of the structure. The line of thrust of R5 is assumed to act through the centre of the wedge. R4 represents friction acting on the base of the foundation beam and F is the applied lateral load acting with eccentricity e. The value of R6 is determined from equilibrium of forces.

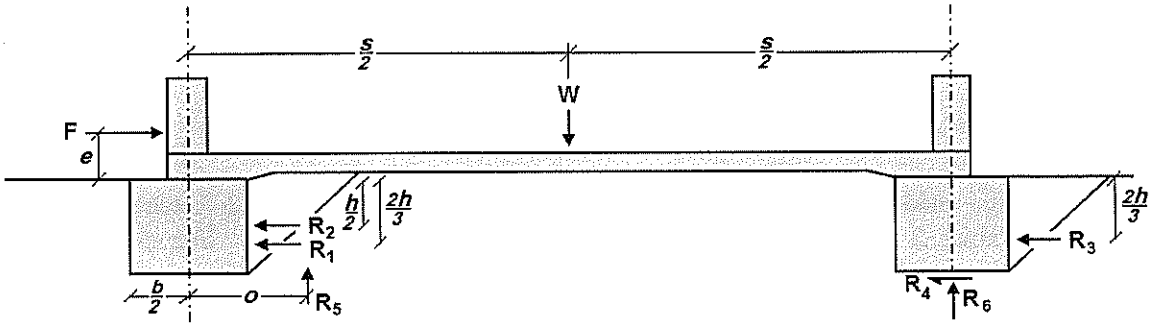

Figure 7. Forces Acting on Structure with Lateral Loading by Force F

Since the left hand beam is moving upwards with the passive soil wedge, there will be no friction acting on the vertical face of the beam and it may be treated as frictionless. Therefore, Rankine's simple theory may be used to compute R_1:

$$R_1 = 0.5K_p\gamma h^2 L \tag{1}$$

$$K_p = \frac{1+\sin\phi_b}{1-\sin\phi_b} \tag{2}$$

in which ϕ_b = the backfill material angle of internal friction, and L is the length of the foundation beam. There will be friction between the right hand beam and the right hand passive wedge of soil. This friction tends to increase the passive resistance R_3 while simultaneously reducing R_6 and the resulting friction R_4. The net effect on the total lateral resistance is probably negligible and so the simplifying assumption of a frictionless wall was applied to the computation of R_3:

$$R_3 = R_1 \tag{3}$$

The remaining reaction forces are given by:

$$R_2 = R_5 K_p \tag{4}$$

$$R_4 = R_6 \tan\phi_g \tag{5}$$

$$W = R_5 + R_6 \tag{6}$$

in which ϕ_g is the interface friction angle between the base of the foundation beam and subgrade. The line of action of R_5 is given by:

$$o = \frac{h}{2}\tan(45^\circ + \frac{\phi_b}{2}) + \frac{b}{2} \tag{7}$$

An explicit expression for R_6 was obtained from consideration of rotational equilibrium of the structure, as follows:

$$R_6 = \frac{(R_1+R_3)(1+\frac{2h}{3e}) - W(\frac{o}{e} - \frac{s}{2e} - K_p(1+\frac{h}{2e}))}{\frac{s}{e} - \tan\phi_g(1+\frac{h}{e}) - \frac{o}{e} + K_p(1+\frac{h}{2e})} \tag{8}$$

The lateral capacity then is given by:

$$F = R_1 + R_2 + R_3 + R_4 \tag{9}$$

Computations were made to predict the measured capacities for Tests 2 and 3 with the results summarised in Tables 2 and 3. Good agreement was obtained in both cases. The slight (6 – 10 percent) underestimate of capacity is probably because of a slight underestimate of the soil strength properties. The test soils were above the water table and were moist and might be expected to show some apparent cohesion. However, the soil strengths used in the computations are what a designer might reasonably estimate and the slight conservatism resulting is considered appropriate.

	W (KN)	L (m)	e (m)	s (m)	b (m)	h (m)	γ (KN/m^3)	ϕ_g (deg.)	ϕ_b (deg.)	F (KN)	F^* (KN)
Test 2	118.1	4.25	0.125	4.0	0.6	0.45	17.2	40	35	263	292
Test 3	233.4	4.25	0.125	4.0	0.6	0.45	17.2	40	35	482	515

Table 2. Comparison of Calculated and Measured Lateral Resistance

* - measured peak loads, average of both directions of loading.

The computations are highly sensitive to changes in the ratio of load eccentricity (e) to width (s). Increasing load eccentricity causes transfer of structural weight from the left hand passive wedge to the right hand beam (in Figure 7). This weight transfer significantly reduces the lateral resistance of the structure because weight applied to the left hand passive wedge is very effective, increasing the lateral earth pressure on the left hand beam by factor Kp (values typically 3 – 4).

With reversal of loading direction, as the structure moved back through its central position, lateral load resistance was observed to decrease to low values as the vertical faces of the foundation beams lost contact with the backfill material. For Test 2, by the third cycle of loading, lateral resistance had dropped to approximately 40 KN. The structure presumably was sliding on the DPC/sand interface with an equivalent friction angle of 19 degrees. For Test 3 the minimum lateral resistance at zero displacement was 114 KN, equivalent to a friction angle of 26 degrees. These friction values are close to the measured values for a slab sliding on a single layer of DPC suggesting that, between displacement extremes, the structure is simply sliding back-and-forth supported by the slab resting "on grade".

These load tests were quasi-static and did not include dynamic effects. Passive soil resistance will be reduced by the inertia of the mass of soil within the passive wedge, although the reduction will be small.

DEEP FOUNDATIONS

As well as contributing directly to the transfer of lateral base shear forces to the structure, deep foundations, when present, may also be required to carry gravity loads and to resist overturning moments induced by the lateral base shear. Such earthquake induced overturning moments generate cyclic axial loads in deep foundations, as shown in Figure 8.

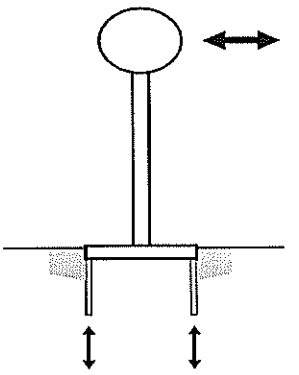

Figure 8. Earthquake Induced Axial Loads on Bored Piles

The effect of cyclic axial loading on the load-displacement behaviour of deep foundations is poorly understood, but of considerable concern. Previous research (e.g. Charlie et. al., 1985, Turner and Kulhawy, 1990, McManus and Kulhawy, 1994) has shown that end bearing capacity of deep foundations is not significantly affected by cyclic loading but that side resistance may be reduced, in

some cases to as low as 8 percent of static capacity. Unfortunately, most available studies have involved large numbers of load cycles appropriate to wind and wave loading of transmission line structures and oil platforms and may not be truly relevant to earthquake loading. Therefore, a study was undertaken to quantify the effect of cyclic axial loading for the reduced numbers of load cycles applied during earthquakes.

Initial testing was of model bored piles in a static (non-shaking) deposit of sand. Firstly, axial loads only were applied and then combined axial and lateral loads were investigated. Next similar models were tested in a laminated box mounted on a shaking table, with simultaneous axial loading of the piles and ground shaking. Finally, some full-size piles were tested in the field at three sites around Christchurch.

Model Study of Axial Loading in Static Tank

Model studies are the most practical way to explore a wide range of parameters economically. Unfortunately, normal scaling laws do not apply to soils because soil properties are highly dependent on overburden pressure. This limitation may be overcome by modelling geotechnical systems in centrifuges, which are able to simulate high gravitational acceleration and thus high overburden stresses. An alternative approach, adopted here, is to make the model as large as possible and consider it to be a small prototype. Also, by using deposits of dry soil, without buoyant effects, a scale factor equivalent to 2 g in a centrifuge may be assumed, and by using loose soil the undesirable effects of excessive soil dilatancy at low confining pressure are avoided.

The first study was performed on model bored piles in static sand deposits. Soil deposits of 1 m diameter by 2 m deep were prepared inside steel tanks by air pluviation of silica sand. The model bored piles, nominally 95 mm diameter by 1450 mm long were constructed by pouring concrete into an embedded steel casing and then removing the casing. Each shaft was reinforced using a single 16 mm diameter deformed steel bar threaded at the top to allow fixing of a load actuator. Additional details of these tests are given by McManus and Chambers (1995).

Loads were applied to the model bored piles by a computer controlled servo-hydraulic actuator. Each "earthquake" consisted of 20 sine wave cycles at a frequency of 1 Hz. Each pile was tested with a different combination of cyclic load amplitude and constant mean (dead) load, either in compression or uplift. Each pile was tested only once.

Failure in uplift was defined either as being complete pullout of the model bored pile (to the limit of the hydraulic actuator) prior to completion of the simulated earthquake, or as an accelerating cycle-by-cycle upwards movement of the shaft with pullout clearly imminent. A definition for failure in compression is always more problematic, even for static load tests. For this study, a limiting displacement of 10 percent of the shaft diameter (9.5 mm) was chosen to define failure in compression

The load-displacement response for Test 21 is shown in Figure 9 and is typical of all the model bored piles which exhibited stable behaviour during simulated earthquake loading. During cyclic loading, the shaft walked slowly down into the soil, but at a decreasing rate per cycle. Immediately after the last cycle of loading, the shaft was deliberately failed in uplift. The uplift capacity was found to be unchanged at 101 percent of static capacity without cyclic loading.

Load Test 22 failed in uplift during the cyclic loading and the load-displacement response is shown in Figure 10. For the first 8 cycles of simulated earthquake loading the response appeared stable, with the shaft slowly walking down into the soil. Then, the shaft started walking upwards at an accelerating rate with the test terminating when the actuator travel was exceeded.

A typical compression failure is shown in Figure 11 for model bored pile Load Test 39. The shaft simply walked down into the soil and exceeded the displacement failure criteria in compression (10 percent of tip diameter).

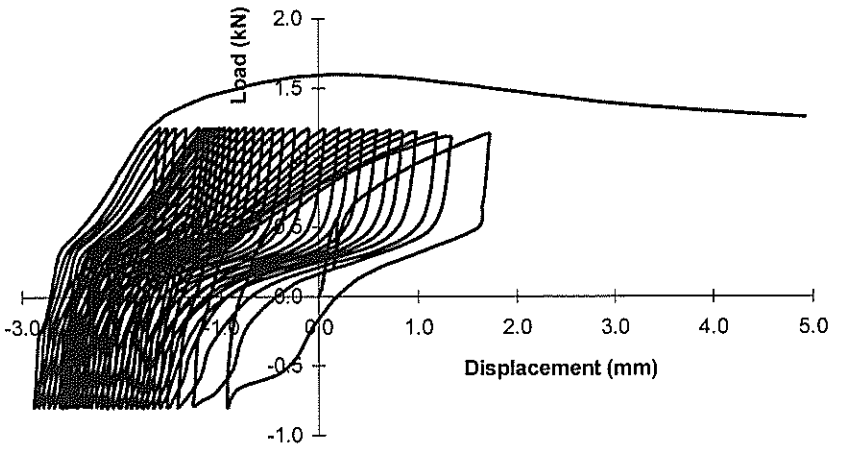

Figure 9. Load Versus Displacement for Simulated Earthquake Loading, Test 21

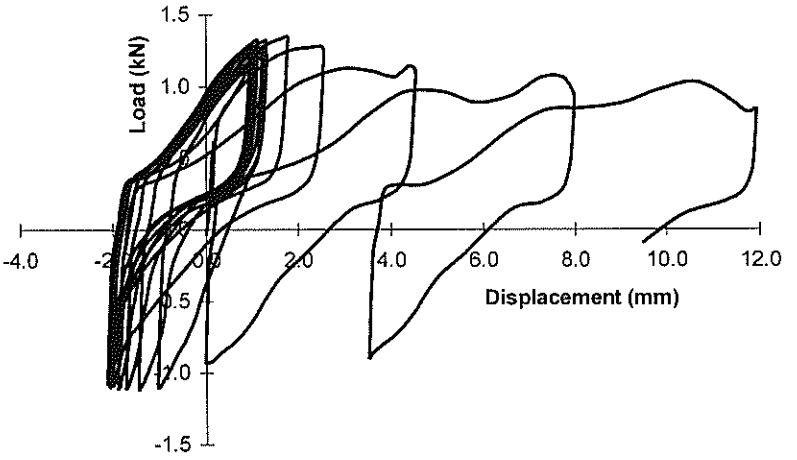

Figure 10. Load Versus Displacement for Uplift Failure, Test 22

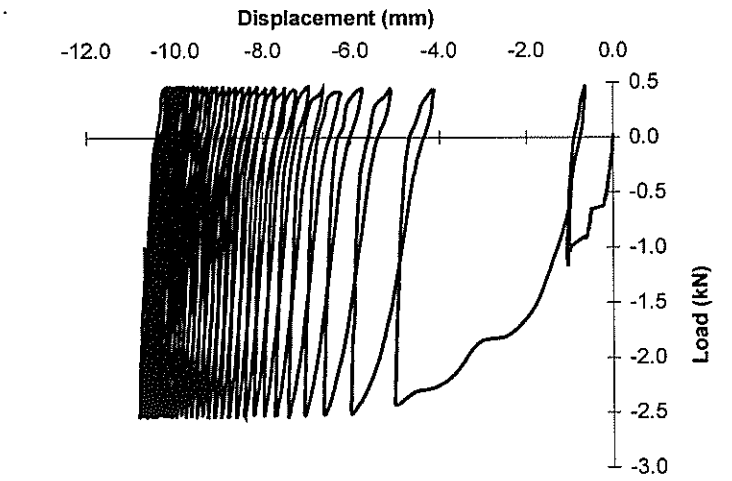

Figure 11. Load Versus Displacement for Compressive Failure, Test 39

A cyclic stability diagram (CSD) for the model bored piles tested in this study is shown in Figure 12. Each individual cyclic load test has been plotted on the diagram by using a small square. The CSD is a useful way of representing all of the possible combinations of cyclic and static axial loads for a pile and the load combinations causing instability. A more detailed explanation of the CSD is given by Poulos (1988).

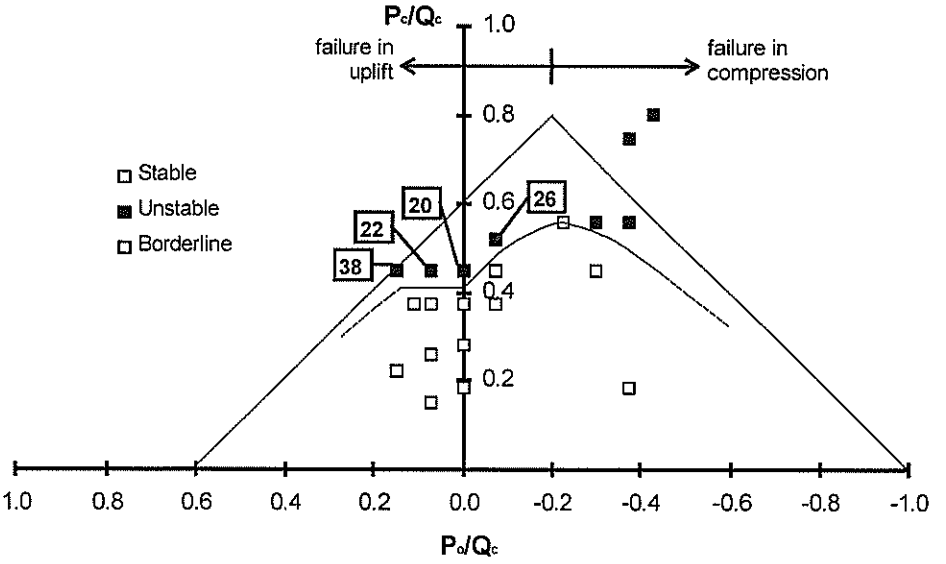

Figure 12. Cyclic Stability Diagram for Model Bored Piles with Simulated Earthquake Loading

The shape of the stable/unstable boundary within the cyclic stability diagram for the model bored piles has a pronounced dip where the boundary crosses the Po = 0 axis. In other words, the worst case for cyclic loading occurred when zero mean load was applied to the shafts. For this case, a cyclic load of 75 percent of static uplift capacity caused failure.

A further conclusion of this study was that the key parameter for cyclic axial loading of piles is the magnitude of load reversal, i.e. the extent to which the direction of loading changes from compression to uplift for each cycle of loading. If no load reversal occurs, then there is little degradation of capacity although some permanent displacements might accumulate. If load reversal does occur, then significant degradation of pile capacity is possible, the amount of degradation being dependent on the amount of load reversal. Additional conclusions are contained in the original paper (McManus & Chambers, 1995).

Combined Axial-Lateral Loading

Most pile foundations will be subjected to some combination of both axial and lateral loading during an earthquake. Generally, repeated or cyclic lateral loading seems to have limited effect on the lateral capacity of pile foundations, although some reduction in stiffness may occur because of gapping.

A model study has been initiated at the University of Canterbury to investigate the effect of simultaneous cyclic lateral and axial loading on both the axial and lateral capacities of piles. The test set-up is complex, requiring computer controlled servo-actuators operating in two axes of motion, as shown in Figure 13. This study is incomplete but early indications suggest that while the lateral loading has little affect on axial capacity, the axial loading reduces the lateral capacity. Further work is required before design recommendations can be made.

Model Study on Shaking Table

In order to truly simulate earthquake conditions it is necessary to test either model or full-size piles in ground that is shaking. Ground shaking during an earthquake induces shear strains in the soil that interact with the pile and are likely to affect pile load-displacement response. Since it is difficult to

know when and where an earthquake is going to occur, the most practical approach to investigating the affect of ground shaking on pile performance is to simulate the earthquake on a shaking table in the laboratory.

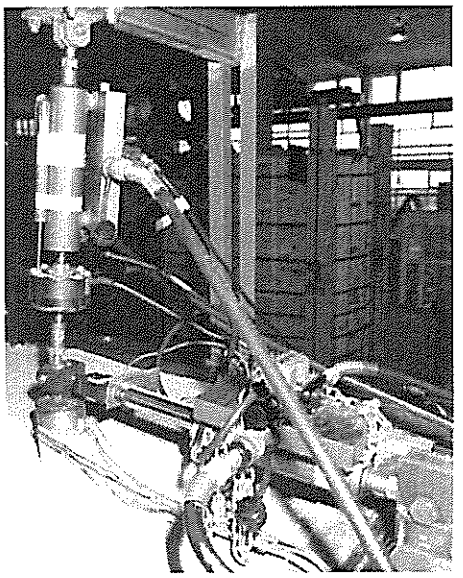

Figure 13. Combined Axial-Lateral Model Load Test

For this study, a large 2 m deep x 2 m long x 1 m wide laminar box was filled with sand and shaken on the Department of Civil Engineering's 20 tonne capacity, single axis shaking table. The tank size was chosen so that similar model piles could be tested as used for the earlier tests in the static tank. The box was laminated so that the soil was free to deform in simple shear simulating free field behaviour. The laminar box and filling hopper is shown in Figure 14.

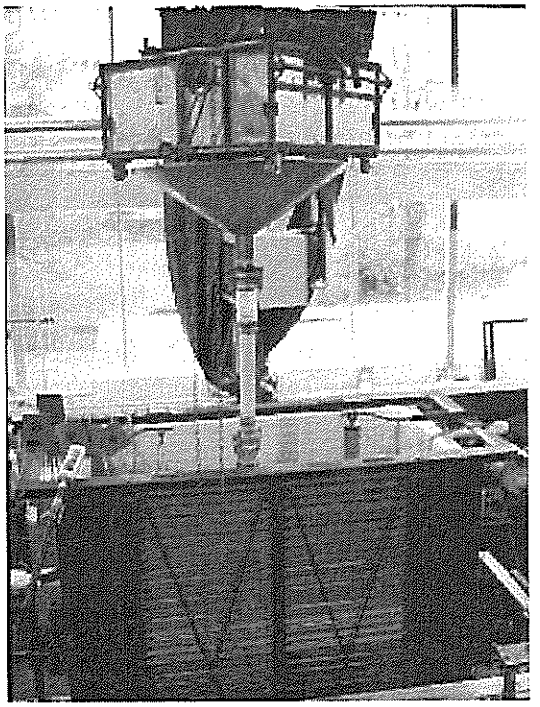

Figure 14. Preparation of Soil Deposit in Laminar Box

Because of the extensive effort required to prepare and test each model pile in the laminar box, only a limited range of parameters were investigated, with the objective being to determine the relative performance of piles in static and shaking soil deposits. Specifically, all tests were axial load only with zero mean load (worst case from the static tests). Simulated "earthquakes" consisted of 20 cycles

at 1 Hz and simultaneous pile axial loads were either in phase with the shaking or out of phase. Some shaking tests were performed without simultaneous cyclic pile loads but with mean uplift loads applied. Full details of the test programme including development of the laminar box are given by Chambers (1999).

The results from the laminar box study are summarised in Figure 15. At low levels of pile cyclic load the piles were stable and settled approximately 30 mm because of the densification and settlement of the soil deposit with shaking. For tests with applied cyclic loads of more than 40 percent of uplift capacity the piles became unstable with large uplift displacements. For tests with cyclic loads applied out of phase with the ground shaking this threshold to instability occurred at approximately 50 percent of uplift capacity. The average peak shear strain in the soil deposit during shaking was between 1.3 to 1.6 percent.

This threshold to instability of between 40 to 50 percent of uplift capacity of the model piles with zero mean load compares with a threshold of 75 percent found for the similar model piles tested in static soil deposits. Apparently, the shaking soil deposit significantly reduced the resistance of the model piles to cyclic axial loading.

Model tests also were performed with static uplift loads applied to the pile during soil shaking and no cyclic axial load component, with the results summarised in Figure 16. For low level shaking (average peak shear strain, APSS = 0.11 percent) the piles remained stable. For higher levels of shaking (APSS = 0.59 and 0.96 percent) the piles became unstable and started to pull out of the soil at applied axial loads of between 50 to 60 percent of uplift capacity.

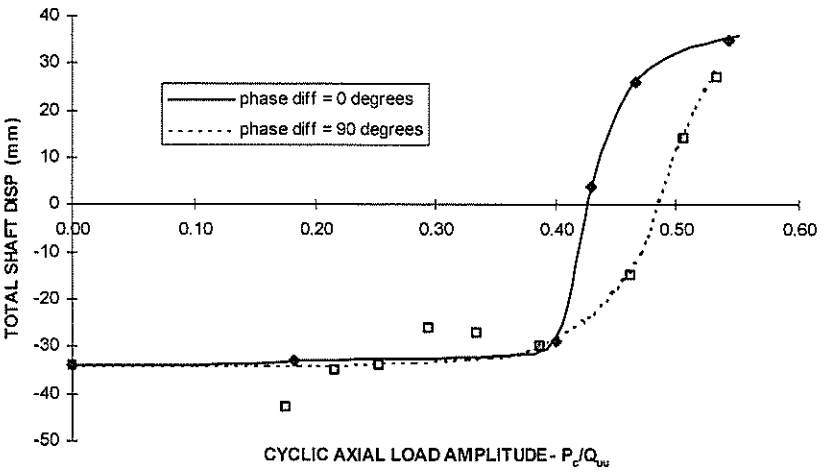

Figure 15. Pile Displacement Versus Cyclic Axial Load Amplitude Normalised by Uplift Capacity for the Shaking Tests (Chambers, 1999)

Full Scale Cyclic Load Tests

The objective of the full-scale pile load tests was to provide general verification of the findings of the model studies. The cost of full-scale field testing precludes a thorough examination of the full range of parameters investigated in the model studies. Also, it is clearly impractical to arrange earthquake magnitude ground shaking to occur simultaneously. However, by checking some of the model predictions at full-scale it allows the model results to be applied with greater confidence.

Three field tests have been performed to date: 750 mm diameter x 6 m deep bored piles in loose sandy gravel at Templeton (McManus, 1997), 275 mm x 275 mm x 8 m long reinforced concrete driven piles at Park Terrace in central Christchurch (McManus, 1999), and 275 mm x 275 mm x 8 m long reinforced concrete driven piles at Salisbury Street in central Christchurch (Lyons, 2000).

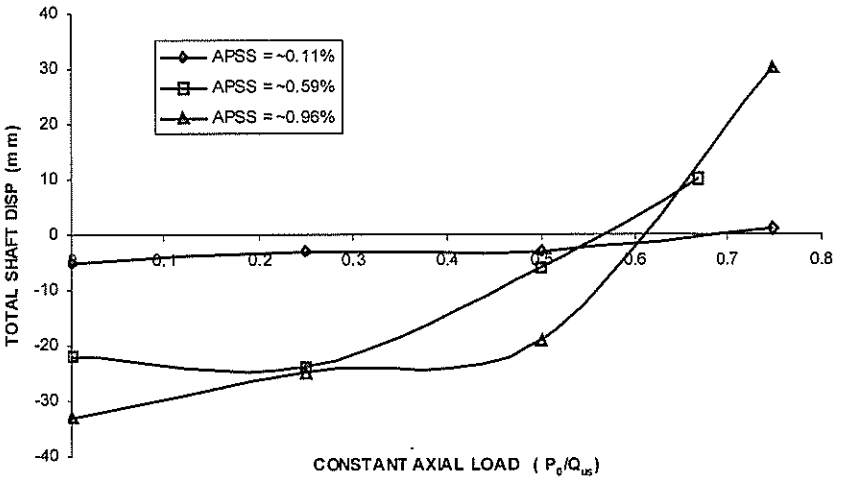

Figure 16. Pile Displacement Versus Constant Uplift Load Normalised by Uplift Capacity for the Shaking Tests (APSS means average peak shear strain for the soil shaking) (Chambers, 1999)

Park Terrace Site

Three 275 mm square reinforced concrete piles were driven 7.75 m into typical Christchurch overbank deposits of soft silts, silty fine sands, and peats, bearing in dense fine to medium sands. Driving of the piles was monitored by using a pile driving analyser and a CAPWAP analysis was performed on one pile giving a prediction for pile ultimate capacity of 930 KN in compression and 495 KN in uplift. The centre pile was subjected to several sequences of cyclic axial loading by a computer controlled, 500 KN MTS servo-hydraulic actuator mounted in a loading frame spanning between the two outer piles, as shown in Figure 17. Amplitudes of up to +/- 350 KN at frequencies of either 1 Hz or 0.5 Hz were applied as simulated "earthquakes" of up to 30 cycles duration. Each "earthquake" was increased in magnitude and the pile was then rested for about one hour.

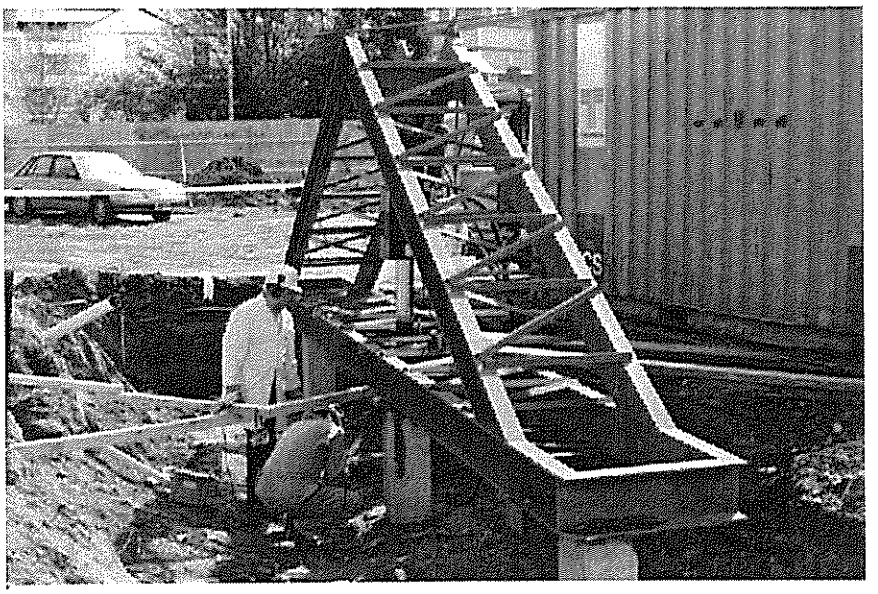

Figure 17. Full-Scale Cyclic Load Test Frame and Actuator

At applied cyclic loads of up to +/- 300 KN the pile load-displacement response was essentially stable with only minor upward displacement creep, as shown typically in Figure 18. However, when the applied cyclic load was increased to +/- 350 KN severe degradation of pile stiffness occurred, exceeding the capacity of the hydraulic loading system, as shown in Figure 19. It proved impossible to increase the cyclic axial load using the available system and 350 KN was taken as the load level

causing onset of pile instability. Monotonic uplift capacity of the pile after completion of the cyclic loading was measured as 300 KN.

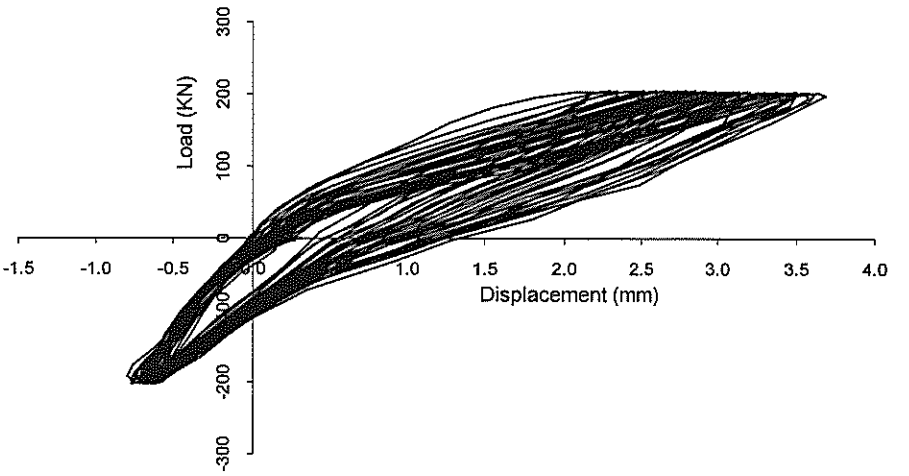

Figure 18. Park Terrace Full-Scale Load Test, +/- 200 KN, 1.0 Hz, 30 Cycles

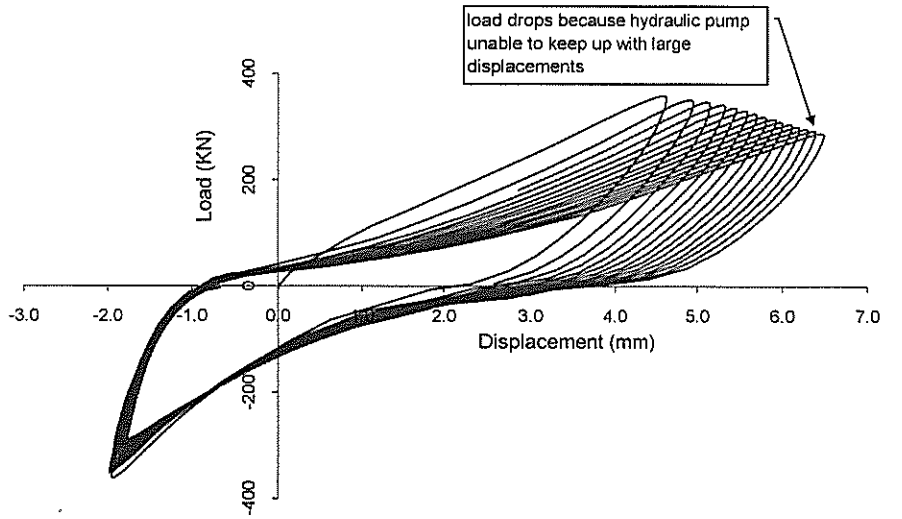

Figure 19. Park Terrace Full-Scale Load Test, +/- 350 KN, 0.5 Hz, 15 Cycles

The two outer piles were then subsequently tested in uplift to determine a reference uplift capacity for the piles without cyclic loading (or at least with half the level of cyclic loading of the test pile and after several weeks "rest".) These uplift tests were crudely performed using a 70 tonne crane and indicated 530 KN capacity at 20 mm displacement with a peak value of 596 KN at 32 mm.

In summary, the level of cyclic axial load causing onset of instability of the pile was found to be approximately 66 percent of uplift capacity (assuming capacity to be 530 KN), which is close to the value of 75 percent for the model pile test it most closely resembles.

Salisbury Street Site

Full-scale cyclic load tests were performed on similar piles at the Salisbury Street site using the same equipment and procedures. The 275 mm square x 8 m long reinforced concrete piles were driven into silts, silty fine sands, and peats, bearing in dense fine to medium sands. The site soils were more competent than at the Park Terrace site and the pile driving analyser predicted higher capacities for the test pile of 2,630 KN in compression and 1,049 KN in uplift.

Again, cyclic load amplitudes of up to +/- 350 KN at frequencies of 1 Hz were applied as simulated "earthquakes" of 30 cycles duration. Each "earthquake" was increased in magnitude and the pile was then rested for about one hour. The load-displacement response of the pile remained stable for all of the load tests. It was not possible to increase the level of cyclic loading above 350 KN , which represents only 33 percent of the presumed uplift capacity of the pile.

The level of cyclic load required to cause instability of the Salisbury Street pile was not determined but the stable behaviour of the pile at applied loads of up to 33 percent of uplift capacity was confirmed.

Templeton Site

Nine bored pile foundations, each nominally 0.75 m diameter by 5.5 m deep, were constructed in a deposit of loose gravel above the water table at a disused gravel quarry at Templeton, near Christchurch. Four of the piles were loaded monotonically to failure in uplift while the remaining five piles were subjected to 30 cycles of 1 Hz sine wave loading at various amplitudes using similar equipment to the Park Terrace and Salisbury Street load tests. The uplift capacity and axial stiffness of the cyclically loaded piles was compared with that of the monotonically loaded piles.

At low levels of cyclic loading (50 percent or less of uplift capacity) the pile response was largely elastic with no significant degradation in strength or stiffness. At higher levels, there was a large reduction in load-displacement stiffness (by a factor of up to 16). The transition from stable to unstable behaviour occurred at a ratio of cyclic load amplitude to axial uplift capacity of about 0.6, slightly less than the value of 0.66 for the driven concrete piles at the Park Terrace site, and 0.75 for the model piles in the static sand deposits.

Design Example 1 - Multi-Storey Building on Shallow Foundations.

The first design example considers the lateral resistance of shallow foundations for multi-storey buildings of various heights, with dimensions shown in Figure 20. The building is founded on shallow beams with integral "slab on grade" construction, similar to the test foundation of Figure 11. The building was assumed to be founded on "intermediate" soils, to be of "limited ductility", to have a natural period of 0.5 seconds, and to be located in Christchurch, giving a seismic acceleration coefficient of 0.3 according to NZS4203 (1992). The lateral capacity of the foundation system for several different building heights was calculated by using the procedure outlined in Equations 1 to 9, with the results summarised in Table 3.

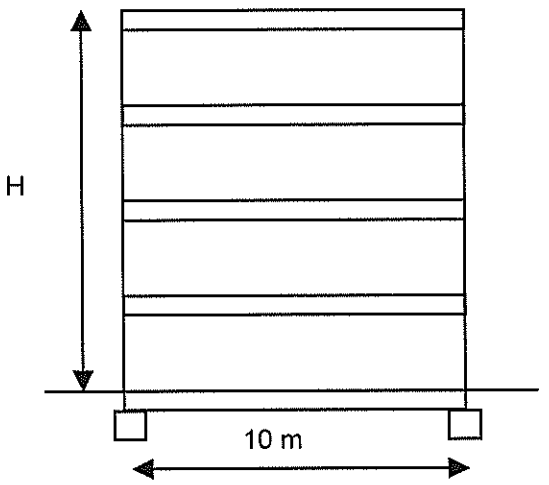

Multi-Storey Building
H = 3 m per storey
EQ Floor load = 1.5 KPa
EQ Roof load = 0.5 Kpa
C = 0.3
e = 2/3 H
γ = 15 KN/m^3
ϕ = 35 degrees
b = 0.6 m h = 0.45 m

(Refer to Figure 11 for key)

Figure 20. Design Example 1

The vertical bearing capacity of the foundation during the earthquake must also be given careful consideration. Overturning moments may significantly increase vertical loads applied to the foundation elements, and the simultaneous application of lateral loads significantly reduces the bearing capacity. Ground shaking may further reduce bearing capacity because of the inertia of the soil failure wedge and overburden.

For Design Example 1 the bearing capacity of the foundation beams was checked two ways: using conventional, quasi-static analysis including load inclination factors (e.g. McCarthy, 2002), and by using seismic bearing capacity factors (e.g. Ghahramani and Berrill, 1995). The bearing capacity is highly dependent on the ratio of applied horizontal to vertical loads. For Example 1 the seismic acceleration coefficient was 0.3, and so the ratio of horizontal to vertical loads for the quasi-static analysis was set to 0.3, assuming that most of the lateral load would be resisted initially by friction under each foundation beam. The seismic bearing factor method assumes implicitly that lateral loads are directly in proportion to the vertical loads factored by the acceleration. The resulting factors of safety for both methods are given in Table 3.

No. Storeys	W	R_6 (max reaction)	F (ultimate lateral resistance)	R_4/F (proportion as beam friction)	FS (lateral load)	FS (bearing) (quasi-static)	FS (bearing) (seismic factors)
	(KN/m)	(KN/m)	(KN/m)	.	.		
1	20	17.5	32.8	0.37	5.5	9.8	7.0
2	35	34.2	38.2	0.63	3.6	5.1	3.6
3	50	50	46.2	0.76	3.1	3.2	2.3
4	65	65	56.7	0.80	2.9	2.3	1.6
5	80	80	67.2	0.83	2.8	1.7	1.2
6	95	95	77.7	0.85	2.7	1.3	1.0

Table 3. Ultimate Lateral resistance for Design Example 1

For the one and two storey buildings the failure mode under lateral loading is as per the cartoon of Figure 6. The high factors of safety (5.5 and 3.6) imply that for the design earthquake acceleration (0.3 g) displacements will remain small and there should be no significant rotation of the building. A large proportion of the lateral resistance of the foundation for the one storey building is provided by passive resistance of the soil trapped between one foundation beam and the slab, with a lesser proportion being provided by friction beneath the opposing beam (R4/F = 0.37) and by passive soil resistance against the leading beam. For the three storey and higher buildings the failure mode is tipping, with rotation about one foundation beam, with most of the lateral resistance being provided by friction under the beam (R4/F = 0.76 - 0.85). The factors of safety for these taller buildings are reduced (3.1 - 2.7) but are still healthy.

The shallow foundations of Example 1 seems adequate for up to four storeys, assuming that soil liquefaction is not an issue for the site and that settlements are satisfactory. For five or more storeys it would seem prudent to use deep foundations because of the increasing risk of a bearing failure (FS 1.7 or less).

Design Example 2 - Multi-Storey Building on Pile Foundations.

The second example considers the same simple multi-storey building of Figure 20, but supported on driven concrete piles beneath the foundation beams. For convenience, the piles will be similar to those tested at the Park Terrace site since the capacity and cyclic behaviour are reasonably well understood. A building height of 10 storeys was chosen for consideration because such a building will tip under the design earthquake acceleration of 0.3 g, requiring the restraint of pile foundations.

First, a conventional pile design was made by considering structure gravity loads for the load case 1.2G + 1.6Q, as shown in Figure 21. The pile capacities were taken from the results of the CAPWAP

analysis with a geotechnical strength reduction factor $\Phi_g = 0.85$ applied, as recommended by AS 2159 (1995). A pile spacing of 7 m under each foundation beam was determined.

10 Storey Building

$KN := 1000\,N$

$Floor_{dead} := 5 \cdot \frac{KN}{m}$ $Floor_{live} := 10 \cdot \frac{KN}{m}$ $Roof_{dead} := 5 \cdot \frac{KN}{m}$ (all per m length of building)

$G := 10 \cdot Floor_{dead} + Roof_{dead}$ $Q := 10 \cdot Floor_{live}$

$\alpha F_{gravity} := 1.2 \cdot G + 1.6 \cdot Q$ $\alpha F_{gravity} = 226 \frac{KN}{m}$

Pile Capacity: $Q_c := 930\,KN$ $Q_t := 495 \cdot KN$ $\Phi_g := 0.85$ (from CAPWAP)

Pile Spacing: $S := \frac{\Phi_g \cdot Q_c}{0.5 \alpha F_{gravity}}$ $S = 6.996m$ (say 7 m)

Figure 21. Conventional Gravity Pile Design

Next, the earthquake load case $G + Q_u + E_u$ is considered. Since any earthquake will generate cyclic axial loads in the piles (as in Figure 8), the first step is to generate a cyclic stability diagram for the piles in order to fully understand the interaction between the cyclic and non-cyclic components of loading on the capacity of each pile. A cyclic stability diagram for the Park Terrace piles is shown in Figure 22.

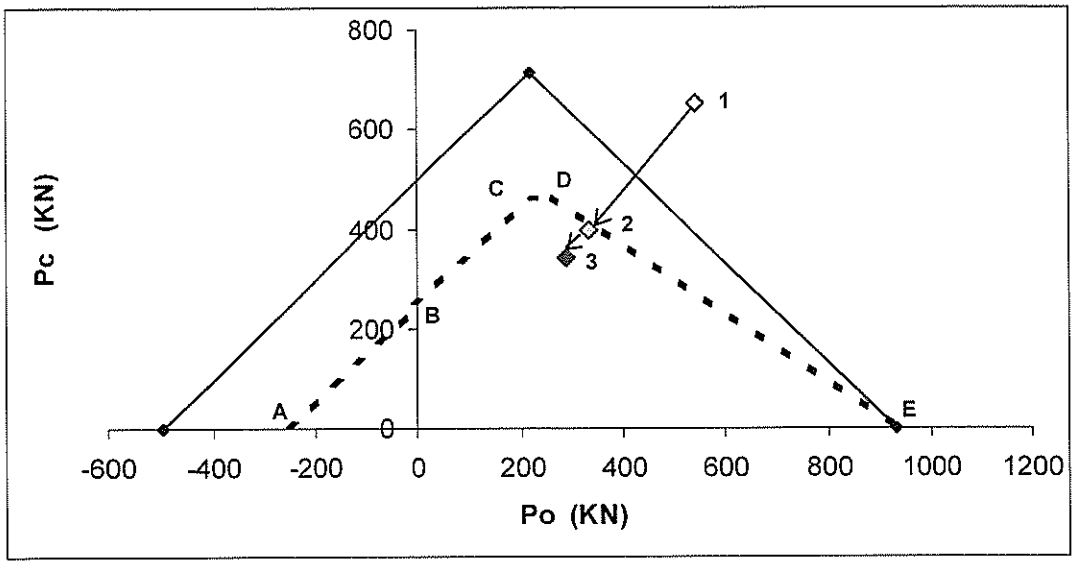

Figure 22. Cyclic Stability Diagram for Piles of Design Example 2

Inside of the triangle represents the range of load combinations (cyclic and non-cyclic) that would be possible if there were no cyclic or dynamic effects on pile capacity. The coordinates of the triangle were determined from the un-factored compression and uplift capacities from the CAPWAP analysis (Q_c = 930 KN, Q_t = 495 KN). The dashed line represents the failure envelope for the pile including the cyclic and dynamic effects of earthquake loading on pile capacity and was constructed as follows: Point A was determined from the model testing in the laminar box, which showed that uplift capacity of a pile in shaking ground without simultaneous cyclic loading was reduced by a factor of 0.5 to 0.6. Point B, the cyclic capacity at zero mean load, was set at Q_t reduced by a factor of 0.4, also taken from the model testing in the laminar box and somewhat confirmed by the full-scale cyclic load testing at the Park Terrace site.

Points C, D, and E were taken from the model test results shown in the cyclic stability diagram of Figure 12. From point B to C the envelope rises at a slope of 1:1 because the increase in mean compression load allows a corresponding increase in cyclic load magnitude without increasing the amount of cyclic load reversal. Point C is under the triangle apex (balanced failure), C to D is flat (transition), and D to E is tentatively set at a factor of 0.7 of cyclic capacity, although there is little experimental data within this range.

Each pile foundation will have a unique cyclic stability diagram, depending on the particular soil conditions, the type of pile construction, the pile depth to diameter ratio, and pile relative stiffness. The cyclic stability diagrams for the piles considered in this study have been assumed to be generally similar in shape because all of the piles, both model and prototype, are relatively short and stiff and are in predominantly loose, granular soils. Guidance for developing cyclic stability diagrams for other conditions are available (e.g. Poulos, 1988).

Design calculations for the earthquake load case are shown in Figure 23. The assumption is made that the piles resist all of the vertical loads and the overturning moment with no contribution from the foundation beams. The initial design from gravity loads of piles spaced at 7 m is clearly inadequate, with the piles likely to fail in compression. The load combination for this case is plotted as Point 1 in the cyclic stability diagram, Figure 22, and falls well outside the triangle of possible load combinations. For the next trial design, the pile spacing was reduced to 4.3 m, resulting in the load combination shown as Point 2 in Figure 22. Point 2 falls on the failure envelope of the cyclic stability diagram and the piles may fail in compression during the design earthquake. For the final trial design, the pile spacing was further reduced by a factor 0.85 to 3.7 m, resulting in the load combination shown as Point 3 in Figure 23. The factor 0.85 was selected as being equivalent to the geotechnical strength reduction factor, Φ_g ,= 0.85, specified in AS 2159 (1995).

10 Storey Building

$KN := 1000 \cdot N$

$Floor_{dead} := 5 \cdot \frac{KN}{m}$ $Floor_{live} := 10 \cdot \frac{KN}{m}$ $Roof_{dead} := 5 \cdot \frac{KN}{m}$ (all per m length of building)

$G := 10 \cdot Floor_{dead} + Roof_{dead}$ $Q := 10 \cdot Floor_{live}$

Seismic hazard coefficient: $C := 0.3$

Base shear: $V := C \cdot (G + Q)$ $V = 46.5 \frac{KN}{m}$

Overturning moment: $H := 30 \cdot m$ $M_o := V \cdot \frac{2 \cdot H}{3}$ $M_o = 930 \frac{KN \cdot m}{m}$

Pile spacing: $S := 7 \cdot m$ (initial trial)

Pile cyclic load: $Lever := 10 \cdot m$ $P_c := \frac{M_o \cdot S}{Lever}$ $P_c = 651KN$ (+/-)

Pile mean load: $P_o := \frac{(G + Q) \cdot S}{2}$ $P_o = 543KN$

Figure 23. Pile Design Including Overturning Effects for Design Example 2

The lateral load resistance of the foundation system also needs to be addressed. By assuming that the vertical loads and overturning moments are resisted entirely by the piles, the main mechanism of lateral resistance of the shallow foundation elements (friction under the leading foundation beam) has been removed from consideration. Also, the passive resistance of the soil ahead of the leading foundation beam is small relative to the weight of the 10 storey building. However, the soil between the leading and trailing foundation beams is forced to slide with the building because a passive wedge is prevented from forming ahead of the trailing beam by the slab, which is held down by the piles. These mechanisms yield an ultimate lateral capacity for the shallow foundation elements of 32 KN/m for a factor of safety of 0.7.

Clearly, the lateral resistance of the piles, estimated to be 29 KN/m at the 3.7 m spacing, will be mobilised giving a combined ultimate lateral resistance of 60 KN/m for a factor of safety of 1.3. With such a low FS hinging of the piles is likely and the structural capacity of the piles will need to be checked for combined actions by the structural engineer. Exceeding the lateral capacity of the foundation system during an earthquake should not be a major concern, provided the axial load capacity is maintained.

In summary, the consideration of earthquake actions together with cyclic and dynamic effects on pile capacity have doubled the number of piles required for the 10 storey example building. Also, the number of piles required is significantly more than for considering earthquake actions alone without cyclic or dynamic effects on pile capacity. Pile design for axial loads needs to be made with reference to a cyclic stability diagram. The final design for the example structure is considered to be nearly at optimum since the final load combination for the piles falls right under the "peak" of the cyclic stability diagram of Figure 22. If either more or less dead load was carried by each pile then the cyclic load capacity would be reduced.

Key to the design process for Example 2 is a detailed knowledge of the structure and its various load scenarios. An optimum design solution is only possible with close interaction between the geotechnical designer and the structural designer. Regrettably, such interaction is rare in New Zealand today.

Liquefaction Comments for Design Example

The above example assumes that soil liquefaction does not occur in the soil surrounding the piles. In the event of liquefaction, pile axial capacity will be reduced by a loss of side resistance through the liquefied layer and above. A partial loss of side resistance for the pile has already been assumed in the cyclic design process and in preparing the cyclic stability diagram. Also, once soil liquefaction has been triggered, the ground surface and structure will receive some degree of base isolation, reducing the overturning moments that are the source of the cyclic axial loads, and, hopefully, preventing pile failure. The main issue for the piles then becomes one of surviving the associated ground displacements and pile bending loads, which requires adequate ductility, principally.

SUMMARY

Recent experimental research at the University of Canterbury concerned with the load-displacement behaviour of both shallow and deep foundations has been outlined. Issues being addressed include base sliding friction and passive resistance mechanisms of shallow foundations, capacity of deep foundations with cyclic axial and lateral loading, and interactions between shallow and deep foundations. Practical considerations have been discussed including two design examples.

ACKNOWLEDGEMENTS

Cyrille Eude, Pierre Guillou, Luc Barahona, and Laurent Barra, final year students from Ecole Nationale d'Ingenieurs de Saint-Etienne, France, performed many of the model pile tests. John van Dyk constructed most of the shallow foundation field tests, George Clarke and John Maley constructed most of the laboratory model testing apparatus, and Siale Faitotonu assisted with the full-size field pile tests.

The Earthquake Commission provided much of the funding through research grants EQC95/184 and EQC99/423. Daniel Smith Industries generously provided the test piles at the Park Terrace site and also assisted with the testing.

REFERENCES

Australian Standard AS 2159 (1995). *Piling, Design and Installation,* Standards Australia, Homebush, NSW, 52 p.

Burdon, N.R.R. (2000). *Earthquake Resistance of Shallow Foundations*, Masters Thesis, University of Canterbury.

Chambers, A. (1999). *The Seismic Response of Drilled Shaft Foundations*, PhD Thesis, Unversity of Canterbury, 152 p.

Charlie, W. A., Turner, J. P., and Kulhawy, F. H. (1985). "Review of repeated axial load tests on deep foundations," *Drilled Piers and Caissons II*, Ed. C. N. Baker, Jr. ASCE, New York, pp. 129-150.

Ghahramani, A. and Berrill, J. B. (1995). "Seismic Bearing Capacity Factors by Zero Extension Line Method," *Proc. Pacific Conference on Earthquake Engineering*, Nov. 1995, pp. 147-156.

Lyons, C. D. (2000). *Degradation of Pile Capacity from Cyclic Axial Loading,* Masters Thesis, University of Canterbury, 165 p.

McCarthy, D. F. (2002). *Essentials of Soil Mechanics and Foundations, 6th Ed.,* Prentice Hall, New Jersey, 788 p.

McManus, K.J. and Kulhawy, F.H., (1994). "Cyclic Axial Loading of Drilled Shaft Foundations in Cohesive Soil," *Journal of Geotechnical Engineering*, ASCE, Vol. 120, No. 9, Sep. 1994, pp. 1481-1497.

McManus, K.J. and Chambers, A.,(1995) "Stability Of Drilled Shafts Under Earthquake Induced Axial Loads," in *Performance of Deep Foundations Under Seismic Loading*, Ed. J. P. Turner, ASCE Geotechnical Special Publication No. 51, p. 1-16.

McManus, K. J. (1997). *Axial Behaviour of Bored Pile Foundations*, Research Report EQC 95/184, Earthquake Commission, Wellington, 47 p.

McManus, K.J. (1999). "Axial Response of a Driven Pile to Cyclic Loading", *Proc. Tech Conf. N.Z. Soc. for Earthquake Engg*, Rotorua, NZ, March 1999.

McManus, K.J. and Burdon, N.R.R. (2001) "Lateral Resistance of Shallow Foundations", *Proc. Tech Conf. N.Z. Soc. for Earthquake Engg*, Wairakei, NZ, March 2001, Paper No. 6.03, 11 p.

New Zealand Standard NZS 4203 (1992). *Code of Practice for General Structural Design and Design Loadings for Buildings,* Standards New Zealand, Wellington, 134 p.

Poulos, H. G., (1988). "Cyclic stability diagram for axially loaded piles," *Journal of Geotechnical Engineering*, ASCE, Vol.114, No.8, Aug. 1988, pp. 877-895.

Turner, J. P. and Kulhawy, F. H. (1990). "Drained uplift capacity of drilled shafts under repeated axial loading," *Journal of Geotechnical Engineering*, ASCE, Vol.116, No.3, pp. 470-491.

Ignimbrite, Andesite, Landslides and Dam Sites: Engineering Geological Models for Volcanic Terrain

W M Prebble
BSc (Hons), MSc, PhD
Department of Geology, University of Auckland

Abstract: Rhyolitic ignimbrite and tephra deposits in the Taupo Volcanic Zone span a wide range of rock mass and soil properties. Welded ignimbrites form thick, extensive, columnar fractured rock sheets, the unrestrained edges of which are dilated and loosened. Non-welded deposits of tephra are susceptible to piping and tunnel erosion and paleosols between deposits contain sensitive clays and potential basal rupture surfaces. Steep fault scarps and hydrothermally weakened slopes have failed as debris avalanches, debris flows, rock fall and block slide. An extensive debris flow deposit from the collapse of the Tongariro volcano has provided successful dam sites in preference to highly fractured andesite lava. A review of recent studies shows that there have been approximately 42 tephra deposits erupted in the last 50,000 years. Predicting the time and size of the next eruption is considered by some authors to be impossible.

INTRODUCTION

The Taupo Volcanic Zone

The Taupo Volcanic Zone (Fig. 1), in the North Island of New Zealand, is an active volcanic rift in which voluminous rhyolitic ignimbrite deposits have dominated the last 1.6 million years (Pringle, McWilliams, Houghton, Lanphere and Wilson, 1992). These vary from welded, columnar-fractured sheet-like rock masses of vast extent and thickness to non-welded soil deposits of pumice, ash, lapilli and pyroclastic flow deposits, which are referred to collectively as tephra. In the geotechnical sense these are soils. Many tephra deposits have been weathered, eroded, and redeposited by wind and water (Prebble, 2001). They extend beyond the TVZ to Waikato and Auckland.

The zone has many active faults of considerable length with vertical offsets of several hundred metres. Andesite volcanoes are a minor part of the TVZ in terms of their volume but form large elevated massifs, especially in the Tongariro area. Large dams, perched canals, power stations and major roads have been constructed throughout the TVZ and the adjacent plateaus.

Scope of this Paper

Current research into landslides on the Paeroa Fault is presented and compared to a recent study into landslides from andesite volcanoes in the Tongariro area. Some of the geotechnical features of ignimbrites, tephras and andesites, which are critical to dams and canals, are reviewed in terms of an engineering geological model in which paleotopography and geomorphic development are key ingredients. Information on frequency and magnitude of late Quaternary tephras is also reviewed.

FREQUENCY AND MAGNITUDE OF RHYOLITIC TEPHRA ERUPTIONS

Frequency

Froggatt and Lowe (1990) reviewed the stratigraphy and distribution of 36 rhyolitic tephra deposits erupted during the last 50,000 years. These come mainly from the caldera volcanoes of Okataina, Taupo and Maroa (Fig.1). Most of the tephra have a radiocarbon age but at least 10 were not reliably dated at the time of the review. A theoretical frequency of one event every 1400 years is indicated by

the published data but ignores erosion of smaller deposits and those yet to be recognised. Moreover a study of the Taupo volcano deposits in the past 25,000 years (Wilson, 1993) found that there are apparently random relationships between repose periods before or after an eruption and eruption volume. Therefore frequency and the elapsed time (approximately 1840 years) since the last eruption are no guide to either the time or size of the next Taupo eruption. Wilson (1993) concludes that both are impossible to predict.

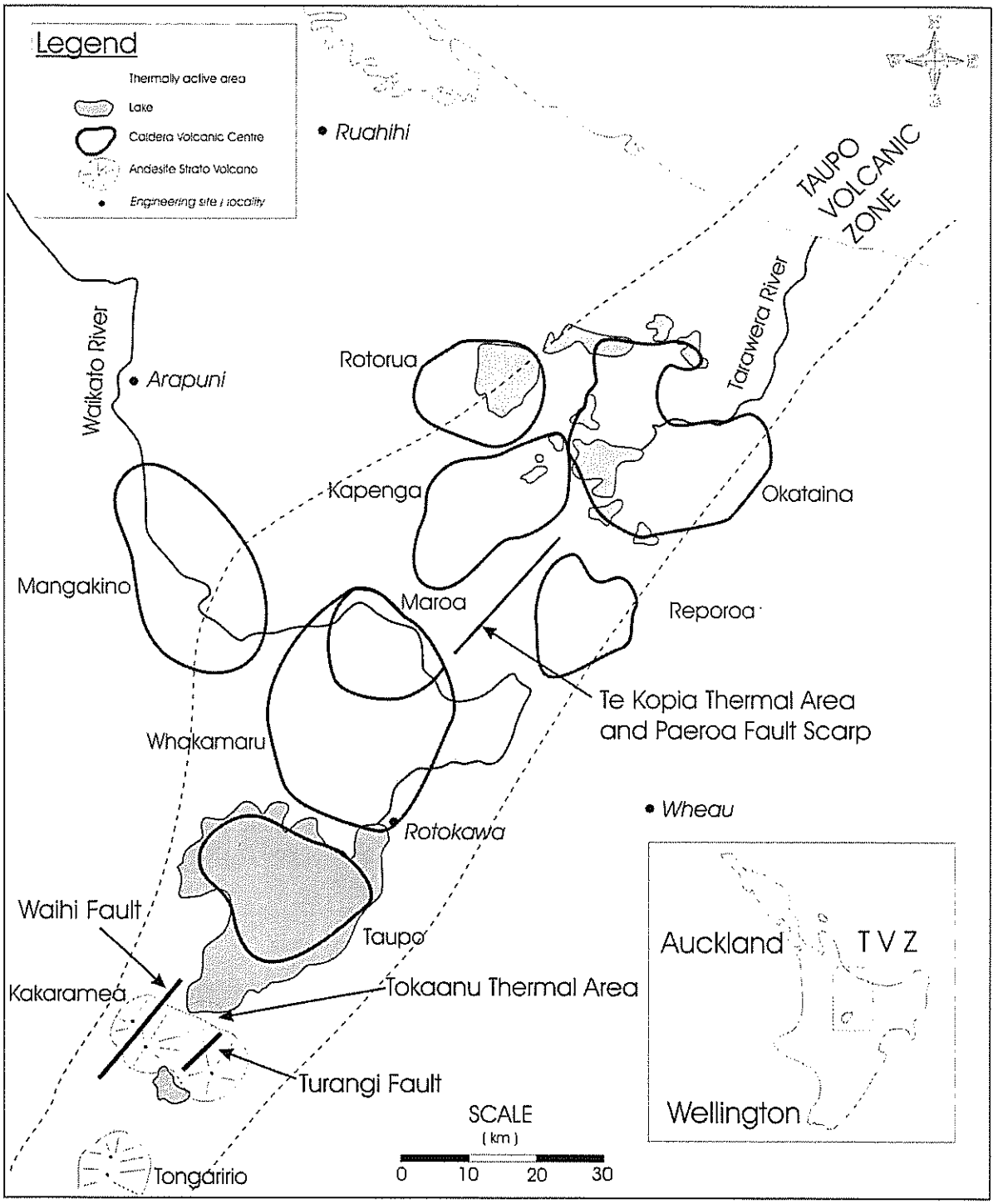

Figure 1. The Taupo Volcanic Zone, Showing the Boundaries of Caldera Volcanic Centres.

Magnitude

Froggatt and Lowe (1990) table a total eruption volume for the last 50,000 years of 816 km^3 but a recent study by Wilson (2001) of the 26,500 years before present (26.5 ka) Oruanui eruption from

Taupo has almost trebled the volume of that event alone to 750 cubic kilometres (km^3). This would increase the total to around 1450 km^3. These volumes are for both airfall and pyroclastic flow tephra but do not include intra-caldera material, which lies beneath the present lake.

Long-Term Activity of the Taupo Volcanic Zone

In contrast to the irregular recurrence of eruptions in the last 26,000 years, Wilson (1993) refers to the more regular long-term activity of the whole TVZ, which is the eruption of very large deposits every 40,000 to 60,000 years. The 26.5 ka Oruanui eruption from Taupo is the latest example. The previous one would be the 50 to 65 ka Rotoiti Tephra from Okataina (Froggatt and Lowe 1990; Wilson, Houghton, Lanphere and Weaver, 1992). The crust of the TVZ is geophysically young and highly fractured and the rate of heat flow is one of the highest in the World. Frequent explosive eruptions are to be expected. Eruption rates from Taupo and Okataina over the last 65,000 years make these the two most productive rhyolite volcanoes in the World (Wilson, 1993).

Geotechnical Significance

The importance from a geotechnical point of view is twofold: complex deposits and a high level of volcanic hazard. The complexity is seen in the highly variable lithology and geometry (Prebble, 2001). Rhyolitic tephra is easily eroded. Over the last 25,000 years erosion has been severe in the TVZ (Wilson, 1993) and weathering has produced clays and paleosols between deposits. This has produced contrasting physical properties in a complex sequence of deposits.

All but 3 of the 28 post-Oruanui eruptions from Taupo have been in the last 12,000 years and many of those in last 20,000 years would have caused relatively minor damage (Wilson, 2001). However, the local impact on the Taupo region would have been serious with potentially serious downstream effects, for instance large hydrothermal eruptions from Rotokawa (Fig 1). In view of the damage from recent small eruptions of Ruapehu, a conservative approach to risk assessment of the smaller eruptions from Taupo or Okataina would be justified. The practice of using a 2000 year return period for earthquake hazard assessment (in Auckland for instance) would suggest that the hazard from rhyolitic eruption in the TVZ should be accorded similar attention in spite of the uncertainties.

The spectrum of geologic hazards in the TVZ is wide and includes other events such as hydrothermal eruptions in populated areas, for instance Rotorua (Slako and Prebble, 2002). Although Wilson (1993) refers to the post-Oruanui deposits at Taupo as eruptive "noise" he acknowledges that the Taupo tephra of 1840 years ago was devastating.

WELDED INGNIMBRITE: COLUMNAR ROCK MASSES.

Ignimbrite Plateaus, Paleotopography and Intervening Soils

Welded ignimbrites form thick, extensive, columnar fractured rockmasses throughout the TVZ, such as the Whakamaru Ignimbrite, which was erupted around 330,000 years before present (Pringle et al, 1992). Rhyolite domes and tephra deposits of the Taupo and Maroa volcanoes post-date the ignimbrites, which are exposed in plateaus on either side of the TVZ and in fault scarps, caldera walls and deep gorges. Locally, thickness varies as a function of the paleotopography. Highly variable paleotopographic contacts between successive deposits (Prebble, 2001) have been observed mainly within tephra but are also present between welded ignimbrites as indicated by boreholes and mapping (Jones, Galloway, Howarth and Ramsay, 1983; Natusch, 1984). Unwelded tephra and alluvium intervene between the rock masses and underlie them.

Dilation, Loosening and Tilting

As a result of erosion the unrestrained edges and narrow ridges of ignimbrite rock masses have dilated and loosened such as at the Wheao canal, giving rise to serious deflections of the concrete penstock intake structure, which was founded on the top of the ignimbrite. It is thought that this allowed water

to penetrate through to the open interconnected fractures and pressurise them (Jones et al 1983). Tilting of the penstocks and power station on an ignimbrite ridge adjacent to the Waikato River was reported at Arapuni (Natusch, 1984). The ridge is a series of fractured ignimbrites and rhyolitic soils. The upper ignimbrite is distinctly columnar, the lower one less so. At the time of the tilting, water was freely issuing from the lower ignimbrite sheet at the back of the powerhouse. De-watering of the headrace system resulted in an almost immediate recovery of two thirds of the tilting. Bearing in mind the evidence from Wheao, it is possible that water wedging of the columns in the ignimbrite at Arapuni could have been a factor in the tilting. Arapuni is the subject of a paper elsewhere in these proceedings.

PIPING, SENSITIVITY AND EARTH SLIDES IN TEPHRA.

Piping and Tunnel Erosion

Non-welded deposits of rhyolitic tephra are susceptible to piping and tunnels erosion, as a result of the low density and the ease with which the material is entrained. Pipes develop in coarse-grained tephra, loess and colluvial gravel on top of cohesive aquitards (Prebble, 2001). At Whaeo pipes and tunnels in these materials lie directly above open fractures in the ignimbrite, with a filling of pumice derived from the tephra above. This indicates that infiltration and seepage is directed through the pipes and tunnels and discharged into the fractured rock aquifer. Piping and tunneling were identified as factors in the collapse of the canal. (Hatrick, Galloway and Howarth 1982; Prebble, 1986.)

Sensitivity and Earth Slides

Earth slides in sensitive rhyolitic clayey silts at Ruahihi (Fig 1) are discussed by Prebble (2001). Similar conditions are found in the Auckland region at Papakura, with perched aquifers in sand and gravel overlying sensitive clayey silts. Slide mounds indicate a run-out of 200 metres on a basal rupture of 2 to 3 degrees dip. There are similar but much smaller mud-spates from rhyolitic deposits at Te Atatu and Hobsonville. South of Auckland on the Waikato coast at Ohuka Stream a large, complex earth block slide has moved on a basal rupture surface in sensitive rhyolitic silts with a perched aquifer immediately above. The overlying dune-bedded sands have been stretched and compressed into a series of blocks and troughs by low angle translation in the silts. This failure is in a bench 15 m above sea level and encompasses an area 200m along the coast by up to 100m inland (van den Bergen, 2002). Table 1 below compares the four localities referred to above.

Locality	Field sensitivity	Stratigraphic position of the sensitive silts	Groundwater regime	Slope failure above
Ruahihi	30 to 60	Successive paleosols in a sequence of rhyolitic tephra	Several perched, confined ribbon aquifers in sands above the silts	Rapid earth block slide – flow beneath canal
Papakura	10 to 20	Layers and paleosols in redeposited rhyolitic tephra	Perched ribbon aquifers above the silts	Earth block slide
Te Atatu – Hobsonville	5 to 15	Thin layers in redeposited rhyolitic tephra	Perched aquifers above the silts	Small earth slides and mud spates
Ohuka	10 to 15	Persistent layer in varied coastal and marine deposits	Perched unconfined aquifer in dune sands above silt	Large complex earth block slide

Table 1. Geotechnical Features of Sensitive Rhyolitic Clayey Silts in Terrace Deposits. Field Sensitivity was Measured with a Geonor Hand-Held Field Shear Vane

LANDSLIDES FROM FAULT SCARPS AND ANDESITE VOLCANOES

Landslides from the Paeroa Fault Scarp

Steep fault scarps, 400 to 580 metres high are seen along the Paeroa Fault near Te Kopia and the Waihi Fault on the Kakaramea Volcano near Tokaanu (Fig 1). Geothermal activity and hydrothermal alteration are evident in the fault scarps at both Tokaanu-Waihi and Te Kopia. Landslides are found along the fault scarps both inside and beyond the current geothermal areas.

Debris Flows

At least four periods of debris flows have been recognised in the apron along the foot of the Paeroa fault scarp (Figs 2, 3 and 4). Newson, Prebble and Browne (2002) identify three welded ignimbrite rock masses in the scarp as the source of the debris, which forms hummocky, tongue-shaped lobes of moderately well packed coarse-grained gravel. The majority of the lobes are clast-supported debris up to at least 6.5 metres thick. Thermal alteration of the gravel clasts indicates that warm groundwater marginal to the geothermal field has been more widespread than previously thought and that this weakened the ignimbrite rock masses in the fault scarp. Head scarp areas (Fig 2) have been identified from geomorphology and are tens to hundreds of metres across. They are found in the upper part of the scarp, with steep narrow chutes leading down from them to the apron below.

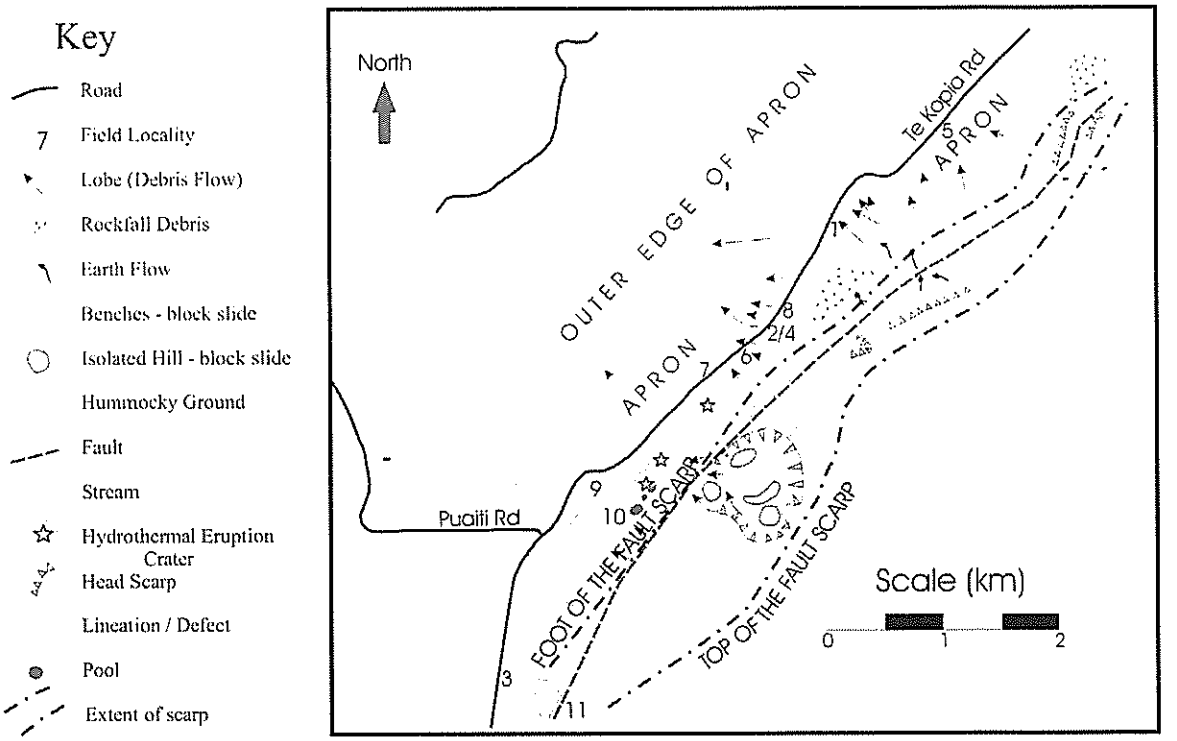

Figure 2. Geomorphic Map of the Paeroa Fault Scarp Near Te Kopia and Puaiti Roads. Refer to Figure 1 for Location Within the TVZ.

Air fall tephra deposits interbedded with the debris lobes provide some age control. At least 4 periods of voluminous debris flows, separated by tephra, have been identified in the last 26,500 years (Figs 3 and 4).

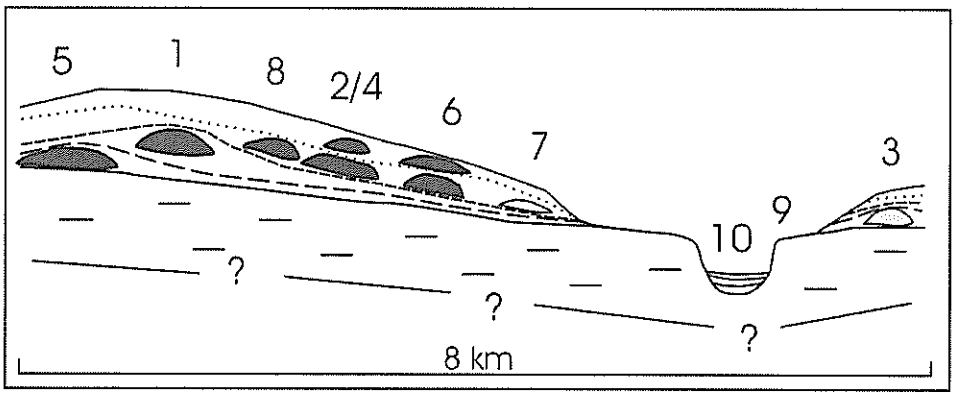

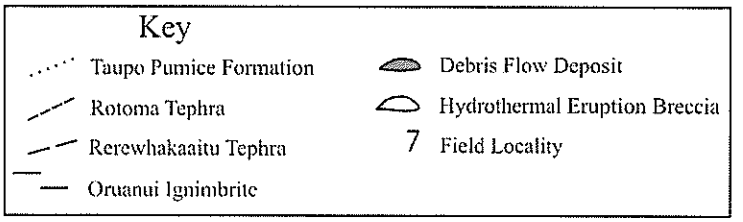

Figure 3. Schematic Section and Stratigraphic Model Through the Apron of the Paeroa Fault Scarp, Parallel to the Scarp. Field Localities are also Shown on Figure 2.

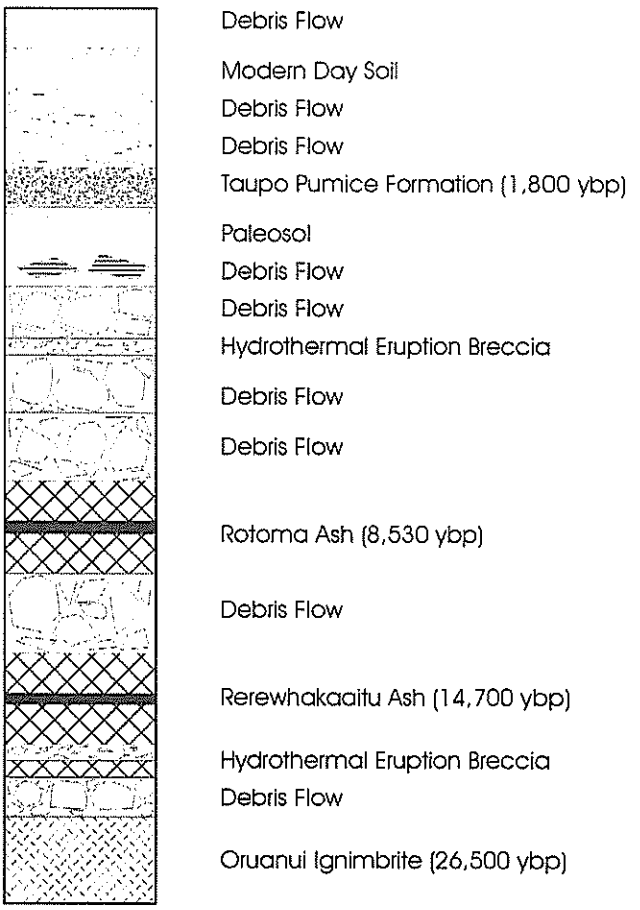

Figure 4. Schematic Stratigraphic Column and Model of the Apron Deposits Exposed Along Te Kopia Road and in Streams Crossing the Apron. Not to Scale.

Recurrence intervals, provided by the tephra ages, are indicated below in Table 2.

Time period ybp = years before present	Recurrence interval
26,500 ybp – present	1 debris flow per 2,944 years
14,700 ybp – present	1 debris flow per 1,633 years
8,530 ybp – present	1 debris flow per 1,218 years

Table 2. Recurrence Intervals for Large Debris Flows from the Scarp of the Paeroa Fault. Flows are Defined by Lobes, Exposures and a Runout of 1.1 km in the Apron Below the Scarp.

Rock Fall, Earth Flows and Block Slides

Rock fall debris is concentrated beneath the steeper, higher parts of the scarp. Block size is an order of magnitude greater than the debris flow clasts- many blocks are from 1 to 3.5 metres in diameter and have run out 150 to 300 metres from the base of the scarp. Earth flows are a frequent event along the fault scarp following high intensity rainstorms. Surficial fine debris and tephra are most susceptible to this type of failure. Block slides are indicated by benches and small isolated hills, in particular those within a large embayment adjacent to the thermal area, east of localities 9 and 10 on Figure 2. Up to 700 metres of translation may have taken place. Some of the geomorphic and geotechnical features of these landslides are given below in Table 3.

Landslides from Andesite Volcanoes in the Southern TVZ

The Te Whaiau Formation (LeCointre, Neall, Wallace and Prebble, 2002) is a large (0.5 to 1.0 km^3) clay matrix-supported debris flow deposit containing very distinctive thermally altered andesite clasts and unaltered megaclasts. It is exposed in the northwestern ring plain of Tongariro volcano (Fig 1), where it is many tens of metres thick. Prebble (2001) pointed out the merits of the deposit as a foundation material and it`s advantages for reservoir containment. Similar but smaller deposits originate from Kakaramea volcano near Tokaanu (Fig 1).

Hegan, Johnston and Severne (2001) describe the historic and disastrous debris flows from the Waihi Fault scarp (Fig 1) and refer to the significance of migrating thermal activity as a destabilising mechanism. They refer to the removal of steam pressure, which allows a higher pore water pressure to return, promoting failure in the thermally altered and weakened material. A similar cycle of conditions probably contributed to the failure of Tongariro Volcano and the generation of the Te Whaiau Formation. These andesitic cohesive debris flows have been included for comparison in Table 3 below.

Landslide type	Debris flows	Rock fall	Block slide	Earth flows	Cohesive debris flow
Source area	Fault scarp	Fault scarp	Fault scarp	Fault scarp	Andesite volcano
Fabric	Clast supported	Individual blocks	Coherent block	Matrix supported	Matrix supported
Lithology of clasts or block	Ignimbrite	Ignimbrite	Ignimbrite	Tephra and slope soils, clays	Andesite, many altered
Landslide Shape	Lobate	Block field	Blocky hillocks	Stream –like, smooth	Lobate to vast area
Heightdrop: run out	1:3 to 1:4	2:1 to 1:1	Uncertain, possibly 1:7	1:60	1:14
Volume ($metres^3$)	15,000 to 700,000	Not applicable	Not available	Up to 360,000 –many less?	Up to 1 $kilometre^3$

Table 3. Some Geomorphic and Geotechnical Features of Landslides from Ignimbrite Sheets on the Paeroa Fault Scarp and from Andesite Volcanoes in the Southern TVZ.

ANDESITE LAVA FLOWS AND AN ENGINEERING GEOLOGICAL MODEL

Lava flows from andesite volcanoes at Tongariro are moderate in size, 10 to 30 metres thick and a few tens of metres wide. As a consequence of the irregular topography over which they have been erupted, individual flows are highly variable in thickness, width, level and direction. They are persistently fractured into continuous irregular columns and blocks. Flow margins and zones of internal shearing are extremely fractured into a mass of loosely interlocked plates.

At the Wanganui Dam site the extremely fractured platey andesite was very loosely interlocked. The rock mass also proved to be too thin and even rose above foundation level on one side of the site, exposing extremely weak alluvial soils. These were unsuitable as a foundation. The site was moved upstream where an earth and rock fill dam was built in the thick and extensive clay-matrix debris of the Te Whaiau Formation. This impermeable, firm, massive landslide deposit proved suitable as foundation material and for reservoir containment. The model presented in Figure 5 is a 2-dimensional cross-section through the ring plain deposits of Tongariro at these dam sites. It is also applicable to the paleotopography of ignimbrite and tephra, as seen at Ruahihi for instance.

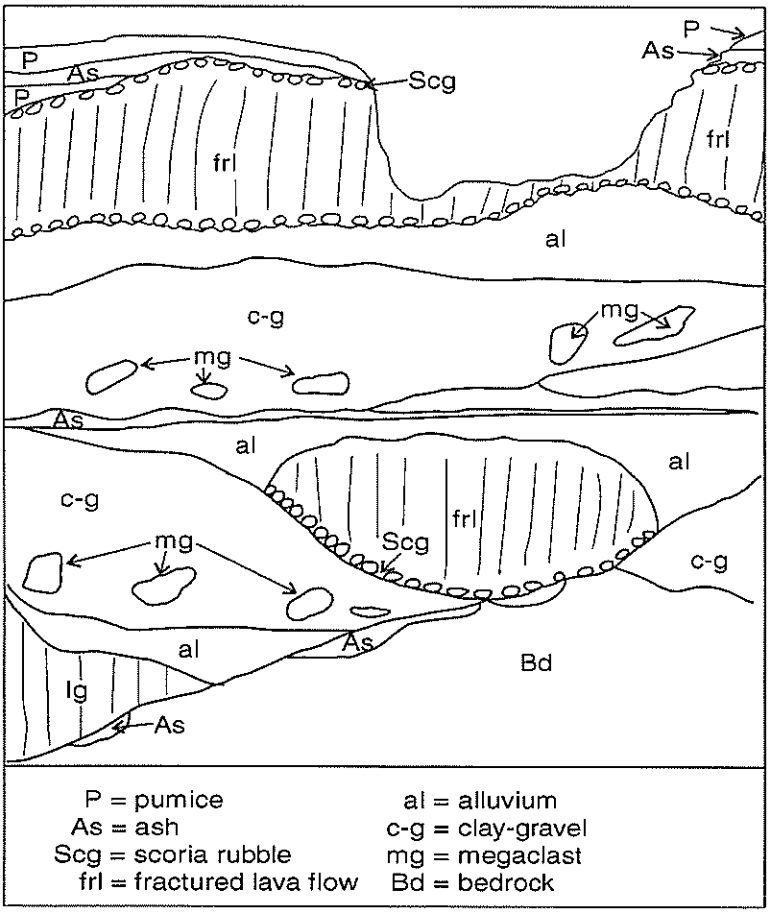

Figure 5. Two – Dimensional Model (cross-section) Through Ring-Plain Deposits of an Andesite Volcano, Such as Tongariro. The Fractured Lava Flows are Approximately 30 m Thick. This Model is Taken from the Vicinity of Wanganui, Te Whaiau and Otamangakau Dam Sites.

CONCLUSIONS

The most recent rhyolitic eruptions from the TVZ have been 42 tephra deposits erupted from 4 rhyolitic volcanoes in the last 50,000 years and with a total volume probably in excess of 1700 km^3. The 26.5 ka Oruanui eruption from Taupo alone contributed 750 km^3.

The relationship between preceding and succeeding repose periods is random. Prediction of both the time and size of the next eruption is impossible. However large eruptions like the Oruanui occur at more evenly spaced intervals of 40 to 60 ka.

Prediction of the scope and time of the next Taupo eruption is formidable and challenging.

The Taupo tephra of around 1840 years ago was devastating over a large region of the North Island.

Tephra and reworked, redeposited, non welded deposits are susceptible to piping and erosion. Sensitivity and slope failure are widespread in rhyolitic silts and clays.

Welded ignimbrites are much older than the tephra (around 330 ka for many of them).

The unrestrained edges of columnar fractured ignimbrites have been subject to wedging and tilting from leaking head race canals.

Steep fault scarps, in welded ignimbrite have failed by debris flows, earth flows and block slides.

At least 4 periods of voluminous debris flows in the last 26.5 ka have been recognised in the apron of the Paeroa Fault scarp. In the last 8,500 years there has been, on average, 1 large scale debris flow with a minimum run out of 1.1 km every 1,218 years.

Rhyolitic air fall tephra and pyroclastic material of known ages have been essential for providing age control on the landslide deposits.

Hydrothermal alteration has been a factor in assisting slope failure.

Andesite volcanoes have failed as a result of hydrothermal alteration, giving rise to cohesive debris flows. At Tongariro, a large (0.5 to 1.0 km^3) and thick clay-matrix debris flow deposit has provided dams sites and reservoirs in preference to irregular and highly fractured andesite lava flows.

Paleotopograhy and geomorphology have been key elements in constructing a model for use in the geotechnical investigation of both extensive areas and specific sites in volcanic terrain.

ACKNOWLEDGEMENTS

The research on landslides of the Paeroa fault scarp is a collaborative research project carried out by Andrew Newson (graduate student), the author and Pat Browne.

REFERENCES

Froggatt, P.C. and Lowe, D.J. (1990). "A review of late Quaternary silicic and some other tephra formations from New Zealand: their stratigraphy, nomenclature, distribution, volume and age," *New Zealand Journal of Geology and Geophysics,* Vol. 33, pp 89-109.

Hatrick, A.V., Galloway, J.H.H. and Howarth, A. (1982). *Report of Committee to Inquire into the Failure of the Ruahihi Canal,* Ministry of Works and Development, Wellington.

Hegan, B.D., Johnson, J.D. and Severne, C.. (2001). "Landslide risk from the Hipaua Geothermal Area near Waihi Village at the Southern End of Lake Taupo," In: *Engineering and Development in Hazardous Terrain,* Ed: McManus, K. IPENZ Proceedings of the Technical Groups, Vol. 29, Issue 2(GM) pp 439-448.

Jones, O.T., Galloway, J.H.H., Howarth, A. and Ramsay, G. (1983). *Report of Committee to Inquire into the Canal Failure on the Wheao Power Scheme,* Ministry of Works and Development, Wellington.

Lecointre, J.A., Neall, V.E., Wallace, R.C. and Prebble, W.M. (2002). "The 55-60 ka Te Whaiau Formation: A catastrophic, avalanche-induced, clay-rich debris flow deposit from Proto-Tongariro Volcano, New Zealand," *Bulletin of Volcanology,* Vol 63, pp 509-525.

Natusch, G.G. (1984) "Arapuni in retrospect," *Transactions ,IPENZ,* Vol 11 (1/CE), pp 1-12.

Newson, A.M., Prebble, W.M. and Browne, P.R.L. (2002). "Landsliding on the Paeroa Fault at Te Kopia," In: *Proceedings of the 24th New Zealand Geothermal Workshop*, Eds; Soengkono, S. and Browne, P.R.L., The University of Auckland, pp 61-66.

Prebble, W.M. (1986). "Geotechnical Problems in the Taupo Volcanic Zone," In: *Volcanic Hazards Assessment in New Zealand,* Eds: Gregory, J.G. and Watters, W.A., New Zealand Geological Record 10, pp 65-80.

Prebble, W.M. (2001). "Hazardous Terrain – An Engineering Geological Perspective," 11th Geomechanics Lecture, N.Z. Geotechnical Society. *New Zealand Geomechanics News,* Issue 62, December 2001, pp 45-69.

Pringle, M.S., McWilliams, M., Houghton, B.F., Lanphere, M.A. and Wilson, C.J.N. (1992). $^{40}Ar^{39}$ Ar dating of Quaternary feldspar: examples form the Taupo Volcanic Zone, New Zealand," *Geology*, Vol 20, pp531-534

Slako, M.A. and Prebble, W.M. (2002). "Geotechnical Properties and Geothermal Instability Hazards of Kuirau Park, Rotorua," *Proceeedings of the 5th Australia- New Zealand Young Geotechnical Professionals Conference, Rotorua New Zealand,* Ed: Davies, T., pp 213-220.

van den Bergen, J. L. (2002). "Geotechnical properties, stratigraphy and slope movement at Ohuka Stream, Port Waikato." *BSc Honours dissertation, in Geology,The University of Auckland.*

Wilson, C.J.N., Houghton, B.F., Lanphere, M.A. and Weaver, S.D. (1992). "A new radiometric age estimate for the Rotoehu Ash from Mayor Island Volcano, New Zealand," *New Zealand Journal of Geology and Geophysics,* Vol 35, pp 371-374.

Wilson, C.J.N. (1993). "Stratigraphy, chronology, styles and dynamics of late Quaternary eruptions from Taupo volcano, New Zealand," *Philosophical Transactions Royal Society London,* A 343, pp 205-306.

Wilson, C.J.N. (2001). "The 26.5 ka Oruanui eruption, New Zealand: an introduction and overview," *Journal of Volcanology and Geothermal Research,* Vol 112, pp 133-174.

Kaimai Tunnel
A Geological Section Through an Ancient Volcano

B D Hegan
Engineering Geologist
Tonkin & Taylor Ltd
(formerly NZ Geological Survey)

Abstract: The Kaimai Tunnel, the longest rail tunnel in New Zealand at 8.9 km was holed through in June 1976 following nearly seven years of tunnelling. Conditions met while driving the tunnel produced a number of challenges, all of which were required to be overcome.

The challenges came in the form of squeezing ground in unstable brecciated volcanic lava and weak volcaniclastic sediments, high groundwater inflows and a high geothermal gradient producing ground temperature up to 38° C. These ground conditions were the result of the tunnel passing through a comparatively young strataform volcanic pile of lavas and tuffs overlain on the eastern side by a series of ignimbrite flows.

This paper discusses investigations carried out for the tunnel and the tunnelling conditions experienced.

INTRODUCTION

The 8.9 km long Kaimai rail tunnel holed through in June 1976 completing excavation of one of the most challenging tunnels in New Zealand. The tunnel is the longest rail tunnel in New Zealand and was driven through a stratified sequence of andesitic lavas and overlying ignimbrites. Tunnelling conditions ranged from excellent to extremely difficult in both headings. Excavation of the 6.4 metre diameter tunnel was by drill and blast excavation in the west and a full face TBM from the eastern side. The tunnel crews faced rock temperatures approaching 40°C and when an ancient buried land surface now altered to swelling clay was encountered excavation was forced to multiple drifts. A long section of the tunnel is shown on Figure 1. More detailed descriptions of construction of Kaimai Tunnel are given by Bennian (1976), Bennian and Hegan (1977) and of the tunnel engineering geology by Hegan (1977).

GEOLOGICAL SETTING

The Kaimai Range is part of a major volcanic block that extends south from the Coromandel Peninsula to the Mamaku Plateau. To the west of the Kaimai Range is the Hauraki Depression. Separating the two and defining the western flank of the range is the steep scarp of the Okauia Fault. To the east the Kaimai Range slopes gently down towards the Tauranga Basin.

Geological mapping by Healy (1967) indicated that from west to east the tunnel would pass through alluvial material before encountering the Okauia Fault, after which the tunnel would be driven through volcanic rock consisting mainly of andesitic lava and breccia. On the eastern side of the range the andesite volcanics are overlain by a series of younger ignimbrite sheets, pumice breccias, tuffs and interbedded sediments which slope gently down into the Tauranga Basin.

GEOLOGICAL INVESTIGATIONS

West Portal

The first geological investigations reported in 1963 selected the present alignment from three alternatives. The first problem identified was the safe excavation of the tunnel through the Okauia Fault on the western side of the range. Two portal locations were investigated by seismic, resistivity, magnetic and gravity surveys. Following drilling investigations starting in 1965, the more northerly

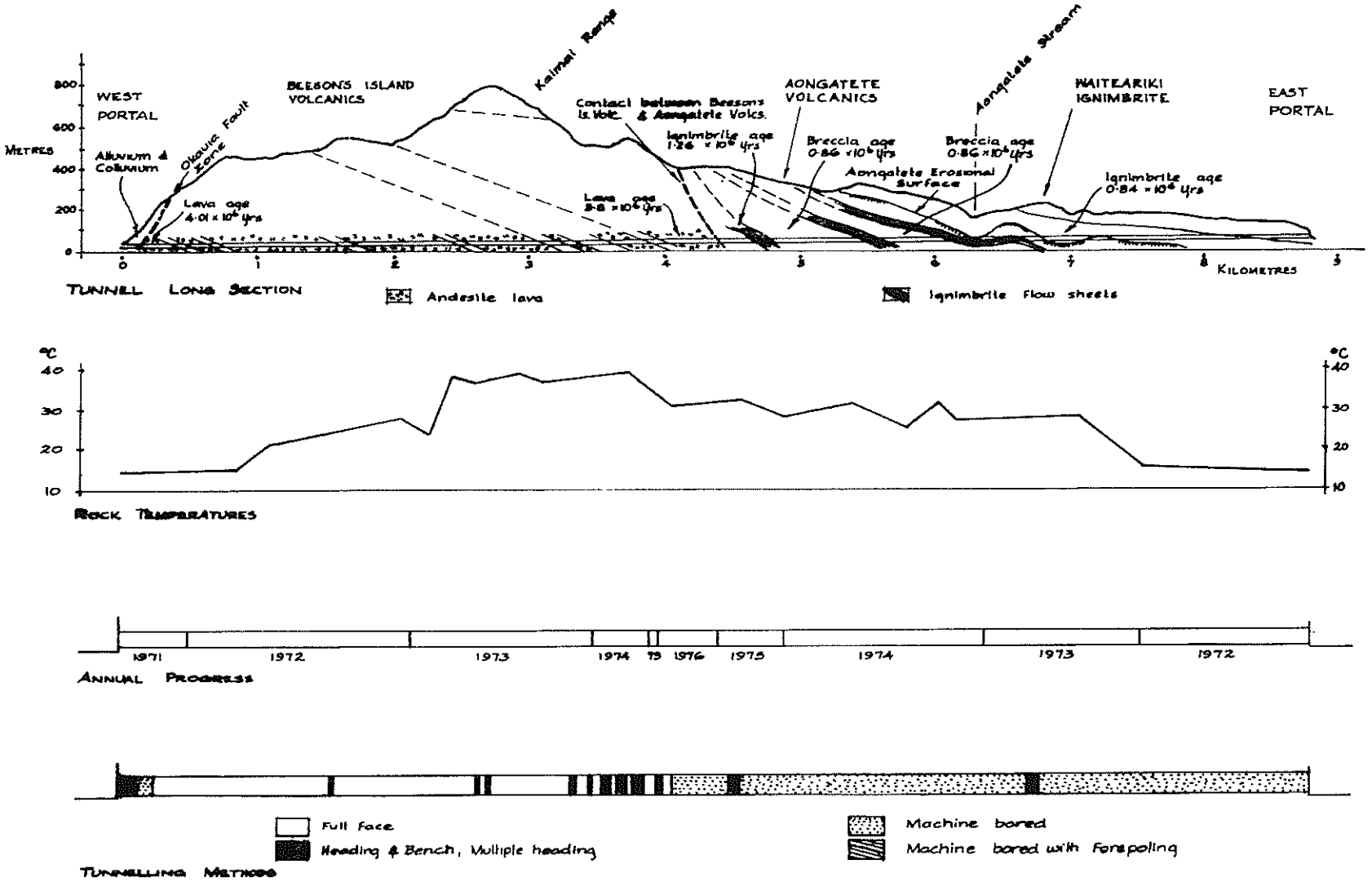

Figure 1: Kaimai Tunnel Longsection (note: radiometric dates shown for the ignimbrite flow units have been recently revised increasing all dates)

portal location was selected to lessen the tunnelling distance through the loose and broken rock associated with the Okauia Fault. Small exploratory drives at the West Portal were commenced in 1969.

Healy (1967) reported that the interpretation of the seismic survey at the western portal area was in general agreement with the later drilling investigations that showed that geological conditions were complex. Faulted blocks of volcanic breccia, sandstone, tuff and a wide zone of andesitic fault breccia and gouge separated alluvial deposits to the west from the main Kaimai Range rock mass.

Central Part of the Kaimai Range

As the tunnel line was approximately 61 metres above sea level, and the Kaimai Range rises to a height of 814 metres in thickly bushed steep country, the geology of the central part of the range at tunnel level could only be inferred from surface geology. Healy (1967) showed the core of the Kaimai Range as Beeson's Island Andesite. He postulated that interbedded solid andesitic lava and flow breccia dipped west based on mapping which showed the dacite lava at the summit dipping west. With this interpretation the Kaimai Range would be a tilted block dipping west. The origin of the eastern scarp between the andesite and younger ignimbrites was also uncertain and Healy considered the possibility of an eroded fault scarp separating the two rock series.

Subsequent mapping over the tunnel line during construction showed that the andesite and dacite lava flows dipped to the east. Engineering geological mapping of the tunnel also recorded chilled lava margins and the tuffaceous beds dipping east throughout the central part of the range. This confirmed that the core of Kaimai Range was composed of an easterly dipping stratified sequence of andesitic lava, autoclastic breccia, tuff and locally derived volcaniclastic sediment. This suggested that the lavas were erupted from a centre now lying in the Hauraki Depression and downthrown by more than 800 m by movement on the Okauia Fault.

Eastern Flanks of the Kaimai Range

Healy investigated the sequence of ignimbrites, breccias, tuffs and interbedded sediments dipping east into the Tauranga Basin by means of eight partially cored diamond holes in 1967. The drill holes were spaced along an alignment between the present east portal location and the southern west portal location. This alignment was later shifted slightly by rotation about the east portal to the more northerly of the west portal locations. With the combination of surface exposure and core from the drillholes Healy was able to recognise that the Waiteraiki Ignimbrite was separated from the underlying Beeson's Island Andesite by an older sequence of ignimbrites and associated tuffs and breccias which he named as the Aongatete Volcanics. Healy subdivided the Aongatete Volcanics into three main units, the Lower Tuffs and Breccias, Aongatete Ignimbrite, and Upper Tuffs and Breccias.

Seismic refraction surveys carried out on the eastern flank of the Kaimai Range were able to trace the contact between the less compacted and the welded part of the Waiteariki Ignimbrite near the eastern portal. However the later drilling investigations showed that the seismic survey was less accurate to the west where the degree of welding decreased as the ignimbrite flow units thinned against the andesite volcanics.

Following the decision to shift the Java TBM to the Eastern Portal a total of eight fully cored drillholes spaced along the eastern half of tunnel were drilled to tunnel level using conventional NMLC coring equipment with N rods. The deepest drillhole was 277 m in length. A total of 1083 metres of drilling were completed with a core loss of 45 m. The drillholes were all vertical except for one angled drill hole at the Aongatete Stream crossing. This angled hole was to investigate a streambed eroded into Aongatete Volcanics and later buried by the Waiteariki Ignimbrite. The drill hole encountered gravel alluvium at a level well above the tunnel crown level and no further investigations were undertaken in this area.

There was sufficient overlap of individual ignimbrite flow units between drillholes to allow further subdivision of the sequence within the Aongatete Volcanics. Eight units comprising breccias, welded

ignimbrites, tuffs and volcaniclastic sediments were recognised and a geological long section was prepared based on this data. The long section proved to be essentially correct for the initial 3.8 km of tunnel from the east portal. Beyond this point the interpretation had assumed that Beeson's Island Andesite would be encountered based on an andesitic breccia being encountered at the base of the western-most deep drillhole. However, as tunnel excavation proceeded past this drillhole and the breccia, further ignimbrite flow units of the Aongatete Volcanics were encountered. The Beeson's Island Andesite was in fact encountered 4.3 km from the East Portal.

As the ignimbrite flow units within the Aongatete Volcanics were strongly welded there was concern that the TBM may have had trouble cutting through these materials. As a consequence a total of 88 samples from drill core were tested to determine the uniaxial compressive strength, Youngs Modulus and wet density of the various units within the Aongatete Volcanics. The strengths measured were all well within the boring capabilities of the TBM and there was confidence that excavation from the East Portal would reach the half way mark.

Groundwater observations in the investigation drillholes had recorded artesian conditions within the ignimbrite flow units. Down-hole water pressure testing was carried out using a single Triefus packer and a permeability of 10^{-5} metres/sec was recorded in the jointed welded ignimbrite. Observations during construction showed that each of the ignimbrite flow units had its own groundwater regime with the intercalated ash beds acting as aquicludes.

GEOTHERMAL GRADIENT

Groundwater temperatures profiles were recorded in the deep drillholes on the eastern side of the Kaimai Range with the highest groundwater temperature of 30°C measured in the western most drillhole in andesitic breccia near the base of the Aongatete Volcanics. Healy (1967) had predicted that the maximum temperature in the central parts of the Kaimai Range could reach 53°C based on the geothermal gradient measure in the drillholes in the Tauranga and Bethlehem Districts.

TUNNELLING CONDITIONS ENCOUNTERED

In 1969 tunnelling commenced in the alluvium on the west side of the range. The material consisted of saturated gravels, sands, silts and clays and provided very difficult tunnelling conditions. Early in 1970 a disastrous fall occurred in this section claiming four lives and a construction delay of several months.

After the tunnel was driven through the Okauia Fault and into the Beeson's Island Volcanes the Java TBM was assembled to bore the remaining section of the tunnel. The TBM encountered very hard, strong andesite lava shortly after it started boring. The combination of extreme hardness and widely spaced fractures in the lava prevented it successfully boring through the rock. The decision was made to shift the TBM to the eastern end of the tunnel.

On the western side conventional full face tunnelling methods were used in the harder andesitic lavas and breccias. Some of the softer altered tuffs and volcanic breccias caused stability problems in the tunnel, especially where swelling clays were present and bench and heading methods were used.

In the central part of the tunnel an easterly dipping ancient buried land surface characterised by swelling clays was encountered, complete with fragments of trees that had been charred by hot lava. Radiometric dating of the overlying lavas gave an age indicating that the forest grew some four million years ago. Tunnelling through this zone required a multiple drift method of excavation with support pressures of 530 tonnes / metre required. These conditions were unforeseen and this section took almost a year to complete. In hindsight the engineering geological mapping over the tunnel line had located bedded tephra and sediments within the lava sequence with an easterly dip that, if projected 2 km to tunnel depth, would have been encountered close to this zone.

In the central part of the range rock temperatures rose to 38°C requiring the use of refrigeration to lower working temperatures. These temperatures were within the range predicted by Healy

On the eastern side the Java TBM made spectacular tunnelling progress reaching 31.7 m per day and 105 m per week in the soft Waitearíki Ignimbrite. The TBM bored through the Aongatete Volcanics with comparative ease although difficulties were experienced with overbreak in the crown of the tunnel in the very weak bedded tuffs and breccias. At one location overbreak reached one tunnel diameter above the crown. To control overbreak a method of spiling ahead of the face was developed. This involved drilling a fan of upward angled 150 mm diameter holes 10 m ahead of the face above the crown and inserting 100 x 100 x 19 column section steel spiles. The spiles were progressively supported by steel sets placed at 1.2 m centres behind the cutter head.

The eastern TBM driven section of the tunnel was driven at 1 in 300 down grade and water at the face was an ever-present problem. The largest flows occurred in the open jointed welded ignimbrites with total flows in excess of 600 m^3/hr (Bennion, 1976). It proved essential to keep the face dry as once water collected at the face in the softer materials the peripherally mounted much buckets had trouble collecting the fluid slurry and the conveyor muck transporting system was prone to spillage.

DISCUSSION

The initial geological investigations for the Kaimai Tunnel carried out in the 1960's were mainly concerned with the distribution of rock types along the tunnel. The early drilling focussed on the geological structure especially at the west portal within the Okauia fault zone. Drilling investigations to characterise rock mass strength and defect spacing on the western side of the Kaimai Range were limited to the portal area by the rapid increase in cover over the tunnel alignment. Consequently little was known of the actual rock mass conditions within the andesite lavas and this was shown when the full face TBM experienced cutting difficulties soon after excavation started. However it should be appreciated that selection of a full face TBM for excavation of the Kaimai Tunnel had been a bold move in the 1960's as machines of this size were fairly new on the construction scene.

When the TBM was shifted to the eastern portal additional fully cored drilling was carried out to give the full range of rock mass characteristics that could be expected from the ignimbrites. Core was logged to the then (1971) engineering geological standards noting rock strength, RQD, and defect spacing and nature. Strength testing of selected sections of the core was also undertaken. Strength testing (uniaxial compressive strength) was carried out systematically on cores taken from the tunnel sidewalls as excavation proceeded on the eastern heading.

The early 1970's saw the introduction of many of the rock mass classification systems with some attempting to predict the loads on the tunnel support systems. Following this line of research a programme of estimating support loads by measuring deflection on strain gauges fitted to selected steel sets was started along with detailed engineering geological logging of these sections of the tunnel. Results were summarised by Rutledge (1977), however much of the data was difficult to analyse due to the irregular blocking of the sets back to the rock mass.

ACKNOWLEDGEMENT

The Ministry of Works constructed the Kaimai Tunnel for New Zealand Rail. The assistance of John Bennion (Project Engineer) and reference to New Zealand Geological Survey data is gratefully acknowledged. The assistance of Tonkin & Taylor in preparing this paper is also acknowledged.

REFERENCES

Bennion J.D., 1976: *The Kaimai Tunnel, New Zealand – a case history.* Paper 1 in *Tunnelling '76 Symposium.* The Institute of Mining and Metallurgy, London

Bennion J. D., Hegan B.D., 1977: *Kaimai – Some Tunnelling Problems* in "Symposium on Tunnelling in New Zealand", 1977, Vol.3(G), Proceedings of Technical Groups, NZIE.

Healy J., 1967: *Geological Report on Proposed Tunnel Line, Kaimai Railway Deviation. New Zealand* Geological Survey unpublished report.

Hegan B.D., 1973: *Eastern Side Geological Investigations: Kaimai Tunnel: Kaimai Railway Deviation.* New Zealand Geological Survey unpublished report.

Hegan B.D., 1977: *Engineering Geology of Kaimai Tunnel.* 1977 NZIE Transactions

Rutledge J.C., 1977: *Engineering Classifications of Rock for the Determination of Tunnel Support,* in "Symposium on Tunnelling in New Zealand", 1977, Vol.3(G), Proceedings of Technical Groups, NZIE.

Engineering Geological Aspects of the Ruahihi Power Scheme, Tauranga

D A Burns
MSc (Earth Science)
Engineering Geology Manager, Meritec Ltd, Auckland
A J Cowbourne
BE (Hons) BSc MSc (Hons) MIPENZ CPEng
Senior Geotechnical Engineer, Tonkin & Taylor Ltd, Tauranga

Abstract: The Ruahihi Hydroelectric Project is constructed in a complex sequence of Pleistocene-age pyroclastic flows and airfall deposits. The principal pyroclastic units are Waiteariki Ignimbrite, Grey Ignimbrite (informal), Waihou Ignimbrite (tentative correlation) and Waimakariri Ignimbrite. Major periods of erosion and weathering followed deposition of each unit, resulting in a spatially complex distribution of materials. Lithological variability within units is typical and, combined with complex paleotopography, leads to problems of stratigraphic identification and correlation.

The engineering geological characteristics of the main pyroclastic and airfall tephra units are described in some detail, and factors that may have contributed to the 1981 canal failure are discussed.

INTRODUCTION

The Ruahihi Hydroelectric Project, located in the lower Kaimai Range (Figure 1), is constructed in volcanic terrain dominated by Pleistocene-age pyroclastic flows and airfall deposits of predominantly rhyolitic composition. The variability and complex distribution of the primary materials, and also of their weathering products, had a significant impact on the design and performance of the project works.

Difficulties were encountered both during construction with highly variable, wet and sensitive materials and also soon after commissioning in September 1981 when a canal buttressing fill failed. A consequence of that failure was unique exposure of many of the geological units encountered during construction of the project works. Prebble (2001) highlighted the variability and difficult geotechnical properties of some of the materials exposed in the failure.

This paper examines some aspects of the engineering geology of the Ruahihi project area to illustrate the complexity of this type of volcanic terrain and the potential problems that can be encountered in the design and construction of engineering works.

The discussion is based principally on geomorphological mapping, engineering geological descriptions of exposed materials, investigation drillholes and geophysical surveys.

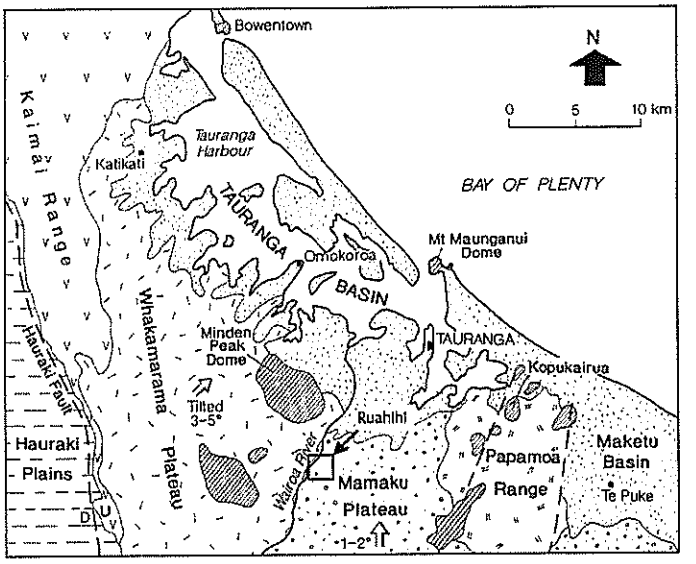

Figure 1: Physiography of the Tauranga Region (after Briggs et al 1996)

GEOLOGICAL AND GEOMORPHOLOGICAL SETTING

The geology of Tauranga Basin and hinterland is mapped at a scale of 1:50,000 by Briggs *et al* (1996). The basin, a major region of Pleistocene deposition, is infilled with terrestrial and estuarine sediments intercalated with pyroclastic flows and airfall deposits. The sediments are principally derived from non-welded and poorly welded pyroclastics and airfall volcanic materials eroded from the surrounding elevated land.

The limits of Tauranga Basin (Figure 1) are defined by Papamoa Range to the east, Mamaku Plateau to the south and Whakamarama Plateau - Kaimai Range to the west. The general dip of Mamaku Plateau is north at about 2° and Whakamarama Plateau northeast at about 4°. Mamaku Plateau, the youngest of these physiographic units, is constrained to a relatively narrow corridor by the older and more elevated Papamoa Range and Whakamarama Plateau (Figure 1). The Mamaku Plateau is characterised by linear, steep-sided drainage courses and broad concordant interfluves, while the Whakamarama surface is much more eroded and dissected.

Wairoa River is located in the valley formed by the contact between the Whakamarama and Mamaku plateaux. It is likely the converging dip of these surfaces has forced the river to migrate eastward into the weaker pyroclastic materials underlying Mamaku Plateau. Ruahihi Canal runs parallels to the river close to the northwestern extremity of the plateau (Figure 2).

Mamaku Plateau in the project area is mapped (Briggs *et al,* 1996) as being underlain by Waimakariri Ignimbrite, a variably welded rhyolitic pyroclastic flow most probably originating from the Rotorua caldera a short time prior to eruption of Mamaku Ignimbrite (Fransen, 1982). The latter overlies Waimakariri Ignimbrite a little to the south. A fringe of non-welded massive sandy ignimbrite (Te Ranga Ignimbrite) mapped along the southern side of Wairoa River, is considered by Briggs *et al* (1996) to be older than Waimakariri Ignimbrite and have a local (Tauranga Basin) source. This unit and Mamaku Ignimbrite were not encountered in the Ruahihi project works.

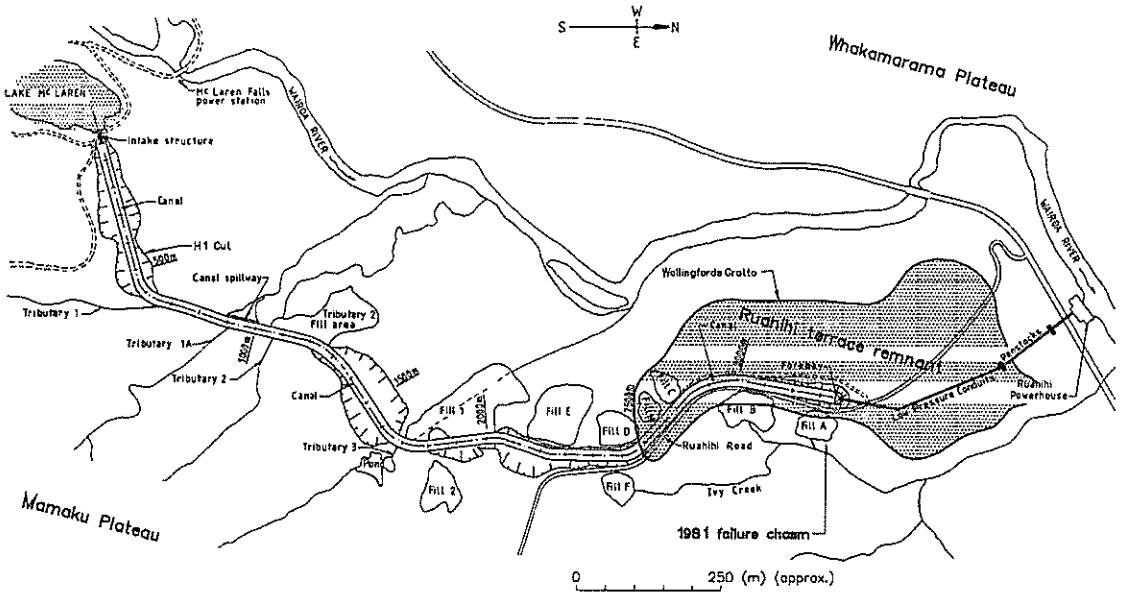

Figure 2 : Ruahihi Scheme Layout

Two distinctive geomorphic units characterise the landforms in the local power scheme area. The southern two-thirds of the canal (to distance 2500m, Figure 2) is located in dissected topography with steep, narrow ridges rising to elevations of 120m. This topography is likely to represent the northern limit of Mamaku Plateau, complicated by intersection with the underlying strongly dissected paleosurface of the Whakamarama Plateau, which rises to the southwest (Figure 1).

This elevated, dissected topography contrasts with the gently undulating terrace remnant to the north on which the northern end of the canal and headrace pipeline are located (Figure 2). The terrace is a narrow, elongated remnant of a larger surface at about elevation 80m that is concordant with similar remnants to the east.

PROJECT GEOLOGY & STRATIGRAPHIC CORRELATION

Table 1 summarises the lithological units encountered in natural exposures, excavations, drillholes and the 1981 failure chasm. Formal and informal stratigraphic names are assigned to the units, however many remain tentative.

Identification and correlation of the different units at Ruahihi has been problematic for a considerable period, including the many years during which elements of the final scheme were investigated (1955 to 1975). Healy (1955 and 1956) described a number of pumice breccia and mixed volcanogenic sedimentary units in the area, including what was later named Waiteariki Ignimbrite, although he did not attempt rigorous correlation with known units.

Lloyd (1965) correlated units with the stratigraphy of the then recently published 1:250,000 Rotorua sheet of the Geological Map of New Zealand. He defined two major units, Upper Mamaku Ignimbrite and Lower Mamaku Ignimbrite, separated by an erosional break. The upper sheet is considered by Briggs *et al* (1996) to be Mamaku Ignimbrite proper, and the lower sheet Waimakiriri Ignimbrite.

Carryer (1975) in a report on drilling investigations for the Ruahihi project, did not attempt to assign stratigraphic names to any of the drilled lithologies other than Waiteariki Ignimbrite.

Cowbourne (1985) described a number of pyroclastic units exposed in the failure chasm that are not formally identified. He tentatively correlated the massive non-welded ignimbrite underlying the Waimakariri Ignimbrite with Waihou Ignimbrite of Fransen (1982) but other units remain unidentified. Although this correlation remains tentative, the name Waihou is used here as a convenient identifier for this unit.

The fact that identification of many of the geological units at Ruahihi remains unresolved illustrates the considerable difficulties that investigators encountered when mapping the site and predicting ground conditions along the canal route.

ENGINEERING GEOLOGY OF PRINCIPAL UNITS

The following is a discussion of the engineering geology of some of the principal materials encountered during construction of the project works. The discussion is confined to the mainly pyroclastic materials that were exposed by canal excavations and the 1981 canal failure. Descriptions are from the youngest unit to the oldest.

Ash Cover

Beds of variably weathered Quaternary airfall tephra form a thin cover on all surfaces in the area except the youngest river terraces. They have been substantially eroded from steep slopes. The older beds are generally thought to be part of the Hamilton Ash Formation (150,000 to 350,000 years), although no correlation has been demonstrated. The age of Rotoehu Ash, at the base of the younger beds, is considered to be about 60,000 years (Lowe and Hogg, 1995).

The two sets of tephra are readily distinguished by the dark paleosol at the top of the Hamilton Ash beds and the coarse ash and lapilli bed at the base of the shower-bedded Rotoehu Ash (Figure 3). The Hamilton Ash beds are weathered to stiff plastic clay (halloysite and kaolinite, Oborn *et al*, 1982). Although water content and degree of sensitivity increase with depth, these beds generally present few problems in handling and compaction as an engineering material.

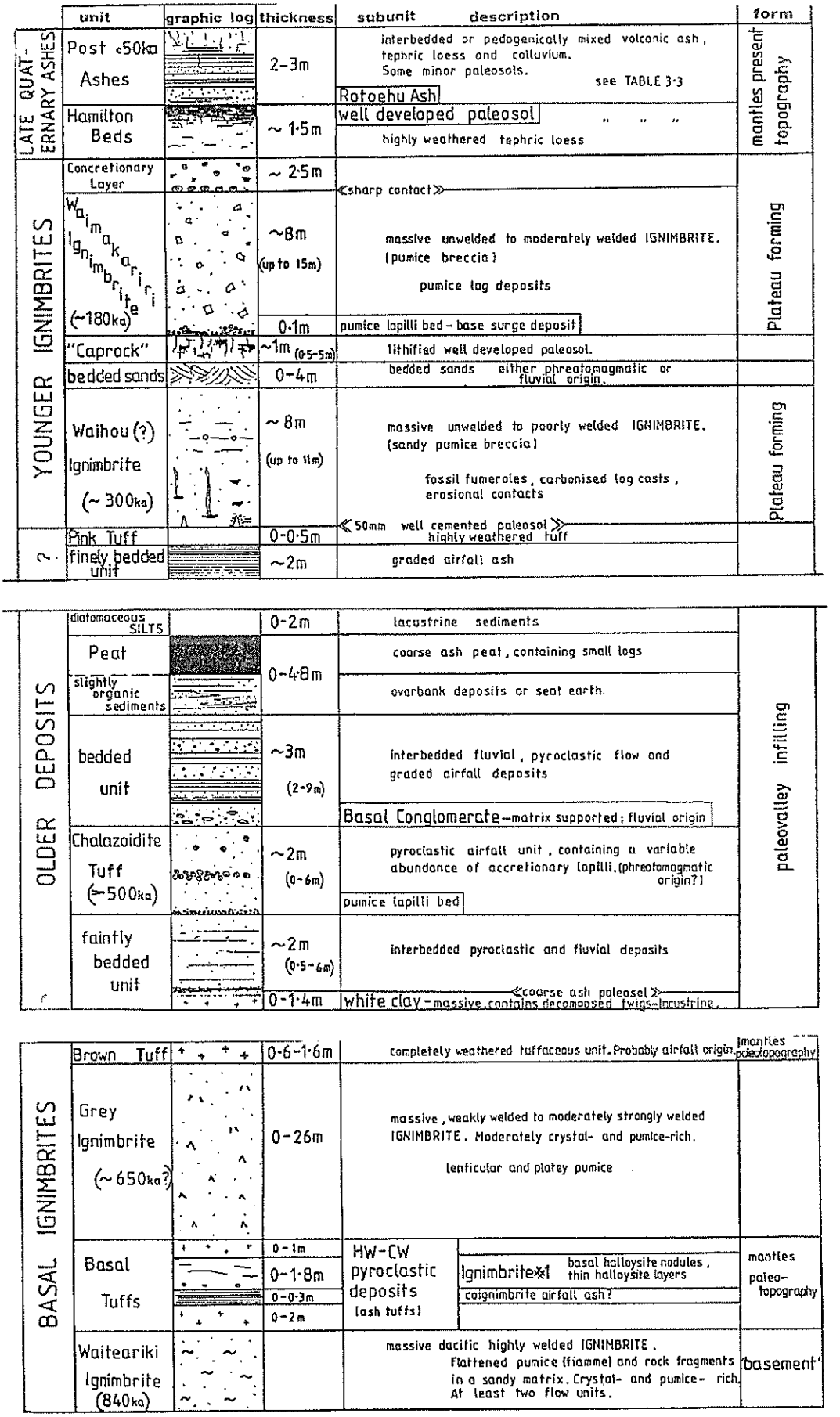

Based on Table 3.2 in Cowbourne (1985). Note that insufficient exposure means that the relationship between the sediments and tuffs of the Ivy Bridge Section (Healy 1955) and the Waimakariri and Waihou(?) Ignimbrites remain unclear.

Table 1 : Summary of Stratigraphy, Ruahihi Area

Rotoehu Ash is thinly bedded, loose gravel, sand and silt (1m thickness) overlain by 0.5m of weathered ash. Overlying Rotoehu Ash is about 1m of firm orange brown clayey silt, which is moderately sensitive, wet and greasy when worked and includes some recognisable pumice lapilli (probably Mangaone Sub-Group, Froggatt and Lowe, 1990). The uppermost 1m of ash is firm clayey silt characterised by relatively strong aggregation of the constituent allophane clays (Parfitt, 1990) producing a free-draining texture.

Waimakariri Ignimbrite

This unit is widespread over the project area, and forms one of the more important materials encountered in the engineering works. When emplaced, it substantially inundated the pre-existing topography. It is variable in thickness, lithology, degree of welding and weathering products. Characteristic features are a topography-mantling, thin basal bed of coarse ash and pumice lapilli, and a ubiquitous zone of red weathering in the uppermost 2m to 6m.

The red weathered zone is unusual. The ignimbrite is completely weathered to bright reddish and orange brown clayey silt with some sand (quartz, feldspar, glass) that is greasy and wet when worked. The clay dominated by halloysite with some allophane (Cowbourne, 1982). The transition to the underlying completely/highly weathered ignimbrite is sharp and very irregular forming pseudo-flame structures and 'blobs'. Hard elongate tubes and spherical 'concretions' comprising halloysite shells with an iron/manganese oxide core are common, particularly at the base.

Waimakariri Ignimbrite is massive, sandy and the content of pumice is variable. In general it grades with depth from a completely weathered upper zone through a middle section of commonly highly sensitive, pale yellow clayey silt, to a lower zone of pale pink, compact pumiceous silty sand. The concentration of pumice blocks increases towards the base and pumice is particularly abundant in paleovalleys, where some stratification is evident (Figure 4).

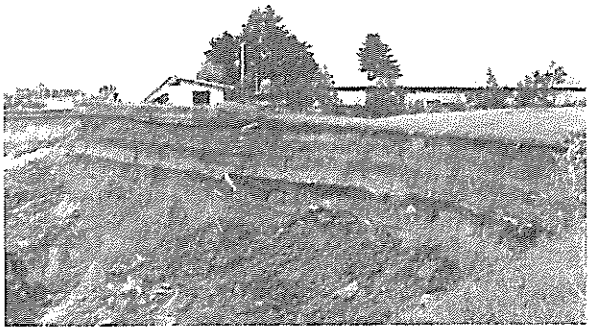

Figure 3 : Quaternary Tephra Exposed in Western Scarp of Failure Chasm

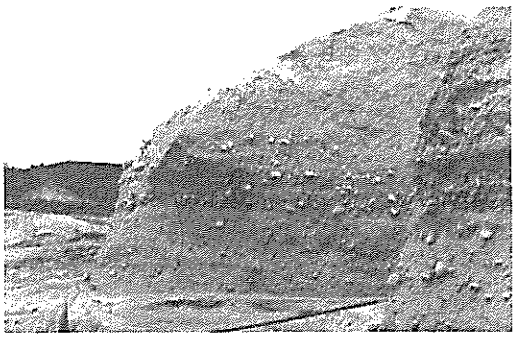

Figure 4 : Weak Stratification Near Base of Waimakariri Ignimbrite

Lateral and vertical variability is characteristic of Waimakariri Ignimbrite. Although predominantly unwelded, isolated welded zones occur (e.g. the northeastern extremity of the collapse scarp), forming a columnar-jointed weak rock. Lateral changes to unwelded, weathered, sensitive material can be abrupt (over less than 2m) accompanied by little visual change in appearance. At the upstream end of the canal, in the cut 500m east of Lake McLaren, the ignimbrite is compact, predominantly unweathered and stands in subvertical cuts to heights of 20m (Figure 5). In contrast, in canal cuts between 1km and 2km to the north, the ignimbrite is completely weathered and sensitive to the base.

The sensitive middle and upper parts of the ignimbrite were widespread in the canal excavation and were difficult materials to excavate, transport and place in spoil dumps. The sensitive materials were also widespread in the failure area and lead to regression of the failure scarps away from the initial canal breach as support to the material was progressively lost.

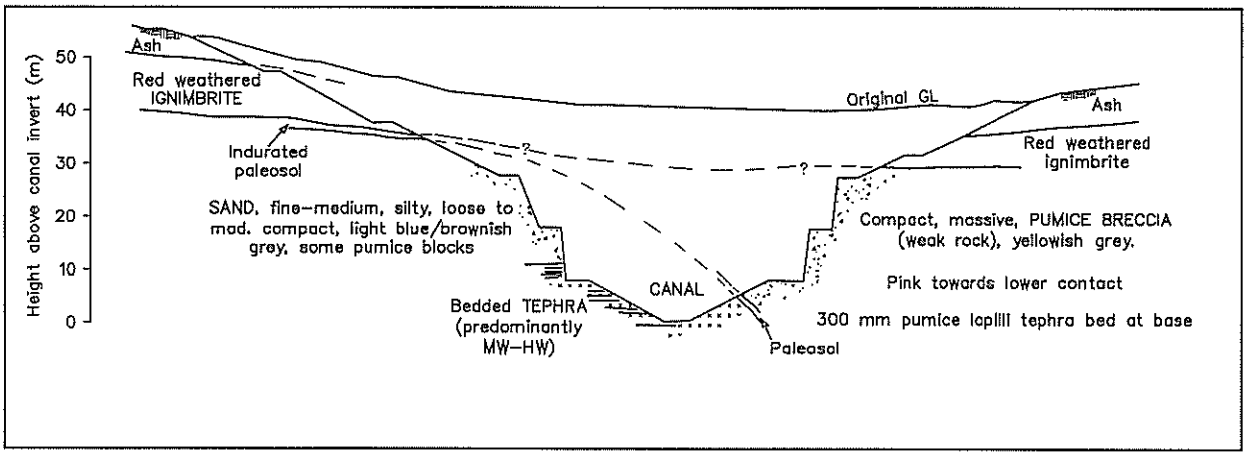

Figure 5: Example of Paleotopography, H1 Cut, Chainage 540m

Lithified Paleosol

An un-named ignimbrite that ranges in thickness up to 5m (generally 1m) is widespread in the failure exposures but less prominent in the canal excavations. The ignimbrite is unwelded, compact, moderately weathered and is capped by a lithified paleosol that has well-developed, polygonal, vertical joints, some infilled with iron and manganese oxides. At the top of the paleosol is a thin layer of greenish clayey silt that although hard is slightly sensitive and greasy when worked.

Bedded Sands

This unit was observed only in the failure exposures and comprises up to 8m of loose silt, sand and gravel (pumice and rock fragments) that in places is distinctly bedded (planar and cross-bedded, Figure 6). Mostly, bedding is diffuse and, although generally flat-lying, the sands mantle topographic highs. The sands appear to be pyroclastic in origin although a fluvial mode of emplacement is possible.

Waihou Ignimbrite

An unwelded sandy ignimbrite exposed in the failure chasm and in the 20m high cut on the southern side of the canal 500m east of Lake McLaren (Figure 3). The unit is up to 15m in thickness, is slightly to moderately weathered and comprises massive, loose, pale grey gravelly sand with pumice blocks scattered throughout. The gravel comprises pumice lapilli and rock fragments. The basal 3m to 4m is compact.

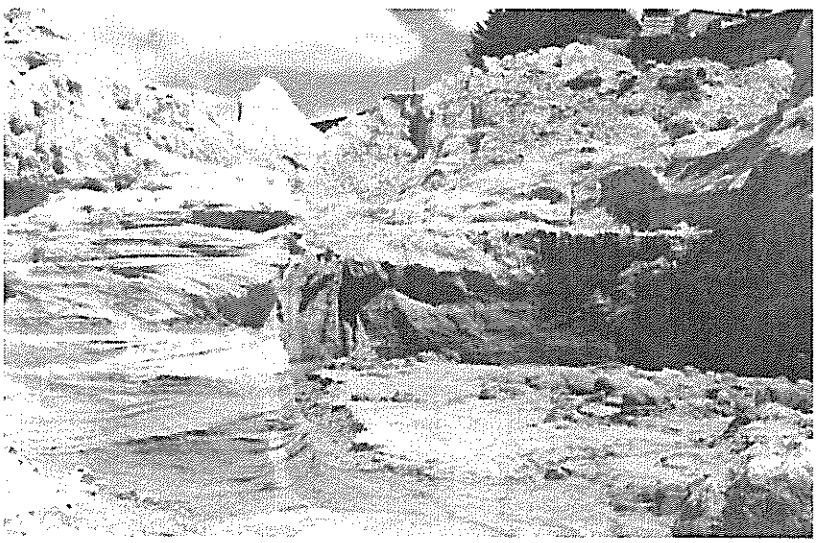

Figure 6 : Cross and Planar Bedding in the 'Bedded Sands', 1981 Failure Chasm

In the failure exposures, log casts are common near, and at the base of the flow (Figure 7). The casts are empty, subhorizontal, up to 300mm in diameter, 0.5m to 2m long and some are lined with iron and manganese oxide. Elongate fossil fumaroles infilled with loose coarse sand also are common near the base of the flow.

Discontinuous, subhorizontal, erosive contacts and thin seams occur at different levels throughout the unit. A line of log casts is associated with one of the contacts. Other features noted include a scour channel infilled with blocks of intact, slightly more compact ignimbrite. It is likely that these features are associated with the mode of emplacement of the flow.

Although predominantly a loosely packed sand this material has performed satisfactorily in the well-drained 20m high subvertical cut east of Lake McLaren. Given its relatively open structure however, it is susceptible to internal erosion (piping) and potential for collapse by densification on wetting.

Graded Tuffs

In the canal failure area the Waihou Ignimbrite rests unconformably on a series of tuffs that form a paleosurface with relief in excess of 10m. These materials are likely to form part of the Older Deposits (Table 1).

The tuffs are the lowermost unit exposed in the failure area and comprise a 2.5m sequence of 100mm thick graded beds of pumice lapilli fining upwards to fine ash (Figure 8). The beds are very compact and are capped by 0.5m of pinkish white, hard clayey silt that is slightly sensitive and greasy when worked. Underlying the tuff beds is massive brown/grey hard clayey silt at least 2m in thickness.

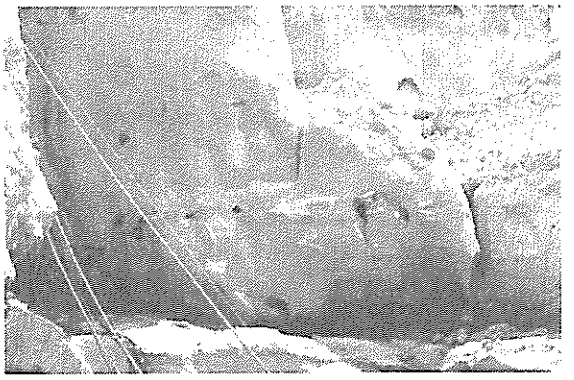

Figure 7 : Log Casts Along Flow Contact Near the Base of the Waihou Ignimbrite

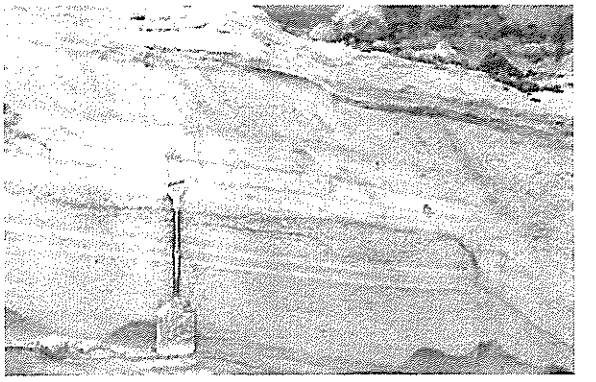

Figure 8 : Compact Graded Tuffs, the Lower-Most Unit Exposed in the Failure Chasm

The tuffs may correlate with a sequence of topography-mantling weathered airfall beds underlying Waihou Ignimbrite in canal exposures east of Lake McLaren and midway along the canal. Although occupying the same stratigraphic position, the characteristics of the deposits are distinctly different.

Grey Ignimbrite

An un-named, massive, grey, sandy ignimbrite of 1 to 5MPa compressive strength was the lowermost unit encountered along the middle sections of the canal excavation. It was also encountered midway down the penstock slope excavation and Cowbourne (1985) correlated it with a grey ignimbrite exposed by the failure flood in Ivy Creek. The rock weathers to reddish brown slightly sensitive clay. The transition from unweathered to completely weathered rock commonly is abrupt.

Waitearikí Ignimbrite

Basement in the Ruahihi area is a strongly welded unit of the Waitearikí Ignimbrite, a Plio-Pleistocene-age dacitic to rhyolitic flow from the Coromandel Volcanic Zone that underlies Whakamarama Plateau (Briggs *et al*, 1996). It is exposed in rapids and waterfalls along the Wairoa

River and was encountered at shallow depth at the canal intake and power station excavations. It was not however, conclusively identified in drillholes and excavations along the canal alignment.

PALEOTOPOGRAPHIC CONTROLS

Paleotopography has been a fundamental factor controlling the distribution and variability of geological units at Ruahihi. Major periods of erosion and weathering followed deposition of each of the principal pyroclastic flow deposits, i.e. Waiteariki Ignimbrite, Grey Ignimbrite, Waihou Ignimbrite and Waimakariri Ignimbrite.

Airfall material is common between each of the flow deposits. Weathering of the ignimbrite and ash materials resulted in the development of clay-rich soils (paleosols) at the top of each ignimbrite unit. The paleosols have an important influence on groundwater movement as they generally act as aquicludes between the more permeable sandy ignimbrite flows. They can concentrate flow in paleovalleys and trap groundwater behind paleoslopes. Measurement of spring flows around the perimeter of the terrace remnant (undertaken prior to significant horticultural development) indicates the total discharge is at least 15% of the maximum possible infiltration recharge. This is unexpectedly high, given the highly dissected nature of the terrace remnant and the presence of a thick, stratified ash soil mantle. Additional groundwater recharge may be occurring from a paleovalley aquifer or from the underlying jointed Waiteariki Ignimbrite.

The paleotopographic controls on groundwater are likely to be responsible for an apparent association with internal erosion and cavity formation. A particularly good example is Wallingford's Grotto on the western side of the terrace remnant, a cave feature more than 2.5m wide and 1.4m high, formed at the base of an ignimbrite unit.

Paleotopography is likely to have been a significant control on the formation of the terrace remnant. The near flat surface of the terrace contrasts with the more elevated and rugged relief immediately to the south. Waimakariri Ignimbrite was the last major event to significantly alter landforms in the area. It mantled, and in places infilled the considerable paleotopography that developed on the underlying Waihou Ignimbrite and older units. The gentle dip of the terrace remnant suggests that the northern fringe of Waimakariri Ignimbrite was contained (ponded), possibly against the adjacent older rocks of the Whakamarama Plateau.

The Wairoa River and its tributaries substantially removed the larger surface, leaving the narrow terrace remnant. Subsurface modelling using drilling and geophysical surveying (Cowbourne, 1985) suggests a ridge of Grey Ignimbrite, and possibly Waiteariki Ignimbrite, underlying the northern end of the terrace remnant has partially protected the terrace remnant from erosion by the Wairoa River.

1981 CANAL FAILURE

Paleotopographic control on the distribution of materials and groundwater flow is considered to have been a significant contributor to failure of the canal at Fill A (Figure 2). The fill was constructed to buttress the eastern canal embankment at a location where the canal was judged to be too close to the steep slopes along the eastern side of the terrace remnant. The fill is mainly cohesive material from the canal excavation.

The committee reporting on the failure (Hatrick et al 1982) concluded that failure was promoted by build-up of pressure under the relatively impermeable fill, destabilising the fill and allowing it to separate from natural ground at the head. The removal of support resulted in settlement of the canal embankment leading to its overtopping and eventual breaching. Erosion of the weak materials underlying the canal by escaping water, in addition to regressive failure of the scarps in the sensitive weathered Waimakiriri Ignimbrite, led to development of the extensive failure chasm.

The critical materials and factors contributing to the failure were:

- The presence of Waihou Ignimbrite underlying the 'seat' of the fill (Figure 9). The ignimbrite thins to the north and south due to the paleotopographic controls of the overlying lithified paleosol and underlying graded tuffs, both resistant, relatively impermeable units.
- The open structure of the loose silty sands of the middle and upper parts of the Waihou Ignimbrite. The sands are susceptible to internal erosion and potential collapse (densification) on wetting.
- The resistant graded tuffs form a 'floor' in the failure washout in the fill area and are close to foundation level of the lower part of the fill. It is likely therefore that part of the fill was founded on, and essentially formed a seal against the tuffs.
- The widespread occurrence of the sensitive, weathered Waimakiriri Ignimbrite, which was a major factor in determining the actual extent of the failure chasm.

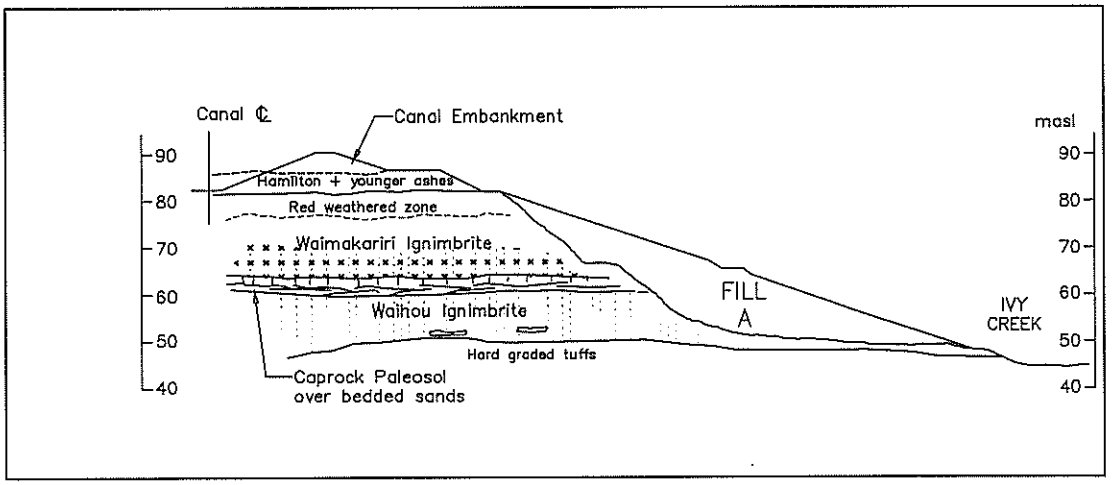

Figure 9 : Geological Section Through 1981 Failure Chasm

Construction of the fill is likely to have prevented free drainage from the Waihou Ignimbrite, allowing groundwater levels to rise in that material, promoting development of cavities and piping erosion. The seal that resulted from placing fill against the graded tuffs prevented relief of pressure at the toe. Pressures eventually created sufficient buoyancy to destabilise the fill, which moved eastward as a coherent mass, removing support to the canal. This model essentially supports the findings of the inquiry committee.

ACKNOWLEDGEMENTS

Trustpower is acknowledged for the use of information collected during the course of construction of the project and subsequent repairs. The second author undertook research at Ruahihi in partial fulfilment of the requirements for an MSc, University of Auckland, 1985.

REFERENCES

Briggs RM, Hall GJ, Harmsworth GR, Hollis AG, Houghton BF, Hughes GR, Morgan MD, Whitbread-Edwards AR, 1996: *Geology of the Tauranga Area, Sheet U14, 1:50,000.* Occasional Report No 22, Department of Earth Sciences, University of Waikato, NZ.

Carryer SJ, 1975: *Geologic Report on the detailed investigations for the Ruahihi Hydroelectric Scheme.* Unpub. Report. 5pp.

Cowbourne AJ, 1985: *Aspects of Engineering Geology and Geophysics, Ruahihi, Tauranga.* Unpublished MS Thesis, University of Auckland.

Fransen PJB, 1982: *Geology of the western Mamaku Plateau and variations in the Mamaku Ignimbrite.* Unpublished, University of Waikato, Hamilton.

Froggatt PC, Lowe DJ, 1990: *A review of late Quaternary silicic and some other tephra formations from New Zealand: their stratigraphy, nomenclature, distribution, volume, and age.* New Zealand Journal of Geology and Geophysics 33:89-109.

Hatrick AV (chairman), 1982: *Report of Committee to Inquire into the Failure of the Ruahihi Canal.* Ministry of Works and Development, Wellington, NZ.

Healy J, 1955: *The Ivy Bridge Section, Lower Kaimai.* NZ Geological Survey unpublished report.

Healy J, 1956: *Geological report on the proposed Lower Kaimai hydro development.* NZ Geological Survey unpublished report.

Lloyd EF, 1965: *Geological report on the proposed Omanawa – Mangapapa – Opuiaki hydro-electric scheme.* NZ Geological Survey unpublished report.

Lowe DJ and Hogg AG, 1995: *Age of the Rotoehu Ash.* Letter to the editor in New Zealand Journal of Geology and Geophysics, 38:399-402

Oborn LE, Northey RD, Beetham, RD & Brown IR, 1982: *Engineering Geological Factors Related to Collapse of Ruahihi Canal.* Submission to Ministry of Works Committee to Inquire into Ruahihi Canal Failure, NZ Geological Survey, DSIR.

Parfitt RL, 1990: *Allophane in New Zealand – A Review.* Aust. J. Soil Res., 28, 343-60.

Parton, I. M. & Olsen, A.J. (1980). "Properties of Bay of Plenty Volcanic Soils.". *Proc. 3rd Australia New Zealand Conference on Geomechanics,* Welllington. Vol.1, pp. 165-169

Prebble WM, 2001: *Geomechanics Lecture 2001, Hazardous Terrain – An Engineering Geological Perspective.* NZ Geomechanics News No 62, NZ Geotechnical Society

Contingency Plan: Auckland Volcanic Field

A L Williams
MSc (Hons), GSL
Senior Engineering Geologist, Beca Carter Hollings & Ferner Ltd
C M Wright
MSc (Hons)
Engineering Geologist, Beca Carter Hollings & Ferner Ltd
A Linzey
MSc (Hons)
Senior Environmental Planner, Beca Carter Hollings & Ferner Ltd
L Chick
MSc (Hons)
Team Leader – Hazards Management, Auckland Regional Council
G McKean
DIP IS
Emergency Management Analyst, Auckland Regional Council

Abstract: The Auckland Metropolitan area is built on a potentially active volcanic field. Geological evidence indicates there is a 5% probability of another eruption occurring from the Auckland Volcanic Field (AVF) within the next 50 years, and that the next eruption is likely to be from a new and currently unknown location. While an eruption from the AVF will result in destruction of a relatively small proportion of the region (less than 80 km^2), indirect impacts on industry, lifeline services, economy and social well-being are likely to have a much wider geographic extent. A well-managed response is essential to ensure that the far-reaching infrastructural, social and economic issues associated with such an event are considered. This paper demonstrates how an understanding of the hazards and risks specific to the AVF has been fundamental to development of the Contingency Plan for the Auckland Volcanic Field.

INTRODUCTION

The Auckland Region, located in the North Island of New Zealand, has a land area of 5,024 km^2. Auckland is home to about a third of New Zealand's population and has the highest population density in the country (Figure 1a). The Auckland Metropolitan area is built on a potentially active volcanic field (Figure 1b). Auckland's Central Business District, and key infrastructure such as ports and international airport are located within the Auckland Volcanic Field (AVF). Geological evidence indicates there is a 5% probability of another eruption occurring from the AVF within the next 50 years, and that the next eruption is likely to be from a new and currently unknown location.

The Volcanic Contingency Plan, VCP (Auckland Regional Council 2002) prepared for the Auckland Region is set in the context of the National Civil Defence Plan, which identifies actions to be undertaken by Government, local authorities and other Civil Defence and Emergency Management (CDEM) agencies in preparation for and response to a volcanic episode. The VCP establishes a co-ordinated CDEM framework to specifically facilitate preparedness, response to and recovery from eruptive activity within the AVF.

The aim of the VCP is to provide for continuity of operations and functions through an eruptive event. This has been achieved by:

- Establishing protocols for the timely and efficient warning of volcanic activity;
- Initiation of immediate communication and public information activities;
- A transparent process of declaration;
- Appropriate deployment of information for the management of a civil defence emergency; and
- Appropriate prioritisation and allocation of regional resources in the event of eruption.

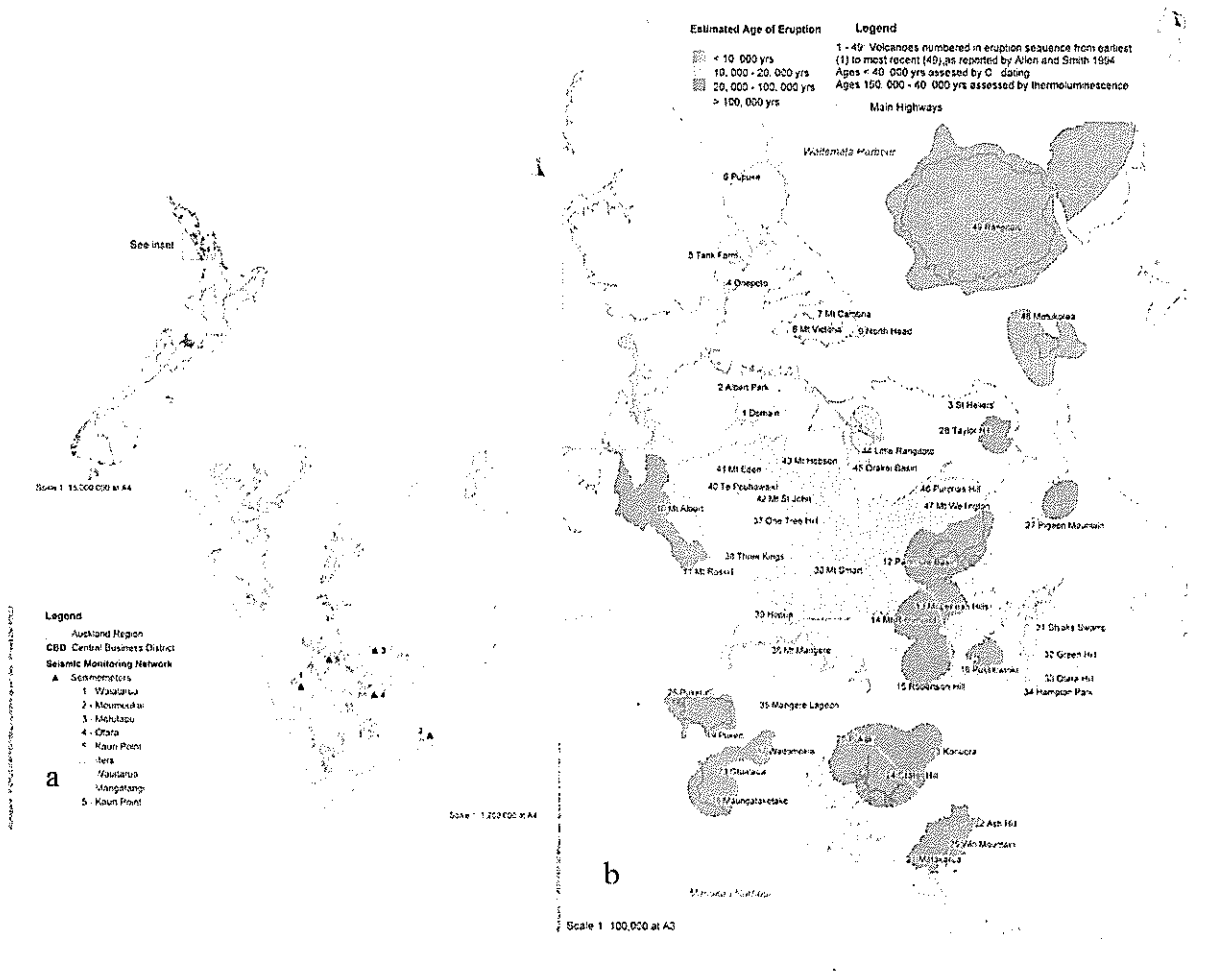

Figure 1: a) The Auckland Region; b) The Auckland Volcanic Field

The success of the VCP is in part dependant on an understanding of the special character of the AVF and the nature of the associated hazard (that is, the geology and engineering geology) and formulation of interim and long-term technical solutions (engineering).

THE AUCKLAND VOLCANIC FIELD

The geologic record indicates that the AVF is a monogenetic volcanic field, in which activity has formed 50 volcanoes within the past 140,000 years over an area of 360 km^2 (Smith and Allen 1993; Smith and Wood 1997) (Figure 1b).

Most of the volcanoes are small cones of less than 150m in height, which developed by eruption over periods of a few months or years. In most cases a single cone resulted from the eruption, but there is evidence that some eruptions have built several adjacent cones. The monogenetic nature of Auckland's volcanoes means that in the event of a future eruption, a new volcano will be formed, rather than an existing volcano re-activated. Therefore, the VCP needs to be sufficiently flexible to be applied to a hazard of unknown location.

Volcanic activity in the AVF is due to a hot spot (hot rock) located about 100km beneath Auckland City (Smith and Allen 1993). Basalt magma has a low viscosity, which allows it to rise relatively quickly through the crust (estimated speeds of 5km/hr). This means that the warning period for impending eruption is likely to be short, perhaps only a few days. The rise of magma is likely to be controlled by the location of faults within the crust. However, because the position of such faults is not known, these indicators cannot be used in predicting the site of a future eruption.

The character of eruptions from the field varies according to the availability of water to the eruption site. Wet (phreato-magmatic) and dry (magmatic) activity often alternate from the same event as the availability of water (groundwater, surface water, seawater) changes. With high water input, activity is dominated by production of a vertical eruption column and the development of base surges. With low water input, activity is dominated by ejection of cooled magma as scoria, tuff and ash, and lava flow. This means that the VCP needs to address a wide range of volcanic hazards and hazard interactions.

The return period between past events has ranged from hundreds to thousands of years. The latest eruption occurred some 600 to 800 years ago. A future eruption may therefore occur at any time in the future. Ages of Auckland's volcanoes determined from carbon dating and thermo-luminescence techniques indicate a trend of increasing size of eruption over the last 20,000 years (Smith and Allen 1993). However, trends in timing and location of eruptions have not been established and it is therefore difficult to predict where and when future activity might occur within the field.

In summary, the following characteristics specific to the AVF need to be addressed in the VCP:

- The site of future eruption cannot be predicted;
- There will be a relatively short pre-eruption period (possibly only a couple of days);
- There may be more than one eruption vent (although it is expected that any vents in a multi-vent episode will be in relatively close proximity);
- Unlike many other natural hazards in New Zealand, volcanic activity will occur over a relatively long time period (a period of months up to a year or more); and
- Volcanic activity will give rise to a number of hazards which will have minor to severe impacts both in terms of damage and geographic extent.

ASSESSMENT OF VOLCANIC HAZARDS AND RISKS

A Volcanic Hazard Matrix was developed to allow a qualitative assessment of the likely nature and impact of hazards associated with an AVF eruption, and to identify those hazards for which mitigative action might be viable. An extract from the Hazard Matrix is presented as Table 1. The matrix combines the findings of hazards and risk studies with the anticipated effects on key lifelines services and structures identified by stakeholders as part of the Auckland Engineering Lifelines Project (AELP). Key inputs include:

- The geological record of Auckland's 50 volcanoes;
- The likely design factors of safety for different structures;
- Volcanic hazard scenarios developed as part of the AELP (Auckland Regional Council 1999);
- Observed performance and recovery of similar structures in other volcanic eruptions (Capelinhos, Azores 1957/58; Surtsey, Iceland 1964; Taal, Philippines 1965; Heimaey, Iceland 1973 and Surtsey and Kalapana, Iceland 1990) (Nairn and Scott 1995; Manville et al 2000).

Risk

A Risk Matrix (Table 2) (where risk = hazard x vulnerability, and vulnerability is a function of the perceived effect on the Auckland community and infrastructure) was developed from the Hazard Matrix. The Risk Matrix identifies the level of risk likely to be associated with each hazard and broadly evaluates those hazards for which mitigative solutions could be considered. For example, crater formation poses a severe risk, but there are no known options for mitigation (other than evacuation with sufficient prior warning). Whereas lava flow and airfall tephra pose high and moderate risks, against which some mitigative options are available for risk reduction. Particular consideration can be given in planning to those hazards that potentially pose a high or severe risk for which some mitigation options are available. These matrices together provide the understanding of the hazards and risks necessary to allow responsibilities and contingency planning to be allocated and implemented.

Hazard[1]	Area Affected	Infrastructure Damage	Damage to Life	Warning	Recovery[2]	Mitigation
Airfall Tephra and Eruption Column	Ash plume may rise 6 – 15km resulting in the deposition of up to 1 million m^3 of tephra spread up to 100km from the vent (although at 100km, there will be no risk to infrastructure other than air traffic). Ash distribution will depend on eruption size, prevailing winds (direction and strength) and particle weight. As westerly winds predominate in Auckland, tephra is most likely to be deposited thickest to the north-east and east of a vent. Tephra thickness is likely to range from a few mm to 600mm.	■ **Domestic and Commercial Structures** Abrasion; enters buildings through broken windows etc; tephra loading may lead to collapse of roofs, walls or columns ■ **Communications** Emergency generation and air conditioning plants vulnerable to abrasive dust and over-heating resulting in service interruption; potential for damage to CBD fibre optic ring and isolation due to power failure; land lines more vulnerable than cellular system; congestion of services ■ **Transport** Temporary road closure, impaired visibility, vehicle damage; blockage of drains resulting in flooding; engine damage resulting in disruption of port activity; closure of air-space, airports. ■ **Energy** Electricity supply restriction and outages due to insulator flash-overs at transmission and distribution systems; minor affect on petroleum or gas pipeline valve controls and petroleum SCADA systems; heavy ash fall may sink floating roofs on petrol tanks causing spills and creating hazardous vapour cloud with risk of explosion ■ **Water Supply** Suspension of ash in water supply reservoirs and leaching of contaminants (eg F), lowering of pH, disruption of treatment process; interference with electrical equipment, filter stations overloaded; damage to pumps ■ **Wastewater and Stormwater** Pipe blockage and local flooding, damage to pumps and plant equipment, interference with treatment process; operational, maintenance and odour problems, overload bypassed to land or harbour with consequences for sanitation	Hinder visibility resulting in accidents. Inhalation of gas and particles causing respiratory problems. Burial of crops and damage to fruit.	An eruption column will be generated following commencement of the eruption. Tephra will be produced within hours over the wider area. Prediction of wind directions critical to defining likely hazard zones. Earthquakes a few hours and up to a few days prior to eruption due to upwelling may provide an indication of the area likely to be affected by these hazards at that time. (Established at SAL 5, Table 3).	■ **Domestic and Commercial structures** Dependent on availability of water supply and access ■ **Communications** May be hindered by ability to access sites and high temperatures. Full recovery within 2 to 7 days ■ **Transport** Regular removal of ash from roads, rail, port and airport; increased maintenance of aircraft to exclude ash from engines and machinery. Full capacity within 1 week of cessation of ash fall ■ **Energy** Temporary repairs and alternative supplies in place within 1 week ■ **Water Supply** Turbidity and acidity of water returns to normal levels within a few hours to days of cessation of ash fall. Essential water supply recovered within 1 week; non-essential supply provided by tanker ■ **Wastewater** Full recovery within 1 week of cessation of ash fall A contingency plan for disposal of ash must be prepared to avoid restricting recovery.	Clean-up and removal. Develop and maintain hospital equipment and products required to treat severe burns. ■ **Commercial structures** Prioritise key structures (eg hospitals) and check for likely ash loading; upgrade to withstand as necessary ■ **Communications** Fit temporary pre-filters to internal/ external air-conditioning units within exchange centres; Seal off exchange centres during the event to minimise ash effects ■ **Transport** Remove from roads and stockpile during eruption; Minimise driving movements; Install extra air filters in vehicles operating within ash fall-out zones ■ **Energy** Encapsulate gas gate stations and shut down gas supply prior to eruption ■ **Water Supply** Prevent ash ingress to water pumping stations, cover filters; Monitor water quality ■ **Wastewater** Bypass and/or shut down vulnerable parts of the plant during ash fall

[1] A description of each hazard is given in Appendix 1
[2] Following cessation of volcanic activity

Table 1. Extract from Hazard Matrix for the Auckland Volcanic Field

Hazard	Area Affected[2]	Immediate Risk	Ongoing Risk	Anticipated Loss	Mitigation	Recovery Period
Earthquake	3 – 5	Low	Nil	Small	Not applicable	Not applicable
Crater, Cone or Ring Formation	0.3 – 1.5	Extreme	Low	Extreme	None	Several months to years
Fire Fountaining[1]	0.2 – 0.5	High	Low	Extreme	Minor	1 week to months
Lava[1]	3 – 5	High	Low	High	Moderate	Weeks to months
Base Surge	3 – 5	High	Low	Extreme	None	1 week to months
Shock Waves	3 – 5	High	Low	High	None	1 week to months
Lava bombs[1]	0.4 – 0.5	Moderate	Low	Moderate	Minor	1 week to months
Airfall Tephra	3 – 100	Low	Moderate	Low	Moderate	1 week to months
Gas	3 – 5	High	Moderate	Moderate	Minor to Moderate	Not applicable
Lightning	3 – 100	Low	Low	Low	None	Up to 1 - 2 days
Tsunami	1	Low	Nil	Low	Moderate	Up to 1 - 2 days

1 Events which are likely to be repeated over a period of time (weeks to months) following the initial event
2 Radial distance from vent, km

Table 2. Volcanic Risk Matrix

WARNING

Physical Warnings

The next AVF eruption will occur when magma presently forming beneath Auckland rises to the surface. As the magma rises through the crust, it will generate small tremors which can be detected using seismometers and later, earthquakes which can be felt. Volcanic eruption is expected to occur after a period of earthquakes lasting a few days to a few weeks. Results of seismometer monitoring to date indicate a very low level of background seismicity, which improves the likelihood of detection of an impending eruption and eventual location of its vent.

Auckland Volcano-Seismic Monitoring Network

The AVSN comprises five sites at which seismic activity is monitored continuously (Figure 1a). The AVSN is designed to monitor seismic activity associated with the onset of volcanic activity, but also detects non-volcanic earthquakes. By recognising a change in the prevailing seismic pattern that might signify magma movement within the volcanic field, some warning of impending volcanic eruption can be given.

Under the National Contingency Plan – Volcanic Eruption, the Institute of Geological and Nuclear Sciences (GNS) are responsible for the interpretation of the data and preparation of Surveillance Reports and Scientific Alert Bulletins containing the allocation of appropriate Scientific Alert Levels (SALs).

Scientific Alert Levels

SALs define the status of the volcanic field at any time. The SALs applied to Auckland's Volcanic Field are those developed for "reawakening" volcanoes, and are also applied to a number of other volcanic centres such as Ruapehu.

Because the basaltic volcanic activity in the AVF is likely to develop over a relatively short time, and Auckland is an area of high population and infrastructure density, warning periods appropriate to the AVF have been assessed for each SAL and warning phases assigned, to assist in contingency planning (Table 3). The periods indicated in Table 3 do not reflect either the minimum or maximum duration of each level, but provide an indication of a realistic lower bound time period between warning levels. These periods are an indication of the mobilisation or resourcing time that can be anticipated. The durations suggest that early changes in seismicity (SAL 0 to 1) provide the most valuable warning of impending eruption because such changes occur over a time period in which mitigation can be reasonably implemented. This is also the period where emergency managers have an opportunity to prepare for response to a volcanic eruption. Once volcanic activity progresses beyond SAL 1, hazardous effects could be experienced within hours, and full-scale eruption within as little as a day.

SAL[1]	Indicative Phenomena	Volcano Status	Period[2]
0	Typical background surface activity; deformation, seismicity, and heat flow at low levels.	Usual dormant or quiescent state. **Advisory Phase**	Not applicable
1	Apparent seismic, geodetic, thermal or other unrest indicators.	Initial signs of possible volcanic unrest. No significant eruption threat. **Alert/ Warning Phase I or II**	A few days and up to a few weeks
2	Increase in number or intensity of unrest indicators (seismicity, deformation, heat flow etc).	Confirmation of volcano unrest. Eruption threat. **Warning Phase II**	Up to 1 to 3 days
3	Minor steam eruptions. Relatively high and increasing trends shown by unrest indicators. Significant effects in eruption area and beyond.	Commencement of minor eruptions. Real possibility of hazardous eruptions. **Warning Phase III**	A few hours to 1 day
4	Eruption of new magma. Sustained high levels of unrest indicators, significant effects beyond volcano.	Hazardous local eruption in progress. Large-scale eruption now appears imminent. **Warning Phase IV**	Up to a few hours
5	Hazardous volcanic eruption in progress. Destruction within HZO Zone 1, major damage beyond active volcano. Significant risk over wider areas.	Large hazardous volcanic eruption in progress. **Warning Phase IV**	Not applicable

[1] Scientific Alert Level

[2] Warning periods assessed for the Auckland Volcanic Field. Periods have been assigned to Scientific Alert Levels (SALs) as a tool for planning purposes only. The SAL may rise to 1 and then return to 0 and is not intended to be a predictive tool.

Table 3. Scientific Alert Levels

The warning system proposed for the AVF therefore utilises the established SALs, but because of the likely rapid progression through the levels beyond SAL 1, sets the SALs in the context of warning phases (Table 3) as follows (see also Figure 3):

- Advisory Phase: The status quo (AVSN monitored by GNS and reported to ARC).
- Alert Phase: Activated with an SAL 1 announcement. Possible volcano-seismic activity has been detected.
- Warning Phase I: Commences within SAL 1 once a general vent area is identified.
- Warning Phase II to IV: Generally coincident with the SAL stages, but in areas of high population density or significant infrastructure risk, Warning Phase II may be issued during SAL 1.

Hazard Zone Overlay

One of the key requirements for civil defence emergency management is to understand the risks associated with an event, and the areas most likely to be at risk. As the future site/s of volcanic eruption in Auckland cannot be predicted, predicting the hazards and risks associated with volcanic eruption in the AVF is more difficult. That is, hazards from volcanic eruption will depend on whether the eruption occurs on land or below water and the risks will depend on the location of the eruption in the AVF.

Eruption scenarios have been effectively used in Civil Defence planning and the Auckland Engineering Lifelines Project (AELP) to identify the hazards and risks that are likely to be associated with future eruption within the AVF, and to model the potential effects of these on Auckland's key infrastructure (Auckland Regional Council 1999). As part of this work, generalised hazard zones were modelled (see "Area Affected", Table 1) based on the geological record for the existing AVF volcanoes. These hazard zones provide a visual perception of the potential distribution of hazards associated with eruption. The scenario examined as part of the AELP was selected because it impacts both land and water and therefore displays the range of eruption styles seen in Auckland volcanoes, and because it is centred within the central business district, the area of highest daytime population and commercial density within Auckland.

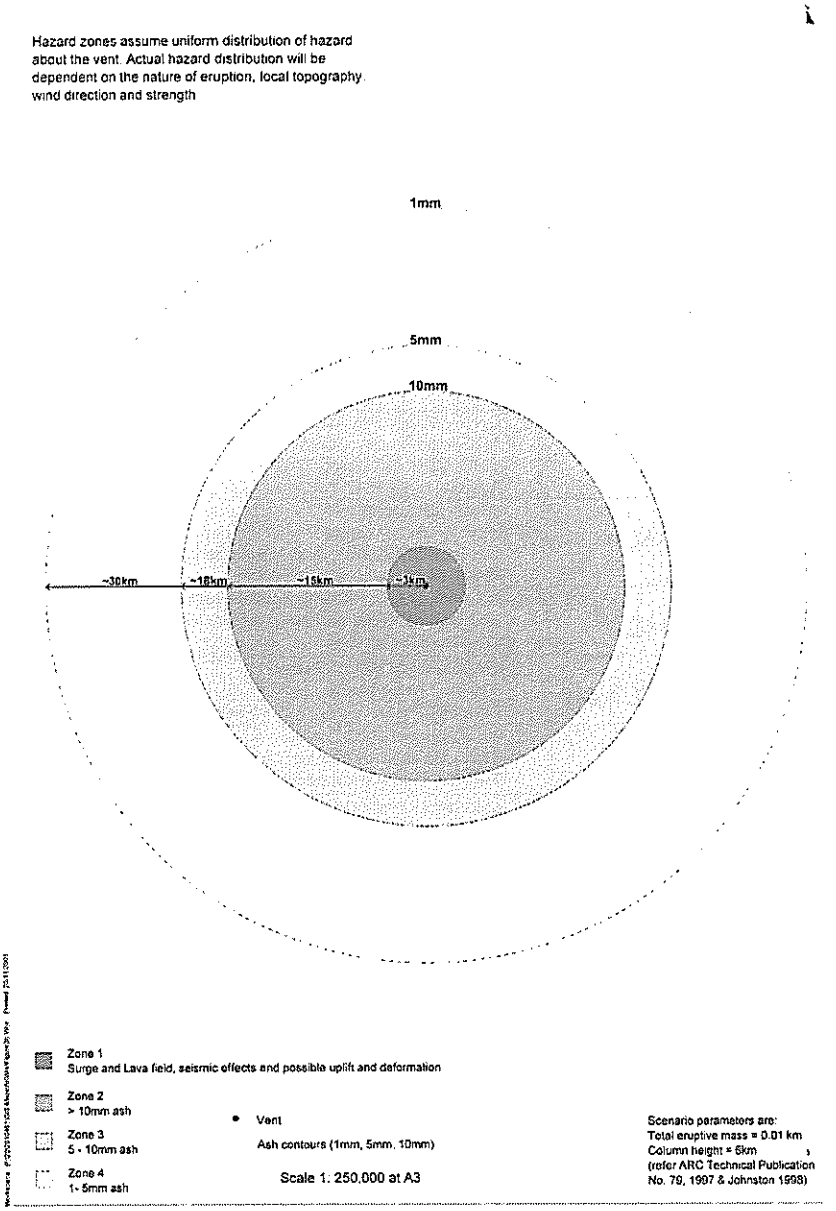

Figure 2. Hazard Zone Overlay

For contingency planning, the hazard zones identified for the scenario eruption have been adopted, but have been modified to show a uniform distribution of hazard about the vent, (ie no prevailing wind direction has been inferred, and no lava flow route identified) (Figure 2). The actual hazard distribution will be dependent on factors such as the nature of the eruption, local topography, wind direction and strength. Key hazard controls are described in Table 4.

Volcano Parameter	Hazard Variable
Rate of magma rise and availability of water	Type of eruptive activity
Volume of magma	Magnitude of hazard zones
Topography	Extent and shape of hazard zones
Wind direction and wind speed	

Table 4. Hazard Controls

As the centre of a future eruption is not clear, a uniform hazard approach allows the hazard distribution to be used as a template for superposition over any other potential vent location once the likely eruption area or site has been identified. This template or Hazard Zone Overlay (HZO) forms a very broad first estimate of the potential area that might be affected by volcanic hazard, and allows response planning to be immediately focussed on the areas most likely to be affected by high risk impacts.

Recognising that the HZO is a tool for *initial* assessment of the likely area at risk from volcanic eruption following detection of a change in seismicity by the AVSN, it has been recommended that a volcanic Scientific Advisory Group (SAG) be established which would be mobilised following detection of atypical seismicity. The SAG will assess and map areas of hazard impact as eruption progresses and provide advice to the lead Civil Defence Emergency Management agencies.

At SAL 1, a Technical Advisory Group (TAG) would be convened to provide advice to stakeholders on mitigation or response options. The TAG will include those able to provide recommendations for temporary engineering works such as works to mitigate lava flow, bypass or repair works and on structural recovery of buildings. The warning system developed for the AVF is presented in Figure 3.

Advisory Phase	**SAL 0**	GNS – Monitoring AVSN ARC and Ministry CDEM – Receive Reports EMO, CEG, SAG and TAG established and meet Review, monitor and amend VCP as appropriate	→ EMO, SAG and TAG established
Alert Phase	**SAL 1**	Inform key organisations (within region) HZO to identify general area potentially affected Convene EMO, TAG and Nominate Lead Agency Public Information Commences	→ CEG, SAG and TAG convened
Warning Phase I	**SAL 1**	Area of volcanic activity/possible vent identified CDEMG identified as Lead Agency (consider alternative) Consider Declaration	
Warning Phase II	**SAL 1 & 2**	Evacuation of HZO 1 Area Review Lead Agency Consider Declaration... (as above)	
Warning Phase III	**SAL 3**	Evacuation of HZO 1 Area SAG mobilised to monitor hazard and hazard effects TAG mobilised to respond to hazards (resource mobilisation)	
Warning Phase IV	**SAL 4 & 5**	Emergency responses to eruption SAG continues monitoring hazard and hazard effects TAG continues to respond to hazards (resource mobilisation)	

Figure 3. AVF Warning Systems

CONCLUSIONS

Auckland city is located within a potentially active volcanic field. The next eruption will be from a new, presently unknown location at some unknown time in the future. Development of a contingency plan for eruption from an unknown centre has been possible through a pragmatic consideration of the geological history and engineering geological issues (hazards and risks) associated with the AVF.

In summary:

- The Auckland Volcano-Seismic Network (AVSN) monitors volcanic earthquakes in the region and could warn us of volcanic activity some days or perhaps weeks before an eruption.
- Changes in the status of Auckland's volcanic field will be identified by Geological & Nuclear Sciences (GNS).
- Once atypical seismicity is indicated, the Hazard Zone Overlay (HZO) will be used as a preliminary tool to rapidly assess the areas potentially at risk.
- Disruption to most lifeline utilities is anticipated, but will depend on the vent location. Direct effects could require evacuation of up to 200,000 people. More people may need to be evacuated if lifeline services are disrupted for any length of time.
- Scientific and Technical Advisory Groups (SAG and TAG) will be mobilised to monitor changes in the volcanic field and advise of technical solutions to mitigate hazards as these arise.
- The VCP outlines the roles and responsibilities of local authorities, GNS, the ministry of CDEM and other key organisations, SOE's and Utility providers. It outlines how command and control will work in eruption response, resource requirements, the process of issuing warnings and declaring a civil defence emergency, evacuation processes and welfare considerations.
- Testing and maintaining the Plan will be key to its success.

REFERENCES

Auckland Regional Council (1999). "Auckland Engineering Lifelines Project, Final Report – Stage 1." Auckland Regional Council Technical Publication No. 112.

Auckland Regional Council (2002). "Contingency Plan for the Auckland Volcanic Field." Auckland Regional Council Technical Publication No.165.

Environment Bay of Plenty, Bay of Plenty Regional Council (1993). "Volcanic impacts report – the impacts of two eruption scenarios from the Okataina Volcanic Centre on the population and infrastructure of the Bay of Plenty, New Zealand. Resource Planning Publication 93/6.

Environment Bay of Plenty, Bay of Plenty Regional Council (1997). "Volcanic contingency plan – Okataina Volcanic Centre, Mount Edgecumbe volcano." Resource Planning Publication 97/4.

Johnston, D. (1997). "The impact of recent falls of volcanic ash on public utilities in two communities in the United States of America." Institute of Geological and Nuclear Sciences, Science Report 97/5. Lower Hutt, 21pp.

Johnston, D. (1997). "The impact of recent falls of volcanic ash on public utilities in two communities in the United States of America." Institute of Geological and Nuclear Sciences, Science Report 97/5, Lower Hutt, 21pp.

Latter, J. (1993). "Volcanic hazards in the Waikato Region." Institute of Geological and Nuclear Sciences, Client Report 93/15.

Latter, J. (1989). "Estimated quantitative volcanic risk: A comparison between Auckland and New Plymouth." DSIR Contract Report No.123, Wellington.

Manville, V., Johnstone, D., Stammers, S., Scott, B., (2000). "Comparative preparedness in New Zealand and the Philippines for response to, and recovery from, volcanic eruptions: case studies from the 1991 Pinatubo eruption and the 1995-6 eruptions of Ruapehu." Bulletin of the New Zealand Society for Earthquake Engineering, Vol. 33, No. 4, pp. 445-476.

Nairn, I. and Scott, B. (1995). "Scientific management of the 1994 Rabaul eruption: lessons for New Zealand." Institute of Geological and Nuclear Sciences, Science Report 95/26, 46pp.

Neild, J. et al. (1998). "Impact of a volcanic eruption on agriculture and forestry in New Zealand." MAF Policy Technical Paper 99/2.

Smith, I. and Allen, S. (1993). "Volcanic hazards at the Auckland Volcanic Field." Ministry of Civil Defence, Volcanic Hazards Information Series No. 5.

Smith, I. and Wood, I. (1997). "Multi-vent eruptions in the Auckland Volcanic Field: evidence, consequences, response. Auckland UniServices Limited.

Taranaki Regional Council (2000). "Taranaki regional volcanic contingency plan."

APPENDIX 1 – Description of Volcanic Hazards

Hazard	Description
Volcanic Earthquake[1]	Ground shaking caused by movement of magma through the crust both before and during eruptions.
Crater, Cone or Ring Formation	Maars, tuff rings and tuff cones may be produced during an eruption. **Maars**: vertical-walled craters cut into pre-eruption country rock and surrounded by low rims. **Tuff rings**: constructional craters lying mostly on or above pre-eruption surface. **Tuff cones**: smaller cones with higher rims.
Fire Fountaining[2]	Eruption of hot magma which may rise hundreds of metres above an active vent. Lumps of cooled magma are deposited as ash, lapilli and bombs. Restricted to a vent or series of vents along a fissure. Preserved at 77% of AVF volcanoes.
Lava[2]	Streams of magma which flow by gravity into and along topographic lows; hot (1000°C or more); associated with 61% of AVF volcanoes. Generated by dry eruptions. May comprise: ▪ continuous and voluminous discharge of highly fluidised lava, often with gas-driven fire fountaining of scoria to hundreds of metres above the vent; or ▪ lava flows produced directly from primary or secondary vents; possibly associated with partial cone collapse or breaching.
Base surge	Ground-hugging turbulent mixtures of steam and solid ejecta that flow out laterally from the base of the eruption column in phreato-magmatic eruptions. Surges range from wet to dry and cool to hot. May develop rapidly as lateral blasts without an associated eruption column. Multiple explosions at short time intervals. Associated with 73% of AVF volcanoes.
Shock Waves	Sound and pressure waves associated with energetic eruptions.
Lava Bombs[2]	Blocks and bombs (cobble to boulder sized material >60mm) follow ballistic trajectories from the vent and are released from the eruption column at 100 – 500m height. Includes both cooler country rock and hot lava.
Airfall Tephra and Eruption Column	**Eruption Column:** Explosive reactions generate an eruption column of pyroclastic material rising several kilometres into the air. In phreatomagmatic eruptions, steam condensation in the eruption plume produces ash rainout. **Airfall tephra:** Includes all volcanic products aerially ejected from the vent (ash <2mm, lapilli 2 - 64mm and bombs >64mm, derived from fire fountaining, ballistic projectiles and fall-out from the eruption column).
Gas	CO, CO_2 and HF may escape from vents. CO_2 generated by burning vegetation may become concentrated in low-lying areas. Boiling of seawater due to flowing lava creates dense white clouds of HCl aerosols (laze) carried downwind at low elevation. Discharge of SO_2 gas adjacent to lava flows. SO_2 and laze generate acid rain. Steam hazard.
Lightning	Pulses within the eruption column generated as a result of electrically charged ash in a convecting eruption column.
Tsunami	Long-period waves generated by updoming of the seafloor or coastal area, fall-out of the lava column into a body of water, base surges and accompanying shock waves, pyroclastic flows impacting on water and submarine explosions.

[1] Earthquakes may also be generated by fault movement. Such earthquakes are tectonic earthquakes, not caused by volcanic processes.
[2] Hazards which are likely to be repeated over a period of time (weeks or months) following the initial event

Geotechnical Engineering of the Northland Allochthon

G E Winkler
MSc (Hons) Engineering Geology
Senior Engineering Geologist, Tonkin & Taylor Ltd

Abstract: The Northland Allochthon, previously known as "Onerahi Chaos Breccia", is well known in the geotechnical engineering circles for its susceptibility to slope instability, soil creep, and its problematic effects on houses, roads, and other engineering structures. This paper summarises some of the key geological and geomorphological characteristics of slopes formed within the parts of the Northland Allochthon that are most susceptible to slope instability, including the close correlation between geomorphology, lithology, and rock mass strength. Slope movement styles and mechanisms are described, as are stabilisation methods and some of the difficulties experienced in doing so. Cut slope engineering is also summarised, as are other geotechnical aspects, such as foundation depths to avoid shrink-swell effects, and effluent disposal techniques and problems. Appropriate investigation methods are also described.

INTRODUCTION

Northland is fast becoming a sought after place to live. But residential, industrial and commercial development, roading and other infrastructure within the area are commonly plagued by the widespread presence of the Northland Allochthon (see Figure 1) and all its inherent difficulties, mainly relating to slope instability. It is a particularly troublesome group of materials in terms of geotechnical and civil engineering, resulting in a significant added cost to the Northland economies.

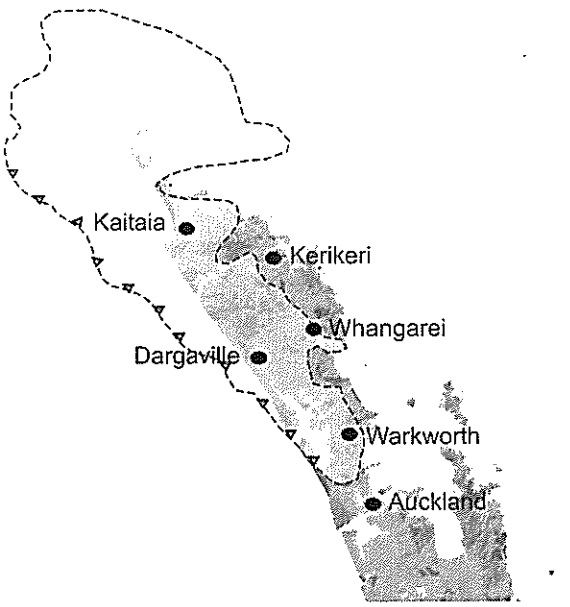

Figure 1. Location of the Northland Allochthon (After Issac, 1996)

The objective of this paper is to present a summary of key geotechnical aspects of the problematic sedimentary rocks within the Northland Allochthon that has been gained from numerous projects within the Northland area, previous work, and study carried out on the allochthonous sedimentary rocks within the North Island, New Zealand. More specifically the following general aspects are described;

- Geology of the allochthon, including its formation, distribution, general rock and soil mass properties, and material properties

- Typical geomorphology, and distinguishing features of various lithologies within the Northland Allochthon
- Suitable methods for investigation
- Typical problems
- Engineering solutions, and their effectiveness

This paper is intended to provide a general summary of information for engineering geologists and geotechnical engineers to assist them in dealing with investigations within the Northland Allochthon. The key theme of this paper is the use of geomorphology of the site and the surrounding area as the main provider of geological and geotechnical information for the particular project.

GEOLOGY

Background

For many years the Northland Allochthon was known as the Onerahi Chaos or Onerahi Chaos Breccia, with the "chaos" and "chaos-breccia" being a fitting description for many zones within the allochthon. However, many parts of the allochthon are not chaotic (although can still be highly shattered, sheared and crushed), and it also includes very large blocks of volcanics. To be technically correct and more applicable to the recent understanding of the geology of the Northland area, the Onerahi Chaos and Onerahi Chaos Breccia were therefore abandoned by geologists and replaced with "Northland Allochthon". Despite this name change, the term Onerahi Chaos is still in widespread use by engineers and the general public at large. Onerahi Chaos is therefore still considered to be appropriate for geotechnical engineering purposes.

The Northland Allochthon comprises a complex of Late Cretaceous (90Ma) to earliest Miocene (25Ma) predominantly sedimentary rocks, with some submarine basaltic volcanics that accumulated offshore to the northeast of Northland (Isaac et al, 1994). The submarine basaltic volcanoes (known as the "Tangihua Complex") developed more than 150km off the Northland coast forming a submarine high. During this period, sediments accumulated within the intervening basin, with sands deposited on the continental shelf adjacent to the eroding Northland landmass, and muds forming further out to sea in deep water. These rocks ranged from non-calcareous to calcareous and siliceous sediments. Later, during the Oligocene period the seas became very calcareous, and these sediments were buried by limestones, calcareous sandstones and mudstones.

During the earliest Miocene times (about 25million years ago) the Pacific Plate began to subduct in a SSW direction beneath the Northland continental crust that comprised mostly Waipapa Group greywackes (Rait, 2000). The sediments that had accumulated in the submarine basin were then shunted and thrusted SSW up and over the submerged continental crust assisted by the high of submarine volcanoes attached to the Pacific Plate further out to sea (Figure 2). Eventually parts of the high of submarine volcanoes were torn off the plate and thrust up and over the submerged continental crust. The emplacement of the Northland Allochthon is understood to have taken about 3 million years (Issac et al., 1994).

Since then the Northland continental crust has been uplifted and tilted to the west as the subduction zone shifted further to the east towards its current position along the East Coast of the North Island. Uplift subsequently resulted in the deep erosion and removal of much of the allochthon. The heights of the ranges formed of the submarine basaltic volcanics, such as the Tangihua Range (627m), Maungataniwha Range (744m), and the Waima Range (781m), give some indication of the original thickness of the Northland Allochthon.

The Northland Allochthon can be subdivided into three main "complexes", generally based on their age of original deposition (Issac et al, 1994). These are;

1. Tangihua Complex (i.e. submarine basaltic volcanics, about 90Ma to 65Ma)

2. Mangakahia Complex (i.e. variably calcareous and siliceous mudstones and sandstones that were initially deposited during Paleocene to Eocene times, about 65Ma to 38Ma)
3. Motatau Complex (i.e. predominantly calcareous limestones, mudstones and sandstones that were deposited later during the Oligocene period, about 25Ma to 38Ma)

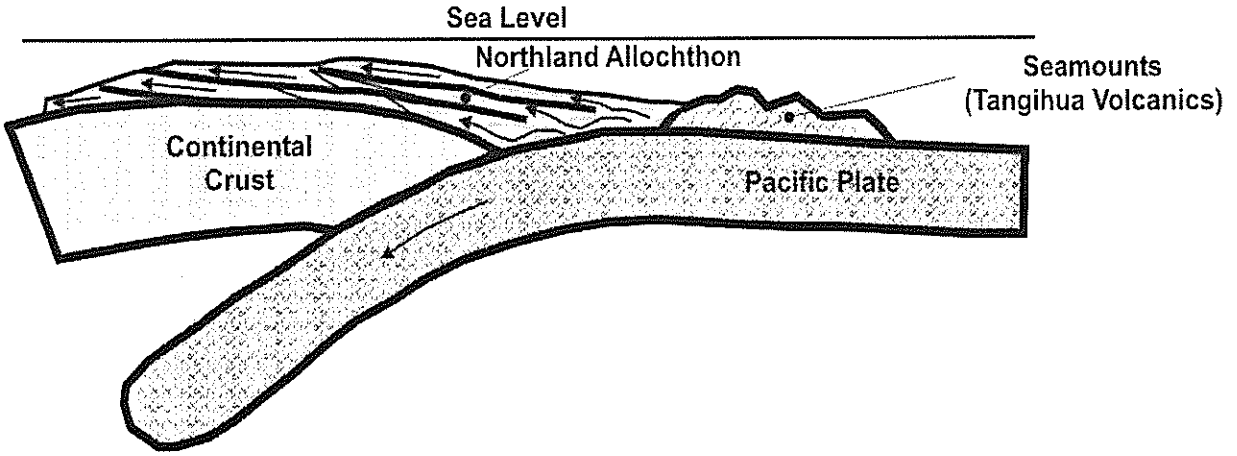

Figure 2. Schematic Diagram of the Model for the Emplacement of the Northland Allochthon

Most of the Mangakahia Complex is what many geotechnical engineers refer to as being "Onerahi Chaos", and is the most disrupted and problematic group of materials within the Northland Allochthon. These multicoloured rocks underlie the bulk of the countryside that typifies the Northland Allochthon ; this being long, low angle (~7° to 15°) hummocky slopes.

The calcareous Motatau Complex includes the Mahurangi Limestone, which is an economically important rock within the Northland area. While there are some geotechnical problems also associated with these rocks, and also within the more competent Tangihua Complex rocks, they are not described further here.

Individual formations have been recognised within the Northland Allochthon, and the key formations within the Mangakahia Complex are the Hukerenui Mudstone (non-calcareous grey, green, red, or dark brown, clay rich, typically highly to pervasively sheared mudstone), and the Whangai Formation (dark grey siliceous mudstone and dark grey to bluish grey calcareous mudstone). Geological details of these formations and the complexes that form the Northland Allochthon can be found in the IGNS monograph "Cretaceous and Cenozoic Sedimentary Basins of Northland, New Zealand (Issac et al., 1994). Published IGNS Q-Maps (1:250000) for the Kaitaia area and the Auckland area also provide good descriptions of the main individual formations that make up the Northland Allochthon.

Rock Mass Characteristics

Due to their low shear strength, most of the displacement of the Northland Allochthon took place within the weak soft non-calcareous mudstones (e.g. Hukerenui Mudstone). These materials have suffered the most deformation and are typically highly to pervasively sheared throughout. They form major "melange zones" (mixed zones) within the allochthon and typically are the major thrust faults between the allochthonous sheets. The pervasive shearing has essentially reduced the overall shear strength of the mudrock to that of a hard soil. Commonly incorporated within the melange are elongate fragments or blocks of more competent lithologies (usually more calcareous sandstones and mudstones). These blocks can be relatively large (i.e. 10 to 20m or even greater). The sheared fabric is usually at a relatively low angle, due to the low angle emplacement of the thrust sheets. Subsequently broad areas are underlain by these zones and they are widely distributed throughout Northland. The more calcareous and siliceous lithologies (such as the Whangai Formation) are also generally highly

shattered sheared and crushed, although to a lesser degree. Some of the shattered nature of these rocks is also related to the fissility of the mudrocks.

The degree of shearing and disturbance generally shows a relatively close correlation to the intact strength of the rock. As a general rule of thumb, the more calcareous, siliceous or sandy the rock is (i.e. the greater intact rock strength) the lesser the degree of shearing. Low angle persistent sheared defects (minor thrust faults) are common, with contorted, chaotic and rotated rock material between the sheared defects.

Soil Mass Characteristics

The soils that develop above the Northland Allochthon are generally relatively thin, with the thickness generally controlled by the permeability of the underlying parent rock. As a general rule the more calcareous and siliceous the parent rock mass, the greater the rock mass permeability and the thicker the depth of the weathered soil mantle. The pervasively sheared non-calcareous mudstones and melange zones within the allochthon (e.g. Hukerenui Mudstone) are the least permeable, and in many cases practically impermeable. Consequently the soil mantle that develops over these materials is the thinnest, generally ranging between 1.5m and 2m thick. The soils tend to grade sharply down into the underlying less weathered parent rock, with a broken zone and a sheared contact with the underlying parent rock. The soil is almost always nearly saturated. The soil mantle overlying the more siliceous and calcareous allochthonous rocks (e.g. Whangai Formation) tends to be deeper (up to 6 to 8m), and commonly with a deeper zone of oxidation due to their greater permeability of the parent rock mass.

In general, the soil mantle that develops over the Mangakahia Complex lithologies tends to comprise an upper and a lower zone. The upper zone commonly comprises light coloured stiff to very stiff plastic silty clay. These clays are typically of low permeability, and so water tends to perch above the clays within the topsoil layer. These are typically wet to saturated for much of the year, and support reeds that would normally grow in flat swampy areas or around springs.

The lower zone generally tends to comprise silty clays and clayey silts, with gravel sized fragments of the more competent materials derived from the underlying parent rock. The soils also tend to generally retain the sheared and chaotic fabric of the underlying parent rock. This zone is generally of relatively higher permeability than the upper zone, and also the underlying parent rock in the case of the melange zones and non-calcareous rocks within the allochthon.

MATERIAL PROPERTIES

Results from a number of ring shear tests, direct shear tests parallel to shearing and back-analyses of failed slopes show that the residual friction angle along sheared surfaces and within the sheared fabric of the highly to pervasively sheared mudstones is typically very low. In general the non-calcareous Hukerenui Mudstones of the Mangakahia complex (i.e. typical Onerahi Chaos) have the lowest residual friction angles of between 10° and 13°, and as low as 8°. Friction angles within sheared zones within the more calcareous and siliceous rocks are higher, generally increasing up to 20°. This is due to the increased proportion of sand sized particles and other fragments within the sheared zones within these stronger rock masses. In these stronger rock masses the shear strength parameters perpendicular to the sheared fabric of the rock mass are much higher. This results in an anisotropic rock mass containing pseudo bedding plane defects (i.e. shears) as would exist in an interbedded sedimentary strata.

The soil mantle that develops over the Mangakahia Complex lithologies are generally subject to high shrink swell behaviour. This is due to the generally high percentage of smectite group clays within the parent rocks, particularly the mudstones. Linear shrinkage is commonly in excess of 15%. Liquid limits can vary widely, although are generally high. It is not uncommon to obtain laboratory test results showing liquid limits in excess of 80%.

The high proportion of swelling clays within the parent rocks results in the softer mudstones and sandstones readily slaking on wetting and drying. However, the calcareous and siliceous formations within the allochthon are cemented enough to limit the degree of slaking of these rocks.

GEOMORPHOLOGY

The geomorphology of slopes underlain by the Mangakahia Complex of the Northland Allochthon is very distinctive and easily identified in the field and in aerial photographs. The "classic" geomorphology is of long and gentle to moderately grading broad hummocky slopes, with hummocks generally extending all the way from the toe of the slope to the crest of the ridge, and side spurs (Figure 3). The hummocks are typically broad generally ranging between 5m and 20m wide. They also tend to be oval and aligned parallel to the surface contours. Hummocks on steeper slopes above stronger rock masses tend to have greater relief.

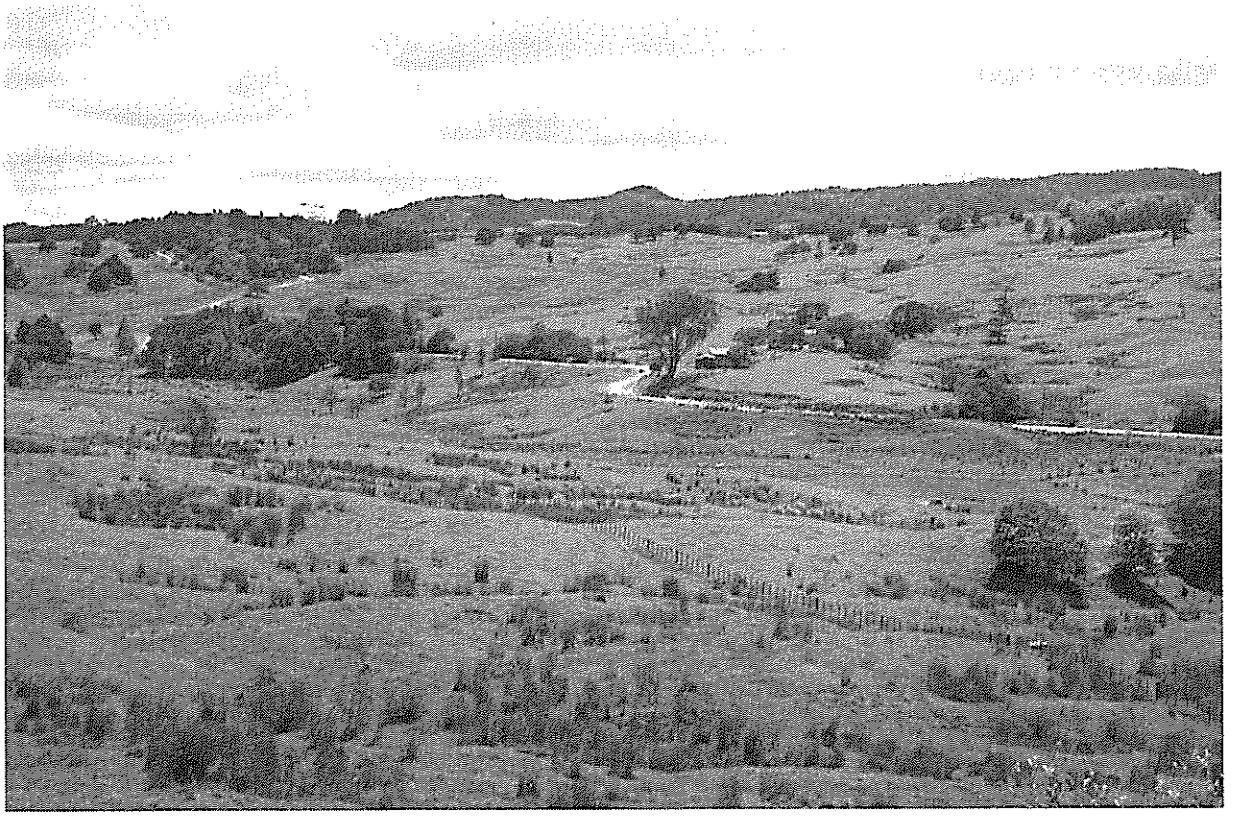

Figure 3. Typical Geomorphology of Slopes Formed Above Northland Allochthon Mangakahia Complex Rocks. Note Long, Broad, Hummocked Slopes, Reeds, and Absent Dendritic Drainage Pattern.

Steep sided incised gullies and their associated dendritic drainage patterns that commonly form above most other non-allochthonous lithologies such as greywacke are almost non-existent in the slopes underlain by the Mangakahia Complex lithologies. Slip scars are also not very common, apart from the steepest of slopes. Sharp and distinct landslide headscarps or lateral scarps are also not common. The widespread presence of swamp reeds growing over the slopes due to the very low permeability of the soil mantle is another good indicator in the field to help distinguish underlying Northland Allochthon from other lithologies.

The geomorphology, and in particular the gradient of slopes formed within the Northland Allochthon is very closely related to the rock mass strength and lithology of the underlying materials. The general rule of thumb here is "the gentler the slope; the less calcareous or siliceous the underling rock mass and the lower the rock mass strength". Slopes underlain by the non-calcareous mudstones and melange stand at the lowest gradients (<12°), reflecting the low residual shear strength of the soil / rock

transition. The weakly calcareous rocks stand at gentle to moderate slopes (12 to 20°), and the calcareous, siliceous and sandstone allochthonous rocks stand at moderate slopes (20° to 26° or more).

Again a very good indication of what underlies the slope can be gained from the geomorphology. Smooth elongated mounds, spurs, or knobs surrounded by hummocky gentle slopes are likely to represent the surface expression of a floater or block of more competent allochthonous material incorporated within softer and sheared matrix of a melange zone (mixed zone of highly sheared rocks). Springs also tend to be present along the contact between the harder, more competent and permeable rock masses, and the highly sheared less permeable and weaker rock masses.

Asymmetric landscapes can form from the direction of the predominant sheared fabric within stronger anisotropic rock masses within the allochthon (i.e. the calcareous and siliceous lithologies). This can form long dip slopes that are parallel to shearing, with much steeper slopes that are perpendicular to the predominant sheared fabric. These exist in the same way as they do in sedimentary strata such as the Waitemata Group.

CAUSES OF INSTABILITY

The characteristic geomorphology that has developed above most of the Mangakahia Complex rocks is that almost all of the slopes have been subject to some form of slope instability and creep over time. This is due in part to the low strength and generally sheared fabric of the soil mantle that has developed over the parent rock. The soil mantle is also generally thin and in many cases overlies impermeable parent rock. Water also tends to perch above the parent rock within the sheared low strength soil mantle.

Where the mantle is thin, the potential for it to saturate is much greater following rainfall events than it is for deeper soil layers. Furthermore, the high shrink swell potential of the less calcareous and siliceous soils results in the general development of large cracks at the surface during the summer months. These then swell with the ingress of water during the remainder of the year resulting in a greater net downwards migration of the near surface soils over slopes over time than more stable soils.

While deep-seated landslides that have displaced within the parent rock mass do exist, the bulk of the characteristic geomorphology is a result of slope instability within the soil mantle. Discrete individual landslides don't tend to form within the slopes as they do above most other lithologies. Instead numerous lobes form over the slope. When one lobe displaces, the lobes behind the initial lobe tend to move slowly towards it to reach equilibrium. As is the case with most low strength slopes, even minor changes in slope conditions can upset the equilibrium. What results is a slope with a number of active lobes that move at different times, rather than all together at once.

The more depressed and centralised parts of the slopes are more active overall, as they are closer to equilibrium due to higher groundwater levels in those areas than towards the spurs and ridges. Nevertheless most, if not all of the slopes may be subject to some degree of movement over time due to likelihood of intense cyclonic events, and the gradual loss of toe support from movement further downslope.

Deep-seated slope failures also exist, although can be difficult to recognise due to the tendency of the headscarps and lateral scarps to regrade resulting in the loss of definition of the original feature. Many of these larger features probably developed by displacement over laterally persistent low angle shears and thrust faults within the allochthon. Many have developed as a result of lithological contrasts, such as relatively permeable siliceous mudstone over impermeable pervasively sheared mudstone.

INVESTIGATION METHODS

Analysis of the geomorphology (also known as "terrain evaluation") is one of the most important and useful aspects of any geotechnical investigation, especially those involving the Northland Allochthon.

It is also a very cost-effective technique for a preliminary investigating a site, and in minimising construction costs, and long term geotechnical risk. The main reason for this is the Northland Allochthon geomorphology provides a very good indication of what lies beneath the surface, its existing engineering behaviour, and how it is likely to behave in the long-term.

In general, the best method for investigating the subsurface conditions of sites affected by typical Northland Allochthon geomorphology is the use of machine excavated test pits, as the nature, orientation and continuity of defects can be obtained with relative ease. Handaugered boreholes are generally of low value, unless information such as undrained shear strength and moisture content profiles are required.

Deeper-seated landslides or ground proposed for large cuts include investigation using machine boreholes. Drilling can be problematic however, due to the swelling potential of the sheared mudstones, and rod-wedging within the more calcareous and siliceous rocks. Gravel and boulder sized blocks or floaters of more competent rocks incorporated within melange zones also tend to be difficult to get past. Drilling should therefore be expected to take longer and to be more expensive than usual.

CIVIL ENGINEERING PROBLEMS

Buildings and civil engineering infrastructure sited on slopes formed in the Mangakahia Complex lithologies of the Northland Allochthon are commonly affected in some form or another. Of all the problems, roads crossing allochthonous country show the most obvious deformation as a result of slope instability. The most common roading problems are underslips, which tend to affect wide areas of the carriageway. This is because many of the slopes can move at relatively gentle gradients compared to more stable country, and relatively minor slope displacements can therefore result in the deformation of large areas of carriageway. Surface runoff from the road surfaces can exacerbate the problem, especially if a large area of surface is channelled through culverts to one point of discharge. These culverts commonly discharge to the depressed areas of the slope below the road, which can be the most sensitive to water in terms of slope stability. Overslips also occur, mainly due to the cut in the slope to form the road. However, these are not as common as underslips. The damage they cause is also usually small (e.g. the gradual blockage of a table drain), although some large overslips can result in the blockage of the road.

Many buildings that are constructed on gentle slopes underlain by the Northland Allochthon rocks have been affected by the gradual creep and slope movements occurring within the soil mantle over time. Buildings don't tend to be damaged by spectacular failures completely demolishing the dwelling. Instead, deformation occurs slowly over time and may go generally unnoticed until some threshold is reached. As a result of the movement of the buildings footings (which usually tend to be shallow), the floorboards of the building tend to warp, and doors and windows may no longer shut. Cracks also develop in masonry surfaces, and concrete pavements distort and tilt. Cracking along joints within the walls are also common, and the warping of the roof is also fairly typical. Other common features of ongoing slope movement are the development of new depressions in lawns, which may pond water after heavy rainfall.

In many cases it is difficult to determine whether the deformation to a building is a direct result of downslope movement, or due to shrink-swell effects of the soils. As most older houses have been constructed on typically very shallow foundations (e.g. less than 300mm below ground level) they are particularly prone to seasonal changes in the moisture content of the swelling clay-rich soils. Large cracks can appear to buildings during the summer months, only to close up again in the winter.

Conventional effluent disposal systems installed in the allochthon soils tend to degrade and malfunction at a much greater rate than those installed in soils above more stable rock types. The plumbing can often become separated by ground movements, and the tank itself can become distressed from higher lateral loads than designed for. Another problem with conventional effluent disposal systems is that in many cases the effluent does not readily seep away. This results in the saturation of

the trenches during heavy loading, and even seepage at the surface resulting in the development of bad odours.

ENGINEERING SOLUTIONS

Foundations

The detrimental effects of excessive shrink-swell behaviour of some of the highly plastic mudstone residual soils can be substantially reduced by increasing the depth of footings to greater than 0.6m. The depth that shrinkage can be expected to affect footings can be estimated by measuring the depth of the desiccated zone within the soil profile in the test pit exposures. In many cases this is greater than 1m. Building platforms should be limited to ridges and spurs that have a low potential for slope instability. Fill platforms on sloping ground almost always require a toe key to provide the necessary stability.

Where possible, roading over mudstone terrain should be kept to ridge crests to avoid crossing areas affected by slope instability.

Slope Stabilisation

Drainage of slopes formed in the allochthon that are subject to slope instability can be difficult, especially in the non-calcareous mudstone units and melange. This is because of the general low permeability of these units, and also because of the very weak, commonly clay-rich nature of the soil and rock masses. Conservative reductions in groundwater levels should be assumed for any drainage measure that is adopted.

Buttress drains are ususally the most effective drainage measure, mainly as a result of the large surface area of the drains. Buttress drains can be also the most practical and simplest method of slope drainage due to the generally thin soil mantle that forms over the most problematic allochthonous materials. However, the construction of buttress drains can be difficult as the trench walls often tend to collapse, even for excavations less than 5m in length. Drains therefore should be excavated in short sections, with the drainage materials installed as quickly as possible to support the side-walls. Drains also need to be fairly closely spaced (generally 2 to 4 x depth) to provide effective drainage across the slope. Buttress drains should therefore be expected to be time consuming and costly to install.

Horizontal drains tend to only work effectively in the calcareous and siliceous allochthonous rocks due to the much greater rock mass and soil mass permeability, and also due to the thicker soil mantle that generally exists over these rocks. They do not tend to be as effective in the non-calcareous mudstones and melange zones due to the very close spacing required between the holes to achieve effective drainage, unless there is a broken zone between the soil profile and the parent rock. The soil mantle above the non-calcareous mudstones and melange zones is also typically thin, and the underlying parent rock mass is generally dry. Problems with horizontal drains occur due to the low surface area of the holes, and also from the smearing of the hole walls as a result of the drilling process and the subsequent reduction in wall permeability.

Slope Regrading, Toe Buttressing, and Shear keys

The regrading of slopes by the reduction of material at the head of the landslide and the placement of fill at the toe is generally not an effective stabilisation option, unless the landslide has developed at the base of the slope. This is because of the reduction of material at the head of the identified movement area could result in the regression of movement further up slope. Also, placement of fill at the toe of a landslide located up from the base of the slope can also result in problems by loading the area below the landslide initiating additional slope displacements.

Shear keys are an effective stabilisation measure to stop slope movement, as the failures are usually relatively shallow so excavation can be achieved by normal excavation methods. Additional normal

loading can be applied to the slope by increasing the thickness of the shear key resulting in the formation of a shear key buttress. If the stabilisation of a slope is going to rely solely on a shear key care must be taken to ensure that the engineering geological model is correct, and that movement isn't initiated along any surfaces beneath the shear key. In any case, if slope regrading, buttressing or the construction of a shear key is going to be used it should be rigorously analysed and checked.

Palisade Walls

The use of palisade walls (or buried pile walls) is probably the most expensive yet most robust measure for stabilising many slope failure problems that develop within the Northland Allochthon. Piles are usually installed into the ground at a distance out from the building that is greater than the width of the active wedge. The piles are usually spaced at centres that are less than or equal to three times the pile diameter. This causes the soil between the piles to bridge should the ground move down slope from the wall. A capping beam across the top of the piles greatly increases the strength of the wall although they can be expensive. Tie-backs can also be incorporated to limit displacements at the top of the wall.

The use of palisade walls incorporated with some form of subsurface drainage is recommended. This reduces the potential loads acting on the wall, and subsequently the risk of excessive wall deflection. It also can reduce the size of the piles required and therefore the overall cost.

Cut Slopes

The natural slope gradient of the hillside is an excellent and very important indicator of the most effective stable slope gradients for long term cut slopes within the Northland Allochthon. This is because the geomorphology of the slopes formed within the allochthon closely reflect the long term shear strength of the rock mass and the soil mantle that forms over it. Consequently these gradients generally need to be relatively low and as close as possible to the natural slope profile, otherwise failures within the cut can be expected. Where steeper cut slopes are proposed careful investigations are required to identify whether low strength continuous defects are present within the rock mass. Defect surveys followed by stability analyses are required to determine possible failure modes and allow engineering solutions to be developed. Trial cuts can be carried out to test the stability of various slope gradients, however the length of time that is required for the slope to reach its "long-term" condition may be too long for the project and slopes that are very close to failure may erroneously be selected. Terrain evaluation is still the most effective method for determining cut slope gradients in the allochthon.

Effluent Disposal

Conventional septic tank systems and trench disposal methods are not generally recommended for effluent disposal in Northland Allochthon country. This is because these methods rely on subsurface soakage into the soils, which are typically of low permeability, especially above the Mangakahia Complex lithologies. In addition, the method essentially injects water into the soil mantle, which reduces its stability and increases the likelihood of soil saturation following heavy rainfall events.

The methods that are most suitable for effluent disposal are dripper irrigation systems installed on the surface or within the topsoil layer. These should be placed in areas that are expected to exhibit high rates of evaporation, such as north facing slopes or on spurs. Alternatively, the disposal field could be laid out beneath trees (e.g. a bushy gully), or surrounded by vegetation that has a high water demand. Another option is the use of evapo-transpiration beds that do not rely on any soakage of underlying soils.

CONCLUSIONS

Slopes that are underlain by Northland Allochthon rocks are generally easy to recognise due to their distinctive geomorphology. In addition, the subsurface geology and landslide geometry can usually be

identified with relative ease based on their landform. These factors, combined with the knowledge and understanding of the various geotechnical problems and engineering solutions can greatly assist in addressing the problems associated with the Northland Allochthon.

REFERENCES

Isaac, M.J. et al. (1994). "Cretaceous and Cenozoic Sedimentary Basins of Northland, New Zealand", Institute of Geological and Nuclear Sciences monograph 8

Isaac, M.J. (compiler)(1996). "Geology of the Kaitaia Area", Institute of Geological and Nuclear Sciences 1:250,000 geological map 1.

Edbrooke, S.W. (compiler) (2001). "Geology of the Auckland Area", Institute of Geological and Nuclear Sciences 1:250,000 geological map 3

Rait, G.J. (2000). "Thrust Transport Directions in the Northland Allochthon", New Zealand Journal of Geology and Geophysics, 2000, Vol.43.

Winkler, G.E. (1994). "Engineering Geological Characterisation of Cretaceous-Tertiary Rocks and their Relationship to Landsliding, Waiapu District East Cape": Unpublished MSc Thesis, University of Canterbury.

Generic Responsibilities of Engineering Geologists in General Practice

F J Baynes
Bsc(Hons), Msc, DIC, PhD, CGeol, CPEng
Consulting Engineering Geologist, Australia

Abstract: Engineering geologists in general practice assume a series of generic responsibilities that relate to their core activities of understanding and communicating the geological conditions. It is suggested that these fundamental responsibilities are: observation and investigation of the geology, geological model development, establishing standards for the geological activities, geological information management and communicating the geology. The key competencies that relate to the generic responsibilities are explored and some comments made regarding the state of practice.

INTRODUCTION

Responsibilities in practice are those matters and/or duties for which a practitioner is answerable, liable or accountable, such as the scope of work, suitable standards, the successful implementation or execution of various aspects of a project or the effective management of staff. The *generic responsibilities* of engineering geologists in general practice will be those distinct matters and duties for which an experienced engineering geologist should be held ultimately accountable, although these can depend upon how a project is managed. Meeting those responsibilities can be expected of what the lawyers would call "a reasonably competent engineering geologist". An ability to fulfill those responsibilities forms the core competencies of professional practitioners of engineering geology.

ARE ENGINEERING GEOLOGISTS INTERESTED IN RESPONSIBILITIES?

In October 2002 a questionnaire was sent to all Australasian IAEG members and also those engineering geologists who are not members but who have nominated to be on a database of engineering geological practitioners in the region ie Australia, New Zealand and PNG. Issues that have been raised by practitioners within the region over the last few years were listed and participants were asked to indicate the importance of the issue by using a scale where 5 = very important and 1 = inconsequential.

ISSUE	IMPORTANCE
Promoting the status of engineering geologists as competent responsible professionals authorised to sign off on various issues, making representations to industry or government, engineering geology as a "brand name".	4.2
Improving the quality of practice in engineering geology in the region through training, Continuing Professional Development courses, workshops etc for both engineering geologists and geotechnical engineers, at a regional and local level	4.1
The need to be able to register as a professional. There are various alternative pathways to registration that could be explored and facilitated.	3.9
The availability, content and status of university education in engineering geology and geology for engineers at an undergraduate and postgraduate level within the region.	3.9
The establishment of technical working groups or regional commissions to generate standards, guidelines or position papers eg for site investigation, geological models, dealing with uncertainty etc	3.5

Table 1. Questionnaire Results

The questionnaire went to about 450 people and 132 replies were received. The results were collated and the values given in the importance column in Table 1 are the average values from the 132 replies for the five issues that were rated the most important.

It would appear that the most important issue facing engineering geologists in the region is "to promote the status of engineering geologists as competent responsible professionals authorized to sign off on various issues and make representations to industry or government". This does not seem an unreasonable aspiration for a group of professionals, provided that there is an appreciation of the responsibilities. Consider what actually happens in the areas of practice where those responsibilities are fulfilled.

AREAS OF PRACTICE

There are no significant differences in the way that understanding and communicating the geology is achieved between civil, mining, offshore, environmental or any other type of ground engineering. Similarly, wherever ground engineering takes place throughout the world, whilst there may be differences in project procurement, the training and education of the individuals involved, or their roles and professional backgrounds, there are no innate differences in the way that projects are implemented and in the generic responsibilities associated with understanding and communicating the geology that have to be fulfilled. But who is taking the responsibility for the geology?

Where some reliance in the project engineering is placed upon knowledge of the geological conditions someone must be responsible for understanding and communicating the geology. In general practice, understanding and communicating the geology is usually the responsibility of people who are also involved to varying degrees in providing some of the engineering expertise required to implement the project, typically in those areas of practice into which engineering geology merges, such as:

- Rock mechanics
- Soil mechanics
- Hydrogeology
- Risk assessment
- Environmental science
- Site supervision
- Site investigation

In Australasian practice the person responsible for the geology may be an engineering geologist, a geological engineer, a geotechnical engineer, a civil engineer or a project manager with some geological knowledge. Occasionally it happens that those in positions of responsibility have no geological knowledge whatsoever, but on those projects it is probably only the lawyers that profit!

It is the premise of this paper that there are some generic responsibilities that only an experienced engineering geologist can properly fulfill, that those generic responsibilities may be established, and that those generic responsibilities epitomize the general practice of engineering geology. Clearly those generic responsibilities have legal, professional and commercial ramifications.

THE NATURE OF RESPONSIBILITIES

There have been numerous attempts of varying excellence to explore, define or delineate the area of practice of engineering geology eg Berkey (1929), Burwell & Roberts (1950), Moye (1966), Arnould (1970), Dearman (1971), Rawlings (1972) Stapledon (1982, 1983), AEG (1993), Fookes (1997), IAEG (1998), Baynes (1999), Morgenstern, (2000), Hungr (2001), AEG (2002), and Knill (2002). Some of these papers are referred to in the authoritative discussions on the subject by Morgenstern (2000) and Knill (2002), to which the interested reader is directed. Unfortunately, descriptions of roles, definitions of activities or delineations of areas of practice of engineering geologists do not constitute an adequate description of the *generic responsibilities*, because, if you care to think about it, responsibilities are different from roles or activities.

Simplistically, activities are what occupy you during the day, whilst responsibilities are what keep you awake at night! In other words, the distinctive thing about responsibilities is that they intrinsically oblige individuals to achieve some level of competency in their work, and in general practice they are often onerous, weighing heavily on the shoulders of those who take them on. Responsibility for assessing the risk of loss of life from landslide in a reasonable and defensible manner, or for considering the adequacy of an investigation for a large dam upstream of a community, are not matters that are undertaken lightly.

The generic responsibilities of engineering geologists are not the same as personal ethics or professional codes of practice. Personal ethics relate to personal beliefs and the religious and social norms of the time and do not necessarily relate to geology. Professional codes of practice for geologists (AEG 2002, Anon. 2003) indicate various responsibilities to the public, to society, to clients, to colleagues and to the profession but they could equally apply to many other professions and do not necessarily relate to geology. Job descriptions for geologists may indicate responsibilities but they are usually restricted to employer-employee interchanges and are often written in terms that could equally apply to many other professions.

Thus although there is much sage advice in the literature about the practice and profession of engineering geology, this review suggests that there is less that specifically relates to the concept of the *generic responsibilities* of engineering geologists. However, there is very little that has not been said before and so, in an attempt to elucidate the concept, the past words of wisdom of eminent engineering geologists were picked over.

GLEANING THE RESPONSIBILITIES

The generic responsibilities of engineering geologists in general practice may be gleaned from a careful re-examination of the available literature and consideration of the essentials of what actually happens in practice. Berkey (1929) considered the geologists' responsibility in engineering projects thus:

> *"It is his duty to discover, warn and explain without assuming the particular responsibility of the engineer who has to design the structure and determine how to meet all the conditions presented and stand forth as the man responsible for the project"*

Although these days the person ultimately responsible for the project is most likely to be some form of blue suited bean counter, this early analysis alludes to the investigative role, the importance of the identification of geological hazards and the need for communication of the geology to the engineer. Judd (1967) wrote about communication problems and noted the responsibility to describe the geology in easily understood terms:

> *"the burden generally is on the engineering geologist to use language that is readily understandable by his client – the civil engineer".*

Henkel (1982) concluded that Berkey's original analysis was correct and also likened the interface between geologists and engineers to the Escher painting, "Sky and water" in which birds and fishes are separate and distinct when in their own element but are indistinguishable at the interface between sky and water. Separate and distinct identities are needed to sustain Escher's image. Analogously, separate and distinct responsibilities for engineering geologists and engineers need to be established for both parties to operate successfully together as an integrated team.

James and Kiersch (1991) reinforced the necessity for the engineering geologist to understand the engineering in order to be able to communicate the significance of the geology:

> *"The mature engineering geologist -...- is responsible for understanding the broad needs of a project builder and for effectively communicating his relevant geologic findings and ideas"*

Fookes (1997) succinctly stated:

> *"the main role of the engineering geologist is to get the geology right"*

which quite clearly and properly indicates the fundamental responsibility for correctly assembling and presenting the geo-scientific knowledge. He went on to allocate responsibility for communication of that knowledge:

> *"the engineering geologist must make precise communication leading to the thorough understanding of his views by his project colleagues"*

Knill (2002) reiterated the responsibility for standards of investigation:

> *"The assessment of the adequacy of the investigation and its reporting is probably the single most important procedural function of the engineering geologist"*

These luminaries reinforce what a common sense view of practice tells us, ie engineering geologists are broadly responsible for understanding and communicating the geology to the engineer. However the gleanings also contain some more specific advice, which, if considered in the context of current practice, suggest that five generic responsibilities may be discerned.

FIVE GENERIC RESPONSIBILITIES

It is proposed that understanding and communicating the geology can be categorized into five distinct areas of generic responsibilities that relate to associated, but different, functions. These are:

- Observation and investigation of the geology in engineering projects
- Engineering geological model development
- Establishing standards and scope for the engineering geological activities
- Engineering geological information management
- Communicating the geology to engineers

To better understand the nature of the five fundamental areas of generic responsibility they have been expanded into a series of key competencies, which are set out in Table 2. These areas of generic responsibility are discussed in more detail below, together with some personal concerns about the current state of practice.

Observation and Investigation of the Geology

In order to understand the geology, the site or the project area must be investigated, observed and characterised. This involves going into the field and actively collecting information, often using specialized techniques, encoding that information in an appropriate language and adding the information to the existing database. This active collection of information usually extends through construction and operation. Investigations are driven by objectives and involve cost effective methodologies. Techniques peculiar to direct and to remote geological, geomorphological and geophysical observation all exist and must be used appropriately. Investigations of the ground are exercises in geological characterization and should be the responsibility of the engineering geologist.

Rengers et al (2002) concluded that the most important bottleneck in information technology is not the calculating power of computers but the detail with which input parameters can be determined in the field. However many observers consider that there is a trend towards reducing the amount of field studies in projects (Hamel and Adams, 2000) and have noted that less field skills are taught during tertiary education (Hathaway, 1998). Field work is more costly and time consuming than office studies and field work is often carried out more cheaply by using inexperienced juniors even if it is an inherently ineffective approach.

Generic Responsibility	Key Competency	Explanation
Observation and investigation of geology in engineering projects	Investigation techniques	A suite of investigation techniques should be chosen for cost effective collection of information
	Characterization methods	All relevant information should be encoded using standard symbols and languages and all geological information should be retained in the process
	Field studies	Field observations and investigations are fundamental and essential and should always be carried out
	Observing and recording	Observation should be insightful and acute and driven by an initial understanding or preliminary site model, but also capable of recording features that are not understood
Engineering geological model development	Geological knowledge	A total geological approach should be adopted in which site conditions are viewed as resulting from the total geological and geomorphological history
	Encapsulate an understanding	The understanding should be encapsulated by the model and should have qualitative, quantitative verbal and graphic components represented in 3D space, plus time
	Anticipation	There should be knowledge of what might be encountered even if the particular geological conditions have not been sampled
	Uncertainty	The uncertainty and level of confidence in the knowledge base should be expressed. Risks should be identified.
	Geohazards	Geohazards should be identified or anticipated and characterized
Standards and scope for engineering geological work	Determination of scope	The extent of studies within reasonable budgets should be determined by those responsible for the activities
	Technical Standards	The quality of the technical work should meet appropriate standards
	Codes of Practice	The professional aspects should meet the clients' and society's requirements and expectations
	Education and Training	Less experienced engineering geologists should be trained in order that they can assume their responsibilities
Engineering geological information management	Collection and collation	All relevant information should be identified, located, collected and incorporated into the project database, processed to establish significance and collated for assimilation
	Reporting and referencing	Information should be separated into observation, interpretation and opinion, the source and quality of the information clearly identified and the report well written and illustrated
	Storage, access, retrieval	The minimum requirement is to store all information for the design life of the project but for the ultimate benefit of society key information should be accessible in perpetuity
Communication of geological conditions to engineers	Engineering knowledge	There should be sufficient knowledge of project engineering to know what is relevant and important geologically
	Transforms	Geological information should be converted or transformed to engineering information prior to being communicated
	Message transfer and feed back	Information should be encoded in a form suited to the engineer and confirmation sought that the message has been received and understood
	Personal qualities	The project manager may be unwilling to listen or accept information that adversely affects the project so credibility and persistence are important qualities in the communicator

Table 2. Generic Responsibilities and Key Competencies

That most basic of techniques, engineering geological mapping, has become underused to the extent that the Geological Society of London recently published a Volume on Mapping in Engineering Geology with the stated aim of introducing the technique to a new generation of practitioners! (Anon., 2002). For extensive high quality field studies to be an axiomatic component of any project their fundamental importance needs to be constantly emphasized

Model development

All of the information must be understood and incorporated into a model of the site that encapsulates the understanding. The model can take the form of profiles, maps, sections, block diagrams, visualizations, time related descriptions, text, explanatory notes or any combination of these. Within that understanding there must be some ability to anticipate geological conditions that have not necessarily been sampled but which might reasonably be foreseen to occur. The understanding must be accompanied by an indication of information source, the degree of uncertainty and the basis for various inferences or anticipations. Geohazards and risks to the project need to be clearly identified. There needs to be qualitative knowledge assembled as well as quantitative knowledge. Developing a model that reflects an understanding of the ground should be the responsibility of the engineering geologist.

The importance of engineering geological models (Fookes 1997, Fookes, Baynes and Hutchinson 2000, 2001) has been clearly identified but the methods for developing those models have yet to be thoroughly explored and documented (ibid, Knill 2002). Fookes, Baynes and Hutchinson (2000) reviewed 32 case histories and previous studies and concluded that there has been a systematic failure to anticipate geological conditions due to the failure to create a geological model of the site.

Standards and scope

The client, the employer, other professionals and society as a whole have a reasonable expectation that the scope of any studies and the technical quality of those studies should meet some appropriate standards. Scope will essentially be driven by the need to answer questions about the geology but also by knowledge of the engineering requirements of the project and appreciation of what level of knowledge is appropriate for satisfactory engineering. The quality of studies should reflect the state of practice. Where those studies are primarily of engineering geology it should be the responsibility of the engineering geologist to determine an appropriate scope and standards within a reasonable budget.

In a study of cost overruns on 71 hydropower schemes involving "enormous amounts of money" Hoek and Palmieri (1998) found that inadequate site investigations were a major contributor to geotechnical risks eventuating. A significant area of concern is where scope is determined by a project manager with a limited budget and little or no understanding of the engineering geological requirements of the project. In these circumstances the engineering geologist must strive to perform in a responsible manner. If the budget is not reasonable and responsibilities cannot be discharged then the project manager should not only be informed, but persuaded as to the error of his ways.

Information Management

On most, if not all projects, there will be existing information relating to the geological and geotechnical characteristics of the site that needs to be collected, collated, accessed, reported, archived and generally managed. In many cases there will be very large amounts of information of enormous value. Additional information is usually collected during investigations and construction and operation and must also be managed. If the project ends up in dispute then the geological information, especially the detail, may well be vital to the resolution of that dispute. Management of this information must be accomplished effectively and where the information is primarily geological in nature this should be the responsibility of the engineering geologist.

Phased investigations starting off with a desk study for the collection and collation of existing information might be thought of as responsible practice. However a recent survey of practitioners in the UK found that only 39% of site investigations included a desk study (Anon 1999).

Multidisciplinary engineering organizations which manage large projects tend to keep records only whilst a project is alive and even then geological information often is of a difficult size or format for electronic record keeping, and may end up piled on a desk. Upon project completion geological records that are no longer treasured by an engineering geologist often end up being trashed because no-one realizes their worth. Utilities often end up losing priceless records during privatization or the latest re-organization. All of this represents a loss of information worth huge amounts of money both to the organizations involved and to society in general.

Communication

The understanding of the site and all of the information must be communicated to the engineer. This requires knowledge of the engineering, so that the information can be transformed to be understood by the engineer, and also so that the significance of the information can be properly transmitted. A personality suited to effective communication and the delivery of what is often crucial advice is necessary. Communicating the understanding of the geology to the engineer is clearly the responsibility of the engineering geologist.

In a combined review of the catastrophic failure of 20 dams, 4 major landslides and 6 tunnels, James and Kiersch (1991) and Kiersch and James (1991) concluded that in the earlier part of the 20th Century a lack of engineering knowledge on the part of geologists was a major contributing factor to the failures. They went on to note that nowadays currently mature engineering geologists generally fulfill this responsibility, probably because they graduated and trained as engineering geologists and have taken on the responsibility of acquiring engineering knowledge. The same authors (ibid) also concluded that poor management was a major contribution to a large number of the failures in that geological advice was not sought or, if proffered, was ignored. If advice was not sought or ignored then engineering geologists have a responsibility to address that problem effectively and their personal qualities are particularly relevant to their ability to succeed in discharging those responsibilities.

CONCLUDING REMARKS

Most engineering geologists fulfil their responsibilities very ably, possibly without ever having thought much about it. Successful projects are implemented effectively and deliver what society requires. Unfortunately, good quality responsible work by engineering geologists involved in successful projects will largely go unnoticed unless it is actively promoted.

Wise people know the value of geology in ground engineering, but for some time a number of experienced commentators have lamented the reduction of the geological content in training and practice in engineering and the commensurate diminution in the role of geology and the engineering geologist (Slosson et al 1991, Fell 1995, Stapledon 1986, 1996,). There is also a feeling that the practical application of the subject of engineering geology has not been matched by the development of a scientific rationale (Knill 2002). This is not a good trend and, if it is not countered, everybody involved in ground engineering will be the lesser for it.

One reason for this situation may be that the *generic responsibilities* of engineering geologists have not been clearly understood, either by practitioners or by engineers and managers, and have not been clearly articulated. Unless those responsibilities are understood and formally recognised by all of those involved in ground engineering then the trend towards a diminution of the role of geology may well continue. This paper is one small attempt to redress this trend but a more profound cultural change is clearly necessary. Globally, what is required is the ongoing promotion of the profession of engineering geologist; my personal preference is to achieve this through the excellence of our work. However in Australasia reliance upon excellence may not be enough and may have to be bolstered with a more systematic approach to professional registration of engineering geologists to establish a formal profile. This may well be the forthcoming challenge to practitioners in Australasia, if we are to contribute to ground engineering in proportion to our worth.

ACKNOWLEDGEMENTS

I am grateful to Peter Fookes, David Stapledon, Alan Moon and Bruce Riddolls for discussing this paper with me.

REFERENCES

AEG, (1993). *Professional Practice Handbook,* 3rd Edition, Special Publication No.5 (eds) Brown & Proctor first edition, Hoose S.N. 3rd edition.

AEG (2002), *AEG News*, Association of Engineering Geologists, Vol. 45, Annual Report and Directory, p 18.

Anon., (1999). "Time to Investigate". *Ground Engineering,* magazine of British Geotechnical Society, Vol.32, No.11, pp 52-54.

Anon. (2002). Key Issues in Earth Sciences: Vol. 1: Mapping in Engineering Geology. *Geological Society Publishing House, London.* compiled by Griffiths, J., 294p.

Anon., (2003). Code of Conduct, Geological Society of London, www.geolsoc.org.uk.

Arnould, M., (1970). The International Association of Engineering Geology, History-Activity. *Bulletin of the I.A.E.G.* Vol. 1: pp 22-28.

Baynes F. J. (1999), Engineering Geological Knowledge and Quality, *Proceedings of the Eight Australia New Zealand Conference on Geomechanics*. Volume 1 Hobart, Institution of Engineers Australia, pp 227 – 234.

Berkey, C.P., (1929). Responsibilities of the geologist in engineering projects. *Tech. Publs. Am. Inst. Min. Metall. Engrs.*, No. 215, pp 4-9, quoted and cited in Henkel (1982).

Burwell, E.B. and Roberts, G.D., (1950). The geologist in the engineering organization. *Application of Geology to Engineering Practice,* (ed). S. Paige, Geological Society of America, pp 1-10.

Dearman, W.R., (1971). Introductory statement to regional meeting of the Engineering Group of the Geological Society Dublin. *Q. Jl Eng. Geol* Vol. 4, No.3, pp 187-190.

Fell R (1995). Geotechnical education, *Australian Geomechanics,* No 27, pp 26-28.

Fookes, P.G. (1997), Geology for Engineers, the Geological Model, Prediction and Performance - *Quarterly Journal of Engineering Geology*, Vol. 30: pp 293-424.

Fookes, P.G., Baynes, F.J. & Hutchinson, J.H., (2000). Total Geological History: A Model Approach to the Anticipation, Observation and Understanding of Site Conditions, *International Conference on Geotechnical and Geological Engineering, Melbourne, Australia* Technomic, Vol.1, pp 370-460.

Fookes, P.G., Baynes, F.J. & Hutchinson, J.H., (2001). Total geological history: a model approach to understanding site conditions, *Ground Engineering*, magazine of British Geotechnical Society Vol.34, No 3, pp 42-47.

Hamel, J.V., & Adams, W.R., (2000). Engineering geology for the new millennium: stick with the basics, to be published in a special issue of *Journal of Nepal Geological Society*, 27p.

Hatheway A.W. (1998). Engineering geology and the environment. *8th International Congress of I.A.E.G., Vancouver, Canada, 21-25 September*, Vol. IV, pp 2269-2277.

Henkel, D.J. (1982). Geology, geomorphology and geotechnics. *Geotechnique,* Vol. 32, No. 3 pp 175-194.

Hoek, E. & Palmieri, A. (1998). Geotechnical risks on large civil engineering projects. *8th International Congress of I.A.E.G., Vancouver, Canada, 21-25 September*, Vol.1, pp 79-88.

Hungr, O., (2001). Task force on the promotion of geological engineering and engineering geology in Canada: preliminary report, *Geotechnical News, BiTech Publishers Ltd*, Vancouver, Vol. 19: pp 60-61.

IAEG (1998), Frontispiece, *Bulletin of engineering geology and the environment*, Vol. 57 No. 1.
James, L.B., and Kiersch, G.A., (1991). Failures of engineering works. *The Heritage of Engineering Geology; The First Hundred Years,* Geological Society of American, Centennial Special Vol. 3, pp 481-516.

Judd, W.R., (1967). Geotechnical Communication Problems; Alex L. du Toit Memorial Lectures No.10. *The Geological Society South Africa*, annexure to Vol. 70, 45p.

Kiersch, G.A. and James, L.B., (1991). Errors of geological judgment and the impact on engineering works. *The Heritage of Engineering Geology; The First Hundred Years,* Geological Society of American, Centennial Special, Vol.3, pp 517-558.

Knill, J., (2002). Core Values: The First Hans-Cloos Lecture. *Proceedings of 9th International Congress of the IAEG, Durban, South Africa, 16-20 September.* (eds.) van Rooy J.L. & Jermy C.A, South African Institute of Engineering and Environmental Geologists.

Morgenstern, N.R., (2000). Common Ground - *International Conference on Geotechnical and Geological Engineering,* Melbourne, Australia Technomic, Vol. 1, pp 1-30.

Moye, D.G., (1966). Engineering geology. *paper presented to Symposium on undergraduate geological training, A.N.U. Canberra* quoted and cited in Stapledon (1982)

Rawlings, G.E., (1972). The role of the Engineering Geologist during construction. *Q.Jl Engng Geol.* Vol. 4, pp 209-220.

Rengers, N., Hack, R., Huisman, M., Slob, S., & Zigterman, W., (2002). Information Technology Applied to Engineering Geology. *9th International Congress of I.A.E.G., South Africa, 16-20 September*, (eds)van Rooy J.L. & Jermy C.A. pp 83-105, South African Institute of Engineering and Environmental Geologists.

Slosson, J.E, Williams, J.W., & Cronin, V.S., (1991). Current and future difficulties in the practice of engineering geology. *Engineering Geology* Vol. 30, part 3, pp 3-12.

Stapledon D.H. (1982). Subsurface engineering – in search of a rational approach. *Australian Geomechanics News,* Vol. 4, pp 26 – 33.

Stapledon D.H. (1983). Towards Successful Waterworks, *Proceedings Symposium for Dams and Canals*, Alexandra, Institution of Professional Engineers, New Zealand, pp 1.3 – 1.15.

Stapledon, D., (1986). Let's Keep the "Geo" in Geomechanics. *Specialty Geomechanics Symposium,* Adelaide, 18-19 August 1986, pp 18-31.

Stapledon D.H. (1996). Keeping the "Geo"; Why and How, the John Jaeger Memorial Address, *Proceedings of the Seventh Australia New Zealand Conference on Geomechanics,* Adelaide, South Australia, Jaksa, Kaggwa & Cameron (eds), Institution of Engineers, Australia, Canberra, pp3-18.

A Deterministic Method for Assessing the Liquefaction Susceptibility of the Heretaunga Plains, Hawke's Bay, N.Z.

G D Dellow
MSc (Hons)
Engineering Geologist, Institute of Geological and Nuclear Sciences, Lower Hutt
P R Barker
NZCS
Scientist, Barker Consulting, Lower Hutt
R D Beetham
BE(Civil); MSc; FIPENZ
Engineering Geologist, Institute of Geological and Nuclear Sciences, Lower Hutt
D Heron
BSc
Scientist, Institute of Geological and Nuclear Sciences, Lower Hutt

Abstract: Since 1840, at least five earthquakes have produced shaking intensities ≥ MM7 on the Heretaunga Plains in Hawke's Bay. Historical reports of liquefaction from these earthquakes were assessed by assigning the damage description to a *liquefaction damage rating*, mapping each report to a geological unit and noting the MM shaking intensity at which the damage occurred. This enabled a *liquefaction susceptibility class* to be assigned to each geological unit and a regional *liquefaction susceptibility map* to be produced. The *liquefaction susceptibility map* is used to develop *liquefaction opportunity maps* for specific scenario earthquake events. *Liquefaction opportunity maps* show the extent and severity of liquefaction-induced ground damage that might be expected during specific earthquake events.

INTRODUCTION

Liquefaction *potential* is assessed by comparing the distribution of *susceptible* deposits and the *opportunity* for strong ground shaking to identify the areas in which liquefaction is likely to be triggered during a given earthquake. Liquefaction potential is site-dependent. Certain soils are more susceptible to liquefaction than others. Youd (in Ziony, 1985) describes liquefaction as: "the process by which water-saturated sediment temporarily loses strength, usually because of strong shaking, and behaves as a liquid". At low levels of ground shaking (e.g.~0.15g), liquefaction is most likely to occur in saturated, relatively uniform fine sands or coarse silts in a loose state, at depths of less than 20 m, where the groundwater level is within about 5 m of the ground surface. However, liquefaction can occur in other less susceptible deposits during periods of stronger ground shaking, or periods when the ground shaking is of longer duration or when resonant effects occur.

Generally the assessment of liquefaction **potential** involves two steps:

- *Evaluation of liquefaction **susceptibility***. This involves the identification of those areas or layers which have the physical characteristics of a liquefiable soil; and
- *Assessing the **opportunity** for strong ground shaking.* This involves identifying seismic sources that are capable of generating moderate to large magnitude earthquakes. The ground shaking generated by these earthquake sources is then modeled and combined with the liquefaction susceptibility map to locate areas where the shaking is strong enough to generate liquefaction in susceptible materials.

EVALUATION OF LIQUEFACTION SUSCEPTIBILITY

Developing a liquefaction susceptibility map for the Heretaunga Plains involved three steps:

(1) Preparation of a detailed geological map delineating Quaternary deposits of different age, depositional environment, and texture at 1:50 000 scale;
(2) Locating and assigning each historical report of liquefaction a *liquefaction damage class* based on the type and extent of ground damage and the Modified Mercalli (MM) shaking intensity at which it occurred; and
(3) Using the *liquefaction damage rating* distribution to assign a liquefaction susceptibility class to each mapped geological unit.

Quaternary Geological Mapping

Understanding the age of the Quaternary deposits and landforms is critical in establishing a Quaternary stratigraphy, and in assessing the susceptibility of a deposit to liquefaction (Youd *et al*, 1975). Most known cases of liquefaction and extreme amplified ground motion in coastal areas have occurred in geologically young (generally Holocene age) sediments (Youd and Hoose, 1978; Tinsley and others, 1985). Over time, sediments become increasingly consolidated and densified, and may develop cementation.

A Quaternary surface geology map of the Heretaunga Plains at 1:50 000 (Dravid and Brown 1997) was used as the geology base map. Topographic-map and aerial-photograph interpretation techniques were used to delineate landforms, such as stream terraces, swamps, estuaries, and floodplains likely to be underlain by uniform deposits with respect to age, and environment of deposition. Historical topographic maps were used to assess the changes resulting from urbanization, and major base-level changes following the 1931 earthquake, to delineate areas of filled, reclaimed ground adjacent to the coastline, and major river systems.

Modifications were made to the geology base map. These changes involved the present river channels being subdivided on the basis of grain-size into two separate units (a coarse and a fine) and the over-bank flood deposits being subdivided into three units on the basis of depositional environment (moderate river gradient, low river gradient and swamps). The resulting map is presented as Figure 1.

Historical Liquefaction Record

Sand boils and water ejections are the most common and unambiguous historical evidence of liquefaction in New Zealand. However, it is likely that other types of ground damage such as the settlement and spreading of embankments and river banks, have been caused by liquefaction, but have not always been recognised as such. In historical records, emphasis has been placed on recording the more obvious effects of earthquakes on buildings, although the unusual and often spectacular earthquake fountains (sand boils or `volcano' features), so common in the epicentral areas of large earthquakes, were usually noticed and reported. On alluvial plains, such features are often the only visible manifestation of liquefaction on areas that appear otherwise undamaged.

Generally, the *intensity threshold (Modified Mercalli (MM) Intensity) for liquefaction* in New Zealand was found to be MM7 for sand boils, and MM8 for incipient lateral spreading (Hancox *et al*, 1997). Liquefaction-induced ground damage is most common at MM8-10, at epicentral distances of 10-100 km (Hancox *et al*, 1997). As the shaking intensity increases at a site, the severity of the reported liquefaction also increases. This observation is used as the basis for classifying the type and extent of liquefaction-induced ground-damage in terms of a *liquefaction damage rating* (Table 1). For example, in the vicinity of the Tutaekuri River (f8 (fine) & f5 (swamp)) sand boils were reported at MM7 (liquefaction damage rating 1) and widespread lateral spreading occurred during MM10 shaking (liquefaction damage rating 4).

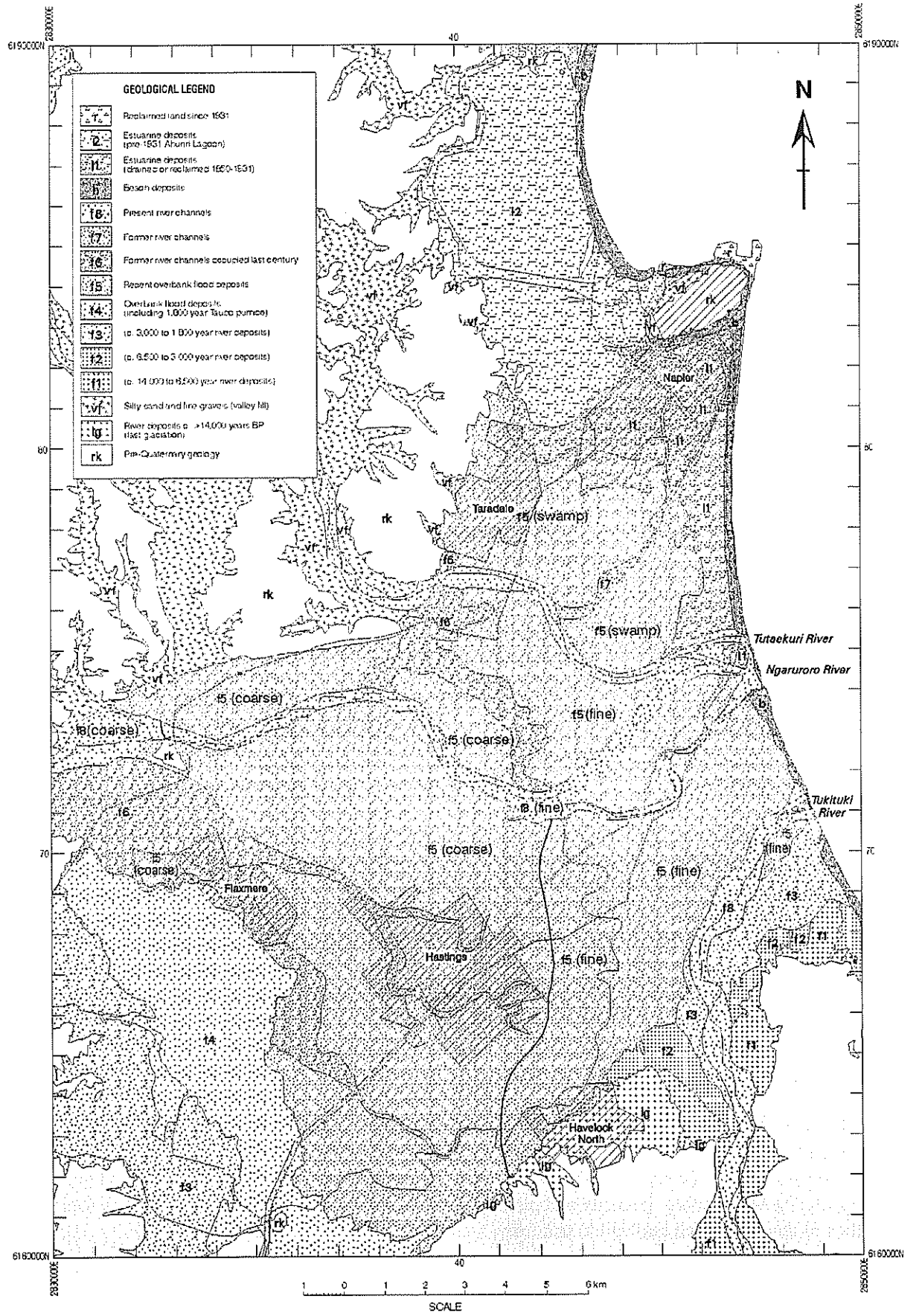

Figure 1. Quaternary Geology of the Heretaunga Plains, Hawke's Bay (after Dravid and Brown, 1997).

Liquefaction Damage Rating	Description of expected liquefaction induced ground damage
0	No liquefaction damage is seen.
1	A few sand boils and minor fissures. Estimate up to 10% of total area affected.
2	Sand boils and moderate fissuring – more extensive near basin edges and in waterlogged areas: banks of rivers broken up, and embankments slumped. Settlements of up to 0.2 m. Estimate 10-20% of total area affected.
3	Lateral spreading common, with many fissures in alluvium (some large), slumping and fissuring of stopbanks, common sand boils. Settlements of up to 0.5 m. Estimate 20-50% of total area affected.
4	Lateral spreading widespread, with extensive fissures and horizontal (and some vertical) displacements of up to 10 m common especially near channel edges. Settlement of uncontrolled fills by up to 1.0m. Estimate >50% of total area affected.

Table 1. Descriptions of Expected Liquefaction Induced Ground Damage for Liquefaction Damage Ratings.

Linking the historical occurrence of liquefaction to liquefaction susceptibility classes allows changes in liquefaction potential for various earthquake scenarios to be assessed across the study area. At the triggering threshold for a particular unit ground damage is generally minimal (damage rating 1 – see Table 1 above). Table 2 sets out the liquefaction damage ratings associated with each liquefaction susceptibility class for a range of MM shaking intensities.

Liquefaction Susceptibility Class	MM Intensity				
	MM6	MM7	MM8	MM9	MM10
Very high	0	1	2	3	4
High	0	0	1	2	3
Moderate	0	0	0	1	2
Low	0	0	0	0	1
None	0	0	0	0	0

Table 2. Liquefaction Damage Ratings Assigned to Liquefaction Susceptibility Classes at Different MM Shaking Intensities.

Liquefaction Susceptibility of Geologic Units

Since 1840, at least five earthquakes have produced shaking intensities of MM7 or greater on the Heretaunga Plains in the Hawke's Bay. The historical reports of liquefaction from these earthquakes were assessed by assigning each report a *liquefaction damage rating,* mapping each report to a geological unit, determining the MM shaking intensity and plotting the results (Table 3). *Liquefaction susceptibility classes* were then assigned for each geological unit using the definitions given in Table 2.

The analysis of liquefaction occurrence during historical earthquakes provides a means of establishing the MM intensity threshold values for the appearance of liquefaction in the various geological units. Using *liquefaction susceptibility classes* forms a basis for predicting the extent and magnitude of liquefaction-induced ground failure expected at different shaking intensities.

Geological Unit	Modified Mercalli Intensity					Comments	Liq. Sus
	6	7	8	9	10		
f8 (coarse)			**0**	*1*	*2*		M
f8 (fine)	**0**	**1**	**2**	**3**	*4*		VH
f7	*0*	**1**	*2*	*3*	**4**		VH
f6			*0*	*1*	**2**		M
f5 (swamp)	*0*	**1**	*2*	**3**	**4**		VH
f5 (low grad)		**0**	*1*	**2**	**3**		H
f5 (med grad)			*0*	*1*	*2*		M
f4				**0**	*1*	No liquefaction recorded	L
f3				**0**	*1*	No liquefaction recorded	L
f2				**0**	*1*	No liquefaction recorded	L
f1				**0**	*1*	No liquefaction recorded	L
vf		*0*	*1*	**2**	*3*		H
lg					**0**	No liquefaction recorded	None
l1	**0**	**1**	*2*	*3*	**4**		VH
l2	**0**	**1**	*2*	*3*	**4**		VH
b		**0**	**1**	**2**	**3**	Amount of settlement used	H
r	*0*	*1*	*2*	*3*	*4*	Not shaken since 1931	VH
rk					**0**	No liquefaction recorded	None

Bold numbers are for historical observations, while the italic numbers are assessments made for where no historical data exists.

Table 3. Liquefaction Damage Ratings/Liquefaction Susceptibility Classes Assigned to Each Geological Unit Based on Historical Liquefaction Records.

The resulting liquefaction susceptibility map is presented as Figure 2. The map illustrates the general susceptibility of an area to liquefaction, if ground shaking above the triggering threshold were to occur. This threshold varies depending on the nature of the ground being shaken. In brief, materials that have a very high susceptibility have a low (MM7 or less) triggering threshold, and materials that have a low susceptibility have a high (MM10) triggering threshold.

ASSESSING LIQUEFACTION OPPORTUNITY

The liquefaction opportunity of the Heretaunga Plains is assessed for two scenarios by overlaying ground-shaking isoseismal maps on the liquefaction susceptibility map for the area. The isoseismal maps were produced by calculating the shaking intensity at grid points located throughout the Heretaunga Plains, given the scenario earthquake's location and magnitude and the distance of the grid point from the earthquake epicentre. This calculation uses the ground-shaking-attenuation equation of Dowrick and Rhoades (1999) for the Mohaka and Poukawa fault events.

Liquefaction may occur in areas where the MM shaking intensities generated by the earthquake modeling equal or exceed the liquefaction threshold intensity. These maps (Figures 3 & 4) depict the type and extent of liquefaction-induced ground-damage that can be anticipated on the Heretaunga Plains for a particular earthquake scenario. The earthquake scenarios were selected because they represent realistic large-magnitude events that have a high probability of occurrence.

Mohaka Earthquake Scenario

The Mohaka fault forms part of the North Island Shear Belt, a major fault system that extends along the length of the North Island, and is composed of a number of large active fault segments. The structures are predominantly right-lateral strike-slip faults with a normal component of motion. Single event displacements on these faults appear to range up to 4-5m.

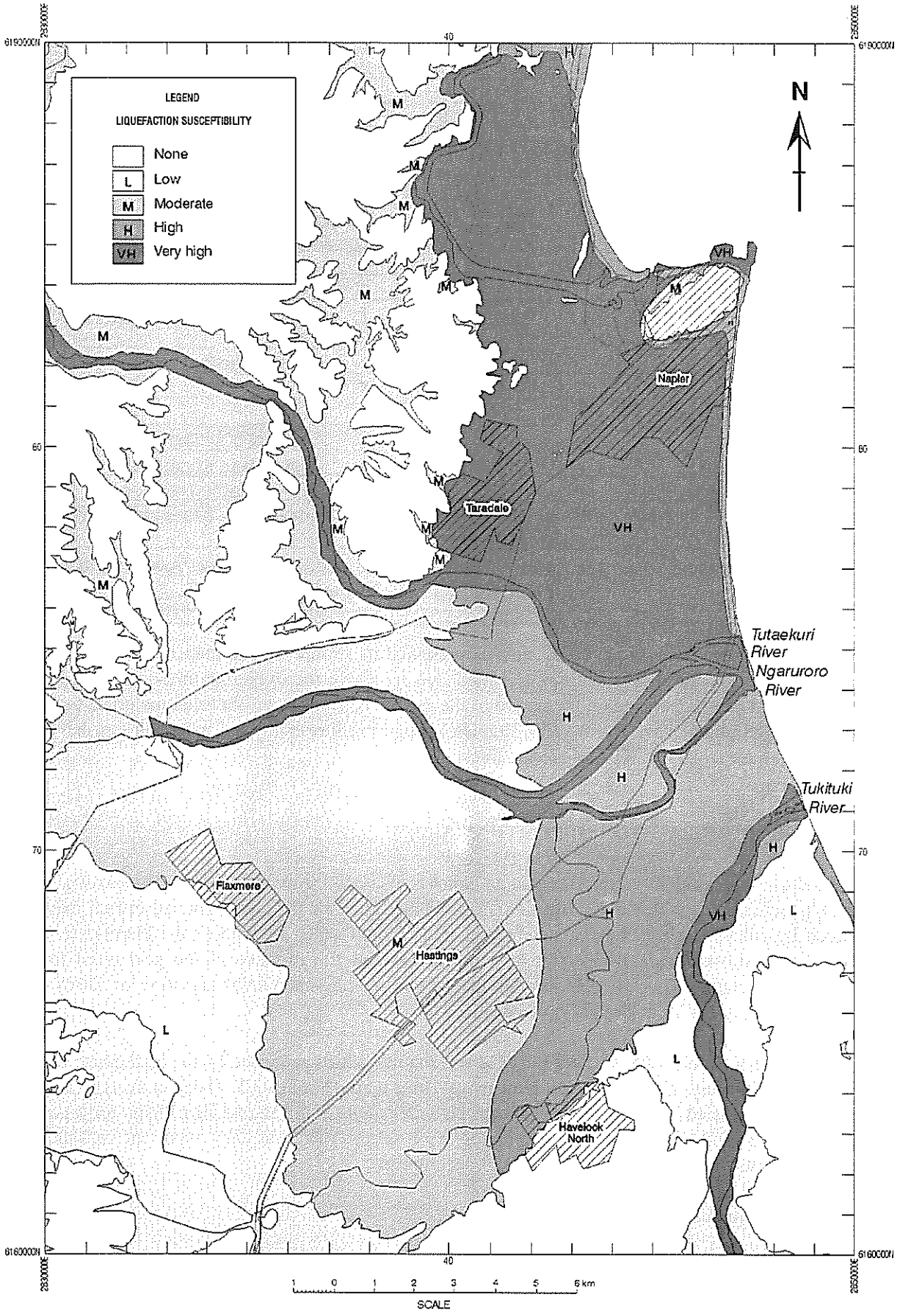

Figure 2. Liquefaction Susceptibility Map of the Heretaunga Plains, Hawke's Bay.

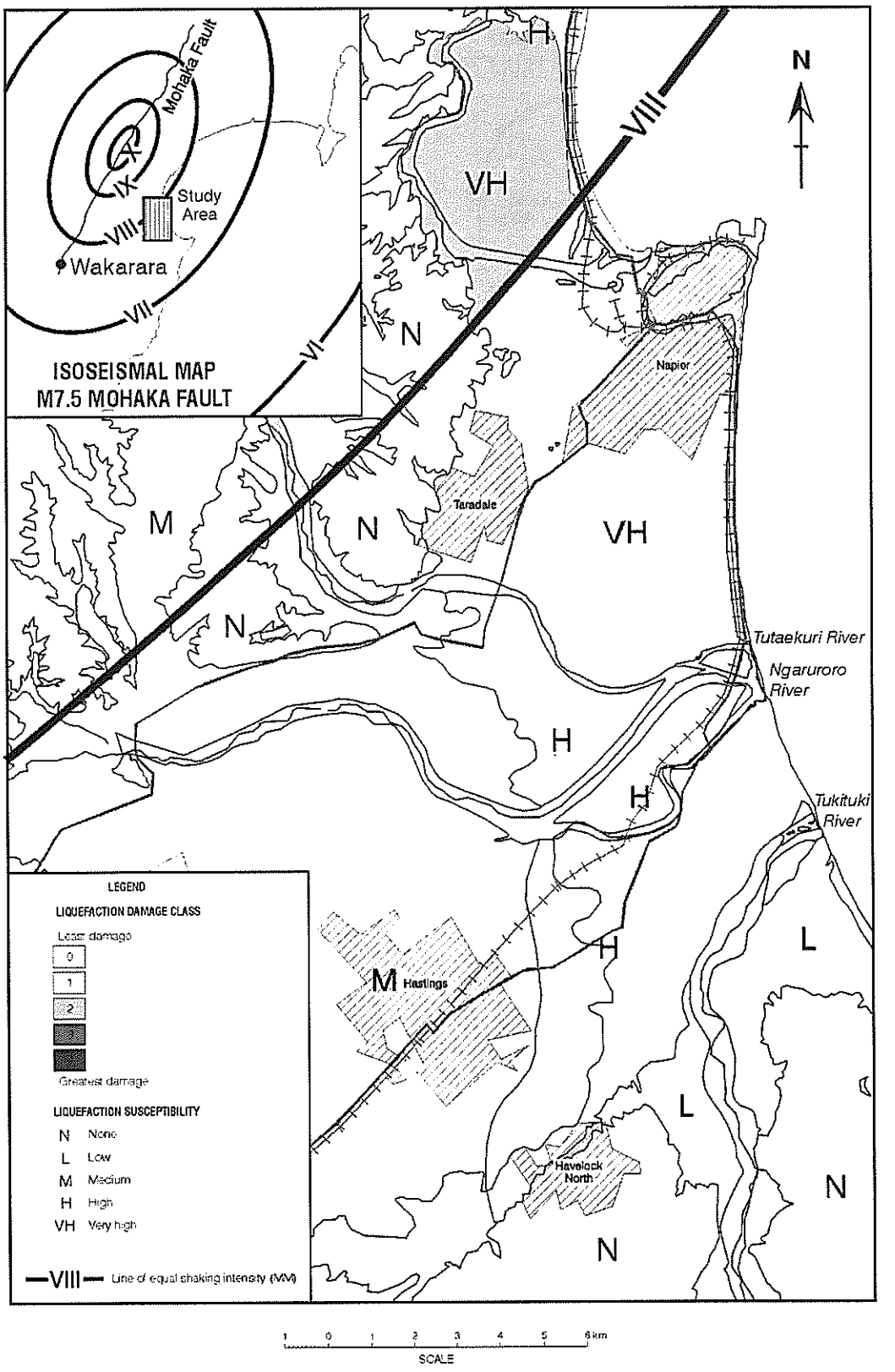

Figure 3. Liquefaction Damage Map of the Heretaunga Plains, Hawke's Bay for a Shallow, Magnitude 7.5 Earthquake on the Mohaka Fault.

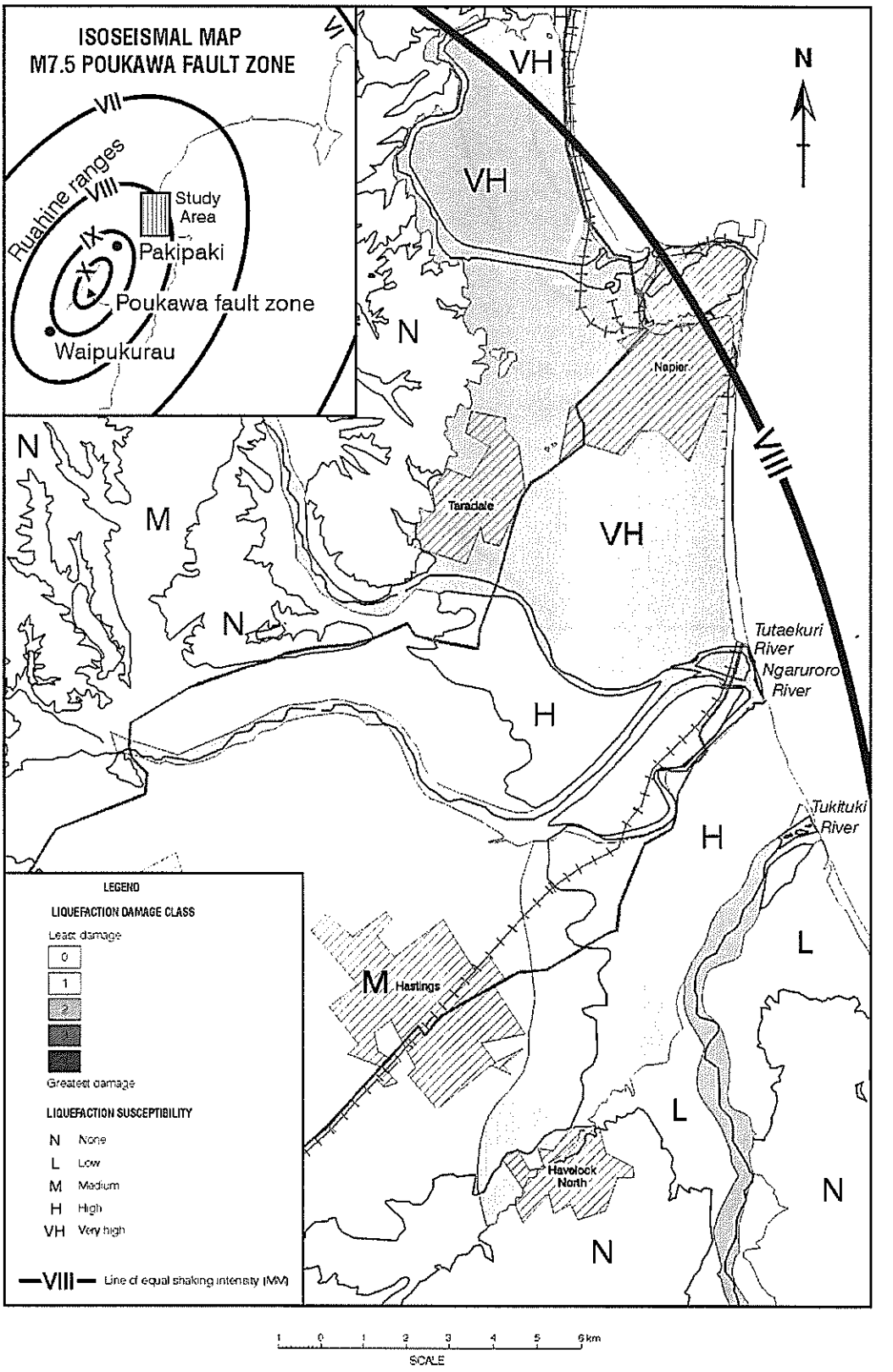

Figure 4. Liquefaction Damage Map of the Heretaunga Plains, Hawke's Bay for a Shallow, Magnitude 7.5 Earthquake on the Poukawa Fault.

Although a large earthquake has not occurred on the Mohaka fault in historical times, geological evidence indicates of late Cenozoic and Quaternary deformation. Raub *et al* (1987) conclude that events on the Mohaka fault have a recurrence interval of *c.* 1000 years. The average right lateral slip rate of the Mohaka fault is about 3 mm/year. Radiocarbon dating of wood fragments from a trench across the fault in the Wakarara area indicates that the last surface rupture is less than 1200 years old (Raub *et al,* 1987). A magnitude 7.5 earthquake on this fault has been selected because previous work (Hancox and Berryman, 1986) has estimated that this is a realistic Maximum Credible Earthquake.

This earthquake would generate MM8 in the northwestern part Heretaunga Plains and MM7 in the southeast (Figure 3). In the MM8 zone, geological units with a very high susceptibility to liquefaction are expected to produce ground damage equivalent to liquefaction damage rating 2, and those units with a high susceptibility would produce ground damage equivalent to liquefaction damage rating 1. In the MM7 zone only the geological units with a very high susceptibility to liquefaction are expected to produce ground damage (liquefaction damage rating 1). All other areas are unlikely to experience liquefaction-induced ground-damage during this scenario.

Poukawa Earthquake Scenario

The Poukawa fault zone extends from Waipukurau to Pakipaki. The surface expression of the Poukawa fault zone is approximately 35 km long and trends parallel to the Ruahine Range that lies approximately 30 km to the west. The geological evidence of past earthquakes indicates that the fault has a dominant reverse style of deformation (Kelsey *et al* 1998). Paleoseismic investigations along the fault suggest a recurrence interval for large surface rupturing earthquakes of about 3000 to 7500 years (Kelsey *et al* 1998). The M_S 7.8, 1931 Napier earthquake occurred along the northern projection of the Waipukurau-Poukawa fault zone, on the Napier-Hawke's Bay fault segment. This earthquake and evidence of several past earthquakes indicate that this fault zone is capable of producing large damaging events (Kelsey *et al* 1998). Because the 1931 event probably released most of the strain along the Napier/Hawke Bay segment of the Waipukurau Poukawa fault zone, the next closest segment of the fault zone to the Napier-Hastings area was selected as an appropriate earthquake scenario.

A magnitude 7.5 earthquake has been selected as a realistic scenario for the Poukawa fault. As shown on Figure 4, this event would generate MM8 throughout most of the Heretaunga Plains with the MM shaking intensity attenuating to MM7 in the northeast. In the MM8 zone geological units with a very high susceptibility to liquefaction are expected to produce ground damage equivalent to a liquefaction damage rating of 2, and those units with a high susceptibility would produce ground damage equivalent to a damage rating of 1. In the MM7 zone only the geological units with a very high susceptibility to liquefaction are expected to produce ground damage, with a liquefaction damage rating of 1. All other areas are unlikely to experience liquefaction-induced ground-damage in this scenario.

LIMITATIONS, CONCLUSIONS & RECOMMENDATIONS

A general assessment of the susceptibility to and likelihood of soil liquefaction effects and ground damage on the Heretaunga Plains in the Hawke's Bay region has been made. The maps from this assessment provide a basis for broad regional engineering and planning, but are not intended for use in place of site-specific investigations. Site-specific geotechnical investigations should be carried out in accordance with the generally accepted standards of practice for important and/or sensitive facilities located in areas that are susceptible to liquefaction.

The historical earthquake record for the Hawke's Bay region shows that liquefaction phenomena have occurred during strong ground shaking of at least MM7. At higher shaking intensities (MM8 – MM10) the occurrence of liquefaction phenomena becomes progressively more widespread and potentially more damaging in the more susceptible areas.

Priority should be given to compiling and maintaining a database of subsurface geotechnical information. The collection and collation of geotechnical data would allow identification of the geotechnical parameters

controlling liquefaction in each of the susceptibility classes to be quantified. This would enable future refinement of the liquefaction hazard model for the Heretaunga Plains.

ACKNOWLEDGEMENTS

GNS acknowledges the support and assistance of the Hawke's Bay Regional Council and the Wanganui District Council for their assistance during this study. The authors thank Gaye Downes for her help providing historical information. Reviews by John Scott, Mauri McSaveney and Gaye Downes helped in ensuring consistency and clarity in the text.

REFERENCES

Dowrick, D.J., Rhoades, D.A., 1999: Attenuation of Modified Mercalli Intensity in New Zealand Earthquakes. *Bulletin of the New Zealand Society for Earthquake Engineering 32(2)*: 55-89.

Dravid, P.N., and Brown, L.J., 1997: Heretaunga Plains groundwater study: Hawke's Bay Regional Council and Institute of Geological and Nuclear Sciences; 2 volumes.

Hancox, G.T., and Berryman, K.R., 1986:Interim assessment of seismotectonic hazards at possible hydro-electric power development sites on the Mohaka River, Hawke's Bay. *EG Immediate Report 86/036, New Zealand Geological Survey, 39p.*

Hancox, G.T., Perrin, N.D., and Dellow, G.D., 1997: Earthquake-induced landsliding in New Zealand and implications for MM intensity and seismic hazard assessment. *GNS Client Report 43601B, December 1997.*

Kelsey, H.M., Hull, A.G., Cashman, S.M., Berryman, K.R., Cashman, P.H., Trexler, J.H. (Jr.), and Begg, J.G., 1998: Paleoseismology of an active reverse fault in a forearc setting: the Poukawa fault zone, Hikurangi forearc, New Zealand. *Geological Society of America Bulletin 110(9)*: p1123-1148.

Raub, M.L., Cutten, H.N., and Hull, A.G., 1987: Seismotectonic hazard analysis of the Mohaka Fault, North Island, New Zealand. *Proceedings of the South Pacific Regional Conference on Earthquake Engineering (January 1, 1987)*

Tinsley, J.C.; Youd, T.L.; Perkins, D.M.; and Chen, A.F.T., 1985: Evaluating Liquefaction Potential: in Evaluating earthquake hazards in the Los Angeles Region, J.I. Ziony ed.: US Geological Survey Professional Paper 1360: 263-316

Youd, T.L., Nichols, D.R., Helley, E.J., and Lajoie, K.R., 1975: Liquefaction potential. *US Geological Survey Professional Paper* (January 1, 1975)

Youd, T.L., and Hoose, S.N., 1978: Historic ground failures in northern California triggered by earthquakes. *US Geological Survey Professional Paper 1978: 177 p*

Ziony, J.I., 1985: Evaluating earthquake hazards in the Los Angeles Region; US Geological Survey Professional Paper 1360 pp.

Foundations and Ground Replacement Taranaki Combined Cycle Power Station

G Saul
BE (Hons), MSc (Lond), DIC, MIPENZ, Regd Engr
Senior Geotechnical Engineer, Opus International Consultants Ltd, Wellington
D Jennings
BE(Hons), MSc (Lond), DIC, FIPENZ Regd Engr
Chief Operating Officer, Opus International Consultants Sdn Bhd, Kuala Lumpur

Abstract: The natural gas fuelled, 360 MW, Taranaki Combined Cycle Power Station is constructed on the volcanic ring plain surrounding Mount Taranaki, a dormant volcano in the North Island of New Zealand. The underlying geology comprises tephra including volcanic ash and grits, lahar deposits and organic lenses. The groundwater level was indicated to be within 3m of the ground surface. The main power train was to be founded on a 59 m long and 11 m to 30 m wide monolithic foundation, which was very sensitive to differential settlement.

This paper describes geotechnical aspects of the project including investigations, assessment of foundation settlement and liquefaction risk. In addition to analysis of the fines content and particle sizes of the deposits, geotechnical assessment of liquefaction risk included the Sugawara and seismic shear wave velocity methods. The effects of both earthquakes and the dynamic loads from the power plant were considered.

Settlement performance was influenced by the presence of organic sediments within the complex volcanic deposits. The overlying laharic deposits and short construction time precluded piling and ground replacement was adopted to manage the settlement risk.

Aspects of the ground replacement with selected granular fill from andesitic rock sources and compaction control during construction are discussed.

INTRODUCTION

Opus International Consultants were commissioned by ABB Power Development to carry out site investigation and foundation assessment for a 360 MW combined cycle gas turbine power plant at Stratford in Taranaki. This work followed on from the involvement that Opus had with the site development feasibility investigations.

The site was adjacent to the Stratford Power Station located on East Road (SH43) to the east of Stratford township. The site (Figure 1) is relatively flat and the small Kahouri Stream separates the two power plants. The Kahouri stream is incised some 8 m below the surrounding ground and the bed comprises boulders of up to 0.5 m in size.

The site is located on a gentle dipping radial plain on the south eastern side of Mount Taranaki, a volcano cinder cone. The site is underlain by, volcanic deposits from successive ring plains formed around the volcano. The ring plain formation comprises thick inter-bedded sequences of detrital volcano-clastics, including tephra, lahar, debris avalanche material, breccia, conglomerates and other intermixed terrestrial sediments and organic deposits.

Seven significant earthquakes (Richter Magnitude >5) have occurred within 50 km of the site in historical times (since 1850) and the region is therefore considered to be reasonably seismically active. The nearest faulting is the Norfolk / Inglewood fault system which is 17 to 22 km from the site. Previous earthquakes of moment magnitude Mw = 7.1 are estimated to have occurred on this fault system in the past and a recurrence interval of about 4,000 years was estimated in a seismic hazard study carried out for the plant, by the Institute for Geological and Nuclear Sciences.

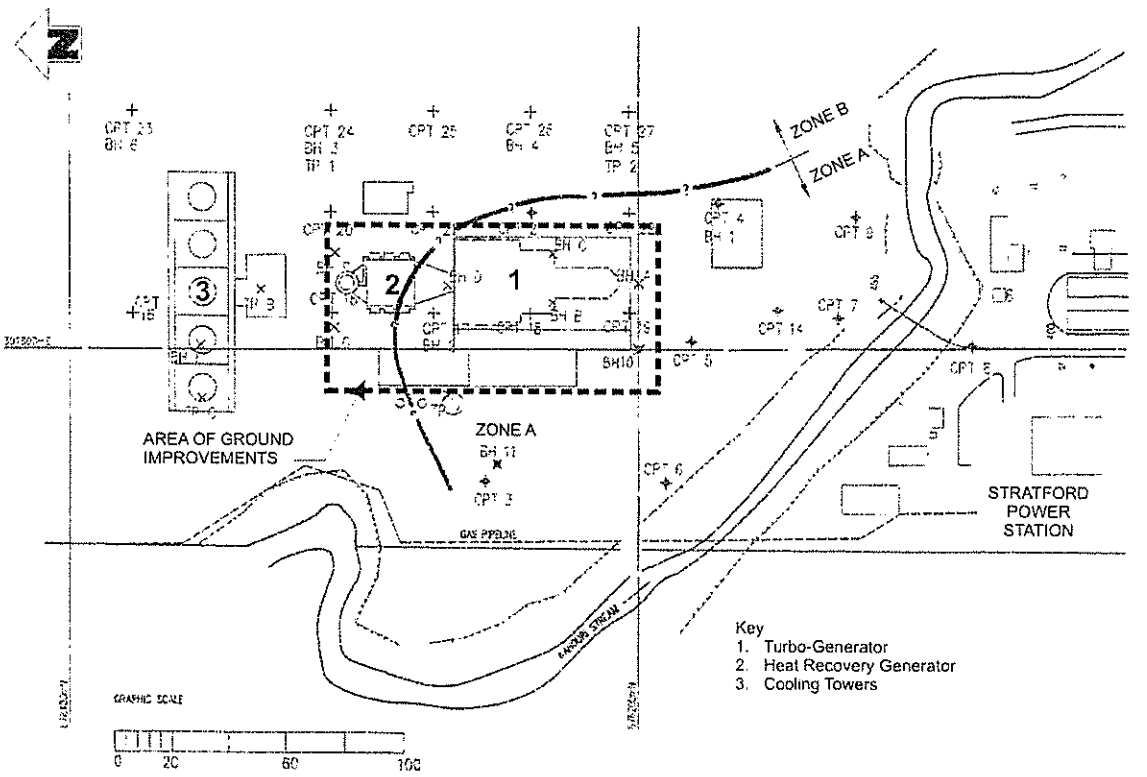

Figure 1. Site Plan.

The proposed structure foundations were designed for the following peak ground accelerations :

- Operating Basis Earthquake (OBE) a max = 0.31g
- Maximum Design Earthquake (MDE) a max = 0.48g

A key feature of the plant was the continuous shaft of about 59 m in length, which demanded tight settlement control. The turbo generator foundation was between 11 m and 30 m wide. The adjacent heat recovery steam generator foundation was 38 m long and 15 m wide.

The plant involved foundations and structures for the main turbo-generator train, heat recovery steam generator (Figure 2), feed water tank and pumps, mechanical draft cooling tower and water pump building, plus a number of ancillary structures.

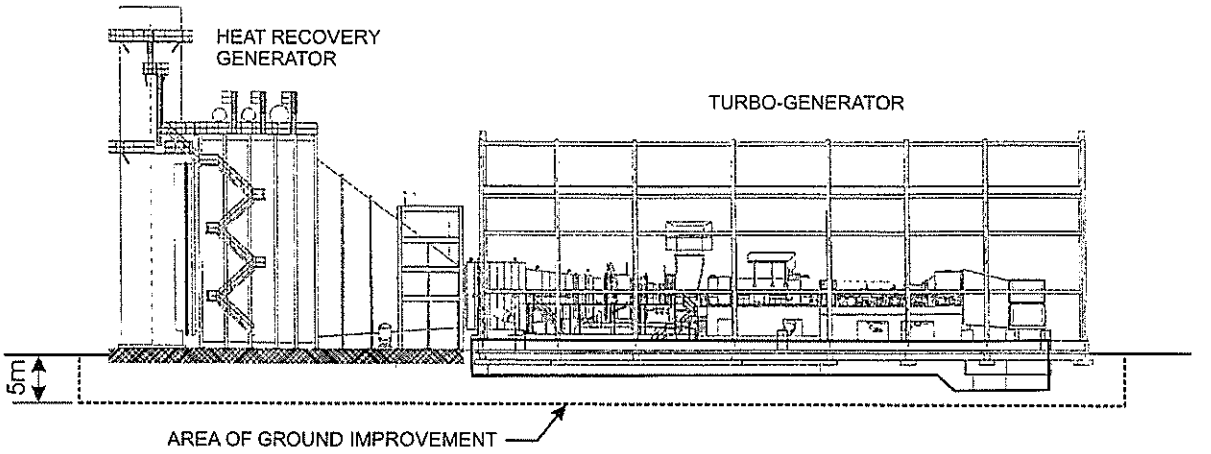

Figure 2. Section Through Main Plant.

SITE INVESTIGATIONS

Site investigations commenced in 1993, and were carried out in a number of stages associated with the development feasibility assessment and the subsequent design. The investigations comprised:

- 11 cored boreholes of up to 20 m depth, but with one to 41 m depth
- 32 Dutch Cone Penetrometer tests (CPT)
- 2 downhole seismic shear wave tests and 2 cross hole seismic tests
- Monitoring of groundwater levels in piezometers installed in 3 boreholes for up to 1 year

Laboratory testing including:

- Water content and compaction tests
- Consolidated undrained triaxial tests for shear strength
- Index tests (particle size analysis and Atterberg limits)
- Oedometer tests to determine consolidation characteristics

Further investigations were undertaken immediately prior to construction to evaluate material sources for the ground replacement under the turbo-generator foundation.

GROUND AND GROUNDWATER CONDITIONS

The stratigraphy was fairly uniform across the site and comprised two units; "Taranaki Brown Ash" and "Inter-bedded Ash and Laharic Materials". These surface materials and the topography of the site were significant in the initial site development planning and the selection of development platforms.

Taranaki Brown Ash is a generic term applied to the surface deposits of ash and lappilli found throughout the Taranaki Region. At the site this varied from 1.5 m to 3.2 m in thickness and consisted of silt and sandy silt. It was indicated to be soft to firm (Su = 30 to 60 kPa), highly plastic (PI = 50%) and sensitive to disturbance. The oedometer tests indicated a preconsolidation pressure of 280 to 520 kPa, indicating an apparent over consolidation ratio of greater than 10 and a volume compressibility (m_v) of 0.3 m^2/MN for the 10 to 100 kPa vertical effective stress range. The over consolidation ratio is inconsistent with the lack of any geological evidence for previous surcharging but is consistent with other studies in Taranaki Brown Ash (e.g. Millar, 1986). Dynamic stiffness properties at small strain were interpreted from the typical shear wave velocities in this material of 70 – 130 m/s, including shear modulus G of 7 to 17 MPa and an undrained modulus of elasticity E_u of 20 MPa.

The "Inter-bedded Ash and Lahar" underlies the Taranaki Brown Ash and continues down to the base of the investigation boreholes. It generally consists of inter-bedded layers of silt / silty sands and gravelly sands / sandy gravels which are inferred to be Ash (possibly re-deposited), organic silts and lahar. Presence of lahars is clearly apparent from the boulder deposits in the bed of the adjacent Kahouri stream. The organic silt was indicated to be soft and hence was assessed to be normally consolidated. The age of these deposits is indicated as 11,700 years BP from carbon date testing of wood fragments recovered from the foundation excavation some 8 m below natural ground level.

To the south and west of the site (Zone A, Figure 1), where the turbo-generator base was located, sandy gravels predominate with few layers of sandy silts / silty sands of between 0.3 to 2.0 m thickness, and soft organic silt of 0.6 m to 1.5 m thick. Loose to medium dense sands and sandy gravel layers of up to 2 m thick were encountered under the surface ash in the vicinity of the turbo-generator base.

To the east and north of the site (Zone B, Figure 1) sandy silts / silty sands predominate with some isolated layers of sandy gravels / gravelly sands of up to 2 m thickness. Occasional cobbles and boulders of andesite are encountered below 11.5 m depth in the south and west of the site.

Water levels were indicated to vary seasonally between 1.5 m and 4.0 m below ground level. (which was surprising given the adjacent incised Kahouri Stream).

GEOTECHNICAL ASSESSMENT

The main geotechnical issues affecting design of the power plant included settlement of foundations and in particular differential settlement of the sensitive turbo-generator foundation, and liquefaction potential under the design earthquake.

Foundations

The three main items of plant, the gas turbine, generator and steam turbines were to be supported on a rigid foundation slab varying in width between 30 m for the gas turbine to 11 m, which apply between 50 kPa and 100 kPa of load to the foundations under static conditions. A maximum acceptable differential settlement of 20 mm between the Turbo-Generator power train end of the foundation and the heat recovery steam generator end was adopted.

Machinery loads were supplied by ABB for the main items of plant. Seismic inertia forces were calculated for the MDE ($a_{max} = 0.48g$).

Ground conditions in the immediate vicinity of the turbo-generator train, were defined by 6 boreholes. The ground conditions varied between the north and south end of the slab particularly in the upper 6 m. The shallow foundation slab would be located on gravelly sands at the southern end (BH10, BHA) and on sandy silts at the northern end (BH2, BHD). Settlement of the slab located on these materials would vary from 20 to 60 mm, giving an unacceptable level of differential settlement.

The issues associated with static settlement were considered together with options to address seismic liquefaction issues (discussed below) in selecting the foundation solution.

Liquefaction Hazard

Young, ie. <10,000 years, saturated sands and silty sands are typically associated with liquefaction. Earthquake induced ground shaking causes pore water pressures to increase and, as the pore water pressures approach the soil confining stresses, the soil loses strength leading to liquefaction and associated settlement.

The susceptibility of a soil deposit to liquefaction is dependent upon a number of factors including soil particle size distribution, density, in-situ stresses, groundwater conditions and the duration and intensity of ground shaking expected at the site. The potential for liquefaction at the Taranaki Combined Cycle site was assessed recognising that:

- Loose to medium dense gravelly sands occur in part of the upper 20 m of the ground profile,
- Groundwater is encountered at a shallow depth of 2 m to 4 m below the original ground surface and water levels may rise by up to 2 m in winter,
- The Taranaki area is subject to strong seismic shaking.

The site is underlain by at least 43 metres of moderately dense sediments. It is therefore considered that the site would be classified as "intermediate" based on the criteria outlined in NZS 4203 (Standard New Zealand, 1992) and that amplification of basement rock shaking is unlikely to occur.

A liquefaction assessment was carried out for the site based on the results of all site investigations, and the design ground shaking, assuming a magnitude M7 earthquake. The assessment is summarised in Table 1 and was based on the following information :

- groundwater level

- Particle size and Plasticity
- SPT "N"
- CPT data (Sugawara , 1989)
- Shear wave velocity, (National Research Council, 1985)
- Geological observations

The assessment identified some layers of loose silty sands and soft sandy silts up to 3m thick between 1.5 m and 5.5 m depth below the Turbo-Generator in Zone A that were potentially liquefiable. Typical fines contents were indicated to be in the range of 30% to 50% and did not preclude liquefaction. The risk to the foundations was assessed to be low in the operating basis earthquake and moderate in the maximum design earthquake.

The risk of liquefaction at depths of greater than 6 m in Zone A was assessed to be very low in the operating basis earthquake and low in the maximum design earthquake. The risk was considered to be sufficiently low that ground damage would not be expected.

Based on the various analyses it is considered that some liquefaction was also possible in Zone B at the northern and eastern end of the site, and a moderate risk of liquefaction was assessed.

The Heat Recovery Generator structure, Mechanical Draft Cooling Tower Structure and associated water pump house were the main structures in Zone B. A number of pipes and services also run between structures. The moderate level of risk of liquefaction and the indicated level of subsidence suggested that consideration should be given to mitigating the risk of liquefaction induced ground damage to the Heat Recovery Generator and any other important plant and services.

Foundation Strategy

The investigations indicated variable founding conditions both in depth and areal distribution and the site was categorised into two areas of relatively consistent soil and foundation characteristics Zone A and Zone B (Figure 1).

The most important structures are, the Turbo-Generator building located within Zone A, and the Heat Recovery Generator located in the transition area between Zone A and Zone B.

Zone A had variable loose/medium dense soils down to a maximum of 6 m depth overlying dense to very dense sandy gravels. The soils in the upper 6 m had both significant static settlement potential and subsidence potential due to liquefaction under seismic loading.

Mitigation options were considered for the soil below the Turbo-Generator and Heat Recovery Generator structure including:

- Dewatering the site to greater than 6 m depth. This would have to be maintained in the long term and would induce soil settlement which would influence the performance of the structures.
- Short piled foundations of about 10 m depth.
- Excavate the foundations to a depth of about 5 m and replace with compacted rock fill below the main structures. An extension of this treatment involving excavation to 2 m depth and replacement over the remainder of the platform was also considered which would remove some of the silty sands.
- Provide a cellular wall foundation system founded on dense sandy gravels at a depth of about 6 m.
- Ground improvement with stone columns down to about 6 m depth.

Ground improvement involving removal and replacement was assessed to be the most cost effective for the main Turbo-Generator and Heat Recovery Generator buildings. Also, subsoil drainage could

be incorporated at the base of the excavation, with gravity drainage to the Kahouri Stream to provide additional protection for the area of ground improvement and the wider area influenced by drainage.

It was proposed that the soils in the upper 5 m be excavated and replaced to provide a reliable foundation for the Turbo-Generator and the Heat Recovery Generator structures. Time, cost and risk issues were critical in the foundation decision. Piling was rejected because of delivery time and pile driving uncertainty. Ground replacement for the turbo generator foundation involved the replacement of some 40,000 m^3 of foundation soils to RL 263 m, 5 m depth below the construction platform (Figure 2). The actual depth was locally adjusted to ensure removal of any soft organic silt near the base of the proposed excavation, as this was a significant contributor to the assessed foundation static settlement.

It was considered that the anticipated seismic risk and displacements were acceptable for the ancillary structures and raft/footing foundations were adopted. Footings for individual structures were tied together for continuity.

GROUND REPLACEMENT CONSTRUCTION

Ground replacement for the Taranaki Combined Cycle Power Plant was a critical path activity. Sourcing and proving of the ground replacement granular fill took place in parallel with the excavation of the site. Final selection of the fill materials was made after a compaction trial was undertaken at the base of the excavation.

The ground replacement was required to deliver an elastic modulus of greater than 35 MPa when measured by plate bearing tests. The challenge was to provide a compaction specification that would deliver this performance when the actual materials were up to 65 mm in size (AP65) and were too large for conventional laboratory tests, which were typically limited to a maximum size of 19 mm (AP19).

Several local andesite rock sources were used to achieve the delivery supply rates necessary to meet the construction schedule. The compaction trial included field compaction and plate bearing tests of both AP19 and AP65 materials. This indicated satisfactory performance of the larger AP65 material. The use of material with larger particle sizes than those tested in the laboratory required an adjustment in the target field densities to ensure that the performance targets were met. Theoretical target densities were calculated (Jennings et al., 1998) to allow for the higher percentage of stone in the actual fill and were higher than the results achieved on the AP19 fraction in the laboratory. The contractor consistently achieved 100 to 108% of the laboratory maximum dry density (based on AP19) and exceeded the target of 98% NZ Heavy Compaction (NZS 4402:1986), but was typically only 90% or more of the theoretical maximum dry density.

The critical performance parameter for the ground replacement was the achievement of an elastic modulus, which would provide the required settlement performance. A series of plate bearing tests on the completed fill surface demonstrated modulus values well in excess of the 35 MPa required. The reload cycle of all plate bearing tests exceeded 80 MPa and were considered more representative than the initial load cycle because initial bedding effects were removed.

A permanent deep drain geotextile wrapped gravel drain was installed around the perimeter of the excavation with gravity drainage to the adjacent Kahouri Stream. The drainage had a site wide influence on ground water levels and provides a measure of liquefaction mitigation for the secondary components of the station.

CONCLUSIONS

From this project a number of interesting aspects related to geotechnical engineering in volcanic terrain have been reinforced:

- The volcanic brown ash soils exhibit a high OCR, which is inconsistent with their geological setting. Soft organic silt layers were encountered at 3 m to 8 m depth and are considered to be normally consolidated.
- The soils are geologically recent. This was confirmed by the age (11,700 years BP) of wood fragments recovered from the foundation excavation some 8 m below natural ground level.
- The soils of the Taranaki ring plain are a complex mix of airfall, fluvial, lahar and organic materials and while some of the materials such as Taranaki Brown Ash are liquefaction resistant, others such organic silts and sandy laharic deposits could liquefy in large earthquakes.
- The combined cycle power station presented demanding settlement performance requirements related to the long continuous turbine shaft configuration. Uniform foundation performance was critical.
- Practical construction considerations, including time, are important in the consideration and selection of foundation solutions, particularly when the ground conditions are complex.
- The ground replacement for the turbo-generator foundation is one of the largest projects of this nature in NZ involving 40,000 m^3 of excavation and controlled replacement.
- Construction of deep granular fills requires careful specification and construction quality control to achieve the performance required.
- Ground replacement proved to be an effective solution. which has delivered the necessary performance for the power station.

ACKNOWLEDGEMENTS

The authors acknowledge the inputs of ABB and other Consultants involved in the design of the Taranaki Combined Cycle Power Station. The views represented in this paper are those of the authors and do not necessarily represent those of ABB Power Development or Opus International Consultants Ltd. The authors wish to thank Natural Gas Corporation. the current owners of the plant, for permission to publish this paper.

REFERENCES

Burland, J.B. and Burbridge, M.C. (1985) " Settlement of Foundations on Sand and Gravel" Proceedings of the Institute Civil Engineers.

Jennings, D.N, Cunningham, J.K, and Thrush, M. (1998): "Practical Aspects of Basecourse Construction Control" Proc Roading Geotechnics 1998, NZGS Symposium, Auckland 1998.

Millar, P.J. (1986). "Taranaki Brown Ash: A Discussion of the influence of Iron Oxide Bonding on Engineering Performance " Ministry of Works and Development, Central Laboratory Report.

National Research Council , (1985) "Liquefaction of Soils During Earthquakes" National Academy press Washington DC.

Standards New Zealand, (1992) "NZS4403: Code of practice for general Structural Design and design of Loadings for Building".

Sugawara ,N. (1989). "Empirical Correlation of Liquefaction Potential Using CPT" Int. Conf. Soil Mech. & Foundation Engineering, Vol 12, No1.

The Design and Construction of a Bridge with MSE Abutments on Seismically Liquefiable Ground

K-C Cheung
PhD, MEng, BSc, MIPENZ, MASCE
Director, Peters and Cheung Ltd
D Peters
BScEng, MIPENZ
Director, Peters and Cheung Ltd
A Blackler
BEng
Engineer, Fletcher Construction Ltd

Abstract: The Tahuna Road Bridge is part of the State Highway 1 Rangiriri to South of Ohinewai Four-Laning project south of Auckland. The bridge crosses the future motorway over seismically liquefiable ground near Ohinewai. Mechanically stabilised earth [MSE] abutments provide shallow founding for the bridge. A low-displacement Y-shape vibratory probe was used to densify the sandy soil underlying the bridge site to a depth of 6~8m to satisfy the seismic design requirements of the Transit New Zealand Bridge Manual. It is the first time that resonant vibratory compaction technique using a low-displacement probe has been employed on a relatively large scale for a bridge project in New Zealand. The successful application of a resonant vibratory probe on the project demonstrated that it is significantly more economical than other ground improvement methods commonly used in the country. The paper presents the design considerations and construction methodologies for the ground improvement and MSE abutments works. Construction aspects are also discussed.

INTRODUCTION

The Tahuna Road Overbridge forms part of the Transit New Zealand State Highway SH1 Rangairiri to South of Ohinewai Four Laning (RSO4L) design-construct contract which was awarded to the Fletcher Higgins Joint Venture.

The site is situated near Ohinewai about 70km south of Auckland and 30km north of Hamilton. The overbridge is a slightly skewed two 19m spans bridge designed to carry 2 lanes of rural traffic over the new four lane SH1 currently under construction. The site is underlain by an alluvial deposit of over 40m thick which is susceptible to seismic liquefaction.

Fletcher Higgins, on the advice of Peters and Cheung Ltd acting as a sub-consultant to the lead consultant, Sinclair Knight Merz, made the decision to use the resonant vibratory compaction technique and a Y-shape low-displacement vibratory probe for the first time on a large scale in New Zealand to treat the liquefiable bridge foundation soils. The foundation improvement works, combined with the use of spread footing and two 8m high mechanically stabilised earth (MSE) bridge abutments, provide founding for the bridge and eliminate the need to pile foundations. A typical cross section of the bridge is shown in Figure 1.

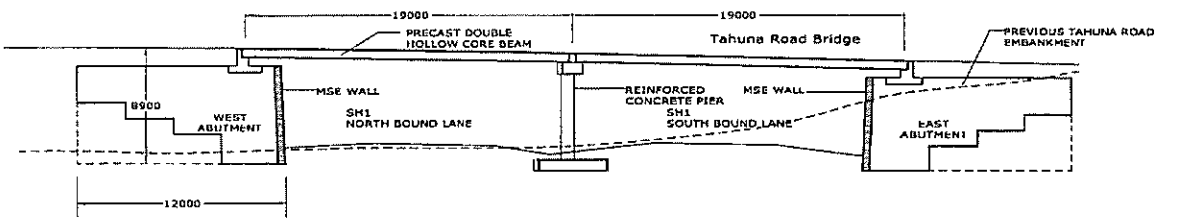

Figure 1. Typical Cross Section of Tahuna Road Overbridge Crossing State Highway SH1

The resonant vibratory compaction technique was found to be effective and economical for the ground conditions at the bridge site. The ground treatment of 1700m^2 area to 6~8m depth was completed within 18 days. The two 8m high Keystone MSE bridge abutments reinforced by steel ladders were founded within the densified area. Extra seismic safety measures in addition to the New Zealand Bridge Manual requirements were incorporated into the bridge and abutment design by adopting the Limited Permanent Displacement Design Concept. The paper presents the design considerations and construction methodologies for the ground improvement and MSE abutments works.

GROUND CONDITIONS

The site is underlain by over 40m thick of alluvial deposits with firm to stiff silt and clay generally present below 18m depth. The upper 6m of the soils are relatively recent, loose, fine gained, pumiceous sands. A layer of medium dense pumiceous sands which slightly increases in strength with depth is present between the upper loose sand and the lower silt and clay layers. Table 1 presents a summary of the typical soil profile of the site and the soil properties in terms of cone penetration resistance, qc, and friction ratio, R_F. Ground water surface is present at about 1.5m below the ground surface in summer lifting to within 0.5m in winter.

Depth (m)	Soil Description	CPT Measurement
0 - 3m	Light brown, fine grained, pumiceous sand	qc = 1 ~ 3MPa R_F = 0.5<~ 0.8%
3 - 6m	Grey, fine grained, loose, pumiceous sand interbedded by thin layers of sandy silt between 4.5m and 6m	qc = 2 ~ 3MPa R_F = 1<~ 1.5% (Generally 1%, except thin silt layers > 2%)
6 - 8m	Grey, dense, pumiceous sand	qc = 8 ~ 10MPa R_F = 1%
8 - 18m	Grey, medium dense, pumiceous sand	qc = 4 ~ 10MPa R_F = 0.5%
Below 18m	Firm to stiff silt and clay	qc = 1 ~ 3MPa R_F = 3 ~ 4%

Table 1. Typical Soil Profile at Tahuna Bridge Site

SITE SEISMICITY

At the request of Peters and Cheung Ltd, the Institute of Geological and Nuclear Sciences undertook a site specific seismicity assessment of the bridge site. Ohinewai is located about 30km north of Hamilton and is located within a moderately low seismic region in New Zealand. Key findings from the assessment were that (i) the site is not susceptible to fault movement related earthquake shaking and (ii) the seismicity of the site for the 475 year and 700 year return period earthquakes is similar and is mainly contributed from earthquakes with local magnitudes in the range of M_L 5.25 to 6. Furthermore, the estimated peak ground accelerations, a_{max}, are in the range of 0.1 ~ 0.2g.

SELECTION OF SEISMIC DESIGN CRITERIA

In accordance with Transit New Zealand Bridge Manual, the Tahuna Overbridge is considered as a motorway structure. In the project, we have chosen the following seismic design criteria for the design of the bridge structure and its abutments.

(i) Serviceability Limit State - M_L 6 & a_{max}= 0.12g, 150 years earthquake return period
(ii) Ultimate Limit State - M_L 5.5 & a_{max} = 0.22g, 475 years earthquake return period
(iii) 1000 years earthquake return period - M_L 6 & a_{max} = 0.22g

LIQUEFACTION ASSESSMENT

The key findings from our liquefaction assessment of the project site are summarised below.

- Serviceability limit state
  - The site is not susceptible to seismic liquefaction during earthquakes with a 150 year return period.
- Ultimate limit state
  - Under no surface surcharge loading condition, the pumiceous sands at 3m-6m and 8m-14m depths are subject to liquefaction or exhibit a marginal factor of safety against liquefaction.
  - Under a 8m high bridge abutment surcharge loading condition, the entire soil profile exhibits a factor of safety against liquefaction, FoS, of generally above 1.5.
- 1000 years earthquake return period
  - Under no surface surcharge loading condition, the soil layers at 3m-6m and 8m-14m depths are subject to liquefaction.
  - Under 8m high bridge abutment surcharge loading condition, the soil layer at 3m-6m depth is subject to liquefaction while the material at 8m-14m generally has a FoS in the range of 1.2-1.5 against liquefaction.

The results above suggest that ground improvement is required to minimise the effect of liquefaction on the performance of the bridge structure and the abutments. Methods for liquefaction assessment for deriving the above conclusions are presented below.

Estimation of Liquefaction Resistance of Soils

Figure 2, NCEER (1997), presents a commonly used CPT cone penetration resistance-based chart for the estimation of liquefaction resistance of clean sands with less than 5% fines content. The data in the chart presents a co-relationship between the capacity of the soil to resist liquefaction, expressed in terms of the Liquefaction Cyclic Resistance Ratio (CRR_1) and the Normalised Cone Resistance (qc_1) for earthquakes with local magnitude (Richter magnitude), M_L, of 7.5. The subscript 1 following CRR and qc denotes their, respectively, equivalent values at a vertical effective stress σ'_v of 1 atm unit (1atm $\approx$ 100kPa). For normally consolidated sand deposits, (qc_1) can be calculated from (qc_1) = qc / $(\sigma'_v)^{0.7}$. It is noted that both qc and σ'_v are given in terms of atm units.

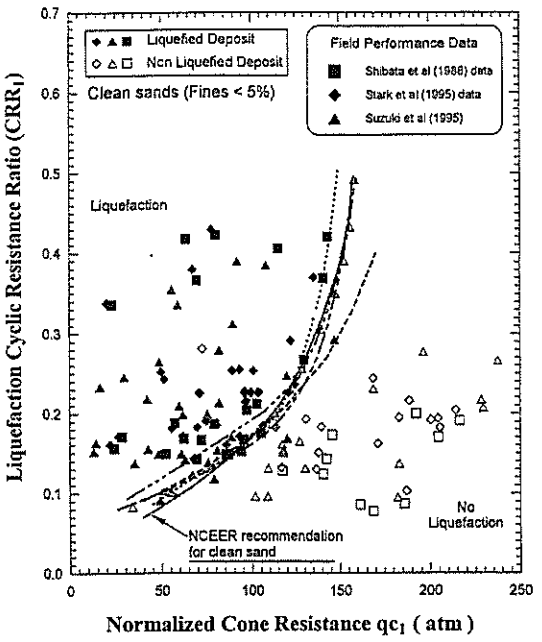

Figure 2. CRR_1 vs qc_1

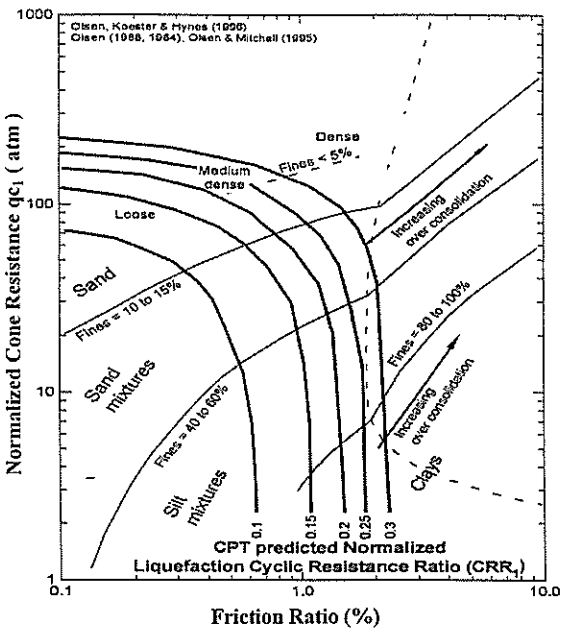

Figure 3. CRR_1 based on Both qc_1 and R_F

Artificial boundary lines proposed by various researchers to approximately separate the liquefaction and non-liquefaction soil deposits were also compared in Figure 2. All lines generally agree well with each other, except where CRR_1 is larger than 0.25. The boundary line proposed by NCEER (1997) is now commonly adopted in engineering practice.

Both cone penetration resistance qc and friction ratio R_F are measured as a routine part of CPT testings. However one of the shortcomings of Figure 2 is that the effects of the friction ratio of a soil on its liquefaction resistance cannot be assessed from the chart because it is entirely based on the measured qc values.

Figure 3 presents a CPT Soil Characterisation Chart proposed by Olsen et al (1996) for the estimation of CRR_1 in terms of both qc_1 and R_F values. It shows that the CRR_1 of a soil increases rapidly as its friction ratio increases. The chart indirectly includes the effects of soil types and the influence of fines content. Thus it is suitable for estimating the liquefaction resistance of both clean sands and soils with high fines contents. Figure 3 was also adopted for the liquefaction assessment of the bridge site.

Earthquake Magnitude Scaling Factors

Figures 2 and 3 were developed from data collected from sites where liquefaction did or did not occur during earthquakes with magnitude near M_L 7.5. For earthquakes with a magnitude smaller or larger than M_L 7.5, it is necessary to scale up or down the CRR_1 values estimated from Figures 2 and 3 by a Magnitude Scaling Factor (MSF) initially introduced by Seed and Idriss (1982). However, later research considered that the MSF values proposed by Seed and Idriss in 1982 were too conservative, and subsequently NCEER(1997) suggested that the upper and lower bound MSF values in Table 2 be adopted.

Magnitude	**5.5**	**6.0**	**6.5**	**7.0**	**7.5**	**8.0**
Upper bound	2.8	2.10	1.60	1.25	1	Uncertain
Lower bound	2.2	1.76	1.44	1.19	1	0.84

Table 2. Earthquake Magnitude Scaling Factors

Factor of Safety against Liquefaction

During an earthquake, the average shear stress, τ_{av} within the soil caused by the earthquake is represented by the cyclic shear ratio, CSR, calculated from the following simplified equation.

$$CSR = \tau_{av}/\sigma'_v = 0.65\,(a_{max}/g)\,(\sigma_{vo}/\sigma'_{vo})\,r_d \qquad (1)$$

where a_{max} and g denote the peak horizontal ground acceleration and the gravity, respectively, while σ_{vo} and σ'_{vo} represent the total and effective overburden pressures, respectively. r_d is a stress reduction factor for flexibility derived from the soil as a correction for assuming total rigidity of the overlaying soil. Alternatively, τ_{av} may be calculated using a computer program such as SHAKE by modelling the soil profile with appropriate soil parameters with appropriate seismic input records.

The factor of safety, FoS, of a soil against liquefaction can be calculated from CRR, CSR and MSF as follows:

$$FoS = (CRR_{7.5} * MSF) / CSR \qquad (2)$$

where $CRR_{7.5}$ is the CRR_1 determined for magnitude 7.5 earthquake using either Figure 2 or 3.

Seismic Induced Excess Porewater Pressure

During seismic excitation, excess porewater pressure builds up within a soil regardless of whether liquefaction occurs or not. For many soils, the seismic induced excess porewater pressure, u_G, can be expressed by Equation (3), Seed et al (1975).

$$u_G / \sigma'_{vo} = (2/\pi)\,\sin^{-1}(N/N_L)^{1/20} \qquad (3)$$

where θ is in the range of 0.5 ~ 0.9 and 0.7 is usually adopted. N_L is the number of uniform stress cycles causing initial liquefaction of the soil at a given CSR, cyclic shear ratio. N is the accumulated number of significant stress cycles during an earthquake. To enable us to calculate the seismic induced excess porewater pressure from Equation 3, the N_L value of the soil need to be determined. We have compiled the CRR_1 and qc_1 relationship from Figure 2, and MSF values from Table 2 into Figure 4 so that N_L values of soils with various cone resistance subject to various levels of cyclic stress ratio can readily be calculated. Figure 4 also presented the number of equivalent stress cycles, N_{Eq}, of various earthquake magnitudes proposed by Seed et al (1975). It should be noted that if N_{Eq} of a given earthquake exceeds N_L, the soil will subject to liquefaction.

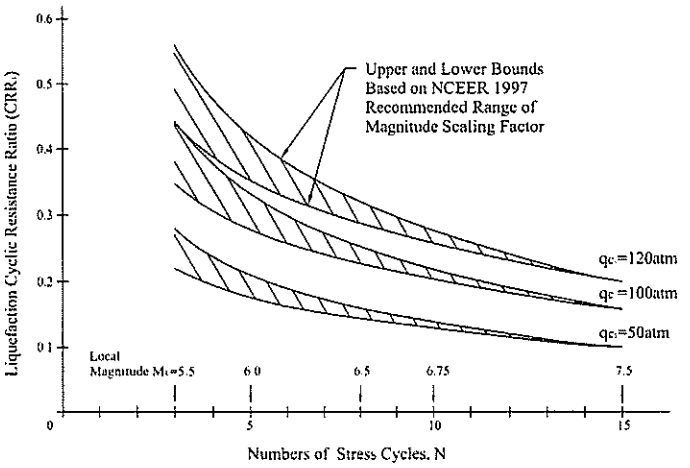

Figure 4. Relationship between Liquefaction Cyclic Resistance and Number of Stress Cycles

DESIGN PHILOSOPHY

During the tender design stage, two bridge options and four ground improvement techniques were considered. It was found that the two span option with the bridge deck founded on shallow strip foundations located immediately behind the MSE abutments and a central pier founded on a strip foundation was the cheapest option. Figure 5. The significant design features comprise the following:

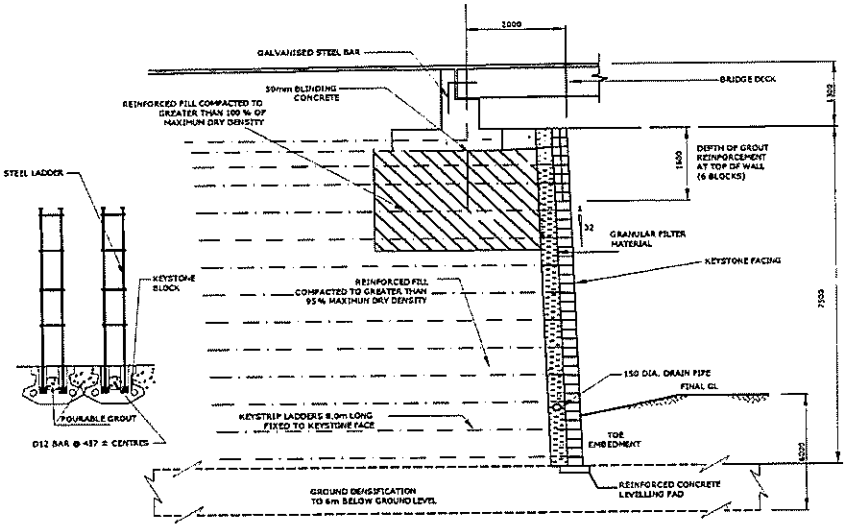

Figure 5. Tahuna Bridge Steel Ladder Reinforced Abutment with KeyStone Facing

- Ground Improvement - Extensive analyses indicated that ground improvement of the upper 6m above the non-liquefiable dense sand layer at 6-8m depth extending to an the area 5m outside the bridge and abutment footprint, Figure 6, was sufficient to satisfy the seismic design criteria outlined in Section 4 and the New Zealand Bridge Manual requirement. The improvement target was to densify the upper 6m soil to exhibit a minimum FoS of 2 against liquefaction for the 1000 year earthquakes, (M_L 6 & a_{max} = 0.22g). The minimum 6m deep improvement was also required

to maintain the static stability of the abutments following severe earthquakes during the period that the seismic induced pore water pressure had not been fully dissipated. The improvement strategy was to form a 8m thick non-liquefiable soil raft underlying the entire bridge site.

- Resonant Vibratory Compaction ground improvement - The insitu sand has a fines content of 5-7%. Vibratory compaction is suitable for the soil and is the cheapest option because the Y-shape vibratory probe, comprising three 10m long steel plates, Figure 7, could be economically made for the project. The contractor had a suitable vibration hammer readily available. The resonant frequency of the ground can be measured to optimise the densification efficiency.
- Mechanically Stabilised Earth (MSE) Bridge Abutments - Inextensible MSE abutment walls have demonstrated excellent seismic performance, exhibit extremely good ductile behaviour and also have a pleasing appearance. High tensile strength geotextiles are also laid below the steel reinforcement zone to enhance the structural ductility of the abutments.
- Bridge foundations - The bridge is founded directly on strip footings at the two MSE abutments and the central pier. The bridge footings at the abutments have approach slabs and are tied into the abutment fill with steel ladders to ensure that the bridge responds elastically under the design seismic loadings. Transverse seismic loads are be resisted by friction between the abutment footings and approach slabs and the underlying granular material in the abutment fill.
- Bridge Deck - The deck comprises prestressed double hollow core beams connected with transverse prestressing designed to distribute traffic and parapet impact loadings. The two spans and the central pier and the abutment footings are tied together by galvanised reinforcement.
- Limited Permanent Displacement Design Concept - The bridge and abutment design extended the ductility concept within the framework of the Ultimate Limit State design for structures to include foundations on sands subject to seismic influence. Significant investigation of the bridge deck and seat interface was undertaken to evaluate the acceptable level of seismic induced movement of the abutments and their influence on the bridge deck. If the Ultimate Limit State design earthquake loading is significantly exceeded, (for example the 1000 year earthquake is exceeded) the abutment movement is limited to less than 200mm. The passive soil wedge behind the bridge seat is designed to fail and act as an energy absorption mechanism to dissipate the earthquake energy transferred from the bridge deck to the abutment so that the integrity of the entire bridge structure is maintained.

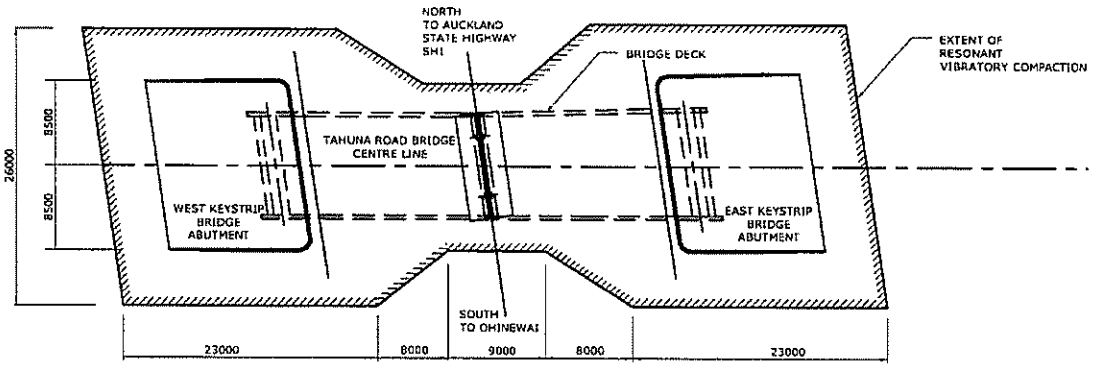

Figure 6. Resonant Vibratory Compaction Area

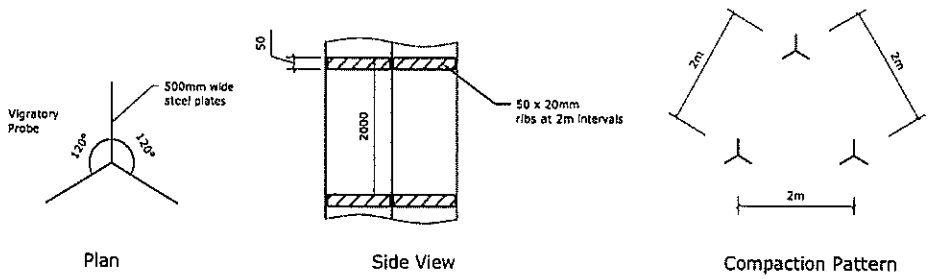

Figure 7. Vibratory Probe Configuration and Compaction Pattern

GROUND IMPROVEMENT OPTIONS

Four ground improvement techniques including (a) stone columns, (b) dynamic compaction, (c) dewatering, excavation and re-compaction, and (d) resonant vibratory compaction were considered. The densification covers an area of 1700m^2 extending 5m outside the bridge and MSE abutment footprints as shown in Figure 6. The costs of the four options range from $78k to $250k. The resonant vibratory compaction method was selected because (i) it was the cheapest option, (ii) it required the shortest construction time and (iii) it had very little environmental effects outside the densification area.

DESIGN METHODS

Resonant Vibratory Compaction Densification

Resonant vibratory compaction is generally suitable for granular soils with a fines content less than about 10% or CPT friction ratio lower than 1%. The soil within the densification zone is generally within this category. The technique has been employed overseas. Some background information can be found in Neely et al (1991) and Van Impe et al (1994). For soils with higher fines contents, vibro-replacement such as stone column densification may be needed.

The configuration of the Y-shape vibratory probe is shown in Figure 7. The probe comprises three steel plates of 500mm wide, 16mm thick and 10m long welded together at 120 degrees. It has 300mm long x 50mm high x 20mm thick ribs welded to both side of the plates at 2m vertical intervals.

The compaction points were arranged in an equilateral triangular pattern at 2m centre to centre spacing covering the entire densification area. A 4 tonne variable frequency vibration hammer was selected for driving and withdrawing the vibratory probe from the ground during the ground improvement process. For the selected 2m compaction point spacing, the surging method was found to develop the most effective compaction effect during the initial field trials. This involved inserting and extracting the probe 5 times to its 6-8m full depth at a rate of 2m per 15 second, with one minute steady state vibration at its full depth before each withdrawal.

MSE Abutments

The seismic induced porewater pressure distribution within the soils beneath and outside the bridge abutment areas caused by the serviceability and ultimate limit states, and the 1000 years return period earthquakes as given in Section 4 were calculated using the methods presented in Section 5. We assumed that the effective angle of friction was $\Phi' = 35^\circ$ for the upper densified pumiceous sands. Below the 8m depth, the effective angle of friction for the unimproved soils was assumed to be $\Phi' = 30^\circ$. We also assumed that the total density of the unimproved pumiceous soil was 16kN/m^3 and that it increased to 18kN/m^3 after the densification.

Using the calculated seismic induced porewater pressure distribution in addition to the static groundwater pressure and the assumed soil parameters, a series of stability analyses were undertaken for the abutment design. The abutments were designed to exhibit a minimum factor of safety of 1.5 to maintain the static stability of the abutments following the ultimate limit state design earthquakes during the period that the seismic induced pore water pressure had not been fully dissipated. Our model predicted that no/insignificant seismic induced abutment movement is caused by the design earthquakes.

For the 1000 year design earthquake, the abutments are designed to have a static factor of safety of at least 1.3 after the seismic induced pore water pressure is fully developed within the soil. We have conservatively estimated that the seismic induced permanent abutment movement is unlikely to exceed 200mm. The passive soil wedge behind the bridge seat is designed to fail and act as an energy absorption mechanism to dissipate the earthquake energy transferred from the bridge deck to the abutment so that the integrity of the entire bridge structure is maintained.

CONSTRUCTION

Resonant Vibro-compaction Field Trial

At the beginning of project, field compaction trials were undertaken partly within an area previously pre-loaded by the old 3m-6m high Tahuna Road Rail Overbridge embankment which was removed prior to the ground improvement work. At the time of the trial, groundwater level was at 1.3m below the ground surface.

To determine the natural frequency of the ground and to maximise the compaction efficiency, the vibratory probe was inserted into and extracted from the ground by the vibration hammer at various rotational frequencies. Vibration monitoring was undertaken at a 2.5m distance from the centre of the vibratory probe on the ground surface. Maximum ground response was measured at about 20Hz (0.05 second) corresponding to the rotational frequency of the vibration hammer at 1600-1700rpm (26Hz). Visually, when the vibratory probe was operated at the 1600-1700rpm hammer rotational frequency, the induced ground settlement and the influence zone of the probe is significantly larger than those induced at other rotational frequencies. It was therefore decided that all subsequent compaction would be carried out at 1600-1700rpm hammer frequency.

During the initial trials, for the selected 2m compaction spacing, it was found that the vibratory compaction surging method as discussed in Section 8 was the most effective method. During the 5 repeatedly surging and steady state vibration cycles, the ground within a 1.5m radius from the centre of the probe settled by 250mm. Subsequent compaction at the surrounding compaction points caused additional 100mm settlement making a total of 350mm settlement.

Spectral Analyses of Surface Waves (SASW) tests were undertaken immediately after the compaction trials to determine the changes in the shearwave velocity properties due to the resonant vibratory compaction. It was generally found that the vibratory compaction immediately increased the shearwave velocity from 80m/sec to 125m/sec. It is equivalent to an improvement of the small strain shear modulus, G, by a factor of 2.

Ground Improvement Results

Ground settlement induced by the vibratory compaction was surveyed as the densification work was in progress. It was observed that the compaction induced settlement characteristics of the ground were different in the areas inside and outside the previous Tahuna Road Rail Over-Bridge embankment footprint.

In the area directly under the previous 6m high embankment at the eastern end of the site, the densification process induced settlement in the order of 250mm. In areas outside the removed embankment, the induced settlement was in the order of 600mm. The difference in their characteristics is due to the pre-consolidation history of the ground.

Depth (m)	Before Densification	After Densification
0 - 3m	qc = 1 ~ 3MPa R_F = 0.5<~ 0.8%	qc = 3 ~ 5MPa (Typical 4MPa) R_F = 1 ~ 1.5% (Up to 2%)
3 - 6m	qc = 2 ~ 3MPa R_F = 1<~ 1.5% (Generally 1%, except thin silt layers >2%)	qc = 3 ~ 4.5MPa R_F = 1.3 ~ 2.0% (Little improvement of qc and R_F in silt layers)

Table 3. Comparison of CPT Test Results Before and After Densification

40 CPT tests were undertaken as part of the QA requirement for the verification of the ground improvement. We have summarised the CPT test results before and after the vibratory compaction in Table 3. Generally, after the compaction, all treated soils exhibited a minimum FoS of 2 against liquefaction for the 1000 year return period earthquake, except for a few thin layers at two CPT

locations where the FoS is slightly below 2. Our detailed analyses of the CPT results using Figure 3 indicated that the increase in the friction ratio due to the compaction could contribute to the improvement in seismic liquefaction resistance of the treated soil as much as the increase in the cone resistance does. Furthermore, the results generally suggest that very little increase in both cone resistance and friction ratio for materials with high silt and clay contents, say F_R>2%.

MSE Abutment Wall Settlement

During the construction of the MSE abutments settlement pins were installed and settlement of the abutments were monitored during and after construction of the bridge. The 8m high eastern abutment is partly located within the previous 6m high Tahuna Road Rail Overbridge embankment area. The total settlement measured was 50mm.

The western abutment is located outside the previous embankment area. A total settlement of 100mm was measured. The majority of the settlement occurred during the 4 week MSE wall construction period. This enabled the immediate start of the bridge concrete works without delays to allow settlement.

The reconstructed Tahuna Road rail embankment adjacent to the bridge site was also monitored for settlement. The embankment is about 7.5m high and was built outside the vibratory compaction zone. The embankment has settled in the order of 300mm. The result indicated that the resonant vibratory compaction has effectively eliminated about two-thirds of the bridge abutment settlement.

Central Bridge Pier Settlement

The central bridge pier is founded on a 4m wide x 10m long strip footing with a 1m embedment depth. The footing is subject to a 150kPa bearing pressure under the serviceability limit state load. The construction of the bridge deck load on the central pier induced insignificant settlement.

DISCUSSIONS & CONCLUSIONS

Key findings from the project are discussed below:

Vibratory Probe Compaction

- An extensive literature survey appears to suggest that it is the first time resonant vibratory compaction technique has been used for the densification of pumiceous sands.
- Overseas published resonant vibratory compaction data for sands mainly employs cone penetration resistance qc as a sole parameter for the evaluation of the effectiveness of the densification process. No published information on the friction ratio is available for comparison with our data. However, the friction ratio is an important parameter for the evaluation of the liquefaction resistance of soils.
- Generally, the increases in the qc values of pumiceous sands due to the densification are not as much as those in published data for non-pumiceous sands. However, with the consideration of improvement from both qc and F_R values, the resonant vibratory compaction increases the liquefaction resistance of the pumiceous sands in terms of CRR_1 at least 80~100%.
- Available data supports the view that the resonant vibratory compaction technique is only effective for materials with CPT friction ratios less than 2% or fines content less than 10%. Our measurements indicated that very little differences in both qc and F_R are noticed before and after vibratory compaction when the silt & clay contents are high.
- CPT results appear to indicate that, although the pumiceous sands are highly permeable and the ground settlement occurred immediately during the vibro-compaction stage, it took at least three days for the ground to develop its full densified strength.
- On average 30 compaction points were completed within one working day during the construction period in summer. The speed of the construction is essentially limited by the safe operating temperature of the vibration hammer which should not exceed 90°C. The production rate can be significantly improved in cold or rainy days.

- The densified ground effectively reduced the 8m high bridge abutment settlement from 300mm to 100mm when compared with the induced settlement of the re-constructed Tahuna Road/Rail Overbridge embankment outside the densified zone.
- Resonant vibratory compaction was found to be an economical and environmental friendly ground improvement technique for the project site.

MSE Bridge Abutments

- The construction of the two 8m high MSE abutments was completed in 4 weeks without the need for heavy cranage and can be considered relatively efficient when compared to other construction methods such as adding two extra bridge spans with normal bridge approach earthfill embankments.
- There are only a few contractors with sufficient experience for the construction of large MSE walls in New Zealand and the labour cost component of MSE wall construction still appears to be relatively high.
- Compaction of the structural fill within the reinforced zone near the MSE wall face to 95% of the maximum dry density is relatively difficult and should be undertaken with extreme care. Over compaction with a heavy roller could cause distortion at the bottom of the wall face.
- The MSE bridge abutments have been designed to deal with the seismic requirements of the New Zealand Bridge Manual. Extra seismic safety using the Limited Permanent Displacement Design Concept was also introduced in the bridge design. If the Ultimate Limit State design earthquake loading is significantly exceeded, (for example the 1000 year earthquake is exceeded) the abutment movement is limited to less than 200mm. The passive soil wedge behind the bridge seat is designed to fail and act as an energy absorption mechanism to dissipate the earthquake energy transferred from the bridge deck to the abutment so that the integrity of the entire bridge structure is maintained.

ACKNOWLEDGEMENTS

Fletcher Higgins Joint Venture was the head contractor the project. Brian Perry was the specialist ground stabilisation sub-contractor undertook the ground improvement works. Sinclair Knight Merz was the lead consultant of the project engaged by Fletcher Higgins. Peters and Cheung Ltd was the specialist bridge designer responsible for the design of the bridge, abutments and ground stabilisation.

REFERENCES

NCEER (1997) Proc. NCEER Workshop on Evaluation of Liquefaction Resistance of Soils, Ed. T L Youd, and I M Idriss. National Center for Earthquake Engineering Research, Technical Report NCEER-97-0022.

Neely, W. J. and Leroy, D. A., (1991) "Densification of Sand Using a Variable Frequency Vribratory Probe", Deep Foundation Improvement: Design, Construction, and Testing, ASTM STP 1089. Melvin I Esrig and Robert C Bachus, Eds., American Society for Testing and Materials, Philadelphia.

Olsen R S, Koester J P, and Hynes M E (1996) "Evaluation of Liquefaction Potential using the CPT", Proc. 28th Joint Meeting of the US-Japan Cooperative Program in Natural Resources - Panel on Wind and Seismic Effects, US National Institute of Standards and Technology, Gaithersburg, Maryland, May 1996.

Seed H B, and Idriss I M (1982) in National Research Council, Committee on Earthquake Egnineering-Liquefaction of Soils During Earthquakes published in 1985.

Seed H B, Martin P P, and Lysmer J (1975) "The Generation and Dissipation of Pore Water Pressures During Soil Liquefaction," Earthquake Engineering Research Centre, Report No. EERC 75-26.

Van Impe, W. F., De Cock, F., Massarsch, R., and Menge, P., (1994) "Recent Experience and Developments of the Resonant Vibrocompaction technique", 13th ICSMFE, New Delhi, India.

Case Studies of Delayed Failure Due To Liquefaction

M E Jacka
BE (Hons), ME (Dist)
Geotechnical Engineer, Tonkin & Taylor Ltd.

Abstract: Delayed failure due to ground liquefaction is investigated, where failure occurs some minutes or hours after earthquake shaking has ceased. Several historical examples of delayed failure are outlined, as are potential mechanisms proposed in the literature to explain their occurrence. The delayed failure of a bridge approach is chosen as a case study to develop a simple model for analysis of such failures. The software packages Plaxis and Slope/W are used to evaluate the stability of the embankment as excess pore pressures dissipate upwards from the liquefied material into the overlying crust. This analysis shows that the surface crust was strong enough to maintain embankment stability immediately following the earthquake, but after 15 minutes the increase in pore pressure in this layer reduced the available strength to the point where static equilibrium could no longer be maintained.

INTRODUCTION

The phenomenon of ground liquefaction has been responsible for a great deal of damage experienced in a large number of earthquakes around the world. The strength loss associated with liquefaction can lead to foundation, slope and embankment failures, whilst lateral spreading deformations often cause significant damage to lifelines and other structures. This investigation focuses primarily on the phenomenon of delayed response to liquefaction, where failure or significant deformation occurs some minutes, hours or days after the main earthquake shaking has ceased.

The issue of earthquake damage to embankments is significant both in terms of the cost of repairs and the disruption to services and lifelines. Often embankments are part of essential structures such as roads, railways, bridges, flood-control works and dams. Delayed embankment failure was observed at the Landing Road Bridge, Whakatane, New Zealand, after the 1987 Edgecumbe earthquake. This case study is used to examine how the occurrence of delayed failure could be explained and modelled.

HISTORICAL EXAMPLES OF DELAYED LIQUEFACTION FAILURE

In past earthquakes there have been a number of examples of liquefaction failures that have occurred some time after the end of seismic shaking. Three such failures are summarised here, to give a background to the problem of delayed liquefaction failure.

Lower San Fernando Dam

A near-catastrophic slide failure occurred in the Lower San Fernando Dam as a result of the 1971 San Fernando, California earthquake, as shown in Figure 1. Seed et al (1975) conclude that liquefaction occurred in a large zone of hydraulic fill at the base of the embankment, upstream of the clay core. The material overlying the liquefied layer broke up and slid as a number of intact blocks, leading to a substantial reduction in the available freeboard. The failure occurred relatively slowly, and did not start until approximately one minute after the earthquake.

Castro (1987) and Seed et al. (1975) consider the possible role of pore water migration in the delayed failure. They point out that the upstream toe of the dam was originally a starter dyke for hydraulic filling, and so was compacted to a dense (dilative) state. In this state, the undrained strength is greater than the drained strength. They suggest that as the liquefied material lost strength, the material at the toe was subjected to higher shear stresses, causing a tendency for dilation. If this soil was permeable enough to allow water to be drawn into the voids a volume increase would have occurred, resulting in

a stress path reaching the steady state line at a higher void ratio, and thus a lower steady state strength. The one minute delay before failure corresponds to the time required for sufficient drainage to occur to instigate such a loss of strength.

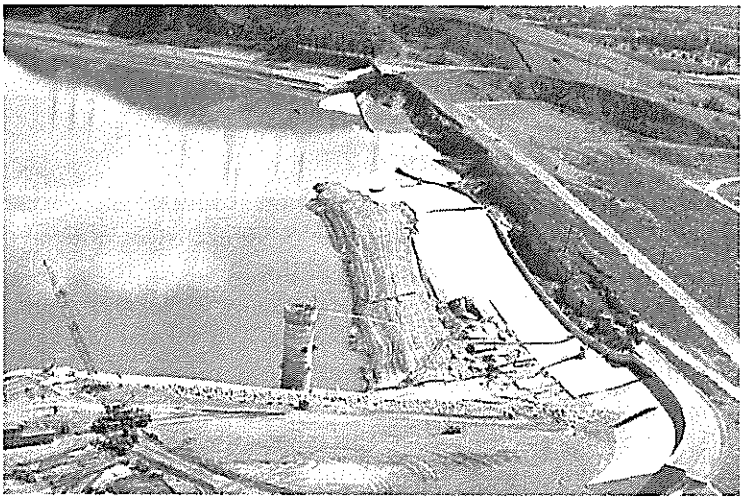

Figure 1. Damage to the Lower San Fernando Dam (Steinbrugge Collection, EERC, UC Berkeley)

Mochikoshi Tailings Dam

As a result of the January 1978 earthquake at Izu-Oshima, Japan, two tailings dams at the Mochikoshi gold mine collapsed. Cross sections of the dams before and after failure are shown in Figure 2.

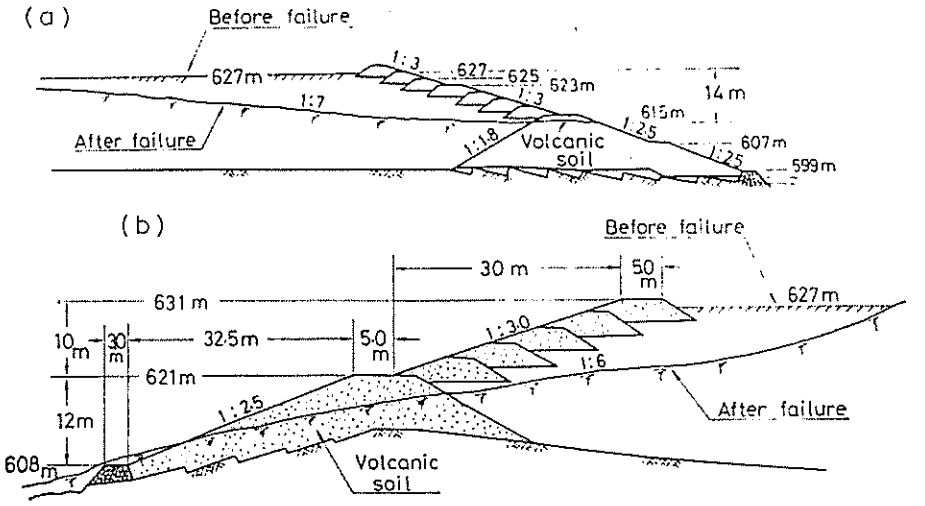

Figure 2. Mochikoshi Tailings Dam No. 1 (a) and No. 2 (b). (Ishihara, 1984)

After about 10 seconds of shaking the crest of Dam No. 1 had settled excessively, and the silty sand tailings had liquefied. This enabled the tailings to breach the dam and sweep away much of the upper part. Approximately 24 hours after the earthquake Dam No. 2 also failed (Ishihara, 1984). Delayed failure may have been due to gradual upward movement of the phreatic surface, resulting from the liquefaction of the tailings. The subsequent increase in pore pressure in the volcanic silt body of the dam would have reduced the effective stresses, and thus the strength available to resist deformation. Ultimately this reduction in strength was sufficient to allow failure under static driving stresses.

Prefectural Apartment Buildings, Niigata

As a result of the 1964 earthquake at Niigata, Japan, a number of buildings at the Prefectural apartment complex suffered rotational foundation failure, as shown in Figure 3. Residents of the

building reported that this was a very slow and smooth failure.

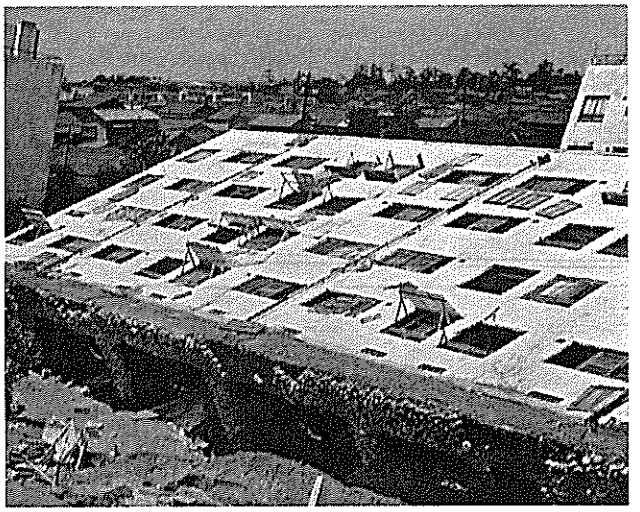

Figure 3. Overturned Prefectural Apartment Building. (Kawasumi, 1968)

The absence of any upthrust ground around the building, and the pattern of cracking in the crust suggest that this was not a conventional "slip-circle" type failure, but rather a case of the building rotating as it sank into the liquefied ground. Failure occurred some minutes after the end of the earthquake (Kawasumi, 1968), suggesting that the soil supporting the foundation did not suffer the immediate loss of strength that would be expected if it had liquefied as a direct result of earthquake shaking. It is suggested that liquefaction initiated at some depth beneath the building and then gradually moved upwards until it caused the failure of the building's foundations.

MECHANISMS OF DELAYED FAILURE

The magnitudes of any deformations which might occur as a result of liquefaction generally depend on the relative magnitudes of the available soil strength and the stresses required to maintain equilibrium. In some cases the immediately available undrained strength of the liquefied and non-liquefied soils may be only just sufficient to ensure stability. In these cases it is possible that any reduction in strength that might occur over time after the earthquake could eventually lead to significant displacements or failure.

Whitman (1987)

Whitman (1987) proposes the two mechanisms for localised strength reduction shown in Figure 4. In the first, a layer of sand is subjected to cyclic straining, causing a tendency for the particles to settle. Thus the upper part of the layer becomes looser while the lower part becomes denser. Although the layer as a whole experiences no volume change, these local changes result in a potential reduction of the steady state strength of the upper part.

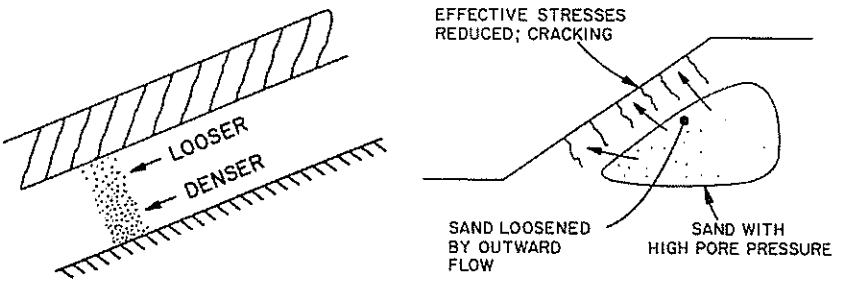

Figure 4. Void Redistribution and Pore Water Migration. (Whitman, 1987)

The second mechanism shown in Figure 4 occurs as a result of high excess pore pressures in an area of liquefied material. The excess pore pressures are relieved by the outwards and upwards migration of pore water. This causes the pore pressure in the overlying layer to increase, reducing the effective stress - and thus the strength that the soil can develop by frictional means is reduced.

Seed et al. (1975, 1987)

Seed (1987) discusses situations where liquefaction develops near the end of earthquake shaking, so failure is driven almost completely by static forces. In these cases he recommends that consideration be given to the effects of gradual pore water redistribution, which may cause failure a considerable time after the end of the earthquake.

As detailed in the previous sub-section, Seed et al. (1975) propose a possible explanation for the one minute delay between the end of earthquake shaking and the failure of the Lower San Fernando Dam. In this case enough drainage may have occurred to allow the dense soil in the embankment toe to dilate to a looser state as it was forced to carry greater forces as a result of the liquefaction of looser material.

Kutter (1997)

Kutter (1997) suggests that migration of pore water can result in a redistribution of void space in a liquefied soil. He argues that a considerable hydraulic gradient is present in a liquefied soil, and that this forces an upwards flow of water. In regions with outwards flow of water a reduction in void ratio is able to occur, while an increase in void ratio can be expected in areas of pore water inflow. This process is often referred to as void redistribution.

Considering that the steady state strength of a soil is strongly related to the void ratio, the process of void redistribution can be expected to reduce the strength of the upper part of a soil profile. Kutter presents a rough calculation using typical parameters to show that in a medium sand sufficient flow could occur to fully soften a 1m thick zone in approximately 15 minutes. This figure is similar to the delay calculated in the analysis of the Landing Road Bridge site, presented in the section 'Stability During Pore Pressure Migration'.

Scott & Zuckerman (1973)

During their laboratory-based research into sand boils resulting from liquefaction, Scott & Zuckerman (1973) witnessed the occurrence of "induced" or "secondary" liquefaction of a coarse-grained dense layer overlying a liquefied material. They observed that from the instant that liquefaction commences soil grains begin to settle out of suspension. Thus at some time after the initiation of liquefaction there exists a layer of re-solidified soil, overlain by a region of soil particles suspended in the pressurised pore fluid. Meanwhile if there exists an overlying non-liquefied layer, it is now left supported only by the soil and water mixture. If this overlying layer lacks apparent cohesion then it may begin to unravel at its lower surface. Thus a liquefaction interface moves upwards through the overlying layer.

Castro (1987)

Castro (1987) agrees with the hypothesis of Seed et al. (1975) presented in the earlier section 'Lower San Fernando Dam', that pore water migration can affect stronger, dilative zones of material. He goes on to recommend that in cases where the soil is permeable enough to allow pore water migration, design for stability should not rely on undrained shear strengths which are greater than drained strengths.

Seed et al. (2001) agree with this approach, reasoning that the significant tendency for dilation required to provide increased strength tends to localise the zone of shearing. As a result, pore water is able to quickly travel the short distance required to permit volume change to occur, and the high undrained strength can persist only briefly.

DELAYED FAILURE OF THE LANDING RD BRIDGE APPROACH EMBANKMENT

Christensen (1995) presents an eyewitness report that suggests delayed failure occurred in the northwestern approach embankment of the Landing Rd Bridge as a result of the 1987 Edgecumbe earthquake. Shortly after the earthquake the motorist was able to cross the bridge, however upon returning roughly one hour later the bridge approach was heavily cracked, and differential settlement between the bridge and the abutment had rendered the bridge impassable by car. Typical damage to the embankment can be seen in Figure 5. The embankment has a maximum height of 3m, and is 23m wide at the base. A generalised soil profile at the site is shown in figure 6.

Figure 5. Damage to the Landing Rd Bridge Approach Embankment. (Courtesy of J. Berrill)

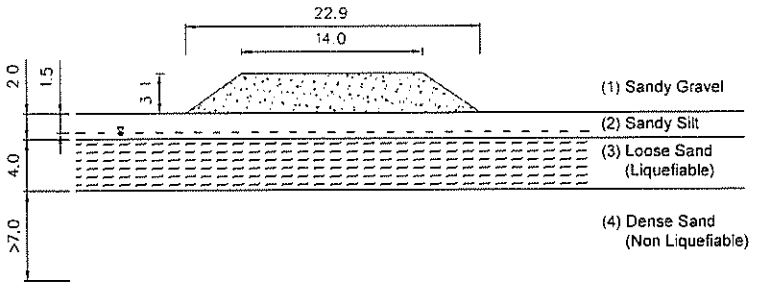

Figure 6. Generalised Geometry & Soil Profile for Analysis of the Landing Road Bridge Approach.

Taking into account the general understanding of possible mechanisms of delayed failure summarised above, the following hypothesis is proposed to explain the delayed failure at the Landing Rd site:

During the earthquake shaking, liquefaction occurred beneath the embankment in a layer of loose sand, approximately 4m thick (Christensen, 1995). Between the embankment and the liquefied layer was a sandy silt layer roughly 2m thick, which did not liquefy. This study proposes that the strength and thickness of this unliquefied crust was only just sufficient to maintain "rafting" stability of the embankment during and immediately after the earthquake.

It is hypothesised in this investigation that as time passed after the earthquake, the excess pore pressures in the liquefied material caused pore water to gradually seep upwards into the unliquefied sandy silt. This reduced the strength of the upper layer to the point where the observed moderate displacements were able to occur. Two mechanisms that could possibly be responsible for this strength loss are:

- If the overlying material is considered in terms of its steady state behaviour, then void redistribution could lead to a reduction in the steady state strength.
- If the strength of the overlying material is considered in terms of the Mohr-Coulomb failure criterion, the increase in pore pressure leads to a decrease in effective normal stresses between soil grains. This decreases the frictional resistance and thus the drained strength available to maintain static equilibrium.

It should be noted that it is not suggested that the delay in failure is due to any delay in the occurrence of liquefaction, nor in this case due to any change in the strength of the liquefied material that may occur through time. It is proposed that the delay in failure is simply due to the time taken for void and pore water redistribution to occur sufficiently for the overlying non-liquefied soil to be weakened to the point where failure is possible.

ANALYSIS OF THE LANDING RD BRIDGE APPROACH EMBANKMENT

As outlined in the previous section, the northwestern approach embankment of the Landing Road Bridge was damaged by deformations that occurred up to an hour after the earthquake. The primary aim of this analysis is to demonstrate the manner in which migration of excess pore water could cause the observed delayed failure.

Four key stages were considered:

1. Pre-earthquake conditions, with full drained strength for all soils.
2. Immediately post-earthquake stability, considering both zero strength and steady state strength in the liquefied soil.
3. Pore pressure migration, where pore water migration into the upper soil layer is modelled.
4. Stability during pore pressure migration, where the stability is re-analysed under the pore pressure conditions expected at various time intervals after the end of the earthquake.

The investigation made use of two specialist geotechnical software packages - Plaxis and Slope/W. Plaxis is a finite element analysis tool for evaluating deformations and stability of geotechnical structures. This was the primary tool used to model the deformation of the embankment and dissipation of excess pore pressures. Slope/W is a limit equilibrium geotechnical analysis package which uses a variety of slip-circle based methods to provide an estimate of the Factor of Safety against failure (FOS).

Excess pore pressures were introduced into the liquefied layer and the consolidation features of Plaxis used to model the dissipation of excess pore pressures resulting from liquefaction. The initial excess pore pressure to be generated in the sand layer was chosen such that a condition of zero effective stress (ie. liquefaction) would occur at the midheight of the layer.

Ideally, a full stability analysis would be carried out at each time step in the pore pressure dissipation calculation. However, the iterative consolidation algorithm used by Plaxis fails to converge as the structure approaches failure, so this option was not feasible. To circumvent this limitation, it was necessary to use a two-step process, firstly calculating the pore pressure distributions at a number of time steps, and then manually introducing these pressures into a conventional stability analysis. In future, it is planned to also perform the analysis in FLAC, as its explicit finite difference formulation tends to remain stable as the structure reaches failure.

The transition from the material properties and pore pressure conditions immediately after the earthquake (Series 2) to those some time later (Series 4) was implemented using a series of four staged construction steps. These steps represent the pore pressure distributions at 0.5, 4.9, 14.1, and 42.4 minutes after the end of earthquake shaking.

ANALYSIS RESULTS

Pre-Earthquake Conditions

Using Slope/W, factors of safety were determined on three failure surfaces of interest. The predicted critical failure surface for pre-earthquake conditions (FOS = 2.04) reaches down to approximately the midheight of the sandy silt layer. Using a ϕ-c reduction process, Plaxis estimates a critical failure region which is in good agreement with the critical surface proposed by Slope/W, with a similar level of safety (FOS = 1.99).

These results show that the embankment possessed ample stability before the earthquake, and that medium-scale failure of the embankment gravel and the upper part of the sandy silt layer was initially critical. It is encouraging to see that there is good agreement between the results from Plaxis and Slope/W for the critical case.

Immediate Post-Earthquake Stability

By setting the strength of the liquefied layer to zero we can determine if a strength contribution from the liquefied material is required to maintain static equilibrium. For this condition Slope/W predicts failure on a surface reaching the bottom of the liquefied sand (FOS = 0.72). Plaxis analysis also predicts large displacements. These results suggest that some strength contribution was indeed required from the liquefied material to provide the immediate post-earthquake stability that was observed.

A best-estimate value for the sand's undrained steady state shear strength (c = 11 kPa + 1.3 kPa/m) was determined using a weighted average of various SPT and CPT correlations (Seed & Harder, 1990; Stark & Mesri, 1992; & Robertson, 1999). Using this strength, both Slope/W and Plaxis analyses show that embankment stability can be maintained immediately after the earthquake. A sensitivity analysis showed that only small reductions in strength are required to trigger failure, therefore the potential reduction in strength due to pore water migration and void redistribution becomes of great importance.

Pore Pressure Migration

The results of the pore pressure dissipation analysis are shown in Figure 7. In general, excess pore pressures of up to 10-20 kPa are predicted to occur in the lower part of the surface sandy silt layer approximately 15 to 60 minutes after the end of earthquake shaking.

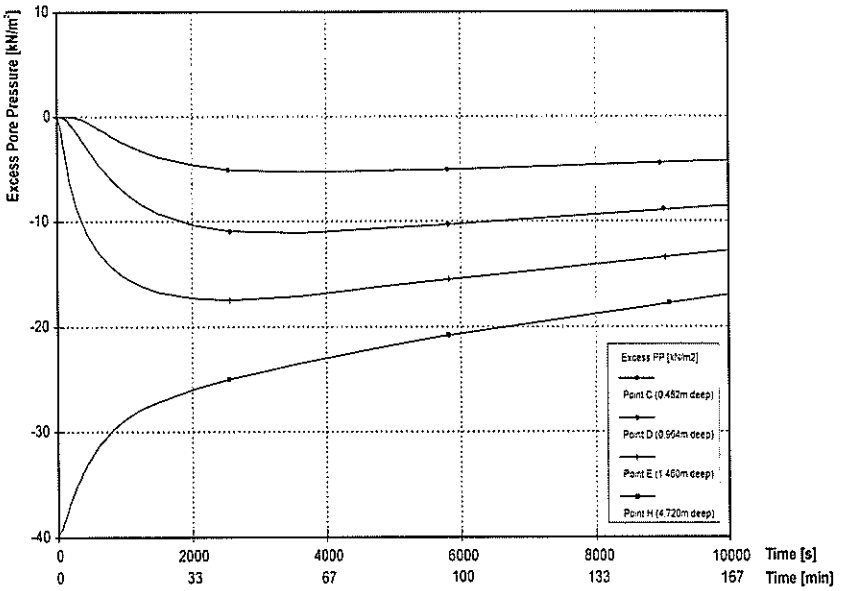

Figure 7. Pore Pressure vs. Time at Various Depths, as Calculated by the Plaxis Dissipation Analysis.

Stability During Pore Pressure Migration

Slope/W analyses (Figure 8) show that dissipation of excess pore pressures from the liquefied layer reduces the factor of safety against failure by almost 10%, enough to effect a change from marginally stable to marginally unstable conditions. The upwards movement of the critical failure surface as pore pressures spread confirms that the observed reduction in FOS is due to a reduction in the strength contribution of the surface layer. Based on these results, failure or significant deformation of the embankment could be expected to occur roughly 15 minutes after the end of earthquake shaking.

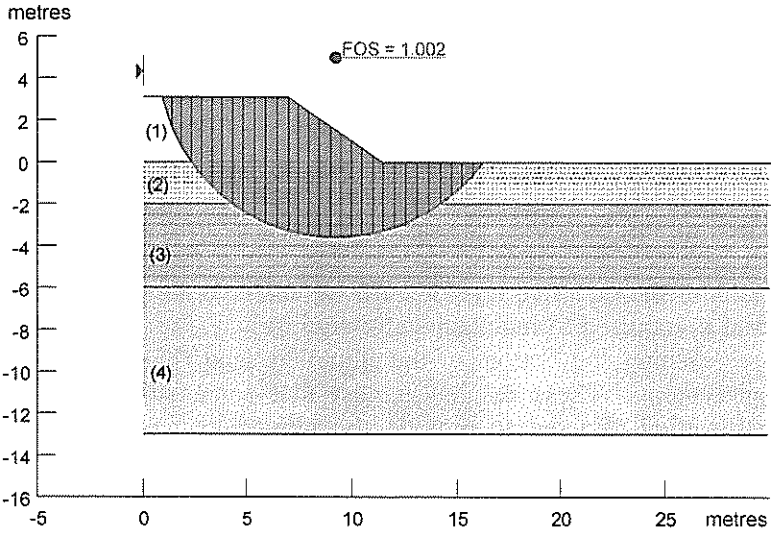

Figure 8. Slope/W Critical Failure Surface After 14 min. of Pore Pressure Dissipation.

The results of the Plaxis analysis are in good agreement with those from Slope/W. Displacements of approximately 5mm are predicted as the pore pressures are raised to the level corresponding to 4.9 minutes of dissipation, however the embankment retains overall stability. The next calculation phase (Figure 9) attempts to raise the pore pressures further, to the level expected 14.1 minutes after the earthquake. Global instability of the embankment develops just before the target pressures are reached, thus Plaxis predicts that failure or significant deformation of the embankment will occur roughly 14 minutes after the end of earthquake shaking.

A maximum total displacement in the order of 150mm is predicted up to the point at which the Plaxis calculation is unable to proceed due to instability. In the 1987 earthquake, large scale collapse of the embankment did not occur, however it was heavily damaged by cracking and subsidence in the order of several hundred millimetres. This suggests the predicted displacement magnitudes are realistic.

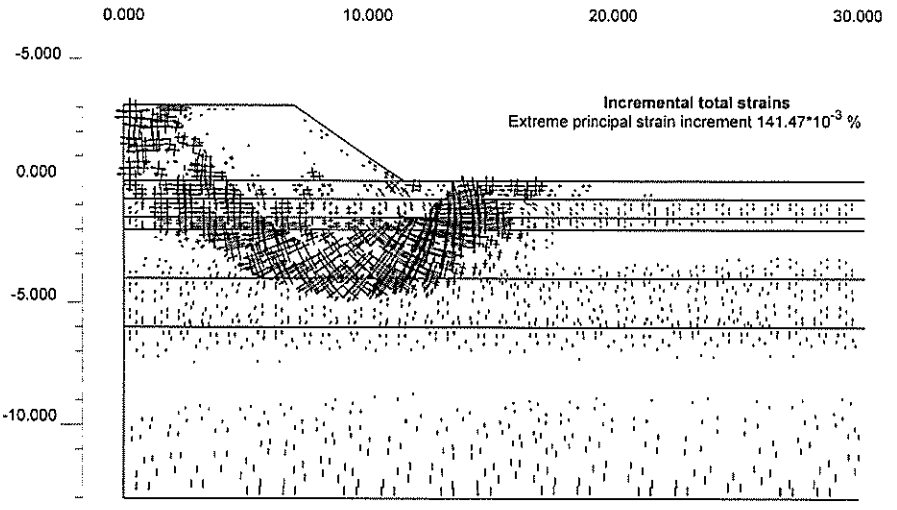

Figure 9. Plaxis Plot of Incremental Shear Strain at Failure, after 14 min. Pore Pressure Dissipation.

Inspection of the effective stress plot in Figure 10 confirms the role of increased pore pressures in the collapse – with the effective vertical stress approaching zero in the lower part of the surface sandy silt layer.

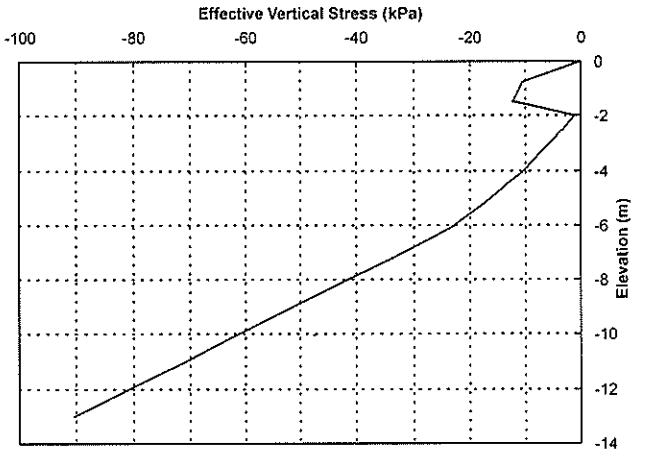

Figure 10. Plaxis Plot Showing Effective Vertical Stresses at Failure.

CONCLUSIONS

The analyses summarised in the previous section support the theory that the embankment would remain marginally stable after the loose sand liquefied, providing that the liquefied material contributes its steady state strength to assist in resisting static driving forces.

Analysis of the dissipation of excess pore pressures from the liquefied layer suggests that the pore pressures in the surface sandy silt layer reached a maximum roughly 45 minutes after the earthquake, with a substantial build up of pressure occurring within the first 15 minutes. In the lower part of the surface layer the resulting total pore pressures would have approached the total overburden stress, leading to a state of near-zero effective stress.

Stability analyses performed using the pore pressure distributions calculated at selected time intervals show that the embankment remains stable up until approximately 15 minutes after the earthquake. At this time the decrease in effective stress in the surface layer is sufficient to reduce the available frictional strength to the point where static equilibrium can no longer be maintained. The predicted 15 minute delay between the end of the earthquake and the appearance of damage is within the upper bound of one hour indicated by the eyewitness account.

Many inter-related theories have been proposed that can be used to explain delayed failures such as observed at the Landing Road Bridge. In general these conceptualise the mechanism as either the gradual redistribution of voids within the soil leading to reduced steady state shear strength, or the movement of pore water reducing effective stresses and thus frictional strengths.

This investigation has shown how a simple model of strength loss can be used in a quantitative framework to assess susceptibility to such secondary failures. This is particularly relevant to the designer in cases where a relatively dense material overlies a potentially liquefiable soil. If the conditions are such that excess pore water from the liquefied material may be readily available to feed a dilative shear zone in the overlying crust then it would be unwise to allow post-liquefaction "rafting" stability to rely on maintaining an undrained strength greater than the drained strength.

ACKNOWLEDGEMENTS

The research summarised in this paper was made possible by the generous financial assistance provided by the New Zealand Returned Services' Association, the New Zealand Society for Earthquake Engineering, Tonkin & Taylor Ltd, and the University of Canterbury. This investigation was supervised by Dr John Berrill, who is thanked for the wealth of experience brought to the project and the invaluable guidance and support he provided.

REFERENCES

Castro, G. (1987) "On the behaviour of soils during earthquakes". In: *Soil Dyn. and Liquefaction*, Ed: Cakmak, A.S., Elsevier. pp. 169-204.

Christensen, S.A. (1995) *Liquefaction of cohesionless soils in the March 2, 1987 Edgecumbe earthquake, Bay of Plenty, New Zealand, and other earthquakes*. ME Thesis, Uni. Canterbury, NZ. 373p.

Ishihara, K. (1984) "Post-earthquake failure of a tailings dam due to liquefaction of the pond deposit", *Proc. 1st International Conf. on Earthq. Engrg.*, Madrid, pp. 1407-1412.

Kawasumi, H. ed. (1968) *General Report on the Niigata Earthquake of 1964*, Tokyo Electrical Engrg. College Press.

Kutter, B.L. (1997) "Strength of liquefied soil is not a material constant; liquefaction is a boundary value problem", *Pre-workshop written statement, Shear Strength of Liquefied Soils*, April 17-18 1987, Urbana, Illinois. Online. Available: http://www.conted.uiuc.edu/ci/soil/. 6 March 2001.

Robertson, P.K. (1999) "Estimation of minimum undrained shear strength for flow liquefaction using the CPT", *Proc. 2nd Int. Conf. on Earthq. Geotech. Engrg.*, A.A. Balkema, Vol. 3, 1999. pp. 1021-1028.

Scott, R.F., & Zuckerman, K.A. (1973) "Sandblows and liquefaction", *The Great Alaskan Earthquake of 1964 - Engineering Volume*, Committee on the Alaska Earthquake, Nat. Academy of Sciences, Washington, D.C., pp. 179-189.

Seed, H.B., et al. (1975) "The slides in the San Fernando dams during the earthquake of February 9, 1971", *J. of the Geotech. Engrg. Div.*, ASCE, 101(7), pp. 651-688.

Seed, H.B. (1987) "Design problems in soil liquefaction", *J. of Geotech. Engrg.*, ASCE, 113(8), pp. 827-845.

Seed, R.B., & Harder, L.F. Jr. (1990) "SPT-based analysis of cyclic pore pressure generation and undrained residual strength", *Proc. H.B. Seed Memorial Symposium*, May 1990, BiTech Publishing., Vancouver, Vol 2, 351-376.

Seed, R.B., et al. (2001) "Recent advances in soil liquefaction engineering and seismic site response evaluation", *Paper No. SPL-2*, Nat. Inf, Service for Earthq. Engrg., UC Berkeley.

Stark, T.D., & Mesri, G. (1992) "Undrained shear strength of liquefied sands for stability analysis", *J. of Geotech. Engrg.*, ASCE, 118(11), pp. 1727-1747.

Whitman, R.V. (1987) "Liquefaction - the state of knowledge", *Bull. Of NZ Nat. Soc. For Earthq. Engrg.*, 20(3), pp. 145-158.

Liquefaction Hazards in the Western Bay of Plenty

P Brabhaharan

B Sc Eng (Hons), M Sc Eng, MIPENZ, MICE, MIEAust, C Eng, CP Eng, Registered Engineer
Principal, Geotechnical Engineering & Risk, Opus International Consultants Limited, Wellington

J Thrush

BE (Hons), GIPENZ
Civil Engineer, Opus International Consultants Ltd, Wellington

Abstract: Liquefaction hazard mapping was carried out for the Tauranga and Western Bay of Plenty Districts as part of an earthquake microzoning study for the Western Bay of Plenty Engineering Lifelines Group. Liquefaction potential was assessed using current semi-empirical procedures, based on past site investigation information collated and supplemented by additional investigations to fill gaps in the information. Liquefaction hazards were mapped from the point estimates and the geology of the area, using a geographical information system (GIS).

The liquefaction hazard is variable with a high potential for liquefaction in the recent estuarine / marine / alluvial sediments including pumiceous sands and a low potential in the coastal sand deposits. Volcanic ash is generally resistant to liquefaction. Ground damage (subsidence and lateral spreading) from liquefaction was also mapped, as this is an important contributor of damage to lifelines. The hazard maps provide a basis for assessment of the risk to lifelines from liquefaction.

INTRODUCTION

Lifelines such as road, rail transportation, communications, electricity, gas, water supply, sewage systems are critical to the survival of communities after natural hazard events such as earthquakes. Therefore it is important to ensure that these facilities can survive or can be readily brought back into service after such events. The Western Bay of Plenty Engineering Lifelines Group is facilitating risk management for lifelines in the area comprising the Tauranga and Western Bay of Plenty Districts. As part of their strategy to promote the management of risks to lifelines, Opus International Consultants (Opus) and the Institute of Geological and Nuclear Sciences (GNS) were engaged to undertake an earthquake microzoning study for the Western Bay of Plenty area.

The microzoning study will provide information to assess the risk from earthquakes to lifelines in the region. The microzoning study included assessment and mapping of the earthquake hazards – active faults, ground shaking and liquefaction. Earthquake induced slope failure and tsunami hazards will be the subject of separate studies. This paper presents the assessment and mapping of the liquefaction hazards for the study area.

DEFINITION AND MECHANISM

Liquefaction includes all "phenomena giving rise to a loss of shearing resistance or to the development of excessive strains as a result of transient or repeated disturbance of saturated cohesionless soils" (National Research Council, 1985). Ground shaking associated with earthquakes gives rise to an increase in the porewater pressure in saturated, loose, mainly cohesionless soils, leading to earthquake-induced liquefaction. In soils where the increasing porewater pressures cannot dissipate rapidly, and become equal to the overburden stress, the soil particles no longer have inter-particular friction, and the soil liquefies, losing most of its strength. Sufficient strength and duration of shaking are necessary to cause significant porewater pressure increase in the soils and to reach the state of liquefaction.

Liquefaction most commonly occurs in saturated loose sands and silty sands. Increasingly it has become apparent from observations in earthquakes that loose sandy gravels and low plasticity sandy silts and silts can also liquefy (Brabhaharan et al, 1994).

LIQUEFACTION HAZARD MAPPING METHODS

Level of Mapping

Liquefaction hazard mapping has gained importance in areas subject to earthquakes, given the high level of damage that can result from liquefaction. This has been widely used for a variety of purposes such as land use planning and risk assessment. In New Zealand, hazard maps have been used for lifeline risk assessment, insurance loss studies and land use planning. A summary of the literature on liquefaction hazard mapping was reviewed as part of the 1992-1993 liquefaction study for the Wellington Region (Brabhaharan et al, 1994).

A *Manual for Zonation on Seismic Geotechnical Hazards* was prepared by the technical committee for earthquake engineering (TC4) of the International Society for Soil Mechanics and Foundation Engineering (Japanese Society for Soil Mechanics and Foundation Engineering, 1993) to provide guidance on standard approaches to the assessment of geotechnical earthquake hazards. This manual classifies zoning for geotechnical earthquake hazards into three grades :

- Grade – 1 General method using existing historical information and geology maps (low cost).
- Grade – 2 Detailed method using aerial photos, field studies and interview (moderate cost).
- Grade – 3 Rigorous method using geotechnical investigation and analysis (higher cost).

The grades represent different grades of zonation depending on the information used, and the potential use of the maps, and represent different levels of cost of preparation.

The Wellington study (Brabhaharan et al, 1994) methodology, adapted for Western Bay of Plenty study, used a combined approach with geotechnical engineering assessment using investigation data, verification of liquefaction based on historical records of liquefaction, and extrapolation of the point assessments using the geology and geomorphology of the area. The approach is similar to the Grade-3 level. However, the map was to a smaller scale appropriate for regional risk assessments, and the method minimises the cost of the zonation by making maximum use of available information on ground investigations from public and private sources, with only limited additional geotechnical investigations.

State-of-the-Art Liquefaction Assessment Methods

The liquefaction assessment methods have been further developed since the Wellington study. A workshop was held by the National Center for Earthquake Engineering Research (NCEER) based in the State University of New York at Buffalo, to bring together experts with knowledge of recent developments, and to put together the state-of-the-art methods for assessing liquefaction hazard (NCEER, 1997). The method using Standard Penetration Tests and Cone Penetration Tests adopted in the workshop is that proposed by Robertson and Wride (1998).

The Robertson and Wride method uses the Seed and Idriss semi-empirical approach, but has improved it based on a larger database of liquefaction records in past earthquakes. It incorporates correction factors for the fines content of the soil and plasticity.

Methodology Adopted for Western Bay of Plenty

The methodology adopted for the Western Bay of Plenty liquefaction hazard study was that developed for the Wellington study (Brabhaharan et al, 1994), tailored to incorporate recent refinements to the liquefaction assessment methods, and tailored to suit the information available and the requirements of this study.
This approach comprised:

- Review of historical records of liquefaction
- Data collection and additional geotechnical investigations
- Identification of areas susceptible to liquefaction

- Selection of key site investigation locations
- Selection of ground shaking hazard information
- Assessment and mapping of the potential for liquefaction
- Assessment and mapping of liquefaction induced ground damage.

REVIEW OF HISTORICAL RECORDS LIQUEFACTION

Johnston and Scott (2000) summarised a review of the available natural hazards information for the Western Bay of Plenty. In recorded history (since c. 1840), the largest shallow earthquakes in this region were the 1891 Waikato Heads earthquake and the 1932 Bay of Plenty earthquake, which had Richter magnitudes of about 6.0. The 1932 Bay of Plenty earthquake caused Modified Mercalli V (MM 5) intensity in Tauranga.

Fairless (1984) compiled case histories of liquefaction throughout New Zealand. No records of liquefaction in the Western Bay of Plenty area were identified in that study. This could be attributed to the lack of strong earthquake shaking in the Western Bay of Plenty study area during the relatively brief recorded history of European settlement in New Zealand. There are many historical records of liquefaction in New Zealand, including observations in the adjacent Whakatane District in the 1987 Edgecumbe Earthquake (Jennings et al, 1988, Pender and Robertson, 1987).

DATA COLLECTION AND GEOTECHNICAL INVESTIGATIONS

Data on ground conditions from past geotechnical investigations and studies were collected from the Councils and other organisations, with the assistance of the lifelines group project manager. Information held by Opus and GNS were also collated. The information collated and reviewed as part of this study included over 200 geotechnical / groundwater reports and well bore records from Environment BOP. The information was reviewed in relation to the known lifeline corridors, and gaps in the available information were identified. Further information was collected from other organisations by targeting these gaps. The locations were mapped in a geographical information system (GIS). A programme of geotechnical investigations, comprising comprised four boreholes with Standard Penetration Tests, nineteen Static Cone Penetration Tests (CPT) and laboratory classification tests, were carried out to fill remaining gaps in information along important lifeline corridors in areas identified as being susceptible to liquefaction.

LIQUEFACTION SUSCEPTIBILITY BASED ON GEOLOGY

Geology Maps

The geological map compiled by GNS was used to characterise the areas susceptible to liquefaction. The geology was compiled from three published geological maps of Healy et al (1964) at 1:250,000 scale, Briggs et al (1996) at 1:50,000 scale and Edbrooke (2001) at 1:250,000 scale. For the geological units that weren't common to all three maps, the legend of Edbrooke was adopted because of its finer subdivision of the Quaternary and Holocene Age geological units. The geology of the area comprises various ignimbrite flow sheets, which have been subsequently mantled by alluvium and volcanic ash. Soft estuarine sediments and alluvium have been deposited in flood plains and incised gullies that extend inland from the coast.

Liquefaction Susceptibility of Major Soil Units

The major soil types in the study area were characterised for liquefaction susceptibility.

Estuarine Deposits: Large areas of estuarine deposits are present in the study area, and comprise sands, silts and clays. The dominant silts and sands are susceptible to liquefaction, and a thickness of 5 m to 20 m or more of loose sediments are present in these areas.

Although fine-grained soils (silts) are more resistant to liquefaction, it is now recognised that low plasticity fine-grained soils such as silts can liquefy. For example, ground damage observations in Wellington during the 1855 Wairarapa Earthquake indicate that fine-grained soils liquefied in that earthquake (Brabhaharan et al, 1994). Even when liquefaction of very soft fine grained soils does not occur, these soft soils can undergo severe loss of strength during ground shaking, and can give rise to ground strains and lateral spreading similar to classic liquefaction.

Volcanic Ash Deposits: The terrace areas from Tauranga to Katikati are covered with volcanic ash deposits, which comprise clays, silts and some sand layers. These are generally firm to stiff or medium dense. These materials are generally considered to be resistant to liquefaction due to the fine-grained plastic nature and the presence of some "welding effects" due to their volcanic origin.

Volcanic Grits and Pumiceous Sands: Coarser grained pumice deposits have been shown in recent studies to be susceptible to liquefaction (Shimizu, 1998 and Marks et al, 1998). Observations during the 1987 Edgecumbe Earthquake in the Eastern Bay of Plenty also showed that sand with significant pumiceous material had liquefied (Pender and Robertson, 1987). Therefore, localised loose sand layers that are present among the volcanic ash deposits may undergo minor liquefaction under strong ground shaking.

Older terrace deposits: The older terraces such as in the Te Puke area include sand deposits, which are moderately dense and are of limited thickness. The older deposits tend to have a lower susceptibility to liquefaction due to ageing effects, which could lead to some inter-particle bonding. These areas are only likely to liquefy in larger events and the associated thickness is smaller.

Coastal sand deposits: The coastal sands are generally medium dense to dense, consistent with their higher energy depositional environment. These are generally resistant to liquefaction, but may experience some liquefaction in large earthquake events.

Residual Soil from Ignimbrite Sheets: Various ignimbrite sheets are present in the area, and near the surface, they are completely weathered and are indicated to be clays and sands. There is limited information from these areas to assess the liquefaction. In some locations these comprise loose sands and silts which are likely to be susceptible to liquefaction. However, these may be localised and the predominantly these residual soils are likely to be dense or stiff and resistant to liquefaction. Given that there are limited lifelines through these areas, this uncertainty is less important.

LIQUEFACTION ASSESSMENT

Selection of Key Locations

Key locations of geotechnical information were selected from the large database of ground investigation locations, based on their quality, the susceptibility based on geology, and the lifeline corridors. Seventy-five key locations were chosen, and some assumptions, particularly regarding groundwater levels and particle size distributions were made to supplement the factual information.

Ground Shaking Hazards

Ground shaking hazards were compiled by GNS as part of the earthquake microzoning project. Peak ground acceleration maps had been derived for two uniform hazard scenarios of 10% probability of exceedance in 50 years (return period of 475 years) and 2% probability of exceedance in 50 years (return period of 2500 years). The uniform hazard ground shaking maps were used for the liquefaction assessment. Liquefaction depends on the magnitude of the earthquake and associated duration of shaking. The contribution to the uniform hazard comes from earthquakes with different

magnitudes. Therefore, it is not appropriate to use the uniform hazard peak ground accelerations directly for the analyses. A method of weighting proposed by Idriss (1985), to modify the peak ground accelerations depending on the earthquake magnitude, was used by GNS to derive *magnitude weighted peak ground accelerations*. The magnitude weighted values then allow the use of the standard liquefaction charts based on an earthquake magnitude of 7.5.

Analyses

The liquefaction analysis was based on empirical correlation of cyclic stress ratio with Standard Penetration Test 'N' values or Static Cone Penetration Test cone resistances (q_c), for soils which liquefied and those which did not liquefy in past earthquakes (NCEER, 1997).

$$\text{Cyclic stress ratio} = 0.65 \cdot a_{max} \cdot \sigma_o \cdot r_d / \sigma'_o \cdot g \qquad (1)$$

where,

a_{max}	peak ground acceleration
σ_o	total overburden stress at the depth under consideration
r_d	stress reduction factor that reduces from 1 at the ground surface
σ'_o	effective overburden stress at the same depth
g	gravitational acceleration

The penetration test values were corrected for energy differences in the Standard Penetration Tests and overburden pressure. The fines content and Plasticity Index of the soils were used (and where not available assumed) to adjust for the increased liquefaction resistance associated with the proportion of fines and higher plasticity. The analysis indicated thickness of soils that are likely to liquefy at each of the key sites, and their potential for liquefaction.

Classification and Mapping

Liquefaction potential was mapped into the five classes in Table 1, depending on the likelihood of liquefaction in the two uniform ground shaking levels, the liquefaction thickness and extent of associated ground deformation.

Class	Liquefaction Potential	Description
1	No Liquefaction	Liquefaction unlikely in any scenario, except locally such as in stream deposits or fill.
2	Localised Liquefaction	Liquefaction is generally unlikely but there may be limited areas that are likely to liquefy in a large earthquake event.
3	Minor Liquefaction	No liquefaction likely in a 10% in 50 year earthquake shaking, but liquefaction of limited layers may occur in a 2% in 50 year shaking.
4	Moderate Liquefaction	Liquefaction is likely in both 10% and 2% in 50 year earthquake shaking, in localised areas or leads to limited ground damage.
5	Widespread Liquefaction	Liquefaction is likely to be extensive in both 10% and 2% in 50 year earthquake shaking and could lead to significant ground damage.

Table 1. Liquefaction Potential Classes.

The liquefaction hazard was then mapped by considering the point assessments of liquefaction potential and the extent of liquefaction based on the geographical spread of the point estimates and the geological extent of the soils. Part of the liquefaction hazard map is shown on Figure 1.

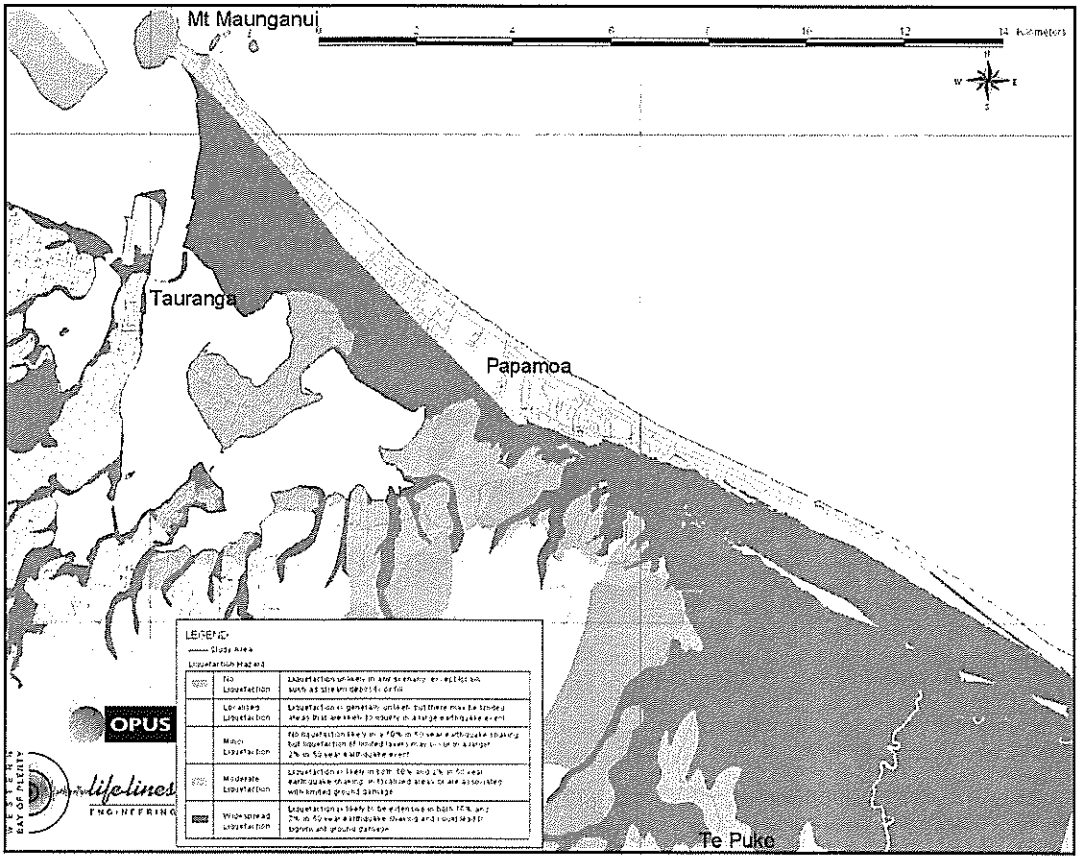

Figure 1. Part of Liquefaction Potential Map

LIQUEFACTION GROUND DAMAGE

Consequences of Liquefaction

The following consequences of liquefaction can cause damage to lifelines :

- Ground damage – subsidence, lateral spreading, flow failure, slope failure
- Bouyancy on buried facilities, exacerbated by flooding from ejection of water and sand / silt
- Foundation failure due to reduction / loss of bearing capacity
- Settlement of structures on liquefied materials

Liquefaction induced ground damage is an important contributor to the damage to most lifelines. The other consequences will depend on the form of the lifeline structures and their foundations.

Types of Ground Damage

Liquefaction can lead to ground damage in the form of :

- Subsidence of ground underlain by liquefied soils
- Slope failure or flow failure of liquefied ground
- Lateral spreading of liquefied ground, and of embankments on liquefied ground

Liquefaction resistant surface layers can reduce ground surface damage from liquefaction of underlying layers. However, such non-liquefiable surface layers may not preclude lateral spreading. Recent studies have indicated that lower permeability, liquefaction resistant layers overlying liquefiable soil layers may lead to the formation of water films at the interface, and can result in liquefaction of the overlying layers and increased lateral spreading.

The ground damage will depend on the liquefiable soils, their thickness, and the topography.

Ground Subsidence

Subsidence of the ground due to liquefaction was assessed using the method proposed by Ishihara and Yoshimine (1992), for each key location chosen for liquefaction assessment. These very approximate subsidence estimates range from less than 10 mm to over 1 m. Indicative magnitudes of ground subsidence for the different liquefaction potential classes in a 10% in 50 year earthquake shaking are given in Table 2.

Class	Liquefaction Potential	Order of Magnitude of Subsidence (mm)
1	No Liquefaction	None
2	Localised liquefaction	Variable but likely to be small.
3	Minor Liquefaction	Less than 100 mm
4	Moderate Liquefaction	100 mm to 300 mm
5	Widespread Liquefaction	Greater than 300 mm (possibly over 1 m)

Table 2. Liquefaction Induced Subsidence.

Lateral Spreading

Lateral spreading of ground has the potential to cause a greater magnitude of ground damage and consequential damage to lifelines. This could occur where liquefied ground can displace towards free surfaces such as river or stream banks and the shorelines. Any embankments (including bridge approaches) built on liquefiable ground are also likely to undergo lateral spreading. Severe damage to a road embankment due to liquefaction related lateral spreading during the 1931 Napier Earthquake is shown on Figure 2.

Figure 2. Lateral Spreading of Road Embankment in Napier Earthquake, 1931

The extent and magnitude of lateral spreading is difficult to assess for regional scale mapping. However, simple rules as to the magnitude and extent of lateral spreading, based on observations in historical earthquakes, were used to provide an indication of the lateral spreading ground damage that may occur, recognising that this is indicative only.

Classification and Mapping Liquefaction Ground Damage

The liquefaction ground damage hazards was mapped using ground damage (subsidence and lateral spreading) assessments, the liquefaction hazard and the proximity to river and significant stream banks. The liquefaction ground damage hazard classification is presented in Table 3.

Liquefaction Ground Damage Zone	Class Description	10% in 50 years	2% in 50 years
A	None	No liquefaction ground damage	
B	Localised minor	Localised minor subsidence	
C	Minor	Minor subsidence (less than 100 mm)	
D	Limited	Moderate subsidence (say 100 mm to 300 mm)	
E	Moderate	Large Subsidence (say greater than 300 mm)	
F	Large	Minor lateral spreading and moderate subsidence	Significant lateral spreading and moderate subsidence
G	Major	Significant lateral spreading and large subsidence	
H	Widespread	Significant lateral spreading and moderate subsidence.	Extensive lateral spreading and moderate subsidence
I	Extensive	Extensive lateral spreading and large subsidence	

Table 3. Liquefaction Ground Damage Classification.

Notes : Lateral spreading definitions

- Minor 10s of millimetres to 200 mm
- Significant 100s of millimetres to 1 metre
- Extensive up to few metres

The classification in Table 3 was used to prepare a map of liquefaction ground damage hazards. This provides a useful resource for the assessment of damage to lifelines. A section of the liquefaction ground damage hazard map is shown in Figure 3.

It is worth noting that significant lateral spreading damage was experienced in the 1995 Kobe Earthquake in Japan, and lateral spreading of the river banks were observed during the 1987 Edgecumbe Earthquake in the eastern Bay of Plenty.

SPATIAL INFORMATION MANAGEMENT AND MAPPING

The earthquake microzoning study involved collection and management of a large amount of information. The data was obtained in digital form or mapped, and managed within a geographical information system (GIS), in this instance ArcView. This enabled the information to be processed efficiently. The maps were produced in GIS format and are available for use in spatial GIS format, to facilitate the overlay of lifeline assets and assessment of the risk.

The maps were printed to a scale of 1:50,000 for the Tauranga urban area, with 1:250,000 scale maps showing the whole study area.

The maps have been prepared from a district scale study and can be used for the assessment of risk to lifeline networks at a district level. While they show areas of liquefaction and ground damage hazard, they should not be used to assume liquefaction or no liquefaction at specific sites. The maps should not be used as a substitute for site-specific investigations and assessments for individual sites and facilities. The classification of liquefaction and ground damage is indicative only. Identification of the limitations is important, so that hazard maps are not used out of context.

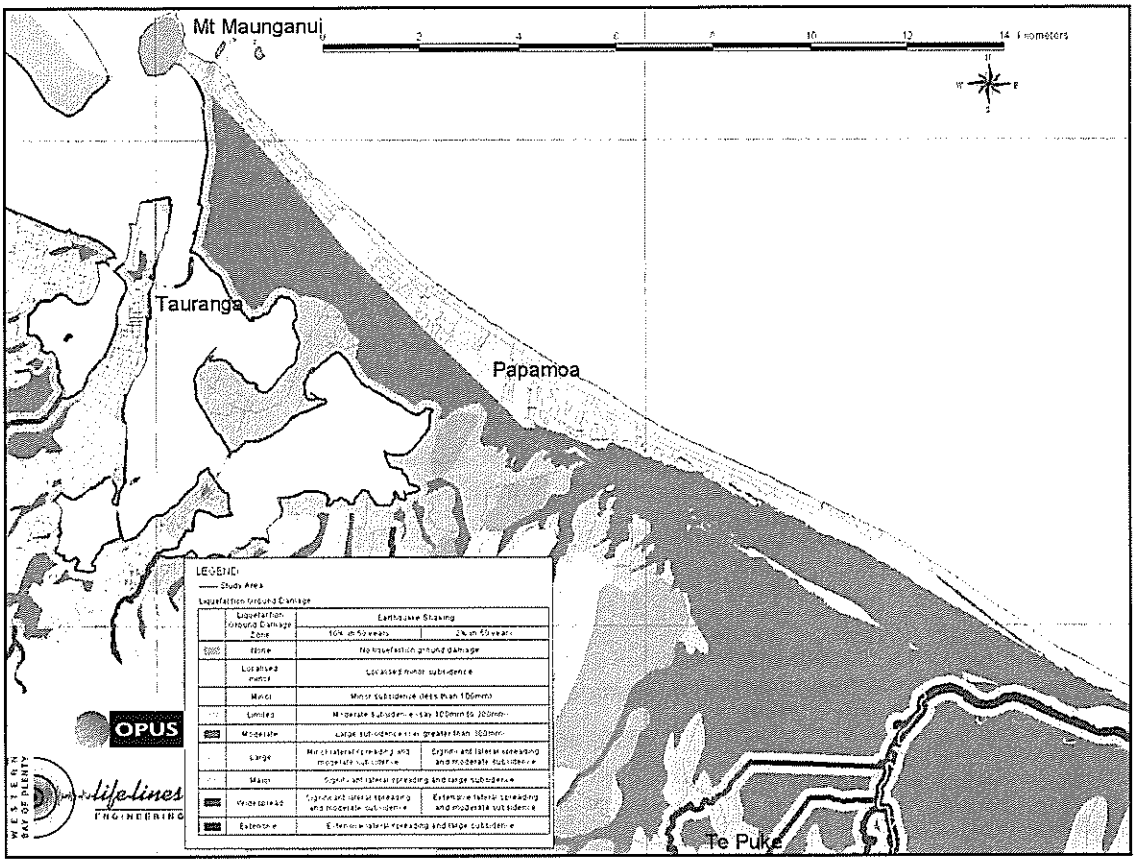

Figure 3. Part of Liquefaction Ground Damage Map

CONCLUSIONS & RECOMMENDATIONS

The geology of the Western Bay of Plenty area is complex with predominantly volcanic, estuarine, marine and alluvium deposits. The liquefaction assessment is based on a robust and efficient methodology, which was used to assess and map the liquefaction hazard using geotechnical information and the geology and topography. The liquefaction performance of volcanic soils is variable, with fine-grained volcanic ash deposits generally being resistant to liquefaction, and pumice sands generally being vulnerable to liquefaction. A key feature of the area is the presence of large areas of estuarine deposits that are vulnerable to liquefaction. Liquefaction induced ground damage was also mapped as lifelines are generally vulnerable to ground damage.

The methodology used provides a rational approach to prepare liquefaction hazard information suitable for the assessment and management of the risk to lifelines.

Further research into the liquefaction performance of volcanic soils, in particular the volcanic ash deposits would be valuable in refining the liquefaction hazard in volcanic regions.

ACKNOWLEDGEMENTS

The authors wish to acknowledge the significant contribution to the study from John Scott, Lifelines project manager (Tauranga District Council) who collected a large amount of geotechnical records, and Grant Dellow, Graeme McVerry and Peter Wood of GNS for the geology and ground shaking inputs used in the study. The contribution of Roger Lynch who prepared the GIS database and maps is also acknowledged.

Permission to publish this paper from the Western Bay of Plenty Lifelines Group and Opus International Consultants Limited is also acknowledged.

REFERENCES

Brabhaharan, P, Hastie, W J, and Kingsbury, P A (1994). "Liquefaction hazard mapping techniques developed for the Wellington Region, New Zealand". *Annual NZNSEE Conference*, Wairakei, 18-20 March 1994.

Briggs, R.M., Hall, G.J., Harmsworth, G.R., Hollis, A.G., Houghton, B.F., Hughes, G.R., Morgan, M.D., and Whitbread-Edwards, A.R (1996). "Geology of the Tauranga area, Sheet U14 1:50,000". Occasional Report No. 22, *Dept of Earth Sciences*, University of Waikato, Hamilton, New Zealand.

Edbrooke, S.W. (Compiler) 2001. "Geology of the Auckland area". *Institute of Geological and Nuclear Sciences* 1:250 000 geological map 3. 1 sheet + 74p. Lower Hutt, New Zealand: Institute of Geological and Nuclear Sciences Limited.

Fairless, GJ (1984). "Liquefaction Case Histories in New Zealand". Report No 84/18. September 1984. 73p. Dept of Civil Engineering, *University of Canterbury*, Christchurch, New Zealand.

Healy, J., Schofield, J.C. and Thompson, B.N. (1964). "Sheet 5 Rotorua" (1st Ed.). "Geological Map of New Zealand 1:250,000". *Department of Scientific and Industrial Research*, Wellington, New Zealand.

Idriss, I.M. (1985). "Evaluating seismic risk in engineering practice". Proceedings of the *11th International Conf on Soil Mechanics and Foundation Engineering*, San Francisco, 1: 255-320.

Ishihara, K and Yoshimine, M (1991). "Evaluation of settlements in sand deposits following liquefaction during earthquakes". *Soils & Foundations* 32, No 1, pp173-188.

Japanese Society of Soil Mechanics and Foundation Engineering (1993). "Manual for Zonation on Seismic Geotechnical Hazards". Prepared by the Technical Committee for Earthquake Geotechnical Engineering, TC4, of the *International Society for Soil Mechanics and Foundation Engineering*. 149p.

Jennings, DN, Edwards, MC and Franks, CR (1988). "Some observations of sand liquefaction in the 2 March 1987 Edgecumbe (New Zealand) Earthquake". Proceedings of the *5th ANZ Geomechanics Conference*, Sydney, August 1988.

Johnston, D and Scott, J (2000). "A review of natural hazards information for the Western Bay of Plenty". Stage 1 Report. December 2000.

Marks, S, Larkin, TJ and Pender, MJ (1998). "The dynamic properties of a pumiceous sand". *Bulletin of the New Zealand National Society for Earthquake Engineering*. 31(2). pp86-102.

NCEER (1997). "Proceedings of the NCEER workshop on evaluation of liquefaction resistance of soils". Edited by TL Youd and IM Idriss. *Technical Report No NCEER-97-0022*. National Center for Earthquake Engineering Research.

Pender, MJ and Robertson, TW (1987). "Edgecombe Earthquake : Reconnaissance Report". Edited by Pender and Robertson. Bulletin of the New Zealand National Society for Earthquake Engineering, Vol20, No 3, September 1987.

Robertson, PK and Wride (1998). "Evaluating cyclic liquefaction potential using the cone penetration test". *Canadian Geotechnical Journal*. 35 : 442-459.

Shimizu, M (1998). "Geotechnical features of volcanic ash soils in Japan". *Int Symposium on Problematic Soils*. IS-Tohoku'98 (Sendai, Japan), pp907-927. Balkema, Rotterdam.

The Legal Implications of Risk

A M G Green
LLB, CoP Environmental Law, Partner, Brookfields, Auckland
E Y-H Tan
BCom, LLB, Solicitor, Brookfields, Auckland

Abstract: Where hazards are identified, for example subsidence arising from historical mining or the collapse of a road due to the presence of weak in situ materials territorial local authorities are bound by statute to assess the public safety risk (including individual and societal risk values). Where unacceptable risks are found to exist those authorities must look to their empowering legislation for authority to ensure the safety of the public and individuals. Such actions can give rise to damages claims arising from, among others, the loss of value of real estate, the closing down of businesses.

INTRODUCTION

Legal risks are significant issues for territorial local authorities ("Council(s)"); sources of such risks come from the general concept of a duty of care which arises when a function is performed (or, as the case may be, not performed).

This paper focuses on the legal implications of risk and, as such, concentrates on the consequence of risk and not the likelihood of risk. In this paper, examples are given of the types of liability which Councils can attract. Of particular interest are actions in negligence.

Negligence has the following elements: there must be a duty of care; that duty must be breached; and the person (plaintiff) must suffer a loss. In other words, these elements must be established when a claim is advanced in negligence. A claim in negligence therefore can become somewhat difficult to mount. Simply stating these elements begs the question of what that actually means.

To complicate matters, Councils are not only exposed to liability at common law, but also when they perform (or fail to perform) their statutory functions. Councils are bound by statute to take positive action to protect the safety of the public. It is this duty which gives rise to further implications which this paper considers, namely Councils' exposure to liability once positive action is taken or, in other circumstances, Councils' exposure to liability if they fail to take the appropriate steps once hazards (such as subsidence arising from historical mining, or the collapse of a road due to the presence of weak in situ materials) are identified.

This paper is structured as follows:

Councils' obligations and powers at common law and under the statutory regime

Concept of the duty of care

- General Approach
- Historical and social reasons for the imposition of duties of care on Councils
- Limitations on duties of care
- Defences – Discretionary function immunity

Illustrative examples – case law

COMMON LAW AND STATUTORY DUTIES

Civil liability is derived from common law principles, such as duties of care, the genesis of which is attributed to the general maxim that one "must take reasonable care to avoid acts or omissions which [one] can reasonably foresee would be likely to injure [one's] neighbour".[1]

Council's duties and powers are also supplemented, or qualified, by various pieces of legislation. Reference is made, by way of example, to the Local Government Act 1974 and the Local Government Act 2002, the Health Act 1956, the Resource Management Act 1991, the Building Act 1991 and the Civil Defence Emergency Management Act 2002.

Councils in New Zealand are under statutory obligations to take steps to ensure the safety of the public.[2] This in turn necessarily means that when hazards are identified, Councils are bound by statute to assess the risks posed.

CONCEPT OF DUTY OF CARE

General Approach

Generally speaking, the following tests establish whether Councils owe a duty of care:

(a) the foreseeability of the harm that ensues;

(b) the nature of the relationship between the parties, usually called "proximity"; and

(c) whether it is fair, just and reasonable that the law should enforce a duty of care, sometimes referred to as "policy reasons".

Historical and Social Justification

In general terms, Courts have imposed duties of care on Councils in the New Zealand social and historical context, and at least in the context of undertaking building inspections, for the following reasons:[3]

- High proportion of owner occupied housing
- Housing construction which was undertaken by small scale cottage builders for individual purchasers
- Substantial responsibility accepted by the state for financing low-cost housing
- Surge in housing development in mid 1970's
- Wider central government and Council support for private house building as regards planning and building controls
- Lack of any common practice for new house buyers to commission their own architectural and engineering surveys, particularly in the context of low cost housing

It is those general community standards and expectations (and, more particularly, the perception thereof) which demands an imposition of a duty of care on Councils.

The concept of reliance has been held to be an important element in establishing if a duty of care exists. There has been found a doctrine of "reliance" or dependence upon Councils' performance of their functions, and that reliance has been affirmed by the Privy Council in **Invercargill City Council v Hamlin**[4] in view of the local conditions.[5] **Hamlin** was a case which dealt with negligent

Council inspection of buildings, Hamlin having sued the Council for having negligently inspected his house when it was built in the early 1970s.[6]

This doctrine has been held to be inappropriate in other jurisdictions. Reference is made, in this connection, to the Australian decision **Pyrenees Shire Council v Day**,[7] in which the doctrine was rejected for being no more than indicative of a duty of care (rather than determinative of such a duty).

Limitations of Duties of Care

There are limitations on Councils' duties of care. Generally speaking, Councils owe a duty of care to landowners and successors in title but not to persons interested in the land (e.g., creditors, guarantors etc). For example, the duty that Councils owe in relation to the issue of consents for a development is owed to the developer, not to those financially interested in the developer, either as shareholder, if the developer is a company, or creditors of the development company.[8]

Defences - Discretionary Function Immunity

In assessing the impact of those obligations that arise from statutes, there is a need to differentiate between breaches of statutory duty and liability at common law. It is firmly established, at least in the New Zealand context, that a duty of care will not always arise in the performance of all Council functions. In other words, it will not always be the case that a breach of statutory duty will give rise to a claim in damages.[9] Generally speaking, the question of whether Councils will be liable in damages for a breach of that duty will depend on whether there can be detected in the words of the statute an intention by Parliament to allow individuals (or a class of persons) to sue. Case law has demonstrated that the Courts will only do this in limited circumstances. Put simply, the plaintiff must show the following:[10]

(a) that the circumstances are such that there is a duty of care at common law;

(b) that a statutory duty gives rise to a common law duty for the Council to do or refrain from doing a particular act; or

(c) that, in the course of carrying out that duty, the Council has brought about such a relationship between itself and the plaintiff as to give rise to a common law duty of care.[11]

There are policy reasons for and against the imposition of such duties on Councils. In this connection, there is a distinction between "policy" and "operational" decisions. More particularly, a well established (although criticised),[12] line of decisions holds that it is necessary to distinguish between complaints against public bodies about the broad merits of a decision which is made in the exercise of a statutory power ("policy"), and complaints about the manner in which that discretionary power has been implemented ("operational"). A duty may be owed in "operational" decisions. Unfortunately, this distinction is not always clear. In other words, Councils could be exposed to liability if, in the implementation of policy decisions, there is some failure to discharge the duty to take reasonable care to avoid injury.

In addition, it has also been held that no duty is owed in respect of decisions or conduct within the ambit of statutory discretion.[13]

Examples of policy decisions include a Council's discretion to rezone certain parcels of land. Arguably, the extent to which a Council should commit its resources or not be committed to the investigation of the suitability of land to be developed is a policy decision and as such, and speaking in general terms, no duty of care is owed in respect of its actions. If, on the other hand, a Council comes into knowledge that certain parcels of land are unsuitable for, say, residential occupation, then it is obliged to look to its empowering legislation and take the appropriate measures.

Examples of operational decisions include Councils' grant of subdivision consents for the development of certain areas of land.

Illustrative Examples – Case Law and Working Examples

The exception of liability in respect of those decisions at policy level or where there are policy reasons justifying the prima facie failure to act appropriately within the operational sphere is important.

Anns v Merton London Borough Council[14] recognised this exception and, more particularly, the case recognises that it must be for a Council to determine the appropriate resources to apply to the various activities in which it is involved or, in some cases, to decide where its priorities lie.[15] In **Anns**, the subsequent owners of a defective building claimed that the Council had been negligent in the exercise of its statutory powers to inspect the building work while it was constructed. As a consequence, the building was built on foundations that were too shallow and subsequently the building suffered cracking and subsidence. Their Lordships were unanimous in finding that a duty of care was owed. Note, however, Lord Wilberforce's recognition that the distinction between "policy" and operational" decisions was a question of degree.[16] Lord Wilberforce said that "many "operational" powers or duties have in them some element of "discretion". It can safely be said that the more "operational" a power or duty may be, the easier it is to superimpose on it a common law duty of care."[17]

While **Anns** deals primarily with Council liability in respect of defective buildings, their Lordships' observations can be appropriately applied, especially as to Councils' discretion as to the way in which resources are allocated.[18]

Coastal erosion

Many will be familiar with the issue of coastal erosion in New Zealand. The issue has become more of an imprecation now that the mean sea level rise is increasing and there appears to be no long term means by which to mitigate against the hazards posed by this.[19] Coastal erosion is an issue which attracts debate as to the extent to which there may be a duty on Councils to prevent land movements forming part of geological development. Traditionally, liability will follow if there has been some positive act to withdraw or remove support. Failure to act is insufficient to found liability. Note the following facts in **Leakey v National Trust for Places of Historical Interest or Natural Beauty**.[20] Over a period of many years, soil and rubble fell from the bank of a mound on to the plaintiff's land, which fall was due to natural weathering and the nature of the soil. It transpired that the defendant knew of the instability of its land and, in particular, it knew that the instability was a threat to the plaintiff's property. Some correspondence ensued between the parties during which the defendant's attention was directed to the danger to the plaintiff's house. The defendant was found liable. If the principles in **Leakey** were applied, then a failure to act when there is a known risk of subsidence affecting land will be enough.[21]

It will be interesting to see if such cases could be similarly applied to New Zealand in the context of coastal erosion. Once again, there needs to be some recognition that the statutory regime here is different to what exists in other jurisdictions. In this regard, the High Court in **Falkner v Gisborne District Council**[22] considered whether the English common law (with regard to the issue of the protection of land from the encroachment of the sea) could apply to New Zealand. The statutory scheme in New Zealand and, in particular, the Soil Conservation and Rivers Control Act 1941 and the Resource Management Act 1991, meant that it did not follow that the duties imposed elsewhere had to be adopted in view of the conditions here.

Subsidence is a reality which those in coastal settlements must accept. Subsidence will occur and it is merely a question of when. If the land upon which residential settlement suddenly collapses, which collapse is foreseeable (and, by implication, loss in value of real estate and possibly physical harm and damage are equally foreseeable), what then are Councils' responsibilities? What liabilities arise and what should Councils do to minimise any such liability?

A Council is obliged, under the Building Act 1991 and the Health Act 1956, to ensure the safety of buildings and those who live within them, as well as to "improve, promote, and protect public health

within its district".[23] Depending on the risks posed to members of the public, it may be appropriate in some circumstances to vacate buildings and in some circumstances, for example, to put up hoardings or fences to caution those visiting or entering the area of the hazard posed. Reference is made, in this regard, to Councils' discretionary powers under, say, section 65 of the Building Act 1991.[24]

If applications for building consents are made *before* the land subsides, Councils may be liable if their record keeping and information monitoring functions are not properly discharged under section 35 of the Resource Management Act 1991. In fact, the High Court in **Bronlund v Thames-Coromandel District Council**[25] awarded the plaintiff general and special damages for negligently issuing a building permit. Comments were also made a Council is unable to claim a policy defence and, in particular, it will not always be appropriate to point to a scarcity of resources to justify a Council's failure to carry out a clear statutory duty. The Court declined, in this case, to see how financial considerations could justify a departure from statutory obligations. In addition, the Court saw the importance of the Council's functions being properly carried out. In order for the Council to perform its function properly it was absolutely vital that the record cards have recorded on them any relevant planning information.

Once the collapse occurs, the issue arises as to when and to what extent Councils have to take positive action to ensure the safety of the public. The legislation is silent in terms of the extent to which a Council must investigate and monitor hazards once they have been identified. Guidance is gained, however, from the over-riding principles and purposes in the Building Act 1991 and the Health Act 1956.

Lord Wilberforce's observations in **Anns** also lend some assistance in determining the extent to which a Council is obliged to take positive action when hazards are identified. According to Lord Wilberforce, it is for a Council to decide on the scale of resources which it could make available in order to carry out its statutory functions.[26]

In the context of coastal erosion, which damage is foreseeable, it will be vital as a first step for Councils to adequately notate LIM and PIM records and to make contrary information available.[27]

Once there has been subsidence, and taking on board Lord Wilberforce's recognition that Councils should be free to decide on the scale of resources, it is suggested that, as a first step, Councils allocate some resources in investigating and identifying hazards (which necessarily includes an identification of the areas affected) and the risks posed by such hazards (which necessarily includes individual and societal risk calculations). Such investigations and identifications will involve geotechnical experts. The terms of reference of such works must be sufficiently wide in order for Councils to sufficiently discharge their obligations at law. It is useful, in this regard, for geotechnical reports to indicate whether the risks posed are at an unacceptably high level or otherwise.

Once such reports are commissioned and the levels of risk are identified, it may be appropriate to make this information available. In this connection, LIM and PIM reports as well as Council property files should make reference to such reports so that the public are adequately informed (which is the purpose behind provisions such as section 35 of the Resource Management Act 1991).

It makes sense that Councils should be able to determine how geotechnical experts should be used (i.e., with what expert qualifications, what tests should be carried out).[28] A plaintiff complaining of negligence (and who brings proceedings for loss of value in real estate, or, in the context of businesses, a loss of profits) must prove that the actions taken by Councils were outside the limits of a discretion bona fide exercised before the plaintiff could begin to rely on a common law duty of care.[29] Note too that where a person suffers loss as a result of conduct by, say, a Council officer[30] which is malicious or which is known to be beyond power, that loss is recoverable in the tort of misfeasance in public office, which tort is concerned with the control of abuse by persons in authority of their position of power over members of the public.[31]

Therefore, once the reports are commissioned, and as long as a Council can point to a valid trail along which it can demonstrate that some resources have been allocated to identify the risks posed by certain

hazards (which identification is necessary under the common law and the statutory regime), it is suggested that a Council should not be exposed to liability unless it can be shown that it has acted outside the ambits of power.

Councils will always have to balance the competing interests once it is known that the risks posed by certain hazards are unacceptable. If it can be shown that the reports upon which a Council relies are valid and defensible (in this connection, it is suggested that there may be some merit in getting reports peer reviewed), and such reports point to an unacceptable level of risk, then it would not be unreasonable for a Council to, say, resolve to issue warrants under section 70 of the Building Act 1991 to require residents to vacate from their properties. Such actions will of course attract the threat of proceedings (loss of profits as a result of the closure of certain businesses, and the loss of value in real estate). Provisions such as section 70 of the Building Act 1991 protect a Council to some degree as it is stated that no liability will lie on the part of a Council if warrants are issued in good faith. It is for that reason that it is suggested that expert reports be commissioned and that such reports be independently reviewed.

Mining

Companies which operate in areas of land subject to subsidence (as a result of, say, previous underground mining) may wish to continue operations notwithstanding a Council's resolution to have people vacate certain areas. In this connection, there may be some suggestion that such companies could demonstrate to a Council that no risk (or a low risk) is posed in terms of certain areas of operations.

In this regard, it may be appropriate for risks to be quantified. By way of example, risk calculations for residential areas may be different to the risk posed in relation to current mining areas. To this end, the calculation of individual and societal risk values for buildings and activities within hazard areas could be qualified by treated/untreated risks and interim risk in relation to the times of exposure and populations at risk.

It may be advisable in these circumstances for Councils to require further reports to be commissioned by those companies, which reports can be independently reviewed by Councils' experts.

Highway hazards

In **Stovin v Wise**[32] the House of Lords (England) once again considered whether it was appropriate to find liability when Councils are exercising statutory functions. The facts were as follows. The plaintiff was riding his motorcycle along a road when a car, driven by the defendant, emerged from a junction into his path. The plaintiff was unable to stop in time and a collision occurred in which the plaintiff suffered serious injuries. The trial judge found that the Council had known that the junction was dangerous (there being accidents at the junction in 1976, 1982 and 1988) and had been negligent in failing to take steps to make it safer.

What made matters worse at the junction was that the view was obstructed by a bank of earth topped by a fence.

Interestingly, the Council's computerised records would have given the junction the status of a "cluster site" or an accident black spot had there been five personal injury accidents within three years. Three accidents in 12 years, however, did not merit special attention under the Council's policy for dealing with hazardous stretches of road. A road safety committee had taken up the matter and before the plaintiff's accident, the committee had approached British Rail, who owned the land upon which stood the obstructing bank and fence. A suggestion was made by British Rail for the junction to be realigned. Upon inspection, Council's traffic movement expert thought that the removal of the bank would be the best solution. Some correspondence followed between the Council and British Rail. Unfortunately, nothing had happened by the time the plaintiff suffered his injuries.

In reversing the Court of Appeal's decision, the House of Lords commented that it was not irrational for the highway authority (the Council) to remove the bank or have it removed, since it was under no duty in common law to undertake the work. Such works were matters of discretion for a Council. Their Lordships found that even if, as a matter of public law, there was a requirement to effect the works, there were no grounds upon which it could be said that the public law duty[33] gave rise to an obligation to compensate persons who suffered loss because that duty was not performed. Again, it was emphasised that it must be demonstrated that the circumstances were such that it would have been irrational for a Council not to have exercised the power.

Stovin was distinguished in the recent English case **Kane v New Forest District Council**[34] on the basis that the Council in **Kane** had created the source of danger since it had required the construction of the footpath and knew that the sightlines to the road made it dangerous to use.

Placing of warning signs

The New South Wales Court of Appeal considered recently the factors relevant in establishing a breach of duty based on the failure to erect appropriate warning signs. In **Waverley Council v Lodge**[35] (where a person walking along a path between a tidal rock pool and concrete steps slipped and fell on rocks), the trial judge had found a breach of duty in that the Council had failed to erect an appropriate warning sign to warn of the potential danger of the rocks. Of interest are the factors to which the Court referred in commenting on the difficulties in establishing a breach in these circumstances:

"Everyday experience does not support attributing talismanic force to signs as a means of averting danger. It is commonplace to see warning signs ignored. An attempt to analyse considerations supporting and adverse to erecting signs of this kind is made difficult by the obvious nature of the information which they would convey."

In particular, such considerations highlight issues which may be potentially the subject of evidence but rarely addressed forensically (such as the impact of signs on human behaviour and the extent to which they are read and complied with).[36] A significant element in **Waverley** was the unchallenged finding that the person who slipped on the rocks had failed to take reasonable care for his safety. The Court found no evidence of any conduct on the part of the Council promoting or encouraging the public use of the tidal rock pool as a venue for swimming and, in those circumstances, the scope of the Council's duty did not extend to erecting signs to warn of something which would do no more than state the obvious.

In the English Courts recently,[37] the Court of Appeal held that common law liability for failure to take safety measures, for example by providing warning signs, could only arise where Council has acted outside its discretion under the English Road Traffic Act 1988 to take appropriate measures to prevent accidents. In other words, the failure on the part of the Council to provide warning signs additional to the two "Give Way" signs at the mouth of the junction was not unreasonable.

CONCLUSION AND RECOMMENDATIONS

The implications to arise when hazards are identified can be severe for a Council, as it is exposed to liability for damages if a duty of care exists and there are no justifications to excuse the way in which a Council has acted, or failed to act. Having said that, however, if it can be demonstrated that a Council exercised its discretion appropriately by, at the very least, commissioning reports so that an accurate level of risk can be identified, then any subsequent actions (or inactions) of a Council can be defended on policy reasons. The judicial debate as to whether this is appropriate and indeed desirable continues and will no doubt be heightened in times when a Council's empowering statutes are under review.[38] It is suggested that, in any event, it will be difficult for a claimant to mount a claim against a Council in negligence when a Council can demonstrate that it allocated its resources in the first instance to identify the risks posed to the safety of the public.

[1] *Donoghue v Stephenson [1932] AC 562 at 580 as per Lord Atkin*

[2] *In the Australian context, Councils are under what is described as a "self-imposed" duty of care to take measures to protect the safety and interests of the public. See, in this regard, Hemmings, N., QC, (1995) "Development Approvals and the Duty of Care." Local Government Law Journal (1995) p 30.*

[3] *Hamlin v Invercargill City Council [1994] 3 NZLR 513(CA) as per Richardson J. Note that arguably, there may be some scope for a shift in attribution of liability and the imposition of duty of care, since, in the context of Hamlin, the Court of Appeal was referring to the distinctive and long-standing features of the New Zealand housing scene at that time [i.e., mid 1970s to 1980s]. For a more comprehensive discussion on duties of care imposed on Councils, see Todd et al (3rd ed, 2001) "The Law of Torts in New Zealand" at 5.4.2.*

[4] *[1996] 1 NZLR 513 (PC). See also the Court of Appeal's decision [1994] 3 NZLR 513 (CA)*

[5] *[1996] 1 NZLR 513 at p 519 line 53, p 520 line 17, p 521 line 31, p521 line 40, p 522 line 9 and p 522 line 44*

[6] *The decisions which deal with negligent inspections of buildings by Councils have been through vigorous judicial debate. The English Courts started the move towards liability (see Anns v Merton London Borough Council [1978] AC 728(HL)) but retreated from this position and ultimately reversed Anns (see Murphy v Brentwood District Council [1991] AC 398(HL)). In New Zealand, the Courts seemingly embrace Anns. In Hamlin, the Court of Appeal and Privy Council pronounced the unique set of conditions within which homeowners and Councils operate in New Zealand and quite emphatically stated that New Zealand must be free to develop its own common law in this regard. Notwithstanding the doctrine of reliance on Councils to ensure the safety of buildings, see the discussion under Defences: Discretionary Function Immunity, in which it is noted that the allocation of resources and the way in which priorities are determined are matters for the Council. It would be quite awkward for the Courts to superimpose their views on how Councils should spend ratepayers' money.*

[7] *(1998) 192 CLR 330 (HC)*

[8] *South Pacific Manufacturing Co Ltd v New Zealand Security Consultants & Investigations Ltd [1992] 2 NZLR 282 (CA), where the Court declined to find a duty to the creditors and investors of the insured.*

[9] *Private law remedy.*

[10] *Todd et al (3rd ed, 2001) "The Law of Torts in New Zealand") at 5.6.*

[11] *X (Minors) v Bedfordshire County Council [1995] 2 AC 633 at 735 (HL).*

[12] *See supra note 10 at 5.6. See also Lord Hoffman's judgment in Stovin v Wise [1996] 3 All ER 801 at p 804 line j, p 826 lines d, g to j and p 827 line e.*

[13] *See supra note 10 at 5.6.1*

[14] *[1978] AC 728*

[15] *Ibid as per Lord Wilberforce at pp 754 A-B,755 C-F, 761 A-B, 762 A-E,771H-772A*

[16] *Ibid*

[17] *Ibid*

[18] *This is the reality where Councils have a limited budget and the allocation of resources must be an aspect of Councils' discretion.*

[19] *For a summary of mean sea level rise in New Zealand, see Bell, R., Hume, T. and Todd, D. (2002) "Planning on rising sea level?" Planning Quarterly, No 145, July 2002*

[20] *[1980] QB 485 (Eng CA)*

[21] *See also Holbeck Hall Hotel Limited v Scarborough Borough Council [2000] 2 All ER 705 (Eng CA)*

[22] *[1995] 3 NZLR 622*

[23] *See section 23 of the Health Act 1956.*

[24] *"65 Powers of territorial authorities in respect of dangerous or insanitary buildings*

(1) Without limiting its powers under Part 5 of this Act, a territorial authority, on being satisfied that any building is a building deemed to be dangerous under section 64 of this Act, may—

(a) Put up a hoarding or fence so as to prevent persons approaching nearer than is safe"

[25] *Unreported, High Court, Hamilton, CP48/94, Tompkins J, 2 April 1998*

[26] *Supra note 10 at 5.6.1*

[27] *Note also Councils' obligations under section 36 of the Building Act 1991 in the context of applications for building consents. Under section 36, there are steps which a Council must follow if the land upon which a building consent relates is subject to erosion, inundation, falling debris etc... The interpretation of section 36 has been subject to some judicial attention in recent years. The current interpretation of section 36 is as follows (as enunciated by the Court of Appeal in Logan v Auckland City Council (2000) 4 NZ ConvC 193,184):*

"[26] Section 36(1) and (2) are to be read in sequence, not with subs (2) coming first, as the Council was at one time inclined to suggest. On a natural and straightforward reading, subs (1) requires a territorial authority to refuse a building consent if either condition (a) or (b) is present unless satisfied that provision for adequate protection is made in respect of (c) or (d). If (c) or (d) as the case may be is satisfied, the building consent issues. But if in terms of the subsection a building consent is otherwise to be refused, then the opening words of the subsection "except as provided for in subsection (2)" come into play. In that situation the territorial authority is entitled to grant the building consent only where each of the paras (a), (b) and (c) of subs (2) is satisfied."

The section enables a consent to be issued in the event that the strict requirements of section 36(1) cannot be met, that is that the land and building must be adequately protected from the named hazards. It is suggested that section 36(2) enables one or the other to be protected, and this interpretation does not mean that the Council can issue a consent knowing that at some future time the building on the land will be affected by the hazard.

Having said that, the wording of section 36(2) could of course be clearer in that it is arguable that it enables an owner to take the risk without protecting the land or building in any way. It simply cannot have been the Legislature's intention because it would fly in the face of the Building Act 1991's purposes and in the face of provisions such as section 64 of the Building Act 1991 as to dangerous and insanitary buildings.

[28] *Supra note 10 at 5.6.1*

[29] *Ibid.*

[30] *Note also actions in negligent misstatements which are statements made which induce reliance by another person and results in him or her suffering financial loss. See supra note 10 at 4.6*

[31] *See, in this regard, the recent case in the Court of Appeal Chisholm v Auckland City Council (unreported, Court of Appeal, CA 032/02, Tipping, Hammond, William Young JJ, 29 November 2002)*

[32] *[1996] 3 WLR 388 (HL)*

[33] *the encumbant duty of care which Councils must exercise as a local authority*

[34] *[2002] 3 All ER 914*

[35] *[2001] NSWCA 439 (NSW CA)*

[36] *Debevec, I. (2002) "To Warn or Not to Warn? A Dilemma for Local Authorities", Local Government Law Journal Vol 7, no.3 February 2002, p 131*

[37] *Larner v Solihull Metropolitan Borough Council [2001] PIQR 248 (Eng CA)*

[38] *Reference is made, in this regard, to the review of the Building Act 1991 in light of the "leaking buildings" problem in New Zealand.*

REFERENCES

Bell, R., Hume, T. and Todd, D. (2002) "Planning on rising sea level?" Planning Quarterly, No 145, July 2002

Debevec, I. (2002) "To Warn or Not to Warn? A Dilemma for Local Authorities", Local Government Law Journal Vol 7, no.3 February 2002, p 131

Hemmings, N., QC, (1995) "Development Approvals and the Duty of Care." Local Government Law Journal (1995) p 30

Todd et al (3rd ed, 2001) "The Law of Torts in New Zealand"

Embankments at Hazardous Extremes

T J E Sinclair
MA, MSc, DIC, FIPENZ, MICE, C.Eng
Principal, Tonkin & Taylor Ltd

Abstract: Whilst embankments are relatively simple engineering structures for most design conditions, two factors are commonly neglected. The first of these is the amplification of earthquake ground motions by the embankment itself. The paper examines the significance of this effect and concludes that any moderate to high embankment has the potential to amplify ground motions such that crest accelerations could be as high as four times the peak ground accelerations but that this is rarely significant in terms of displacement. The second commonly neglected factor is that of embankment cracking due to the difference in stiffness between embankment and foundation materials. Examples are used to show where this is critical and concludes that cracking will appear for embankment heights less than normally indicated by stability analyses only where foundation shear strengths are less than about 40 kPa. This means very low embankment on soft foundation may appear to have failed when normal stability considerations are theoretically adequate.

INTRODUCTION

The purpose of this paper is to illustrate what special design measures may be necessary for embankments on the volcanic edge. The hazards associated with volcanic areas, particularly the Taupo Volcanic Zone, are various but earthquakes and soft soils would likely be the most significant with respect to embankments. Earth dams and transportation routes (road and rail) make up the major part of the embankment group, but there could be other important facilities such as landfills included.

The paper first considers the relatively high embankments (say greater than 15 m) that are the characteristic of moderate to large dams, but could include the higher road embankments. Such embankments tend to amplify earthquake ground motions, to give crest accelerations possibly as much as four times the peak ground accelerations. The recognised methods for assessing the earthquake effects are summarised, and typical examples given to illustrate the trends and show when the factors become significant. The author notes that designs rarely take account of the amplification effect, despite the fact that many of the relatively modest embankments (e.g. roads and bridge abutments), have natural periods in the range of 0.15 to 0.3 seconds, generally corresponding with the peak of the response spectrum.

At the other end of the geometric scale, relatively low embankments are frequently employed in areas of soft soils. Whilst soft soils generally occur in all environments, the volcanic ashes are particularly important in our own national setting because they have reasonably favourable strength properties but relatively high compressibility. Stability and settlement are generally addressed to a high level of sophistication and often in great detail, but the issue of embankment cracking is usually overlooked. This cracking occurs due to the difference in stiffness between foundations and embankment soils. In the volcanic context, pumice soils provide excellent lightweight fill for embankments on soft ground but the compacted materials is relatively stiff and brittle. The paper provides simple means of checking the critical heights for cracking as well as stability and shows trends for typical embankment geometries and ground conditions.

EMBANKMENTS AND EARTHQUAKES

It is now common practice in the design of dams to take account of the amplification of earthquake ground motions by the dam embankment. Whilst this may be common practice, it is still not universal and certainly was not considered for dams designed more than 25 years ago. Allowing for

embankment response appears to be neglected for other lower embankments such as employed for transportation or landfills.

The purpose of this section is to examine whether this apparent neglect is of any consequence.

Methods of Response Analyses

There are various ways of assessing the response of embankments to ground shaking, falling into the following categories:

a) Dynamic numerical models
b) Simplified methods

The former involve special purpose computer codes (e.g. Kuwano & Ishihara, 1988; Finn et al, 1986; Finn, 1991; Mejia and Seed, 1983), requiring extensive preparation and detailed analysis, and generally not worth while except for large, costly and highly critical structures.

The simplified methods now reduce almost totally to that proposed by Makdisi and Seed (1979). This relies on the "shear beam" concept which leads to the following results:

- The embankment response depends primarily on the first three fundamental natural periods of the embankment, together with the response spectra.
- The fundamental natural periods are derived assuming a prismatic wedge but are otherwise independent of the shape of the embankment (side slopes, aspect ratio).
- The fundamental natural periods, therefore, are dependent only on the height of the embankment and the average shear modulus (G).

The method is described by Makdisi & Seed (1979), but is summarised as follows:

i) The crest acceleration (a_c) is approximated by the "square-root-of-the-sum-of-squares" (SRSS) of the contributions of the first three fundamental response modes (a_{c1}, a_{c2} and a_{c3}), i.e.

$$a_c = (a_{c1}^2 + a_{c2}^2 + a_{c3}^2)^{0.5} \quad (1)$$

ii) The contributions of the first three response modes are as follows:

$a_{c1} = 1.60.\ S_{a1}$
$a_{c2} = 1.06.\ S_{a2}$
$a_{c3} = 0.86.\ S_{a3}$

where S_{a1}, S_{a2} and S_{a3} are the spectral accelerations at the fundamental natural periods T_1, T_2 and T_3 respectively

iii) The fundamental natural periods may be approximated as follows:

$$T_1 = \frac{\pi h}{1.2 v_s} = \frac{2\pi}{\omega_1} \quad \text{i.e.} \quad \omega_1 = \frac{2.4\, v_s}{h} \quad (2)$$

$T_2 = 0.43.\ T_1$
$T_3 = 0.28.\ T_1$

where h = height of embankment

v_s = average shear wave velocity = $\sqrt{\frac{G}{\rho}}$

ρ = density

and ω_1, ω_2, ω_3 are the fundamental natural frequencies.

The computation of crest acceleration, therefore, is relatively simple. The complications arise because the shear modulus (G) or shear wave velocity (v_s) tend to decrease as strain increases (i.e. as level of shaking increases) and the degree of damping increases as strain increases. The first of these tends to increase the natural periods as shaking increases, and the second changes the spectral accelerations. Much of the Makdisi & Seed (1979) paper is concerned with this issue and how to ensure the parameters and strains are compatible.

First Approximations

Before addressing the complication due to shear modulus softening with strain, it is of interest to look at the first approximations, assuming constant values.

A typical value for the shear wave velocity of a compacted well graded clayey gravel would be 400 m/s. A 30 m-high embankment of such material would therefore have a first natural period of about 0.2 seconds. This happens to be close to the peak of the typical acceleration spectra. In addition, it would be reasonable to assume that the spectral accelerations for lesser periods would also be close to the spectral peak.

This would give crest acceleration:

$$a_c = S_{a1} (1.60^2 + 1.06^2 + 0.86^2)^{0.5}$$
$$= 2.1\ S_{a1}$$

Now peak spectral acceleration is approximately 2.5 to 2.75 times the peak ground acceleration (PGA), giving a crest acceleration therefore of something over five times the peak ground motion.

The same conclusions would apply to a high road embankment of say 15 m height, constructed of clayey fill with a typical shear wave velocity of 200 m/s.

Clearly, if this were realistic, it would be almost impossible to prevent some form of yield at the crest of any moderate sized embankment for ground accelerations more than about 0.1g.

Further Refinement

It has been noted that actual amplifications are nowhere near those indicated by the above first approximations. The method of Makdisi & Seed (1979) provides for a more realistic assessment, allowing for softened shear modulus and higher damping. The method requires the following:

- Determine small-strain shear modulus (G_{max})
- Allow for "degradation" of G by use of a relationship for G/G_{max} versus strain.

Much research has gone into both of these issues, and time/space do not permit detailed discussion. However, applying the recommended method and relationships to a range of embankment heights, with a range of material stiffnesses (shear wave velocity, v_s = 100 m/s to 800 m/s) and two levels of shaking typical of the "volcanic edge" (central North Island), trends are evident in Figures 1 to 4. For these typical examples, the two design PGA's chosen were 0.22g as an arbitrary "Operating Basis Earthquake" (OBE) and 0.35g as an arbitrary "Maximum Credible Earthquake" (MCE). Some of the simplifying assumptions may not apply at the extreme ends of the height or stiffness ranges, but the following conclusions are clear.

- Amplifications between peak ground acceleration (PGA) and crest accelerations can be as high as 4.5 for typical dam or transportation embankments.
- Amplifications tend to be insensitive to the levels of shaking.

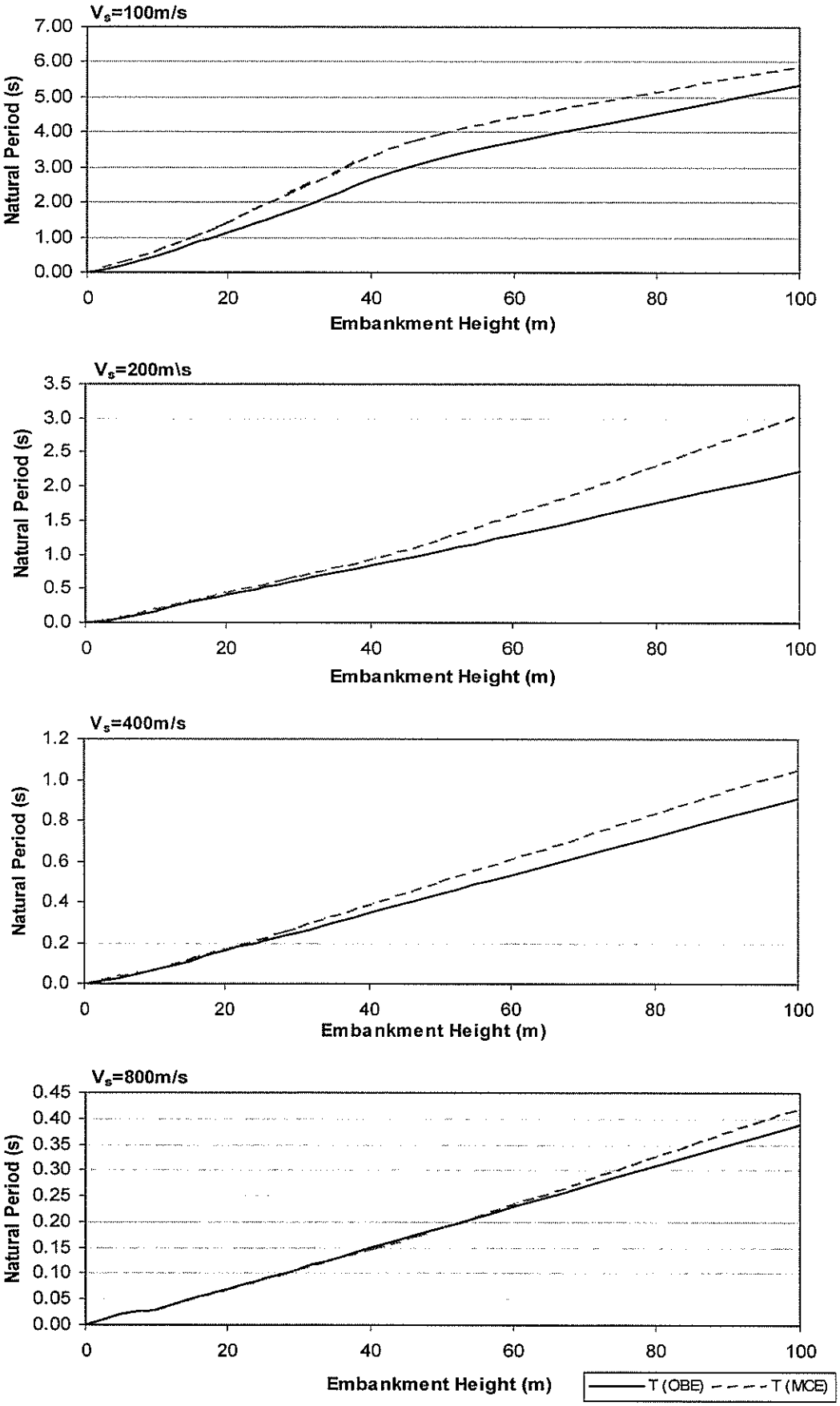

Figure 1. Variation of Natural Period with Embankment Height, Allowing for Strain Under Large Earthquake

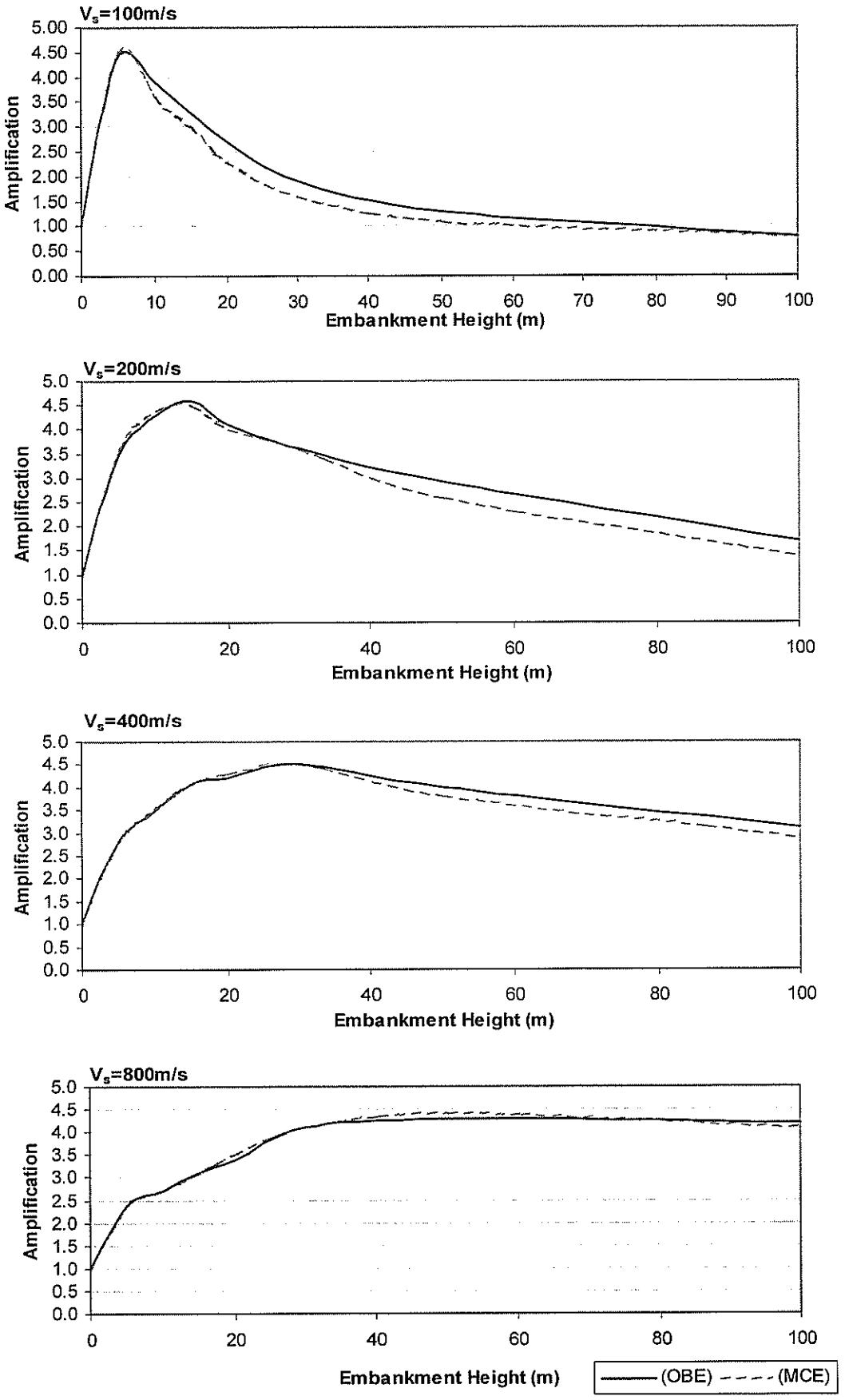

Figure 2. Variation of Amplification with Embankment Height

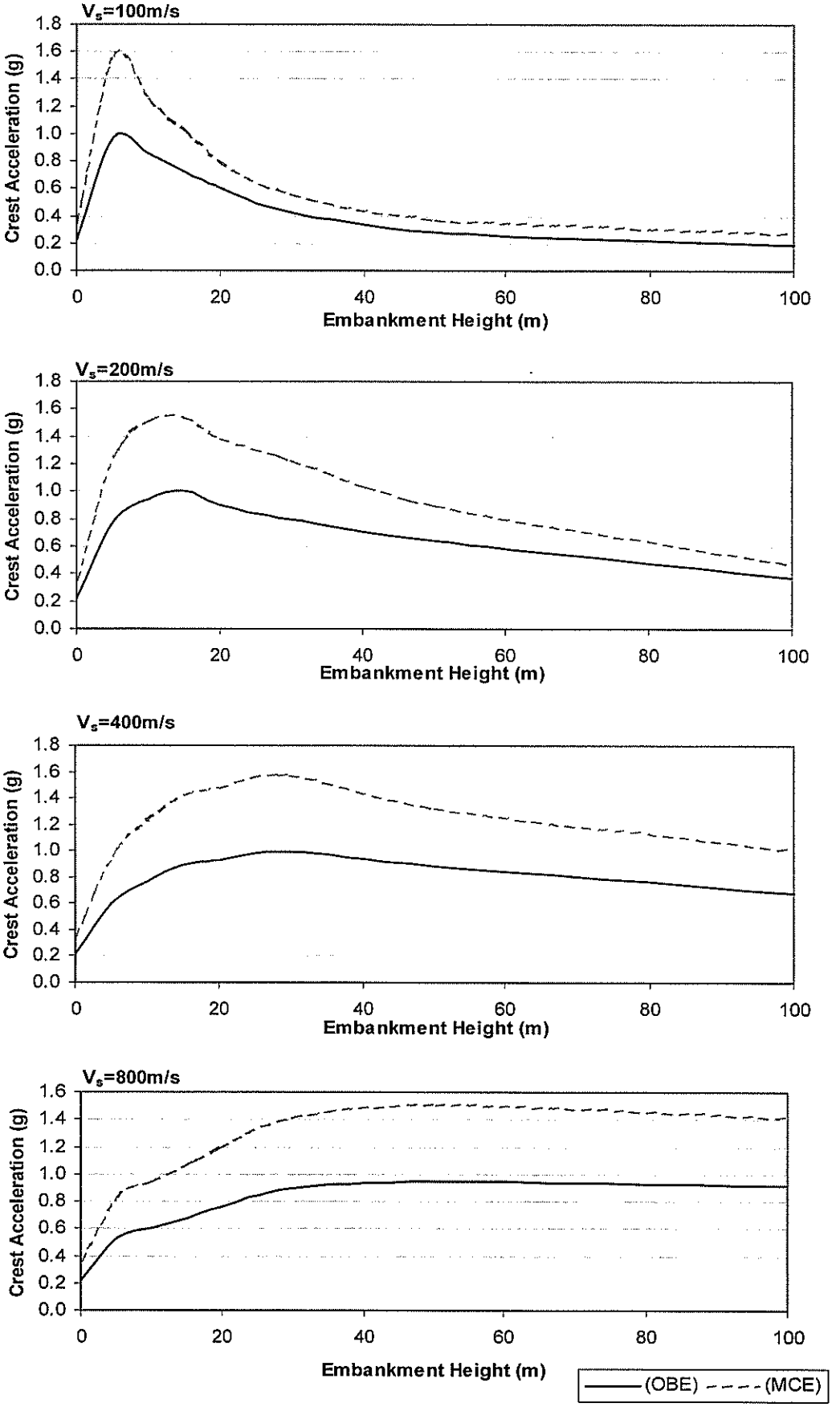

Figure 3. Variation of Crest Acceleration with Embankment Height

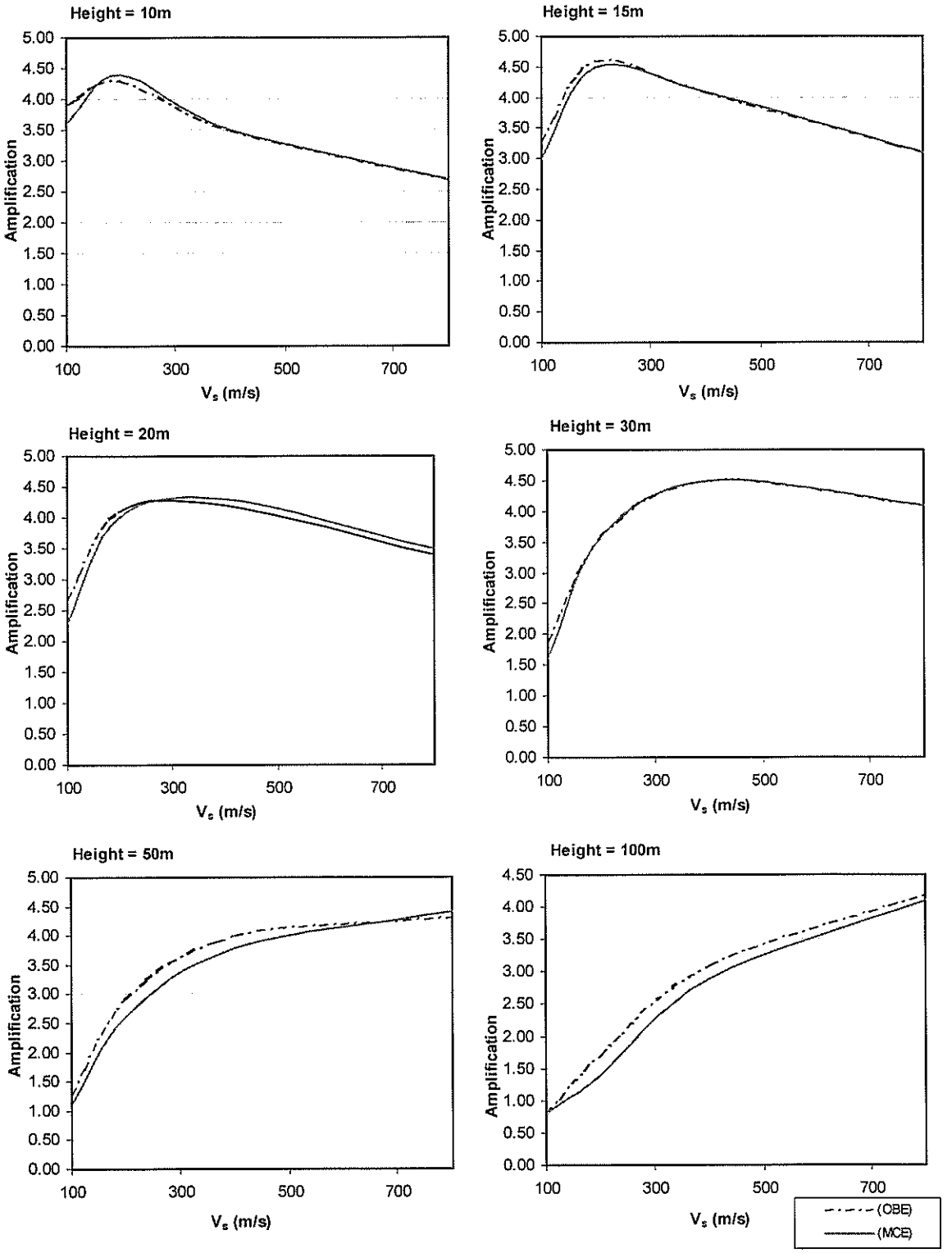

Figure 4. Variation of Amplification with Shear Wave Velocity

Implications of Amplifications

Whilst such amplifications are still higher than measured in practice, the effect is dramatic enough to mean it cannot be ignored. The question now is how much does it matter?

Makdisi & Seed (1978) present a curve to show how the average acceleration reduces with depth of a potential slip surface below the embankment crest (Figure 5). From this it can be seen that the following approximations would be reasonable.

Proportion of Embankment	Average Acceleration of Slip Mass as Proportion of Crest Acceleration	Possible Amplification of Ground Acceleration
Top Third	80%	3.6
Top Half	60%	2.7
Whole Embankment	35%	1.6

Table 1: Amplification for Various Proportions of Embankments.

So, with a design acceleration of (say) 0.2g, typical almost anywhere in New Zealand, the theory suggests the top third of the high embankment could be as much as 0.7g, almost certainly causing yield.

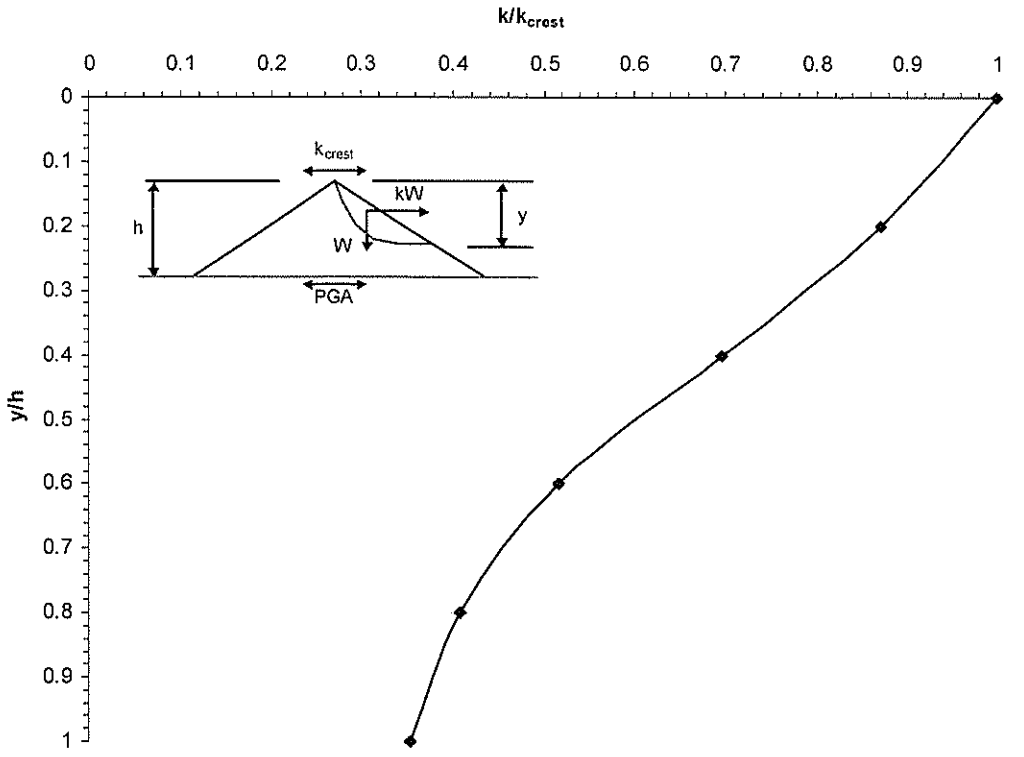

Figure 5. Slip-Mass Acceleration as Proportion of Crest Acceleration (Makdisi and Seed, 1979)

However, it is also well known that "yield" under earthquakes loading does not necessarily mean "failure". Due to the rapid and reversing nature of earthquake loads, repeated but momentary reductions of the factor of safety below unity tend to result in limited displacements rather than complete failure. Makdisi & Seed (1978) present a means of estimating such displacement based on a method originally proposed by Newmark (1965). Many others have explored the problem (e.g. Kuwano and Ishihara, 1988), but possibly the simplest to apply is that proposed by Ambraseys and Menu (1988). Figure 6 shows their curve for estimating displacement on sloping ground due to an

earthquake of about Magnitude 7 (M_s = 6.9 ± 0.3). It can be seen from this that a maximum acceleration of about three to four times the yield or "critical" acceleration (i.e. $k_c/k_m \approx 0.3$) still only results in displacements on the order of 100 mm. So, as an approximate "rule of thumb", displacements of about 100 mm should be expected if the yield acceleration for (say) the top third of an embankment is about the same as the PGA.

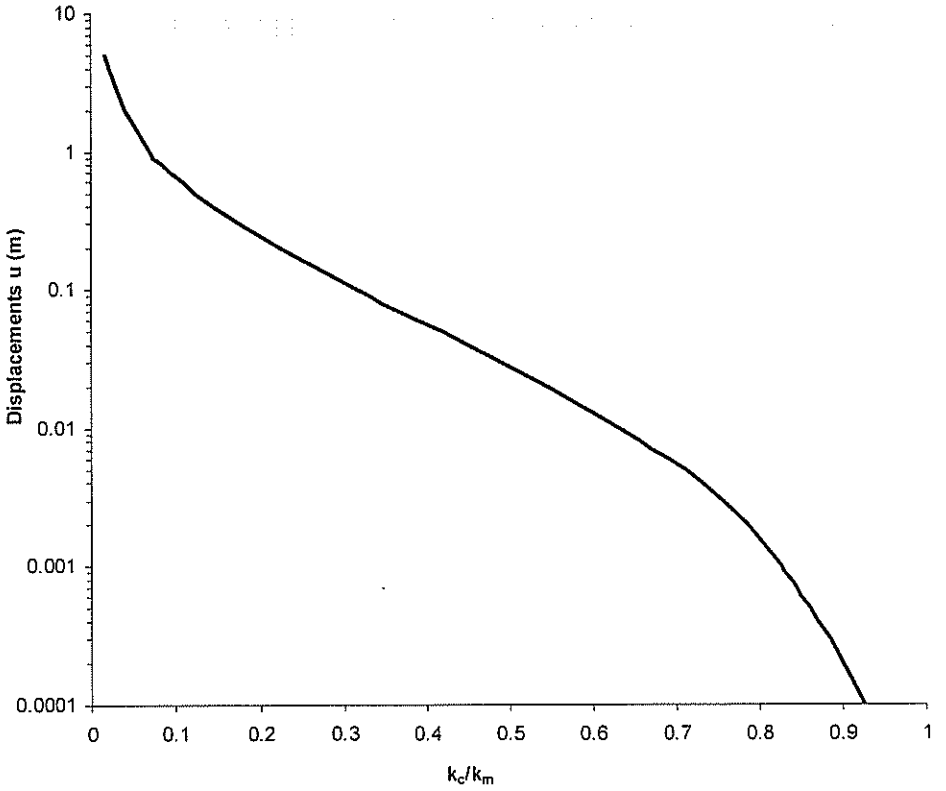

Figure 6. Predicted Unsymmetrical Displacements (from Ambraseys and Menu, 1988)

Significance

Our current theories of soil mechanics indicate that modest sized dam embankments at the higher road or rail embankments can be subjected to very high acceleration near the crest. There is little point in carrying out pseudo-static stability analyses without taking the amplification effect into account. On the other hand, even with very high accelerations, the resulting displacements tend to be reasonable, bearing in mind that the causative events are likely to be extreme events. A dam could be designed to tolerate a few hundred millimetres without compromising the short term security. Likewise, road embankments would still be serviceable. Rail embankments, however, may be more critical.

LOW EMBANKMENTS

Introduction

The volcanic regions produce their share of soft soils. There is an obvious need to build road and rail embankments on such soils and the usual concepts of soil mechanics apply for design and construction. Stability and/or bearing capacity is checked in the normal way; often with computer programmes that can model the foundation profile and the embankment materials in great detail. However, rarely is the strain compatibility between foundation and embankment taken into account. Computer programmes such as FLAC or PLAXIS would do this with reasonable effort but would generally not be justified for design of low embankments.

Embankment Cracking

Longitudinal cracking of embankment comes about due to the difference in stiffness between the foundation soils and embankment materials. Often the latter has high strength but is relatively stiff and brittle (e.g. pumice). Tensile strains at the base of the embankment cause cracks initiating at the base and working up to the top, very often well after the pavement is in place and despite the 'stability' being checked exhaustively. This may not technically be 'bearing failure' but it certainly looks like it to the owner!

A chart developed by Chirapuntu and Duncan (1975) provides a useful simple check on potential for cracking, reproduced here as Figure 7. Incidentally, the curves for N_T in Figure 7 can be approximated very closely by the relationship :

$$N_T = 5.11\left(\frac{k_E}{k_F}\right)^{-0.757}\cdot\left(\frac{w}{D}\right)^{0.25} \qquad (3)$$

where the terms are defined in the figure.

Also, the foundation modulus number (k_F) can be represented by the equation:

$$k_F = 640\,(PI)^{-1.3}\,S_u \qquad (4)$$

where S_u is average foundation undrained shear strength in kPa and PI is the Plasticity Index.

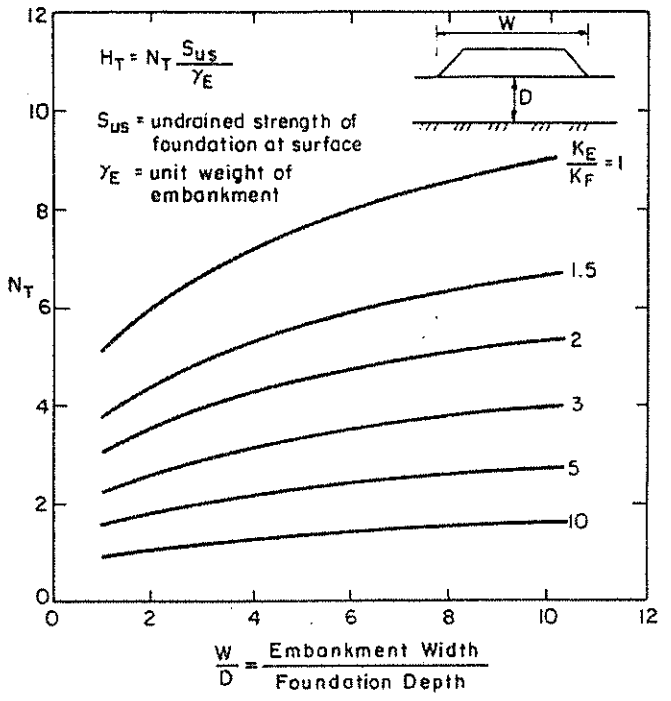

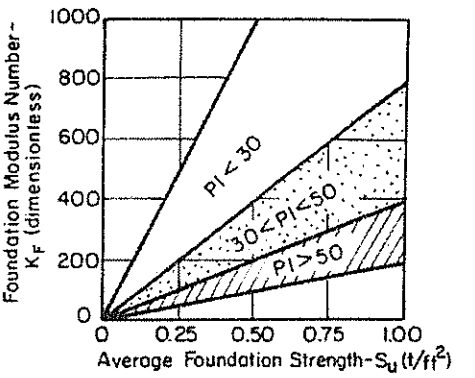

Typical values of K_E for compacted fills

Unified Class.	Compaction Water Content		
	Optimum - 3 %	Optimum	Optimum + 3 %
GC	300 - 1200	200-500	75 - 300
SP	400 - 1000	400-1000	400-1000
SM	300 - 750	300 - 750	300 - 750
SC	250 - 1000	150 - 600	50 - 250
ML	250 - 1000	150 - 600	50 - 250
CL	250 - 1000	100 - 400	30 - 200
CH	100 - 400	50 - 200	20 - 100

Values shown apply to fill materials compacted to dry densities from 90% to 95% of the Std. AASHO maximum. In general, the value of K_E increases with increasing dry density at a given water content.

Figure 7. Chart for Estimating Height of Embankment (H_T) When Cracking Begins (after Chirapuntu & Duncan, 1975)

Stability

As mentioned above, the stability or 'bearing' capacity of the embankment is easily analysed using any of the available slope stability software.

A useful quick check for stability of an embankment of one material type on a foundation of another is given by Bak-Kong Low (1989). The factor of safety is given by:

$$F = N_1\left(\frac{c_a}{\gamma H}\right) + N_2\left(\frac{c_m}{\gamma H} + \lambda \tan \Phi'_m\right) \tag{5}$$

Where: N_1, N_2 and λ are constants dependent on the ratio of soft soil thickness (D) to embankment height (H) and the embankment slope angle (β and $b = \cot \beta$)

c_a = average undrained shear strength of the foundation.
c_m and $\emptyset'_m$ = effective stress strength parameters of embankment material.
γ = unit weight of embankment material.

The reference gives relationships for the three stability numbers (N_1,N_2, and λ) which can then be computed easily with a spreadsheet calculation. Alternatively they may be obtained from Figures 8, 9 and 10 of this paper.

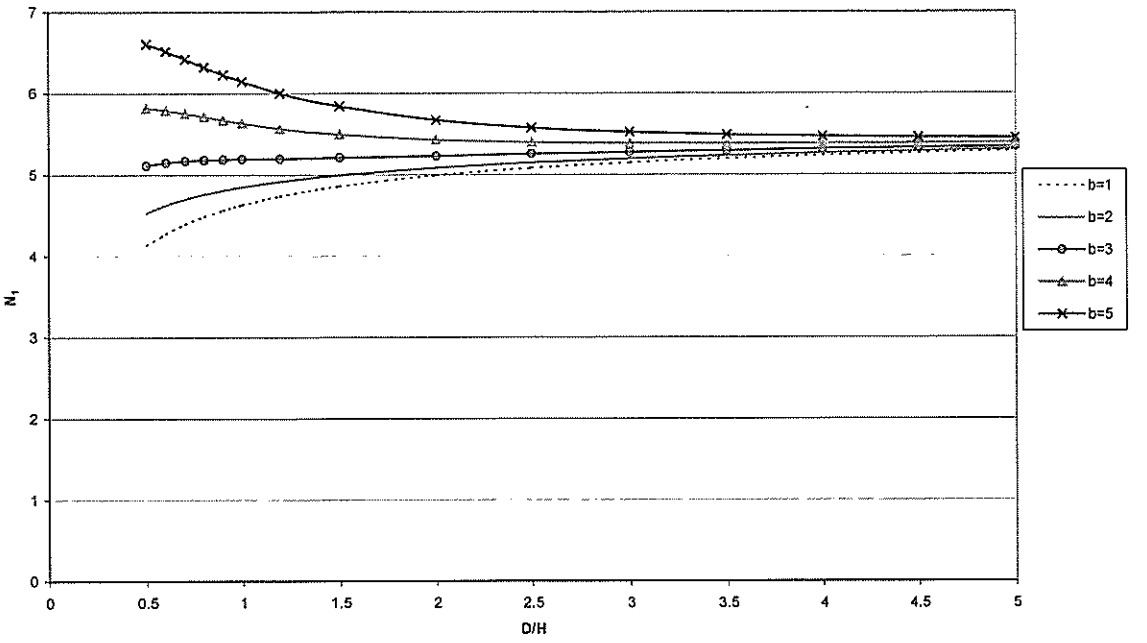

Figure 8. Factor N_1 for Embankment Stability.

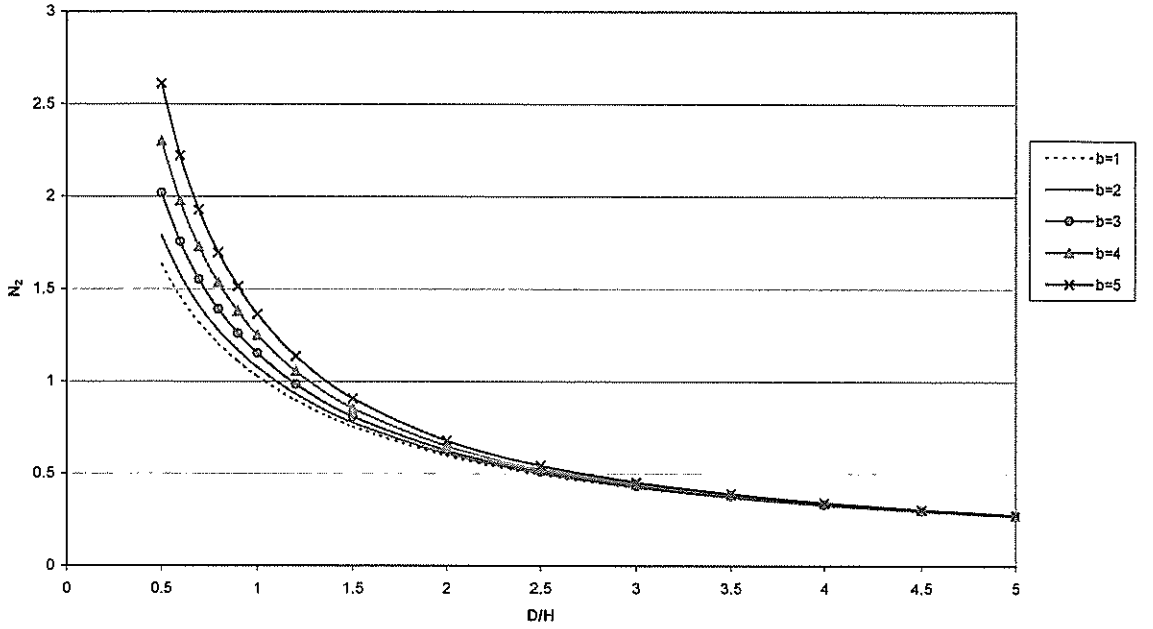

Figure 9. Factor N_2 for Embankment Stability.

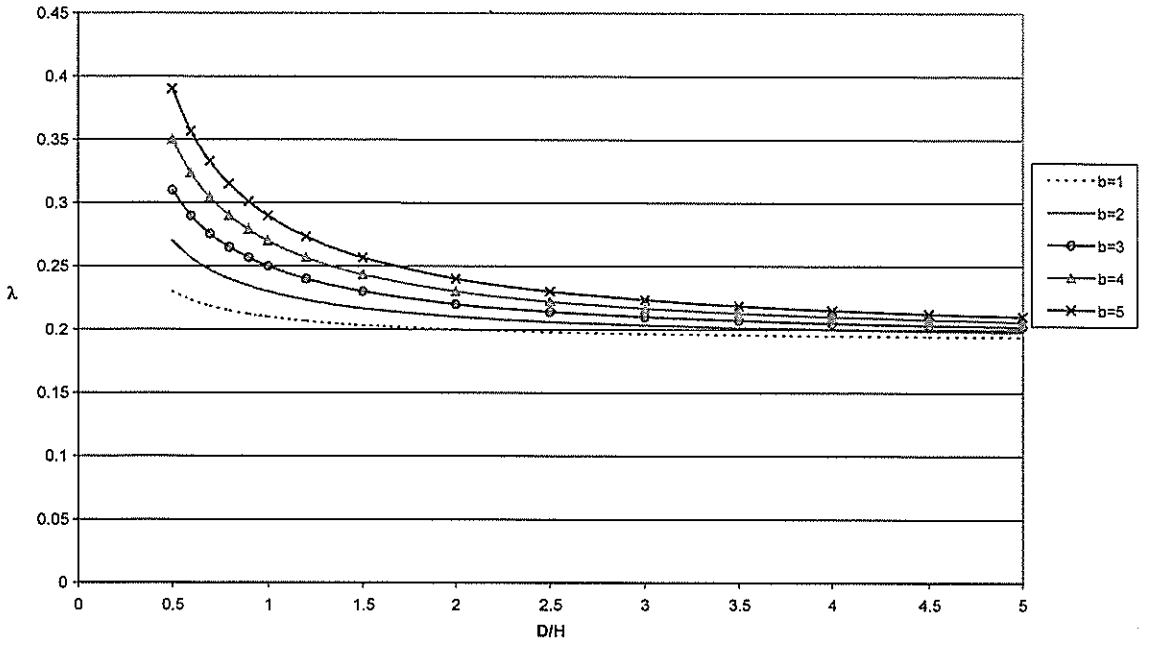

Figure 10. Factor λ for Embankment Stability.

Example

To see where cracking might appear before stability becomes an issue, an example calculation can be carried out with the aid of the above relationships. Figure 11 shows the critical heights of embankment for both cracking and stability (F = 1.0 and F = 1.3), for a typical embankment on a soft soil of about 5m depth, given as a function of average foundation shear strength.

It can be seen that cracking controls only at very low average foundation shear strengths. The results will depend on depths of soft soil and other factors, but if these calculations are repeated for different

depths, allowing for increase in strength with depth, it will be found that the critical height for cracking is less than the critical height for (say) a factor of safety of 1.3, only when the average foundation shear strength falls below about 40 kPa.

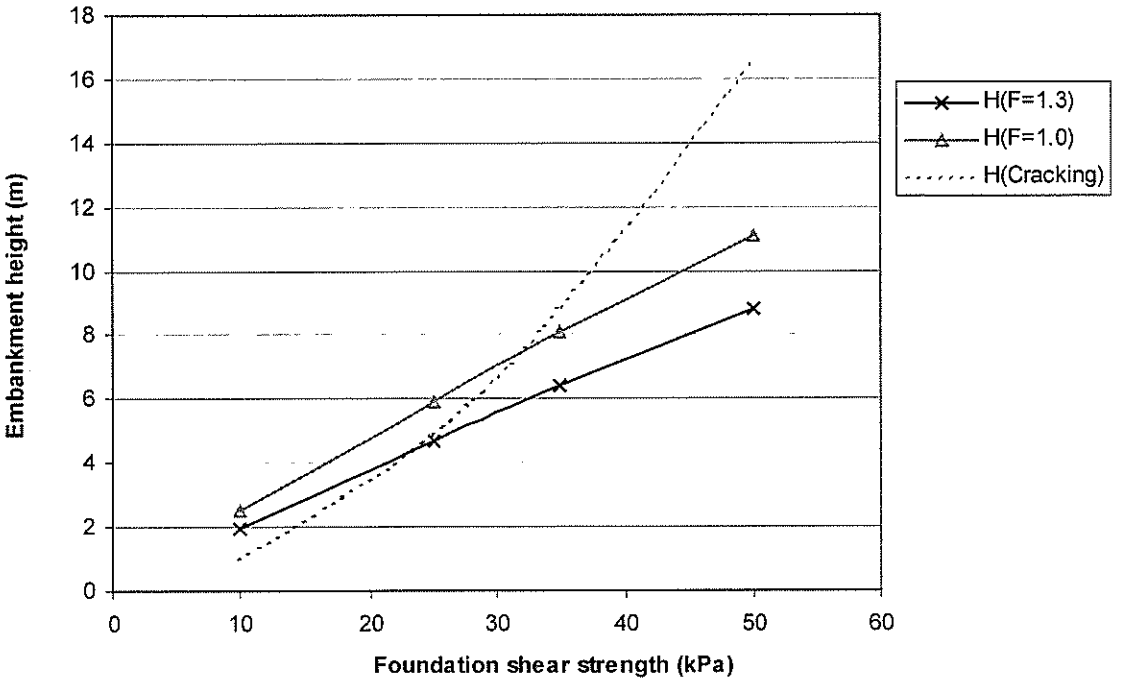

Figure 11. Critical Embankment Heights for 5m of Soft Soil

CONCLUSIONS

There are just two primary conclusions from this paper:

I : Any moderate to high embankment has the potential to amplify ground motions such that crest accelerations could be as high as four times the peak ground accelerations. This may or may not matter with respect to yield displacement, but, almost certainly anywhere in New Zealand, it will not be possible to justify design suitability on the basis of an acceptable factor of safety.

II : For soft foundation soils of (say) less than 40 kPa average shear strength, cracking will appear in the embankment at heights less than normally indicated by stability requirements. Beware: This cracking is often delayed until the most inconvenient time! Geosynthetic reinforcement appears to work well in limiting the potential for cracking but must be present under the central portion of the embankment base.

REFERENCES

Ambraseys, N.N. and Menu, J.M. (1988). "Earthquake induced ground displacements". *Earthquake Engineering and Structural Dynamics*. Volume 16, 985-1006.

Bak-Kong Low (1987). "Stability analysis of embankments on soft ground". ASCE. *Journal of Geotechnical Engineering*, Vol. 115, No.2, Feb.

Chirapuntu, S. and Duncan, J.M. (1975). "The role of fill strength in the stability of embankments on soft clay foundations". *Geotechnical Engineering. Research Report.* Dept. of Civil Engineering, University of Cal., Berkeley.

Finn, W.D.L., M Yodendrakumar, N. Yoshida and H. Yoshida 1986. TARA-3: A Program to Compute the Response of 2-D Embankments and Soil-Structure Interaction Systems to Seismic Loadings. *Dept. of Civil Engineering., University of British Columbia, Vancouver, Canada.*

Finn, W.D.L. (1991). "Estimating how embankment dams behave during earthquakes. *Water Power & Dam Construction,* April.

Kuwano, J. and Ishihara, K. (1988). "Analysis of permanent deformation of earth dams due to earthquakes". *Soils and Foundations,* Vol.28. No.1, 41-55, March.

Makdisi, F.L and Seed, H.B. (1979) "Simplified procedure for evaluating embankment response". ASCE, *Journal of Geotechnical Engineering.* Vol.105, No.12

Makdisi, F.A. and Seed, H.B. (1978) "Simplified procedure fore estimating dam and embankment earthquake-induced deformations", ASCE, *Journal of Geotechnical Engineering.* Vol. 104, No.GT7, July.

Mejia, L.H. and Seed, H.B. (1983) Comparison of 2D and 3D dynamic analysis of earth dams. *ASCE Journal Geotechnical Engineers,* Vol 109, No11.

Newmark, N.M. (1965). "Effects of earthquakes on dams and embankments". *Geotechnique* 15, 139-160.

Seed, H.B. and Idriss. I.M. (1970). "Soil moduli and damping factors for dynamic response analyses". Report No. EERC70-10 *Earthquake Engineering Research Center*, University of California, Berkeley.

Piping Failure of the Poihipi Reservoir

D R Tate
Director, Riley Consultants Ltd, Auckland

Abstract: The Poihipi Reservoir formed a water storage for fire fighting purposes at the Poihipi Geothermal Scheme located near Taupo. Soon after initial filling of the HDPE lined reservoir, the reservoir breached by a piping mechanism. The nature of the failure was remarkable in several respects. The outflow from the breach occurred at two separate locations, located 500m and 300m respectively from the reservoir in opposite directions. The failure seepage path followed a linear active fault which was present beneath the footprint of the reservoir.

This paper describes the mechanism of the piping process, the investigations which were carried out for an alternative reservoir site and the design solutions adopted. A discussion of recent research by Australian researchers on piping failures in the context of this failure is also presented. This event highlighted many risk factors associated with seepage from water retaining structures in general, and specific risks associated with water retaining structures in volcanic terrain.

INTRODUCTION

The original reservoir was located on the top of a hill about 300m west of the power station. It was constructed from local pumiceous gravel, sand and silts. The majority of the reservoir was constructed in natural material with fill used to increase the height of the embankment to the required level on the south side. The reservoir was about 6m deep and was lined with HDPE to prevent water leakage. All seams were site welded. Three pipes penetrated the liner for inlets and outlets (Figure 1).

DESCRIPTION OF RESERVOIR FAILURE

The reservoir began filling in early March 1996. It was noted by site staff that the reservoir was losing a significant amount of water prior to the collapse, particularly in the week prior to the failure. The breach was first noticed at midday on 11 April. Failure is believed to have occurred during the preceding night. Moisture was also noted at the face of the embankment about three weeks prior to the collapse.

The visual evidence of the failure was remarkable. At the reservoir site, a very deep trench occurred diagonally through the centre of the reservoir, and the HDPE liner had been torn completely along the line of the trench (Figure 2). The trench was estimated to be at least 10m deep and up to a few metres in width.

Extensive linear ground cracking, subsidence and heave extended some 500m to the southwest and 270m northeast of the reservoir. The eastern corner of the reservoir wall had collapsed over a width between 4 and 10m, where the service pipes were located. Beyond this point the line of cracking and subsidence veered away from the service pipe trench.

The reservoir water discharged at two main "break-out" locations well away from the reservoir. Beyond the eastern corner a long line of slumping and cracking was visible on the ground surface extending to drill pad 64. This pad was a large flat area created by cut and fill. A series of "erosion pipes" were observed in excavations clearly showing the erosion path (Figures 3, 4).

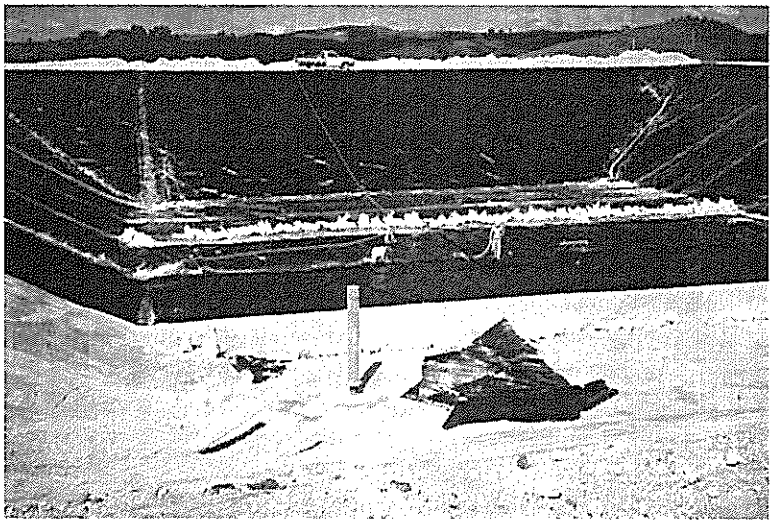

Figure 1. Original Reservoir During Construction

Figure 2. View Along Failed Reservoir from Eastern Corner

Figure 3. Breakout Point on Drill Pad 64

Figure 4. Erosion Tunnel at Drill Pad 64. The Tunnel was Encountered on the Reservoir Side of the Break Out Point

The reservoir water also discharged to the west of the reservoir. A line of slumping was visible down to the base of a ridge about 250m away. No cracking or slumping was visible until the breakout point at the base of a valley about 500m from and 55m below the reservoir (Figures 5, 6).

Figure 5. Subsidence Extending Southwest from the Western Corner of the Reservoir. The Gully in which the Water Exited (Figure 6) is Beyond the Far Ridge with Trees

A line of ground cracking was also observable running roughly at right angles to the southeast of the two features described above. The cracking could be followed to the base of a small hill about 50m from the reservoir. Ground cracking was also observed on the opposite side of the hill but there was no indication of a breakout from the reservoir in the area of these cracks.

Figure 6. View Towards South Showing the Main Southern Water Outlet Area and the Flow Path Across the Valley Floor Marked by Sediment

Figure 7 shows the location of the breakout zones and prominent ground cracking relative to the reservoir. A cross-section is shown on Figure 8.

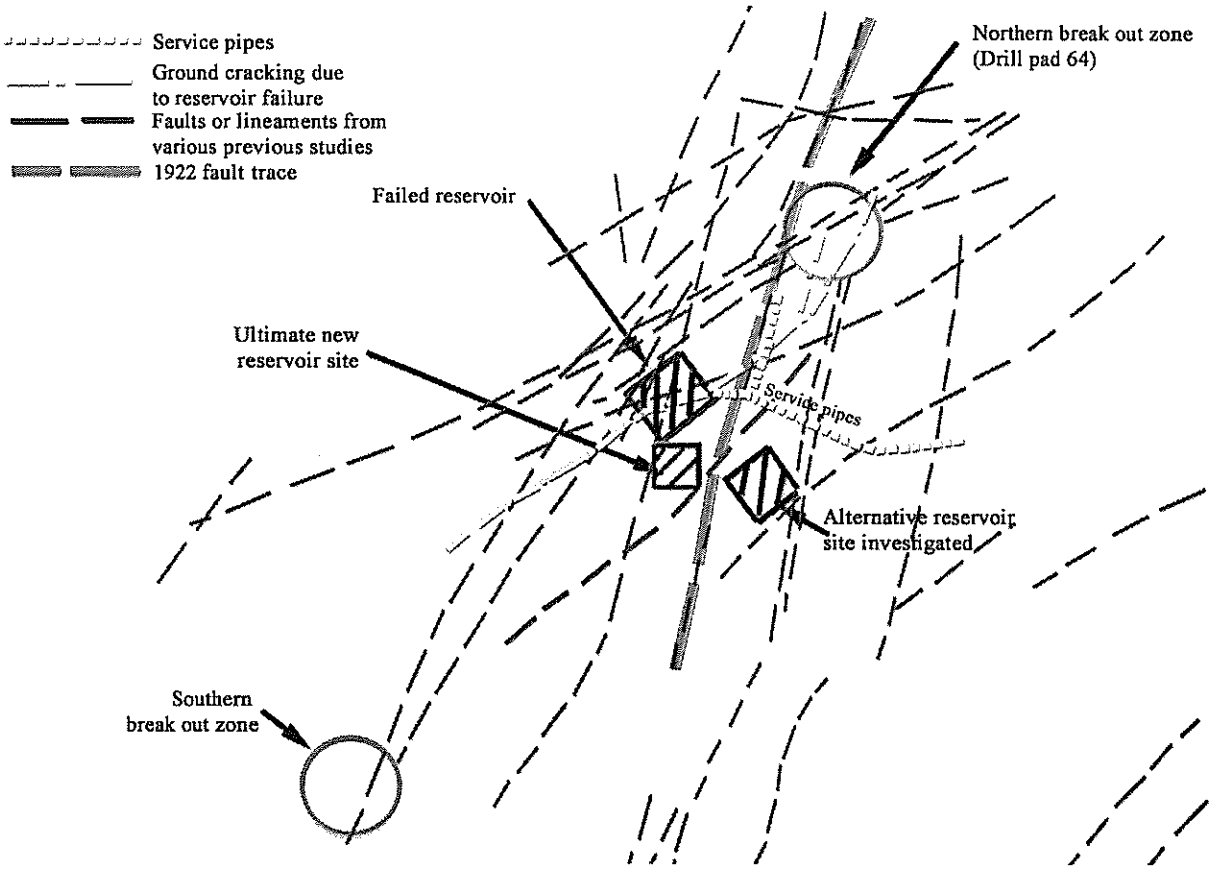

Figure 7. Previously Indicated Faults and Lineaments

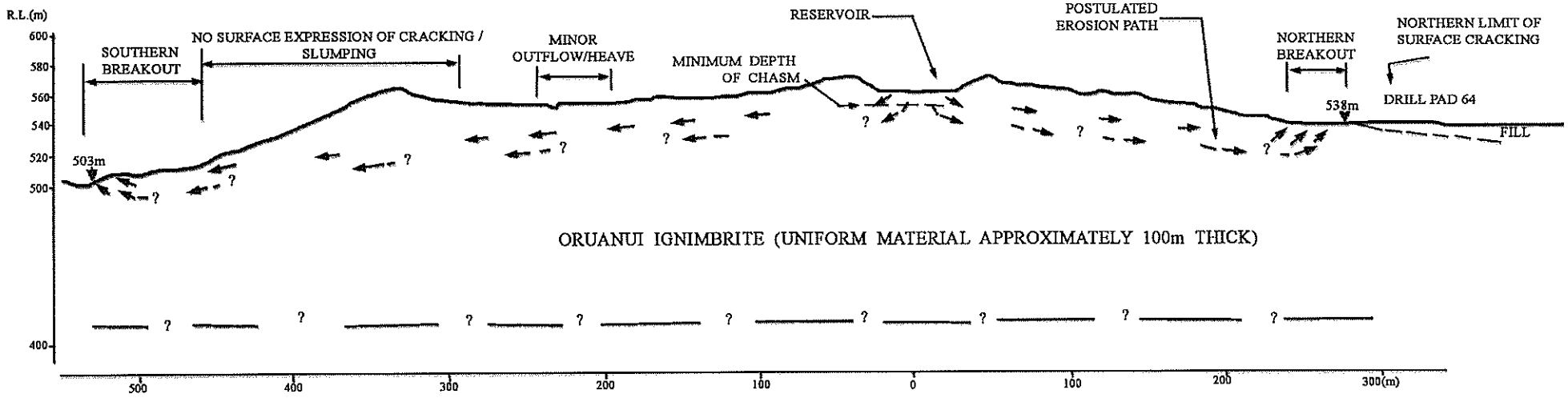

Figure 8. Cross Section along Failure Path

GEOLOGICAL CONDITIONS

General

The geological conditions at the Poihipi site are typical for the area, where the soils are predominantly tephra erupted from the Taupo Volcanic Centre. At the reservoir site there is a sequence of silts, sands to highly permeable pumice gravels. The site is also transected by a series of relatively closely spaced faults, many of them active. Investigations carried out at the powerhouse and subsequent to the reservoir failure confirms this.

Subsoils at Reservoir Site

Photographs taken during construction show a complex distribution of materials in the excavation. The materials exposed in the reservoir walls comprised young surficial tephras (layers of loosely packed pumice gravel and sand alternating with silty sand layers), loess and, at lower levels, Oruanui Ignimbrite. The ignimbrite forms the engineering basement of the area. This material was typically a tightly packed gravely sand.

The floor of the reservoir was partly on the surficial tephras and partly on loess and/or Oruanui Ignimbrite. The contact was interpreted to be a fault coinciding with the position of the service pipes and the chasm produced by the failure.

Relationship to Faulting

Previous studies for the site specifically addressed geological and seismic hazards. These studies identified possible faults on various orientations in the vicinity of the reservoir. Sections of the ground cracking/slumping coincide with previously identified faults, but none coincided precisely with the failure over its entire length. Figure 7 shows the proximity of the ground features to previously identified or suspected faults.

The faults on the site typically contain a persistent shear plane a few millimetres wide on the up thrown side and a network of discontinuous secondary shear planes on the downthrown side.

REASONS FOR FAILURE

Postulated Mechanism of Failure

The fundamental cause of the reservoir failure was an uncontrolled concentrated leak from the reservoir, which led to internal erosion between a "breakout" point or points and the reservoir. The internal erosion occurred along the weakest line of resistance. The narrow linear nature of the erosion paths over extremely long distances indicate the erosion occurred along faults. The most likely sequence of events leading to the failure is summarised below:

- An initial leak occurred through the liner, most probably in the area where the pipes penetrated the liner.
- Seepage occurred at depth, along paths of low resistance provided by the fault. High pressures occurred because of the confined nature of the seepage path along a thin zone, and the rapid fall in ground contour away from the reservoir.
- Parallel cracking occurred on the ground surface coincident with the leakage paths. This cracking occurred by hydraulic fracturing, which is a phenomenon whereby water pressure exceeds the horizontal stress in the ground and cracks enlarge and propagate to the ground surface. Faults and the junction of the access trench (for the pipes) with natural ground are points of low horizontal stress. The tendency for cracking at the ground surface decreased as the overburden stress increased ie when the seepage path went beneath a hill

- The seepage water broke out at the ground surface when the overburden stress decreased ie at the toe of the slope at the drill pad and/or the valley base. The heaved ground is evidence of high water pressure at depth.
- Internal erosion occurred backwards from the "breakout" point(s) forming a "pipe", progressively back to the reservoir.

- When the erosion pipe reached the reservoir, material was lost directly beneath the HDPE liner, removing support.
- The liner tore where the support was lost. Leakage then increased rapidly. Multiple flow paths with subsequent erosion were created, leading to total draining of the reservoir.

Reasons for Initial Leak

The most likely point of the initial leak is around the inlet/outlet pipes. At this position several adverse conditions existed:

- The pipes penetrated the liner at several points. The pipes penetrated the liner at a low level, and thus the area around them was subject to maximum hydraulic loads of about 6m of water.
- The trenches carrying the pipes were potential areas of differential settlement, because of the likely difference in compressibility of the trench backfill and the surrounding ground. The differential settlement would put the liner under considerable tension.
- The pipe locations coincided with the fault zone and contact between surficial tephra and loess and the more compact Oruanui Ignimbrite which could also lead to differential settlement.

DISCUSSION ON RECENT RESEARCH ON PIPING FAILURES

International statistics on dam incidents indicate that 2% of embankment dams have historically experienced a piping incident. About 40% have occurred in the foundation and almost half are associated with conduits through the dam. About 64% of failures occur on first filling or in the first five years of operation. In New Zealand, a number of piping incidents and failures have occurred in volcanic materials and the hazards are well known. Statistics on dam incidents in New Zealand indicate that inadequate attention to drainage and presence of volcanic materials are the major causes. 57% of serious incidents occurred in volcanic materials, mostly within the Taupo Volcanic Zone (Riley, 1997). None of the incidents have been directly due to active faulting.

Recent research by Australian engineers has produced a framework to estimate risks of piping for both existing and new dams (Foster and Fell, 2000, Bell et al, 2001). The process of internal erosion and piping is broken up into four phases; initiation of erosion, continuation of erosion, progression to form a pipe, and formation of a breach. The influence of the various factors for the Poihipi Reservoir failure is shown in Table 1. Although the Poihipi Reservoir is only a very small dam (water depth 6m, height of fill embankment <5m), the concept is applicable.

The research and accepted practice indicates that many of the risk factors associated with the site geology and the design adopted were high. However there was a high likelihood of avoiding the breach if expert advice was sought given that seepage was observed and the reservoir was losing water. This reinforces the desirability of expert overview of the commissioning process; even for a reservoir such as this which appears quite innocuous.

There are some features of this failure which are unusual, even in a global context. The predominant unusual feature is that piping occurred along an active fault. A similar mechanism occurred at the Baldwin Hills Reservoir failure which occurred in California in 1963 with the loss of a number of lives (Sherard et al, 1974). Similar site conditions were apparent with cohesive soil overlying a more permeable horizon. This is a dangerous combination for a water retaining structure. The clay layers

were sufficiently cohesive to allow very large erosion tunnels to form in the sand layers below. This mechanism was also very evident at the Poihipi site.

At Poihipi, the main influence of the fault is that it provided a low resistance seepage path, and promoted hydraulic fracturing or cracking. Hence minimal head loss due to seepage occurred and the hydraulic gradient associated with the failure is very low at about 0.1. It is thus apparent that hydraulic gradient alone is not a good indicator of the likelihood of a piping failure, especially in these highly erodible volcanic soils. This is also highlighted in Australian research where piping failures and accidents have occurred at gradients as low as 0.05.

Phase of Process	Factors	Assessed Influence or Likelihood	Overall Probability
Initiation of Erosion	Conduit penetrating liner with poor sealing detail	More likely	High
	Differential settlement of trench back fill, vertical sides	More likely	
	Hydraulic fracturing due to low stress zone in active fault	More likely	
	Continuous feature	More likely	
	Silty low permeability layers overlying high permeability layer	More likely	
	Factor of Safety low for blow-out (only in retrospect)	More likely	
Continuation of Erosion	No filter or drainage zones	More likely	High
Progression to Formation and Enlargement of Pipe	Silty materials support a roof of a pipe	More likely	High to Moderate
	Erodible fine sands	More likely	
	Dispersive soil	Unknown probably unlikely	
	Hydraulic Gradient low (less than 0.2)	Less likely	
	No restriction on flows by upstream zones	More likely	
Formation of Breach Mechanism	Small storage	Unlikely	High as occurred but less likely if monitoring procedures were adequate
	Intervention to prevent breach	In hindsight was possible	
		Overall Likelihood	High

Table 1. Influence of Factors on Piping Mechanism

NEW RESERVOIR

It was immediately apparent that the existing site was not suitable. Accordingly an alternative site was investigated on a hill some 100m south of the failed reservoir. A series of trenches were excavated. The main finding was that three closely spaced active faults were encountered. One of the faults, displace the Rotongaio Ash by a small amount; this ash is one of the deposits resulting from the most recent eruption in the Taupo area dated at 1850 years before present. There was evidence of as many as five movements in the past 10,000 years.

The intensity of faulting indicated that it was impractical to avoid the likely presence of active faults; given constraints on reservoir siting. The final site chosen is shown on the site plan, Figure 7.

The geotechnical design principles included the following:

- A continuous 1 metre thick zone of cohesionless filter material was placed as a drainage layer beneath the impermeable liner. This zone also acts as a "crack stopper" because it cannot sustain an open crack.
- The reservoir volume and depth was reduced, compatible with the project requirements.
- Comprehensive monitoring, particularly of first filling, was recommended.

The new reservoir has performed well with no unusual incidents recorded.

CONCLUSIONS

1. The piping failure of the reservoir occurred in volcanic materials in the foundations. A number of similar incidents and failures of water retaining structures have occurred in volcanic materials in New Zealand. Conservative filter and drainage zones for these materials are essential. This point is also emphasised in the New Zealand Society on Large Dams (NZSOLD) Dam Safety Guidelines 2000.
2. This failure associated with an active fault is very unusual. This feature allowed piping failure to occur at a very low hydraulic gradient of about 0.1. The remarkably long failure path lengths of 300m and 500m respectively in opposite directions, is a unique situation with a water retaining structure located at the top of a hill.
3. The following additional factors are highlighted for water retaining structures in volcanic terrain:
    - Cohesive or silty soils overlying permeable strata are a dangerous combination, as they can form a roof to a piping tunnel. Soils with fines content exceeding 15% in the overlying layer are a high risk.
    - Piping failure in these highly erodible volcanic soils can occur at very low hydraulic gradients.
    - The framework for assessing piping risk developed by Australian Researchers is useful for both existing and new water retaining structures. This method is recommended for dam practitioners.
    - Pipe penetrations and conduits penetrating embankments require very careful design.
    - Specialist geological advice should be sought if active faulting is suspected, as at this site they were often very subtle features and could be easily missed. In general, siting similar structures on an active fault should be avoided.

ACKNOWLEDGEMENTS

I acknowledge the permission of Contact Energy to publish this paper.

REFERENCES

Bell, G R., Fell, R. and Foster M. (2001). "Risk and standards based assessment of internal erosion and piping failure – a convergence of approaches," *NZSOLD/ANCOLD Conference on Dams, Auckland.*

Foster, M. and Fell, R. (2000). "Use of event trees to estimate the probability of failure of embankment dams by internal erosion and piping," *ICOLD 20th Congress on Large Dams, Beijing.*

NZSOLD (November 2000). "New Zealand Dam Safety Guidelines"

Riley, P. (1997). "Dam incidents in New Zealand," *ICOLD 19th Congress on Large Dams, Florence.*

Sherard, J.L., Cluff C.S. and Allen C.R. (1974) "Potentially Active Faults in Dam Foundations." *Geotechnique 24,* No 3, Pg 367-428

Project Manukau Landfill Seaward Bund

T Wallis
BE (Hons), MIPENZ, R.Eng.
Senior Geotechnical Engineer, Beca Carter Hollings & Ferner Ltd
D V Toan
PhD, FIPENZ, R.Eng
Technical Director, Beca Carter Hollings & Ferner Ltd

Abstract: This paper describes the design concept and construction monitoring of a 900m long rock bund founded on soft marine deposits to form a new seawall retaining a landfill for 1.6 million cubic metres of dewatered sludge. Design of the bund is largely controlled by stability against a sliding/rotational slip failure through the underlying soft marine clay deposit. The bund was constructed in stages to allow time for the marine deposits to increase in strength before adding the next lift of bund material. The strength gain was predicted during design and was monitored during construction by in situ testing with a large shear vane. Settlement plates were installed and monitored by precise levelling. Four vibrating wire piezometers were installed to monitor the generation of excess pore water pressure with application of bund construction loading and dissipation of excess pore water pressures with time. The results of shear vane tests, settlement monitoring and piezometer monitoring are presented and discussed. The correlation between the time for settlement as shown by the settlement plot and dissipation of excess pore water pressure is discussed.

INTRODUCTION

"Project Manukau" is the upgrading of Auckland's wastewater treatment plant at Mangere. The project has three main purposes – to increase the capacity, to increase the effluent quality and to remove the four oxidation ponds in order to return the pond area to the Manukau Harbour. The latter of these involves the removal of accumulated sludge from the base of the oxidation ponds, partial dewatering of the sludge, and deposition of it in a landfill constructed in one corner of the ponds.

This paper describes the design concept and construction monitoring of a 900m long rock bund constructed on soft marine deposits to form a new seawall retaining the landfill.

PROJECT DESCRIPTION

The treatment plant oxidation ponds were built in the 1960s by enclosing an intertidal mudflat area of around 500 hectares in the Manukau Harbour. The treatment plant upgrade project required a new landfill to be built in the eastern corner of Pond No.2. Prior to commencement of the sludge dewatering, the geotechnical properties of the sludge were not known but its behaviour was expected to resemble a "jelly", ie. very low strength and slightly viscous.

After dredging from the pond floors, the sludge was dewatered in centrifuges from a solids content of around 8% to 20% by weight, resulting in a material with density slightly greater than water and shear strength estimated to be around 1kPa.

The landfill design was based on an assumed angle of repose of the sludge of 1 vertical to 120 horizontal. From the estimated four million cubic metres of dewatered sludge, it was determined that the landfill was required to cover an area of around 50 hectares. A new 900m long bund was required, to 3.6m height above seabed level (approximately at mean sea level, set at RL50m as the project datum) which would become a seawall exposed to the Manukau Harbour upon removal of the oxidation pond bunds. The pond level prior to landfill construction was about RL52m, ie. 2m depth of effluent and sludge.

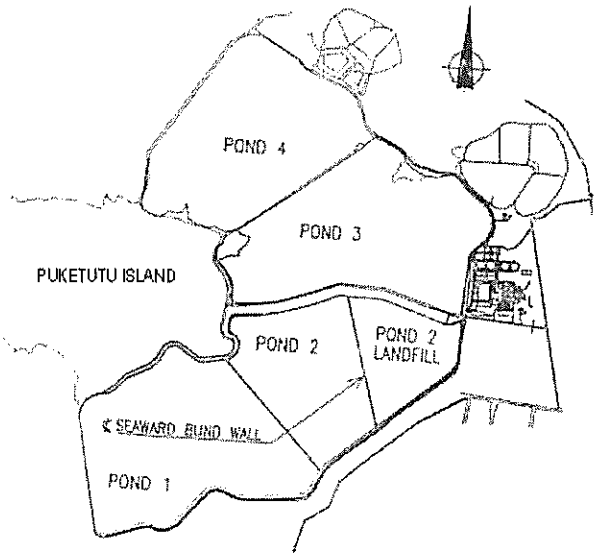

Figure 1 – Site Plan

The seabed generally comprised very soft clayey silt, which was not traffickable by machinery. Sludge placement was achieved by construction of an inclined conveyor founded on driven piles, and aligned in the centre of the landfill. Sludge was dropped off the conveyor at variable positions allowing it to flow outwards towards the edge containment bunds.

GEOLOGY AND SOIL PROFILE

The surficial geology at the treatment plant site includes Holocene (recent) marine sediments, Pleistocene Tauranga Group alluvium and volcanics comprising ash, tuff and basalt. The bund design and construction was controlled largely by the recently deposited marine sediments, which consisted of very soft clayey silt up to 5m thick. This was underlain by the Tauranga Group alluvium comprising stiff peats, silts and clays and sand layers.

Early site investigations had comprised a few boreholes drilled from a barge, which were followed by large shear vane tests to measure the in situ strength.

Later stages of investigation were undertaken through a rock fill starter bund and consisted of more machine boreholes, several cone penetrometer tests (CPT) and further large shear vane tests.

The continuous soil profile record of the CPTs was found to provide a useful guide of the stratigraphy, such as identification of thin sand layers. While it readily identified the thickness of the soft marine muds, the sensitivity was considered insufficient to provide a design value for shear strength. A large shear vane of 100 x 50mm was used to more accurately measure the shear strength.

From the shear vane tests, the marine mud was found to be close to normally consolidated with a shear strength profile of around 4 kPa at the seabed, increasing by around 2 kPa for every metre of depth.

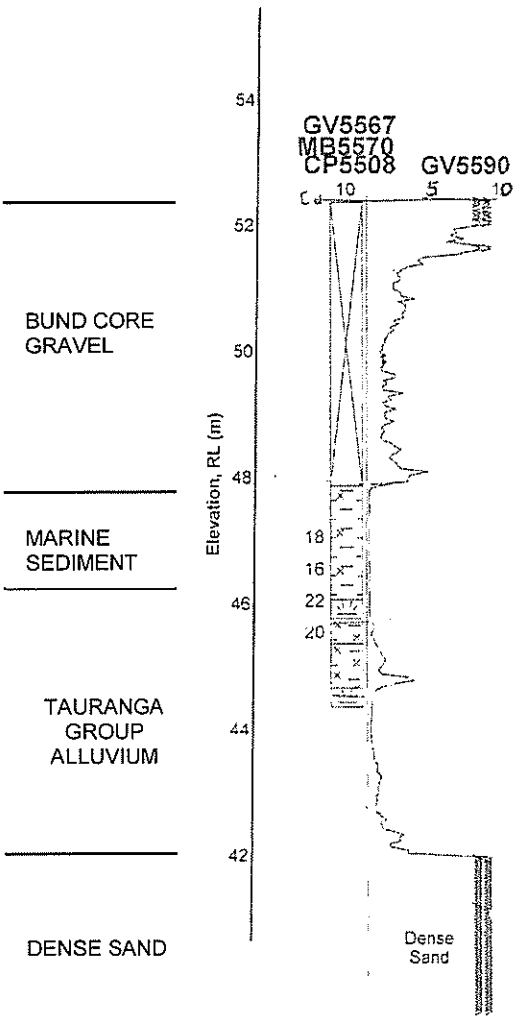

Figure 2 – Typical Site Investigation Results, from CPTs, Large Shear Vane Tests and Machine Boreholes

BUND DESIGN

The bund design cross-section depended largely on stability against a rotational slip failure through the underlying soft marine deposits. Other design criteria were permeability for sludge and leachate containment and armouring for wave protection. Stability was assessed using computer software for calculating factors of safety for circular and non-circular slip surfaces.

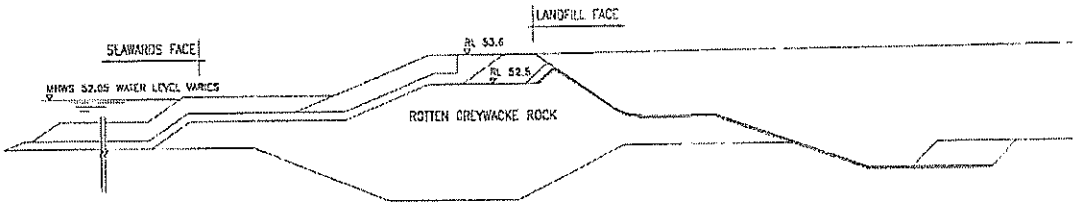

Figure 3 – Design Bund Cross Section

The construction stages were analysed for stability using total stress soil parameters since stability would be critical immediately upon the fill loading.

It was found that for the bund to be constructed to full height in a single operation, the depth of undercut of soft clay and/or overall slope angle required would be excessive. Instead, the design called for staged construction since it was considered that the soft marine mud would increase in strength with consolidation due to the partial bund loading.

The mechanism understood to occur is as follows. The marine sediments have a certain initial undrained shear strength and are in an at-rest effective stress state, ie. the pore pressure equals the head due to the pond level, which is constant. Immediately upon placement of bund fill, the undrained shear strength stays the same but the pore water pressure rises. As the clayey silts have low permeabilities, the excess pore water pressure dissipates gradually. As the water is expelled from the pores, the soil particles press together resulting in consolidation and increase in the undrained shear strength.

The increase in strength was predicted by considering the effective stress that would be applied. In the long term, the shear strength under an applied load should rise to the strength measured in the original soil at a depth with the same effective stress. As the time for such strength gain to occur would be critical to the construction, the design required periodic shear vane testing to verify that the required strength gain had been achieved. Staged construction with lengthy holding periods was a viable solution because the rate of pond dredging required a 2.5 year construction period.

Figure 3 shows the design bund cross-section.

Other design concepts which may have been required if the construction period had been shorter included a deeper undercut, eg. complete removal of the marine sediments, or ground improvement eg using lime stabilised soil columns. Such solutions would have been significantly more costly.

BUND CONSTRUCTION

Preliminary bund design called for a two metre deep undercut of the seabed mud and construction of a starter bund by placing rock fill to 0.5m above pond water level, which was typically 2.0m above the seabed level. An excavator working off a barge completed the undercut and the starter bund was advanced by end tipping rock to form a bund just above water level. The bund core comprised "rotten greywacke", a low-cost, highly weathered rock, which was sufficiently granular in nature to allow placement under water with minimal compaction.

The actual margin of stability was found to be close to that predicted in the design, as indicated by some accidental slumping that occurred during construction. Slumping occurred where material was stockpiled on the bund crest about 1m higher than allowed for in the design.

The landfill construction required dewatering of the landfill area, so the bund's initial work was to resist instability into the dewatered landfill area. Seepage due to the 2m head difference was not excessive, showing the effects of the fines content in the "rotten greywacke" bund core material and where significant flow did occur, it was reduced by placing mud on the outer face.

An HDPE liner was placed on the inside face of the bund for leachate containment.

It was found that the sludge dried to a cake to a depth of a 200 to 300mm and a firm, cohesive fill material could be made by drying the sludge in windrows. The dried sludge could then be placed in layers by tracking with an excavator. Such a layer was placed on the inside face of the bund to form a buffer against the much more liquid sludge. This dried sludge provided toe buttressing for the bund and allowed some construction trafficking.

An excavator working from the bund crest placed a bedding layer and rock armour on the outside face of the bund under water. The excavator was equipped with reach and depth readout equipment to assist with placement of material to the correct lines and levels under water.

INSTRUMENTATION

Instrumentation of the bund comprised settlement plates and three types of piezometer, namely vibrating wire, pneumatic and standpipes.

Settlement Plates

Settlement needed to be measured primarily in order to predict with increasing accuracy the remaining settlement so that the target crest level could be met. An accurate prediction was required because excess fill would be undesirable both from a material quantity/cost perspective and because any excess in fill height had an adverse effect on stability. Conversely, if greater settlement than estimated occurred, additional filling would be required a later date to provide the required seawall crest height.

Monitoring the settlement plates provided the sum of the settlement of all underlying layers at the time of the reading. While the underlying layers settle at different rates due to different thicknesses and permeabilities, the plot of settlement against time or log time would allow extrapolation in order to estimate the long term settlement.

Settlement plates were installed on the base of the undercut and rock fill carefully placed around the rods while under water. Success in protecting settlement rods from construction traffic was less than total, but most plates survived and provided relevant historical settlement records for several locations along the bund for the entire construction period an beyond.

Piezometers

Piezometers were installed in the soft clay layer to monitor the excess pore water pressure developed under the bund loading. The results were not expected to be used in stability analyses since total stress parameters were used in the design. However, the dissipation of excess pore water pressure provided a measure of the degree of consolidation and therefore the time for settlement could be predicted.

Both pneumatic and vibrating wire type piezometers were installed to provide cross checking of data and backup in case of their failure. The vibrating wire piezometers were selected with a response range to suit the maximum expected pore pressure. The lowest pressure range piezometer was selected since the accuracy is a percentage of the maximum pressure. The accuracy of the selected piezometers was reported by the manufacturer to be ±0.5% of the 170 kPa range, ie. ±87mm of water head and the resolution as 0.025% of the 170 kPa range, ie. ±4.3mm of water head. The former of these specifications provides an indication of the absolute measurement of pressure, while the latter indicates the repeatability of the results. One vibrating wire piezometer was installed above ground and used as a barometer so that the piezometer readings could be corrected for changes in atmospheric pressure.

The pneumatic piezometers and readout unit were found to be unable to provide sufficiently accurate readings to be useful in measuring a few metres of excess pore pressure.

Standpipe piezometers were installed and screened within the bund core (relatively permeable material) in order to give the static ground water level in the bund, ie. the piezometric level to which the excess pore pressure in the underlying clay layers would eventually dissipate.

MONITORING RESULTS

Shear Vane Results

In March 2001, around 2.5 years after the initial bund loading, the strength of the clay immediately beneath the bund was found to have increased, refer Figure 4. The trend line inferred from the scatter of results was 23 kPa, which was constant with depth. This equates to a strength gain of 15 kPa at 2m depth and 11 kPa at 4m depth below seabed. The applied load was around 75 kPa.

The greater strength gain at shallower depth can be explained by the higher degree of consolidation due to the shorter drainage path nearer the base of the bund.

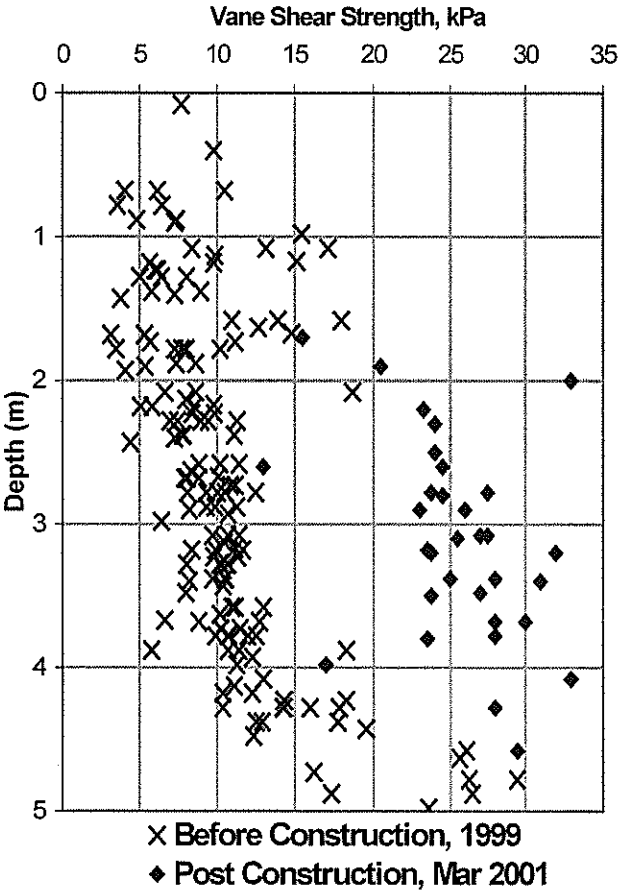

Figure 4 – Shear Vane Results

Settlement Results

Figure 5 shows the settlement versus time plot for a typical settlement plate. The initial loading of around 40 kPa resulted in around 400mm of settlement, the rate of which became minimal by about February 2000, some 18 months after commencement of construction. The rate of settlement then increased again with more load application. The latter stages of loading were the order of another 40 kPa, with additional settlement approaching 250mm recorded to date.

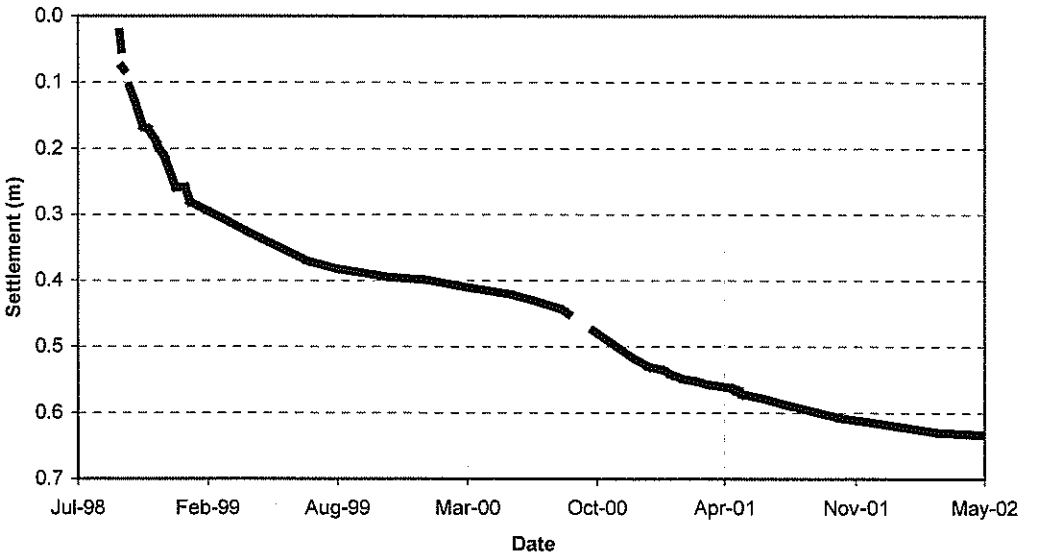

Figure 5 – Settlement Monitoring Results

Piezometer Results

Figure 6 shows the piezometric level for a typical vibrating wire piezometer along with the adjacent standpipe screened with in the bund core. In order to relate the pressure level to the construction levels, the elevation of the piezometric surface is plotted, ie. as a reduced level in metres to the same datum as the bund construction (note that the site datum is RL50m at mean sea level).

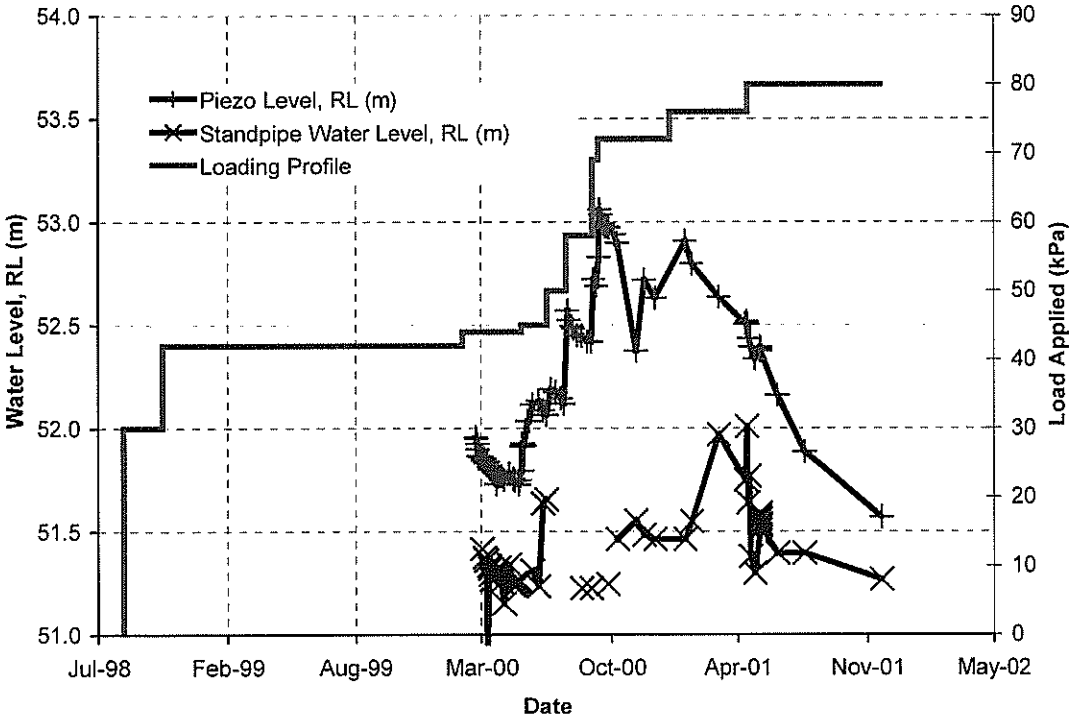

Figure 6 – Applied Load and Piezometric Level

The plot shows the response of pore water pressure to the each of the applied loading steps, followed by dissipation. Between May and September 2000, the pore pressure increased by about 1.3m or 13 kPa, while at the same time dissipation of around 7 kPa occurred (estimated from inspection of the plot), ie. a total of 20 kPa pore pressure increase in response to about 26 kPa of applied load.

It is noted that the piezometer result will be affected by settlement of the piezometer tip. This effect was not allowed for in the results provided. To accurately correct for this effect, a settlement cell would have been required at the same location as the piezometer tip.

The importance of timely instrument readings can be seen from the piezometer plot. For example, there is a rise in pore pressure between 8 December 2000 and 25 January 2001, but sparse data over this period means that the date of the increase and the peak level to which the pressure rose cannot be determined.

The break coincides with the Christmas break. Clearly, readings were needed immediately before and immediately after any load placement to collect the most useful information. A preferred method of instrumentation would have been to use data logging equipment, which is becoming more readily available at reasonable cost.

If load had been applied in a single stage, or if more complete dissipation had occurred between loading stages, it would have been possible to assess the "degree of consolidation" for that loading stage. The coefficient of consolidation, c_v, could therefore have been calculated, and hence more accurate estimates of time for settlement. In the case described above, consolidation due to each of the multiple loading stages overlapped making the interpretation less accurate.

SUMMARY

A landfill containment bund has been designed comprising rock fill placed under water onto soft marine sediments to a height of 3.6m above the seabed. Staged construction was required with holding periods to allow time for consolidation and strength gain of the soft clay. Construction was successfully completed when breaching of the outer seawall exposed the bund to tide and waves about 18 months after commencement.

Construction monitoring instrumentation comprised settlement plates, vibrating wire piezometers and standpipes. In addition, shear vane testing was undertaken to verify the predicted strength gains. The vibrating wire piezometers were found to produce accurate, reliable results over an 18 month construction period in a coastal environment. The pore pressure and settlement monitoring programme has proved valuable in assessing the bund performance compared with the design requirements, in particular the time for settlement.

ACKNOWLEDGEMENTS

The authors wish to thank Watercare Services Ltd and Manukau Wastewater Services Ltd for the permission to publish this paper. Thanks are also given to Dr D P Carter for guidance during the project.

Performance of Steep Reinforced Fill Slopes in Seismic Environments

C R Lawson
BE, ME, MIEA, MASCE
Managing Director, Ten Cate Nicolon Asia, Malaysia

Abstract: The relative performance of two steep reinforced fill slopes, containing the same fill type, subjected to earthquake loads are presented. One slope performed exemplary while the other failed. The lessons learned from these two case studies enables conclusions to be drawn concerning what is good practice. Steep reinforced fill slopes containing fine-frictional fills can perform well in seismic environments provided adequate care is taken during design and construction.

INTRODUCTION

From an economic perspective reinforced fill slopes provide an ideal solution because they maximize the use of locally available fill material. In many instances the local fill material may be fine-frictional and/or cohesive in nature. For good performance of reinforced fill slopes the long term shear characteristics of the proposed fill must be well understood.

Jewell and Wroth (1987) have shown that all soils may be reinforced, with the poorer quality soils requiring more reinforcement in order to obtain a given stability improvement. Taken to the extreme this could be construed to mean that any soil type could attain any required level of internal stability provided enough reinforcement was included. In practice this is not the case. For reinforced fill slopes economics dictate that only approximately 20% to 25% of the total internal shear resistance is provided by the reinforcement with the remainder provided by the compacted reinforced fill. Thus, the reinforcement is a minor, but important, contributor to internal shear stability.

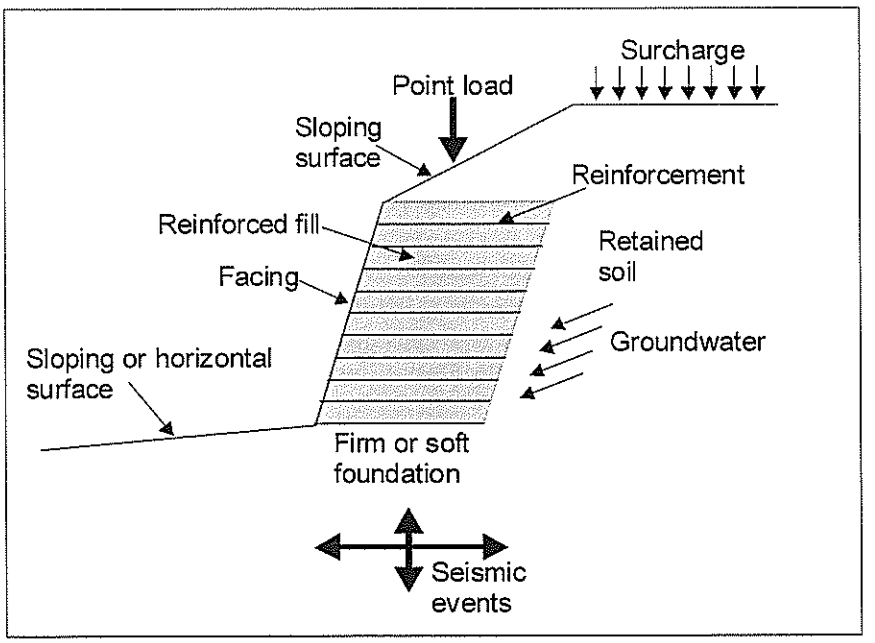

Figure 1. Typical Features of a Steep Reinforced Fill Slope.

The typical features of a steep reinforced fill slope are shown in Figure 1. What must be borne in mind is that the reinforced zone is only one component of the overall slope (although a major one). Other components also impact the performance of the reinforced slope, such as, climatic conditions (temperature, rainfall, etc.), external loads, local geomorphology, groundwater effects, reinforced soil geometry and the construction procedure. All these components need to be considered when designing reinforced fill slopes.

Steep reinforced slopes are defined as those having a slope face angle greater than or equal to 45°. At this slope angle it is considered that the tension generated in the reinforcement cannot be dissipated before it reaches the slope face and consequently, the slope facing has to have some form of structural characteristics. Common forms of slope facing are wrap-around facings with soil bags (the most common), angled steel mesh facings, and gabion facings (the least common).

The majority of reinforced fill slopes utilize local fill. In Asia this has meant the widespread use of soils with significant percentages of fines. These "fine-frictional" fills range from relatively uniform, granular, clay-cemented sandstone to very well-graded residual soils to "cohesive" deposits of partially weathered shales and clay-gravels. While this covers a wide range in terms of soil gradation, when compacted properly all these fine-frictional fills have adequate shear strength, with the worst exhibiting $\phi' \approx 30°$. Many of these soils have compacted $\phi'_p \geq 35°$. Of prime importance when using these fine-frictional fills in reinforced slopes is the degree of compaction attained and the consistency of compaction throughout the slope. Good and consistent compaction of these fills is essential from the viewpoint of maximizing shear resistance and minimizing ingress of water.

In general, the performance of reinforced fill slopes subjected to earthquake loadings has been good, e.g. Tatsuoka et al. (1996). In a small number of instances localized collapse or excessive deformations have occurred, but these have been invariably ductile in nature, and have resulted in negligible collateral damage. For a reinforced slope to collapse on a significant scale it requires a combination of high earthquake loading coupled with deficient design and construction.

TWO STEEP REINFORCED SLOPE CASE STUDIES

To illustrate the extremes in performance that are possible for steep reinforced slopes subjected to seismic loadings two case studies are presented. Both case studies are from Taiwan. The reinforced fill used for both slopes was a clay-gravel that is prevalent in this particular region of Taiwan. The reinforced slope at Nan-Hua performed excellently during an earthquake while the reinforced slope at Chi-Nan failed.

Clay-gravel soils of Taiwan

Large areas of the Western plains and foothills of Taiwan consist of gravel and clay-gravel deposits. These deposits consist of an uncemented gravel matrix in-filled with sand, silt and clay particles to varying extent – clay contents can be as high as 25%. With age, insitu laterization has occurred within the fine fractions of the deposits and consequently, natural and excavated slopes in these deposits may approach the vertical. When remoulded, stable slopes approaching 40° may be constructed with these fills provided good compaction is performed and water ingress is prevented.

The clay-gravel fills are extremely heterogeneous with regard to shear properties due to the presence of the large-sized gravel fractions and the lateritic nature of the undisturbed material. Observed shear properties can range from $c' = 10$ kPa to 120 kPa and $\phi' = 20°$ to 50° depending on the presence of the coarse gravel fraction and the lateritic condition, Woo et al. (1982).

Many steep reinforced fill slopes have been constructed using these clay-gravel fills, with reinforced slopes over 25 m in height not uncommon. Normally, on site, some of the gravel fraction is separated from the fill and is used in subsurface drains, etc. The remaining finer fractions are incorporated into the fill slope. Good compaction of this fill can be attained provided the fill does not become wet. Having become wet, this fill is very difficult to compact and behaves in a semi-plastic manner.

For consistent, long term performance it is important that water not penetrate the fill. In tropic, wet environments good surface drainage and subsurface drainage measures should be installed when using these fills.

Nan-Hua reinforced slope

The steep reinforced fill slope at Nan-Hua, in the South West of Taiwan, was constructed during 1998 to provide an extra parking and services area for a large hillside development. The reinforced slope at its highest point is 50 m and consists of a maximum 6 reinforced soil tiers, each of 8 m in height and 2:1 face slope, Figure 2. The bottom 5 tiers have reinforcement lengths of 20 m, with the top tier having a reinforcement length of 16 m. This yields a reinforced zone width to effective height ratio of 20/50 = 0.4. The reinforced fill used was the local clay-gravel material described previously.

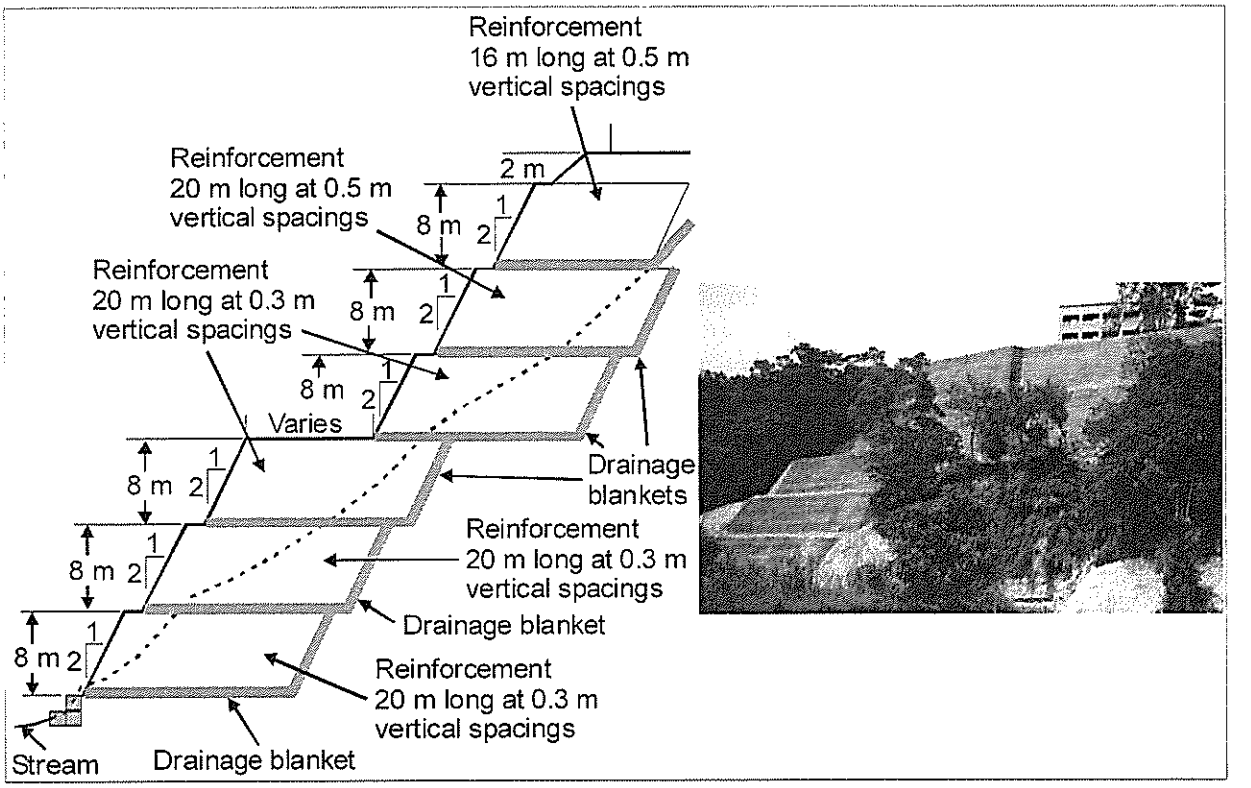

Figure 2. Steep Reinforced Fill Slope, Nan-Hua, Taiwan.

The reinforcement used in the reinforced slope was a polyester geogrid with a short-term tensile strength of 90 kN/m. In taking into account design earthquake loadings of 0.3g the reinforcement vertical spacing was limited to 0.3 m in the bottom 4 tiers and 0.5 m in the top 2 tiers. Design earthquake loadings were also considered in determining the horizontal extent of the reinforcements in the reinforced zones.

The facing for the reinforced slope consisted of soil-filled bags with wrap-around geogrid. The wrap-around geogrid was extended a further 1.5 m into the slope at the top of each reinforced layer to ensure adequate local bond. Grass seed was added during filling of the soil bags to enable ready vegetation growth. Within 3 months of completion much of the slope face was covered with extensive vegetation.

Extensive subsurface drainage measures were employed because of the occurrence of groundwater in the existing earth slope. These consisted of drainage blankets, consisting of geotextile filters with drainage aggregate and porous pipes, placed along the base and extending up the rear of each reinforced tier.

Close attention was paid to the compaction of the clay-gravel fill to ensure consistent compaction densities approaching 90% of Standard Proctor were achieved throughout the reinforced fill mass. Overall, construction quality was excellent.

For monitoring purposes a series of deformation targets were installed along the slope crest and at selected positions in the parking and services area.

On October 19, 1999 an earthquake with a magnitude of 6.4 struck the South Western area of Taiwan, centred near the city of Chiayi. This earthquake occurred a month following the infamous Chichi earthquake, and while not as destructive, considerable damage and injuries were reported. In the vicinity of Nan-Hua, around 20 km to the South of the earthquake epicentre, a number of natural slope failures occurred, including one slope adjacent to the reinforced slope.

Following the earthquake, an evaluation of the reinforced slope was carried out by means of an extensive visual inspection. Little deformation occurred at the crest and on top of the slope with results from the deformation targets showing maximum permanent horizontal movements of 2 cm, with most movements less than 1 cm. Some narrow cracks were observed in the asphalt pavement of the car park on top of one part of the slope at the rear of the top reinforced tier. Overall, the performance of the reinforced fill slope proved exemplary.

Chi-Nan reinforced slope

This steep reinforced fill slope was situated at the entrance to Chi-Nan University, near Puli in the Central West of Taiwan, and served as part of the slope construction measures carried out to construct the main access entrance into the University. The reinforced slope was designed and constructed as a competitive alternative to an original reinforced fill slope proposal. The original reinforced slope proposal, which consisted of more-substantial reinforced zones, was more costly than the alternative design, and hence, in preference, the alternative was adopted.

The overall geometry of the slope is shown in Figure 3a, which comprised a 15 m high natural slope of face angle 1:1, followed by 4 reinforced tiers, each of 10 m height with slope face angle of 2:1, followed by a 15 to 25 m high natural slope of face angle 1:1.5. The total maximum slope height was 80 m. The bottom reinforced tier had reinforcement lengths of 13 m, with second tier having 10 m reinforcement lengths, the third tier having 7 m reinforcement lengths, and the top tier having only 4 m reinforcement lengths. This yields a reinforcement zone width to effective height ratio of 13/45 = 0.29. The reinforced fill used was the local clay-gravel material described previously.

Several types of polyester geogrids were used as the reinforcement in the slope. In the bottom tier the geogrid used had a short-term tensile strength of 105 kN/m while the geogrids used for the remaining tiers had short-term tensile strengths of 60 kN/m. Vertical reinforcement spacings of 0.5 m were used in the bottom two tiers with 0.75 m spacings in the upper two tiers.

Geogrid wrap-around facings with soil-filled bags were used for the reinforced slope facings. The geogrid wrap-around was extended 1 m into the slope at the top of each reinforcement layer to provide adequate local bond. As with the Nan-Hua reinforced slope, grass seed was added during filling of the soil bags to enable ready vegetation growth. Within 3 months of completion much of the slope face was covered with extensive vegetation.

Construction of the Chi-Nan slope began in 1994. Near completion of the construction a fairly large failure occurred in one part of the reinforced slope, which was most likely due to groundwater effects. The failed section of the slope was reconstructed with subsurface drainage being included (this was the only part of the slope that had subsurface drainage). The slope was completed in 1996.

On September 21, 1999 a major earthquake of magnitude 7.6 struck the Central West area of Taiwan, the epicentre being near the town of Chichi. Peak ground accelerations as high as 1.0g were recorded near the epicentre. The earthquake was very destructive with up to 2,500 fatalities and much collateral damage.

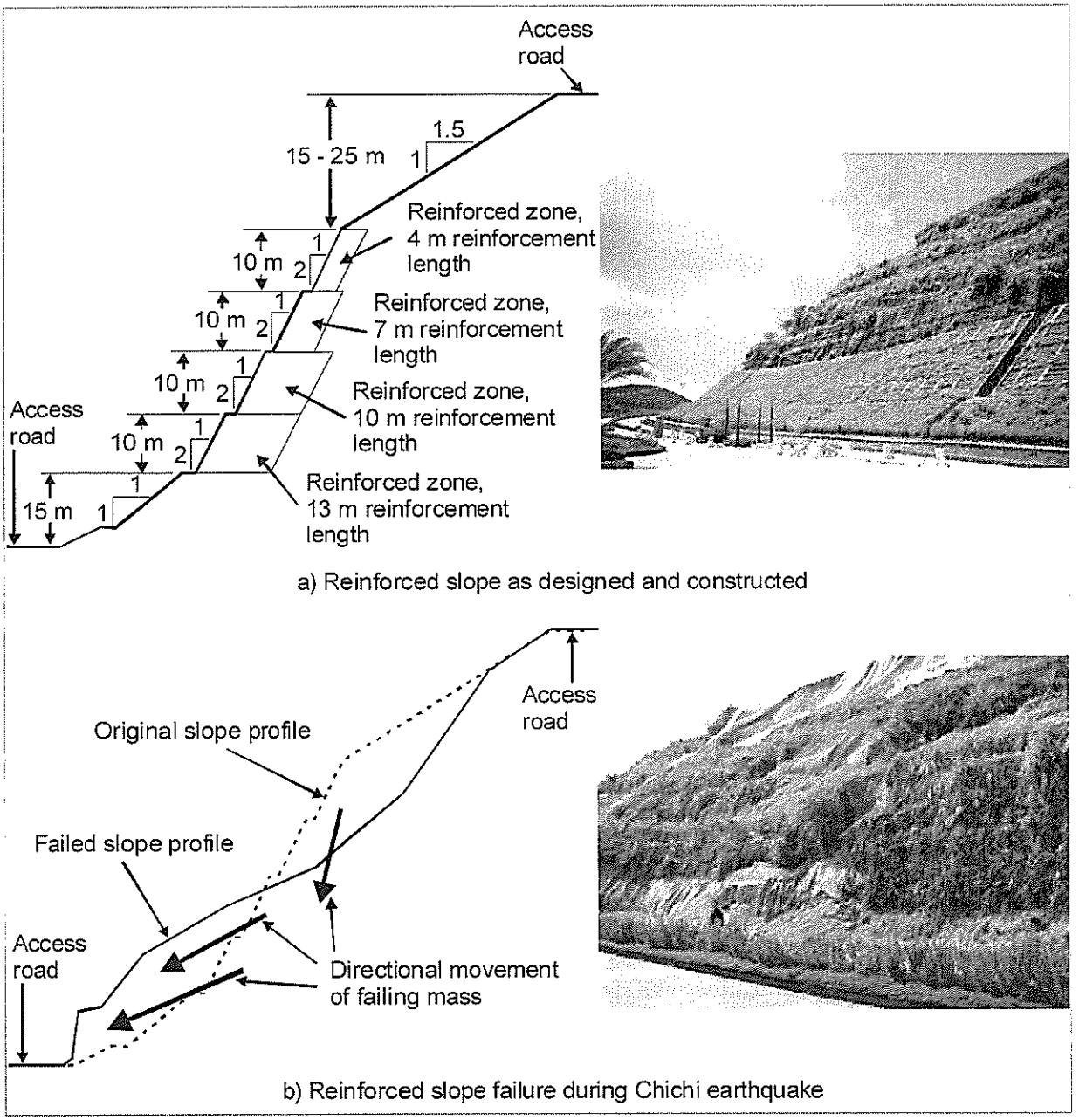

Figure 3. Steep Reinforced Fill Slope, Chi-Nan, Taiwan.

In the vicinity of the Chi-Nan slope, approximately 20 km to the North East of the earthquake epicentre, severe peak horizontal ground accelerations of 0.60g and peak vertical ground accelerations of 0.28g occurred.

During the strong ground motions the reinforced slope moved outwards and down the toe slope, Figure 3b. The mode of failure was en-mass sliding of the reinforced soil zones. The lower two tiers moved en-mass 20 m down to the bottom of the 1:1 slope to come to rest at the edge of the access road. The upper two tiers collapsed en-mass into the void left by the horizontal displacement of the lower two tiers. In the gross movements of the reinforced mass much of the reinforced slope facing was highly deformed with the result that the geogrid wrap-around facing was pulled out of the soil mass and was left hanging down the face of the slope.

A back-analysis of the failed slope using limit-equilibrium methods calculated failure at a horizontal acceleration of 0.3g and a vertical acceleration of 0.2g. This assumed that the shear parameters of the clay-gravel reinforced fill were $c' = 20$ kPa and $\phi' = 35°$. These back-analysed accelerations at failure

are less than those recorded in the vicinity of the slope thus, slope failure would appear inevitable under the peak accelerations recorded.

FUNDAMENTAL CRITERIA FOR STEEP REINFORCED SLOPES IN SEISMIC ENVIRONMENTS

Observations on the fundamental performance criteria for steep reinforced slopes in seismic environments are possible using lessons from the two-presented case studies. These are highlighted as follows.

Basic design procedures used for reinforced slopes

Reinforced slope design methodologies based on two-part wedge or log-spiral procedures are well proven. Simple, standard slope geometries can be designed using chart or spreadsheet methods. More complicated slope geometries and loading regimes require computer programs that can account for these variables. Reinforced slope programs that account for seismic loads in terms of a pseudo-static approach are also increasingly common.

Suitable reinforced fills

The fundamental criterion for reinforced fill is its internal shear resistance characteristics over time when placed in the reinforced slope. From a design perspective, it is imperative that the internal shear resistance of the reinforced fill remains above the value used for design over the full design life of the reinforced slope.

As stated previously, all soils may be reinforced, however, poorer quality soils require a greater amount of reinforcement to achieve a given improvement in stability. In many instances, poorer quality fine-frictional fills are used for reinforced fill because they are locally available and economical. These fills are suitable for reinforced fill provided their internal shear behaviour, over time, is known.

The prime attribute affecting the performance of fine-frictional fills in reinforced slopes is the degree of compaction attained and the consistency of compaction throughout the slope. Good and consistent compaction of these fills is essential from the viewpoint of maximizing shear resistance and minimizing ingress of water. For the Nan-Hua reinforced slope compaction control was very good. This, in conjunction with good drainage, enabled the reinforced fill to perform very well. However, for the Chi-Nan reinforced slope compaction control was considered to be variable with the result that partial failure of the slope occurred near completion of construction due to water ingress into the reinforced fill. This was corrected by the use of subsurface drainage measures in this location and replacement of the failed reinforced fill.

In a temperate, wet environment it may be difficult in practice to place and compact in a consistent manner the finer gradation soils. Rainfall during construction results in pore water pressures within the "compacted" fill thereby reducing its effective shear strength. Unless the fill can be allowed to dry out additional quantities of reinforcement may be required to achieve the design level of internal shear resistance.

Poor compaction quality also enables easy ingress of water into the fills following construction. Water may enter by way of surface infiltration and groundwater flow. Water ingress results in soil erosion and the development of pore water pressures within the fill. As stated already, pore water pressure reduces the shear strength of the fill, but it can also decrease the strength parameters associated with soil softening. The control of soil erosion is best carried out by good attention to slope facing and surface drainage details. The control of pore water pressure build-ups is best carried out by the extensive use of subsurface drainage (see below). Indeed, when dealing with reinforced slopes containing fine-frictional fills drainage is just as important as the reinforcement.

The reinforcement, its vertical spacing and extent

The fundamental criteria for the reinforcements are that they retain a required strength over a specific period of time at a specific level of strain within the reinforced fill environment. In addition, the reinforcements must form a good bond with the surrounding reinforced fill. Currently, geogrids would appear to be the most efficient reinforcements in meeting these criteria, but other reinforcement types also may be appropriate. Ease of installation is another advantage for geogrid reinforcements.

Today, much is known about the long-term performance of geogrid reinforcements. Consequently, it is important to take these long-term characteristics into account when determining the appropriate reinforcement type for a specific reinforced slope application.

The long-term strength of the reinforcements, the height of the slope, its slope angle, external loads and the reinforced fill to be used all contribute to the appropriate vertical spacing of the reinforcements. These factors, along with the reinforcement bond characteristics determine the extent of the reinforcements within the reinforced fill.

Seismic occurrences impose greater disturbing loads on reinforced slopes, and if not accounted for may lead to slope failure. Wholesale failure of a reinforced slope is an extreme event and is presaged by extensive deformation, resulting in a ductile mode of failure.

The Nan-Hua reinforced slope's reinforced zone width to effective height ratio was 0.4 whereas the same ratio for the Chi-Nan reinforced slope was approximately 0.3. During the Chiayi earthquake the Nan-Hua slope remained very stable, but during the Chichi earthquake the Chi-Nan slope collapsed. This may give some guidance regarding initial reinforced slope dimensioning in seismic environments with a reinforced zone width to effective height ratio of 0.4 providing a safe solution. Other factors, including magnitude of seismic loading, face slope angle and foundation conditions will also impact the extent of the reinforced zones in the reinforced slope. It is illustrative to note that it took an earthquake of magnitude 7.6 to fail the steep reinforced slope at Chi-Nan with a reinforced zone width to effective height ratio of 0.3. Under static conditions this reinforced slope had remained stable for 3 years previous.

Quality of the slope facing

Slope facings are an integral component of reinforced slopes and, depending on the steepness of the slope, can play an active, i.e. structural, role or a passive, i.e. non-structural, role. Furthermore, the slope facing constitutes the visual component of the reinforced slope and consequently must meet additional criteria in terms of surface erosion resistance and aesthetics. For aesthetics, increasing emphasis has been placed on the use of "green" facings.

For steep reinforced slopes the facings need to be relatively substantial in size compared to the passive facings for shallow slopes because they need to be able to dissipate the residual tensile stresses occurring in the reinforcement at the slope face as well as confine the reinforced fill to enable compaction near the slope face. Three commonly used facings for steep reinforced slopes are shown in Figure 4. These are soil bag facings, angled steel mesh facings and gabion facings. The major advantage with these three facing techniques is that they do not require the use of external formwork to construct the slope facing.

The soil bag facing, Figure 4a, is the most common and consists of soil-filled bags, normally with vegetation seed mix included, placed to form the slope face. The reinforcement is wrapped around the outside of the soil bags and brought back into the slope to provide adequate local bond length. Once placed, it is possible to reshape the soil bags with an excavator bucket to provide a good quality slope finish. The technique is very cost effective and a good quality, green face is obtained. Furthermore, once the vegetation has been established on the slope face the plant and grass root systems provide excellent local stability to the slope face.

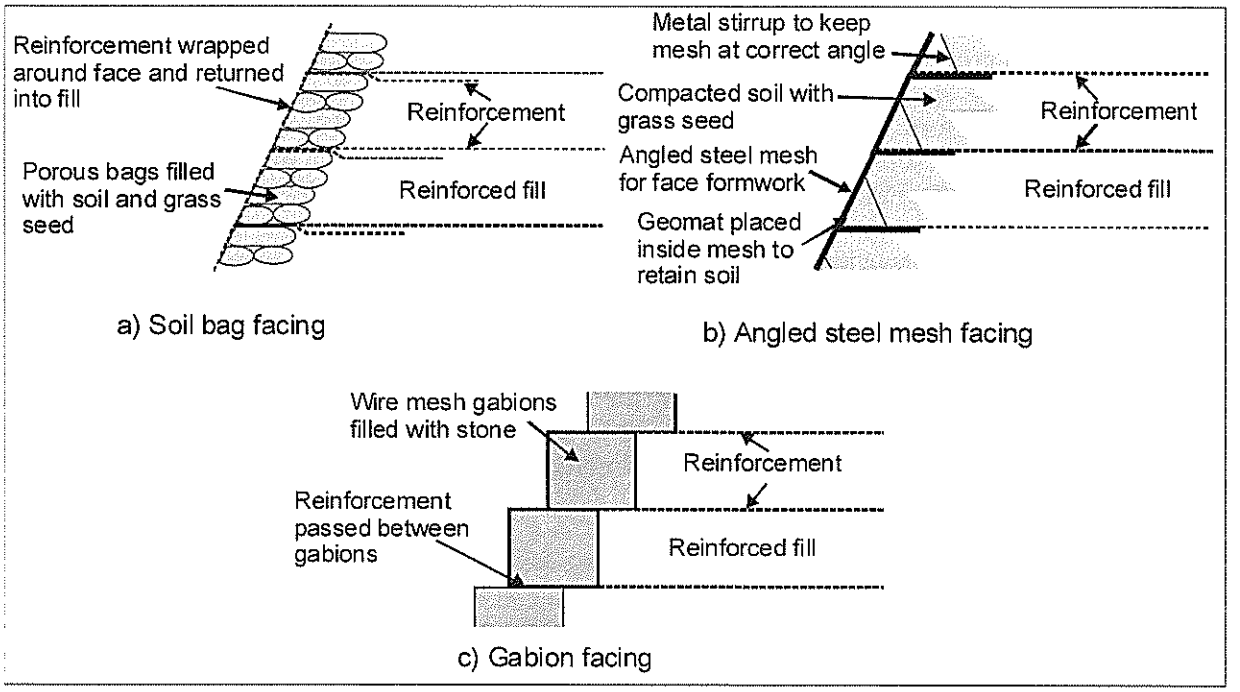

Figure 4. Three Common Facing Techniques for Steep Reinforced Slopes.

The angled steel mesh facing, Figure 4b, consists of steel mesh, prefabricated to the required slope angle, used as a semi-rigid external formwork. The angled steel mesh elements are placed along the extremity of the slope with the reinforcement truncated at the inside base of the angled mesh. To prevent surface erosion and support vegetation growth a geomat is placed down the inside of the face of the angled steel mesh prior to placement, and light compaction, of a soil mixed with grass seed. Behind this front soil layer the reinforced fill is placed and compacted. The angled steel mesh remains in place permanently. In seismic environments it is common to provide a positive connection between the reinforcement and the angled steel mesh facing.

The gabion facing, Figure 4c, consists of wire mesh cages filled with stone as the facing units. The reinforcement can be either physically attached to the gabion cages or passed between adjacent rows of gabion cages. It is possible to have a green finish with gabion facings by including soil and grass seed with the stone in the gabion cages.

The type of slope facing used for both the Nan-Hua and the Chi-Nan steep reinforced slopes was the soil bag facing with geogrid reinforcement wrap-around. This type of slope facing is economical, durable, aesthetic and can be easily shaped to meet specific grade lines and curves. Vegetation growth normally occurs very quickly following construction. Consequently, this type of facing is by-far the most common facing for steep reinforced slopes. In static environments, the magnitude of the geogrid wrap-around embedment should be 1 m, whereas in seismic environments it would appear wise to increase this to 1.5 m to account for any face movements. This has been borne out by the relative performance of the soil bag facings with wrap-around geogrid reinforcement at the Nan-Hua and Chi-Nan slopes.

Importance of good drainage

Good drainage should be an integral part of reinforced fill slopes. The effective use of drainage enables groundwater and surface water to be contained and redirected before it can enter the reinforced slope and cause damage. Where high reinforced slopes are constructed in several tiers surface and subsurface drainage galleries should be included at each tier, with the subsurface drainage galleries extending all the way to the extent of the excavation.

The main function of the subsurface drainage system is to collect groundwater at the rear of the slope and convey it in a controlled manner to exit the slope face. The groundwater collection area for the subsurface drainage system should be founded against the undisturbed part of the excavation area at the rear of the slope with enough exposed surface area to readily collect any groundwater flows. This prevents any pore pressure build-ups occurring behind the lower-permeability, compacted backfill. Well-designed drainage networks should then convey any groundwater to the exit points at the face of the slope.

The choice of the correct materials for the subsurface drains is also important for their long-term performance. Well-selected geotextile filters with the appropriate aggregates and/or pipe drains are critical.

In wet environments, surface catchment drains should be installed along the crest of each tier of the reinforced slope and at the top of the slope crest. The functions of these catchment drains are to gather surface run-off and conduct it away from the slope in a controlled manner; to prevent excess surface run-off from cascading uncontrollably down the face of the slope; and to provide controlled exit points for subsurface drains.

For steep, high, reinforced slopes constructed in a wet environment the proposed drainage system should be well planned before construction commences.

Poor drainage measures may well have been a contributing factor to the collapse of the Chi-Nan slope: it certainly contributed to the partial failure during the original slope construction. In contrast, the drainage measures employed at the Nan-Hua reinforced slope were extensive and detailed.

CONCLUSIONS

Steep reinforced fill slopes utilizing fine-frictional fills can perform well even in severe seismic environments. However, to ensure good performance the correct design procedure must be followed along with attention to construction detail such as the correct placement and compaction of the fine-frictional fill. Good drainage measures should be mandatory.

At the ultimate limit state reinforced slopes behave in a ductile manner with extensive deformations occurring well before collapse. While this limit state is to be avoided, it nevertheless provides an insight into the mode of behaviour of reinforced soil slopes. In general, flexible, ductile structures give better performance in seismic environments than rigid, brittle structures.

REFERENCES

Jewell, R.A. and Wroth, C.P. (1987). "Direct shear tests on reinforced sand," *Geotechnique* Vol. 37(1), pp. 53-68.

Lawson, C.R. (2001). "Performance related issues affecting reinforced soil structures in Asia," *Proceedings IS Kyushu 2001*, Balkema, Vol. 2, pp. 63-99.

Tatsuoka, F., Koseki, J. & Tateyama, M. (1996). "Performance of reinforced soil structures during the 1995 Hyogo-ken Nanbu earthquake," *Proceedings IS Kyushu '96*, Balkema, Vol.2, pp. 973-1008.

Woo, S.M., Guo, W.S., Yu, K. and Moh, Z.C. (1982). "Engineering problems of gravel deposits in Taiwan," *Proceedings engineering and construction in tropical and residual soils*, ASCE, New York, pp. 500-518.

Tailings Dam Performance Assessment Using Finite Elements

M Aravind

BE (Hons) MS CP Eng MIEAust
Senior Geotechnical Engineer, Sinclair Knight Merz, Auckland

Abstract: The Mount Gordon mining site, which is being operated by Western Metals Ltd, has been developed around two major copper ore deposits (Esperanza and Mammoth ores) about 120 kms north of Mount Isa in north-western Queensland. The mines have been in operation since 1927 by open cut and underground methods.

Sinclair Knight Merz (SKM) was commissioned by Western Metals to provide design and construction advice on the tailings dam, saddle dams and spillway and technical advice on tailings management strategy. The design of the tailings dam and the saddle dams was undertaken using finite element modelling. This paper describes the use of finite element modelling using PLAXIS to assess the performance of the main tailings dam and the three saddle dams. The performance of the dams are evaluated in terms of deflections, seepage and long term settlement of the tailings in the Tailings Storage Facility (TSF).

The properties of the tailings and other materials used in the dam construction was assessed from limited laboratory testing and site observations. The results of the finite element analysis were compared with field observations to understand the behaviour of the TSF.

Studies using advanced finite element modelling were performed enabling SKM to recommend cost effective solutions to address concerns regarding in-situ tailings management with negligible impact on the environment.

INTRODUCTION

The Mount Gordon mining site has been developed around two major copper ore deposits about 120 kms north of Mount Isa in north-western Queensland, Australia. The mines have been in operation since 1927 by open cut and underground methods and is being operated by Western Metals Ltd. The process of metal recovery changed from continuous sequential leaching to "Autoclave" pressure leaching to deal with the high volumes and grade of copper as the mining progressed over time.

The tailings dam is located in Conservation Valley, adjacent to the open pit. In 2002, seepage flows from the dam had increased significantly, in the order of 500 m^3 per day, which is far in excess of the initial estimate of about 8 m^3. The quality of the seepage water deteriorated, with low pH, high sulphate, copper and cobalt concentrations, and is currently being pumped back into the tailings dam, rather than being discharged to the environment.

Sinclair Knight Merz (SKM) was commissioned to assess the causes of the high seepage volumes, assess the design and performance of the main tailings dam and the three saddle dams including a spillway and recommend tailings storage strategies including options to increase storage capacity of the Tailings Storage Facility (TSF).

This paper describes the use of finite element modelling using PLAXIS to assess the performance of the main tailings dam and the three saddle dams. The performance of the dams are evaluated in terms of deflections, seepage and long term settlement of the tailings in the TSF.

GEOTECHNICAL ASSESSMENT

Main Tailings Dam

The main tailings dam was constructed in early 1998, predominantly using rockfill material from the Mining Pit with a compacted clay core and filter layer within the upstream portion of the embankment. The dam is approximately 52 m high with a finished crest level of about RL 276 m. The clay core is about 4 m thick with a 2 m thick filter zone on the downstream side of the dam. The rockfill material in the North Waste Dump abuts the dam on the downstream side and buttresses the slope. A simplified section through the main tailings dam is presented in Figure 1.

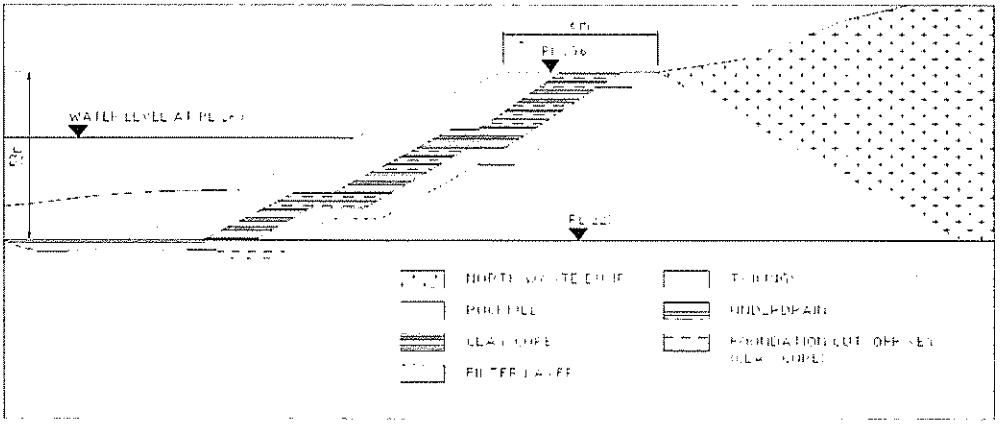

Figure 1. Typical Section Through Main Tailings Dam

An underdrainage system was constructed beneath the tailings on the upstream side of the dam, to enable the removal of pore water from the tailings and accelerate settlement of the tailings.

However, the TSF has been operating differently to what was envisaged during the initial design. The tailing inflow has behaved differently from that anticipated during design stage. Seepage from the TSF was encountered at a monitoring station north of the dam and is currently being pumped back into the TSF at the rate of about 500 m^3/day. In addition to the above, storm water was being discharged in the TSF. Consequently, the water level in the TSF has increased and the tailings deposition is now subaqueous rather than sub-aerial.

Tailings Properties

The tailings storage facility (TSF) provides storage for the fine-grained solid waste from the ore extraction process that is pumped as a slurry of around 50-60% solids upstream of the dam embankment. The solid fraction is allowed to settle out creating a low permeability barrier to seepage of low pH, sulphate and dissolved metal rich fluids to groundwater.

Two types of ores will be mined – Esperanza deposit is being currently mined and mining from the Mammoth deposits will commence in April 2003. The reported (Reference 4 – URS 1998) physical properties of the Esperanza and Mammoth tailings are summarised in Table 1. The sub-aqueous tailings deposition has resulted in some alterations to the tailings properties from those envisaged by others during earlier analyses. The tailings properties were based on the results of the bathymetric survey and limited laboratory testing carried out by Western Metals.

Property	Dry Density	Permeability	Effective Cohesion	Effective Friction	Void Ratio	Specific Gravity	Elasticity Modulus
Units	(kN/m^3)	(m/s)	(kPa)	[°]		g/cm^3	(MPa)
Esperanza Tailings	12.3	1.50E-07	10	25	2.17	3.9	2
Mammoth Tailings	10.0	5.0E-08	10	25	1.70	2.7	2

Table 1: Physical Properties of Tailings

The beaching profile of the tailings was earlier assessed to be at a slope of about 0.5° to 1° based on the assumption that the deposition of the tailings is sub-aerial. However, the present sub-aqueous deposition may have influenced the tailings beaching profile, which is judged to be steeper than 5° in places. The depositional environment is influenced by the high specific gravity and angularity of the particles, which typically results in steeper tailings slopes as observed on site. This effect will be exacerbated when deposition is submerged leading to even steeper angles.

Performance of the Tailings Dam

The performance of the main tailings dam was assessed using the commercial software, PLAXIS, which uses finite element to model non-linear and time-dependent behaviour of soil. The soil was modelled using the 'Hardening Soil' model, which is an elastoplastic type of hyperbolic model and simulates irreversible compaction of soil under primary compression and shear deformation. A selection of soil parameters used for the analysis is presented in Table 2.

Property	Dry Density	Permeability	Effective Cohesion	Effective Friction	Dilatancy Angle	Poisson's Ratio	Elasticity Modulus
Unit	(kN/m^3)	(m/s)	(kPa)	[°]	[°]		(MPa)
HW Rock – Foundation	19	8.50E-08	100	30	0	0.2	150
SW - Fresh Rock	20	1.30E-07	150	30	0	0.2	300
Rockfill	18	1.00E-05	10	45	4	0.2	100
Clay Core	15	1.00E-09	5	30	0	0.28	15
Filter	18	1.50E-06	10	30	0	0.24	20
Waste Dump	20	1.00E-06	10	40	4	0.2	100

Table 2: Geotechnical Model for Main Tailings Dam

The construction of the main tailings dam to a crest elevation of RL 276 m was modelled in 4 stages. A consolidation step at the end of the construction of the main tailings dam was introduced to assess the settlement of the main tailings dam without any external influences. Next, the North Waste dump was modelled on the downstream side of the dam to study its influence on the main tailings dam. The tailings level in the TSF was gradually increased in 5 stages to an ultimate elevation of RL 275 m to study seepage and settlement of the tailings.

The model was analysed under steady state seepage conditions to study seepage through the dam, short term and long term deformation of the dam and tailings and stresses in the main tailings dam. Consolidation steps were introduced at the end of each tailings increment to study short term settlement behaviour. The final consolidation step was set to run until virtually all the excess pore pressures in the tailings was dissipated.

Settlements

Based on our assessment, in the absence of any external influence, the dam is likely to have settled by about 500 mm, most of which would have occurred during construction of the dam. The analysis also indicated that settlements of about 2 m could have occurred as a result of additional loading from the North Waste Dump which abuts the downstream side of the tailings dam. Part of the settlement is attributed to poor compaction of the rockfill (which was modelled as having lower elastic properties in the finite element model) in the main tailings dam. Post construction settlement in the order of about 400 mm was observed in the main tailings dam following the construction of the North Waste Dump.

However, the monitoring of settlement was discontinued and it is possible that long term settlements are occurring in the main tailings dam as a result of additional loading from the North Waste Dump. However, these settlements are less than 5% of the height of the dam and are unlikely to affect the overall integrity or performance of the dam. A typical section through the finite element model of the main tailings dam showing the deformed mesh is presented in Figure 2.

Settlement in the tailings was between 10% and 25% of total tailings thickness. However, the settlement estimate of the tailings is approximate owing to the variation in the tailing properties and in-situ density and moisture conditions. Tailings in its present beached position, at surface elevation of RL 260 m, is likely to settle about 5 m at the end of primary consolidation. However, as the tailing deposition continues and reaches a maximum elevation of RL 275 m, the maximum settlement in the tailings upon completion of primary settlement could be in the range of 10 m to 15 m. The void ratio of the tailings is estimated to decrease from approximately 1.44 to between 1.2 and 0.9. The rate of settlement will depend upon a number of parameters including tailings size, drainage path and overburden load, but is judged to be between 5 to 10 years.

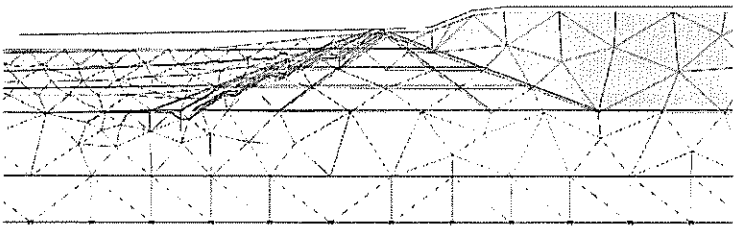

Figure 2. Typical Finite Element Section Showing Deformed Mesh

Seepage

The analysis indicate seepage of about 50 m^3/day through the main tailings dam. This is consistent with what was observed on site. A monitoring station to the north of the North Waste Dump was typically collecting about 30 to 60 m^3/day of seepage until the tailings surface elevation reached RL 240 m. At this elevation, a quartzite ridge cut across the southern portion of the dam establishing a preferential flow path for seepage. Since then, seepage quantities have increased significantly and is now in the order of about 500 m^3/day. Typical section through finite element model of main tailings dam showing seepage flow is presented in Figure 3.

Based on the water balance model and in-situ measurements an average seepage of at least 15,000 m^3 / month is estimated to be occurring from the TSF. Some seepage could also be occurring through surface infiltration of the North Waste Dump. In the long term, it is proposed that the water from the TSF will be re-used for ore processing until there is no free standing water in the TSF. Seepage, therefore, is not an issue for concern in the long term.

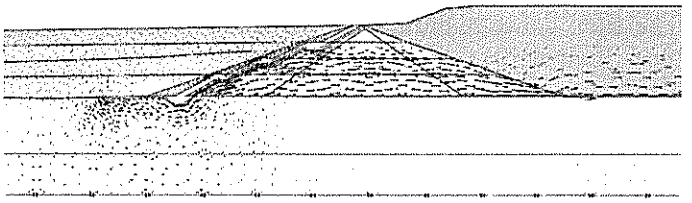

Figure 3. Typical Finite Element Section Showing Seepage Flow

Saddle Dam Characteristics

Two saddle dams on the western side and one saddle dam with a spillway on the southern side was constructed in December 2002 to increase the total storage capacity of the dam to about 6,160,000 m^3. The saddle dams were constructed with a central clay core and with general fill on both sides with a layer of rip-rap for protection of the dam. Typical section through the finite element model of the saddle dam is presented in Figure 4.

The saddle dams and spillway characteristics are summarised as following:

Upstream batter slope – Rockfill, General fill	1.75 H : 1 V (~30°)
Downstream batter slope – Rockfill, General fill	1.75 H : 1 V (~30°)
Slope for Clay core	0.5 H : 1 V (~63°)
Total saddle dam crest width:	6 m
Minimum width of saddle dam clay core at the crest:	4 m
Crest of Saddle Dams (1, 2 and 3):	RL 277 m
Crest of Spillway	RL 276 m
Width of Spillway	20 m

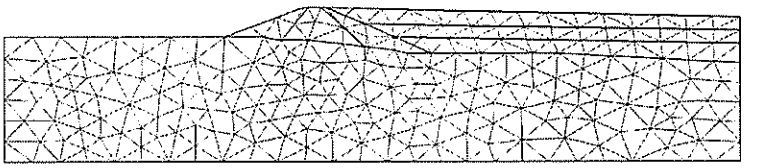

Figure 4. Typical Finite Element Section Showing Deformed Saddle Dam Mesh

Construction of Saddle Dams and Spillway

Majority of the material for the construction of the saddle dam and spillway was procured from the North Waste Dump. The North Waste Dump comprises materials ranging from clay to boulders. The waste material was segregated in-situ to isolate clays, silty soils for general fill (maximum particle size of 150 mm) and rockfill / riprap material (maximum particle size 500 mm). Material removed in the construction of the cut-off key was used as rockfill or riprap material in the saddle dam.

The main objective of the spillway is to safely allow discharge of decant in an emergency situation should the decant level exceed the spillway crest elevation of RL 276 m. Further, the spillway shall also limit the seepage of tailings. HDPE liner was placed on the downstream of the spillway and anchored at the crest to provide a competent surface for uniform discharge with adequate anchorage to prevent tearing of the membrane. The HDPE was protected with a 200 mm thick layer of general fill.

Performance of the Saddle Dams

The saddle dams were analysed using PLAXIS with the geotechnical model presented earlier in the paper. The analysis performed was similar to the earlier described analysis performed for the main tailings dam.

The maximum settlement at the crest of the saddle dam was typically less than 100 mm, most of which would occur during construction of the saddle dams. Post construction settlement in the saddle dams will be negligible.

The seepage through the saddles dams was governed by the permeability of the foundation material and was generally less than 5 m^3 per day, although the presence of faults and other high permeability channels in the foundation layer in the footprint of the saddle dam could substantially increase the seepage through the saddle dam.

During construction of one of the saddle dams, a weak crushed zone was observed in the footprint of the dam. This material was overexcavated to the top of weathered rock and backfilled with clay core material.

CONCLUSION

This paper describes the use of finite element modelling using PLAXIS to assess the performance of the main tailings dam and the three saddle dams. The performance of the dams is evaluated in terms of deflections, seepage and long term settlement of the tailings in the TSF. The TSF has been operating differently to what was envisaged during the initial design with higher than anticipated water level in the TSF and the tailings now being deposited subaqueously rather than sub-aerially.

The analysis indicates that settlements of about 2 m could have occurred as a result of additional loading from the North Waste Dump which abuts the downstream side of the tailings dam partly due to poor compaction of the rockfill. The settlements in the main tailings dam are less than 5% of the height of the dam and are unlikely to affect the overall integrity or performance of the dam.

Settlement in the tailings was between 10% and 25% of total tailings thickness. As the tailing deposition continues and reaches a maximum elevation of RL 275 m, the maximum settlement in the tailings upon completion of primary settlement could be in the range of 10 m to 15 m occurring over a period between 5 to 10 years.

The analysis indicates seepage of about 50 m^3/day through the main tailings dam. However, seepage volumes of about 500 m^3/day was being collected and pumped back into the TSF. The high seepage volume is attributed to the preferential flow path through the quartzite ridge cutting across the main tailings dam, which was not included in the finite element model. In the long term, it is proposed that the water from the TSF will be re-used for ore processing until there is no free standing water in the TSF. Seepage, therefore, is not an issue for concern in the long term.

The maximum settlement at the crest of the saddle dam was typically less than 100 mm, most of which would occur during construction of the saddle dams. Post construction settlement in the saddle dams will be negligible. The seepage through the saddles dams was governed by the permeability of the foundation material in the footprint of the saddle dam and was generally less than 5 m^3 per day.

REFERENCES

GeoCompute (2001), Geochemical Evaluation Report, Water Quality and Storage Integrity, Esperanza Tailings Dam and Esperanza Open Pit, August 2001.

Sinclair Knight Merz (2002), Technical Specification Document for Saddle Dams, Mount Gordon Tailings Dam, July 2002.

URS (2001), Tailings Dam Storage and Contamination Sources Assessment, Mount Gordon Operations, December 2001.

Woodward-Clyde (1998a), Gunpowder Copper Expansion Project – Tailings Dam Design Report, January 1998.

Woodward-Clyde (1998b), Gunpowder Copper Expansion Project Tailings Dam Operations And Maintenance Manual, June 1998.

Seismic Lateral Earth Pressure in a Stiff Cohesive Soil

W Okada
BE (Hons), ME, MIPENZ, Regd Engr
Geotechnical Engineer, Sinclair Knight Merz Ltd

Abstract: Simple procedures are available for calculation of seismic lateral earth pressures in a dry cohesionless soil. The Mononobe-Okabe method is an example of such procedures, and probably the most widely used method. There are, however, few published analytical methods of computing seismic lateral earth pressures on structures retaining stiff cohesive soils. Some published retaining wall design guidelines recommend the Mononobe-Okabe method, which assumes a dry, cohesionless soil, for analysis of lateral earth pressures on flexible retaining structures subject to seismic loading. Some design guidelines, however, do not provide alternative methods for analysis of structures retaining a cohesive soil. This paper presents an example calculation of seismic earth pressures in a cohesive soil via the Saran-Prakash method. The calculated seismic forces on the retaining wall is compared to that obtained through finite element analysis. The calculated forces are in good agreement, suggesting that the Saran-Prakash method is probably applicable to most simple flexible retaining walls in cohesive frictional soils. Analogy with the finite element suggests that the point of application of the calculated pseudo-static forces may be taken as one third of the wall height above the base for practical design purposes. The Saran-Prakash method cannot be directly applied to total stress analysis because Saran and Prakash do not provide the required parameters for undrained conditions.

INTRODUCTION

The Mononobe-Okabe method (Mononobe and Matsuo, 1929), although first proposed over 70 years ago, still remains one of the most popular and commonly used approaches to calculating seismic earth pressures exerted on retaining structures. Several authors have subsequently proposed alternative approaches to calculation of seismic lateral earth pressures, for example, Steedman-Zang (1990).

Although the Mononobe-Okabe method provides a very simple analytical technique for computing seismic lateral earth pressures, it assumes dry cohesionless soil. Where backfill soil is below water table, there is an approximate method of allowing for the soil stresses and water pressures under seismic loading, which is described in the Australian Earthquake Engineering Manual (1993). Nonetheless, modified forms of the widely used Mononobe-Okabe equation that account for cohesive soils appear to be less commonly used. It would be useful for New Zealand geotechnical engineering applications to have similar simple analytical techniques that are applicable to cohesive soils, such as stiff cohesive Waitemata group residual soils in the greater Auckland region.

Saran and Prakash (1968) developed an analytical technique for computing seismic lateral earth pressures in cohesive soils, which is based on a pseudo-static limit equilibrium approach. The pseudo-static method does not incorporate dynamic ground motion, duration and inertial effects. The method may be used to determine yield acceleration. The Saran-Prakash method is considered further in this paper.

CURRENT DESIGN GUIDELINES

Australasia

Design guidelines currently used in Australasia include the Bulletin of the New Zealand National Society for Earthquake Engineering Vol. 13 No. 7 (Matthewson et al, 1980), Transit New Zealand

RRU Bulletin 84 (Wood and Elms, 1990) and Australian Earthquake Engineering Manual. Thes design guidelines categorise retaining walls in terms of whether the wall structures are designed t undergo permanent outward displacement. Non-displaceable walls are further classified into thre categories according to stiffness, namely, rigid, stiff and flexible. For each category, increments o earth pressures under seismic loading are calculated as follows.

Rigid Wall

$$\Delta P_E = k_h \gamma H^2 B \tag{1}$$

Stiff Wall

$$\Delta P_E = 0.75 k_h \gamma H^2 B \tag{2}$$

Flexible Wall

$$\Delta P_E = 0.5 \Delta K_{AE} k_h \gamma H^2 B \tag{3}$$

Where:

k_h = horizontal seismic coefficient

γ = soil unit weight

H = height of retaining wall

B = width of retaining wall

$\Delta K_{AE} = K_{AE} - K_A$

K_{AE} = Mononobe-Okabe active pressure coefficient

K_A = active pressure coefficient

AS4678-2002 Earth-retaining structures (Standards Australia, 2002) prescribes the Mononobe Okabe method as a generic seismic design approach, and does not consider stiffness of the retainin walls. The Bulletin of the New Zealand National Society for Earthquake Engineering Vol. 13 No. and AS4678 do not specify any alternative design approaches for cases where the soil is cohesive and therefore the Mononobe-Okabe method in its original form, as shown in eq. 3, is not valid. Th Australian Earthquake Engineering Manual recommends use of the trial wedge method for suc cases. In addition, the extension of the Mononobe-Okabe method proposed by Saran and Prakas (1968) is referenced as an alternative approach. In Transit New Zealand RRU Bulletin 84, Woo and Elms (1990) present a simplified form of Saran and Prakash's general solution, assuming n tension cracks and no surcharge.

Eurocode 8

The draft No. 5 of Eurocode 8 (2002), which is currently undergoing a review process, specifie similar approaches to seismic design of retaining structures. Dynamic earth pressure increment fc flexible walls is calculated from the Mononobe-Okabe equation, with allowance made for wate pressures where appropriate. The expression used to estimate the earthquake earth pressur increment on rigid walls is virtually identical to that of the Transit New Zealand RRU Bulletin 8 and Australian Engineering Manual. Stiff walls are not considered in Eurocode 8.

ANALYTICAL METHOD BY SARAN AND PRAKASH

Saran and Prakash (1968) proposed a method for calculating earth pressures behind a retaining wall under seismic loading by use of dimensionless parameters. The method replaces a dynamic force with a pseudo-static equivalent force. The method allows for tension cracks, inclined walls, and surcharge. Saran and Prakash considered equilibrium of forces acting on a failure wedge as shown below.

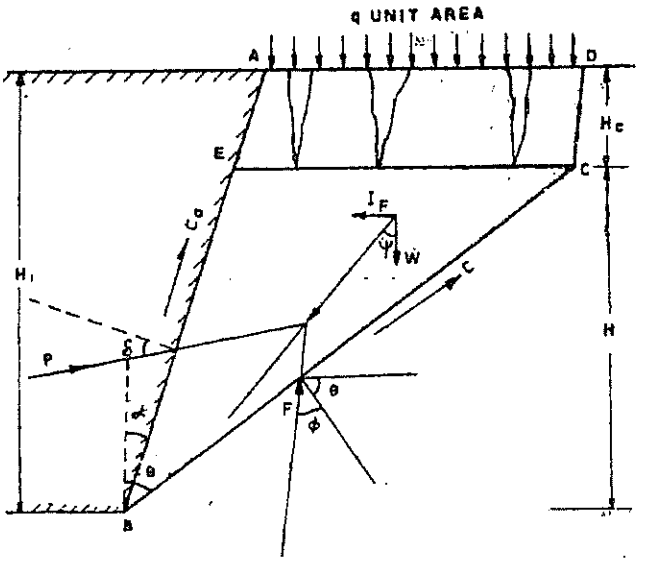

Figure 1. Forces Acting on Failure Wedge (Saran and Prakash, 1968)

By considering the equilibrium of the horizontal and vertical forces acting on the failure wedge, Saran and Prakash derived the following expression for an equivalent force for lateral earth pressures behind the retaining wall:

$$P = \gamma H^2 (N_{a\gamma})_{dyn} + qH(N_{aq})_{dyn} - cH(N_{ac})_{dyn} \qquad (4)$$

Where $(N_{a\gamma})_{dyn}$, $(N_{aq})_{dyn}$ and $(N_{ac})_{dyn}$ are dimensionless parameters. These dimensionless parameters are a function of failure plane angle, θ. Saran and Prakash calculated the value of θ for which each parameter is maximum, and presented the maximum parameters for a range of values of ϕ, k_h, α and n, as shown in Figure 2 and Tables 1 and 2. The values shown in Figure 2 and Tables 1 and 2 correspond to vertical walls. Saran and Prakash also provided a series of dimensionless parameters for inclined walls, and for static case, that is. $k_h = 0$.

The point of application of the calculated equivalent pseudo-static force could not be determined from their method (Saran and Prakash, 1968). Wood and Elms (1990) suggested that it would be reasonable to assume that, for the trial wedge method, the earthquake increment acts at one third of the wall height above the base for flexible walls. Since the trial wedge method forms a conceptual basis for the Saran-Prakash method, this assumption is probably reasonable for their method in most cases.

The Saran-Prakash method may be extended to analysis of saturated clays by carrying out a total stress analysis, that is, by setting $c = c_u$, and $\phi' = 0$ where c_u is the undrained shear strength of the soil (Wood and Elms, 1990). However, $(N_{a\gamma})_{dyn}$ and $(N_{aq})_{dyn}$ parameters were not presented by Saran and Prakash (1968) for $\phi' = 0$. Perhaps total stress analysis of saturated clays may be more readily carried out by the conventional trial wedge method.

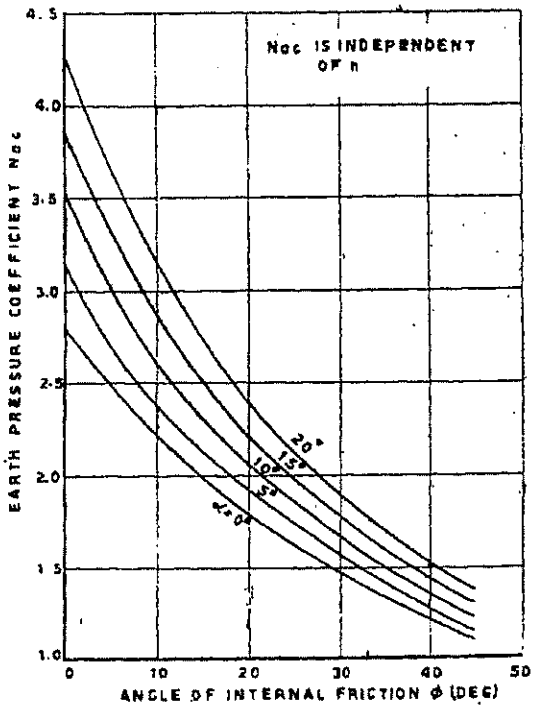

Figure 2. $(N_{ac})_{dyn}$ versus ϕ (Saran and Prakash, 1968)

	Friction Angle ϕ				
Horizontal Seismic Coefficient k_h	**5°**	**15°**	**25°**	**35°**	**45°**
0.05	0.872	0.578	0.396	0.273	0.185
0.10	-	0.634	0.437	0.306	0.212
0.15	-	0.702	0.484	0.342	0.242
0.20	-	0.795	0.538	0.384	0.276

Table 1. $(N_{aq})_{dyn}$ Factors for Vertical Walls (Saran and Prakash, 1968)

		Friction Angle ϕ				
Horizontal Seismic Coefficient k_h	**n[1]**	**5°**	**15°**	**25°**	**35°**	**45°**
0.05	0	0.436	0.289	0.198	0.136	0.092
	0.2	0.610	0.405	0.277	0.191	0.129
	0.4	0.785	0.521	0.357	0.246	0.167
	0.6	0.959	0.636	0.436	0.300	0.204
0.10	0	-	0.317	0.218	0.153	0.106
	0.2	-	0.443	0.306	0.214	0.148
	0.4	-	0.570	0.393	0.275	0.191
	0.6	-	0.697	0.481	0.336	0.233
0.15	0	-	0.351	0.242	0.171	0.121
	0.2	-	0.491	0.339	0.239	0.169
	0.4	-	0.632	0.435	0.308	0.218
	0.6	-	0.772	0.532	0.376	0.266
0.20	0	-	0.397	0.269	0.192	0.138
	0.2	-	0.566	0.377	0.268	0.193
	0.4	-	0.715	0.485	0.345	0.248
	0.6	-	0.874	0.592	0.422	0.303

[1] n is the ratio of the depth of tension cracks, Hc, to uncracked portion of the wall height, H. Refer to Figure 1.

Table 2. $(N_{a\gamma})_{dyn}$ Factors for Vertical Walls (Saran and Prakash, 1968)

EXAMPLE PROBLEM

In order to validate the applicability of the Saran-Prakash method to typical cohesive soils, an example problem is considered. The example shown below is a case study of a proposed retaining wall structure in a stiff cohesive Waitemata group residual soil in Auckland. Although the in-situ residual soil is overlain by a small amount of fill material, it will be ignored to simplify the problem. The dimensions and simplified soil conditions are shown in the figure below.

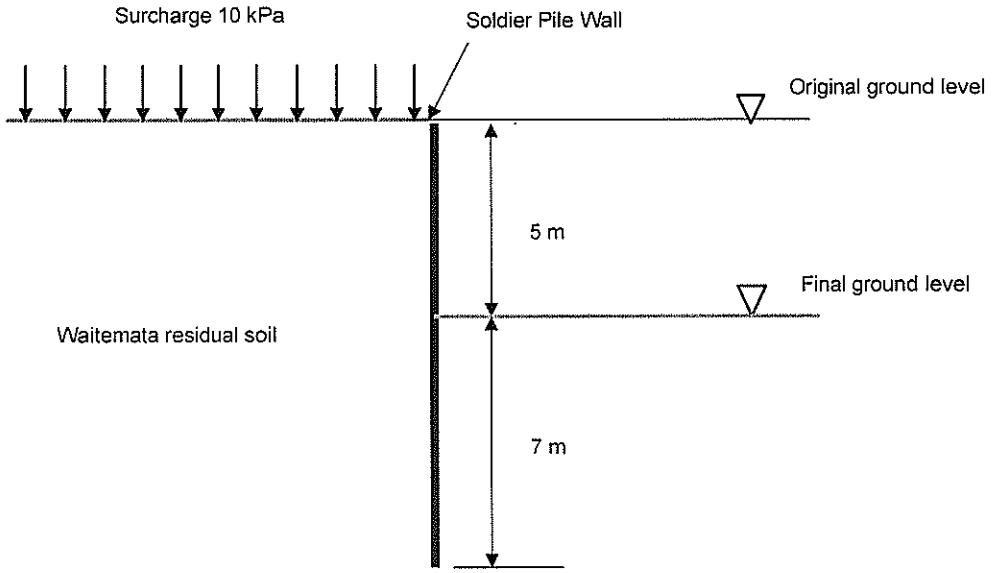

Figure 3. Proposed Retaining Wall and Simplified Soil Conditions

Due to site constraints, the proposed retaining wall will be a soldier pile wall, which will be constructed top-down. It is likely that the proposed soldier wall will comprise 600 mm diameter circular concrete piles spaced at 2 m. The stiffness of the soldier pile wall was taken into account in the finite element analysis. The in-situ cohesive frictional residual soil will remain in place, and unlike cast in-situ walls, will not be replaced with granular backfill or other similar materials. The Saran-Prakash method would be a suitable analysis method for this type of retained material.

The equivalent forces for seismic earth pressures behind the retaining wall have been computed using the Saran-Prakash method and finite element analysis, and the results are compared and discussed below. It is assumed that the retaining wall will be subjected to a surcharge of 10 kPa, which accounts for traffic loading. For the purposes of the example problem, water table is assumed to be well below the base of the retaining wall, and therefore is not considered in the analysis.

The Saran-Prakash Method

The equivalent seismic forces on the example retaining wall have been calculated for a range of horizontal seismic coefficient. The original Saran-Prakash method allows for tension cracks in cohesive soils. Wood and Elms (1990) stated that the tension cracks could be ignored since it is likely that lateral compression at the ground surface from the dynamic inertia forces will offset the tensile stresses that develop because of outward yielding. In this paper, the seismic forces have been calculated with the effects of tension cracks taken into account. The soil parameters are shown in Table 3. The calculated equivalent seismic forces are compared to the results of the finite element analysis in the following section.

Finite Element Analysis

Figure 4 shows the finite element model used for the analysis of the example problem. The analysis was carried out using finite element code PLAXIS version 8.1. The model comprises 15-node triangular elements, which allow cubic interpolation of displacements and stresses. The analysis incorporated staged construction of the retaining wall; that is, changes in soil stress states during construction of the retaining wall were simulated in the analysis. Pseudo-static horizontal loading was applied to the model as horizontal gravity loading for the range of k_h values considered.

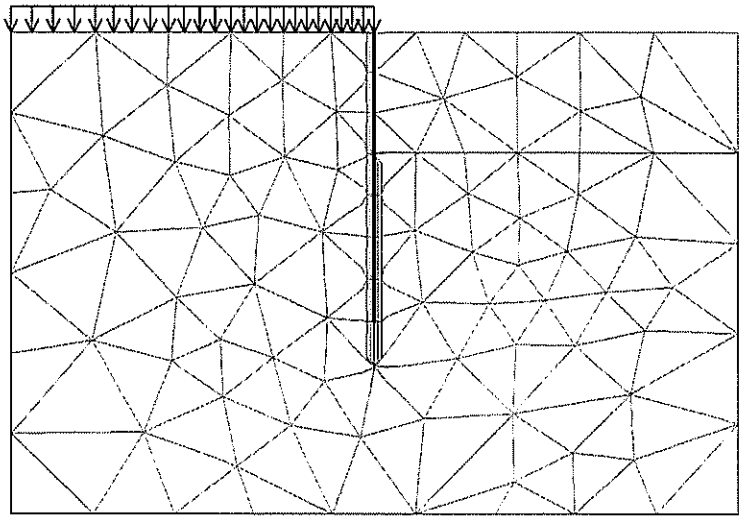

Figure 4. Finite Element Model for the Example Problem

Table 3 shows the soil parameters used in the analysis. The soil was modelled with an elasto-plastic Mohr-Coulomb model.

Geological Unit	Soil Parameters			
	Unit Weight	Friction Angle	Cohesion	Modulus
	γ_b	ϕ'	c'	E
	(kN/m3)	(degrees)	(kPa)	(MPa)
Waitemata Residual Soil	20	33	5	100

Table 3. Soil Parameters for the Residual Waitemata Soil.

The calculated horizontal seismic forces on the retaining walls are shown in the table below:

	Equivalent Seismic Forces on the Wall (kN/m)				
Horizontal Seismic Coefficient, k_h	0[1]	0.05	0.10	0.15	0.20
Saran-Prakash Method	395	448	513	581	658
Finite Element Analysis	492	518	551	613	676

[1] Static Loading

Table 4. Equivalent Seismic Forces Calculated via Saran-Prakash Method and Finite Element Analysis.

The equivalent seismic forces calculated via the Saran-Prakash method are generally smaller than those calculated from the finite element analysis, but are in a similar order of magnitude for values of k_h less than 0.1. For k_h values above 0.1, the Saran-Prakash method and finite element analysis are in good agreement. The discrepancy may be a result of use of the planar failure wedge assumed in the Saran-Prakash method. In addition, the finite element analysis outputs stresses at stress points within the elements. The stress points are spaced at about 0.3 m to 0.4 m in the vicinity o

the retaining wall. The stresses between the stress points were interpolated, and the equivalent force has been calculated by assuming linear variation. This may be a minor source of uncertainty.

Point of Application

Figure 5 shows the distribution of lateral earth pressures on the retaining wall, which have been obtained from the finite element analysis under static and seismic (k_h = 0.2) loading.

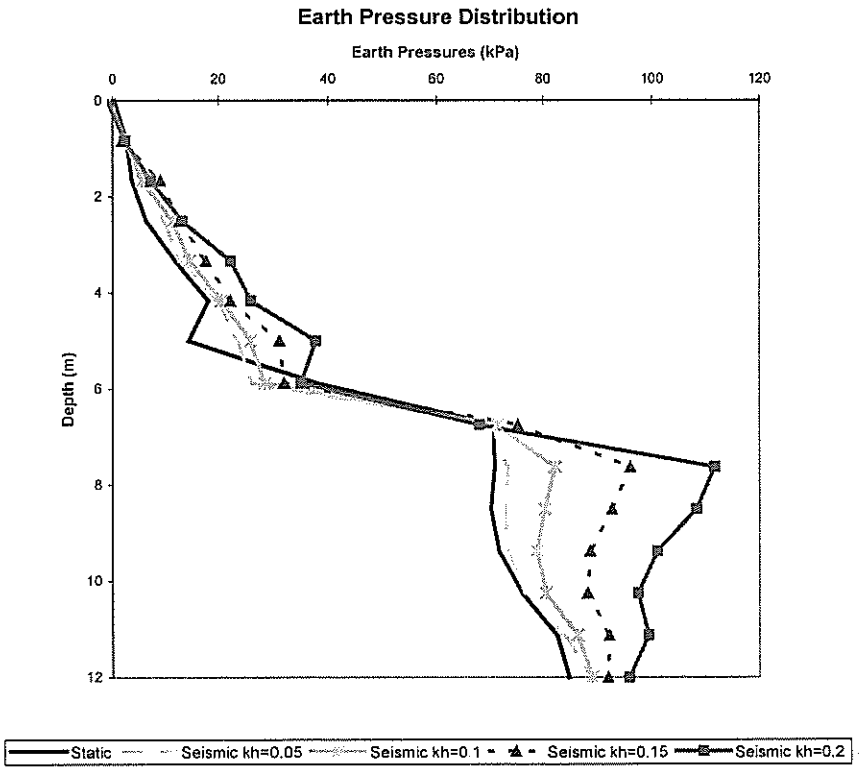

Figure 5. Distribution of the Seismic Earth Pressures Calculated via Finite Element Analysis

The point of application of the equivalent pseudo-static force has been estimated for k_h ranging from 0.05 to 0.2. This was carried out by computing summation of the seismic earth pressures, and taking moment about the base of the wall. The calculated points of application of the equivalent pseudo-static forces are approximately 0.3 H above the base of the wall in all cases where H is the wall height. Given the good agreement between the Saran-Prakash method and finite element analysis, it would be reasonable to assume that the point of application determined in the finite element analysis could be applied to the Saran-Prakash method for simple problems such as the example considered herein. Perhaps the equivalent seismic force may be applied at H/3 above the base of the wall for practical design purposes since this would provide a slightly conservative design force.

CONCLUSIONS AND RECOMMENDATIONS

The Mononobe-Okabe method is widely used for design of retaining walls in cohesionless soils subject to seismic loading. Seismic earth pressures on retaining walls in cohesive soils are not discussed in some of the design guidelines that have been published in Australasia. The analytical technique proposed by Saran and Prakash (1968) is an extension of the Mononobe-Okabe method, and provides a simple analytical method for calculating seismic earth pressures in c-ϕ soils. The

Saran-Prakash method is not directly applicable to undrained loading of saturated clays. Tota stress analysis may be carried out by the conventional trial wedge method.

The Saran-Prakash method has been applied to a simple example problem, and the calculatec seismic forces on the retaining wall have been compared to the results of finite element analysis The equivalent pseudo-static forces obtained using the Saran-Prakash method were in gooc agreement with the results of the finite element analysis, particularly for values of horizonta seismic coefficient, k_h, above 0.1. This suggests that the Saran-Prakash method is probably applicable to most simple retaining structures in cohesive soil. It may be inferred from comparisor with the finite element analysis that the equivalent pseudo-static forces calculated via the Saran-Prakash method may be applied at one third of the wall height for practical design purposes.

ACKNOWLEDGEMENTS

The author wishes to thank Mr G. Murray and Mr. S. Terzaghi for their useful review comments or an early draft of this paper. Special thanks go to Professor M. Pender and Dr J. Berrill, whose guidance provided a starting point for this paper.

REFERENCES

Australian Earthquake Engineering Manual 3rd Edition. (1993). Ed: Irvine, M. And Hutchinson, G.

European Standard (2002). Eurocode 8: Design of Structures for Earthquake Resistance, Part 5: Foundations, Retaining Structures and Geotechnical Aspects, Draft No. 5.

Matthewson, M.B., Wood, J.H. And Berrill, J.B. (1980). "Seismic Design of Bridges Section 9 Earth Retaining Structures," Bulletin of the New Zealand National Society for Earthquake Engineering, Vol. 13 No. 3 September, Pp. 281-293.

Mononobe, N. and Matsuo, H. (1929). "on the Determination of Earth Pressures During Earthquakes," *Proceedings Of World Engineering Conference 9*, Pp. 177-185.

Prakash, S. and Saran, S. (1966). "Static and Dynamic Earth Pressures Behind Retaining Walls," *Proceedings Of The 3rd Symposium on Earthquake Engineering*, University Of Roorkee, India, Vol 1, Pp. 277-288.

Saran, S. and Prakash, S. (1968). "Dimensionless Parameters for Static and Dynamic Earth Pressures For Retaining Walls," *Indian National Society of Soil Mechanics and Foundation Engineering Journal*, Vol. 7, Issue 3, Pp.295-310.

Standards Australia (2002). "AS 4678-2002 Australian Standard Earth-Retaining Structures," Pp. 89-99.

Steedman, R.S. and Zeng, X. (1990). "The Seismic Response of Waterfront Retaining Walls," *Proceedings, ASCE Specialty Conference on Design and Performance of Earth Retaining Structures, Special Technical Publication 25*, Cornell University, Ithaca, New York, Pp. 872-886.

Wood, J.H. and Elms, D.G. (1990). "Seismic Design of Bridge Abutments and Retaining Walls," *RRU Bulletin 84*, Vol. 2, Transit NZ, Wellington

Geotechnical Properties of Two Volcanic Soils

L D Wesley
PhD, MASCE, Regd Engr
Senior Lecturer, Department of Civil and Environmental Engineering, University of Auckland

Abstract: Some of the factors which geotechnical engineers should be aware of in undertaking projects in volcanic country are described by giving an account of the behaviour and properties of two volcanic materials. The first is the allophane clay group; the unusual properties of allophane give these clays very distinctive characteristics. An account is given of their formation and geotechnical properties, and reference made to several projects undertaken involving allophane clays. The second is pumiceous sand, found in various parts of the North Island. The soft (or crushable) nature of the particles means the behaviour of these sands is significantly different from hard grained sands. An account is given of some research work carried out in an attempt to better understand their behaviour.

INTRODUCTION

Many engineering works of a geotechnical nature have been undertaken in the Central North Island volcanic region, the most impressive being the dams and canals constructed as part of major hydroelectric schemes. The Waikato River dams, the Tongariro scheme, and the Matahina dam are the best known examples. In general these projects have been very successful, though not all have been free of problems, either during construction, or after completion. The Arapuni scheme suffered some quite major construction problems, Matahina Dam experienced a significant "incident" during construction, and serious deficiencies in its design or construction became apparent after the Edgecombe earthquake. It has had major rebuilding and upgrading work done on it since then. Actual failures have not occurred on major schemes, but two spectacular failures occurred on small hydro schemes during the 1980s – the Ruahihi and Whaeo canal disasters.

SOME GENERAL COMMENTS

It is not the purpose of this paper to give an overview of the geotechical properties of all the volcanic soils found in the volcanic areas of the North Island. That would be too big a task and beyond the competence of the writer. Rather the paper is restricted to two particular volcanic soil types, the study of which will hopefully highlight some of the general features of volcanic soils that geotechnical engineers should be aware of. These two types are allophane clays and pumice sands. Before proceeding with this some general observations may be useful.

Volcanic soils do not fit comfortably into the range of soils covered by most textbooks or conventional soil mechanics courses in universities. This is because their origin and formation processes are very different from those of "conventional" (ie sedimentary) soils. Fine grained materials of volcanic origin may contain clay minerals not found in other soils. In addition their formation process by situ weathering means that their properties are governed by this process, and not by stress history as with sedimentary soils. They cannot therefore be slotted into the familiar normally consolidated and over-consolidated categories. Coarse grained materials may be essentially the same as any other coarse materials, but they may also be very different. Some volcanic sands and gravels consist of quite weak particles, either because of their inherent nature or because weathering has altered and softened them.

It is important therefore to recognise these differences and not expect volcanic materials to conform to patterns of behaviour associated with conventional sedimentary deposits. In particular, empirical correlations applicable to sedimentary soils may be inappropriate and give misleading pictures when applied to volcanic soils.

ALLOPHANE CLAYS

Occurrence

There are substantial areas in the North Island where clays derived from the weathering of volcanic ash occur. These clays tend to be rich in the clay mineral allophane, which gives them rather unusual and unique properties. They are often referred to as "brown ash" by local engineers. Whether all clays referred to as brown ash contain allophane is not known to the writer; the term is used rather loosely and in some cases may be applied to clays that do not contain allophane. The clays described here are those whose properties are influenced primarily by their allophane content, and will be referred to as allophane clays. Similar clays occur in many parts of the world, including Indonesia, The Philippines, Japan, Central and South America, and Africa.

Formation

The formation and composition of allophane clay is complex, and most of the research and literature on the subject comes from the discipline of soil science rather than soil mechanics. This research and literature has grown enormously in the last two or three decades since the term allophane first found its way into geotechnical literature, and it shows a number of new and interesting findings. Firstly, it shows that allophane seldom occurs by itself. Instead, it is almost invariably found with other clay minerals, especially a mineral called imogolite. It seems to be almost inseparably linked to imogolite, and many papers on allophane are in fact on "allophane and imogolite" rather than on allophane alone. Secondly, it shows that allophane is not strictly amorphous, as early literature asserted. Both allophane and imogolite have some crystalline structure, albeit of a very different nature to other clay minerals.

Allophane clays are derived primarily from the in situ weathering of volcanic ash, although they may be derived from other volcanic material. This parent material may be either basic or acidic in nature. It appears that the primary condition for allophane formation is that the parent material be of non-crystalline (or poorly ordered structure) composition. Volcanic ash meets this criteria; it is formed by the rapid cooling of relatively fine-grained pyroclastic material, the cooling process being too rapid for the formation of well ordered crystalline structures. In the author's experience, the parent volcanic ash from which allophane clays are formed is generally in the coarse silt to fine sand particle size range.

In addition to the above requirement of non-crystalline parent material, it appears that the weathering environment must be well drained, with water seeping vertically downward through the ash deposit. High temperatures also appear to favour or accelerate the formation of allophane clays. Allophane clays may be very deep; in Indonesia the writer has encountered cuts in these materials up to about 30m deep, while site investigation drilling has shown depths of up to almost 40 metres. This thickness results from successive eruptions and associated ash showers, with weathering progressing as the thickness grows. Examination of cut exposures in West Java, Indonesia, shows the individual layer thickness to vary generally between about 100 and 300mm.

Structure

The precise structure of allophane clays is somewhat problematic. Their extraordinarily high natural water contents and void ratios (described in the next section) clearly indicate an unusual material, and call for an explanation in terms of either structure or chemical composition (or both). Various explanations have been offered over the years. As mentioned above, allophane has been described in the past as non-crystalline or amorphous, and "gell-like". However, electron microscopy studies over the past 10 years or so (Wada, 1989 and Jacquet, 1990) show that the material in its natural state does have an ordered structure – consisting of aggregations of spherical allophane particles with imogolite threads "weaving" among them, or forming "bridges" between them.

Figure 1 shows an electron micrograph of the material in its undisturbed state, (taken from Wada, 1989). The concept of approximately spherical particles with thread-like structures spanning between them appears to explain both the very high natural water content, and the changes the material undergoes on remoulding. Remoulding appears to break up the aggregations of particles and threads

spanning between them and turns the material into a homogeneous unstructured mass. This is generally accompanied by some loss of strength and an increase in compressibility, as well as a reduction in permeability.

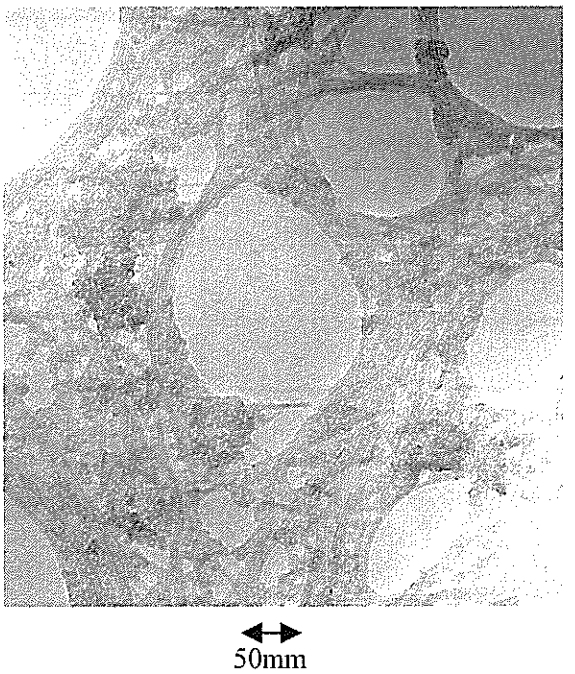

Figure 1. Electron Micrograph of Allophane and Immogolite (after Wada, 1989).

General Comments on Engineering Properties

Before describing particular properties the point should be made that allophane clays are not problem soils. There is still a belief among some geotechnical engineers that the presence of allophane in a soil is something to fear or be concerned about. This should not be the case. Observation of these clays in their natural environment shows them to perform remarkably well. For example, terraced ricefields in Indonesia exist on slopes as steep as 35^{0} and almost up to 40^{0}. They are permanently saturated by irrigation water flowing from terrace to terrace. Many water retaining structures have been successfully constructed from allophane clays. While they ought not to be a cause for concern, it is important that their special properties be understood and taken account of in planning engineering projects involving allophane clays.

Natural Water Content, Void Ratio, and Atterberg Limits

The natural water content of allophane clay covers a very wide range, from about 50% to 300%. This corresponds to void ratios from about 1.5 to 8. It appears that water content is a reasonable indication of allophane content – the higher the water content the greater the allophane content. Atterberg Limits similarly cover a wide range, and when plotted on the conventional Plasticity Chart invariably lie well below the A-line. This means that according to the Unified Soil Classification System they are silts. However they do not display the characteristics normally associated with silt – the tendency to become "quick" when vibrated and to dilate when deformed. At the same time they are not highly plastic like true clays, so they do not fit comfortably into conventional classification systems. Figure 2 shows a plot of the Atterberg limits on the Plasticity Chart.

Influence of Drying

Drying has a very important effect on allophane clays. Frost (1967) gave the first systematic account of this effect for both air and oven drying on tropical soils belonging to the allophane and halloysite group. He showed that clays from the mountainous districts of Papua New Guinea with values of Plasticity Index ranging from about 30 to 80 in their natural state become non-plastic when air or oven

dried. Wesley (1973) describes similar effects from the allophane clays of Java, Indonesia. The properties of the clay described in this paper apply to the clay in its natural state, ie without air or oven drying, unless otherwise stated.

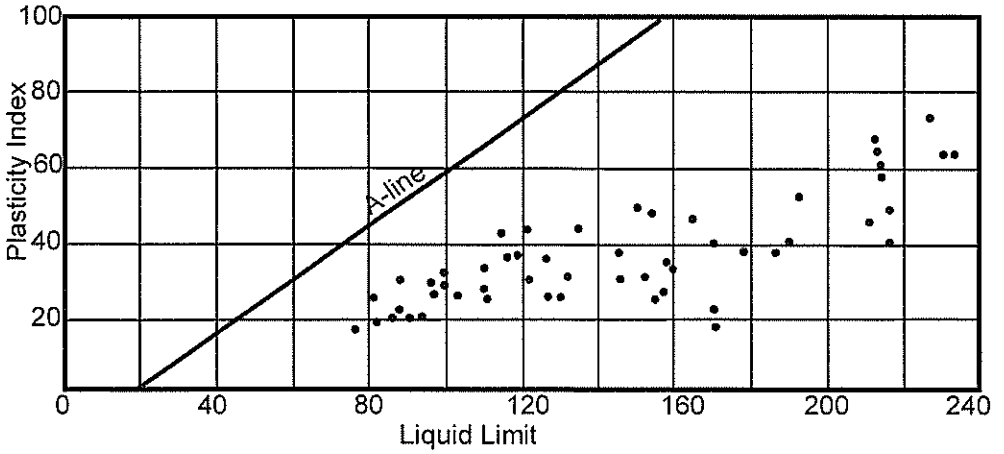

Figure 2. Atterberg Limits of Allophane Clays on the Plasticity Chart.

Identification of Allophane Clays

There are various techniques used by soil scientists to identify allophane: these are primarily X-ray diffraction and electron microscopy. Such methods are not readily available to geotechnical engineers For engineering purposes, sufficient indicators of the presence of allophane are the following:

1) Volcanic parent material
2) Very high water contents
3) Very high liquid and plastic limits lying well below the A-line on the Plasticity Chart
4) Irreversible changes on air or oven drying - from a plastic to a non-plastic material.

If all of these are applicable then the soil almost certainly contains a significant proportion of allophane.

Stiffness and Compressibility

Typical results from oedometer tests on undisturbed samples from Indonesia and New Zealand are shown in Figures 3 and 4. Details of the samples are given in Table 1.

Sample Number	Location Information	Depth (m)	Void Ratio	Water Content (%)	Atterberg Limits		
					L.L.	P.L.	P.I.
I.3	Cipanunjang, Indonesia	1.0	4.76	161.2	187	149	38
I.4	Cipanunjang, Indonesia	3.0	4.72	156.1	179	139	40
I.6	Kamojang, Indonesia	12.2	5.34	190.7	*		
NZ.4	Omata, New Zealand	7.5	2.58	81.3	*		
NZ.6	Omata, New Zealand	7.0	3.20	114.1	*		
NZ.7	Omata, New Zealand	5.1	2.49	88.5	*		

* Atterberg limits not measured on these samples

Table 1. Details of Samples Used for Oedometer Tests.

Figure 3 shows the results as conventional e-log(p) graphs and Figure 4 as direct compression versus stress on a linear scale. The e-log(p) curves suggest that all the samples have similar compressibility characteristics with "pre-consolidation" pressures of varying magnitude. However, when plotted using a linear pressure scale this is no longer the case. Only some of the samples show an apparent pre-consolidation pressure; this is of course not related to stress history. It arises from the structure of the

soil created by the weathering process, and is perhaps better described as a vertical yield pressure rather than a pre-consolidation pressure. Why some samples show a yield pressure and others do not is not known, though it may be related to the original denseness of the parent material.

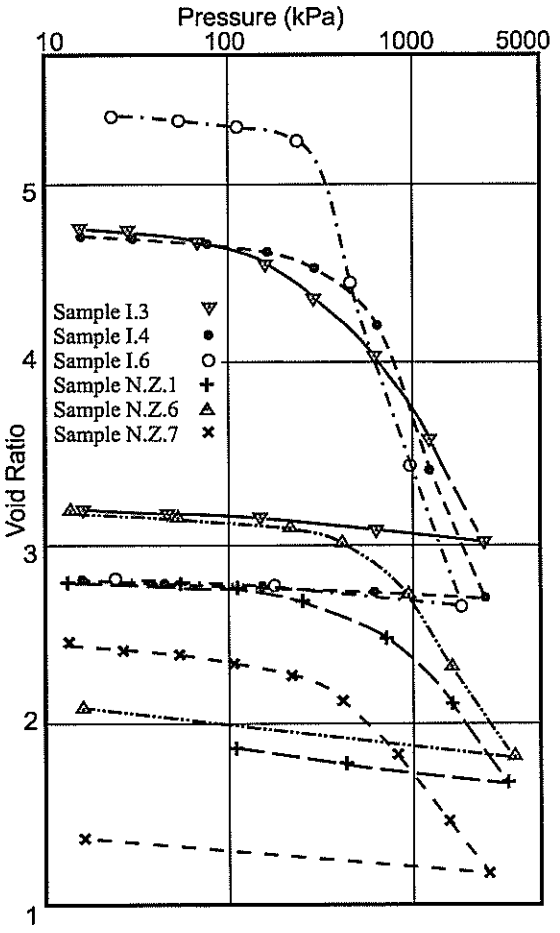

Figure 3. Oedometer Test Results as e-log(p) Plots.

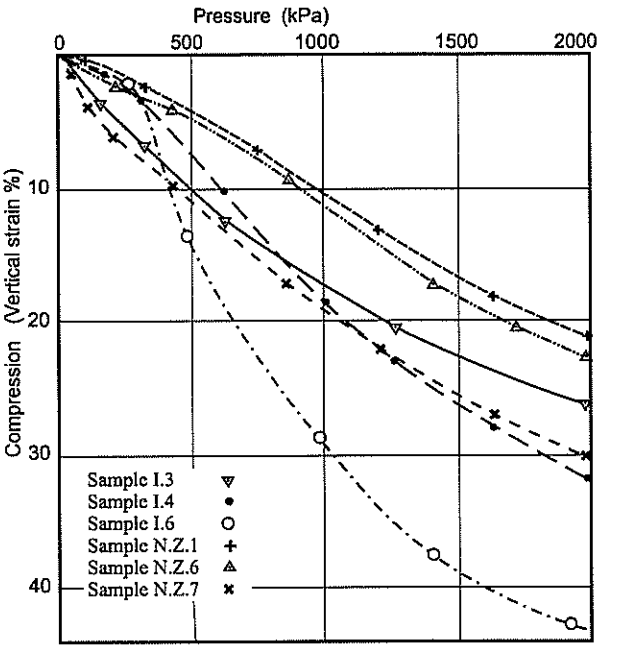

Figure 4. Oedometer Tests Showing Compression Versus Pressure on a Linear Scale.

These graphs illustrate two important points. Firstly, to gain a clear picture of the consolidation behaviour it is necessary to plot the results using a linear scale as well as a log scale. Secondly, the portion of the graph of interest in foundation design is often close to linear with respect to pressure, and favours the use of the linear parameter m_v (or constrained modulus D) for settlement calculations rather than the log parameters C_c and C_s.

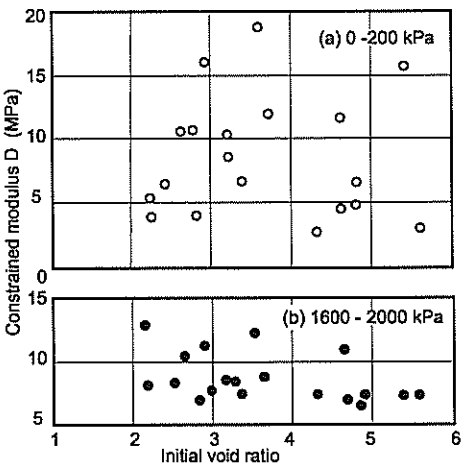

Figure 5. Constrained Modulus (D) Versus Initial Void Ratio.

It is of interest to note that for these clays there does not appear to be any relationship between the initial void ratio and compressibility. Fig. 5 shows the constrained modulus D measured when the sample is loaded from 0 to 200 kPa, and again between 1600 kPa and 2000 kPa, plotted against the initial void ratio. The data shows considerable scatter, but there is no clear trend towards higher compressibility with increase in void ratio from 2 to nearly 6.

Figure 6 shows typical root time plots from oedometer tests. At low stress increments the consolidation rate is clearly very rapid but becomes progressively slower as the stress level rises. To investigate this effect in more detail, pore pressure dissipation tests were carried out using a triaxial cell. Two samples from New Zealand and two from Indonesia were tested. A summary of the c_v values obtained from these dissipation tests is shown in Fig. 7. It is seen that the c_v value decreases by approximately four orders of magnitude as the stress increases from 50 to 1000 kPa. With the New Zealand samples, the tests were repeated after remoulding the soil. It is seen that the c_v value is then consistently low and close to the end value from the undisturbed samples. With the Indonesian samples, permeability measurements were also made between each consolidation stage; the results showed an identical trend to the c_v values. Figure 7 shows that remoulding the soil apparently destroys the open structure of the undisturbed soil, which is believed to account for the high permeability.

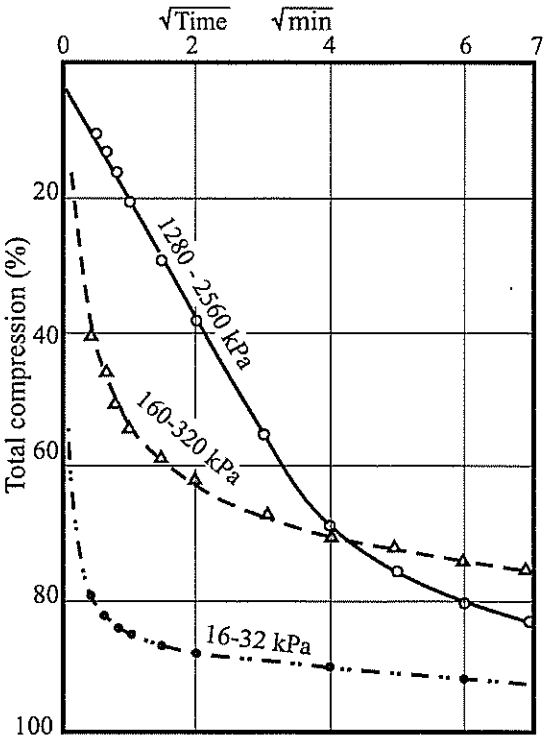

Figure 6. Typical Root Time Plots from Oedometer Tests.

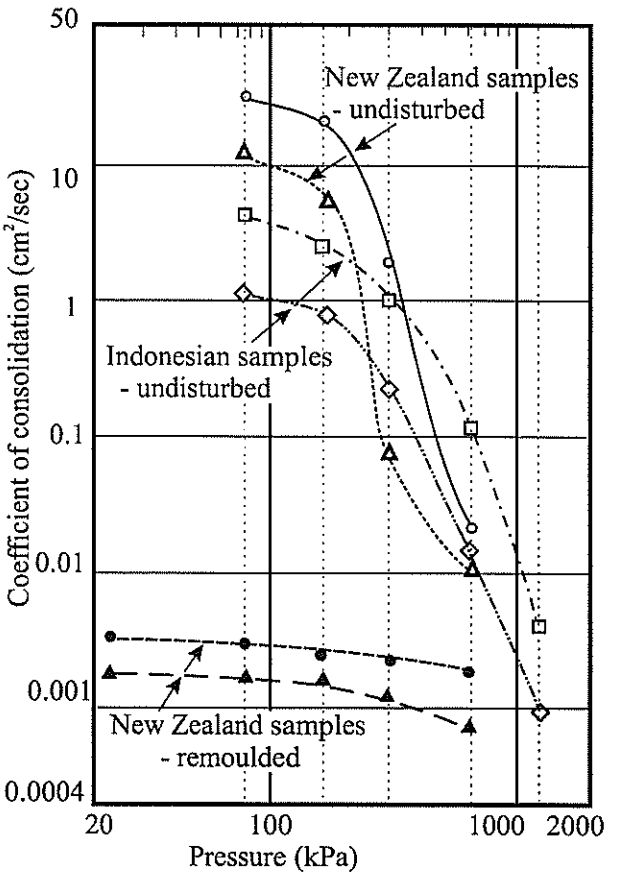

Figure 7. Summary of c_v Values from Pore Pressure Dissipation Tests.

It should be appreciated that with clays of this type it is not possible to determine reliable c_v values from conventional oedometer tests. The drainage path length is too short for pore pressure dissipation to control the deformation rate. The upper limit of the c_v value which can be measured with a conventional oedometer test with sample thickness of 20 mm is about 0.01cm^2/sec. At the relatively low stress levels relevant to engineering situations, the c_v value of allophane clays is normally much higher than this.

The points made above should be kept in mind when dealing with any residual soil. Results of consolidation tests should be plotted using both log and linear scales in order to get a true picture of behaviour. Some samples within a particular soil type may show distinct "yield" pressures, while others may not. Consolidation rates can also vary over wide ranges within any given soil group.

Some layers within the Auckland Waitemata clays have permeability values at the lower end of the range expected for clays, while others may have permeability values normally associated with silts.

Undrained Strength

Figure 8 shows cone penetrometer test (CPT) results from two sites, one in Indonesia and one in New Zealand.

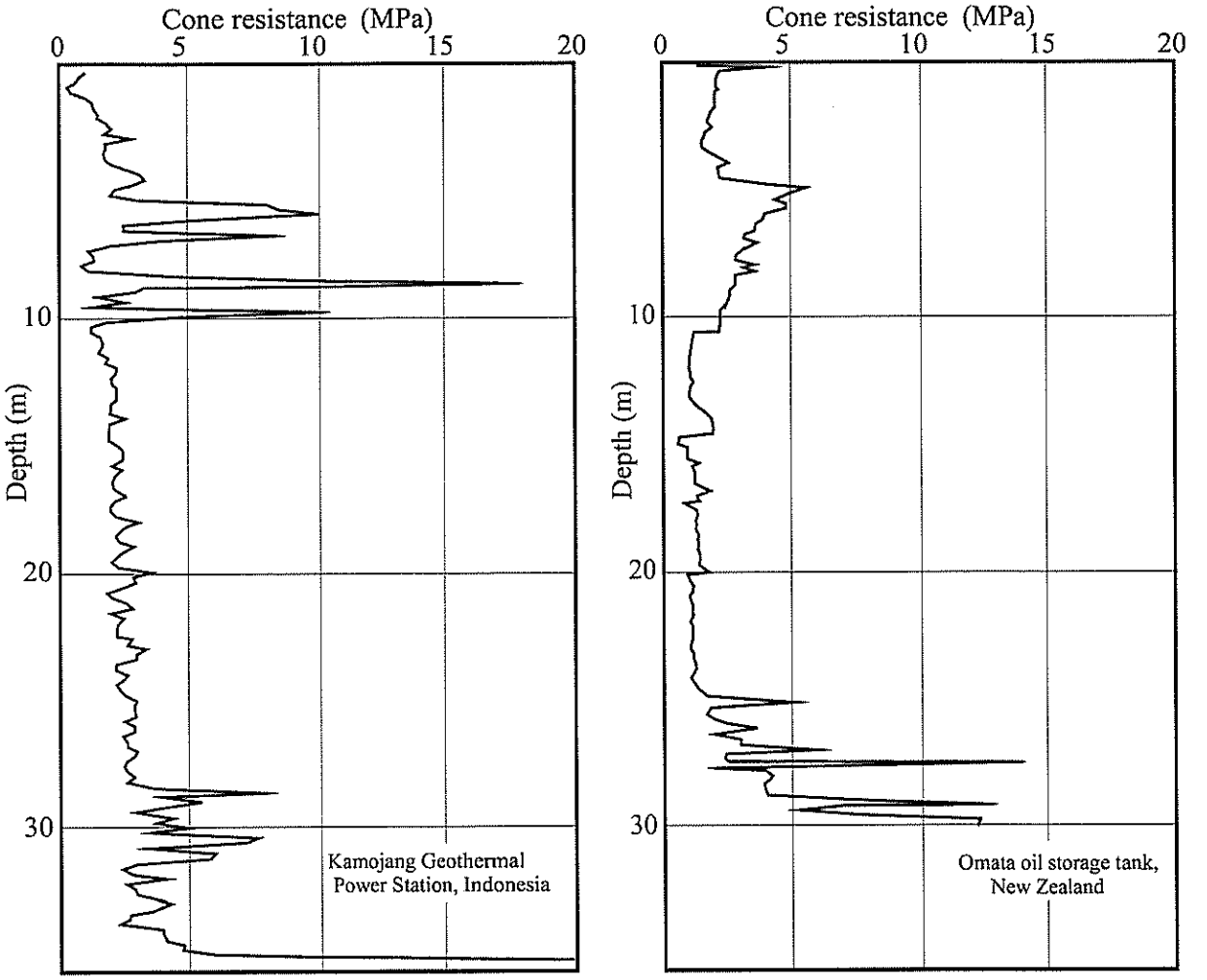

Figure 8. Cone penetrometer Tests from Sites in Indonesia and New Zealand.

These are fairly similar. They show that while the in situ strength is reasonably uniform, it does have small fluctuations over the full profile, and there are some zones with considerably higher values. These are believed to be zones of coarser material within the fine clay. The cone resistance varies between about 1 and 3 MPa. Using a correlation factor (N_k) of 15 this corresponds to an undrained shear strength range of about 65 kPa to 200 kPa. Values of undrained strength obtained from other methods at the Kamojang site ranged from about 50 kPa to 170 kPa, confirming the trend indicated by the CPT tests.

Effective Strength Parameters

The effective strength parameters c' and ϕ' are surprisingly high for a soil of such fine grained composition. This is perhaps not surprising; observation of field behaviour suggests that this must be the case. As mentioned earlier, in Indonesia and other tropical countries, terraced rice fields exist on remarkably steep slopes in areas of allophane clay. These slopes remain stable despite permanent saturation with irrigation water, which flows from terrace to terrace.

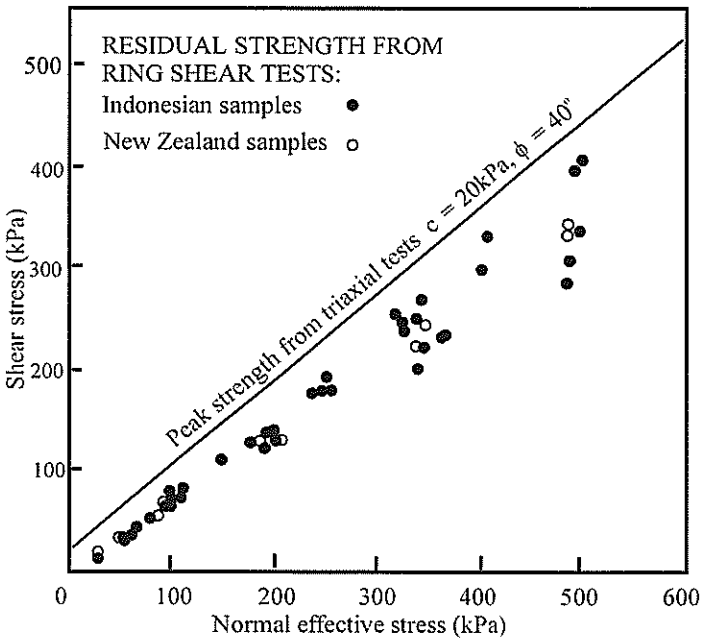

Figure 9. Effective Strength Parameters.

Figure 9 summarises results from laboratory tests on samples from Indonesia and New Zealand. Triaxial tests were carried out to obtain the peak values, and ring shear tests to obtain the residual values. Both values are remarkably high and there is surprisingly little difference between them. Rouse et al (1986) have obtained similar high values from allophane soils in Dominica.

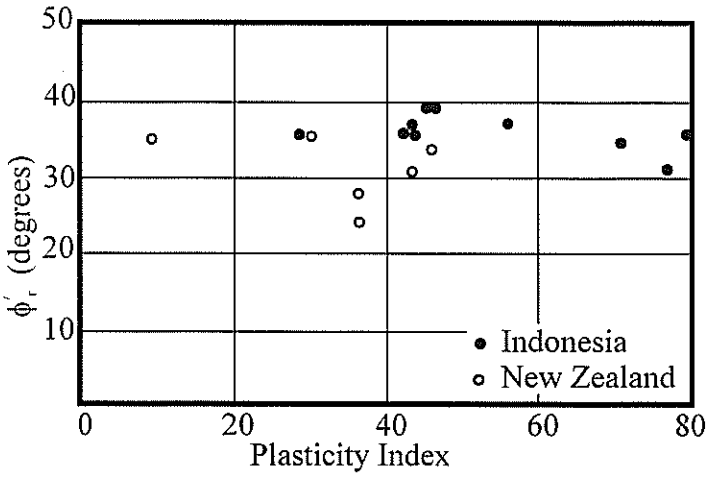

Figure 10. Residual Strength Friction Angle Versus Plasticity Index.

Fig. 10 shows values of the residual angle ϕ'_r plotted against Plasticity Index. It is seen that there is no relationship between the two; ϕ'_r does not steadily decrease with Plasticity Index as is the case with sedimentary clays. With PI values above about 80, sedimentary soils would be expected to have ϕ'_r values of around 10°, whereas the allophane clay has values between 30° and 40°.

Compaction Characteristics

The compaction behaviour of typical allophane clay is illustrated in Fig. 11. This shows a "natural" compaction curve together with curves obtained after drying to varying degrees. The natural water content was 166%. The natural curve was obtained by drying back the soil in steps from this initial water content. Fresh soil was used for each point. The test was then repeated three times, firstly after oven drying, secondly after air drying, and finally after limited air drying (to w = 65%). This was done with large bulk samples. The material was then wetted up in stages, using fresh soil for each point. The results show the dramatic changes caused by drying. When dried from its natural water content

the compaction curve is almost flat, with only a very poorly defined optimum water content. On re-wetting, the behaviour becomes more conventional, with clearly defined optimum water contents and peak dry densities. It is evident from this that almost any result can be obtained if the test involves drying and re-wetting. This result is from an Indonesian allophane clay. Local (ie New Zealand) allophane clays may not show such a dramatic effect because of their lower allophane content.

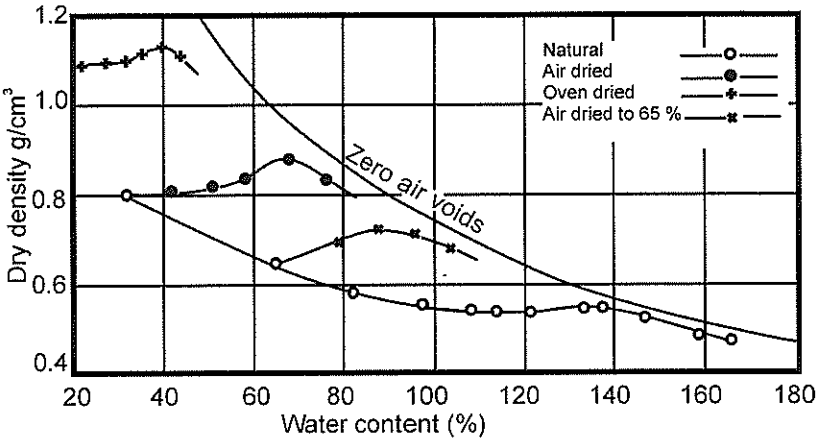

Figure 11. Typical Compaction Behaviour of an Allophane Clay.

Fig. 12 (after Kuno et al 1978) shows the effect of repeated compaction on allophane soils. Some allophane clays are of high sensitivity, and others are not: this is reflected in the curves in Fig. 12. The strength of the soil has been measured after compaction using a series of different (but known) compactive efforts. The compactive effort is indicated by the number of hammer blows. A cone has been pushed into the soil to obtain a measure of strength: this is the "cone index" value shown in the figure. The graphs show that in general there is a marked decrease in strength as the number of blows increases. Presumably the structure of the soil is being progressively destroyed, releasing water and softening the soil, an effect sometimes referred to as "over-compaction".

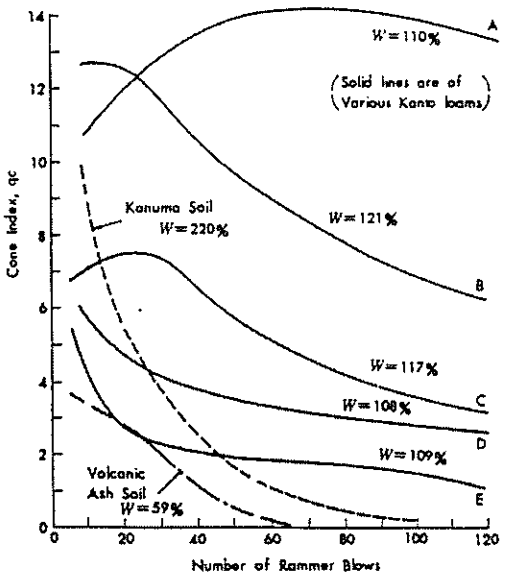

Figure 12. Influence of Compactive Effort on Strength of Compacted Allophane Clays.

The above behaviour illustrates that difficulties can arise in compacting allophane soils if their properties are not understood and taken account of in planning and executing earthworks operations. Specifications can be almost meaningless if excessive drying is allowed before testing is carried out. In countries like Papua-New Guinea and Indonesia the wet climate in which allophane clays occur means that significant drying during excavation and compaction is not very practical. Difficulties

during earthworks operations are described by Parton & Olsen (1980) and Moore & Styles (1988).

These problems can be overcome to some extent in several ways. The first is to recognise that soils can be satisfactorily compacted without recourse to the rigid control methods associated with water content and dry density values. The second is to be clear what objective is aimed for in compacting the soil. For example, the objective with a road embankment is very different from that with a water retaining embankment. With a road embankment it is preferable to keep the compactive effort to a minimum and "press" the soil together with quite light compaction. – enough to get rid of any large voids, but insufficient to destroy the natural "structure" of the soil and cause it to soften. In this way it is possible to retain much of the original strength of the material. With water retaining embankments a rather more rigorous approach is needed, but even for these it is desirable to carefully control the compactive effort. Compaction control, involving control of compactive effort, together with shear strength and air voids testing is generally a better approach than conventional water content and dry density methods.

The Cipanunjang dam in West Java (Wesley, 1974) is an example of successful compaction of allophane clay; compaction here was done using steel rimmed rollers. Some difficulties were encountered due to wet weather and softening of the soil, but the job was completed satisfactorily. The writer has been involved in the compaction of allophane clay at a geothermal site (Kamojang) in West Java, Indonesia. Difficulties were encountered because the very wet climate at the site made it difficult to dry the soil sufficiently to achieve the target undrained shear strength of 150 kPa. The fill was required to form a level platform for a switch yard. The strength requirement was lowered to 90 kPa and the job successfully completed. The fill appeared to "harden" with time, presumably due to the development of negative pore pressure in the soil.

Erosion Resistance.

It is an interesting observation that both in their undisturbed and re-compacted state, allophane clays are remarkably resistant to erosion. It is only when they are cultivated and allowed to partially dry at the surface that they become susceptible to erosion. Observation of road cuttings in Southeast Asia as well as in New Zealand (Taranaki and the central volcanic plateau) shows that negligible erosion occurs from the cut faces. In Indonesia, the drying of the face appears to result in the formation of a hard "crust" which is resistant to erosion. It is also evident in terraced rice-fields that negligible erosion takes place as the irrigation water flows from one terrace to the next terrace.

The report into the Ruahihi canal failure makes some rather sweeping statements about the properties of volcanic soils. Among these are allegations of dispersiveness and erodibility, and susceptibility to "degradation". The statements are very sweeping and no attempt is made to differentiate between different types of volcanic soil. The report prompted the writer to investigate this question of the dispersivity of allophane clays. A final year student, Chan Siew Yan carried out pin-hole dispersion tests on soils from the Ruahihi area, as well as tests on other allophane clays. The results are described by Wesley and Chan (1991). None of these tests showed any evidence of erosion or dispersivity. For a more comprehensive account of allophane clays see Wesley (2002).

Significant Engineering Projects in Allophane Clays.

A number of dams and related water retaining structures have been successfully undertaken making use of allophane clays. An early example is the water supply dam Cipanunjang in West Java, Indonesia, built in 1928 during the Dutch colonial period. This is a homogeneous 30m high embankment with cut-off drains in the downstream slope. It is described in detail elsewhere (Wesley, 1974), and is still a vital part of Bandung's municipal water supply. The Mangamahoe Dam in New Plymouth, and the embankment supporting the supply canal at the Kuratau power scheme (on the western shore of Lake Taupo) are further examples. The Kamojang geothermal power station in West Java, Indonesia, is supported by a raft foundation on about 35m of allophane clay (Figure 9). There have been no problems with its performance. Wesley and Matuschka (1988) describe these examples in greater detail.

PUMICEOUS SANDS

Occurrence and General Description

Pumice sands are found in various parts of the North Island of New Zealand, especially along the lower Waikato River valley and in parts of the Bay of Plenty. Although they do not cover wide areas, their places of concentration in river valleys and flood plains means they tend to coincide with areas of considerable human activity and development. Consequently they are not infrequently encountered in engineering projects and their evaluation is a matter of considerable interest to geotechnical engineers. Not much research has been carried out into the properties of these materials; in recent years the geotechnical group at Auckland University has made some progress towards filling the gap. Some of the results to date have been described by Wesley et al (1999), and Wesley (2000). In this paper the main focus will be on the issue of particle crushing, and the extent to which this influences the behaviour of the sand.

The sand is characterised by the vesicular nature of its particles; each particle contains a dense network of fine holes, some of which are inter-connected and open to the surface, while others appear to be entirely isolated inside the particles. The result is that the particles are light-weight, have very rough surfaces, and are easily crushed, especially when compared to more "normal" hard grained sands such as quartz sand.

One Dimensional Compression and Particle Crushing

To initiate this investigation of particle crushing the results of one dimensional compression (oedometer) tests are illustrated in Figures 13 and 14. Figure 13 shows the particle size curves for the four samples used in these tests. One of the samples is a natural sand obtained from the Waikato River. The other three are artificial sands obtained by crushing coarse pumice particles and then sieving. Figure 14 shows the results of the compression tests, which were carried out to a maximum stress of 8000 kPa. The reason for this high stress level will become apparent shortly – it is of a similar magnitude to the stress level in cone penetrometer tests. A curve from a typical hard grained (predominantly quartz) sand is also shown in this figure. It is immediately apparent that the pumice sands are much more compressible than the hard grained sand. The difference in compressibility is greatest at the lower stress levels, especially between zero and 2000 kPa. In order to investigate the effect of crushing, the tests were actually repeated a number of times to steadily increasing stress levels, and terminated at these levels so that particle size measurements could be made corresponding to each stress level. The stress levels involved were 500, 1500, 3000, 5000, and 8000 kPa.

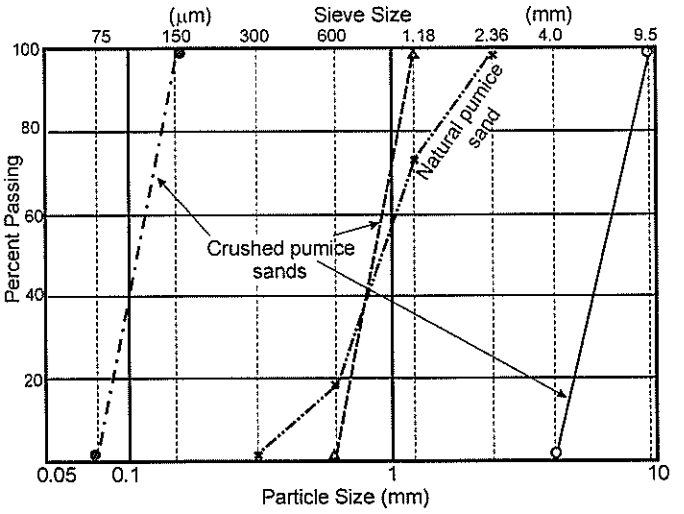

Figure 13. Particle Size Distribution Curves of the Pumice Sands.

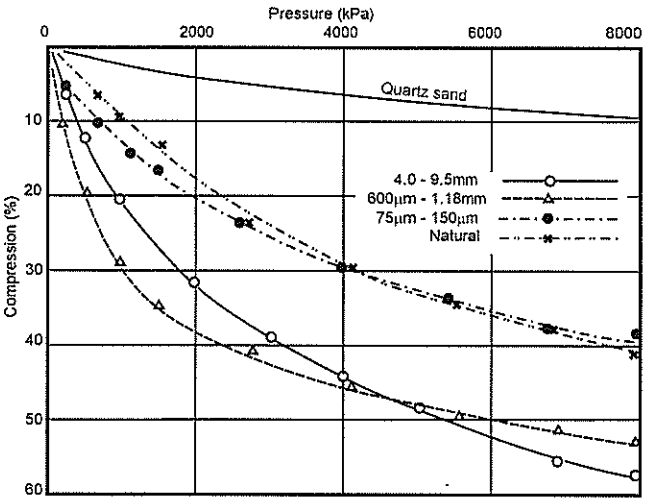

Figure 14. One Dimensional Compression Test Results.

The particle size measurements showing crushing are presented in Figure 15. It is immediately evident that very substantial particle crushing occurs, especially with the two coarser fractions. Crushing in the natural sand and the very fine fraction is much less than in the other fractions.

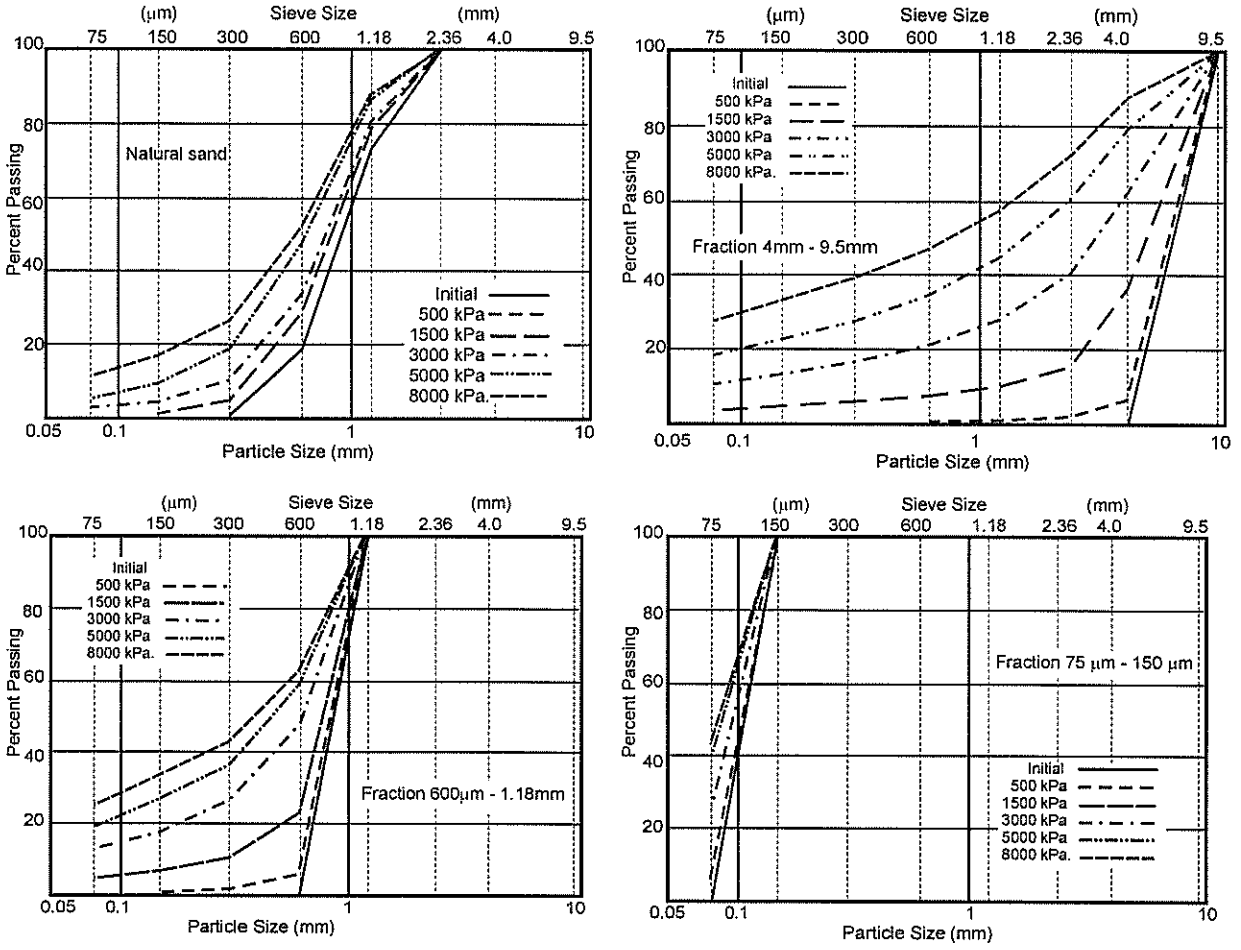

Figure 15. Particle Crushing During One Dimensional Compression.

To further illustrate the crushing effect, Figure 16 has been prepared. This shows a graph of percent crushed against the stress level for each of the four materials. The figure confirms the point mentioned above, namely that crushing is least in the natural sand and the fine fraction, and also suggests that crushing tends to "level off" at higher stress levels. The measure used here to express the degree of crushing (percent crushed) is a fairly elementary one, and more sophisticated measures may show

somewhat different trends. The measure used here has been calculated by simply comparing the amounts retained on each sieve; where reductions have occurred these have been calculated and added up to give the total weight of material crushed. This has then been expressed as a percentage of the total weight.

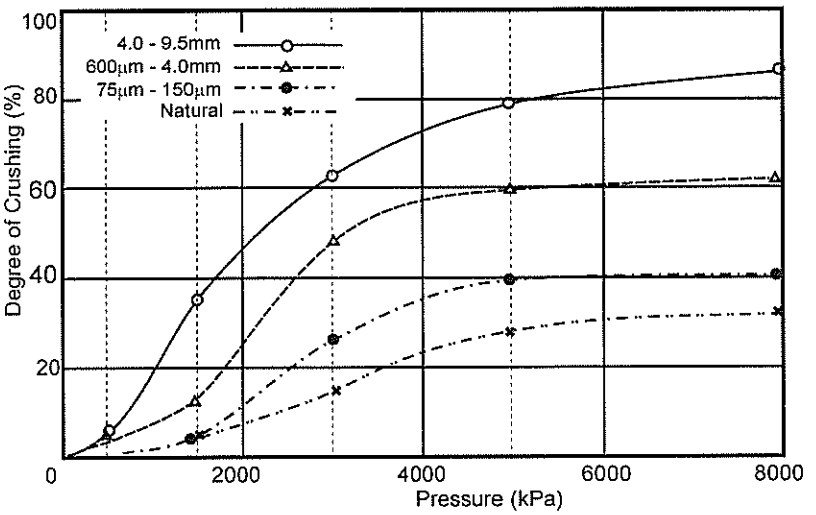

Figure 16. Degree of Crushing in Compression Tests.

Figure 16 suggest that very little crushing occurs at the stress levels involved in most foundation situations. Applied stresses from foundations on sand are unlikely to exceed 1000 kPa. The onset of major crushing appears to be at about 1500 kPa, and then levels off again after about 4000 kPa. At this latter stress level the particle size distribution has changed so much that the materials have become well graded and densely packed, so that contact stresses between particles are greatly reduced (and crushing declines). Despite the impression given by this figure it should not be imagined that no particle breakage occurs at low stress levels. Some crushing probably starts as soon as load is applied: the measured degree of crushing at 500 kPa was between about 2% and 5%. The large difference in compressibility between the pumice sand and conventional hard grained sand can only be attributed to the soft nature of the pumice particles and the consequent crushing, so that even if major breakage does not occur at low stress levels, some minor fracturing is still occurring, probably at the surface of the particles.

The information presented in Figs 15 and 16 is from tests on the sand in its loose state. Tests were also carried out on dense samples; these showed comparable results with somewhat less crushing.

Cone Penetration Tests in a Calibration Chamber

The prime interest in carrying out this research on pumice sands was in the interpretation of conventional cone penetrometer tests (CPTs). For this purpose a large calibration chamber (on loan from Monash University) was used. A diagrammatic view of the chamber is shown in Figure 17. Tests were carried out on the natural pumice sand, and also on a hard grained predominantly quartz sand. The tests were on the sands in both their dense and loose states, using applied vertical stresses of 50, 100, and 200 kPa. The results of these tests are summarised in Figures 18 to 21

Figs. 18 and 19 show typical results for the pumice and quartz sand respectively; these are for the loose and dense states at a vertical confining stress of 200 kPa. In Fig. 20, the cone resistance curves from Figs. 18 and 19 are shown on the same graph so that a direct comparison can be made between the behaviour of the two sands. Fig. 21 summarises all the test results in the form of the familiar graph of q_c versus vertical stress.

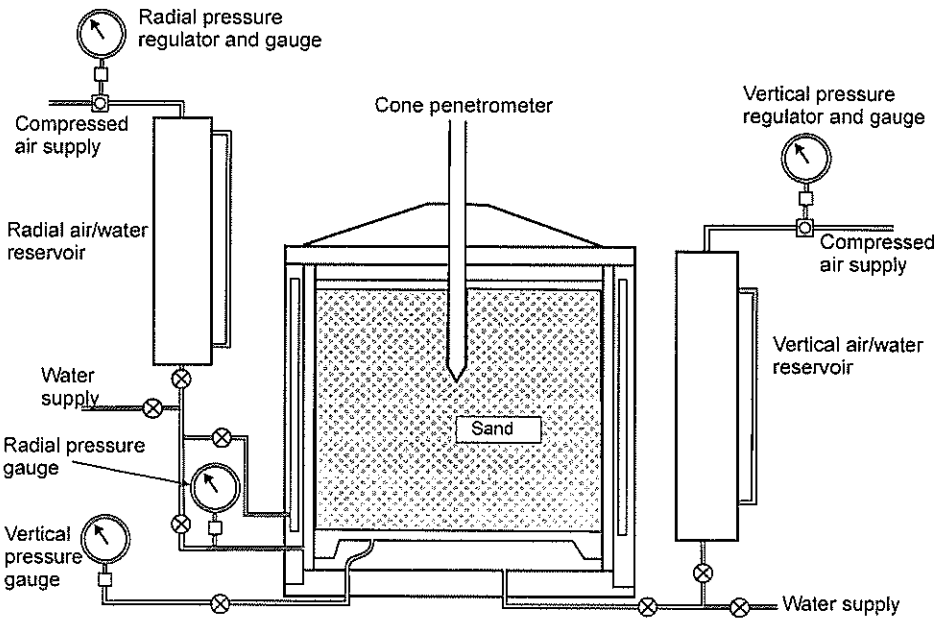

Figure 17. The Calibration Chamber Used for Cone Penetrometer Tests.

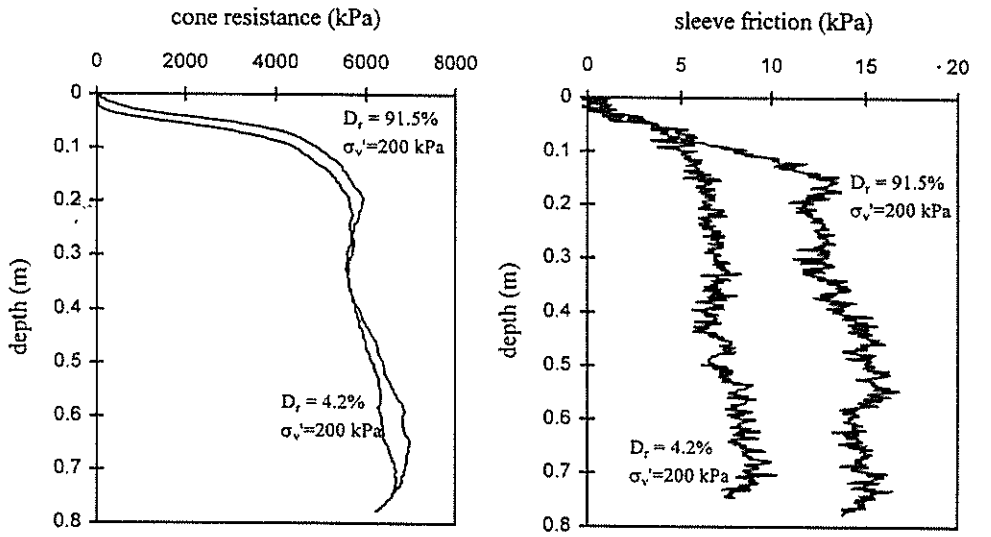

Figure 18. Typical Results from the Pumice Sand.

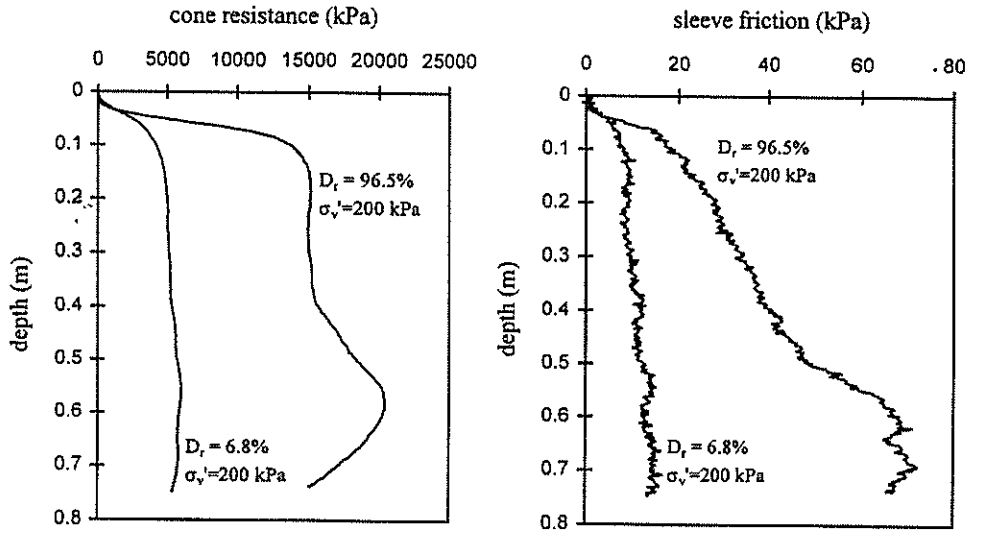

Figure 19. Typical Results from the Quartz Sand.

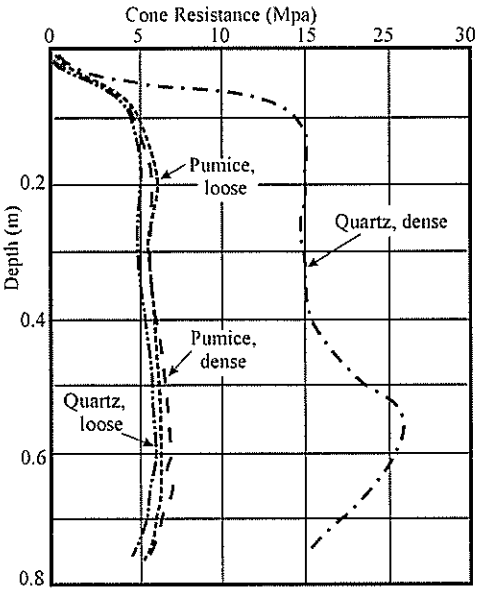

Figure 20. Comparison of Typical Results.

There is a surprising and dramatic difference in behaviour between the two sands as is readily apparent in these figures. The quartz sand behaves as expected, showing large differences in cone resistance between the loose and dense states, and steadily increasing values with confining stress. The pumice sand, on the other hand, shows quite startling behaviour, with the following rather extraordinary characteristics:

1. There is very little change in cone resistance between its loose and dense states, and the increase in resistance with confining stress is less pronounced than with the quartz sand.
2. The penetration resistance of the pumice sand is a little higher than that of the quartz sand in the loose state.
3. Despite showing very little difference in cone resistance, the pumice sand still shows a large difference in sleeve friction, comparable to that of the quartz sand.

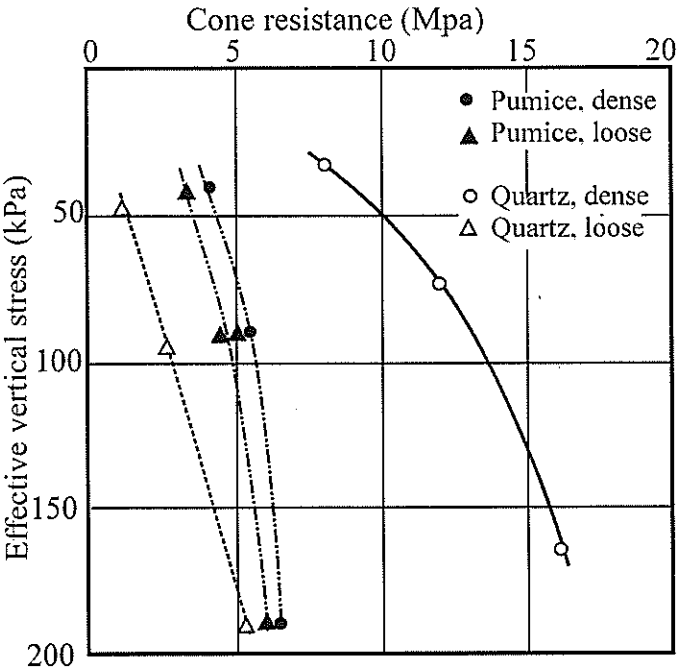

Figure 21. Chart Summarising All the CPT Results.

This dramatic difference in behaviour can only be attributed to the different in particle strength of the two sands. The initial interpretation put on the results was that with the quartz sand failure occurred by

shear displacement, while with the pumice sand failure occurred predominantly as a result of particle crushing. To investigate the extent of particle crushing, samples were taken from the immediate vicinity of the cone when emptying the chamber for the purpose of carrying out particle size measurements. "Immediate vicinity" in this context means a zone extending not more than 1 to 2 cm from the edge of the cone. These particle size measurements showed a surprising amount of crushing with both sands, especially in the dense states, and the crushing is only marginally higher with the pumice sand than the quartz sand. This comparison is purely qualitative, as it was not possible to be sure that the size and location of the samples was the same in each case. With the pumice sand the crushing was similar to that at a stress of 8000 kPa in the oedometer compression test (Figure 16).

Perhaps the explanation for the insensitivity of cone resistance to density with the pumice sand lies in the shear strength behaviour of the pumice sand revealed by drained triaxial tests. Typical triaxial test results, together with those from the quartz sand, are given in Figure 22. These show that with the pumice sand, in both the dense and loose state, the deviator stress slowly climbs towards a peak value, but there is no post peak decline in strength. The strain to reach the peak value is large, generally between 20% and 30%. This peak value is essentially the same regardless of whether the sand is initially in the dense or loose state. The failure values from triaxial tests on the two sands are illustrated in Figure 23.

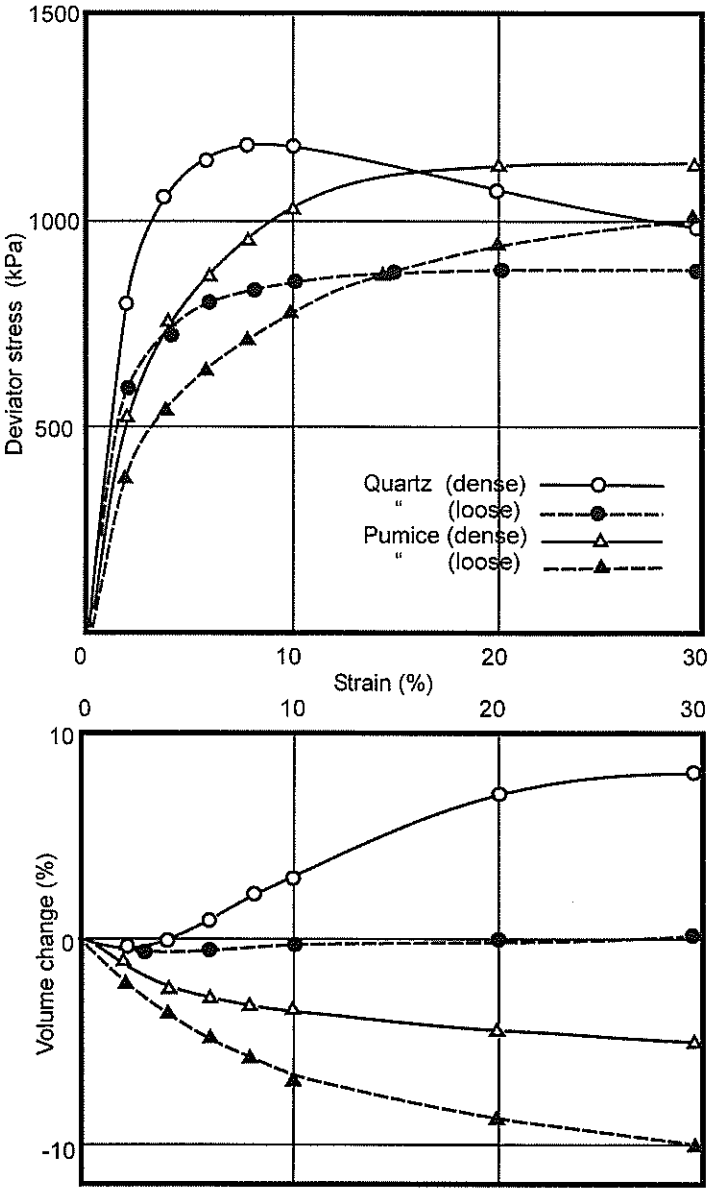

Figure 22. Typical Results of Triaxial Tests on Pumice and Quartz Sand.

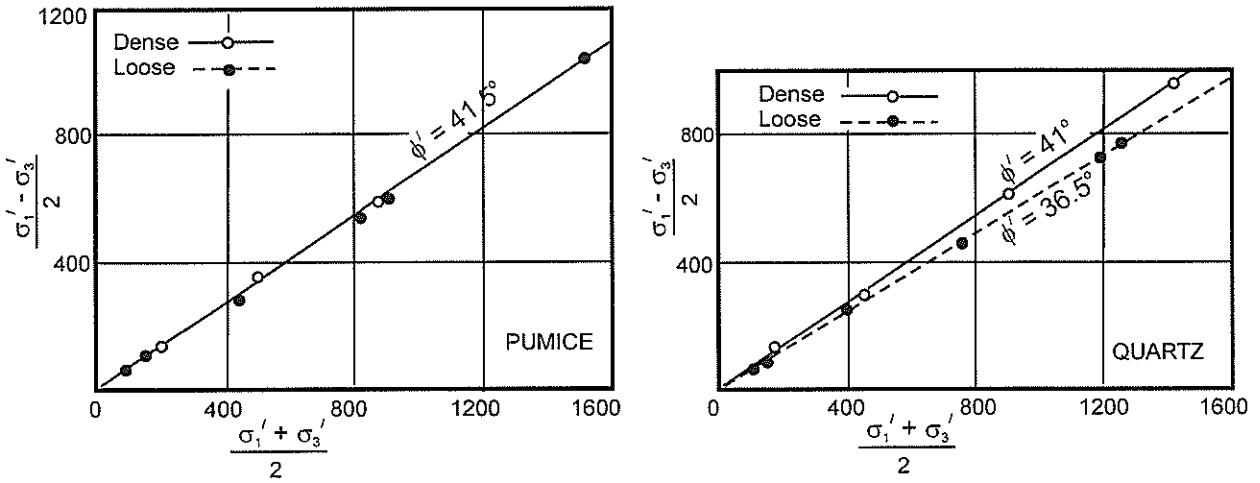

Figure 23. Results of Drained Triaxial Tests on the Two Sands.

The conclusion drawn from these results is that the resistance measured in the cone tests on the pumice sand simply reflects this common "ultimate" state revealed in triaxial testing, and which is little influenced by the initial density state.

HARDENING EFFECT IN COMPACTED PUMICEOUS MATERIALS

To close this paper, the results of another small piece of research are presented. Some materials, especially those of volcanic origin, tend to stiffen up or "harden" quite rapidly after compaction, even though they may be quite soft and displaying substantial "weaving" during compaction. With some of these materials, leaving them undisturbed for only a day or two is sufficient for them to become quite firm or hard. The question investigated here is whether this hardening is the result of some form of chemical reaction creating bonds or cementation between particles, or purely a pore pressure effect. The investigation was carried out by a post-graduate (M.Eng. Studs) student, who has described the work in detail (Kiryakos, 1997). Only the essential details and results are presented here.

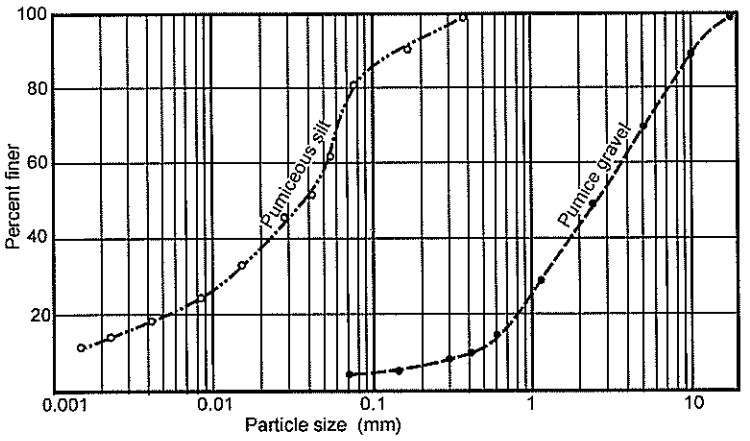

Figure 24. Particle Size Distribution Curves of the Two Materials.

Two pumice material were tested, one a silt and the other a gravel. Particle size and compaction test results are shown in Figure 24 and 25. A number of compacted samples of each material were then prepared by compacting them at identical water contents. The water content was about 2% wet of optimum in each case, this value being chosen so as to produce samples of relatively low strength comparable with those often produced during compaction in the field. The samples were compacted in brass tubes. Strength measurements were made immediately on two samples of each material to determine the initial, or "as-compacted" strength. The strength measurements were made using

unconfined compression tests for the gravel, and undrained triaxial tests (without a confining stress) for the silt.

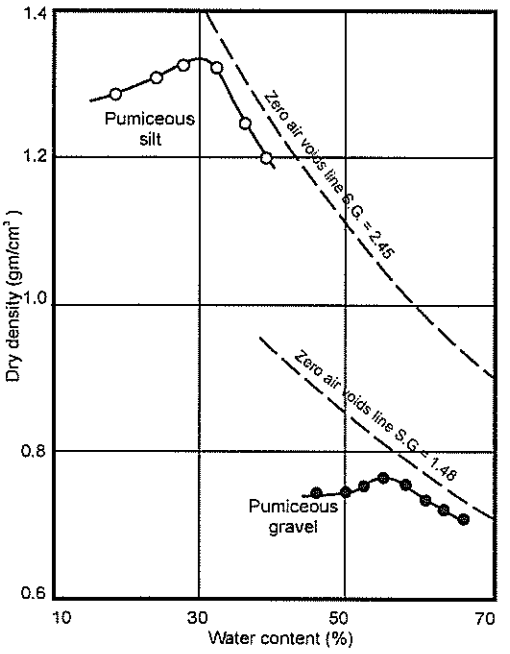

Figure 25. Compaction Test Results for the Two Pumiceous Materials.

One set of samples was then sealed by carefully waxing the tubes, and stored for testing later at specific time intervals. In this way any changes in strength in these samples could only result from chemical effects. The second set of samples was used to investigate changes in pore pressure. With the silt samples this was done by setting up the samples in a triaxial cell and connecting the porous

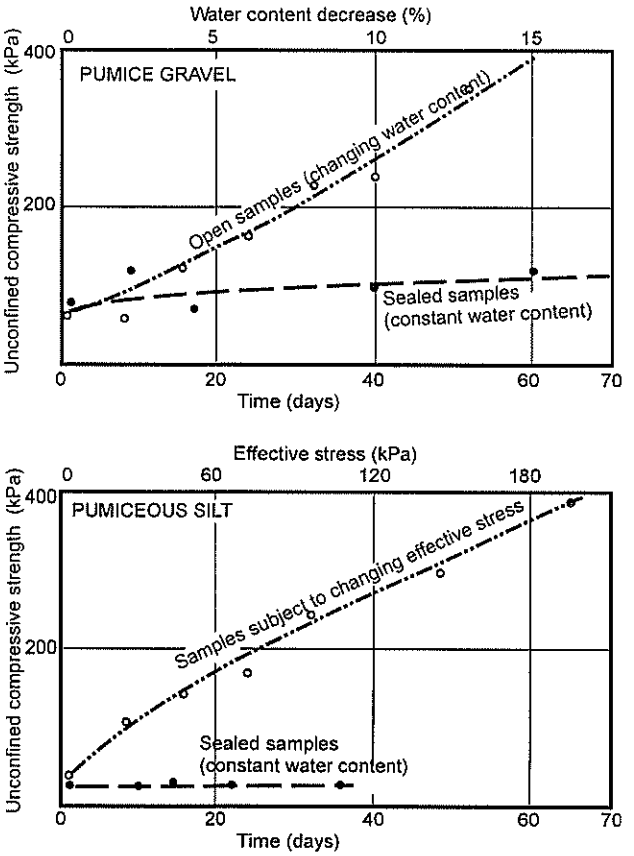

Figure 26. Changes in Strength with Time for the Two Pumiceous Materials.

stone at the base of the sample to a suction pump via a water/air interface. This induced negative pore water pressure (pore water tension) within the samples. Tests were done at pore water tensions from 25 kPa to nearly 100 kPa, this being the maximum value feasible with this technique. Ignoring a small correction because of incomplete saturation, this produced effective stresses in the samples equal to the applied suction. This procedure was used as it was considered to most closely replicate the situation in the field. With a low water table, as is often the case in well drained pumiceous areas, the material compacted at the surface will be subjected to a negative pore water pressure governed by the depth of the water table. To continue the investigation to higher stress levels, several more tests were carried out using cell pressure in the usual way to consolidate the samples.

The compacted gravel samples were very coarse, open materials, containing considerable air, and the technique used with the silt samples was not considered appropriate for the gravel samples. Instead these samples were simply extruded and left open to the air, so that evaporation took place and presumably induced increasing pore water tension within the gravel. Unconfined strength measurements were then made when weight measurements indicated moisture content reductions at 2% intervals. The two sets of sealed samples of both materials were opened at specific time intervals, and tested immediately after opening to ensure no loss of moisture. The results of the tests are shown in Fig 26 in the form of graphs of strength versus time and strength versus either pore water tension (for the silt) or water content reduction (for the gravel).

The results clearly show that strength changes only occur as a result of change in pore water tension or change in water content. The sealed samples tested at time intervals of up to 60 days show no significant or consistent change in strength with time. Hence the hardening characteristic is clearly a purely physical one resulting from changes in effective stress and not from chemical processes. In practice, it is likely that quite high pore water tension develops in both the silt and the gravel when they are left alone after compaction. The silt is frequently a subgrade material lying above a deep water table, so that the pore water tension will be approximately equal to the depth of the water table. The gravel, on the other hand, is often used on forest roads as the main pavement material, and is thus open to the atmosphere. Hence evaporation can occur which would be expected to create high pore water tension within the material.

CONCLUSION

Two particular volcanic soils have been described here, both of which show unusual properties. The clay minerals, allophane and imogolite, impart these distinctive properties to the allophane clay, and the soft grains impart the unusual properties to the pumice sand. The lessons from this study relevant to other volcanic soils are probably the following:

1. Volcanic soils are likely to behave somewhat differently from sedimentary soils. Geotechnical engineers should recognise this and not assume they will conform to preconceived patterns, especially those associated with sedimentary soils.
2. While every effort should be made to develop theoretical or behavioural frameworks to assist us in understanding and interpreting soil behaviour, we ought to recognise the limitations of such frameworks, and not seek to make all soils fit into these frameworks.
3. In evaluating the engineering properties of soils we ought to first observe carefully their behaviour in the field, before looking at their behaviour in laboratory tests
4. Some well established concepts, especially stress history and the use of the e-log p plot for analysing consolidation behaviour, are not necessarily appropriate for all soils, especially volcanic and residual soils.
5. Volcanic soils are so varied that it is unrealistic to expect them to fit into any single behavioural pattern.

REFERENCES

Frost, R.J. (1967). "Importance of correct pre-testing preparation of some tropical soils," *Proc. First Southeast Asian Regional Conf. on Soil Engineering*, Bangkok, pp. 44-53.

Jacquet, D. (1990). "Sensitivity to remoulding of some volcanic ash soils," In: *New Zealand. Engineering Geology* 28(1) pp1-25.

Kiryakos, M.D. (1997). "Investigation of the time hardening effect with two compacted pumiceous materials," *M.E. Project*, University of Auckland.

Kuno, G., Shinoki, R., Kondo, T. & Tsuchiya, C. (1978). "On the construction methods of a motorway embankment by a sensitive volcanic clay," *Proc. Conf. on Clay Fills*, London, pp. 149-156.

Moore, P.J., & Styles, J.R. (1988). "Some characteristics of volcanic ash soil,". *Proc. Second Int. Conf. on Geomechanics in Tropical Soils*. Singapore, pp. 161-166.

Parton, I. M. & Olsen, A.J. (1980). "Properties of Bay of Plenty Volcanic Soils,". *Proc. 3rd Australia New Zealand Conference on Geomechanics,* Wellington. Vol.1, pp, 165-169

Wada, K. (1989). "Allophane and imogolite". Chapter 21 of *Minerals in Soil Environments* (2nd Edition) SSSA Book Series No 1, pp. 1051-1087.

Wesley, L.D. (1973). "Some basic engineering properties of halloysite and allophane clays in Java, Indonesia," *Geotechnique* 23, No 4: 471-494.

Wesley, L.D. (1974). "Tjipanundjang Dam in West Java, Indonesia," *Journal of the Geotechnical Division* ASCE 100/GT5, pp. 503-522.

Wesley, L.D. (1977). "Shear strength properties of halloysite and allophane clays in Java, Indonesia," *Geotechnique* 27, No2, pp. 125-136.

Wesley, L.D. & Matuschka, T. (1988). "Geotechnical engineering in volcanic ash soils," *Proc. Second Int. Conf. on Geomechanics in Tropical Soils*, Singapore Dec. 1988. Vol.1. pp. 333-340.

Wesley, L.D. (1998). "Some lessons from geotechnical engineering in volcanic soils," *Proc. Int. Symposium on Problematic Soils*. Sendai, Japan, Vol.1, pp. 851-863.

Wesley, L.D. and Chan S.Y. (1990) "The dispersivity of volcanic ash soils," *Proc. IPENZ Conference* 1991. Vol. 1, pp.67-76.

Wesley, L.D., Meyer,V.D., Satyawan Pranyoto, Pender, M.J., Larkin, T.J., and Duske, G.C. (1999). "Engineering Properties of a Pumice Sand," *Proc. Eighth Australia New Zealand Conference on Geomechanics,* Hobart.

Wesley, L.D. (2002). "Geotechnical characterisation and properties of allophane clays". *Proc. International Workshop on Characterisation and Engineering Properties of Natural Soils*. Singapore, Dec. 2002.

Trial Loading – An Effective Method of Predicting Settlement

S J Palmer
BE (Hons)
Geotechnical Principal, Tonkin & Taylor Ltd, Wellington
H W Wick
BE (Hons)
Geotechnical Engineer, Tonkin & Taylor Ltd, Wellington

Abstract: Settlement predictions based on geotechnical investigation data can have a high level of uncertainty. This is particularly the case for volcanic ash. The consolidation properties of volcanic ash do not fit the classical model assumed for alluvial soils. This paper presents a literature review of consolidation properties of New Zealand volcanic ash and promotes the use of site-specific monitored trial loading as a means of obtaining information for reliable settlement predictions for volcanic ash and other soils. Three case studies of trial loads are presented; one on volcanic ash and two on reclamation fill.

INTRODUCTION

The methods routinely used by geotechnical engineers to predict settlement of soils include:

(a) Calculations based on parameters derived from oedometer consolidation tests.
(b) Calculations based on estimation of consolidation parameters by correlation with Cone Penetrometer Tests (CPT) cone resistance (qc)
(c) Calculations based on empirical relationships between settlement of granular soils and Standard Penetration Test (SPT) N values (Burland and Burbridge, 1985).

This paper promotes the use of a further method; site specific monitored trial loads. There are instances where the cost and duration of trial loads are not large and the information provided can lead to reliable settlement predictions. Three case studies are presented where trial loads have been used to estimate settlements; one on volcanic ash and two on reclamation fill.

In the case of volcanic soils, information is presented which indicates that the routinely used methods of predicting settlement can provide erroneous information.

The use of trial loads on volcanic soils is promoted. It is often practical to include a trial load in an investigation programme if settlement is critical to design as consolidation of volcanic ash occurs quickly.

VOLCANIC ASH, TARANAKI

Background

In early 2000 Yarrows (The Bakers) Ltd of Manaia, Taranaki proposed to build a coldstore to store dough. Tonkin & Taylor Ltd were engaged to undertake the geotechnical investigation and design.

The proposed coldstore covered an area of 40m x 18m, including four areas of racks for dough storage, which impose an average floor load of 50kPa over an area of 17m x 9m.

The investigations comprised two boreholes, six cone penetrometer tests, hand-augers and Scala penetrometer tests. These investigations indicated the following typical soil profile.

Depth (m)	Description	SPT N (blows/300^{m})	CPT qc (MPa)	Shear Vane Peak/Residual (kPa)
0-0.4	PAVEMENT			
0.4-2.4	ASH Clayey silt with some fine sand, orangish brown	4	0.5 – 1	48/20 98/18 95/33 181/28
	PUMICEOUS SAND			
2.4-6.5	a) Fine to course sand with silt varying from a trace to some, medium dense	11 – 21	2 – 25	
6.5-10	b) Fine to coarse sand with some silt, loose	2 – 9	0.5 – 5	
10+	c) Fine to coarse sand, dense	50 +	10 - 25	

Table 1. Manaia Site Soil Profile

Groundwater was encountered at 2.2 – 2.5m depth. Figure 1 shows a typical CPT record.

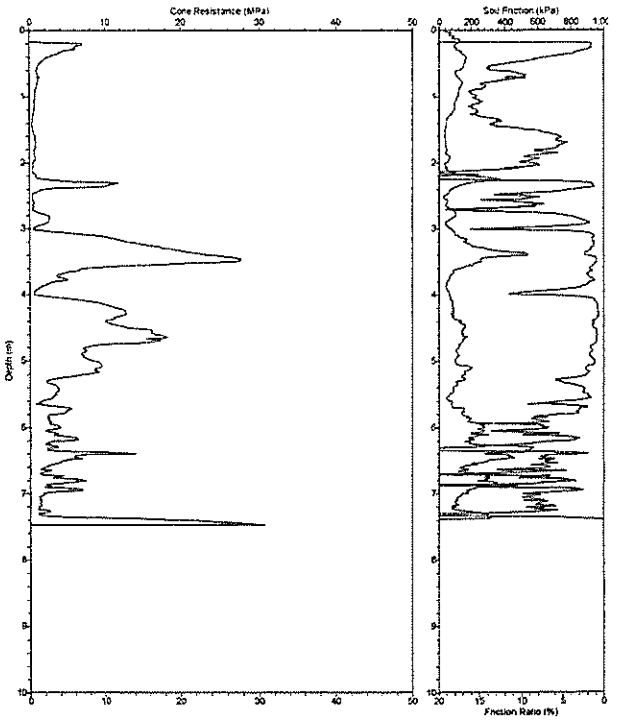

Figure 1. Typical CPT Plot at the Manaia Site.

A piled suspended floor solution offered security against static and possible earthquake induced settlements, but with a cost penalty relative to a floor slab on grade of more than $200,000. Therefore to be able to provide a cost-effective foundation solution it was necessary to predict the settlement potential of a floor slab bearing on the volcanic ash with confidence.

As a first stage of this settlement assessment a literature review on the compressibility of volcanic ash was undertaken.

Literature Review

In 1998 and 1999 M Pender and L Wesley published three useful papers in the NZGS Geomechanics News discussing consolidation parameters of volcanic soils.

Wesley (1999) reports that oedometer tests on volcanic ash have indicated:

a) Coefficient of compressibility m_v = 0.1 to 0.3 MPa $^{-1}$ with no correlation evident with void ratio or water content. (This compares to a typical value of 0.25 MPa $^{-1}$ for a very stiff alluvial silt). i.e. Volcanic ash has relatively low compressibility
b) Coefficient of consolidation (Cv) of the order of 3000 m^2/year or more at the stress level of interest. This compares to a typical value of 10m^2/year for alluvial silt i.e. Volcanic ash consolidates very quickly. Cv reduces with stress.

Pender et al (1998) compared oedometer consolidation tests against CPT cone resistances to test the relationship:

$1/m_v$	=	α_m qc
m_v	=	coefficient of compressibility (MPa^{-1})
qc	=	CPT cone resistance (MPa)
α_m	=	coefficient depending on soil type

This comparison revealed a wide range of α_m values (1.7 to 28.5) for volcanic soils.

In the qc range of 0.5MPa to 1.0 MPa of interest for our coldstore project, volcanic ash m_v values of 0.2 to 0.3 and α_m values of 3.5 to 11 were indicated (α_m coefficient values for alluvial soils are typically in the range of 3 to 5. although not all alluvial soils fit in this range). The range of coefficients indicates that compressibility of volcanic ash is not reliably predicated from cone resistance.

Pender (1999) compares monitored settlements against CPT cone resistance for an alluvial soil site and a volcanic soil site. An α_m value of 3 was concluded for the alluvial soil site and 12.5 to 25 for the volcanic soil site. Again indicating that compressibility of volcanic soils cannot be reliably predicted from cone resistance. The volcanic soil site had cone resistances of typically 0.5 MPa to 1.0 MPa and typically 40 kPa of loading was applied. These values of cone resistance and loading intensity are similar to our coldstore project. m_v values for the volcanic soil calculated back from the settlement records presented by M Pender were 0.1 to 0.2 MPa $^{-1}$ i.e. half of the values reported by M Pender in his earlier paper (Ref 2) on the basis of oedometer tests. The oedometer test results reported by M Pender in Ref 2 were from the same site as the monitored settlement reported in Ref 3. We therefore conclude that oedometer tests can indicate the compressibility of volcanic soil to be higher than the actual insitu condition. This may be due to sample disturbance.

We concluded from this literature review that:

- m_v values predicted on the basis of CPTs for the volcanic ash (qc = 0.5 to 1.0 MPa) at our coldstore site could be 0.1 to 0.2 Mpa^{-1} , although we had no site specific data to confirm this. These values (m_v = 0.1 to 0.2 MPa^{-1}) give predicted settlements for the 50 kPa loaded floor of less than 25mm and within the structures tolerable range.
- Settlement predicted on the basis of oedometer tests could be conservative by a factor of 2 and beyond the acceptable limits for the structure.
- Settlement could not be reliably predicted from CPT cone resistance.
- The settlement could be expected to occur very quickly (within minutes).

Noting the above conclusions it was decided to undertake a trial loading on the site.

Trial Loading

The trial loading was preferred because:

- The trial load was considered to be the only reliable way to predict settlements and confirm the acceptability of the slab on grade solution, saving $200,000 over the piled alternative.
- The trial load could be undertaken relatively cheaply using a stockpile of hardfill material required for the project. A long duration of monitoring was not required because of the high co-efficient of consolidation (Cv) value of volcanic ash.

A 12m diameter 3.5m high truncated cone of hardfill trial load was placed and settlements were monitored before and after the load placement. The location of the weakest CPT record was selected for the trial load site. Up to 15mm of settlement occurred virtually instantly and no further settlement was monitored during the subsequent 2 weeks of monitoring. These results related to an α_m of 10 and an m_v of $0.1MPa^{-1}$ to $0.2MPa^{-1}$. Less than 25mm of settlement was predicted for the proposed loaded floor. The floor was constructed as a slab on grade and has performed well under the load of dough.

RECLAMATION FILL, WELLINGTON WATERFRONT

Background

The Museum Hotel is a 5 storey, reinforced concrete building located on Wellington's reclaimed waterfront. In 1993 the Hotel was pushed a distance of 130m using hydraulic rams on a railway track and boggie system. Ground conditions along the move route comprised up to 7m of reclamation fill overlying 2m to 4m of compact beach sand, which in turn overlies dense alluvium. There were two distinct areas of reclamation fill; an area of end tipped loose granular fill and an area of soft silt hydraulic fill. The move was undertaken in two stages with a 90-degree bend between. At the intermediate point the ninety-one railway boggies and track had to be turned 90 degrees. A process which took one week. The turn site was located on the compressible hydraulic fill.

Settlement calculations

Investigations including boreholes, tests pits and consolidation tests were undertaken along the move route. On the basis of this data settlements were calculated. The settlement calculations not only had to consider the total magnitude of settlement but also the rate of settlement because of the limited duration of loading. Calculated settlements fell into a wide range. At the turn site the top end of the predicted settlement range (more than 150mm) would have left the Hotel in a depression, which it would be difficult to push out of. The predicted settlement at the bottom end of the range (50mm) would be manageable. Trial loads were undertaken to refine the settlement predictions.

Trial Loading

Two monitored trial loads were undertaken. One comprised a railway system located over granular fills and loaded with railway irons. The other comprised 40 tonne of concrete blocks stacked on an area of 2m x 2m located over silt fill. Settlements calculated on the basis of the trial loads were at the lower end of those calculated on the basis of the geotechnical data.

Real Loading

Settlement of the rail boggie system was monitored throughout the move stages and intermediate turning stage. Up to 50mm of settlement occurred at the turn site which was consistent with the calculations based on the trial load.

RECLAMATION FILL, HAVELOCK

Background

Tonkin & Taylor have undertaken two projects in recent years at the Port of Havelock; an extension to the Sanfords mussel-processing factory in 1999-2000 and a current development of approximately 9 hectares of reclaimed land for industrial lots. These two sites are less than 1km apart.

The extension to the Sanfords building, undertaken in 1999-2000, was approximately 30m x 30m with expected dead plus live floor loads of up to 20kPa. The site is located on land reclaimed during the 1950's. Investigations comprised boreholes and CPT's. Predicted settlements calculated on the basis of the CPTs, were greater than tolerable limits under the proposed loading. However, adjacent buildings with shallow foundations showed little or no signs of settlement. It was therefore agreed that trial loading of the site would be undertaken, which would double as pre-loading if the settlements were found to be excessive.

The current reclamation development consists of silt dredgings from the Havelock Marina. During 2001 and 2002 the dredgings were placed over an area of the existing estuary to the south of the Havelock Marina. The soft reclamation silts are highly compressible; therefore pre-loading of the fill was required to reduce the settlement potential.

The soil profile at both the Sanfords and the current reclamation site typically comprise 1 to 3m of soft reclamation silts (qc = 0.25 to 0.5 MPa) overlying estuarine silts interbedded with sandy layers to a typical depth of 8m. Dense alluvial gravels then underlie the reclamation fill. The main difference between the two sites is that the reclamation fill at the Sanfords site has been in place for 50 years compared to typically 1 year at the current reclamation site.

Trial-loading / Pre-loading

Concrete blocks, which were easily accessible at the site, where used as a trial-load at the Sanfords site. The trial loading covered an area of approximately 8m x 8m and imposed a surcharge load of 27kPa. The trial load was moved around the site to pre-load the area of the building extension. Settlement at each trial load area was monitored for approximately 1 to 2 months.

Dredings and gravel stockpiles are being used for pre-loading the current Havelock reclamation development. The pre-load applies a typical surcharge of 30kPa and settlements are being monitored using settlement plates. The pre-load is being used to achieve a target pre-consolidation pressure of 15kPa at the proposed foundation level. It is expected a pre-load surcharge of 30kPa will need to be in place for 3 to 4 months to reach the target pre-consolidation pressure.

Total settlement of 70mm was predicted on the basis of trail loading/pre-loading for the Sanfords site. Settlement of the current Havelock reclamation development is ongoing, however data to date indicates 70mm total settlement under 20kPa of pre-load. These settlement results relate to α_m values of 2.3 to 2.5 for the Sanfords extension and 3.7 to 4.0 for the current reclamation development. These α_m values are within the range of values reported by others for alluvial soils (reference Pender 1999).

CONCLUSIONS AND RECOMMENDATIONS

Undisturbed volcanic ash has a low compressibility and consolidates rapidly, relative to alluvial silt of similar CPT cone resistance or shear vane values.

Settlement of volcanic ash cannot be reliably predicted on the basis of CPT data. Settlement predicted on the basis of oedometer tests may be conservative. Site-specific trial loading can be a practical means of obtaining data for settlement prediction, because settlement of volcanic ash occurs very quickly. It is recommended that site trial loading of volcanic ash be considered as part of an investigation programme if settlement predictions are critical to design.

Similarly on other soil types trial loadings should be considered if settlement is critical to design. The size and weight of the trial load should be selected to provide an increase in stress in the critical soil layer similar to that imposed by the final loading.

REFERENCES

Burland, J.B. and Burbridge, M.C. (1985). "*Settlement of foundations on sand and gravel*", Proceedings of the Institution of Civil Engineers.

Murashev, A. and Palmer, S.J. (1998) "*Geotechnical issues associated with development on Wellington's waterfront*" Proceedings of IPENZ Conference

Pender, M.J., Mayer, V.M., Larkin T.J., Wesley, L.D. and Duske, G.C. (1998) "*Field and laboratory testing of volcanically derived soils*" N.Z. Geomechanics News No. 56.

Pender, M.J. (1999) "*Relationship between settlement & cone resistance at two sites*", N.Z. Geomechanics News No. 57

Wesley, L.D. (1999) "*Some lessons from geotechnical engineering in volcanic soils*", NZ Geomechanics News No. 58.

Laboratory Stiffness and Other Properties of Auckland Residual Soil

M J Pender
BE (Hons), PhD, FIPENZ, Life Member NZGS
Professor of Geotechnical Engineering, Department of Civil & Environmental Engineering, University of Auckland
L D Wesley
BE (Hons), ME, PhD
Senior Lecturer, Department of Civil & Environmental Engineering University of Auckland
B Ni
ME (Fuzhou), ME (Hons) (Auckland)
Research Fellow, Department of Civil & Environmental Engineering, University of Auckland

Abstract: Data on the geotechnical properties of Auckland residual clays are presented in this paper. Information about Atterberg limits and shear strength is included, but the main thrust of the paper is to consider the estimation of Young's modulus in the laboratory using triaxial and oedometer testing. In addition, the estimation of the coefficient of consolidation is considered in the conventional oedometer and in a hydraulic oedometer. The main conclusion from the paper is that the conventional oedometer is not the most suitable device for determining the properties of Auckland residual soils. Another factor that complicates the determination of geotechnical properties is the inherent variability of the soil. Even though the specimens tested were cut from block samples taken from one location, there are substantial variations in the shear strength and stiffness properties from specimen to specimen. A possible explanation for the higher Young's modulus values obtained from triaxial testing is the multiple data points that can be obtained with suitable recording equipment, which means that it is possible to eliminate any bedding effects on the initial parts of the stress-strain curves.

INTRODUCTION

In this paper information about the geotechnical properties of Auckland residual clays is presented. The majority of the test data was obtained from samples taken from the site of the University of Auckland Student Amenities Centre at the corner of Symonds St and Alfred St in Central Auckland. Block samples were recovered from a depth of about 5 m at the base of a digger pit. The blocks were taken from a thick layer of visually uniform residual cohesive soil.

Residual soils derived from in situ weathering of Waitemata group soft rocks are common over much of the Auckland region. They range from highly plastic cohesive soils to low plasticity silty soils, reflecting the composition of the Waitemata group soft rocks which range from sandstone to mudstone. In some cases the residual soils are difficult to distinguish from Pleistocene deposits. In both cases the cohesive soils encountered are categorised as stiff to very stiff.

Particular emphasis is placed on the estimation of stiffness but in addition there is information on Atterberg limits, variability, shear strength properties, and consolidation behaviour. The data for the Student Amenities site is supplemented by data obtained over a number of years on samples from various sites around the city. Properties were determined in triaxial testing (both 38 and 76 mm diameter specimens), the conventional oedometer (specimen 76 mm in diameter and 19 mm thick), a hydraulic oedometer (specimen 76 mm in diameter and 19 mm thick) in which the specimen can be back pressure saturated and the pore pressure dissipation monitored, and a K_o triaxial cell (in effect an oedometer with specimen heights up to 150 mm, which can be back pressure saturated, with drainage from one end and pore pressure monitoring at the other).

The main conclusion from this paper is that the conventional oedometer has limited usefulness for providing parameters for residual soils. Stiffness measurements on triaxial specimens give larger values for Young's modulus than is obtained from the oedometer. The estimation of the coefficient of consolidation requires a specimen thicker than the 19 mm in the conventional oedometer.

SAMPLING AND SAMPLE STORAGE

The samples were recovered from the base of digger pits. Two methods of recovery were used: either cutting blocks by hand or by jacking steel sampling tubes into the ground. The block samples were approximately cubical in shape, typically 300 to 400 mm in size. They were placed temporarily in plastic bags for transport back to the laboratory where they were trimmed, the upper surface marked, wrapped with several layers of cling film, and then placed in double sealed plastic bags. The steel sampling tubes are 220 mm diameter by 220 mm tall and, for pushing into the soil, fitted with a removable cutting shoe having a 10 degree angle. The push is provided by a hydraulic jack reacting against the digger bucket or by thrust from the digger bucket. The tubes are then recovered by hand digging. On recovery the ends of the tube samples are trimmed flush, covered with a layer of cling film and then a piece of rubber sheet 3mm thick, followed by 20 mm plywood end plates which are held in place by four tie bolts. The steel tubes are used for long term storage and the blocks for short term. Soil from the blocks has been tested up to a year and more after sampling, in which time no deterioration is evident. The steel tube samples have been tested up to three years after sampling; even after this length of storage they appear to be in good condition.

ATTERBERG LIMITS AND LIQUIDITY INDEX

In Figure 1 Atterberg limit data is presented for various samples from around Auckland. It is clear that the Atterberg limit values are quite variable with results scattered along the A-line up to liquid limit values in excess of 100%. Consistent with the visual description of these soils as stiff to very stiff, the liquidity index values are less than 0.5, sometimes as low as 0.1.

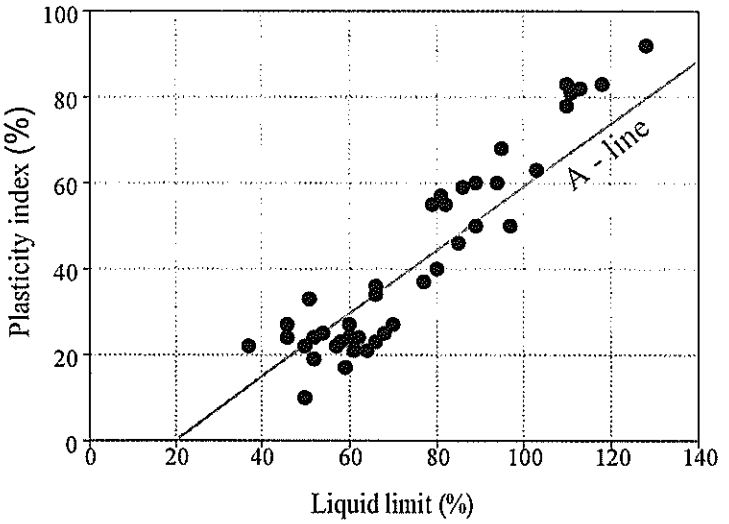

Figure 1. Atterberg Limit Data for Samples from Around Auckland

VARIABILITY

Residual soils are formed by weathering from parent rock in situ, the properties of the Auckland residual soils suggest that this is an inherently irregular process. Figure 2 presents a demonstration of this from the work of Indrawan (1986) who tested soil from a South Auckland site. The undrained shear strength of soil in a tube sample was measured using a laboratory vane apparatus. As can be seen from the photograph a number of vane readings were taken at a given level and small pieces of soil excavated from each vane position for water content determination. This process was repeated at a number of levels in the specimen. In Figure 2 the measured undrained shear strengths are plotted against the corresponding water content. The extent of the variability is evident from the wide range of shear strengths and water contents in a single tube sample having a volume of only about 8 litres. It is clear also that there is no correlation between the vane strength and water content. It is probable that variations in water content reflect changes in plasticity as well, and it is this which is the source of the variations in both shear strength and water content.

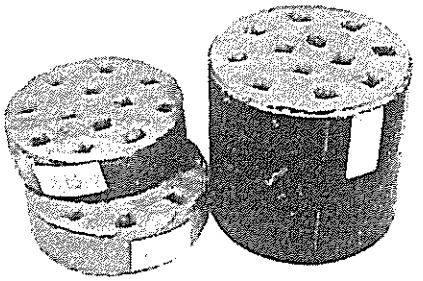

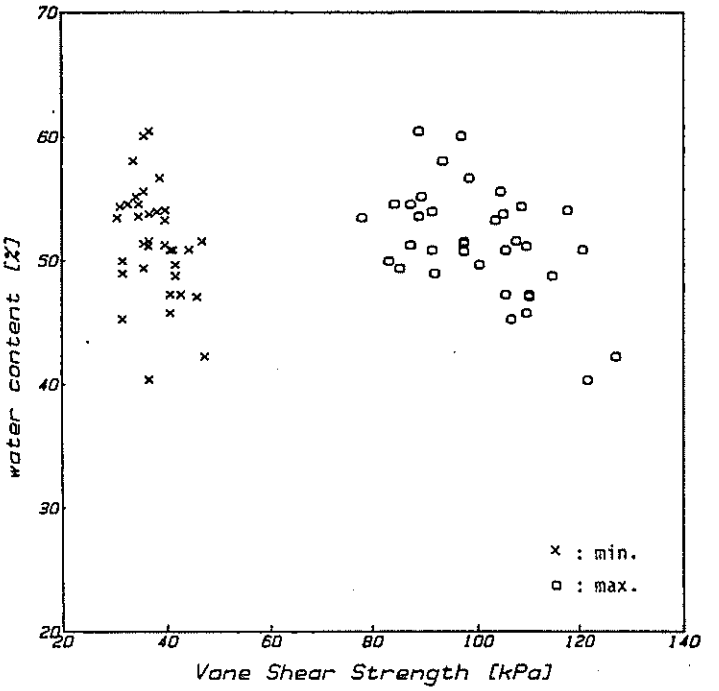

Figure 2. Variability Within a 200mm Tall by 200 mm Diameter Sample. Above: Sample with Vane Water Content Specimens Removed, Right: Vane Shear Strength – Water Content Relation (after Indrawan 1986).

SHEAR STRENGTH PROPERTIES

The soil from the Student Amenities Centre had a Liquid Limit of 110%, a Plastic Limit of 32%, and a liquidity index of about 0.14. Four consolidated drained and fifteen consolidated undrained triaxial tests were done on specimens saturated with back pressure and isotropically consolidated. All the specimens were 38 mm in diameter and 76 mm tall. Figure 3 has the effective stress paths for the consolidated undrained triaxial tests prepared at the lower consolidation pressures and peak stress points for the four drained tests. A failure envelope for $c' = 22$ kPa and $\phi' = 24$ degrees is also shown in the figure. In Figure 4 the stress-strain curves and effective stress paths for all fifteen consolidated undrained tests are plotted. In Figure 5 the sine of the mobilised friction angles at peak shear resistance are plotted against the effective consolidation pressure for each test result. For consolidation pressures in excess of about 500 kPa it appears that the mobilised friction angle settles to a constant value at about 24 degrees.

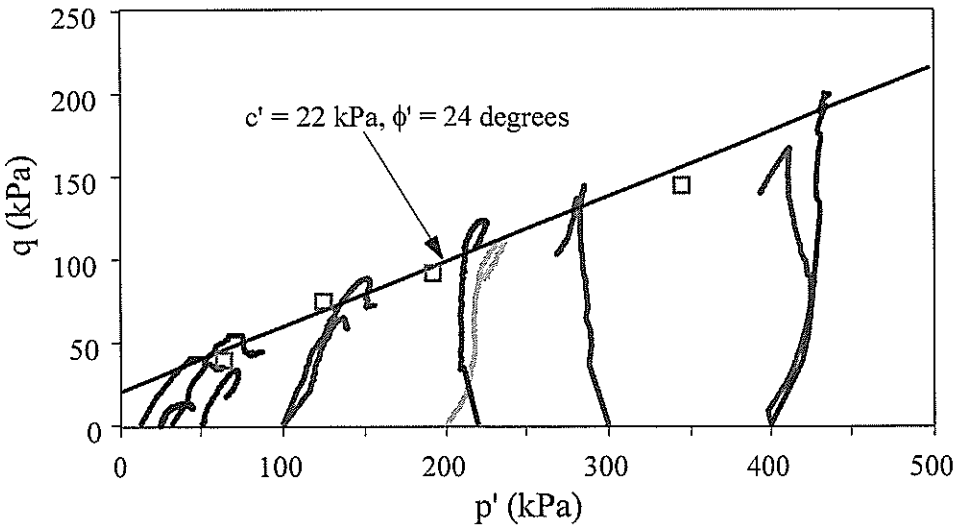

Figure 3. Effective Stress Paths for the Eleven Undrained Triaxial Tests at Lower Consolidation Pressures and the Peaks of the Four Drained Tests (shown with the square box symbol). The Line Defining $c' = 22$ kPa $\phi' = 24$ Degrees is Drawn. ($q = \frac{1}{2}(\sigma'_1 - \sigma'_3)$ and $p' = \frac{1}{2}(\sigma'_1 + \sigma'_3)$)

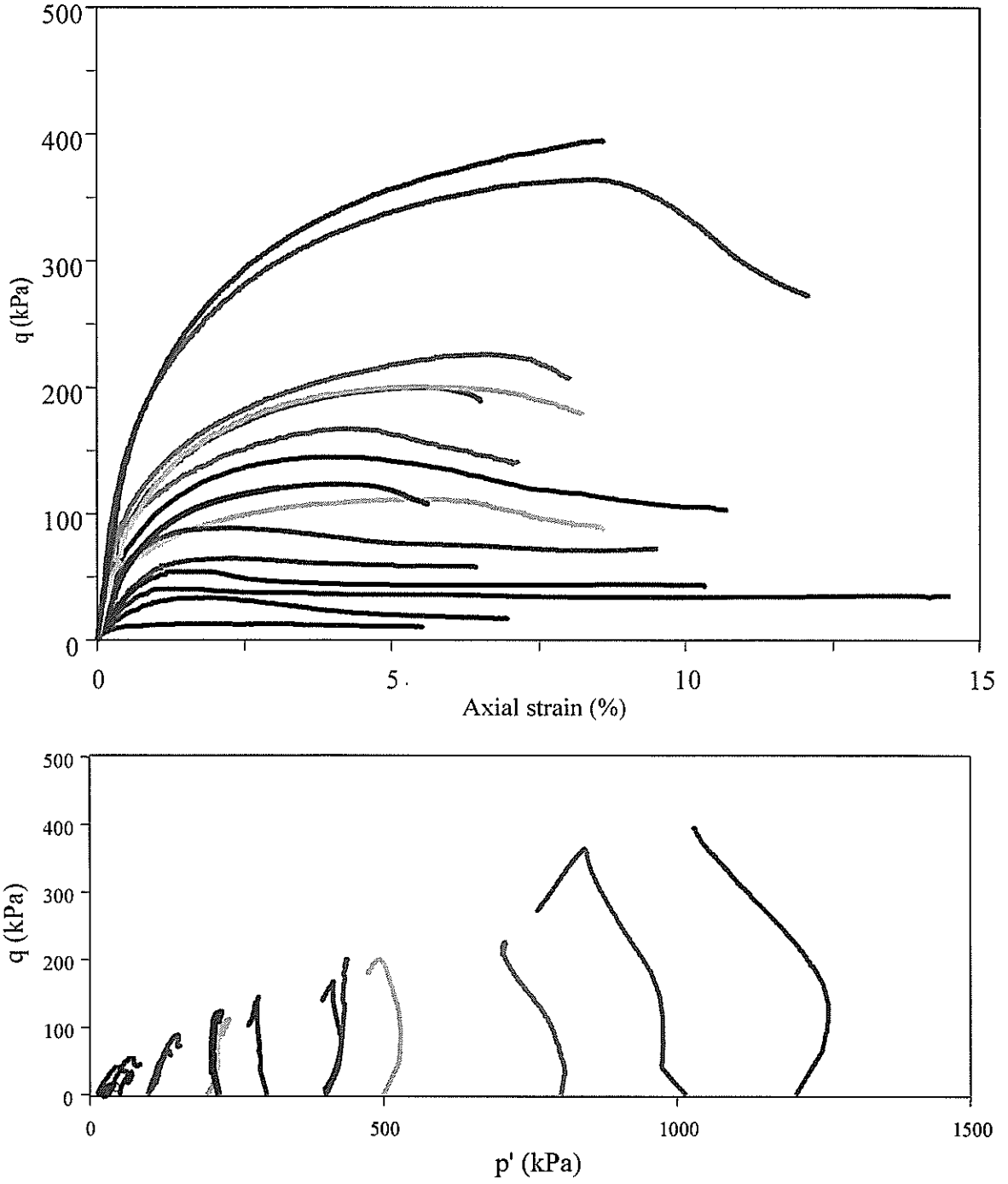

Figure 4. Stress-Strain Curves and Effective Stress Paths for All 15 Undrained Triaxial Tests.

The variability illustrated in Figure 2 is also evident in Figures 3 and 4. All the specimens were cut from block samples taken in close proximity, yet the peak shear strength of specimens with effective consolidation pressures of 25 kPa, 50 kPa and 800 kPa fall well below the general trend of the other results which define a shear strength envelope having $c' = 22$ kPa and $\phi' = 24$ degrees. All the data in Figures 3, 4 and 5 are for triaxial compression curves. In Figure 6 results obtained by Meyer (1997) on soil from a North Shore site are plotted. In this case there are results from drained and undrained triaxial tests, both compression and extension. These results suggest that the strength parameters for compression loading are different from those for extension stress paths. The material tested by Meyer had a Liquid Limit of 60%, a Plastic Limit of 32%, and a liquidity index of about 0.32.

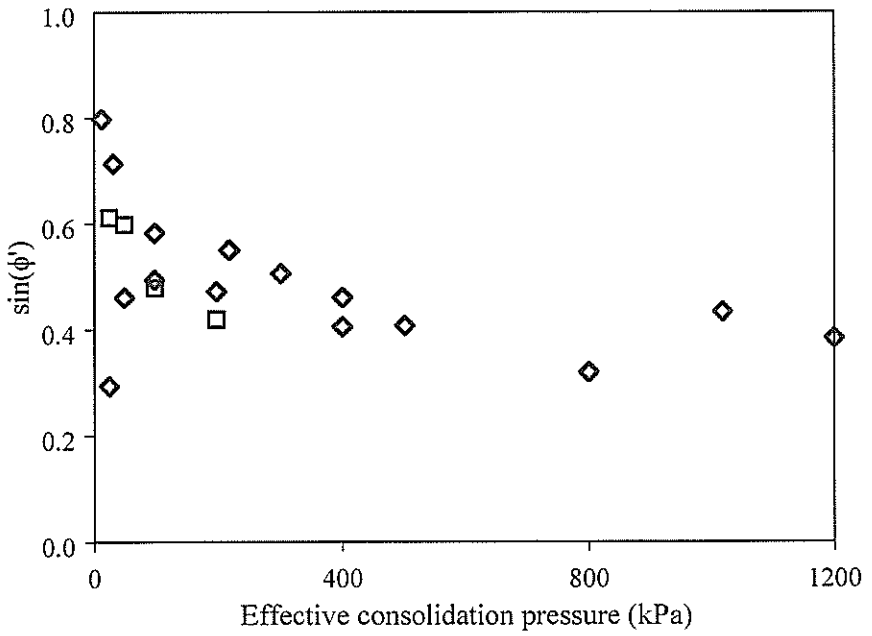

Figure 5. Sine of the Mobilised Friction Angle at the Peak Shear Strength (diamonds – undrained tests. squares – drained tests) (sin(24 degreees) ≈ 0.40)

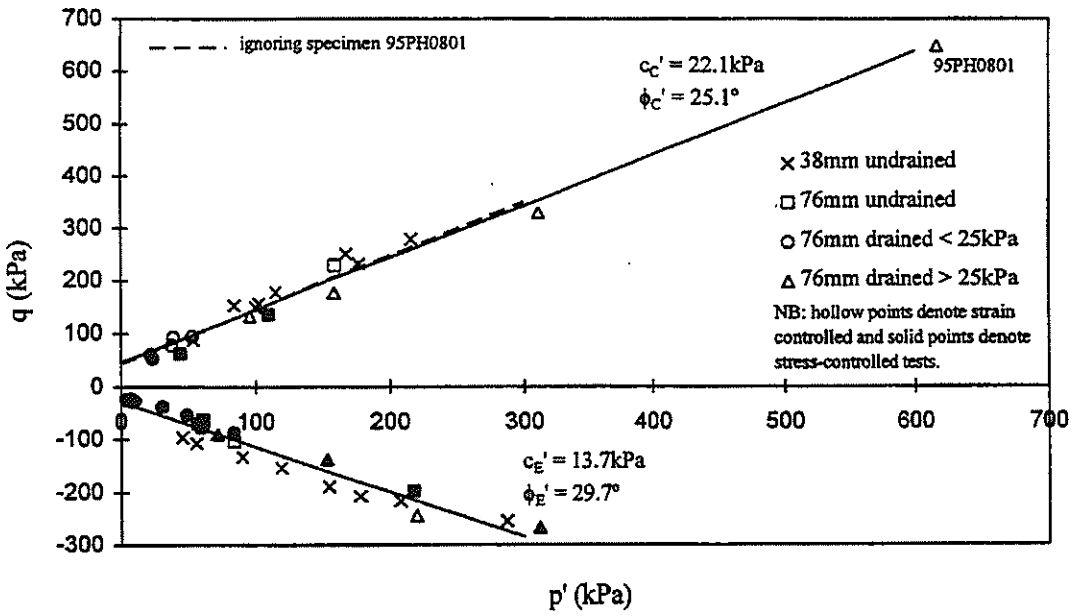

Figure 6. Data from Triaxial Compression and Extension Tests (from Meyer (1997))

STIFFNESS

An appropriate starting point from which to look at the stress-strain behaviour of soil is to consider the small strain range and use the idealisation that the soil behaves elastically. Provided the material can be regarded as isotropic the elastic stress-strain model is useful as values for only two parameters specify the material properties. Oedometer tests with loading in horizontal and vertical directions, Meyer (1997), show that the horizontal and vertical stiffness are very similar in Auckland residual soils, so, at this stage, it is assumed that, at small strains, the soil behaves as an isotropic elastic material.

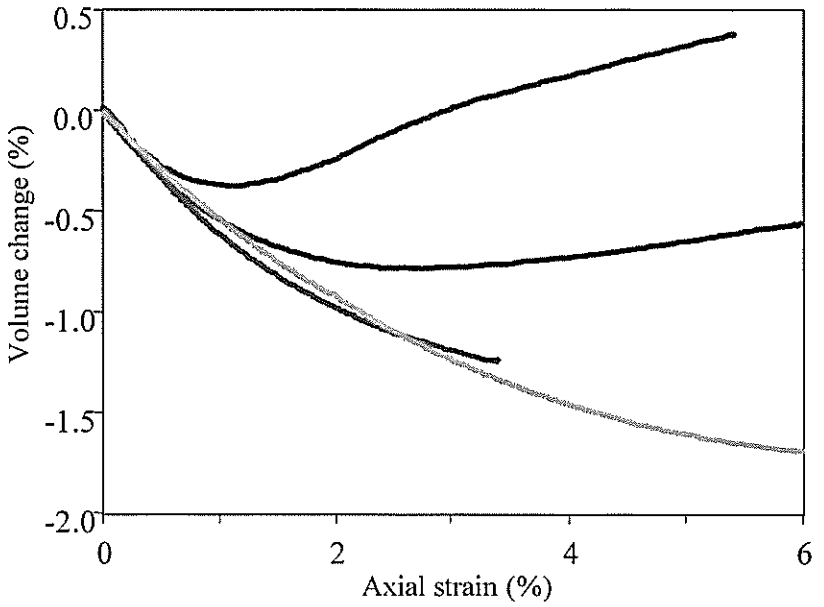

Figure 7. Volume Change Curves for Drained Triaxial Tests (volume decrease is shown as negative). Effective Consolidation Pressures 25, 50, 100 and 200 kPa.

Drained triaxial tests

The slope of the initial part of the volume change data for the drained tests, Figure 7, can be used to estimate Poisson's ratio for the soil. The value obtained is in the 0.20 to 0.30 range.

Undrained triaxial tests

The Young's moduli derived from the initial slopes of the triaxial stress-strain curves are plotted against the effective consolidation pressure in Figure 8 for both drained and undrained tests. The data from the undrained tests are converted to a drained Young's modulus using a Poisson's ratio of 0.25. Despite the scatter a clear trend for an increase in stiffness with increasing consolidation pressure is evident. These stiffness values were obtained from the part of the stress-strain curves up to shear stresses of 10% of the maximum shear stress. To obtain these values the initial part of the stress-strain curve needs to be examined very carefully and any bedding effects removed. This is easily achieved if the tests are done using a data logging system that records many data points in the initial stages of the test. Also one needs a displacement transducer with appropriate sensitivity; the displacement transducers used for these tests had an axial strain sensitivity of 0.02%.

K_o triaxial tests

Three tests were done in a K_o triaxial cell on specimens 76 mm in diameter and 150 mm tall. These were back pressure saturated and consolidated to a small effective consolidation pressure. The apparatus has a loading ram which is the same diameter as the specimen. The K_o condition is imposed by preventing any water flowing in or out of the cell. Measurement of the cell pressure and the pore water pressure enables the effective value of lateral stress, σ'_3, to be obtained. These specimens are loaded at a constant rate of deformation of 0.05 mm/hr. The stiffness obtained from the initial 0.2% axial strain is also plotted in the Figure 8. As these specimens are larger than those for the majority of the tests it was found that only very small amounts of correction were required for the initial part of the stress strain curves.

Oedometer tests

Finally, the stiffness of the initial part of the loading curves obtained from conventional oedometer tests are plotted. From the oedometer the constrained modulus is obtained. Having obtained the constrained modulus, M, Young's modulus, E, is obtained from the following equation:

$$E = \frac{M(1+\nu)(1-2\nu)}{(1-\nu)} \qquad (1)$$

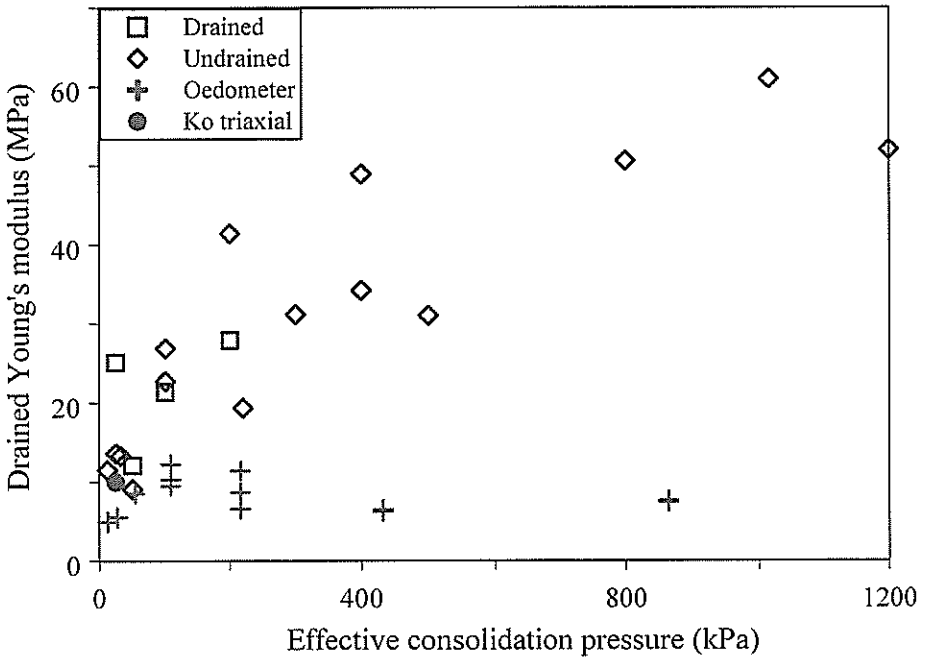

Figure 8. Drained Young's Modulus Values Versus Effective Consolidation Pressure for Undrained, Drained, K_o, and Oedometer Tests. (A Poison's ratio value of 0.25 was used to convert the undrained Young's moduli and oedometer constrained moduli to equivalent drained Young's modulus values.)

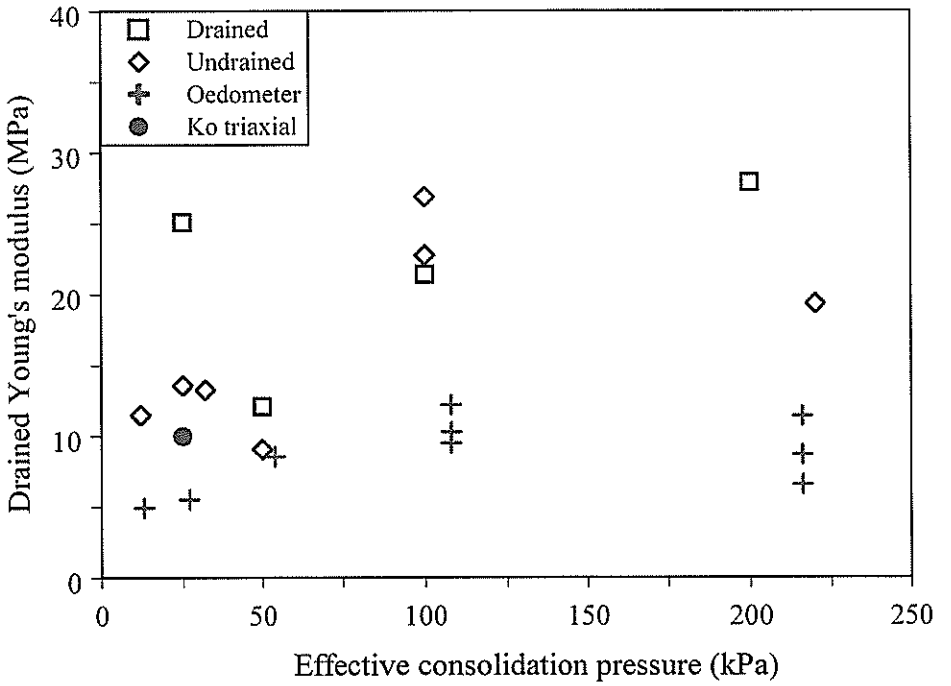

Figure 9. Drained Young's Modulus Values for Tests at Low Effective Consolidation Pressures.

where ν is Poisson's ratio. Using the value of 0.25 for Poisson's ratio obtained from Figure 7 equation (1) gives Young's modulus by dividing the constrained modulus by 1.2. In Figure 9 the Young's modulus values obtained from the various tests are plotted for the lower range of effective consolidation pressures. It is apparent that the modulus values from the conventional oedometer test are less than those from the triaxial testing, this confirms the conclusion reached by Pender at al (2000). There are probably a number of reasons for this. First, as the oedometer specimen height is only 19 mm, any bedding errors will cause errors in the modulus values. Second, as the loading is not

continuous there are no closely spaced data points available for correcting bedding errors as is possible with the triaxial data. Third, the conventional oedometer has no way to ensure saturation of the specimen.

TRANSITION PRESSURE

If oedometer compression – vertical stress data are plotted in a graph with a logarithmic stress scale, a curve is obtained which suggests a preconsolidation pressure. As shown by Pender et al (2000), unless there is a change in stiffness at the same pressure on the plot with a natural stress scale, this preconsolidation pressure is merely an artefact of the scale used on the stress axis. For Auckland residual soils the natural stress scale plot is usually near to linear so there is no preconsolidation pressure. For residual soil one does not expect to find any preconsolidation pressure as the soil formation is not a consequence of stress history; one may however find a "vertical yield stress" or "apparent" preconsolidation pressure arising from other factors. Despite the absence of a preconsolidation pressure in the oedometer results, the Auckland soil still exhibits a change in behaviour as the consolidation pressure in the triaxial tests is increased. Examination of the effective stress paths in Figures 3 and 4 reveals a change in the shape of the undrained effective stress paths. At low effective consolidation pressure the effective stress path moves to the right of the diagram, at high effective consolidation pressures the path moves to the left. Between these two behaviours there is a region in which the effective stress paths rise approximately vertically. From Figure 3 this appears to occur, for the soil from the Student Amenities Centre site, for specimens with an effective consolidation pressure of about 200 kPa.

Another indication of a change in behaviour comes from the constant rate of strain K_o triaxial tests. These were drained from the top of the specimen and the pore water pressure was measured at the base. If the strain rate is sufficiently slow there will be negligible pore pressure increase at the undrained end of the specimen. In fact, the rate of pore pressure increase in relation to the rate of loading and drainage path length can be used to estimate the coefficient of consolidation. Data for three tests are shown in Figure 10. It is apparent that there is a change in the rate of pore pressure rise at axial strains of around 1.5 to 2.5 %. Tracing this behaviour back to the stress path diagram it is seen

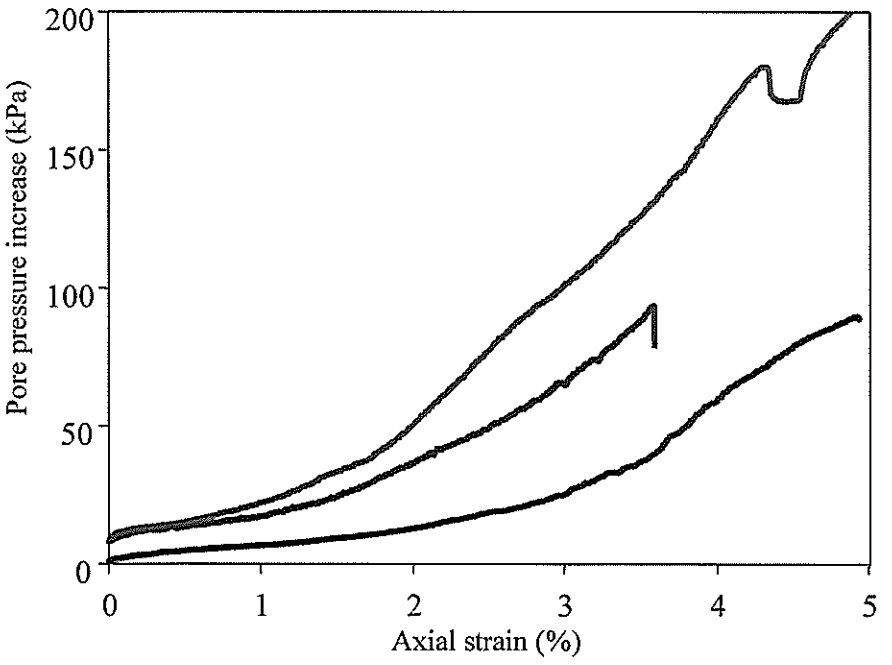

Figure 10. Rate of Pore Pressure Increase at the Undrained End of the Specimen in Constant Rate of Strain K_o Tests. (Change of slope of these curves corresponds approximately to the stress conditions at the transition pressure.)

that this change in pore pressure response occurs at about the stage in the test when p′ is between 100 and 150 kPa, that is at a similar value of p′ at which the undrained effective stress path switches from trending to the right to trending to the left. It is proposed herein to refer to the pressure at which these changes occur as the transition pressure.

COEFFICIENT OF CONSOLIDATION

Above it is explained how the conventional oedometer does not give a good indication of compressibility. We will now consider the merit of the device for determining the coefficient of consolidation, c_v. Auckland residual soils have comparatively high c_v values which are not measured readily in the conventional oedometer. The problem is that the consolidation occurs so quickly that insufficient data can be gathered to define the initial linear part of the compression – square root time curve.

Figure 11 has settlement-square root time curves plotted for conventional odeometer tests in which the compression is obtained by manual reading of the dial gauge. The earliest reading that can be obtained is about 2 seconds after the load increment is applied. The shapes of the settlement square root time curves in Figure 11, for eight vertical stresses between 7 kPa and 864 kPa, show that a significant proportion of the consolidation has occurred by the time the first reading is taken. This test was done on samples obtained from the site of the Auckland North Shore Wastewater treatment plant.

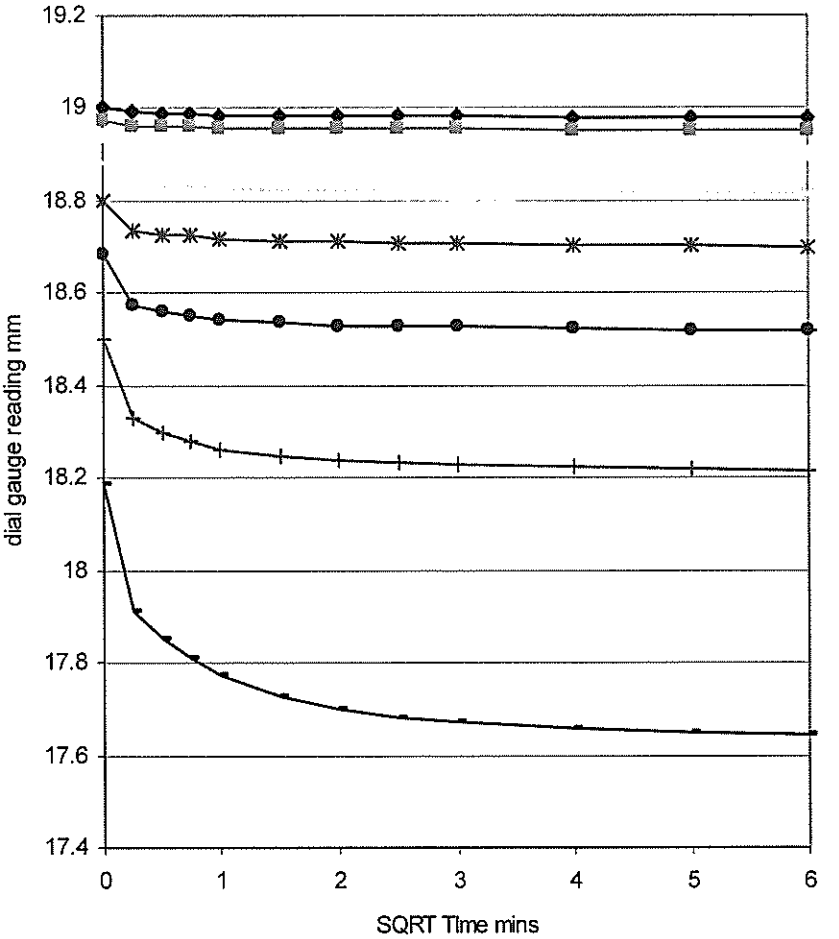

Figure 11. Compression-square root time curves for eight load increments in a conventional oedometer test with manual recording of the compression. The rapid initial compression prevents reliable estimation of the coefficient of consolidation.

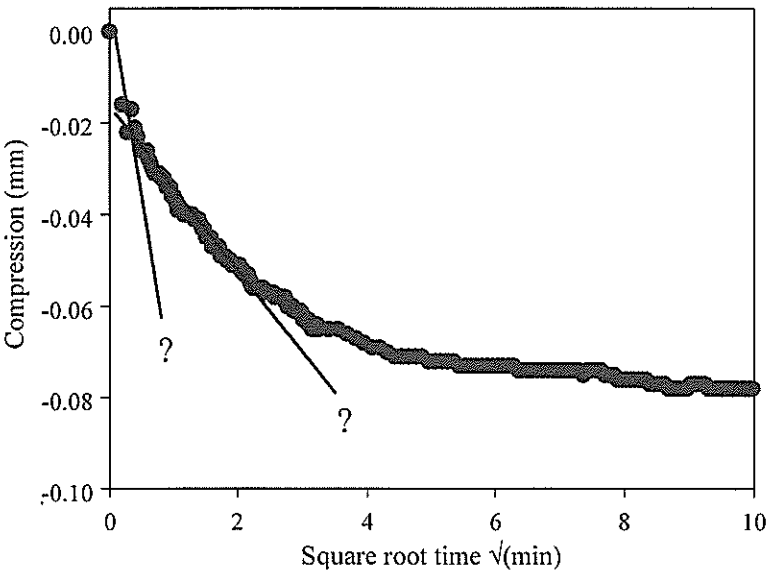

Figure 12. Compression-Square Root Time Curves for a Load Increment in a Conventional Oedometer Test with Automatic Recording of the Compression at an Applied Vertical Stress of 54 kPa. Reliable Estimation of the Coefficient of Consolidation is Still Problematic.

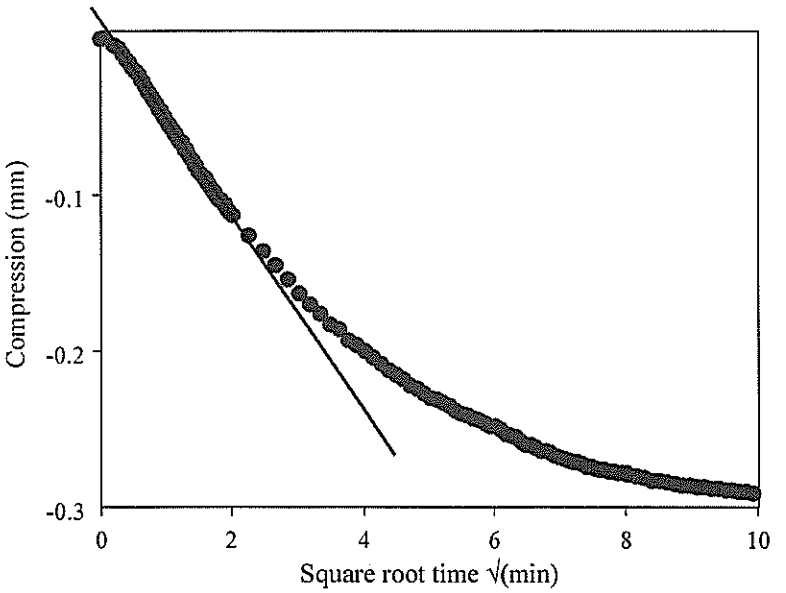

Figure 13. Compression - Square Root Time Curves for a Load Increment in a Hydraulic Oedometer on a Saturated Specimen with Automatic Recording of the Compression. Applied Vertical Effective Stress at the End of Consolidation 50 kPa. The Initial Part of the Curve is Now Well Defined.

In Figure 12, a compression-square root time curve is plotted for a conventional oedometer test on a sample for the Student Amenities Centre. In this case the settlement was monitored with data logger equipment capable of taking readings every second. It is still clear that there is difficulty defining the initial part of the curve, as there appears to be an initial sudden compression when the load is applied. In Figure 13 data is presented for a test in a hydraulic oedometer. The initial height of the specimen is still 19 mm but drainage from one end only doubles the drainage path length and increases the time for consolidation by a factor of 4. The specimen is also saturated with back pressure before the start of the loading. In this case there is considerably better definition of the initial part of the curve.

CONCLUSIONS

We reach the following conclusions:

1. The major conclusion reached is that the conventional oedometer test seems to have limited usefulness in testing Auckland residual soils. While the tests reported here have focussed on Auckland residual clay, it is probable that the shortcomings identified in the oedometer test will apply to any stiff (or very stiff) residual soil.

   Conventional triaxial testing, both drained and undrained, and measurements in a K_o triaxial cell, all give significantly larger values for the Young's modulus along the initial part of the stress-strain curves (Figures 8 and 9). This is believed to be because the relatively small size of the oedometer samples inevitably results in greater disturbance during preparation, and greater bedding errors when the load is applied.

   The small height of oedometer specimens also means that pore pressures dissipate too rapidly to allow useful readings of the settlement rate to be obtained (Figures 11 and 12). A hydraulic oedometer, or testing in a K_o triaxial cell, give better definition of the initial linear part of the compression – square root time curve (Figure 13). Pore pressure dissipation tests in a triaxial cell (not covered herein), would also allow realistic readings to be obtained.

2. Specimen to specimen variability of the soil also contributes to difficulty in defining the shear strength and stiffness properties of the residual soil (Figures 2, 3, 4, 5, 8 and 9).

3. The concept of the transition pressure is introduced as a stress at which there is a change in the shape of the undrained effective stress paths and a change in the rate of pore pressure build up in constant rate of strain one dimensional compression. This transition may or may not be related to a "yield" pressure. In triaxial tests, there will always be a change, regardless of any yield phenomenon, in the shape of the undrained stress paths as the consolidation pressure is increased. However, the change in the rate of increase in pore pressure in the K_o tests, Figure 10, is fairly sudden and does suggest some change in the properties of the soil skeleton.

ACKNOWLEDGEMENTS

The authors wish to acknowledge the financial support of the Foundation for Research, Science and Technology through contract UOAX007 "Essential Geotechnical Knowledge for NZ Infrastructure Development".

REFERENCES

Indrawan, Z (1986) "Stress-strain and strength characteristics of an Auckland soil", PhD Thesis, University of Auckland.

Meyer, V M(1997) "Stress-strain and strength properties of an Auckland residual soil", PhD Thesis, University of Auckland.

Pender, M. J., Wesley, L. D. & Twose, G. R. "Compressibility of Auckland residual soil", *GEOENG2000 Conference, November, Melbourne. CD ROM* Proceedings paper 1082, 2000.

Early Stages of Weathering of Karamu Basalt and Implications for Geomechanical Properties

V Moon
MSc(Hons) PhD (Waikato)
Senior Lecturer, Department of Earth Sciences, University of Waikato
J Jayawardane
MSc (Leningrad) MSc (AsIT)
Department of Earth Sciences, University of Waikato

Abstract: Variations in geochemical and geomechanical characteristics were measured through a basalt weathering sequence exposed at an abandoned quarry at Karamu, near Hamilton. Geochemical measurements show that at the early stages of weathering (fresh to slightly weathered) reductions in the concentrations CaO and MgO are rapid, though are not accompanied by major mineralogical change; at later stages of weathering secondary clay minerals form following well described mineralogical changes. Fresh basalt is strong (uniaxial compressive strength ~ 262 MPa; point load index 5.59) with well-developed, closely spaced columnar jointing. Slightly weathered material is distinguished in the field only by slight discolouration along joint planes, but laboratory tests show a dramatic loss of strength in slightly weathered rock (point load index 0.41; CBR 43 %). A causal relationship between the loss of cations and loss of strength in the early stages of weathering is suggested. This stage of weathering is diffusion controlled whereby cations are lost from the constituent primary minerals and replaced by H^+. This process disrupts the lattice structure and causes a marked loss of strength. Implications are that slightly weathered rock, which appears competent in the field, is likely to have much lower strength and durability than assumed from field evidence.

INTRODUCTION

Weathering of rocks alters their chemical, mineralogical, and physical properties in often poorly-understood ways, creating difficulties for engineering in these materials. In order to develop a better understanding of the impact of weathering on geotechnical behaviour, recent work has concentrated on the geochemical changes in rocks as they weather (Sharma and Rajamani, 2000; Guan *et al.*, 2001: Ng *et al.*, 2001; Duzgoren-Aydin *et al.*, 2002). This paper develops a model for strength loss during the early stages of weathering based on measurements of geochemical and geotechnical properties of basalt specimens of various weathering grades.

KARAMU BASALT PROFILE

An abandoned basalt quarry at Karamu, approximately 17 km southwest of Hamilton, provides a complete weathering sequence from fresh to completely weathered rock. This exposure is part of the Okete Volcanics of the Alexandra Volcanic Group (Briggs and Goles, 1984) and consists of basaltic lava flows and associated scoria material with an estimated age of 2.03 ± 0.03 Ma (Stipp, 1968). The basaltic lavas are overlain by weathered rhyolitic tephra of the Hamilton Ash Formation; the oldest of these tephras is approximately 0.35 ± 0.04 Ma (Kohn *et al.*, 1992).

Figure 1 is a summary log of the quarry profile. The profile was divided into 5 weathering grades based on visual characteristics as defined by the New Zealand Geomechanics Society (1988) standards: *fresh* rock shows no evidence of weathering; *slightly weathered* rock has discoloured discontinuity surfaces; *moderately weathered* rock is discoloured with some soil material; *highly weathered* rock is > 50 % soil material but may contain corestones; and *completely weathered* rock is entirely soil. Sampling locations were selected to obtain a range of materials through the profile. Sample depths were determined as the depth below a horizontal datum above the top of the slope.

GEOCHEMISTRY

Mineralogy and geochemistry of each specimen were determined using crushed samples and thin sections. Major and trace element analyses were undertaken using X-ray fluorescence (XRF), and minerals present in the samples were identified using X-ray diffraction (XRD) and thin sections under

both polarized and reflected light. Scanning Electron Microscopy on broken rock and soil surfaces was used to examine clay minerals. Following NZS 4402 (Standards Association of New Zealand, 1986) the pH of solutions of powdered samples was determined. This measures abrasion pH that gives an indication of the pH of the solid component of the rock, not of the weathering solutions.

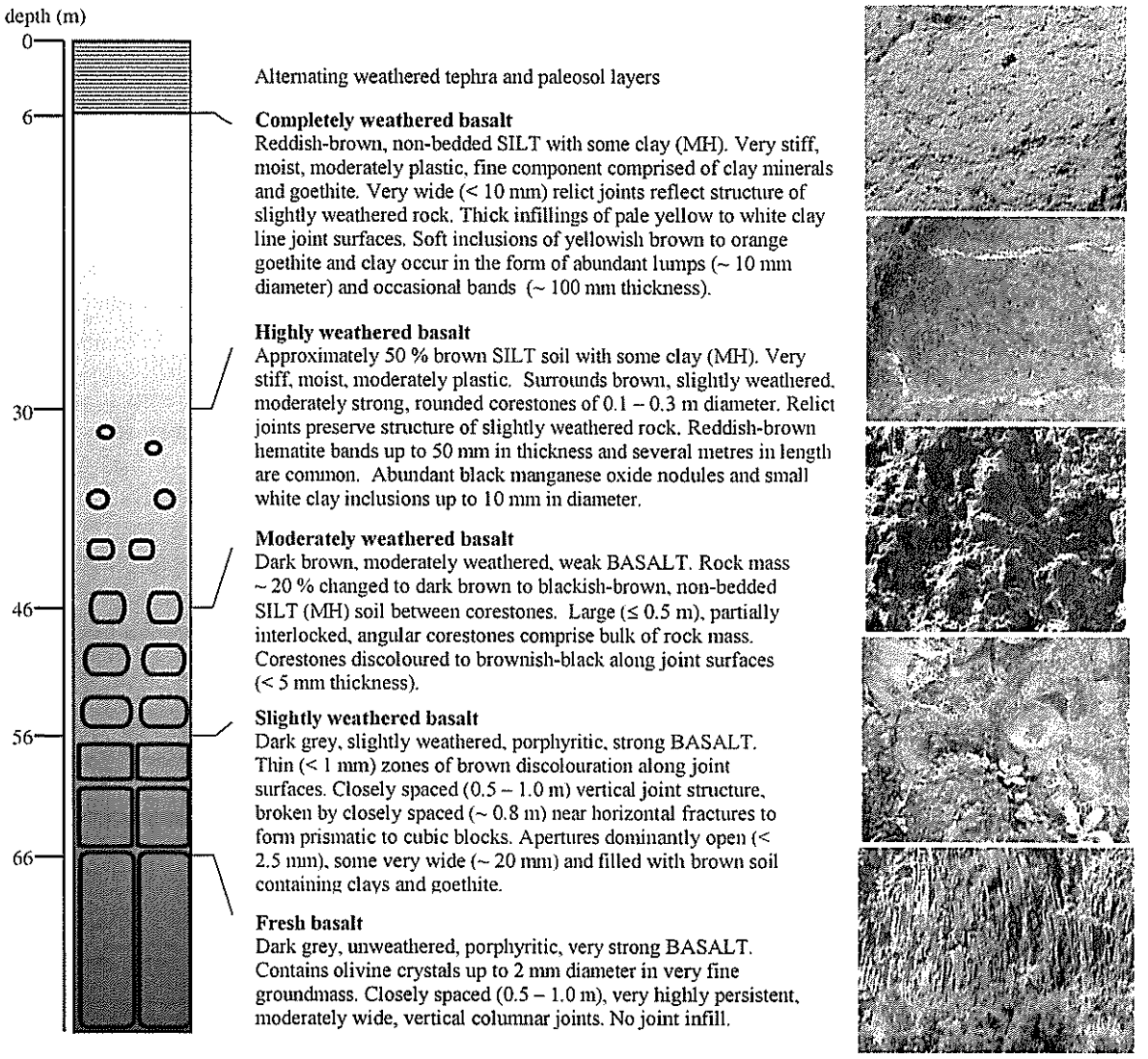

Figure 1. Karamu Basalt Weathering Profile Description.

Chemical Concentrations

Average chemical concentrations for major and trace elements determined using XRF are presented in Table 1; Figure 2 shows major element oxide concentrations plotted against depth, with approximate weathering grade boundaries marked, and Figure 3 presents the same graph for trace element concentrations (error bars represent ± 1 standard deviation). The value of loss on ignition (LOI) is assumed to be the water retained within the mineral structures (H_2O+) which is released on ignition at temperatures above 110°C (Rollinson, 1993).

Major Element Oxides

From Figure 2 it is apparent that at the slightly weathered stage, the concentrations of MgO, CaO and FeO drop markedly from those of the fresh basalt, while Fe_2O_3 and H_2O+ concentrations increase significantly. These trends largely continue through to the moderately weathered stage, by which point the concentrations of MgO, CaO and FeO are essentially zero. From moderately to completely weathered grades there are no further changes in these concentrations when the large error bands are taken into consideration.

	Fresh Basalt	Slightly Weathered	Moderately Weathered	Highly Weathered	Completely Weathered
no. of samples	7	5	12	6	7
SiO_2	42.39 ± 1.66	30.81 ± 30.3	33.29 ± 5.05	32.78 ± 6.13	38.67 ± 7.99
Al_2O_3	12.04 ± 0.23	21.52 ± 4.15	26.83 ± 2.40	27.80 ± 2.28	27.67 ± 3.34
MnO	0.18 ± 0.00	0.32 ± 0.10	0.22 ± 0.13	0.28 ± 0.16	0.07 ± 0.10
MgO	12.53 ± 0.59	3.52 ± 4.61	0.65 ± 0.42	0.37 ± 0.17	0.32 ± 0.36
CaO	10.82 ± 0.31	1.35 ± 2.68	0.08 ± 0.10	0.00 ± 0.01	0.00 ± 0.00
Na_2O	1.30 ± 0.35	0.04 ± 0.08	0.01 ± 0.02	0.00 ± 0.00	0.00 ± 0.01
K_2O	0.70 ± 0.26	0.07 ± 0.10	0.06 ± 0.05	0.06 ± 0.07	0.08 ± 0.09
TiO_2	2.41 ± 0.11	4.32 ± 0.83	2.98 ± 1.42	3.27 ± 1.31	2.23 ± 1.51
P_2O_5	0.39 ± 0.02	0.53 ± 0.11	0.33 ± 0.18	0.53 ± 0.30	0.18 ± 0.18
Fe_2O_3	3.12 ± 0.10	16.32 ± 7.03	14.94 ± 5.67	16.57 ± 4.75	12.91 ± 5.49
FeO	10.46 ± 0.35	5.11 ± 4.36	0.79 ± 0.30	0.87 ± 0.25	0.68 ± 0.29
LOI (H_2O+)	3.68 ± 0.99	13.42 ± 1.09	17.89 ± 1.94	15.08 ± 0.88	15.11 ± 1.14
Nb	40 ± 3	64 ± 11	48 ± 20	50 ± 19	33 ± 23
Zr	201 ± 8	301 ± 43	365 ± 35	366 ± 44	337 ± 122
Th	4 ± 1	9 ± 3	22 ± 7	19 ± 6	24 ± 14
Sr	708 ± 106	48 ± 67	16 ± 8	22 ± 8	8 ± 6
Ba	315 ± 20	697 ± 61	472 ± 144	358 ± 108	187 ± 84
Rb	18 ± 7	5 ± 2	9 ± 3	8 ± 4	12 ± 9
V	297 ± 8	468 ± 71	327 ± 162	501 ± 195	317 ± 161
Cr	726 ± 51	1241 ± 223	694 ± 497	966 ± 556	314 ± 405
Ni	318 ± 25	758 ± 190	427 ± 325	403 ± 216	56 ± 56
Zn	107 ± 3	179 ± 31	104 ± 55	106 ± 53	50 ± 33
La	27 ± 6	71 ± 39	30 ± 34	81 ± 21	26 ± 23
Ce	61 ± 6	84 ± 22	91 ± 21	123 ± 63	63 ± 42
Nd	40 ± 8	95 ± 77	41 ± 20	42 ± 17	16 ± 2
Ga	20 ± 1	32 ± 5	36 ± 1	37 ± 5	39 ± 12
Pb	2 ± 1	5 ± 2	20 ± 12	13 ± 8	28 ± 15
Y	23 ± 0	78 ± 88	22 ± 16	13 ± 4	10 ± 5
abrasion pH	8.09 ± 0.28	5.58 ± 1.03	4.99 ± 0.26	4.25 ± 0.13	4.12 ± 0.14

Table 1. Average (± 1 Standard Deviation) Chemical Compositions of Each Weathering Grade.

Therefore, in terms of major element changes, weathering of these rocks is characterized by a loss of the cations Mg^{2+}, Ca^{2+}, Fe^{2+}, and an increase in Fe^{3+} and water within the mineral structures. Apparently, loss of Mg^{2+} and Ca^{2+} takes place mostly between the fresh and moderate stages of weathering, and likewise, the drop in Fe^{2+} is complete at the moderate stage of weathering. Thus, loss of cations and oxidation of iron is carried out in the first portion of the weathering process. This is in agreement with the Egglington's inclusion of cation loss as an indicator of slight weathering in his recent weathering grade classification (Eggleton, 2001).

Trace Elements

From Figure 3 it is apparent that most trace element concentrations increase from the fresh to moderately weathered grades of weathering. This is true of the Rare Earth Elements and Ba, as documented by Price *et al* (1991) for Australian basalts, but also for a variety of other trace elements (Figure 3A&B). Beyond the moderately weathered stage, the pattern of change shown in these graphs is variable, with most trace element concentrations either falling slightly or remaining constant with further weathering (Figure 3B). Several show a further peak at the highly weathered stage (Figure 3A). This increase in trace element concentrations at the slight to moderate stage of weathering is likely a reflection of the loss of the major elements (Ca, Mg, Fe) and hence an apparent concentration of trace elements, rather than actual influx of these trace elements into the system. Reductions with further weathering likely represent mobilization of trace elements as clay mineral formation proceeds.

Two trace elements, Rb and Sr, follow a similar change in concentration with depth (or weathering grade) to the major element oxides of CaO, MgO and FeO in that their concentration reduces markedly from fresh to moderately weathered rock, followed by little change with further weathering (Figure 3C). These trace elements have an affinity with Ca according to their ionic radii, and are interpreted as being lost from the system in the same way as the major element cations are removed in the early stages of weathering.

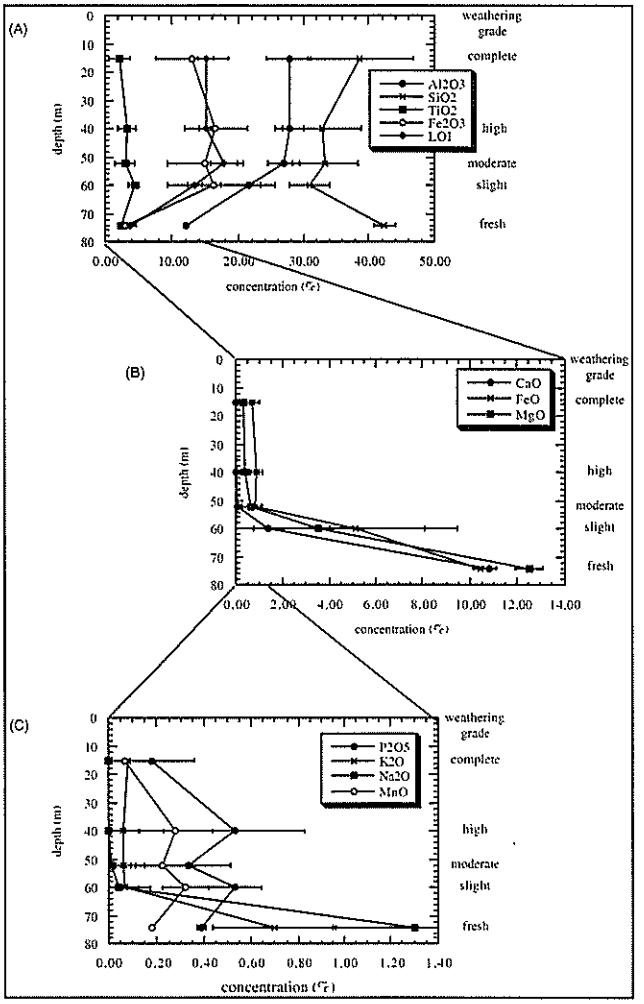

Figure 2: Variations in Major Element Oxide Concentrations with Depth and Weathering Grade.

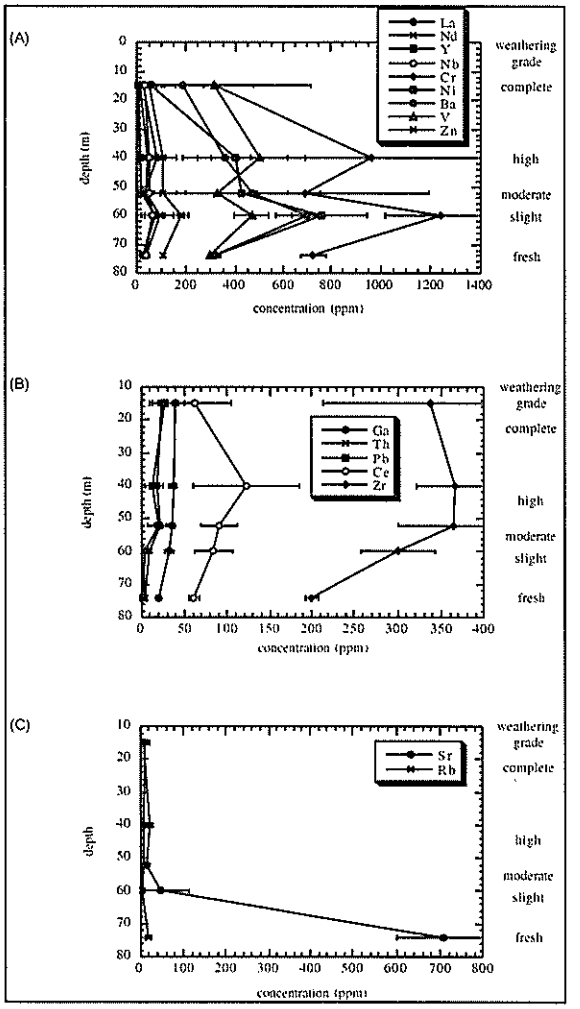

Figure 3: Variations in Trace Element Oxide Concentrations.

Abrasion pH

Abrasion pH is slightly alkaline in the fresh basalt, and falls markedly to be somewhat acidic at the slightly weathered stage. Only a small reduction in abrasion pH is observed after the slightly weathered stage. This reduction in abrasion pH is believed to be related to the observed reduction in cations during this early stage of weathering: in fresh basalt the abrasion pH value of 8.5 indicates that alkaline earth elements (Ca, Mg) are present, while the pH of 5.6 in the slightly weathered rocks suggests that the alkaline earths have been removed, and there is more H^+ in the system.

Mineralogy

Figure 4 summarises the mineralogy observed at each weathering grade. The mineralogy is largely unchanged from fresh to slightly weathered basalt; the original mineral suite is still evident with minor alteration of crystals, and fracturing of both the crystals and groundmass is more apparent. At the moderately weathered stage there is considerable alteration of the primary minerals to clays, and further weathering is characterized by increasing development of clay minerals and sesquioxides.

GEOMECHANICS

Strength and bulk rock properties were determined for specimens from each weathering grade. A range of tests from soil- and rock-mechanics were selected; the main limitation on testing for physical properties is that few tests are suitable across the entire range of material properties.

Natural water content, dry bulk density, and particle density were determined using standard methods (NZS 4402, Standards Association of New Zealand, 1986); 5 specimens from each sampling site were

tested and the results averaged. Permeability of soil materials was determined in the laboratory on small cylindrical specimens using a falling head permeameter. Particle size distribution of soil materials was determined using a combination of wet sieve analysis for the coarse components (>0.6 mm), and laser diffraction for the fine components (≤0.6mm).

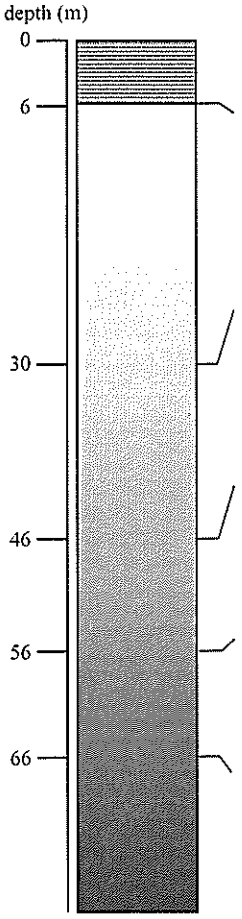

Completely weathered basalt
Mineralogy of completely weathered basalt is complex with clays predominating; only traces of olivine are left. The original porphyritic texture is present as traces only, and the matrix cannot hold the remaining parts of phenocrysts together. Clay minerals identified are: montmorillonite, illite, halloysite, kaolinite, beidellite, saporite and vermiculite. Goethite and hematite are also present.

Highly weathered basalt
Mixture of titanomagnetite, goethite, manganosite and clays, with remnants of the original rock preserved. Because of these remnants of rock, the matrix appears to retain the relict porphyritic texture. Titanaugite is replaced completely, but relict traces of the outlines of olivine crystals are still visible. An extensive crack network exists. X-ray diffraction shows the presence of clay minerals, mainly kaolinite, illite, halloysite, beidellite and montmorillonite.

Moderately weathered basalt
Original porphyritic texture still preserved as a relict texture. Olivine crystals develop orange to brown iddingsite rims up to 30 mm in thickness. Titanaugite phenocrysts show evidence of alteration to hematite in the form of change of colour from p-ale purplish grey to reddish brown. Plagioclase is largely altered to clays. A network of cracks filled with clays, goethite and hematite is apparent. Clay minerals mainly smectite and, in lesser quantities, illite and kaolinite.

Slightly weathered basalt
Original porphyritic texture of fresh basalt retained. Alteration of olivine crystals evidenced by development of orange-coloured iddingsite rims up to 1.7 mm in thickness. Titanaugite crystals reduced in size from fresh basalt due to breakage, and some plagioclase crystals show a turbid or speckly appearance. Fractures more visible and frequent, and some clays evident on fracture surfaces and as alteration products of interstitial glass.

Fresh basalt
Holocrystalline to hypocrystalline, fine grained, porphyritic with phenocrysts of euhedral to subhedral olivine, subhedral titanaugite and rare plagioclase in a groundmass composed of laths of plagioclase, tiny granular titanomagnetite, and glass. Apatite and chromite accessory minerals. Minerals are unaltered except for narrow zones of pale yellow discoloration of olivine crystal edges. Fine linear fractures observed in groundmass.

Figure 4. Summary of Mineralogical Observations Throughout the Karamu Basalt Weathering Profile.

Field index strength measurements were undertaken for both rock and soil materials. All measurements are recorded as index values without conversion to SI units. Schmidt hammer rebound number (R) was determined for fresh and slightly weathered materials following methods described by Brown (1981). Vane shear strength of moderately to completely weathered materials was determined using a Geonor hand held vane tester H-60. Similarly, penetration resistance was determined for these materials using an EL29-3729 Pocket Penetrometer. In all cases, 20 readings were taken for each sample location and the average of the 10 highest values calculated.

Uniaxial compressive strength (UCS) was determined on NX size cores following standard methods described by Brown (1981). A total of 10 specimens was tested from fresh rock material as all other weathering grades proved unable to be sampled and prepared to the tolerances required for compressive strength testing. Point load strength index tests were undertaken on irregular specimens of fresh and slight weathered Karamu Basalt; more weathered materials were too weak for this test procedure. Size-corrected point load strength index ($I_{s(50)}$) was determined following the method described by Franklin (1985). Twenty irregular specimens were tested from each sample location, and average $I_{s(50)}$ values calculated. California Bearing Ratio (CBR) was measured following NZS 4402 (Standards Association of New Zealand, 1986). The CBR was determined at penetrations of 2.5 mm and 5.0 mm and the higher value used. This test spanned all grades of weathering.

Direct shear testing of soil (moderately to completely weathered) materials was carried out following methods of using a direct shear box. Tests were carried out at unconsolidated undrained conditions with a shearing rate of 0.61 mm min^{-1}. Values of cohesion (c) and angle of internal friction (ϕ) were determined for each sample location. Atterberg Limits (liquid limit, plastic limit and plasticity index)

were determined using a cone penetrometer. Following NZS 4402 (Standards Association of New Zealand, 1986) the water content value corresponding to a 20 mm penetration was determined as the liquid limit, and the water content corresponding to 2.8 mm penetration was taken as the liquid limit as defined by Allbrook (1980).

Results

Data obtained from geomechanical testing are summarized in Table 2; graphs of measured parameters with depth are presented in Figure 5.

Parameter	Fresh Basalt	Slightly Weathered	Moderately Weathered	Highly Weathered	Completely Weathered
Water content (%)	0 ± 0	29 ± 9	46 ± 8	43 ± 20	43 ± 9
Dry density (kg m^{-3})	2811 ± 48	2116 ± 241	1908 ± 116	1758 ± 20	1538 ± 43
Particle density (kg m^{-3})	2820 ± 46	2294 ± 176	2225 ± 106	2217 ± 87	2102 ± 72
Porosity (%)	0.32 ± 0.13	7.96 ± 3.98	14.28 ± 2.24	20.61 ± 3.58	25.39 ± 1.78
Permeability (m s^{-1})			0.20 ± 0.05	7.70 ± 0.04	40.3 ± 9.1
Clay content (%)			30 ± 8	32 ± 6	25 ± 14
Schmidt rebound (R)	33 ± 7	19 ± 4			
Point load index ($I_{s(50)}$)	5.6 ± 1.8	0.41 ± 0.28			
UCS (MN m^{-2})	262 ± 47				
CBR (%)	100 ± 0	42.5 ± 3.5	27.5 ± 3.5	15 ± 0	2.5 ± 1.8
Penetration resistance			4.10 ± 0.22	4.15 ± 0.13	4.37 ± 0.04
Vane shear strength			119 ± 32	123 ± 14	115 ± 6
Cohesion (kN m^{-2})			1 ± 1	4 ± 2	5 ± 2
Friction angle (°)			34 ± 1	37 ± 1	35 ± 2
Liquid limit (%)			75.0 ± 7.68	64.14 ± 7.96	73.50 ± 6.59
Plastic limit (%)			60.90 ± 10.74	50.94 ± 4.91	58.72 ± 6.73
Plasticity index (%)			14.09 ± 5.55	13.20 ± 5.97	14.79 ± 6.12

Table 2. Average (± 1 Standard Deviation) Results of Geomechanical Testing for Materials.

For the bulk rock properties that span the range of weathering grades it is apparent that relatively large changes with depth occur from the fresh to moderately weathered grades, and comparatively minor changes occur with further weathering. Indeed, this change is most marked in the change from fresh to slightly weathered rock, where the dry density decreases by some 24 %. This dramatic change in bulk rock properties across the fresh to slightly weathered grades is accompanied by a marked loss of strength as shown by the point load strength index (order of magnitude loss of strength) and CBR (almost 60% loss of bearing capacity).

From moderately to completely weathered the materials are characterized by soil properties: the dry and particle densities continue to fall with increased weathering as clay minerals become dominant. However, from moderately to completely weathered there is little change in the measured shear strength and penetration resistance parameters. Likewise, the Atterberg limits show little consistent change, especially when the error estimates are taken into account.

Therefore, from fresh to slightly weathered basalt the materials retain rock-type characteristics in an engineering sense, but undergo a dramatic and significant loss of intact rock strength. This loss of strength is much greater than would be assumed on the basis of field inspection alone as only some minor discolouration provides evidence of this stage of weathering. At the moderately weathered grade the material develops plasticity, associated with the conversion of primary minerals to secondary clay minerals. Initially the clays are concentrated around corestones; with further weathering the physical characteristics of the clays change very little, but their proportion increases.

STATISTICAL ANALYSIS

Statistical analysis was used to explore possible relationships between measured geotechnical and geochemical parameters. Values of some geotechnical and geochemical parameters overlap in adjoining weathering grades as weathering grades are assigned based on visual appearance. Hence, statistical analysis was undertaken on individual sample results rather than weathering grade means.

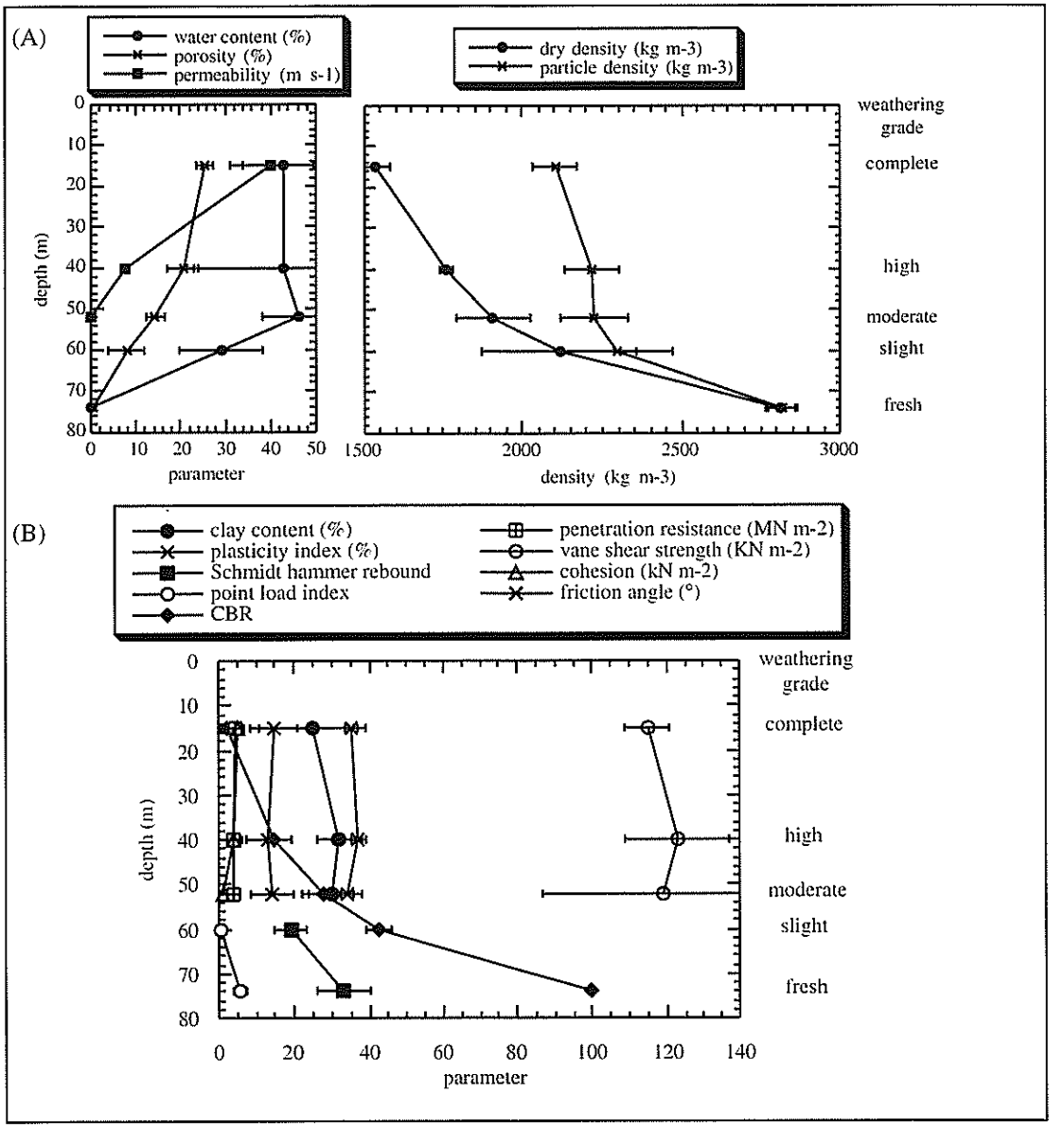

Figure 5. Variations in Measured Geomechanical Properties with Depth and Weathering Grade.

Regression Analysis

Initially linear, semi-logarithmic and second-order polynomial regression analyses were used to identify possible relationships. Regression coefficients (r^2) at the 95% confidence level were determined for all available data. According to Johnson (1984), $r^2 = 0.64$ is considered significant at the 95% confidence level; this was considered as the minimum value for acceptance of a possible relationship. However, relationships with high r^2 values that did not produce convincing plots, in terms of spread of data points, were discarded. Table 3 presents the regression coefficients for significant relationships between geotechnical and geochemical parameters. From this it is apparent that:

(1) CBR and other strength parameters, together with dry density, correlate with cation concentration patterns;

(2) abrasion pH correlates significantly with all bulk material properties (density, porosity and permeability) and CBR; and

(3) none of the soil engineering properties (cohesion, angle of internal friction, Atterberg limits) shows any acceptable relationship with chemical parameters except for cohesion versus abrasion pH.

Principal Components Analysis (PCA)

PCA was undertaken on the geochemical data in order to recognise those components that account for the bulk of the variation in the original data. From this analysis it was determined that CaO and MgO concentrations explain 95% of the variations in the geochemical data. Further, CaO concentration delineates fresh basalt from the other stages of weathering and can be used to delineate fresh basalt: fresh basalt samples have high CaO values; all other weathering grades have low CaO values; MgO concentration, which correlates highly with CaO concentration (r^2=0.97), follows a similar pattern. Therefore, most variations of geochemical data can be explained by the variations of either CaO or MgO concentrations.

	Water Content (%)	Dry Density (Kg M^{-3})	Porosity (%)	Perm-Eability (M S^{-1})	Schmidt Hammer (R)	Point Load $I_{s(50)}$	Cbr (%)	Cohesion (Kn M^{-2})
SiO_2						0.83 poly		
Al_2O_3		0.78 lin					0.85 lin	
MgO							0.88 lin	
CaO		0.86 lin				0.72 poly		
Na_2O					0.72 lin	0.92 lin		
K_2O					0.81 lin	0.91 lin		
FeO		0.86 lin	0.72 poly				0.90 lin	
LOI	0.70 lin							
Th								
Sr		0.86 poly				0.79 lin		
Ba				0.71 poly				
Rb					0.89 lin.	0.83 lin		
V						0.82 poly		
Cr						0.68 poly		
Zn						0.70 poly		
Ga		0.76 poly						
Pb		0.69 lin					0.86 poly	
abrasion pH		0.95 lin	0.92 poly	0.66 poly			0.96 lin	0.84 poly

Table 3. Regression Coefficients (R^2) for Acceptable Correlations Between Geochemical and Geotechnical Parameters (Lin = Linear Regression; Poly = 2nd Order Polynomial Regression).

INTERPRETATION

Figures 2 and 4 indicate that changes in MgO, CaO and FeO concentrations and geotechnical parameters for which a full range of weathering grades is represented (CBR, dry density, porosity, and water content) with depth show a striking resemblance in that they all display a marked break in slope at 50 – 60 m depth (slightly to moderately weathered). A simplified view of these relationships sees each of strength, density and oxide concentrations decreasing in a two-stage fashion: a rapid decrease occurs from fresh to moderately weathered, followed by only slight changes beyond the moderately weathered stage (porosity and water content show mirror images of these trends). A concurrence between these trends is supported by the statistical analysis:

(1) regression analysis indicated significant relationships between dry density and the concentrations of CaO and FeO, porosity and FeO, and CBR and MgO and FeO concentrations; and

(2) PCA indicated that changes in CaO and MgO concentrations accounted for approximately 95% of the variations within geochemical parameters and provided precise discriminators between fresh and weathered basalt.

It is proposed that there is a causal relationship between these trends: a decrease in the absolute quantities of the cations Mg^{2+}, Ca^{2+} and Fe^{2+} leads to a loss of strength of the rocks in the fresh to moderately weathered phase of weathering. The following sections present a hypothesis to explain this causal relationship.

Cation loss and substitution

Measurable mineralogical changes lag behind geochemical changes, and hence the slightly weathered rock still has an identifiable mineralogical suite similar to the fresh rock. Price *et al* (1991), working on basalts of Australia, observed a dramatic change in concentration of Ba and REE in the early stages of weathering with no associated discernable mineralogical changes. Similar trace element behaviour (Figure 3) is recognized in the basalts of this study.

The geochemical changes in the early stages of weathering do not appear to reflect a major change in the mineralogy of the material, but rather indicate subtle changes in the structure of the minerals within the rock caused by the diffusion of Ca^{2+}, Mg^{2+}, and Fe^{2+} ions from the crystal lattice. Removing the cations from their lattice positions creates a charge imbalance within the crystal lattice. This can be remedied by the influx of other cations, such as H^+ which is available in groundwater and is mobile. Abrasion pH measurements indicate that H^+ cations are present in the slightly and moderately weathered samples, confirming an increase in these ions. Hence, abrasion pH becomes a good indicator of weathering grade at this early stage of weathering, in keeping with the statistical analysis where abrasion pH was recognised as correlating with bulk material and strength parameters.

Loss of Intact Strength and Development of Factures

Replacement of Mg^{2+}, Ca^{2+}, or Fe^{2+} with H^+ is believed to involve a weakening of the crystal structure and hence a loss of strength of the crystals because:

(1) the replacement cations have different valencies from the original cations, creating a charge imbalance: and

(2) the ionic radii of the replacement cations (H^+ = negligible (Aylward and Findlay, 1998)) are smaller than those of the original cations (Mg^{2+}=72 pm, Ca^{2+}=100 pm, Fe^{2+}= 78 pm (Aylward and Findlay, 1998)).

A reduction in ionic radius will disrupt the bond angles and interionic spacings within the crystal structure. This, together with altered valency, is likely to lead to reduced bond strength and hence weaker crystals (although the overall mineralogy is unchanged).

There are insufficient published data available to allow genuine calculation of bond strength reduction associated with these changes to primary minerals. However, the changes in crystal strength within the olivine group as the proportions of Mg and Fe vary along the solid solution between forsterite and fayalite illustrate the importance of lattice dimensions and charge imbalance on mechanical properties. In this case, a 1 % decrease in lattice parameters and an 11 % decrease in ionic radius (Deer *et al.*, 1962) is accompanied by a 6.3 % decrease in bulk modulus (Carmichael, 1982). The case of replacement of Mg^{2+} with H^+ in minerals in the Karamu Basalt represents a large decrease in ionic radius. By analogy, it seems reasonable to assume that the observed decrease in mechanical properties in the olivine suite is mirrored in these other minerals.

The imbalance in the crystal lattice induced by the removal and replacement of cations results in a considerable loss of compressive strength in slightly weathered Karamu Basalt. Whilst tensile stresses were not determined, it is assumed that an analogous loss of tensile strength would have occurred. Weakening of the intact material allows microfractures to develop and extend easily in response to lower stresses, and in this case the strength drop observed is believed to be sufficient to allow microfracture extension in response to residual stresses alone. Bock (1979) measured large (>12 MPa in tension; >15 MPa in compression) residual stresses in a basalt column in Australia. Residual stresses of this magnitude are of the same order of magnitude as the predicted compressive strength of the slightly weathered Karamu Basalt. Coalescence of microfractures leads to the development of near-horizontal macrofractures as those aligned favourably with respect to the maximum tensile stress (vertical) direction grow preferentially. The establishment of a network of macrofractures marks the onset of the moderately weathered stage.

Development of Secondary Minerals

Once the available Ca^{2+}, Mg^{2+} and Fe^{2+} ions are essentially removed from the lattice, at the moderately weathered stage, the fracturing process ceases and further weathering largely takes the form of conversion of primary minerals to secondary clay mineral species. No further major strength loss is noted, but with increased weathering the rock mass becomes more typically plastic as a consequence of the increasing proportion of clay minerals. This follows the patterns described for other materials in which soil-engineering behaviours develop as clay minerals evolve.

CONCLUSION

The weathering sequence is often seen as initially fracturing of the rocks by physical processes in the early stages of weathering, followed by the progressive development of secondary minerals that reduce the strength of the material. From this study, it is apparent that an early loss of alkaline earth elements can be measured geochemically before any significant mineralogical change occurs, and is closely linked to a dramatic drop in the intact strength of slightly weathered basalt. This drop in intact strength in turn allows for fracture development in response to residual stresses, after which secondary mineral development occurs following well-established patterns.

A major implication of this is that intact strength loss in these rocks occurs at the slightly weathered stage, before secondary mineral formation is apparent in field expression, and before major macrofracture development is obvious. Slightly weathered material is distinguished in the field simply on the basis of some discolouration, mainly along discontinuity surfaces. From field inspection alone slightly weathered rock appears competent, and simple description would suggest that it is an adequate material for many engineering applications. However, even slight discolouration along joint surfaces (reflecting removal of alkaline earth elements from the rock material) may be an indication that the strength and durability of the intact rock are severely compromised.

REFERENCES

Allbrook, R.F. (1980). The drop-cone penetrometer method for determining Atterberg limits. *New Zealand Journal of Science* 23 pp 93-97.

Aylward, G and Findlay, T. (1998). *SI Chemical Data.* John Wiley and Sons, New York.

Bock, H. (1979). Experimental determination of the residual stress field in a basaltic column. *Proceedings of the International Congress on Rock Mechanics,* Rotterdam, Balkema. pp 45 – 49.

Briggs, R.M. and Goles, G.G. (1984). Petrology and trace element geochemical features of the Okete volcanics, western North Island, New Zealand, *Contributions to Mineralogy and Petrology* 86 pp 77-88.

Brown, E.T. (1981). Rock characterisation, testing and monitoring, *ISRM suggested methods*, Pergamon Press, England.

Carmichael, R.S. (1982). *Handbook of Physical Properties of Rocks.* CRC Press, Inc. Florida.

Deer, W.A., Howie, R.A. & Zussman, J. (1962). *An Introduction to the Rock Forming Minerals.* John Wiley & Sons, New York.

Duzgoren-Aydin, N.S., Aydin, A. and Malpas, J. (2002). Re-assessment of chemical weathering indices: case study on pyroclastic rocks of Hong Kong. *Engineering Geology.* 63 pp 99 – 119.

Eggleton, R.A. (2001). *The Regolith Glossary: Surficial Geology, Soils and Landscapes.* CRC LEME, Australia.

Franklin, J. A. (1985). Suggested method for determining point load strength. *International Journal of Rock Mechanics, Mining Science and Geomechanics Abstracts.* 22 pp 53-60.

Guan, P., Ng, C.W.W., Sun, M. and Tang, W. (2001). Weathering indices for rhyolitic tuff and granite in Hong Kong. *Engineering Geology.* 59 pp 147 – 159.

Johnson, R. (1984). *Elementary Statistics.* Duxbury Press, Boston.

Kohn, B.P., Pillans, B. and McGlone, M.S. (1992). Zircon fission track age for middle Pleistocene Rangitawa tephra, New Zealand: stratigraphic and paleoclimatic significance. *Paleogeography, Paleoclimatology and Paleoecology*. 95 pp 73-94.

New Zealand Geomechanics Society (1988). *Guidelines for the Field Description of Soils and Rocks in Engineering Use.*

Ng, C.W.W., Guan, P. and Shang, Y.J. (2001). Weathering mechanisms and indices of the igneous rocks of Hong Kong. *Quarterly Journal of Engineering Geology and Hydrogeology*. 34 pp 133 – 151.

Price, R.C., Gray, C.M., Wilson, R.E., Frey, F.A. and Taylor, S.R. (1991). The effects of weathering on rare-earth element, Y and Ba abundances in Tertiary basalts from southeastern Australia. *Chemical Geology* 93 pp 245-265.

Rollinson, H. (1993). *Using Geochemical Data: Evaluation, Presentation and Interpretation.* Longman Group, UK.

Sharma, A. and Rajamani, V. (2000). Major Element, REE, and Other Trace Element Behaviour in Amphibolite Weathering under Semiarid Conditions in Southern India. *The Journal of Geology*. 108 pp 487 – 496.

Standards Association of New Zealand (1986). *Methods of Testing Soils for Civil Engineering Purpose.*, Wellington

Stipp, J.J. (1968). The geochronology and petrogenesis of the Cenozoic volcanics of North Island, New Zealand. *Unpublished Ph.D thesis*, Australian National University, Canberra.

Numerical Modelling of Auckland Soils

S Terzaghi
BE (Hons), MIPENZ, Regd Engr
Associate, Sinclair Knight Merz

Abstract: Many of the Auckland soils, including the Waitemata Formation, are known to behave in 'non-standard' ways compared to the traditional soils literature. Conventional approaches to modelling these materials often do not work entirely satisfactorily. An attempt to model residual to completely weathered Waitemata soils are described and some of the key differences in behaviour discussed. A brief discussion on other Auckland soils is also given.

Simulating a 'typical' laboratory test result using a more advanced soil model does indicate that there are significant differences in the behaviour of Auckland residual and pumice soils compared to the textbook and that much more work needs to be carried out to understand these differences. Some of these differences may influence the way that laboratory test results are interpreted to obtain strength and stiffness parameters.

INTRODUCTION

Many of the Auckland soils are unusual, compared to the soils more typically reported in the textbooks and literature. This is due partly to the climatic conditions prevailing around Auckland, in particular a wet and temperate climate, and partly it is due to the relatively complex geologic setting, with many different sources and ages of materials. This includes rhyolitic/acidic material transported from the Taupo Volcanic zone, re-worked material via the Waitemata Group materials, basaltic/basic material from all the small cones around Auckland, also alluvial materials derived from all of these sources. Many of these materials exhibit deep and/or extensive weathering profiles, which are not always apparent. To further confuse matters, it can be difficult to distinguish from the investigation information on any given site between a completely weathered soil and a reworked material (alluvium or colluvium). The fact that both materials are present only becomes apparent once the site is opened up.

Conventional approaches to modelling these materials often do not work entirely satisfactorily. Usually one can match certain aspects of the behaviour with one approach, yet need an incompatible approach somewhere else. Historically, this may not have been important, since one can identify a strength profile that apparently captures the actual strengths, and then one can identify a deformation profile that matches the in situ performance reasonably well. But in terms of linking the two profiles through numerical analysis they are incompatible in terms of conventional correlation and behaviour.

This paper discusses this issue in greater depth with relation to some residual to completely weathered Waitemata Material.

MODELS OF WAITEMATA CLAY

In attempting to describe the behaviour of the "Waitemata Clay" one needs to first address the issues of variability in any set of material property test results. This is demonstrated by a recent project for which some 22 Consolidated isotropic undrained triaxial tests of weathered to residual Waitemata samples that were carried out. All samples were taken from within 10 metres of the ground surface and generally within 5 metres, and all locations are within approximately one kilometre of each other. Samples were tested were recovered and tested by two very reputable companies. Yet the range of E_{50} (secant stiffness at 50% of failure strain) on the first test stage varied from 2,900 kPa to 24,000 kPa, with a corresponding range of strengths represented by c' and ϕ' ranging from 7 kPa to 35 kPa, and 22° to 38° respectively. There is little or no dependency of strength on depth or initial cell pressure.

Similarly the reported coefficients of consolidation (C_v) are widely scattered, from 1 m^2/year through to 2,345 m^2/year.

Such a wide range in properties is, however, not reflected in field behaviour. Many other laboratory tests exhibit similar or greater range of variability (Pender et al 2000). Part of the variability is certainly due to sample disturbance and this may explain the often-reported observation that the stiffness measured in the laboratory and the field are quite different. This makes it difficult to select an average stiffness for numerical modelling. Hence a single 'typical' test is discussed in greater detail to shed some light on these observations.

The triaxial test stress-strain curve and pore pressure plot for the selected sample are shown in Figure 1, with the relevant stress paths shown in Figure 2. The sample was recovered from a depth of 4.5 to 5 metres.

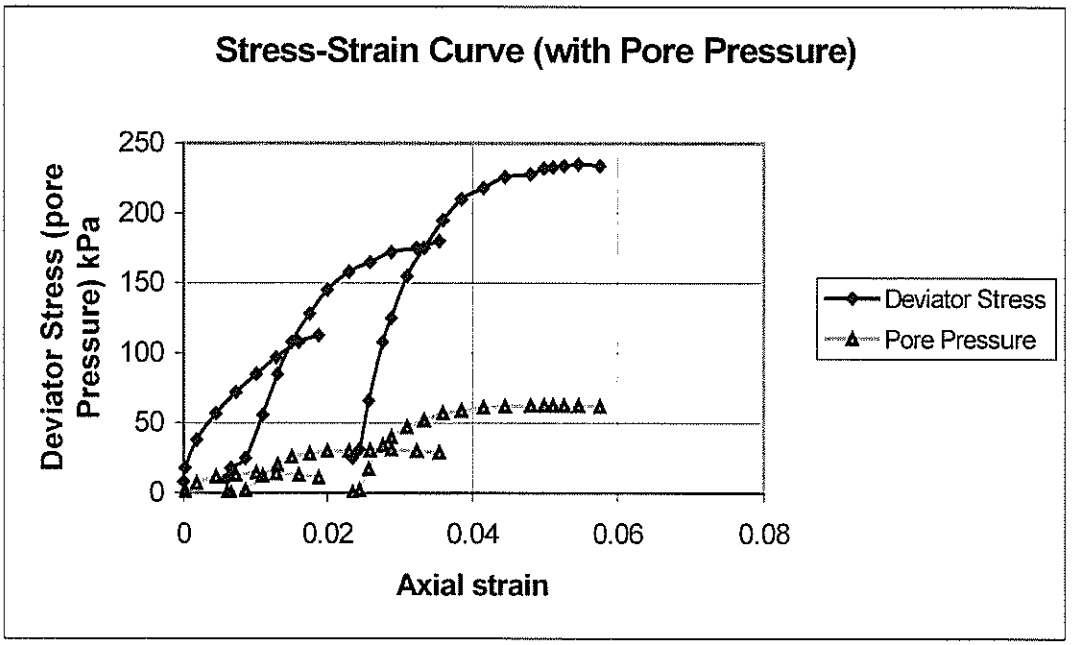

Figure 1. Triaxial Test Stress-Strain Curve

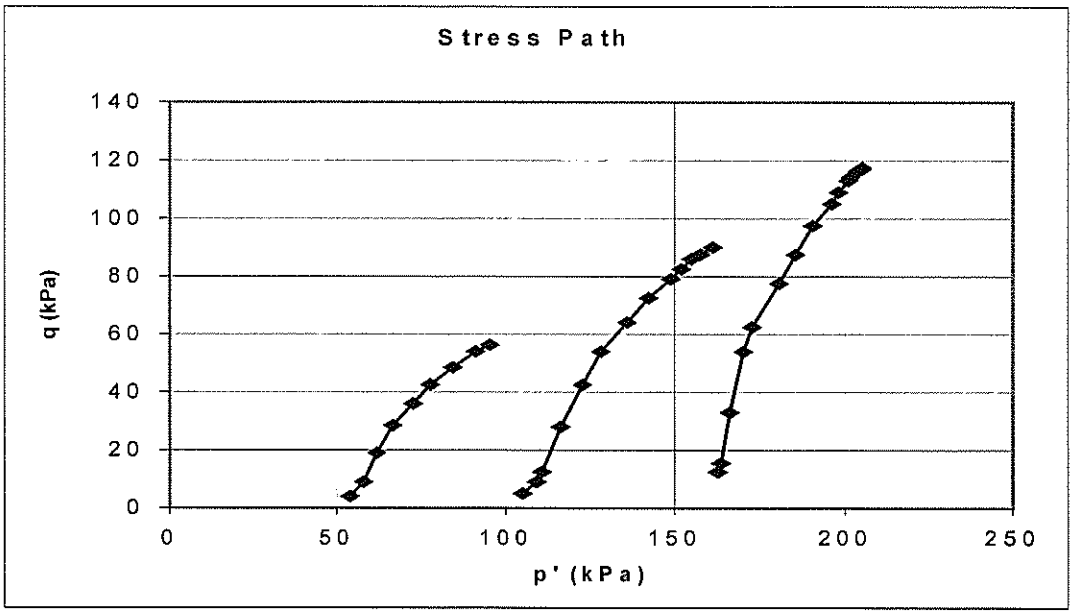

Figure 2. Triaxial Test Stress Path

This particular sample has reported effective stress parameters of c'=10 kPa and ϕ' = 34° based on maximum stress ratio. An E_{50} of 7,500 kPa has been assessed for a reference pressure of 50 kPa. The

stress paths suggest over-consolidated behaviour with very small increase in pore pressure due to shear stress. However, in comparison there was very large volumetric strain during the consolidation phase, typically around 1.5%. This large volumetric strain needs to be examined in greater detail as part of a separate study.

In order to choose a suitable model for use in modelling the soil, one should consider the essential characteristics of the available models compared to the features that need to be simulated. A basic elastic-perfectly plastic model (such as is commonly termed a mohr-coulomb model) would not be suitable as it does not emulate the change in stiffness with pre-failure shear strain,. Equally the pore pressure generation in undrained loading is fixed at a Skempton pore pressure parameter A=1/3. A third issue is it does not model the change in stiffness as a result of increasing confinement. Hence a mohr coulomb model should not be used unless the strain range was sufficiently small such that the assumption of elasticity was justified. A simulation based on cam-clay family of models could also be used. Most of the current models model compaction of a normally to lightly consolidated clay very well, but are less effective a modelling the changes in stiffness or volume as a result of shear strain. Likewise there is the 'Hyperbolic' family of models. These are based on the observation that the stress-strain curve on materials undergoing a tri-axial test matches a portion of a hyperbola. These models tend to match the changes in stiffness as a result of shear very well, though tend not to be so good in matching volumetric compression.

A hyperbolic model (Duncan et al 1980 & Schanz et al 1996) was selected for the numerical model on the grounds that it better represents the volumetric behaviour during triaxial testing which results from shearing rather than compaction. In addition, the modulus is stress dependent with confining pressure. The simulation was set up using a commercial finite element program.

The parameters identified above are used in one round of numerical modelling. Figures 3 and 4 show the resulting stress-strain diagrams and stress path with other parameters set on the programme default values (based on international experience of the program "PLAXIS" use). Whilst the initial moduli and total strength look reasonable, the strain to failure, pore pressures, and the stress paths are suspect.

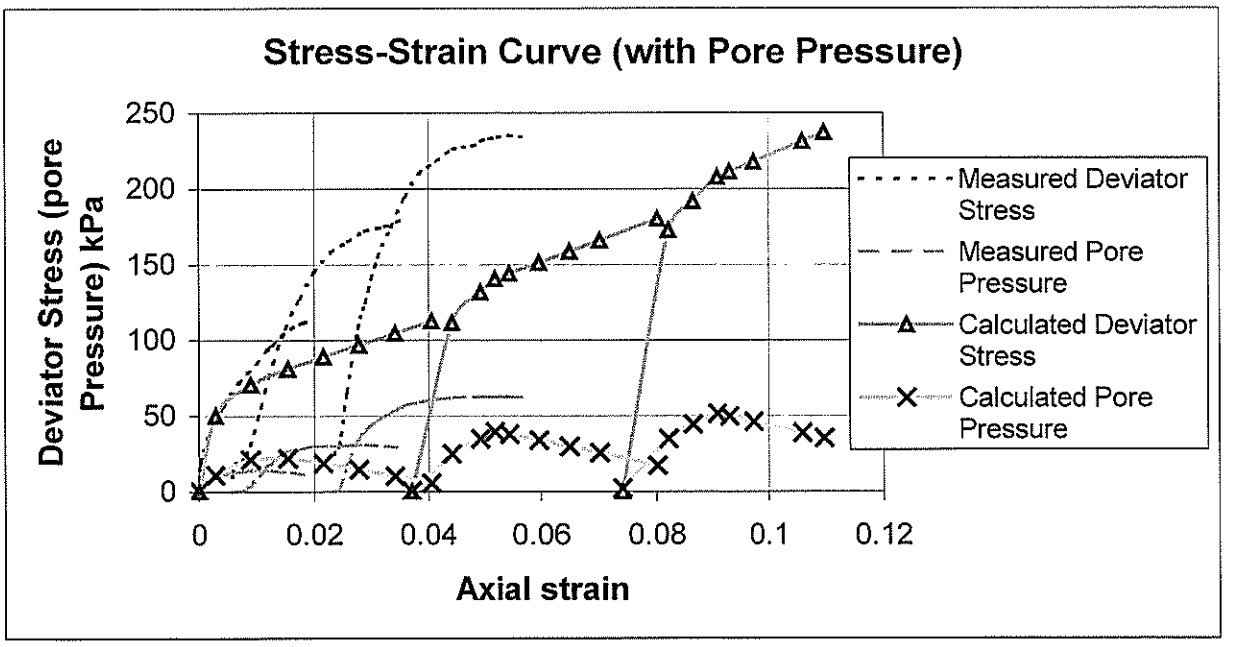

Figure 3. Comparison of Triaxial and Numerical Model Stress Strain Curves (default parameters).

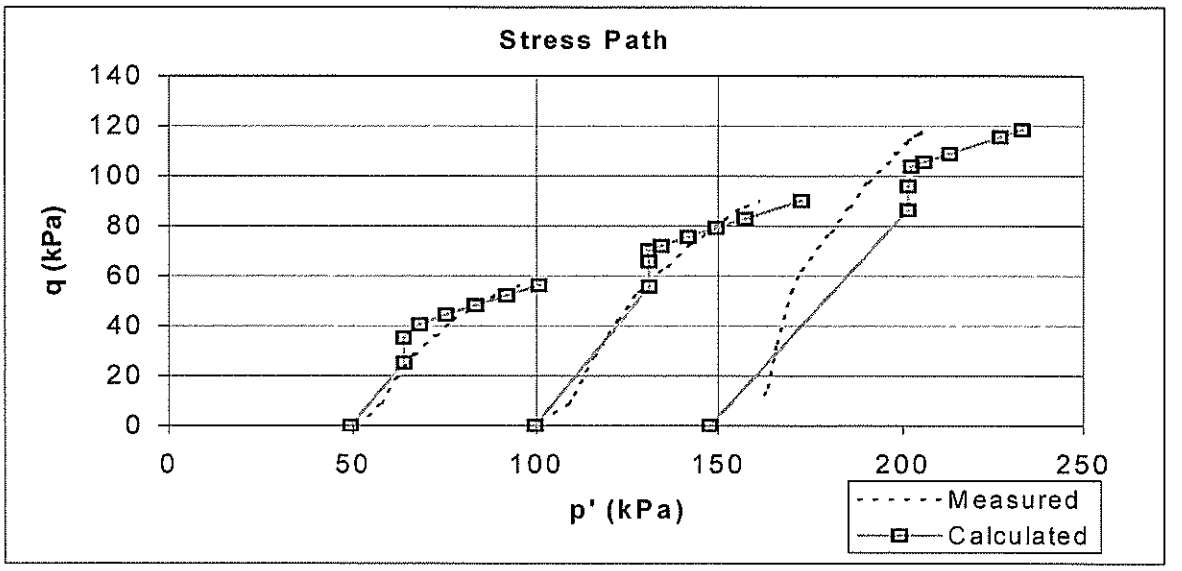

Figure 4. Comparison of Triaxial and Numerical Model Stress Path (default parameters)

This demonstrates that there is a substantial difference between conventional correlations and Auckland materials. This also illustrates the need to select the appropriate modulus for the stress and strain range that will be experienced by the soils under load.

By changing a number of the parameters it was possible to obtain a sufficiently good match to use for a critical deformation/strength analysis, (Figures 5 and 6). The limited match leads one to suspect that the underlying model is not fully effective for these Auckland soils.

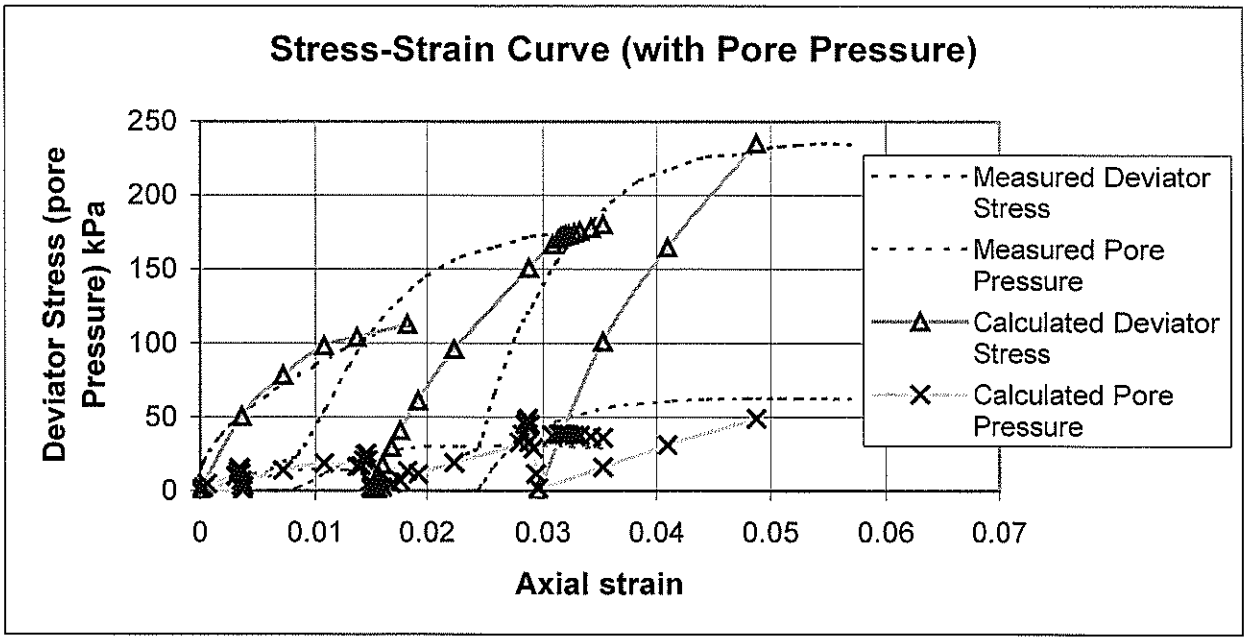

Figure 5. Comparison of Triaxial and Numerical Model Stress- Strain Curve (optimised parameters)

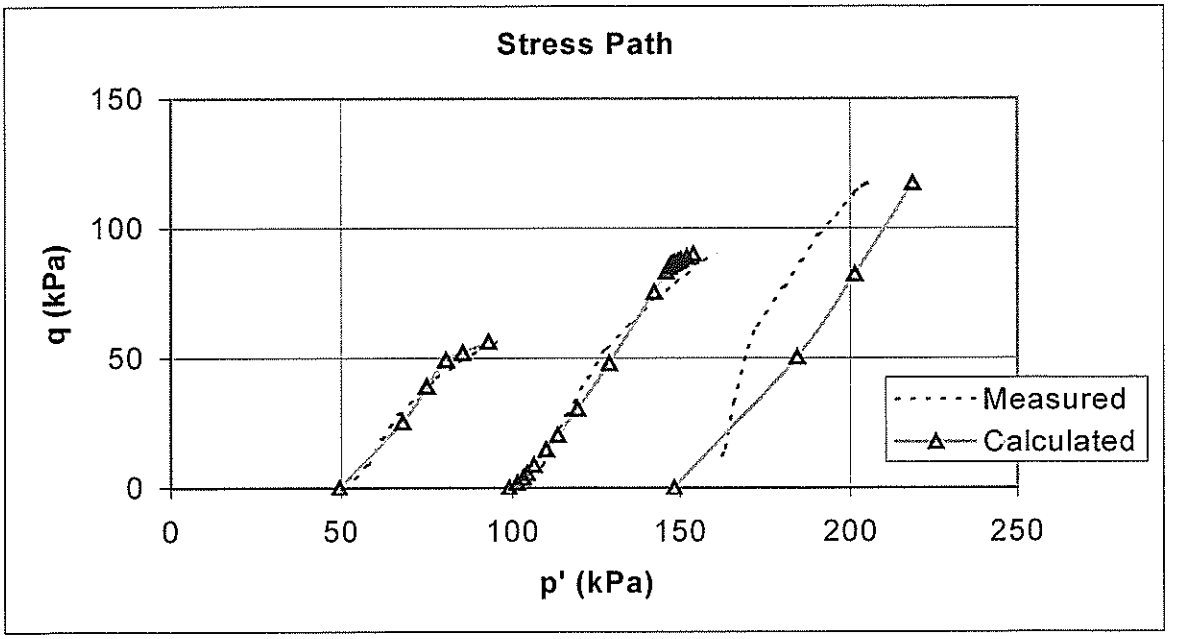

Figure 6. Comparison of Triaxial and Numerical Model Stress Path (optimised parameters)

In order to provide a better match the following model input parameters needed to be adjusted; the stress dependency exponent,, unload / reload modulus and the dilation angle. In the first instance, the stress dependency of the stiffness modulus is small, though significant. This is represented by the equation $E= E_{ref}(\sigma_c/(\sigma_{ref})^{0.2}$. An exponent of around 0.2 was used, compared with an exponent of 0.7 that is more typical. The differential between the in situ modulus and an unload-reload modulus is present, though again smaller than normal. The unload-reload seems to be approximately 1.5 times the E_{ref}, though for this numerical program only a factor of 2 was permissible. A factor of 3 to ten is more usual range for soils.

The angle of dilation is a strength parameter that is commonly ignored. It relates the volumetric change of a sample to the amount of shear strain in drained loading. Interestingly, introducing a large dilation angle was effective in bringing the models closer to the laboratory. test behaviour. This is an element of the Waitemata Clay characteristics that is worthy of further study. If the observations of the dilation angle is correct, it will influence the way that laboratory test data is interpreted. A number of other parameters were also adjusted by small amounts, including the stiffness moduli, friction angle (up), and cohesion (down).

Curvature of the strength envelope is a further element of behaviour not demonstrated well by the numerical model. The final stage is not well represented in the model, and this reflects in part changing strength and possibly a change in material parameters due to increased pressure.

It is now proposed to complete a full scale test of the revised model parameters by comparing calculated behaviour with observed behaviour of a specific monitored site.

CONCLUSIONS

This comparison of numerical model behaviour and laboratory / in situ test behaviour shows that the existing models commonly in use within commercial analysis programmes do not represent well the typical Waitemata material behaviour. It is also evident that much further research needs to be performed to clarify the underlying behaviour of these materials in order to permit the effective modelling of the material. Such modelling is expected to be needed as infrastructure development in the Auckland region increases with the consequent demand that the impact of development be minimal on existing structures and services.

REFERENCES

Duncan, J.M., Byrne, P., Wong, K.S., Mabry, P., Strength, Stress-Strain and Bulk Modulus Parameters for Finite Element Analyses of Stresses and Movements in Soil Masses, Report No UCB/GT/80-01, University of Berkeley, 1980

Pender, M.J. Wesley, L.D. Twose, G., Duske, G.C., Pranjoto, S., Auckland Residual Soil – Compressibility Measurement, New Zealand Geotechnical Society Geomechanics News, Issue 60, December 2000.

Schanz, T., Vermeer, P.A., Bonnier P.G., Formulation and verification of the Hardening soil model, Beyond 2000 in Computational Geotechnics, Balkema, 1999.

Relic Slip Verification Study – Tauranga District

D H Bell
Senior Lecturer in Engineering Geology
University of Canterbury, Christchurch
L Richards
Rock Engineering Consultant
The Old School House, Ellesmere, Canterbury
R Thomson
Consulting Geologist
Cromwell, Central Otago

Abstract: A study carried out by the authors in late 2000 using air-photo interpretation, supplemented by field checking, identified more than 2000 features of actual or probable landslip origin within the volcanic and fluviatile/estuarine deposits of the Tauranga District. Information has been transferred to the Council GIS database using a series of 1:5,000 base plans, and the data analysed to assess debris runout distances and scarp height/depth (V:H) ratios. Earlier studies had shown that a cliff zone defined by a ratio of 1V:2H effectively predicted the area of concern for slope stability assessment, and these so-called hazard zones were adopted by Council despite inevitable plotting errors. Our studies from a much more robust data set have generally confirmed the 1V:2H zone for cliff-top regression, but have also shown a significantly greater travel distance for debris runout than previously anticipated with an overall travel angle between 1V:3H and 1V:4H (18-14°). Although less than 1% of the landslips identified are currently active, the presence of relic slips remains a major issue for land development in Tauranga and reporting guidelines have been developed for geotechnical practitioners.

INTRODUCTION

The study described here was initiated by Tauranga District Council in late 2000, with the specific aims of 1) reviewing the existing landslip data on Council's GIS database; 2) carrying out a photogeological interpretation of various aerial photograph runs flown between 1943 and 1997; 3) transferring the new information to the Council database using 1:5,000 plans with 2m contour interval; and 4) assessing the geotechnical implications arising from these new data. A study by Houghton and Hegan (1980) had previously identified some 250 relic slips in the Tauranga City area which had been plotted onto a 1:40,000 base map, but subsequent errors in transferring this information to Council's GIS database had resulted in plotting errors up to 50m in plan location. The landslip features that had previously been plotted were principally located along steeper cliff lines, either those being actively undercut by wave action or forming abandoned slopes cut originally by marine or fluvial processes. The present study has focused on all landslip features identifiable using an extensive air-photo data set comprising ten different runs flown between 1943 and 1997, and the photogeology was carried out by one of the authors (R Thomson) whilst limited field checks were carried out by two of us (D Bell & R Thomson) as part of the relic slip verification process. Detailed analysis of the data obtained was then completed by the third author (L Richards) to establish vertical height:horizontal distance (V:H) relationships as part of the overall geotechnical evaluation for Council. This study integrates the new data on landslip features with the overall geology of the Tauranga area (Briggs et al, 1996), and an interpretation of landslip failure models derived from work at Maungatapu Peninsula by Oliver (1997).

PHOTOGEOLOGY STUDIES

The geology of the Tauranga area comprises a sequence of older volcanic rocks including dacites, rhyolites and ignimbrites ranging in age from about 2.5 to 0.5Ma, together with associated fluviatile and estuarine sediments of the Matua Subgroup (c.2.0-0.05Ma). Younger airfall tephras, including the Hamilton Ash (0.35-0.1Ma) and Rotoehu Ash (c.50ka), overlie the landscape and drape a series of

terraces reflecting progressive basin development and sea-level fluctuations during the Quaternary. The stratigraphy of the area is complex, and for most practical purposes can be considered (from oldest to youngest) as the Matua Subgroup/Tauranga Group, Hamilton Ash, Rotoehu Ash and the Post-Rotoehu Ash Tephras, each of which has distinctive geological and geotechnical characteristics.

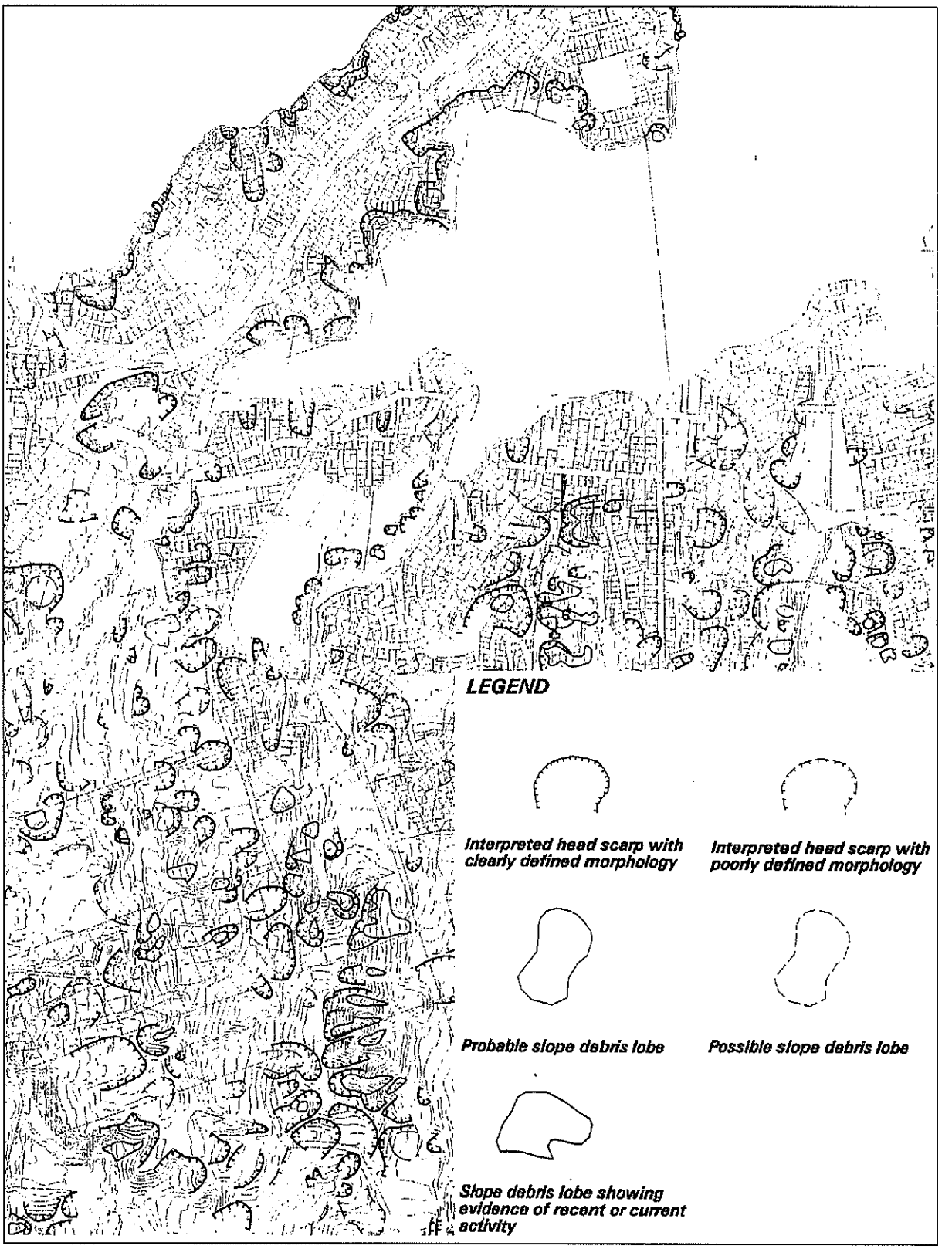

Figure 1. Part of 1:20,000 GIS Compilation for Tauranga Showing Mapping Procedure and Legend. [Note that original map is colour-coded to identify specific feature types].

A total of ten black-and-white aerial photograph sets were provided by Tauranga District Council for this study, these being flown in February 1943, January 1959, December 1971, September 1973, January and June 1975, May 1977, October 1978, March/April 1997, and March/June 1997. Many of the photo scales were between 1:2,000 and 1:6,000, and most were greater than 1:20,000, making recognition of relic landslips relatively straightforward even though many were only arcuate features from which all debris had been removed (Figure 1). The classification system used to describe the relic slips was, after field checking, recorded as follows (Figure 1):

- Possible headscarps and/or debris lobes with poorly defined morphology (~1000 features)
- Probable headscarps and/or debris lobes with clearly defined morphology (~1000 features)
- Active features with evidence for recent or current movement (13 in total)

In total more than 2,000 relic slips were recognised and mapped within Tauranga City and environs during this study, the term *relic slip* being used to mean "*the remnants of a previous landslide which has been inferred from the presence of a headscarp feature and/or hummocky slope debris*". The above terminology was adopted in part for consistency with the earlier study by Houghton and Hegan (1980), in which they used the terms "probable" and "possible" to record a degree of subjectivity as to the certainty with which specific features had been identified as being of landslip origin.

DATA SYNTHESIS AND ANALYSIS

Specific landslide attributes were determined for each of the relic slips, which comprised more than 2,000 recognised headscarp features and over 400 slope debris lobes. Terminology used is shown in Figure 2, and typical analysed profiles based on geometry and interpreted geomorphology are given in Figure 3. The following data were formatted into an Excel™ spreadsheet to enable calculation of scarp and runout angles (the latter where possible) in relation to the 2H:1V (26.5°) hazard "zone" under investigation:

- Relic slip reference number and coordinates in terms of the New Zealand map grid.
- Scarp height, distance and width, together with scarp crest and base RLs (to nearest metre).
- Runout distance (from headscarp) and maximum width, with debris toe and top RLs.
- Slope angles for the scarp segment and the runout zone (defined from headscarp to toe).
- Geological unit data, comment on surface hydrology, and any other relevant factors.

The scarp angle, which is defined by the ratio of the vertical height to the horizontal distance from the head to the toe of the scarp, was found to average about 15° and this equates to a slope of 3.75H:1V. Tait (2002) interpreted the same data set for 2080 landslips, and found that 32% of all relic slip scarps were steeper than 25° (approximately 2H:1V), whilst 31% were flatter than 15° (3.75H:1V), with some variability due to geology. The analysed relic slips do not show the expected decrease of scarp angle with increasing slope height, and the correlation is not good between the location of mapped landslip features and Council's 2H:1V zone. Nevertheless, experience has shown that the 2H:1V criterion does provide a simple screening technique for slopes requiring specialist geotechnical input, as this is equivalent to a lower bound friction angle for the near-surface ash deposits of Tauranga and should give realistic factors of safety greater than 1.5 in conventional stability analysis.

The runout (or travel) angle, which is defined by the ratio of height difference from headscarp crest to runout toe divided by the equivalent horizontal distance, gave a similar mean of about 15° or 3.75H:1V. Four of the six slips shown in Figure 3 include runout debris, and three of these have computed travel angles in excess of 3H:1V consistent with this mean value. Given that the youngest (Rotoehu and post-Rotoehu) ashes of the Tauranga area typically have friction angles of 30° or greater, however, theoretical travel angles of about 1.7H:1V would be predicted. It is suggested that the observed values of about 4H:1V are indicative of much greater mobility of the ash materials due to their low densities at around 1200-1400 kg/m^3, with flow behaviour being induced by rainfall infiltration or saturation due to seepage.

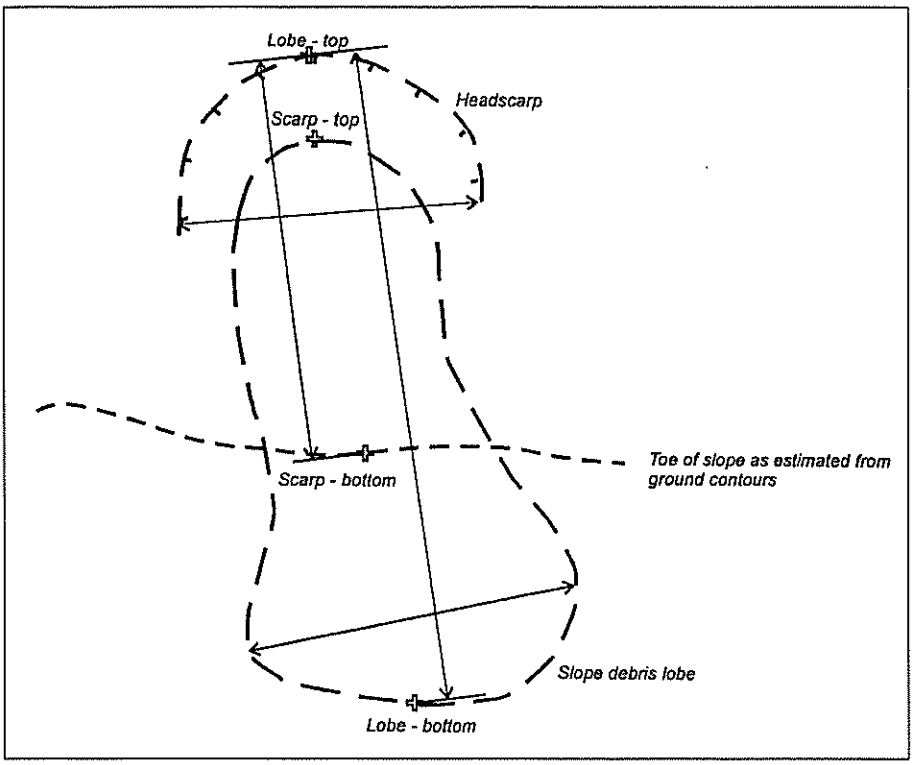

Figure 2. Basic Terminology Used to Define Landslide Attributes for Analysis.

GEOTECHNICAL IMPLICATIONS

In assessing the stability of cliffs or steeper slopes in the volcanic soils of the Tauranga area, the 2H:1V criterion has become an accepted means of identifying and administering concerns regarding slope instability in relation to residential development. Following their investigation of serious coastal instability at Omokoroa (some 10km northeast of Tauranga) in August 1979, Tonkin & Taylor (1980) concluded that slope failures would not extend beyond a 2.25H:1V limit (~24°) and they recommended a setback distance of 6m from the 2.25H:1V "hazard line". Subsequently Houghton & Hegan (1980) recommended a 2H:1V line to define the potential limit of slope instability in the Tauranga volcanic soils, which has now become widely accepted, although again their conclusions appear to have been strongly influenced by the Omokoroa study. Given that the 2H:1V criterion is based on an active-passive wedge geometry (Figure 4 (a)) in which the ash deposits fail above an aquifer within sediments of the Tauranga Group (or Matua Sub-Group) due to pore pressure effects, it is surprising that a number of practitioners continue to analyse for deep-seated circular failures in the volcanic soils of Tauranga (such as the profile shown in Figure 4 (b)).

Bird (1981), and later Oliver (1997), carefully observed and documented slope failures (especially in cliffed areas such as Maungatapu Peninsula), and it is important to reiterate that an appropriate engineering geology model is a necessary pre-requisite to quantitative stability analysis. Oliver (1997) identified four main modes of slope failure in the Tauranga area, these being 1) large-scale block failures, possibly retrogressive and typically $>10^5$ m^3 in volume; 2) piping-triggered block failures, such as those at Omokoroa and Maungatapu; 3) wave erosion-triggered block failures due to active cliff undercutting; and 4) shallow regolith or colluvium/topsoil failures. Of these, it is the piping-triggered block failures that are of particular concern in Tauranga, and there are interesting similarities with the chalk cliff failure model recognised by Hutchinson (1970) at Joss Bay in the United Kingdom. Four geometric models for this type of failure are shown in Figure 4, of which (c) and (d) are considered the most likely to describe the situation where either "blowout" or softening occurs within an aquifer unit between impermeable sub-horizontal beds in the basal Matua Subgroup with consequent steep (60°±) backscarp development in the overlying ashes and sediments.

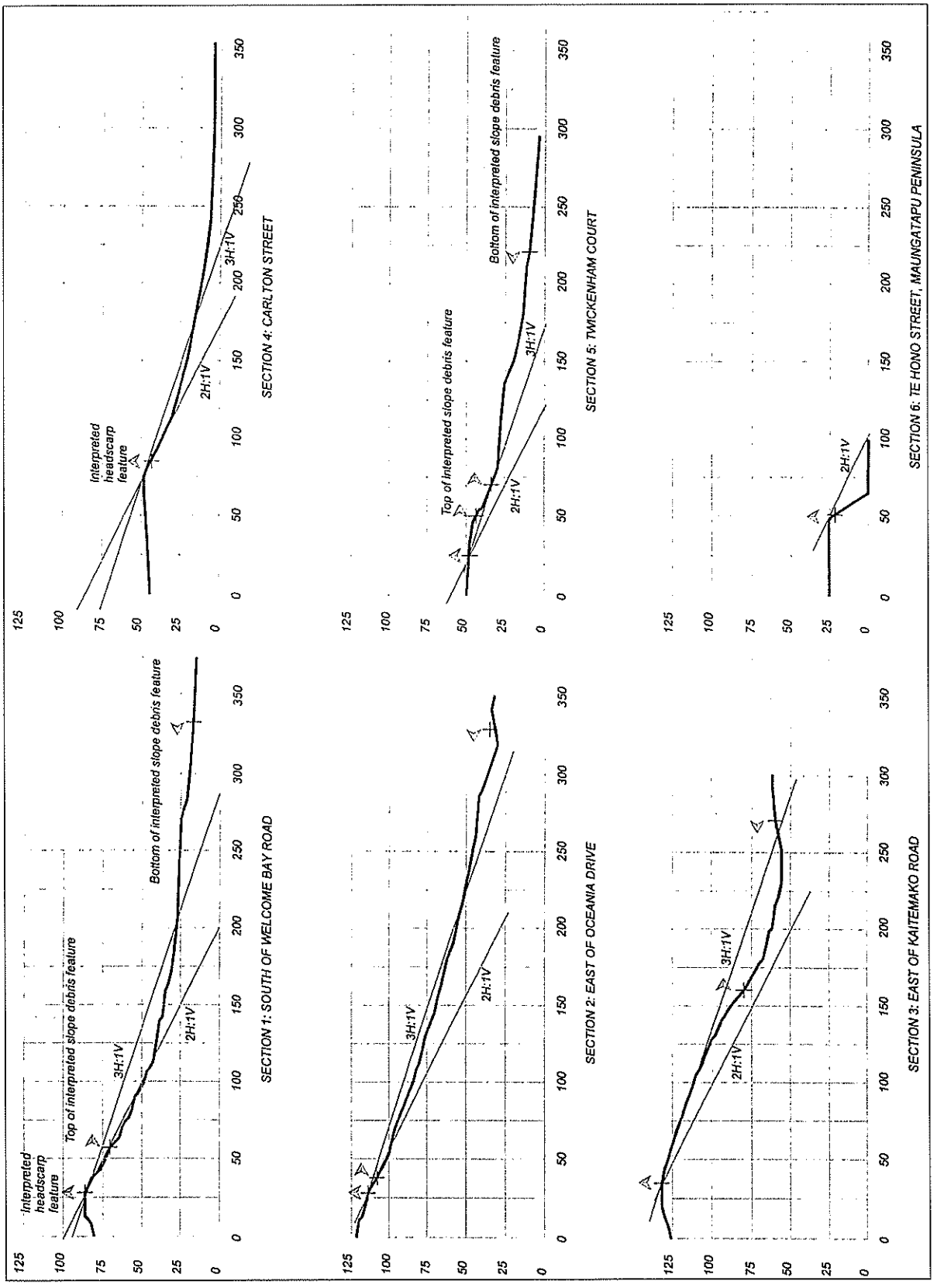

Figure 3. Six Profiles Analysed in Terms of Slope Gradient.

The relic slip verification study has generally confirmed that the 2H:1V slope criterion is still a valid approach to identifying areas where instability may occur on steeper slopes, although it can in no way replace or substitute for site-specific investigation and analysis in conjunction with detailed air-photo studies including use of the landslide inventory maps generated by this study. Instability is more likely in cases where a cliff is being actively undercut by wave erosion, while fluctuating sea-levels of the Late Quaternary have also been a factor as evidenced by the variety of terrace distributions and surface elevations. Further study of the age and development of the Tauranga landscape is clearly warranted, both from a geomorphological perspective and to assist with future urban planning in the district, and the present study has confirmed that geology does have some obvious controls on slope evolution even though that data are not presented or discussed in any detail in this paper.

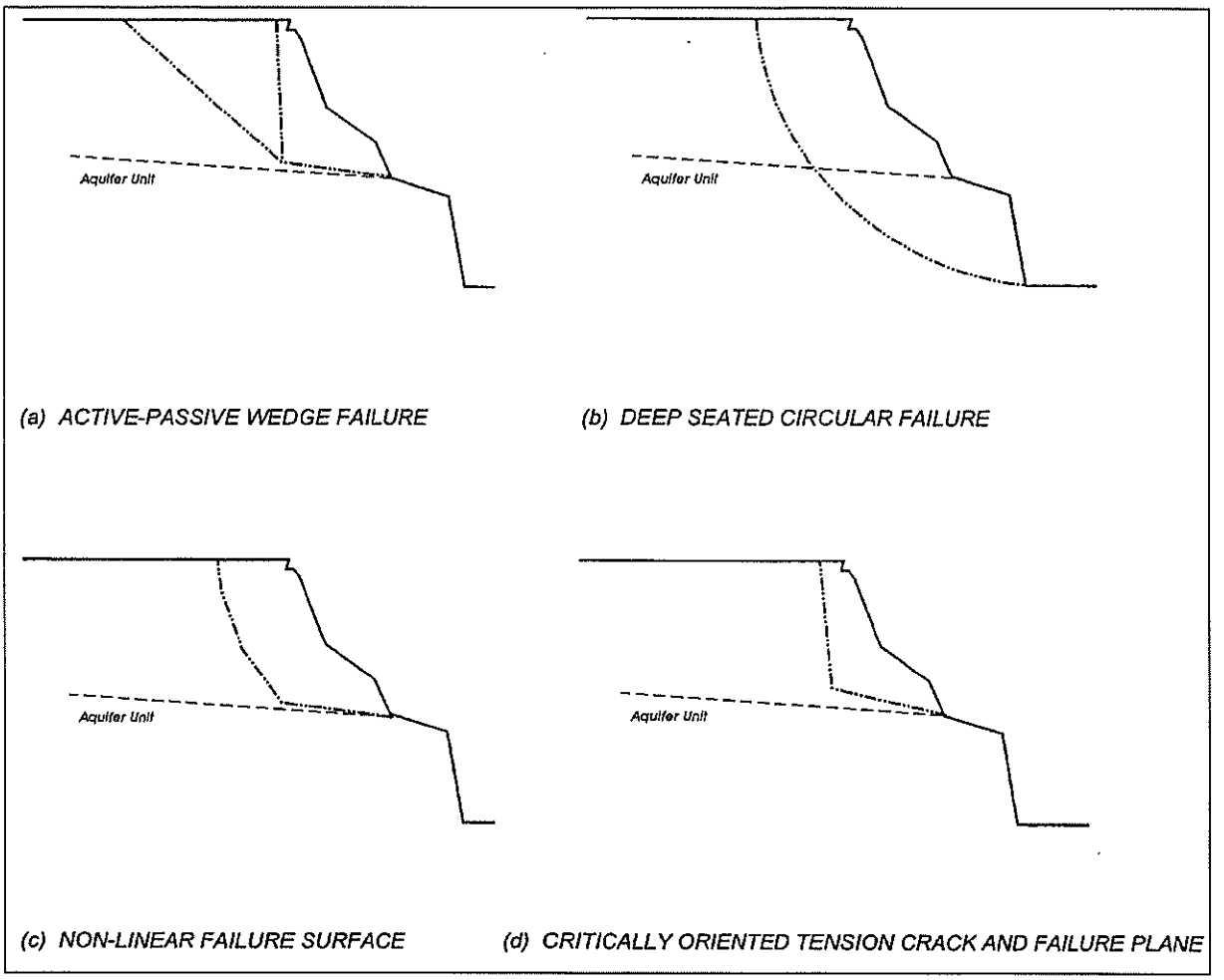

Figure 4. Possible Failure Models for Stability Analysis of Piping-Initiated Block Slides in Tauranga as Used by Local Geotechnical Practitioners. [Refer to text for brief discussion].

The scarp angle only exceeds 30° in 15% of the cases analysed (Tait, 2002), and clearly longer-term degradation post-failure will produce a significantly lower angle especially if seepage is occurring actively from the face. A realistic setback distance from the scarp or cliff top is required, and the original approach developed by Tonkin & Taylor (1980) for Omokoroa (6m beyond the 2.25H:1V hazard line) is probably still appropriately conservative in the absence of existing instability or other information. Our analyses using data from Maungatapu Peninsula suggest that a 2H:1V line from the cliff base should correspond to a factor of safety of about 2.0 for a realistic failure model, although each site must clearly be considered in its own geological, geomorphological and geotechnical context. We note again that the so-called 2H:1V "hazard line" is measured from the crest of the steeper slope segment to its ultimate base, and that the great majority of failures recorded lie within this zone and already incorporate a conservative setback distance.

The issue of toe runout from landslips in the Tauranga area does not appear to have been evaluated fully in previous studies, and the data generated by the relic slip verification study suggest that the runout or travel angle will frequently exceed 3.75H:1V (15°). The travel angle is defined from the crest of the slope to the toe of the runout debris where present (as shown in Figure 2), and this has clear implications for construction of dwellings either within former (= evacuated) landslip features or by siting them close to the toe of a steep cliff where failure might occur. The need to investigate a site well beyond the limits of the building footprint is reiterated, with air-photo interpretation offering an obvious first stage in identifying historical changes in slope geometry or position. The fact that past slope failures appear to have been significantly more mobile than expected, with an implied friction angle of about 15°, indicates that this geotechnical issue requires careful consideration especially for buildings in gully-mouth areas where debris flows could be a significant concern.

Whilst less than 1% of the relic slips studied were considered to be active, and a number have probably been removed by earthworks, one intent of the landslip inventory arising from this study is that both the Council and the practitioner will use the database to ensure that appropriate investigations are designed and carried out where there is any possible issue regarding past slope or land instability. Normal site investigation procedures (desk study; walkover; air-photo interpretation; site mapping; test pits; boreholes; etc) remain the key to successful geotechnical practice in this relatively difficult volcanic terrain, and local experience together with a knowledge of geological precedent are most important factors. We consider in fact that many sites can be at least initially evaluated from careful air-photo study and on-site geological investigation, and that much greater reliance can be placed on this information than on either numerical analyses using unsatisfactory failure models or the use of qualitative pseudo-probabilistic descriptions (for example, as outlined by the Australian Geomechanics Society Subcommittee on Landslide Risk Management, 2000).

PROFESSIONAL CONSIDERATIONS

Since May 1993 Tauranga District Council has operated an accreditation system for geotechnical specialists, whereby both engineering geologists and geotechnical engineers are evaluated in terms of qualifications, relevant experience, level of mentoring, quality of reporting, and responses at a Panel interview. Specialist (Category 1) advisers are accredited to report on any specific matter, in particular the development of steeper slopes, assessing or stabilising existing landslides, and difficult ground conditions (eg land prone to liquefaction): Category 2 specialists are accredited to deal with flatter slopes and/or ground with no evidence for landslip, and there is proviso for them to work on Category 1 sites with appropriate peer review at the client's expense. The rationale behind this approach, and the basis on which it was implemented to deal with perceived difficult ground conditions in the Tauranga area, is detailed by Petrenas (1996): he makes the point that prior to 1993 Council staff relied on their own judgement as to the ability of geotechnical specialists, but that the new system has provided greater transparency and quality assurance in terms of practitioner competence.

Arising from this study we recommend that Category 1 specialist advisers (as presently defined) be required to report on the following in terms of slope stability assessment:

- Sites with probable slope movements showing clearly defined headscarps, hummocky debris, and/or evidence for current/recent activity.
- Sites with possible slope movement features and evidence for either or both poorly defined headscarps and hummocky debris.
- Buildings located within the 2H:1V slope line (ie land steeper than about 26°) or within the 4H:1V runout distance from the slope crest.
- Sites with water seepage or discharge from the slope at any height.

Unless their work is peer-reviewed, Category 2 specialists are restricted to sites where there is no evidence of slope instability within (or in close proximity to) the existing or proposed development, and where the building is located outside the 2H:1V slope line or the 4H:1V runout distance from the slope crest. Category 3 sites are those where there is no requirement for specialist geotechnical or engineering geology data input or assessment.

The system now operating within Tauranga City and environs is designed to ensure that suitably experienced geotechnical practitioners with sound local knowledge are responsible for investigating and reporting on the more difficult sites, and that appropriate levels of mentoring and peer review are available to younger or less experienced engineering geologists and geotechnical engineers. As part of our study assessment guidelines have been developed to assist practitioners, although we do not advocate a "checklist approach" to site evaluation because of the possibility of failing to recognise unusual or critical information. Instead we strongly believe that sound engineering geology, with quality air-photo interpretation, is an essential tool within the Tauranga area and be should be used more widely to develop site-specific models prior to, and at times instead of, quantitative stability analysis. The scarp and runout angle guidelines are also simply another technique to draw attention to possible instability concerns adjacent to steeper slopes or cliff lines, whilst the relic landslip inventory that has been presented here is intended to provide additional guidance for the experienced practitioner and should not be considered definitive in its own right.

The presence or absence of groundwater within a slope, reticulation/disposal or direct infiltration of stormwater, and antecedent rainfall/threshold triggering conditions all remain issues for professional judgement and/or site-specific investigation. Further studies are clearly warranted, including long-term monitoring of groundwater levels and responses within the slopes of Tauranga City, and evaluation of the likely threshold levels of precipitation triggering both piping-initiated instability and shallow regolith failures. The recognition of past instability at a site, and knowledge of groundwater conditions and likely extremes at that site, are the keys to safe design and/or slope remediation where an appropriate engineering geology model has been developed and quantified as required. Ultimately, however, it is the competence and professionalism of the practitioners working in the Tauranga District that will ensure future geotechnical problems are identified, evaluated and remediated or avoided without loss of life or significant property damage.

CONCLUSIONS & RECOMMENDATIONS

1. The present study has identified more than 2,000 relic slip features in Tauranga City and environs, of which approximately equal numbers (~1,000 of each) have been classed as probable and possible on the basis of headscarp or debris lobe morphology: only 13 presently or recently active landslip features with clearly defined surface morphology have been recognised, representing less than 1% of the total number of relic slips.

2. The relic slip features have been recognised primarily using air-photos that were flown between 1943 and 1997, supplemented by limited field checks, and the data have been transferred to Council's GIS database using 1:5,000 field sheets with appropriate topographic and cadastral information: a 1:20,000 compilation map has also been prepared, although further work is required to identify those landslip features which have been removed by later earthworks.

3. Landslip attributes have been measured and analysed, in particular the scarp height/horizontal distance relationship and the debris lobe dimensions where this feature is preserved: our data confirm that 2H:1V (26.5°) is realistic for the scarp angle, as has previously been adopted following work at Omokoroa in 1979-80, and that a runout or travel angle (defined from scarp crest to debris lobe toe) of 4H:1V (14°) is an appropriate measure of potential landslip mobility.

4. We recommend that Council adopt these guidelines for land-use planning purposes, especially for residential building sites, and that these criteria be used in conjunction with the relic slip inventory data to plan and implement site investigations: Category 1 geotechnical specialists should be involved with land steeper than 2H:1V (as at present), within the potential 4H:1V runout zone which does not appear to have been adequately addressed in the past, and where active landslip features are present.

5. In our opinion greater use should be made of engineering geology and photogeology techniques in identifying geotechnical constraints or hazards, and in formulating appropriate site models for quantitative stability analysis where required: whilst assessment guidelines have been developed by us to facilitate such work, it is the competence and professionalism of geotechnical practitioners that is of greatest importance for future land development in the Tauranga area.

6. Future research should involve development of a geotechnical database for Tauranga and adjacent areas, including relic slip information and documentation of future landslips and debris flows as well as the distribution of specific volcanic units from exposure logging and mapping: further study of the geomorphological development of the Tauranga area is also recommended, so that better constraints can be placed on the age of specific landscape features for planning purposes.

REFERENCES

Australian Geomechanics Society Sub-Committee on Landslide Risk Management (2000) *"Landslide Risk Management Concepts and Guidelines," NZ Geomechanics News, Issue 60: 61-92*

Bell, D.H.; Richards, L.; Thomson, R. (2001) *"Relic Slip Verification Study – Tauranga District Council Environs," Unpublished Consultant Report to Tauranga District Council, March 2001*

Bird, G.A. (1981). "The Nature and Causes of Coastal Landsliding on the Maungatapu Peninsula, Tauranga, New Zealand," *Unpublished MSc Thesis, University of Waikato Library.*

Briggs, R.M.; Hall, G.J.; Harmsworth, G.R.; Hollis, A.G.; Houghton, B.F.; Hughes, G.R.; Morgan, M.D.; Whitbread-Edwards, A.R.(1996). "Geology of the Tauranga Area," *Occasional Report No 22, Department of Earth Sciences, University of Waikato.*

Houghton, B.F. and Hegan, B.D. (1980). "Preliminary Assessment of Geological Factors influencing Slope Stability and Landslipping in and around Tauranga City," *NZ Geological Survey Engineering Geology Report EG248, October 1980.*

Hutchinson, J.N. (1970). "Field and Laboratory Studies of a Fall in the Upper Chalk Cliffs at Joss Bay, Isle of Thanet," *Proceedings of the Roscoe Memorial Symposium, Cambridge.*

Oliver, R.C. (1997). "A Geotechnical Characterisation of Volcanic Soils in relation to Coastal Landsliding on the Maungatapu Peninsula, Tauranga," *Unpublished MSc Eng Geol Thesis, University of Canterbury Library.*

Petrenas, B. (1996) "Accreditation of Geotechnical Engineers and Engineering Geologists," *Proc. Tech. Groups IPENZ, Volume 22, Issue 1(G):142-151*

Tait, T.M. (2002). "Slope Stability and Land-Use Planning, Tauranga District, New Zealand," *Unpublished MSc Eng Geol Thesis, University of Canterbury Library.*

Tonkin & Taylor Ltd (1980). "Omokoroa Point Land Stability Investigation," *Unpublished Consultant Report to Tauranga District Council, May 1980.*

Consolidation Testing of Huka Falls Formation – Properties Related to Subsidence at Ohaaki and Wairakei

S A L Read
BSc (Hons)
Engineering geologist, Institute of Geological & Nuclear Sciences Ltd
M J Pender
BE (Hons), PhD, FIPENZ, Life Member NZGS
Professor of Geotechnical Engineering, University of Auckland
P R Barker
NZCS
Scientist, Barker Consulting
S Ellis
BSc (Hons), PhD
Scientist, Institute of Geological & Nuclear Sciences Ltd

Abstract: The Huka Falls Formation comprises sandstones, siltstones, mudstones and pumice breccias, which typically have high void ratios (e >1) normally associated with soils, but strengths equivalent to that of weak rocks (q_u >1 MPa). The results of laboratory consolidation testing of drillhole samples from Ohaaki geothermal field and surface samples from Te Totara Stream at Wairakei generally demonstrate differing coefficients of volume compressibility (m_v) either side of apparent pre-consolidation pressures between 0.5 and 5 MPa. Compressibility values at apparent pre-consolidation pressures appear to be greater in sandier materials (m_v >0.1 MPa^{-1}), decreasing with greater apparent pre-consolidation pressures and in muddier materials (m_v <0.05 MPa^{-1}).

INTRODUCTION

Ground subsidence at the Wairakei and Ohaaki geothermal fields in the central North Island is considered to be controlled by the properties of the Huka Falls Formation (Allis *et al.*, 1997; 1998). At Wairakei, consolidation of pumice breccias was initially identified as the likely cause (Allis and Barker, 1982), while work at Ohaaki focussed more on the behaviour of lower permeability mudstones (Allis *et al.*, 1997). The results of numerical modelling suggest that subsidence is controlled by either shallower horizons in the Huka Falls Formation, in particular mudstones (eg. Allis and Zhan, 2000), or by deeper, more compressible, horizons within the formation (eg. Lawless *et al.*, 2001).

Our objective was to examine the properties of Huka Falls Formation materials by laboratory consolidation testing of samples from both inside and outside subsidence areas at the two geothermal fields. The testing has included aspects related to the duration of each loading stage, influences from slightly elevated test temperatures (<80°C), and petrographic examination of samples before and after testing. Most of the results have been reported in Read *et al.*, (2001), and this paper focuses more on their assessment based on natural scale consolidation pressure plots along with compressibility values at apparent pre-consolidation pressures determined from traditional semi-logarithmic plots. This paper does not include numerical modelling of subsidence behaviour, and is restricted to the consolidation properties determined with some comments on their possible influences on subsidence mechanisms.

HUKA FALLS FORMATION

The Huka Falls Formation is widely distributed between Taupo and Rotorua (Figure 1). It was deposited in a lake, or lakes, existing from about 100,000 years ago until the Oruanui eruptions about 26,500 years ago. Conditions in the lake(s) were influenced by active hydrothermal systems and intrusion of nearby rhyolite domes. Younger eruptive sequences (eg. Oruanui), which may have been up to 100 m thick, form a mantling cover. Surface exposures of the formation are therefore rare, and are present mainly where there has been significant erosion, such as close to the Waikato River.

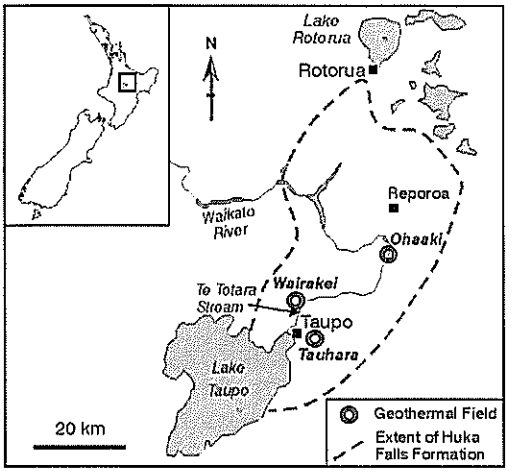

Figure 1: Location Map.

LITHOLOGY

Grindley (1965) recognised four units within the Huka Falls Formation, three being dominated by lacustrine sediments and one by volcaniclastics. The sediments typically range from very fine-grained, diatomaceous or carbonaceous mudstones, to siltstones and fine sandstones. Coarse sandstones and conglomerates are also present locally. The fine-grained sediments are commonly laminated or thinly bedded and include tuffaceous layers, while the volcanic unit is coarser-grained and dominated by vitric tuffs and tuffaceous sandstones.

The formation is up to 350 m thick, and bedding is typically sub-horizontal or shallow-dipping. Geothermal activity before, during, and after deposition has influenced mineral assemblages (Rosenberg and Hunt, 1999), with authigenic minerals dominated by smectite clays (Read *et al.*, 2001). Some thin layers and a few thicker horizons (eg. at the Huka Falls on the Waikato River) may be silicified.

ENGINEERING CLASSIFICATION PROPERTIES

Huka Falls Formation materials typically have low densities (Table 1), with a greater volume of voids than solids (ie. void ratio e >1). In an engineering sense, rock lithology names (eg. mudstone) are appropriate for the materials because their unconfined compressive strength test (q_u) values are greater than those for traditional soil/rock boundary at q_u = 1 MPa. (q_u values for samples from drillhole BRM-12 at Ohaaki - Allis *et al.*, 1997 - are 1.2 to 2.7 MPa).

Void ratios greater than 1 are usually associated with softer, normally consolidated, soil materials (ie. those not previously subjected to stresses greater than the loads from their present overburden). However, the weak rock material strengths of the Huka Falls Formation materials indicate that their properties are controlled by greater skeletal bonding than that created by the effects of overburden pressure alone. In comparison, many New Zealand Tertiary-age sedimentary rocks with similar unconfined compressive strengths have void ratios between 0.4 and 0.6 (Read and Millar, 1991).

Location	Material	Bulk density ρ [1] (t/m^3)	Dry density ρ_d [1] (t/m^3)	Void ratio e [1]	Porosity n [1]
Wairakei, Tauhara					
Robertson (1984)	Sediments	1.57 (0.18)	1.00 (0.24)	1.45 (0.47)	0.58 (0.08)
15 samples	Breccia	1.55 (0.11)	0.97 (0.19)	1.50 (0.45)	0.59 (0.08)
Ohaaki					
Rosenberg & Hunt (1999)	Sediments	1.79 (0.19)	1.36 (0.23)	0.85 (0.38)	0.44 (0.13)
51 samples	Tuffaceous	1.79 (0.21)	1.36 (0.31)	0.85 (0.31)	0.44 (0.12)

[1] Mean (standard deviation). Volumes measured after drying followed by saturation.

Table 1. Classification Properties of Huka Falls Formation at Wairakei, Tauhara and Ohaaki.

CONSOLIDATION TESTING

The testing programme used samples from the 170 m deep drillhole BRM-12 (Allis *et al.*, 1997) located inside the subsidence area at Ohaaki, and from surface exposures at Te Totara Stream (Figure 1), 1 km downstream of Huka Falls and outside the subsidence area at Wairakei. A total of 26 tests have been performed since 1995.

Methodology

Testing was performed in conventional balance-arm oedometer loading frames, using a test procedure based on New Zealand Standard 4402 (NZS 4402, 1986). After recovery, the HQ triple-tube cores from BRM-12 and block samples from Te Totara Stream were double-wrapped in plastic to preserve their close-to-saturation natural ('as received') water contents. Test specimens (20-25 mm thick) were trimmed into a 50 mm diameter ring, and surrounded by water after placement in the loading frame.

Loading was applied in 5 to 7 increasing increments until the apparent pre-consolidation pressure was reached, with two further increments beyond. The load, which was applied approximately normal to bedding, doubled with each increment and the largest pressure applied for each test was between ≈4 and ≈16 MPa (16 MPa is ≈1000m of overburden). Initial testing used a 1 hour loading cycle throughout the test, with an overnight extension at the greatest pressure and a single step unloading. The more recent testing was over longer periods. A 24 hour loading cycle was used at lower pressures, while at higher pressures the cycle was extended until the height change in a 24 hour period was much less than 1% of the height change at that pressure. This took up to 2 weeks, and in some cases was deliberately extended. Unloading reversed the increments, taking several days.

Because standard equipment is not available for conventional testing at geothermal temperatures (>100° C), testing at slightly elevated temperatures (50°-70° C) was performed on 4 samples from Te Totara Stream by connecting the water around the specimen to a temperature-controlled water bath.

Petrographic inspection of test specimens before and after loading was carried out using a scanning electron microscope (SEM). Mineral composition of bulk samples was determined by X-ray diffractometry, complemented by more detailed examination of clays by energy-dispersive X-ray (EDX) and optically on glass slides. These results are reported in more detail in Read *et al.* (2001).

Results

The consolidation test results in Figure 2 are plotted with a conventional logarithmic consolidation pressure scale (eg. NZS 4402, 1986). Both the more recent tests in Figure 2a (Ohaaki and Te Totara) and initial tests in Figure 2b (Ohaaki and some Wairakei) show a consistent response to loading. The Huka Falls Formation lithologies, which have a range of initial void ratios between 1 and 2, show little change in void ratio at lower pressures. At higher pressures they indicate considerable changes in void ratio that give a bi-linear appearance to the overall consolidation curves. The greatest changes, equivalent to about a 25% reduction in specimen height during a complete test, occur for materials with initial void ratios greater than 1.4. The most significant continuing height changes during the initial testing (Figure 2b) tended to be shown by muddier materials. For materials with lower initial void ratios, the changes tended to be less dramatic and more variable, including for the completely altered rhyolite (Ohaaki Rhyolite) at the base of drillhole BRM-12 which has a void ratio less than 1.

Recent experience with residual soils formed from the weathering of Tertiary-age sedimentary rocks in Auckland (Pender *et al.*, 2000, 2003) has shown that such bi-linear appearance can be an artifact of plotting procedure (ie. plotting an arithmetic line on a semi-logarithmic scale results in a curve). Janbu (1963) and Janbu and Senneset (1979) strongly advocated the plotting of consolidation test results with arithmetic (linear) scales as a more robust means of determining the pressure ranges over which material responses to loading are different. For over-consolidated materials, this would be either side of an apparent pre-consolidation pressure, before and after which a significant change in compressibility (or deformation modulus) would be expected.

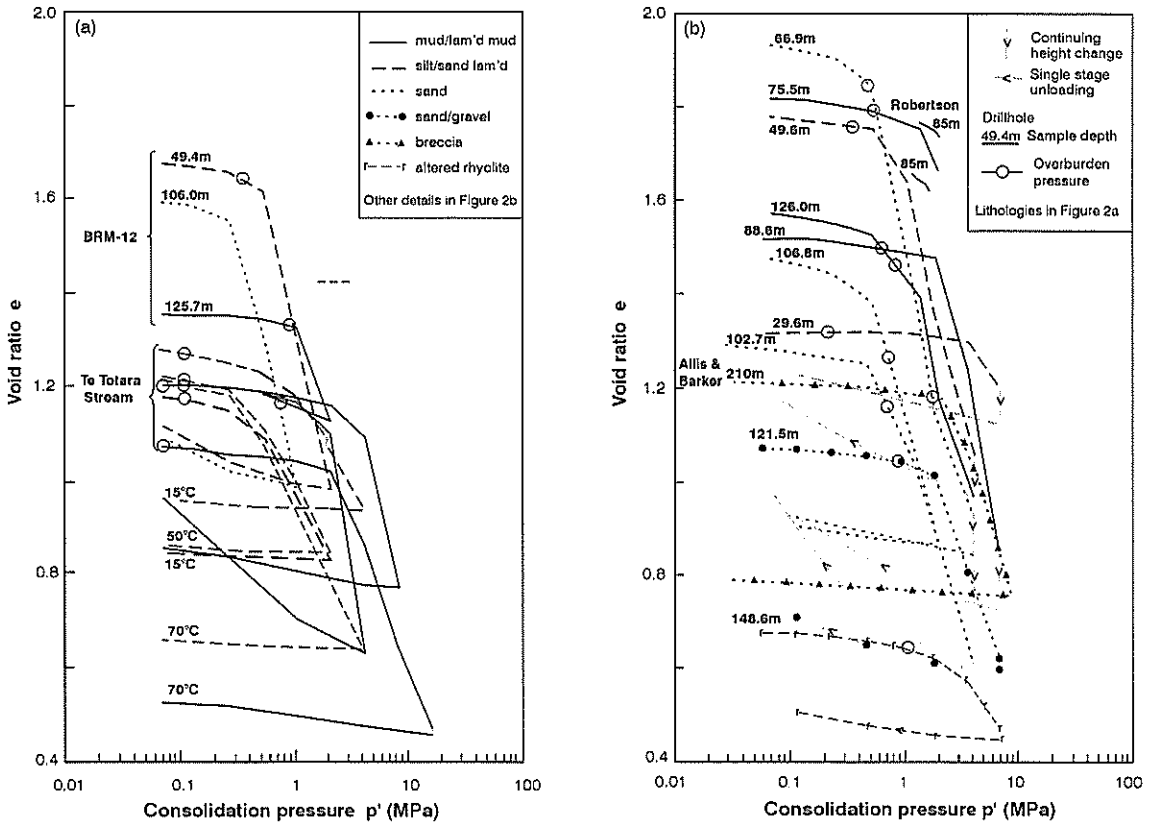

Figure 2. Laboratory Consolidation Test Results Plotted Conventionally. Recent testing (a) from Ohaaki and Te Totara Stream, and Initial Testing (b) from Ohaaki (BRM-12) and Wairakei Including Results in Allis *et al.* (1997), Allis and Barker (1982) and Robertson (1984).

Figure 3 plots the consolidation test results using a linear scale for consolidation pressure. For clarity it excludes some of the results in Figure 2 as well as unloading, but retains representation of material types, including altered rhyolite. Typically there is a change in response with increasing consolidation pressure, with an exception being the altered rhyolite. Over their range of initial void ratios, the Huka Falls Formation materials commonly show a noticeable steepening (ie. increased response with increased pressure) at consolidation pressures between 0.5 and 3 MPa. This is sometimes followed by a shallowing (ie. stiffer response) at even higher pressures. Gradients for sandier materials tend to be steeper than for muddier materials. Commencement of the steepening coincides fairly well with apparent pre-consolidation pressures, which were determined by conventional graphical techniques (NZS 4402, 1986) from the curves in Figure 2 and interpolated between load increments on Figure 3. The coincidence of the changes with the apparent pre-consolidation pressure gives a reasonable basis for further consideration of the materials responses using traditional consolidation methods.

Compressibility is a measure of the capability of a material to consolidate. Figure 4 shows the data from Figure 3 plotted as the coefficient of volume compressibility (m_v – NZS 4402, 1986). Compressibility values are calculated from the height changes following a load increment, and are plotted against the consolidation pressure applied in that load increment. Where the duration of loading was extended (eg. during the greatest pressure during initial testing - Figure 2b) height changes over this extended period are excluded. Values for loads smaller than 0.07 MPa (ca. 10 m of overburden) are also excluded because of their proximity at low pressures at the start of the test. Points for apparent pre-consolidation pressures have been plotted in the same manner as those for Figure 3

The most significant variations in compressibility occur in the vicinity of apparent pre-consolidation pressure values. The more prominent peaks, with compressibility values >0.1 MPa^{-1}, are associated with sandier materials, while at higher pressures (>3 MPa) both sandier and muddier materials show similar, though lower (<0.1 MPa^{-1}), values. Interestingly, the altered rhyolite shows no change in compressibility with increasing pressure. Given that it may be considered as a weathered rock, behaviour more like that noted for residual soils in Auckland (Pender *et al.*, 2000) is not surprising.

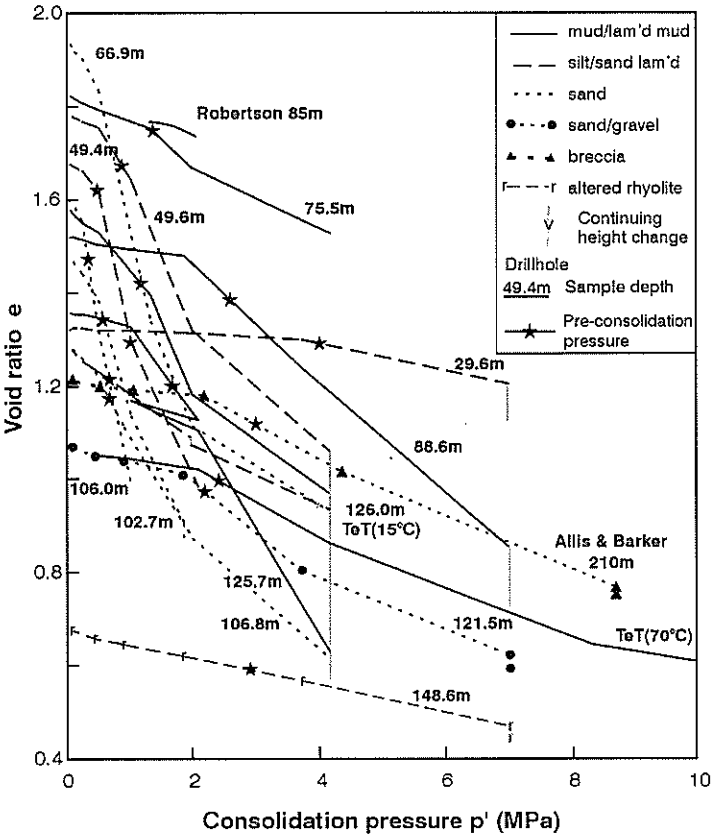

Figure 3. Laboratory Consolidation Test Results Plotted with Linear Axes. Apparent Pre-Consolidation Pressures Determined from Conventional Plots in Figure 2 and Interpolated onto Figure 3.

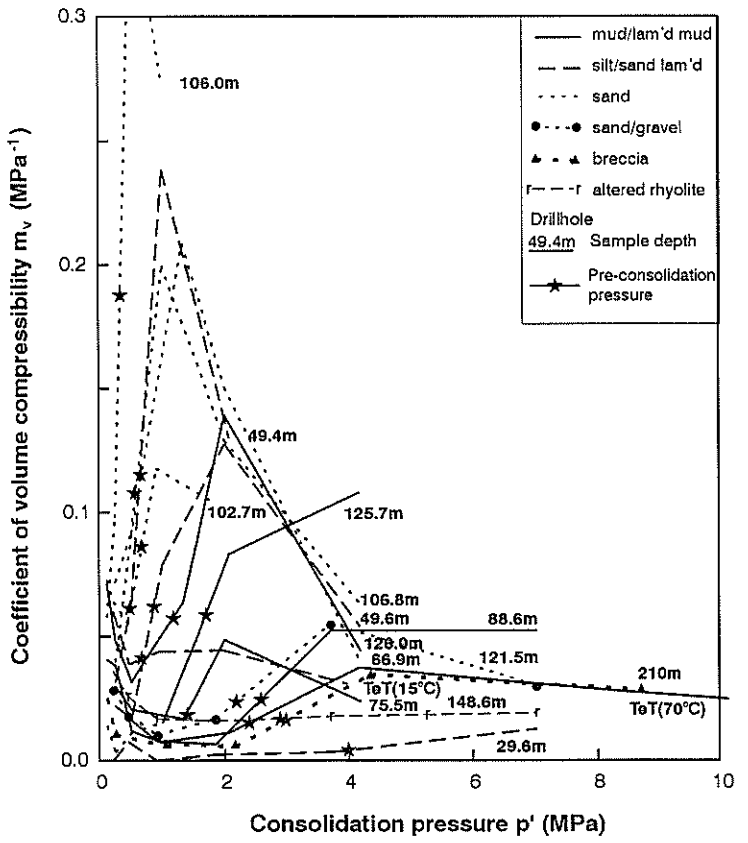

Figure 4. Compressibility Values for the Consolidation Test Results in Figure 3.

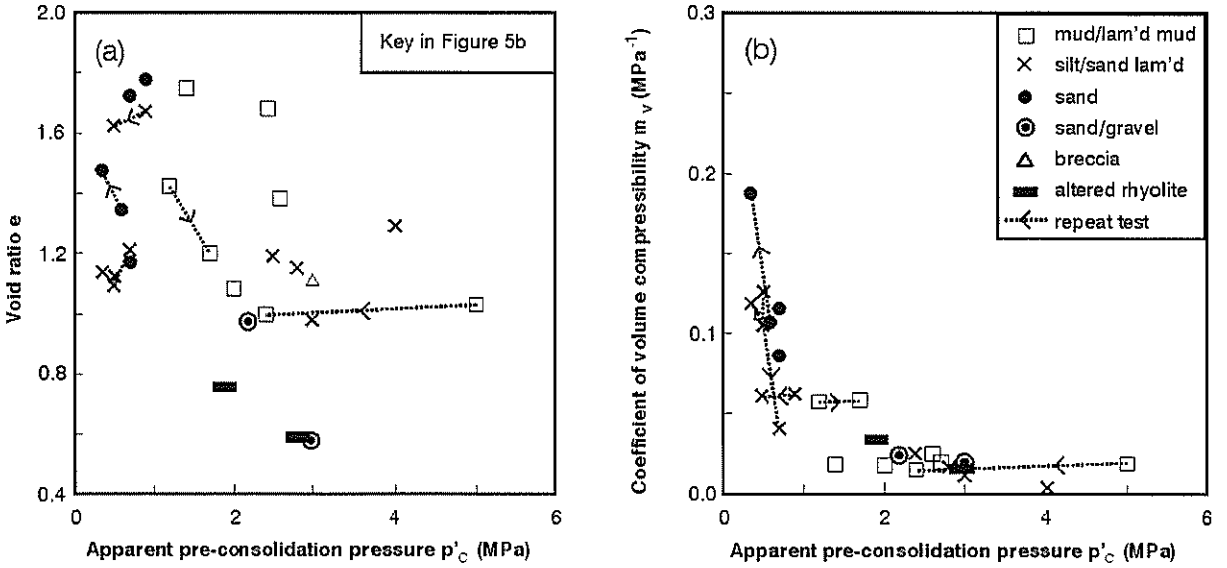

Figure 5. Laboratory Consolidation Test Values at Apparent Pre-Consolidation Pressure. Void Ratio (a) and Coefficient of Volume Compressibility (b) at Apparent Pre-Consolidation Pressures Determined from Conventional Plots in Figure 2 and Shown in Figures 3 and 4.

As changes in compressibility values pressure can be recognised either side of an apparent pre-consolidation pressure, further investigation of consolidation properties of the Huka Falls Formation material at apparent pre-consolidation pressure values is worthwhile. While the incremental doubling of applied pressures during a test means there is a need to interpolate values and the results are sensitive to the calculations, this does not discount the approach. The data in Figure 5, which shows void ratios and compressibilities determined at apparent pre-consolidation pressure for the 26 tests since 1995 as well as one from Allis and Barker (1982), suggests two things. First, void ratio values show a wide range for a given value of apparent pre-consolidation pressure for sands, silts and muds (ie. the two properties are reasonably independent). Second, higher compressibility values appear to be associated with sandier materials that also have lower apparent pre-consolidation values.

Several of the points in Figure 5 are from tests repeated on similar materials (Figure 2a includes the conventional plots for them). The 3 repeat tests from drillhole BRM-12 were on specimens prepared from adjacent cores (<1.0 m apart) of similar lithology, and used longer loading cycles than the first (initial) testing. The 4 repeat tests from Te Totara Stream were on specimens prepared from the same block samples, and 3 were performed at slightly elevated temperatures (50°-70° C).

Figure 5 includes the differences between the repeat tests, showing variations that could be considered due mainly to sample variability. However, it should be noted that the repeat tests from drillhole BRM-12 were carried out four years after the initial testing, and therefore some of the values may need to be treated with caution. The sandier materials (ie. 106 m depth) tend to show a noticeable increase in compressibility, but their overburden pressures shown in Figure 2 are similar to or greater than apparent pre-consolidation pressures. This is indicative of sample disturbance either during coring and/or by stress relief during subsequent storage. The differences for the testing of samples from Te Totara Stream at slightly elevated (50° - 70° C) temperatures (3 tests - two sandy, one muddy) showed no demonstrable change in compressibility at these temperatures (Figure 5). The major difference in the one test on muddier material at 70° C was a markedly reduced apparent pre-consolidation pressure, while the repeat test on sandier material at room temperature showed a greater reduction in compressibility than the slight increases for the two tests at 50° C and 70° C.

Scanning electron microscope images of specimens before and after consolidation testing show the deformation is largely plastic (Figure 6). The void ratio reduction from an original open honeycomb-type structure is accompanied by the flattening of clay mineral sheets and plastic deformation of clay coatings around detrital minerals, with little evidence of brittle fracture (Read *et al.*, 2001).

Before consolidation (natural conditions)

After consolidation (reduced void ratio)

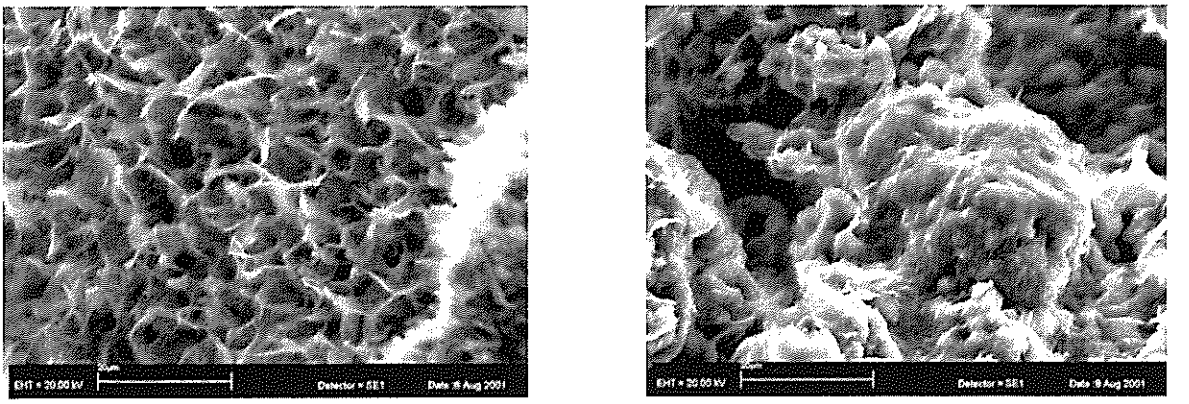

Figure 6. Scanning Electron Microscope Images Before and After Completion of Consolidation Test. Views are in the Direction of Loading for Drillhole BRM-12 Sample at 106.0 m Depth.

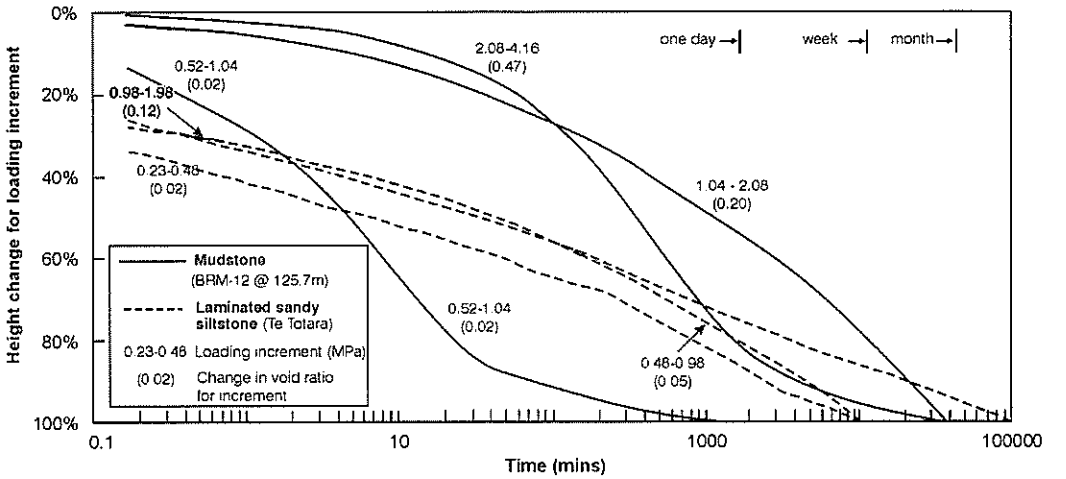

Figure 7. Height Changes for Loading Increments Before, Near and Past Pre-Consolidation Pressure. Void Ratio Changes for Increment Given in Brackets, with Complete Results Shown in Figures 2a and 3.

Figure 7 shows the responses to loading of sandier and muddier materials at different loading increments. The sandier materials show a slightly greater immediate response, followed by a more uniform ongoing height change. Such a response is not dissimilar to that of residual soils from Auckland. The overall response of the lower permeability muddier materials is slower, and with a smaller component of immediate response. When loading increments were near to, or about, the apparent pre-consolidation pressure, height changes sometimes continued over a longer period and resulted in more time being needed to complete that increment (eg. 1.04 – 2.08 MPa for the mudstone in Figure 7 with an apparent pre-consolidation pressure of 1.7 MPa). For that particular test, partial unloading from this point (see Figures 2a and 3) resulted in little rebound (ie. the deformation from loading was permanent). In contrast, unloading from the maximum pressure applied (≈4.2 MPa) resulted in a large rebound. This large rebound from maximum pressure was also noted for the muddier materials during the initial testing (Figure 2b). At that time the behaviour was thought to reflect the rapid loading cycles, but instead appears to be a characteristic of the muddier materials.

Permeabilities of the materials have not been directly measured. When values were derived from the consolidation test results, using procedures in NZ4402 NZS (1986), hydraulic conductivity values were typically low (10^{-8} to 10^{-11} m/sec). These values indicate that slower, rather than rapid, responses to changes in applied pressures might be anticipated. Many of the loading increments also showed some ongoing height changes with time (Figure 7), indicating not only slow responses, but also a degree of secondary consolidation.

DISCUSSION

The Huka Falls Formation materials have some special characteristics. They are geologically young lake sediments with a combination of high void ratios ($e > 1$) and weak rock ($q_u > 1$ MPa) strengths. Petrographic examination indicates that the strength of the materials has been imparted by skeletal bonding by clays and other cementing agents, prior to any significant void reduction by burial close to the time of deposition. The laboratory consolidation testing has confirmed that the Huka Falls Formation materials show behaviour consistent with the existence of an apparent pre-consolidation pressure. This means that they are potentially able to retain their high void ratios, when buried to greater depths, than weaker materials.

Ground subsidence follows changes in sub-surface conditions that result in higher effective stresses (eg. from the lowered pore pressures that accompany a drop in water table level). The laboratory consolidation testing also demonstrates that at pressures greater than the apparent pre-consolidation pressure most of the materials have increased compressibility values. Consequently, given appropriate changes in sub-surface conditions, the consolidation properties of the Huka Falls Formation materials are able to provide a plausible mechanism for ground subsidence occurring at the geothermal fields.

The most marked reductions in void ratio exhibited during the laboratory testing were for materials with higher initial void ratios ($e_o > 1.4$). However, the apparent pre-consolidation pressures do not show a systematic relationship with void ratio (Figure 5a), so void ratio does not appear to be a good proxy for depth over the range of depths sampled (30 - 150 m). A better correlation is indicated by the curved relationship of compressibility with apparent pre-consolidation pressures (Figure 5b, with sandier materials having greater compressibility values. Figure 8. which shows Figure 5b plotted semi-logarithmically, indicates possible linear relationships. Independent of which of the possible relationships may be more useful, Figure 8 suggests that with the higher compressibility values for sandier materials at lower apparent pre-consolidation pressures ($m_v > 0.1$ MPa^{-1}), compressibility values will be lower ($m_v < 0.05$ MPa^{-1}) at greater depths (>250m).

Figure 9 shows the apparent pre-consolidation pressures and the dry densities summarised in Table 1, plotted against the depths of sampling for consolidation testing at drillhole BRM-12 (170 m - Figure 9a) and the overall thickness of the Huka Falls Formation (350 m - Figure 9b) respectively. Figure 9a, which includes the Te Totara Stream results, suggests that apparent pre-consolidation pressure and depth are independent. Results plotting to the left of the overburden pressure curve (assuming the water table is at the ground surface) indicate the possible sample disturbance and stress relief of sandier materials as discussed earlier. Figure 9b shows that below 150m depth dry density values

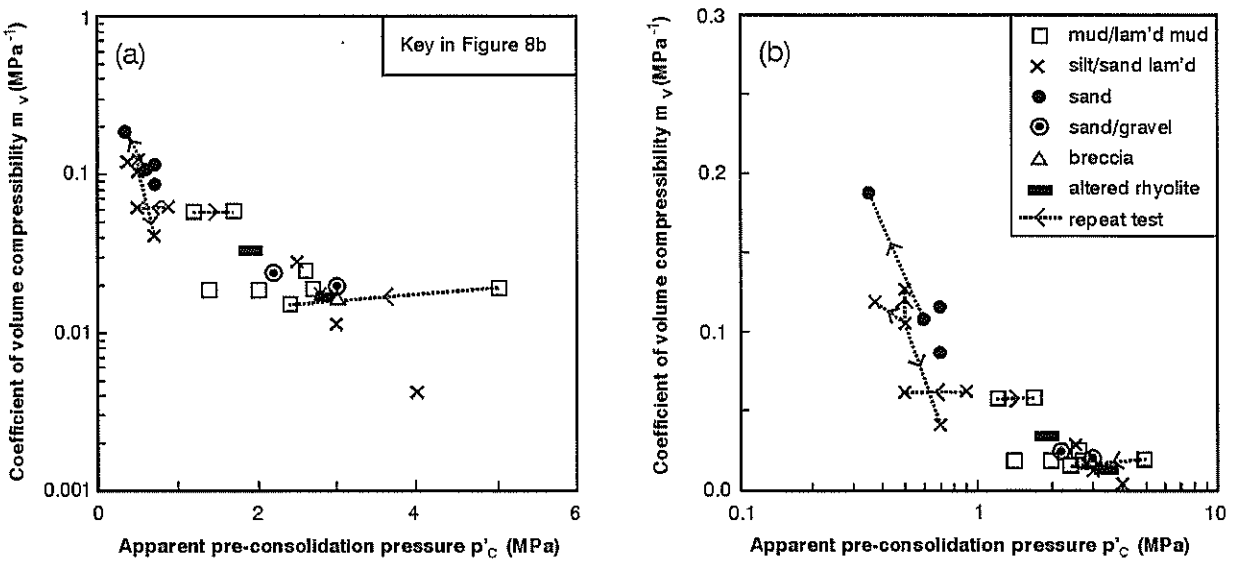

Figure 8. Coefficient of Volume Compressibility and Apparent Pre-consolidation Pressure on Semi-Logarithmic Plots .

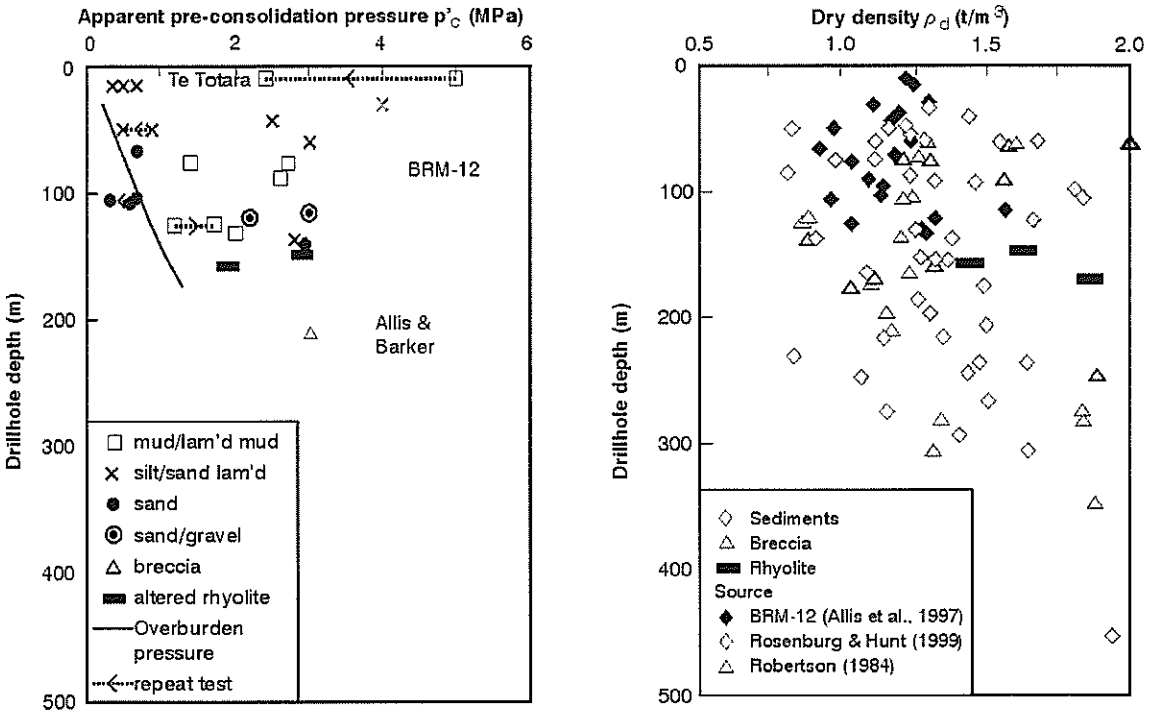

Figure 9. Laboratory Testing Results (Consolidation and Density) for Drillhole Depth. Density Data from Robertson (1984) and Rosenberg and Hunt (1999) Summarised in Table 1.

appear to more systematically increase with depth. The plot also shows that a greater number of the lower density values appear to be for either tuffaceous/breccia materials rather than sediments, and/or from Wairakei/Tauhara rather than Ohaaki. Irrespective of the last point, the greater density values at depths >200 m are not incompatible with the lower compressibility values (m_v <0.05 MPa) indicated in Figure 4 at applied pressures >2 MPa during the consolidation testing.

Further laboratory testing would not only improve our understanding of the properties of the Huka Falls Formation, but also enhance confidence in the input parameters for the numerical modelling of subsidence. As well as compressibility and permeability values, the influences of immediate and continuing responses to pressure changes need to be known. K_0 triaxial testing provides a technique for determining apparent pre-consolidation pressures as suggested by Janbu and Senneset (1979), and provides a possibility of being adapted for testing at temperatures that better duplicate geothermal systems. Consolidation testing to higher loads (eg. 25 MPa) would also better define compressibility trends at depth. As a final point, because of lithological influences on consolidation properties, an accurate definition of material geometries and pressure distributions is important.

CONCLUSIONS

Laboratory consolidation testing of the high void ratio, but high strength and low permeability, Huka Falls Formation materials (sandstones, siltstones, mudstones and pumice breccias) has shown that they generally demonstrate differing coefficients of volume compressibility (m_v) at pressures on either side of apparent pre-consolidation pressures that vary between 0.5 and 5 MPa. Although the most marked reductions in void ratio during testing occurred in materials with higher initial void ratios (e_o >1.4), no systematic relationship between void ratio and depth is apparent over the depths sampled (30 - 150 m).

Compressibility (m_v) data show a non-uniform relationship with apparent pre-consolidation pressure The data indicate that the highest compressibility values (m_v > 0.1 MPa^{-1}) are for sandier lithologies and that compressibilities will be smaller (m_v < 0.05 MPa^{-1}) with greater depth. These results, however, are not seen as likely to contradict previous suggestions that subsidence at the geothermal fields occurs within the Huka Falls Formation.

ACKNOWLEDGEMENTS

We thank Contact Energy (Geothermal) for access to cores and permission to publish the paper, plus support from Environment Waikato. Funding has been provided by the Foundation for Research, Science and Techology through contract CO5X0201. Thanks to those people who have helped at various stages of the work including Rick Allis, Mike Rosenberg, Agnes Reyes in addition to Carolyn Hume for graphics and Peter Millar, Nick Perrin and Colin Wilson for constructive reviews.

REFERENCES

Allis, R.G. and Barker, P.R. (1982). "Update on subsidence at Wairakei". In: *Proceedings 4th N.Z. Geothermal Workshop*, Auckland, Part 2, pp. 365-370.

Allis, R.G. and Zhan, X. (2000). "Predicting subsidence at Wairakei and Ohaaki geothermal fields, New Zealand", *Geothermics*, Vol. 29(4-5), pp. 479-497.

Allis, R.G., Zhan, X. and Clotworthy, A.W. (1998). "Predicting future subsidence at Wairakei field, New Zealand". In: *Proceedings 20th N.Z. Geothermal Workshop*, Auckland, pp. 133-137.

Allis, R.G., Carey, B., Darby, D., Read, S.A.L., Rosenberg, M., Wood, C.P. and Zhan, X. (1997). "Subsidence at Ohaaki field". In: *Proceedings 19th N.Z. Geothermal Workshop*, Auckland, pp. 9-16.

Grindley, G.W. (1965). "The geology, structure, and exploitation of the Wairakei Geothermal Field, Taupo, New Zealand". *NZ Geological Survey Bull. ns75*, NZ Government Printer, Wellington.

Janbu, N. (1963). "Soil compressibility as determined by oedometer and triaxial tests." In: *Proceedings 4th European Conference on Soil Mechanics and Foundation Engineering*, Weisbaden, Vol 1, pp. 19-25.

Janbu, N. and Senneset, K. (1979). "Interpretation procedures for obtaining soil deformation parameters." In: *Proceedings.7th European Conference on Soil Mechanics and Foundation Engineering*, Brighton, Vol 1, pp. 185-188.

Lawless, J.V., Okada, W., Terzaghi, S. and White, P.J. (2001). "New 2-D subsidence modelling applied to Wairakei-Tauhara". In: *Proceedings 23rd N.Z. Geothermal Workshop*, Auckland, pp. 133-137.

NZS 4402 (1986). *Methods of testing for civil engineering purposes.* Standards New Zealand (SNZ) New Zealand Standard (NZS), NZS, Wellington.

Pender, M.J., Wesley, L.D., Twose, G., Duske, G.C. and Pranjoto, S. (2000). Compressibility of Auckland residual soil. In: *Proceedings GeoEng 2000*, Melbourne, Paper GCC1282.

Pender, M.J., Wesley, L.D. and Ni, B. (2003). Laboratory stiffness and other properties of Auckland residual soil. In: *Geotechnics on the Volcanic Edge*, Tauranga.

Read, S.A.L. and Millar, P.J. (1991). "Classification of New Zealand soft sedimentary rock materials". In: *Proceedings 7th International Congress on Rock Mechanics,* Aachen, Vol. 1, pp. 327-331.

Read, S.A.L., Barker, P.R. and Reyes, A. (2001). "Consolidation properties of Huka Falls Formation - linkages to subsidence at Wairakei and Ohaaki". In: *Proceedings 23rd N.Z. Geothermal Workshop*, Auckland, pp. 57-62.

Robertson, A. (1984). "Analysis of subsurface compaction and subsidence at Wairakei geothermal field, New Zealand". *Unpublished MSc thesis, University of Auckland, New Zealand.*

Rosenberg, M.D. and Hunt, T.M. (1999). "Ohaaki geothermal field: some proerties of Huka Falls Formation mudstones". In: *Proceedings 21st N.Z. Geothermal Workshop*, pp. 89-94.

GEONET Landslide Response: The Fatal Cleft Peak Debris Flow of 3 January 2002, Rees Valley, West Otago

M J McSaveney
Institute of Geological & Nuclear Sciences, Lower Hutt
P J Glassey
Institute of Geological & Nuclear Sciences, Dunedin

Abstract: On 3 January 2002, Robin Alan Buxton was killed by a debris flow while attempting to cross a headwater tributary of Rees River, West Otago. The event occurred during a thunder storm. High-intensity rain triggered many shallow landslides in the thin layer of loose, weathered rock debris overlying the steeply dipping schist bedrock on many slopes in the area. These in turn initiated debris flows in many mountain torrents. Mr Buxton and Bevan Thrower had the misfortune to be in a stream channel and about to cross at the time a 2-metre deep debris flow approached them at high speed. Mr Thrower heard it approaching and escaped by the narrowest of margins.

INTRODUCTION

At about 10 am on 3 January 2002, Robin Alan Buxton, 28, was killed by a debris flow while attempting to cross an unnamed headwater tributary of the Rees River, West Otago. He was tramping between Shelter Rock Hut and the Rees Saddle (Figures 1 and 2). The tributary drains from Cleft Peak at the northern end of the Richardson Mountains. The event was witnessed by Bevan Thrower, who narrowly escaped the surging 2m-high wall of rock, water, mud, and debris.

What is the GeoNet Landslide Response?

The non-profit *GeoNet* project was instigated by the Earthquake Commission (EQC) and Institute of Geological & Nuclear Sciences (GNS). EQC funds *GeoNet* to monitor geological hazards and improve the quality of associated data in New Zealand. *GeoNet* collects data on unusually large or complicated landslides. It compiles a database of landslide locations and attributes; and it makes the information available through reports, an annual newsletter, and ultimately through a web-based database. *GeoNet* responds to landslides that have (or have a potential to have) any of the following: (i) death or serious injury; (ii) potential for subsequent catastrophe (such as breaching of a landslide dam); (iii) direct damage of $1,000,000 or greater; (iv) indirect costs (economic losses) of $10,000,000 or greater; (v) threats to public health (eg water supply contaminated, sewage discharge); (vi) significant research interest. Our response to the Rees valley tragedy was made on the first and third of these criteria.

Data Gathering

We flew to the site by helicopter on the morning of 25 January 2002. We inspected and photographed the upper Rees Vvalley from the air and saw evidence of many new debris flows. Most had occurred on the morning of 3 January during a thunderstorm. We saw the sources of many of these debris flows below and between broken cloud cover. All had similar origins. Cloud obscured the source of the fatal debris flow, but we identified which of the upper basins on Cleft Peak was the source of most of the debris. We landed on the fan below the source area to collect a sample of the debris-flow material, and inspect a section of the channel upstream of the accident site. We saw the accident site, and the place where Mr Buxton's body was found from the air. These sites had no important information as to the origins or behaviour of the debris flow, so we did not land to investigate them.

We briefly spoke with Senior Sergeant John Fookes (Queenstown Police), who was involved with the search and body recovery. He arranged for us to see Bevan Thrower's witness statement and the police

scene video. Constable Travis Hughes provided further information and confirmation of some details. Bevan Thrower provided further recollections of his experience in the debris flow.

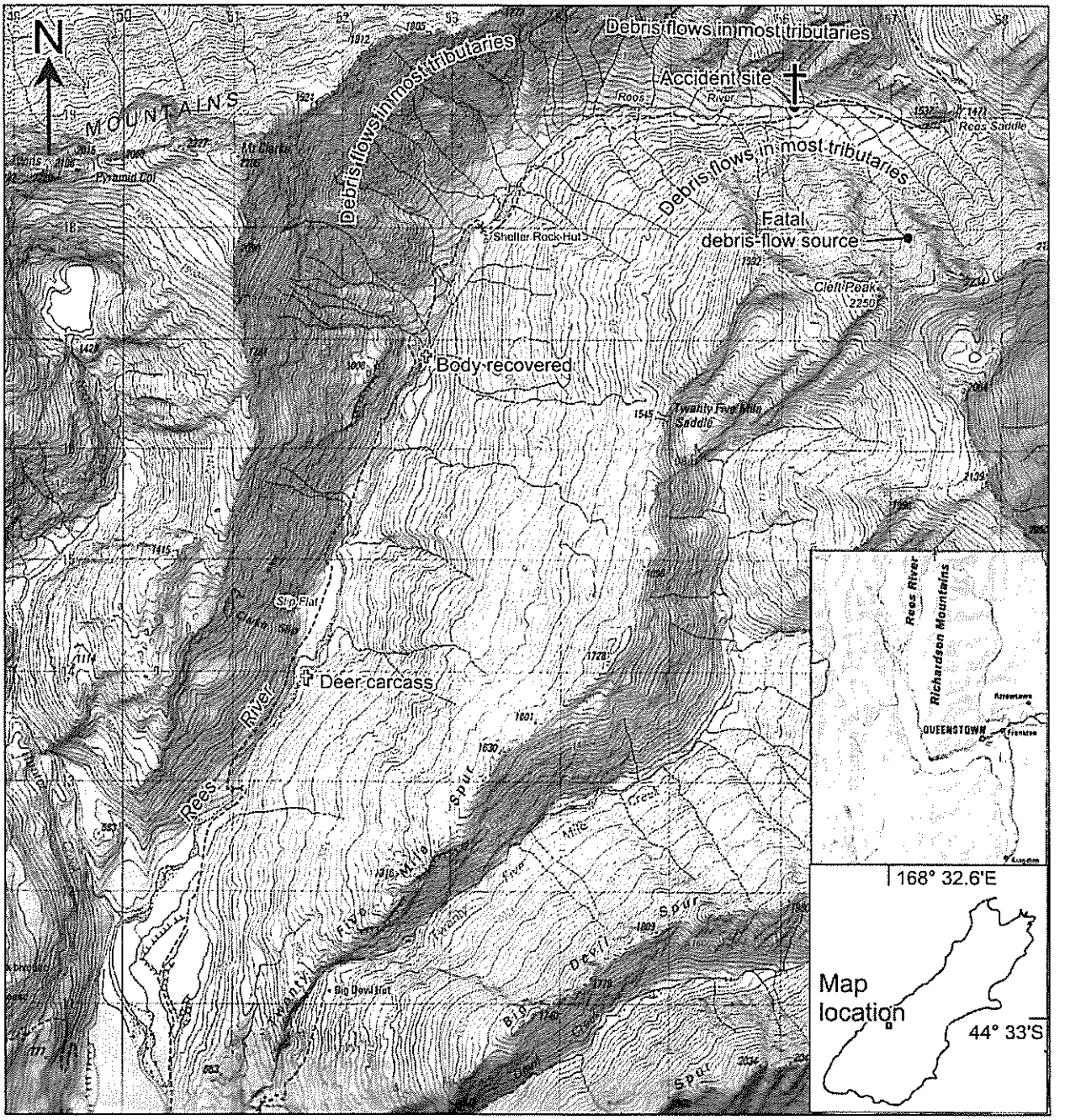

Figure 1. Map of Upper Rees River Valley. Grid is 1 Kilometre Square.
[From Infomap 260-E40 Earnslaw (2000). Fatal debris flow came from the north flank of Cleft Peak (See Fig. 2 for detail). A deer possibly killed by a debris flow was deposited by the river at the south end of Slip Flat]

SITE GEOLOGY

Geomorphology

The upper Rees valley is a U-shaped, formerly glaciated valley and drains to Lake Wakatipu. The valley is floored south of Rees Saddle (Figure 1) by a series of steep coalescing fans from many minor tributary basins. The accident occurred on the largest fan, which has formed from debris eroded from the northern slopes of Cleft Peak (Figure 2). Abundant very large boulders and remnants of raised levees (mostly well vegetated) flanking channels on the fans identify them all as being formed dominantly by infrequent debris flows of similar and larger sizes to the fatal event. Unvegetated levees beside more than half of the active channels indicated many very recent debris flows.

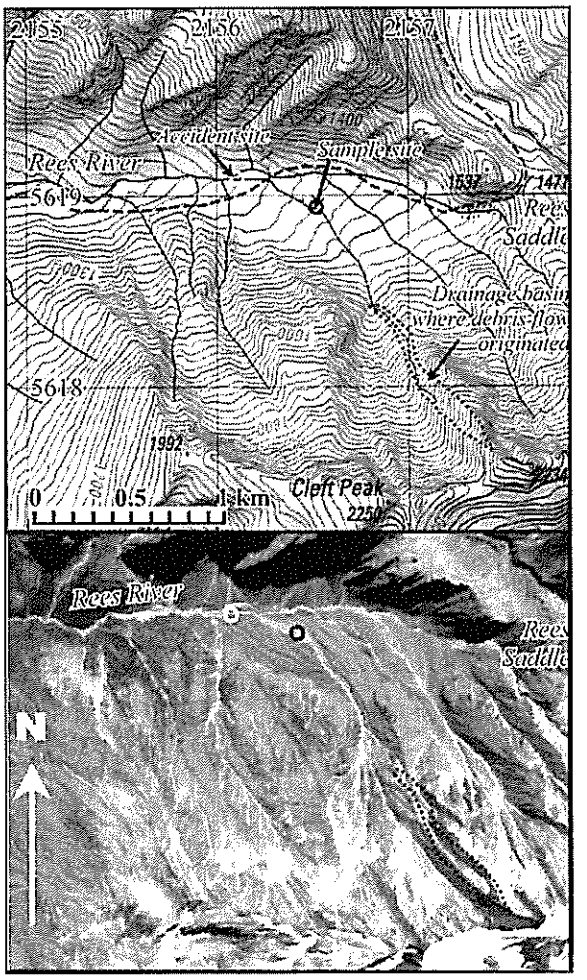

Figure 2. Map and Vertical Aerial Photo of the Site of the Fatal Cleft Peak Debris Flow
[The track passes through the accident site, and is not as shown on Infomap 260-E40. Grid is New Zealand Map Grid. North is uppermost. Aerial photograph (Part of SN3982/18 of 12 March 1966) is partly rectified for distortion and topography.]

Upslope from the site of the accident, the slopes of the northern end of the Richardson Mountains are deeply dissected by a series of narrow gullies leading from minor drainage basins that head at Cleft Peak (2250 m) and several unnamed peaks along the ridge to the north (Figure. 2). This is the largest such set of minor drainage basins in the upper Rees valley in the vicinity of Rees Saddle. Fine gravel thinly deposited over live alpine tussock beside the stream channel, identified the source of the fatal flow as being the true rightmost (most easterly) of the basins (Figure 3). It is an elongate basin about 800 metres long and less than 80 metres wide, perched on the side of the main basin contributing to this tributary. The shape of the basin contributed to the time of concentration of the flow, and hence to the precise timing of it, but there was nothing inherently "special" about the basin that led to anything special about the fatal flow compared to any of the others. On the morning of 3 January 2002, debris flows were the norm, and not the exception, occurring in more than half of the 40 or so tributaries in the upper Rees.

The accident occurred on the lower slopes of the debris-flow fan, at the lower limit of the range of slopes on which a debris flow can flow. There was nothing unusual about the geomorphology of the accident site that might have contributed to the fatality. The site (Figure 4) was a logical and normally safe location to cross the stream.

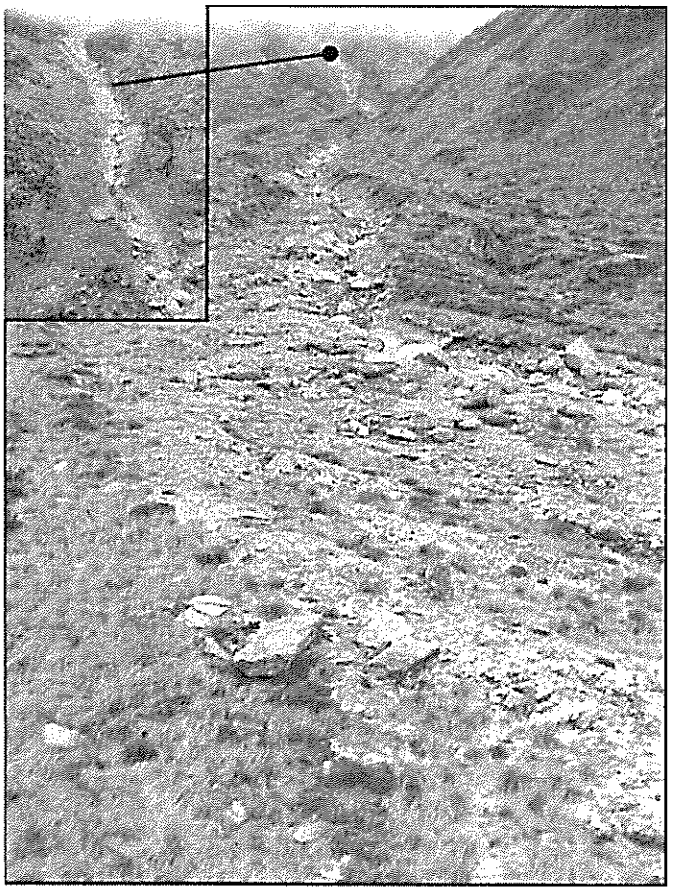

Figure 3. Path of the Cleft Peak Debris Flow on the Upper Portion of the Fan.

[The flow appears to have originated from the true right (left in photo) Tributary at the head of the fan. The flow remained confined to the channel in the upper portion of the fan, but spilled out of it on the lower fan where the channel was less incised. Inset is close view of the tributary that shows evidence (debris over live plants) of the passage of a large debris flow.]

Bed-Rock Geology

The debris-flow source area is cut in highly erodible schist of the Aspiring lithologic association (Turnbull 2000). It is finely segregated, quartz-feldspar-mica schist. The foliation dips steeply to the west-northwest at about 45°, about 8° steeper than the general slope of the mountainside. Although thin greenschist bands cut across Cleft Peak, greenschist is not visibly significant in the debris-flow deposit. The pelitic schist is highly susceptible to physical weathering and is easily eroded. It readily yields sediment particles of all sizes from boulders the size of small cars, to sand and silt.

WEATHER CONDITIONS

A northwest airflow covered much of the country on 3 January 2002, caused by a low of less than 984-hPa southwest of South Island. A series of cold and occluded fronts were embedded in the warm, moist, unstable air. There was light drizzle in the Rees valley on the morning of 2 January, but the afternoon was sunny. About dusk, it started to drizzle again, and rained steadily most of the night (McSaveney & Glassey 2002).

Mr Thrower recollects "steady" rain through the morning of 3 January. Shortly before the accident, however, the rain must have increased, because he noted that streams then were up slightly and discoloured, whereas along the route to the stream crossing, they had been ankle-deep and clear. One thing that stands out in his memory is "the lack of heavy rain, more showery easing to drizzle with patches of hail hitting off and on." Although he did not describe thunder in his statement to police, Mr Thrower recollects that it was "rocking and rolling all that morning." Not long before the accident, he "stopped to admire the awesome show being put on." A particularly severe convective storm cell, with localised torrential rain appears to have reached the headwaters of the Rees River between one and two hours after the two trampers left Shelter Rock Hut and shortly before Mr Thrower reached the

stream crossing – about when he "stopped to admire the awesome show." The particularly torrential part of this cell however does not appear to have crossed his path.

No rainfall intensities in the Rees valley are known. At Dart Hut, 3.3 km north of the debris-flow source, there were 240 mm of rain between 8:00am 3 January and 8:00am 4 January. This is likely to occur every two to three years on average (from Tomlinson 1980). Flows of the larger rivers were not extreme events either. We reason that the duration of very high intensity rain was short, perhaps for only 5–10 minutes. It was enough to trigger many shallow regolith slides. When these entered the steep and now flooded streams they continued as debris flows. The high-intensity rain moved in a narrow band (perhaps only 5 km wide) as a convecting storm cell was swept along in the westerly air flow. The extensive amount of landscape change seen in the upper Rees valley in the form of many shallow landslides, debris flows, and massive deposition along channels in the river bottom is not something to be seen there very often. From the stature of vegetation extensively damaged, a storm of this magnitude had not happened previously for many decades. If the event was something likely to be seen on average only every 50 to 100 years, the likely 10-minute rainfalls were in the range 30–50 mm (Tomlinson 1980).

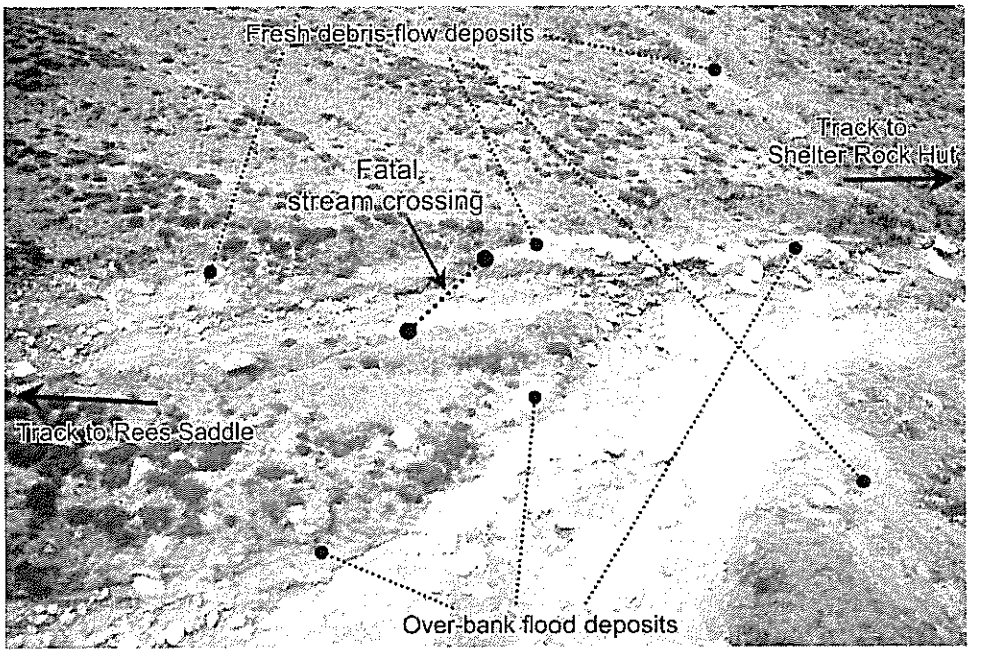

Figure 4. Site of Fatal Stream Crossing on Track Between Shelter Rock Hut And Rees Saddle.
[Rees River flows from centre foreground to right centre. The tributary stream where the accident occurred enters from the left centre. Boulders are up to 2 metres across. Photograph taken on 25 January 2002.]

THE DEBRIS FLOW

Witness Account

Mr Buxton was travelling alone but he joined with Bevan Thrower to cross the stream which was up but not unduly so. They linked arms to make the crossing. Mr Thrower had his parka hood down and, with unimpeded directional hearing, heard a loud rumbling roar from upstream before they had entered the water. He knew immediately that it was not thunder. Without looking to see what might be coming, he scrambled up the bank of the several-metres deep channel (Figure 4). As he was climbing the bank, his feet washed out from under him. Looking over his shoulder he saw Mr Buxton, with hood up, first standing facing upstream, then turning to move. With black water rising up his body, Mr Thrower kept scrambling up the bank. When he reached the top and felt safe, he looked back to see Mr Buxton's pack disappear. He did not see him again. He then ran along the river bank trying to spot Mr Buxton. Some 200 metres downstream, a creek they had crossed safely earlier was now washed out

and impassable. He ascended some 300 metres up its fan before finding a place to cross, and return to Shelter Rock Hut along the walking track to tell others.

Between the time the two were considering crossing the stream, and Mr Thrower reaching safety, the water had gone from dirty brown to black. The noise was a deafening grinding and banging. He had a "tide mark" of sand in his pack and clothes. The debris flow had all but ripped off his gaiters and jammed sand and pea-sized gravel into his boots. The flowing material felt like extremely sloppy, wet concrete (Bevan Thrower, personal communication, 7 March 2002). Afterwards, the wet debris left on the stream banks was like wet concrete, up to his knees, and almost impassable.

Origin of the Debris Flow

The source area of the flow was not able to be inspected, but the formation of debris flows in alpine, schist landscape is well understood. Similar rare high-intensity rainstorms have triggered debris flows elsewhere in the region, such as in the vicinity of Makaroroa River and Lake Wanaka in January 1994 when five bridges on SH6 were destroyed (McSaveney 1995).

The lower slopes of the upper basins around Cleft Peak had been accumulating detritus from physical weathering of the exposed schist bedrock on the slopes above them since they had last been emptied by debris flows some decades earlier. The debris was highly variable in thickness, up to several metres or more, and consisting of boulders and cobbles in a matrix of sand and silt. The bedrock is relatively impermeable to water, and the overlying debris is both porous and permeable. Storm runoff from such steep alpine basins is extremely rapid. Under very high-intensity rain, the loose debris becomes locally saturated and initiates a landslide of the loose layer over the bedrock. Local landsliding also can be initiated when the stream flow is high enough to erode the loose debris in its bed, and so undercut the stream banks. Whatever the exact cause of the collapse, the wet loose debris formed a slurry, like wet concrete, that was able to flow downslope, including down the stream channels. This moving slurry was dense (up to 90% by weight of rock) and highly erosive. It moved faster than the stream flow and picked up further debris from the stream channel, including all of the water.

The exact mix of water and sediment in the debris flow, and the exact range of debris particle sizes present in it are relatively unimportant, because both were changing rapidly as the flow progressed down valley. As the flow approached the track crossing on the lower flanks of the fan it was depositing sediment and not significantly eroding its bed but it was picking up water and becoming more fluid. At the track crossing, a few tens of metres above the tributary's junction with Rees River, the debris flow was described as being like extremely sloppy concrete while flowing. On standing it quickly firmed up as the water drained out, but remained unable to support the weight of a man for some minutes. The matrix of the debris flow a few hundred metres upstream of the track crossing contained 63% pebbles, 25% sand, 11% silt and less than 1% clay particle sizes (McSaveney & Glassey 2002). As a debris-flow material, it had no unusual or distinguishing characteristics.

Dispersal of the Debris Flow Downstream

The raging torrent in the Rees River moved a very large quantity of sediment. Much of this was delivered to the river by the many other debris flows, and other flooded tributaries. Some of the coarser components of the sediment were deposited in the bed of the river channel. The raised bed, in addition to the increased water volume, contributed to a high water surface of the flooded river. Downstream of Shelter Rock Hut, the flooded river undercut the riverbanks in many places and tore out many riverside trees contributing to an increasing load of large woody debris being carried in the flood. Alongside the tributary the deposits set like lobes of concrete, but beside Rees River they were loose and friable because they had much less silt in them. This change indicates that the debris flow did not continue beyond the junction. There appears to have been enough water in the river at this point to dilute the slurry to a hyperconcentrated flow, and then to a "normal" raging water torrent in full flood.

Mr Buxton's body was carried swiftly downstream, initially in the frontal wave of the debris flow, but later simply by the flow of the torrent for most of its journey. Eventually the body lodged on the

outside of a bend in the river flow, by a cluster of large boulders where a substantial flood flow was pouring through a scrubby tree which filtered out all of the larger floating debris passing its way. The large amount of woody debris covering the body, suggests that much of the bank erosion and addition of wood to the floodwaters occurred after the body had passed by on its way to the site where it was trapped.

CONSEQUENCES OF THE DEBRIS FLOW

Damage to Life, Property and the Landscape

The primary damage from the Cleft Peak debris flow was the killing of Robin Buxton and the destruction of the gear he was carrying. His body and pack were recovered separately on 7 January about 4 km downstream of where he had attempted the stream crossing. Body damage was largely percussive (extensive bone fractures), as if from impacting boulders. There was little evidence of massive abrasion of skin, or puncture wounds from woody debris. Although all clothing was torn from the body, avulsion of body tissue was relatively minor (loss of right lower forearm, and part of head). Likewise, Mr Buxton's pack suffered little external damage, although some exposed contents (such as the sleep mat) had been torn away. Given the nature of the debris flow, and how he was caught in it, we believe his escape was impossible and death was close to instantaneous. The coroner found that he died of a head injury. Mr Thrower was exposed only to a much slower velocity of flow at the edge, and was uninjured.

The debris flow did no lasting damage to the walking track or any other DoC infrastructure. It destroyed many plants but created some new geomorphic surfaces in the landscape. As an indication of the sudden onset of damage on 3 January, an adult deer was also killed that morning somewhere in the upper Rees, probably by another of the many debris flows. Its carcass was deposited lower in the Rees valley.

The nominal value of an adult life currently used in costing road accidents is $4,000,000. If this value is accepted for Mr Buxton, the economic cost of the event is likely to have been about $4.2 million inclusive of search and recovery costs, debriefings, report preparation and the coroner's inquest. The event has not affected the popularity of the Rees valley track as a tramping route.

DISCUSSION

Recognition of Areas with Debris-Flow Potential

Debris flows are significant erosion and deposition processes in the shaping of the New Zealand alpine landscape. Although they occur infrequently, marks of their occurrence are widespread and persistent. Many steep channels are mostly shaped by debris flows, and are occupied by streams that do little geomorphic modification between debris flows. Debris flows are not rare, they just occur infrequently in any one stream. Their repeated occurrence leads to a channel form with a characteristic U shape, much like a miniature U-shaped glacial valley. Most of the steep tributary channels in the upper Rees valley are shaped by debris flows and have this distinctive cross profile where they are cut into the schist bedrock.

Debris flows have an ability to carry enormous boulders where they are available (Figure 5). These are far larger than can be transported by a stream in flood. Steep fans covered by lines of scattered boulders, such as occur in the upper Rees valley indicate terrain subject to a severe debris-flow hazard.

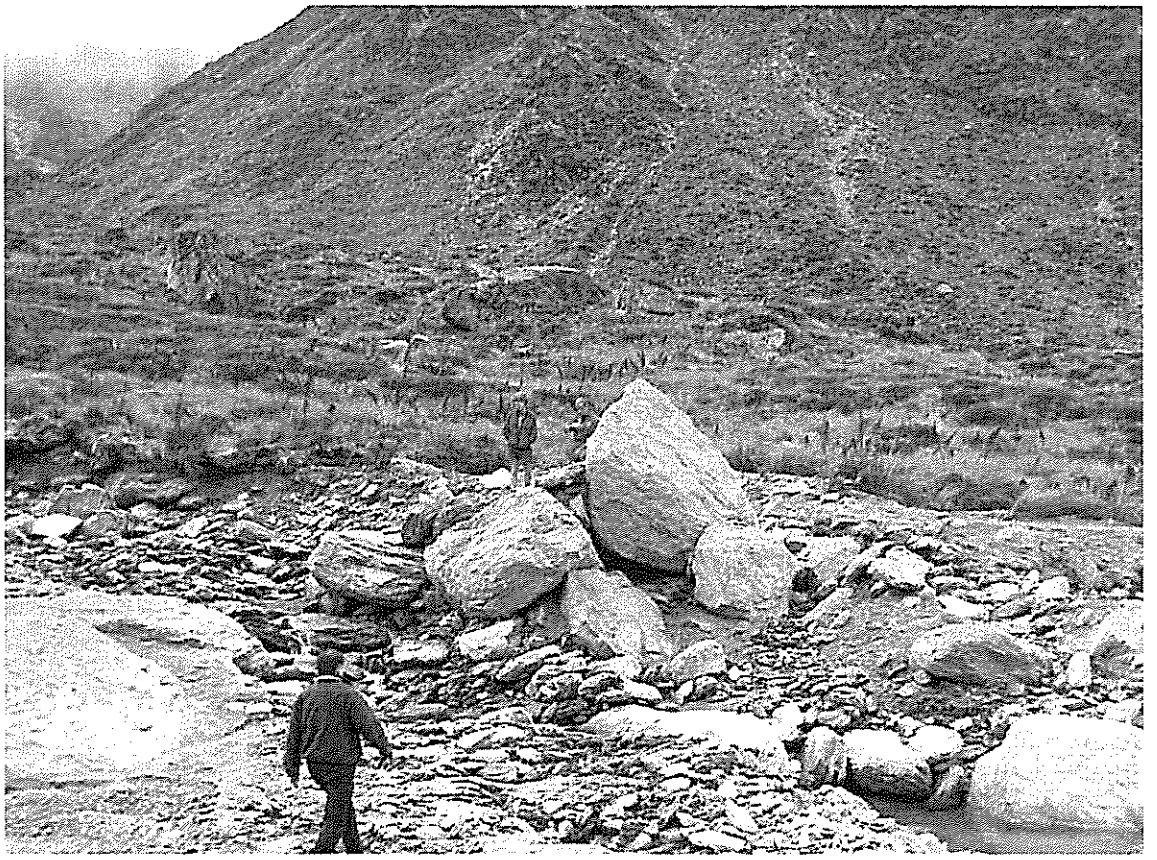

Figure 5. Example of the Boulders Moved Hundreds of Metres By The Debris Flow on the Upper Fan.
[Here a group have accumulated as a stable cluster when each became buttressed against the powerful debris-flow current by its surrounding boulders. In the background are other large boulders from a past debris flow, now overgrown by dense subalpine plant cover.]

Probability of the Debris-Flow Fatality

Debris-flow fatalities are not new in New Zealand. Lahars are simply debris flows on volcanoes, and so New Zealand's greatest single-event death toll from a debris flow (151 deaths) was in the 25 December 1953 Tangiwhai rail disaster. Previous known debris-flow accidents to trampers include fatalities when a debris flow struck the Lake Daniels Hut in the early 1970s, and when a debris flow struck a tent at Klondike Corner in 1978. More recently, a debris flow from a side stream carried away a hut in the upper Motueka River, Nelson, killing the two occupants. These backcountry fatalities arise through the inappropriate siting of a few mountain huts and campsites in areas exposed to a danger of debris flows.

Although there are many more sites where roads and tracks cross debris-flow paths than there are huts and campsites in debris-flow paths, it is unusual to learn of people being killed by debris flows because they have inadvertently strayed into their path. There are a number of reasons for this. The total exposure to debris-flow danger is shorter when people move through the danger zone than when they rest in it. Also, the storm conditions when debris flows tend to be generated may inhibit many people from travelling. But also it is unusual for evidence linking the person to the debris flow to survive. Had Mr Buxton's death not been seen, there is little evidence to link him to any particular stream crossing or to a debris flow.

The coroner found Robin Buxton's death was a rare and unavoidable accident. The more remarkable event was the survival of Bevan Thrower. Although it demonstrated that one can escape from a debris flow through vigilant personal awareness of one's surroundings, and quick appropriate reaction to an unusual warning, the escape was also a matter of luck. Had there not been a survivor to report the loss and its location, a search would not have arisen until the trampers were reported overdue, and missing somewhere between the Shelter Rock and Dart Huts. The deaths would likely have been attributed to the two having been washed away while attempting to cross a flooded stream. There are many rare and unusual ways to meet one's death in New Zealand's mountains, and death by being swept away by a

debris flow while crossing a mountain stream is one of the more unusual. Of similar low likelihood are being killed by lightning strike, falling tree, or earthquake-triggered landslide. Avoidance of these dangers while tramping is a personal and not a societal responsibility. Statistically, to die in a debris flow on a tramp is more likely to occur while asleep in a tent or a mountain hut than while crossing a stream.

Track Location and Stream Crossing

The accident site was a logical and normally safe location to cross the stream. Had the crossing been higher on the fan in the position where it is marked on the topographic map, for example (Figures 1 and 2), this particular accident might not have happened. Mr Buxton would have taken longer to reach the crossing and hence would not have been in the stream channel at the time the debris flow passed through it. Equally, if Mr Buxton had left Shelter Rock Hut some minutes earlier or later, or if he had walked faster or more slowly, the accident might not have happened. However, the debris flow spread more widely higher on the fan and had the two been crossing there at the time the flow passed through it is less likely that anyone would have been able to escape.. The map inaccuracy did not contribute to the accident.

Warnings, Cautions, and Awareness of Danger

DoC staff who accompanied us on 25 January believed that people at Shelter Rock Hut had been warned of the danger of undertaking the journey to Rees Saddle during the storm on 3 January. Statements in the news media on 5 January noted "There was heavy rain and thunder storms on the morning he [Robin Buxton] left and trampers were advised of the danger." Bevan Thrower's witness statement does not mention a warning however. The rain was not unusually heavy, nor the streams in spate, at the times that Mr Buxton and Mr Thrower departed from the hut. If the weather deteriorated to the extent that people at the hut were warned of any danger, it was after Robin Buxton and Bevan Thrower had left. Also, it is likely that any warning would have been of the danger of crossing flooded streams, and the extreme rapidity with which mountain torrents can rise during rain. It is not likely that the warning would have covered the danger of being overwhelmed by a debris avalanche or a debris flow.

There was no reason to issue a warning prior to the tragedy, and it is unlikely that one was issued. In a media statement of 5 January, Sarah Smith, the warden at Shelter Rock Hut, is quoted: "People were very solemn and I think it hit home the seriousness of the river" With a search underway, about 10 trampers decided to head back down the river. About six continued towards the saddle yesterday, she said. "I've just told them to be very careful and turn back if they're feeling unsafe." This appropriate warning may well have been the origin of other media reports about trampers being advised of the danger.

Mr Buxton and Mr Thrower were experienced lone trampers. Their choosing to cross the side stream together when it was in fresh, is evidence that they were aware of and experienced in doing such things. Tramping in rain was unlikely to have been new to either of them. Had they received warning earlier at the hut, they would likely have taken it as a caution – and treated it much as earlier in life they might have treated their mothers' warnings about crossing roads on the way to school.

The event that took Mr Buxton's life was not a flooded stream, but a much rarer and more extreme event – a debris flow. It came upon him with little warning. It happened through conditions that arose only tens of minutes earlier. It could not have been predicted an hour or so before. While it might be useful for more trampers to be aware of the possibility of debris flows, and of the signs to look for in the landscape and the weather to warn of their likelihood, such knowledge has little prospect of saving lives. The event is too rare, too sudden, and too dangerous for such knowledge to be particularly useful. The witness to Mr Buxton's death survived because of the speed of his instinctive reaction to a loud noise perceived as a danger. Mr Thrower's reaction is unlikely to have been different had he known about debris flows.

The conditions that gave rise to the debris flows came upon the two while they were traversing a series of debris-flow fans. Some flows did not follow water courses, and so once the trampers had begun to cross the expanse of fans leading to Rees Saddle, they were as safe from debris flows while continuing their journey as they would have been had they chosen to shelter beside a rock until the rain had eased.

CONCLUSIONS

- During a severe storm on the morning of 3 January 2002, Robin Alan Buxton, 28, was killed by a fast-moving debris flow when he was unable to get out of its way while preparing to cross a stream. His death was a very unusual accident, and not something that he or others could have easily foreseen or prevented. He was simply in precisely the wrong spot at the wrong time during a very rare event.
- Bevan Thrower survived the event because of the speed of his instinctive reaction to an unfamiliar noise that he perceived as a danger. He narrowly escaped death and his survival without injury was as much a matter of luck as it was of survival instinct.
- Mr Thrower's parka hood was down, giving him unimpeded, directional hearing, whereas Mr Buxton's hood was up – as expected in intermittent squalls of hail. There may be a lesson in this.
- The debris flow was rare at the site, but it was typical of schist debris flows in West Otago.

ACKNOWLEDGEMENTS

We gratefully acknowledge the assistance of the New Zealand Police, particularly Senior Sergeant John Fookes, Sergeant Frank Dowle and Constable Travis Hughes for their assistance in this investigation. Denis Egerton was both a safe pilot and a font of information. We also thank Bevan Thrower for sharing with us his intimate knowledge of the debris-flow experience. This study was funded by the Earthquake Commission through GeoNet, and by GNS.

REFERENCES

Mcsaveney, M.J. 1995. Debris Flows and Bridge Losses at Waterfall Creek, SH6 at Lake Wanaka, New Zealand. Institute Of Geological & Nuclear Sciences Science Report 95/21. 35 P. Lower Hutt, New Zealand. Institute Of Geological & Nuclear Sciences Ltd.

Mcsaveney, M.J. and Glassey, P.J. (2002). "The Fatal Cleft Peak Debris Flow of 3 January 2002, Upper Rees Valley, West Otago" Institute of Geological & Nuclear Sciences Science Report 2002/03. 28 P. Lower Hutt, New Zealand. Institute of Geological & Nuclear Sciences Ltd.

Tomlinson, A.I. (1980). "The Frequency Of High-Intensity Rainfalls in New Zealand." Water & Soil Technical Publication 19. National Water & Soil Conservation Organisation. 36 Pp.

Turnbull, I.M. (2000). "Geology of The Wakatipu Area." Institute of Geological & Nuclear Sciences 1:250 000 Geological Map 18. 1 Sheet + 72 P. Lower Hutt, New Zealand. Institute of Geological & Nuclear Sciences Ltd.

Tephra Stratigraphy of Maar Craters: Implications for Ash Fall Hazard and Risk Assessment in the Auckland Region

J L Hoverd
MSc (Hons) Geology
Engineering Geologist, Tonkin & Taylor Ltd

Abstract: Maar craters are a common feature of the Auckland Volcanic Field, often forming freshwater lakes once eruptive activity has abated. A c. 61m core recovered from paleolake sediments that fill Onepoto Basin, a maar crater in North Shore City, Auckland reveals a long, high-resolution record of ash fall from both distal and proximal sources. A detailed chronological framework of the core has allowed volcanic ash fall hazard in the Auckland region to be assessed with greater reliability than has been possible in the past. Drilling of the c. 61m core was completed during November 2001. Detailed logging and analysis of the core identified preservation of 78 distinct ash fall events spanning the time interval 9.5-144ka. The 78 ash horizons represent five individual volcanic sources, including the proximal Auckland Volcanic Field, and distal sources Okataina and Taupo Volcanic Centres, Taranaki volcano, and Tongariro Volcanic Centre.

Detailed chronology of the ash fall events is obtained from correlation of ash fall layers contained in the core with events of known age, combined with new radiometric ages from this study. This new information has enabled the frequency of ash fall events from local and distal sources to be determined. Combining ash fall frequencies in the Onepoto core with those proposed in other studies results in a frequency of 1 event per 500 years in the Auckland region (for the period of well-dated events).

INTRODUCTION

The recovery of a long core record from Onepoto Basin in North Shore City, Auckland was part of a broader investigation of paleolake sediments in the greater Auckland region conducted by the Auckland Maar Lakes Project working group. Members of the Department of Geology and the Department of Geography at The University of Auckland undertook the investigation of cores recovered from Onepoto maar crater. The investigation may be divided into two principal areas of interest: firstly, as a record of palaeoenvironmental change in the Auckland region over the last glacial cycle, and, as is the focus of this study, to contribute to the tephrochronology of northern New Zealand and a volcanic hazard and risk assessment for Auckland City.

Understanding of the types of volcanic hazards and their impacts relies heavily on interpretation of volcanic deposits. Current understanding of temporal relationships is not detailed enough to allow eruption frequencies of the Auckland Volcanic Field (AVF) to be estimated (Smith and Allen, 1993). Earlier work in the AVF has seen several attempts at frequency analysis (Latter, 1990; Nichol, 1986; Searle, 1964). However, without a coherent stratigraphic framework and better age control these simple frequency models are not reliable. Sandiford et al. (2001) calculate frequencies of ash fall from a core recovered from Pukaki Crater, based on good chronology. This study aims to enhance these frequencies by examining a record from the northern extent of the AVF.

Auckland faces an additional threat from several large and productive rhyolitic and andesitic eruptive centers 200–300 km to the south and southeast, including the TVZ, Tongariro Volcanic Center, and Taranaki Volcano (Newnham et al., 1999). The threat from distal volcanic sources has in the past been underestimated. For example, a small magnitude eruption from Ruapehu (1996) necessitated the closure of Auckland International Airport on three consecutive nights (Johnston et al., 2000). Further research into the likely impacts of Quaternary silicic volcanism on Auckland's environment and infrastructure is essential.

This study involved a detailed stratigraphic investigation of 78 tephra (ash layers) identified in a c. 61m core recovered from near the centre of Onepoto Basin.

ONEPOTO BASIN

Onepoto Basin is a 700m diameter, basaltic phreatomagmatic explosion crater in North Shore, Auckland (NZMS 260, map grid reference R11/666866). It is one of about 50 known volcanoes in the Auckland Volcanic Field (AVF). No radiometric ages have been presented for Onepoto, and age control for the entire AVF is poor (e.g. McDougall et all. 1969; Shane and Smith 2000; Sandiford et al. 2001). However, activity is considered to post-date c. 140 ka with the most recent eruption in the AVF occurring c. 600 years before present (Froggatt and Lowe 1990). A fresh water lake occupied Onepoto crater after eruptive activity abated. The crater rim was breached by the rising sea levels c. 9 ka, producing an estuary that rapidly filled with mud up to present sea level. Man-made reclamation has occurred in the last 100 years.

Open barrel piston coring near the center of the basin recovered 36.01m of massive, fossiliferous marine mud overlying 25.33m of finely laminated (mm – cm scale), organic rich freshwater sediments interbedded with tephra horizons. The freshwater sediments are dark grey to dark greyish brown and finely laminated. Their continuity throughout the sequence suggests no post depositional bioturbation and no erosional gaps.

IDENTIFICATION OF VOLCANIC SOURCE

This study recognised 78 macroscopic tephra layers within the freshwater sediments (no tephra were found in the marine muds). Tephra layers ranged in thickness from discontinuous layers <1 mm thick to a 630mm bed (rhyolitic ash fall from Rotoehu eruption in the TVZ). Individual suspect tephra layers were identified visually and sampled for analysis. Distinctive geochemistry of each tephra was determined by energy dispersive spectrometry (EDS) methods using an electron probe microanalyser. The results enabled tephra to be fingerprinted and confirmed as distinct ash fall events, and also allowed a volcanic source to be determined for each event. A total of 78 tephra were identified including seven (7) derived from the local volcanoes of the AVF, 27 from the TVZ, 41 from Taranaki Volcano, and three (3) derived from Tongariro Volcanic Centre.

CHRONOLOGY

Establishing a stratigraphic and chronological framework for tephra in the Onepoto core began with the identification of five key tephra derived from the TVZ. These tephra included Rotoma (9.5 ka), Waiohau (13.8 ka), Rerewhakaaitu (17.7 ka), Okaia (27.5 ka), Tahuna, and Rotoehu tephra. Other rhyolitic tephra of known age were subsequently identified based on stratigraphic position. The paucity of information available in the literature regarding tephra derived from Taranaki and Tongariro, and the nature of that derived from the AVF does not allow reliable correlation of individual tephra from these sources (Shane and Smith, 2000; Cronin et al., 1996; Donoghue et al., 1995). Ages of tephra from available literature are considered reliable up to 36.7 ka (Te Mahoe tephra).

Sedimentation rates throughout the interval 9.5–36.7 ka were calculated using published ages of several TVZ derived tephra identified in the core. Approximate ages were interpolated for previously undated tephra using the calculated sedimentation rates (Table 1).

Depth (m)	Source	Name	Age	Depth (m)	Source	Name	Age
36.28	OVC[1]	Rotoma	**9500**	41.14	Tk		41500
36.31	Tk[2]		9700	41.78	OVC	Rotoehu	44700
36.35	Tk		10000	42.18	Tk		46700
36.38	TVC[3]	Opepe	**10200**	43.72	Tk		54600
36.57	Tk		11400	43.77	Tk		54800
36.72	Tk		12300	44.28	Tk		57400
36.80	Tk		12800	44.83	AVF		60200
36.87	TgVC[4]		13200	45.04	Tk		61300
36.97	OVC	Waiohau	**13800**	47.04	Tk		71400
37.13	Tk		15200	47.80	TVZ		75300
37.31	TgVC		16700	48.55	TVZ		79100
37.42	Tk		17600	48.69	Tk		79800
37.43	OVC	Rerewhakaaitu	**17700**	48.71	Tk		79900
37.62	Tk		19000	48.81	Tk		80400
37.96	OVC	Okareka	**21400**	48.89	TVZ		80800
38.11	Tk		23500	48.99	Tk		81300
38.22	OVC	Te Rere	**25000**	49.24	Tk		82600
38.33	TVC	Kawakawa	**26500**	49.46	Tk		83700
38.43	Tk		26800	49.48	Tk		83800
38.48	Tk		26900	49.53	Tk		84100
38.50	TVC	Poihipi	**27000**	49.61	Tk		84500
38.52	AVF[5]		27100	49.64	Tk		84600
38.58	Tk		27400	49.81	Tk		85500
38.59	TVC	Okaia	**27500**	55.61	Tk		90200
38.88	AVF		29100	56.08	Tk		92600
38.89	AVF		29200	51.90	TVZ		96100
39.94	AVF		35200	51.96	TVZ		96400
40.05	OVC	Unit G?	35800	51.98	TVZ		96500
40.15	OVC	Hauparu	36400	52.01	TVZ		96600
40.20	OVC	Te Mahoe	**36700**	52.20	Tk		97600
40.32	OVC		37300	52.24	TVZ		97800
40.35	OVC		37500	52.36	Tk		98400
40.48	TVC	Tahuna	38100	54.22	TgVC		107900
40.63	OVC		38900	55.24	Tk		113000
40.95	Tk		40500	59.48	Tk		134600
40.98	OVC		40700	59.80	AVF		136200
41.00	Tk		40800	60.98	TVZ		142200
41.01	Tk		40800	61.09	TVZ		142700
41.10	Tk		41300	61.34	AVF		144000

[1] Okataina Volcanic Centre; [2] Taranaki Volcano; [3] Taupo Volcanic Centre; [4] Tongariro Volcanic Centre; [5] Auckland Volcanic Field

Table 1. Sources and Ages of Tephra Identified in this Study. Ages in Bold Font are Derived from the Literature, Remaining Ages are Inferred from Calculated Sedimentation Rates.

A preliminary radiometric ($^{40}Ar/^{39}Ar$) age of 144 ± 18 ka was returned for the basal basaltic tephra in the core. Confirmation of this age is dependent on a replicate run that was not available at the conclusion of this study. Using this radiometric age, sedimentation rates were determined for the section of core inferred to have been deposited in the interval 36.7-144 ka, i.e. outside the range of well-dated tephra. Ages are estimated for tephra occurring in this interval using the calculated sedimentation rate (Table 1).

HAZARD ASSESSMENT

Background

Volcanic hazard is the volcanic phenomenon that poses a threat to persons and/or property in a given area within a given period of time. The risk that volcanic eruptions pose to society has increased sharply in modern times due to increased populations; more developed and diversified economies, and more complex infrastructure (Johnston et al., 2000). On a global scale, and relative to most other hazards, natural or man-made, volcanic and related hazards occur infrequently and affect few people. However, volcanic disasters can have significant short-term human and economic impacts. Volcanic eruptions can cause havoc to life and communities on earth. Ash fall hazard is the furthest reaching of volcanic and related hazards. Rock fragments < 2 mm in diameter (ash particles) that fall from the ash cloud, even at great distances from source, are hard, dense, angular, abrasive and pervasive (Sparks, 1997; Carey and Sparks, 1986). Blong (1996) summarises the likely effects of ash fall of varying thickness on infrastructure, property, humans, and livestock (Table 2).

Thickness	Effects on humans and animals[1]	Effects on property and vegetation[1]
1 mm (Class I)	Little or none. Minor, short-lived respiratory complaints.	Airports closed. Contamination of water supplies. Electronic and magnetic equipment disrupted.
10 mm (Class II)	Little to no visibility. Death of insects and fish. Respiratory tract infections prevalent, asthma. Inflamed and infected eyes	Corrosion of exposed metals. Transport immobilised. Shorting and arching of electrical transformers, associated fires. Large scale power failures. Inoperable stormwater and sewage systems. Protection of food crops required.
10 cm (Class III)	Serious respiratory problems widespread. Associated deaths. Bird life destroyed. Imported feed necessary for livestock.	Complete loss of power. Crops severely damaged or destroyed. Branches stripped from trees. Roof collapse. Major failures of all lifelines.
1 m (Class IV)	Death and serious injury resulting from building collapse. Necessitates the removal and protection of livestock.	Building collapse. Destruction of trees. Total failure of all lifelines. Emergency services inoperative. Significant siltation of drainage systems ports and harbours. Short-term loss of land use.
10 m (Class V)	Massive loss of human life, mostly as a result of building collapse and burial. Total loss of livestock.	Long-term loss of land use. Building collapse prevalent. Drainage systems, ports, harbours permanently altered

[1]Effects adapted from Blong (1996).

Table 2. Summary of Likely Hazardous Effects of an Ash Fall Event. Critical Thickness from Blong (1996). Hazard Classification in Parentheses, as Per Classification System Devised in This Study (Table 5).

The degree to which society's vulnerability to volcanic hazard, particularly ash fall hazard, has increased in modern times is demonstrated by comparing the impacts of ash fall from the two largest eruptions of the twentieth century from Mt Ruapehu, the most recently active vent of the TgVC. Johnston et al. (2000) examine the impact of these two similar eruptions that occurred 50 years apart (1945 and 1995-1996). They concluded that social and economic changes were the key factors that produced significantly greater impacts of the 1995-1996 eruption. Ash fall from the 1995-1996

Ruapehu eruption proved to be the most significant hazard (Johnston et al., 2000). Ash fall from these eruptions was recorded throughout most of the North Island of New Zealand. Auckland International and Domestic airports received < 1 mm of volcanic ash, yet this was enough to necessitate closure of the airport on three consecutive nights. Thickness of ash fall deposits in the Onepoto core

Ash Fall Frequency

Ash fall frequencies are calculated for the time interval that spans 9.5-36.7 ka (Table 3). In this interval ages of rhyolitic tephra are well constrained and ages for undated tephra have been estimated. Published ages for rhyolitic tephra older than Te Mahoe are scarce and the accuracy of these should be treated with caution (there are few ^{14}C ages for this interval and calibration to calendar years is difficult). Sedimentation rates have been used to interpolate ages in the interval 9.5-36.7 ka. During the interval 9.5-36.7 ka there are 29 tephra identified in the Onepoto core including four events from TVC, eight from OVC, 11 from Taranaki (Tk), two derived from TgVC, and four from the AVF.

Source	Calculated frequency
All sources	1 per 900 yrs
TVC	1 per 6800 yrs
OVC	1 per 3400 yrs
Tk	1 per 2500 yrs
TgVC	1 per 13 600 yrs
AVF	1 per 6800 yrs

Table 3. Ash Fall Frequency for all Sources in the Onepoto Core During the Interval 9.5-36.7 Ka.

An $^{40}Ar/^{39}Ar$ age of 144 ± 18 ka for the base of the core allows ash fall frequencies to be calculated for ash fall events occurring outside the range of reliably dated rhyolitic tephra (≥ 36.7 ka) (Table 4). Calculations have shown that ash fall events recorded in Onepoto occur at significantly lower frequencies in this interval. This is consistent with the literature, which states that the TVZ, in particular, was considerably less productive during this interval, especially pre-Rotoehu (Wilson et al., 1995).

Source	Calculated frequency
All sources	1 per 2200 yrs
TVZ	1 per 7100 yrs
Tk	1 per 3700 yrs
TgVC	one tephra
AVF	1 per 33 100 yrs

Table 4. Ash Fall Frequency for all Sources in the Onepoto Core Outside the Range of Reliably Dated Rhyolitic Tephra.

Hazard Classification

There have been few studies in the past that attempt to quantify the likely effects of ash fall hazard. The scarcity of literature in this field reflects both the small number of large eruptions occurring in modern times that provide researchers the opportunity to study the effects, and the fact that most large eruptions of modern times have occurred in remote regions, in poor, developing countries such as Indonesia (Blong 1996). The eruptions of Mt Ruapehu in 1995–1996 highlighted the need for greater understanding of the implications of ash fall events in the Auckland area (Johnston et al., 2000).

The severity of ash fall hazard is directly related to the thickness of the resulting deposit (Sparks, 1997) also demonstrated in Table 2. A hazard classification scheme has been devised (I–V) in this

study that pertains to thickness of ash fall deposits and the likely effects (Table 5). The range of thickness used for classifications (I–V) are based around critical thickness, and effects described by Blong (1996) (Table 2). This hazards classification system is generated such that it may be used to assess the level, or degree of hazard based on the thickness of ash fall and the likely impacts.

Thickness	Class
< 5 mm	Class I
6 – 50 mm	Class II
51 mm – 500 mm	Class III
501 mm – 5000 mm	Class IV
> 5000 mm	Class V

Table 5. Hazards Classification System Proposed by this Study. For Effects See Table 2.

Blong (1996) states that volcanic ash compacts to half its original thickness after a few days, particularly if wet. Thus it is likely that the thicknesses of tephra horizons recorded in the Onepoto core are an underestimation of the "real", or original thickness of ash fall deposits. Tephra thicknesses in the Onepoto core are also subject to c. 40 m of lithostatic load, and this would compact the layers even further.

The degree of the ash fall hazard increases significantly when a corrected thickness is assumed compared to hazards associated with observed thickness. For example, the record of Class II hazard increases from 20% of the total number of ash fall events to 38%, almost twice that for the measured thickness. The record of ash fall preserved in the Onepoto core provides a better opportunity to assess the degree of hazard experienced by Auckland because it is longer than any from earlier investigations. The frequency of each class of hazard has been estimated for the intervals 9.5-36.7 ka and 36.7-144 ka (Table 6, Table 7).

Class of hazard	Frequency
Class I	1 per 1300 yrs
Class II	1 per 3400 yrs
Class III	1 per 9000 yrs

Table 6. Frequency of Ash Fall Hazard (Class I-V) Recorded in the Onepoto Core for the Interval 9.5-36.7 Ka.

Class of hazard	Frequency
Class I	1 per 4000 yrs
Class II	1 per 5000 yrs
Class III	< 1 event in 5000 years

Table 7. Frequency of Ash Fall Hazard (Class I-V) for the Interval 36.7-144 Ka. Rotoehu Tephra (44.7 Ka) is the Only Class IV Hazard Recorded in the Core.

Hazard Profile for Ash Fall in the Auckland Region

A composite hazard profile has been constructed for ash fall in the Auckland region using previous studies (Sandiford et al., 2001; Sandiford et al., in press; Newnham and Lowe, 1991), in combination with findings of the Onepoto core (Table 8). Ash fall hazard frequencies are estimated for the interval 6.7-36.7 ka. Previous studies have yielded 43 individual tephra in the interval spanning 6.7-36.7 ka, representing six volcanic sources (includes Mayor Island). The Onepoto core has revealed 17 additional, previously unrecognised tephra in this period.

Volcanic source	Number of events
Taupo Volcanic Zone (TVZ)	18
Taranaki Volcano (Tk)	20
Tongariro Volcanic Center (TgVC)	7
Auckland Volcanic Field (AVF)	13
Mayor Island	1
Unknown origin	2
Total	60

Table 8. Summary of Tephra Identified in Previous Studies Combined With those from this Study for the Interval 6.7-36.7 Ka.

Volcanic source	Frequency
TVZ	1 per 1700 yrs
Tk	1 per 1500 yrs
TgVC	1 per 4300 yrs
AVF	1 per 2300 yrs
Total	1 event per 500 yrs

Table 9. Ash Fall Frequencies for all Sources Combining Tephra from Previous Studies in the Interval 9.5-36.7 Ka (Table 8).

Tephra thickness provided in previous studies enables the hazard classifications (Table 5) to be placed on events recorded in these sections (Pukaki, Mt Richmond, Lake Waiatarua, and Kohuora Crater). This has allowed a more comprehensive assessment of hazard frequency for tephra occurring in the Auckland region in the interval 6.7-36.7 ka (Table 10).

Class of Hazard	Frequency
Class I	1 per 800 yrs
Class II	1 per 1800 yrs
Class III	1 per 6000 yrs

Table 10. Frequency of Ash Fall Hazard (Class I-V) for Tephra Identified in the Auckland Region, Combining this Study with Previous Investigations for the Interval 9.5-36.7 Ka.

Future Work

Hazard assessments are based on the assumption that the same kinds of phenomena will arise at the same frequency in the future as in the past. Obviously this assumption is not always correct. For many volcanoes the period for which the eruptive behaviour is known may be too short to 'capture' infrequent but high magnitude events. Moreover, eruptive behaviour of a particular volcanic source may change with time. The longer the period spanned by the database used to construct past eruptive behavior, the more useful and reliable the hazard assessment is. Over the last few decades there have been one or two eruptions each year by volcanoes with *no records of historic activity* (Sparks et al., 1997). This is a comment on both the shortness of eruption records that are available and the lengths of repose periods. Reconstruction of past volcanic activity over intervals of millennia or tens of millennia is largely based on stratigraphic study.

This study has highlighted the need of further stratigraphic studies regarding ash fall frequency in the Auckland region. Ash fall deposits from AVF volcanoes have limited dispersal, and thus a single stratigraphic study such as this represents but a small window of AVF stratigraphy. Further studies in the greater Auckland region would be essential to gain a clearer picture of ash fall frequencies from the AVF.

SUMMARY AND CONCLUSIONS

Investigation of the tephrostratigraphy of Onepoto maar crater combined with other similar studies (Newnham and Lowe, 1991; Newnham et al., 1999; Sandiford et al., 2001; Sandiford et al., in press), has confirmed that distal volcanic sources, in addition to local basaltic volcanism, pose a significant threat to Auckland city. Taranaki volcano is recognised as the most frequent producer of tephra in the Onepoto core. In the interval of overlap between Onepoto and other cores, particularly Pukaki (9.5-27 ka) core, there are tephra that do not occur in all sequences. Significant differences exist between records of tephra derived from the AVF. For example, between 9.5-27 ka the Pukaki core contains seven basaltic tephra from the AVF, whilst in the same interval the Onepoto core does not contain any. This feature can be attributed to the limited dispersal of volcanic material from basaltic volcanoes in the AVF.

Combining previous multi-source tephra studies in Auckland with findings of the Onepoto core frequency of ash fall events in the region suggests one event per 500 years from all sources. This includes one event per 1700 years from TVZ, one event per 1500 years from Taranaki volcano, one event per 4300 years from Tongariro Volcanic Center, and one event per 2300 years from the Auckland Volcanic Field.

A Class I hazard potentially causing closure of airports, contamination of water supplies and minor respiratory problems is estimated to occur at a frequency of one event per 800 years. The frequency of Class II hazard with the potential to completely immobilise all forms of transport, destroy electricity reticulation systems, disrupt sewage and drainage systems, and damage commercial food crops is estimated as one event per 1800 years. A Class III hazard that is capable of causing failure of all lifelines, building collapse, serious injury and death is estimated to occur at a frequency of one event per 6000 years.

ACKNOWLEDGEMENTS

Funding for this project was gratefully received from the Foundation for Research in Science and Technology (FRST), Auckland Regional Council, and The University of Auckland Science Faculty. This project would not have been possible without the academic support from my thesis supervisor, Dr Phil Shane.

REFERENCES

Allen, S.R., (1992). "Volcanic hazards in the Auckland Volcanic Field". MSc Thesis, University of Auckland, New Zealand, 153 pp.

Allen, S.R. and Smith, I.E.M., (1994). "Eruption styles and volcanic hazard in the Auckland Volcanic Field, New Zealand". *Geoscience Report Shizuoka University*, 20: 5-14.

Blong, R.J., (1984). *Volcanic Hazards: A Sourcebook on the Effects of Eruptions*. Academic Press, Sydney, 424 pp.

Blong, R.J., (1996). "Volcanic hazards risk assessment". In: *Monitoring and Mitigation of Volcano Hazards*, R. Scarpa and R.I. Tilling (Editors), Springer-Verlag, New York, pp. 675-698.

Carey, S.N. and Sparks, R.J.S., (1986). "Quantitative models of the fallout and dispersal of tephra from volcanic eruption columns". *Bulletin of Volcanology*, 48: 109-125.

Cronin, S.J., Neall, V.E., Stewart, R.B. and Palmer, A.S., (1996). "A multiple-parameter approach to andesitic tephra correlation, Ruapehu volcano, New Zealand". *Journal of Volcanology and Geothermal Research*, 72: 199-215.

Donoghue, S.L., Neall, V.E. and Palmer, A.S., (1995). "Stratigraphy and chronology of andesitic tephra deposits, Tongariro Volcanic Centre, New Zealand". *Journal of the Royal Society of New Zealand*, 25: 115-206.

Froggatt, P.C. and Lowe, D.J., (1990). "A review of late Quaternary silicic and some other tephra formations from New Zealand: their stratigraphy, nomenclature, distribution, volume and age". *New Zealand Journal of Geology and Geophysics*, 33: 89-109.

Johnston, D.M., Houghton, B.F., Neall, V.E., Ronan, K.R. and Paton, P., (2000). "Impacts of the 1945 and 1995-1996 Ruapehu eruptions, New Zealand: An example of increasing societal vulnerability". *GSA Bulletin*, 112(5): 720-726.

Kermode, L.O., (1992). "Institute of Geological and Nuclear Sciences Geological Map 2". *Institute of Geological and Nuclear Sciences*, Lower Hutt, New Zealand.

Lowe, D.J., (1988a). "Late Quaternary volcanism in New Zealand: towards an integrated record using distal airfall deposits in lakes and bogs". *Journal of Quaternary Science*, 20: 111-120.

Lowe, D.J., (1988b). "Stratigraphy, age, composition, and correlation of late Quaternary tephras interbedded with organic sediments in Waikato lakes, North Island, New Zealand". *New Zealand Journal of Geology and Geophysics*, 31: 125-165.

Lowe, D.J., Newnham, R.M. and Ward, C.M., (1999). Stratigraphy and chronology of a 15 cal yr sequence of multi-sourced silicic tephras in a montane peat bog, eastern North Island, New Zealand". *New Zealand Journal of Geology and Geophysics*, 42: 565-579.

McDougall, I., Polach, H.A. and Stipp, J.J., (1969). "Excess radiogenic argon in young subaerial basalts from the Auckland Volcanic Field, New Zealand". *Geochimica et Cosmochimica Acta*, 33: 1485-1520.

Newnham, R.M., Lowe, D.J. and Alloway, B.V., (1999). "Volcanic hazards in Auckland, New Zealand: a preliminary assessment of the threat posed by central North Island silicic volcanism based on the Quaternary tephrostratigraphical record". In: *Volcanoes in the Quaternary*, C.R. Firth and W.J. McGuire (Editors), Geological Society of London, London, pp. 27-45.

Nichol, R., (1986). ""I think I'll put some mountains...here": Volcanic risk in Auckland". *Tane*, 31(133-138).

Sandiford, A., Alloway, B.V. and Shane, P.A.R., (2001). "A 28 000-6600 cal yr record of local and distal volcanism preserved in a paleolake, Auckland, New Zealand". *New Zealand Journal of Geology and Geophysics*.

Sandiford, A., Horrocks, M., Newnham, R.M., Ogden, J. and Alloway, B.V., in press. "Environmental change during the last glacial maximum (c. 25000-c. 16 500 years B.P.) at Mt Richmond, Auckland Isthmus, New Zealand". *Journal of the Royal Society of New Zealand.*

Searle, E.J., (1964). "Volcanic risk in the Auckland Metropolitan district". *New Zealand Journal of Geology and Geophysics*, 7: 94-100.

Shane, P.A.R., (2000). "Tephrochronology: a New Zealand case study". *Earth Science Reviews*, 49: 223-259.

Shane, P.A.R. and Hoverd, J.L., (2002). "Distal record of multi-sourced tephra in Northern New Zealand: implications for volcanic chronology, frequency and hazards". *Bulletin of Volcanology*, 64: 441-454.

Shane, P.A.R. and Smith, I.E.M., (2000). "Geochemical fingerprinting of basaltic tephra deposits in the Auckland Volcanic Field". *New Zealand Journal of Geology and Geophysics*, 43: 569-577.

Smith, I.E.M. and Allen, S.R., (1993). "Volcanic Hazards at the Auckland Volcanic Field". *Volcanic Hazards Series* No. 5, 34 pp.

Sparks, R.J.S., (1997). *Volcanic Plumes*. Wiley, Chichester; New York, 574 pp.

Wilson, C.J.N. et al., (1995). "Volcanic and structural evolution of the Taupo Volcanic Zone, New Zealand: a review". *Journal of Volcanology and Geothermal Research*, 68: 1-28.

Landform Development of the Central Coastal Bay of Plenty Region: An Integrated Study

J H Rae
MSc (Hons)
Network Control Planner, Transfield Services (New Zealand) Ltd.

Abstract: The Central Bay of Plenty contains numerous widespread, lithologically variable geological deposits that have been formed by a dynamic system of volcanic, geomorphic and tectonic processes. The landscape is characterised by alluvial plains and dissected ignimbrite plateaux. Tectonism and processes of deposition and erosion have resulted in a distinctive terraced morphology. Regional morphology is controlled primarily by both lithological and structural attributes, while selected studies show that localised development results from a combination of slope failure mechanisms and surface processes, related to differences in geotechnical properties, lithology and drainage. Recent reworking and re-sedimentation is evident across the region, as indicated by the presence of numerous volcaniclastic units and alluvial terraces. This is indicative of a landform development cycle which is can be summarised by both depositional (constructive) and erosional (destructive) phases.

INTRODUCTION

Volcanoes, particularly when associated with silicic volcanism, are often known for large scale, cataclysmic episodes, resulting in distinctive primary products and features (e.g. pyroclastic flows, caldera formation, ring faulting, cone collapse). The hazards, which result from such eruptive processes and products, vary enormously during the event and the immediate, resultant effect on the community and infrastructure can be devastating. In addition to the initial impact of a volcanic event, secondary processes and effects can continue to affect the surrounding environment as the local system adapts to new materials and alteration. Effects are widespread and can occur hundreds of kilometres from the source. The landform development of such areas can be attributed to primary (syn-eruptive) processes and materials and in addition, secondary (post-eruptive) events where both deposition and erosion are responsible for morphological development. Physical features include: Coastal cliffs; fault scarps; alluvial valleys and terraces; coastal plains and dune formations. The central coastal Bay of Plenty is a region defined by such distinct geological and geomorphic features.

In order to further an understanding of regional history and landform development an integrated study involving stratigraphic, lithological and geomorphic analysis was performed. This study was conducted for a thesis at the University of Waikato and incorporated description of both regional and localised processes. Initial field work and mapping was conducted in conjunction with Environment Bay of Plenty Regional Council. The study involved detailed analysis of a field area located within the central, coastal Bay of Plenty region (Figure 1.), extending from Matata in the east and to Pukehina in the west, and inland to Pongakawa and Manawahe. Detailed mapping was undertaken within this 250 km^2 area and landform development processes interpreted as a result of this field study.

REGIONAL GEOLOGY

The geology of the central coastal Bay of Plenty is dominated by a variable series of deposits, representing the products of a dynamic system of volcanic, geomorphic and tectonic processes. These deposits vary in source, lithology, thickness and distribution. Located on the edge of the Whakatane Graben, west of the Taupo Volcanic Zone (TVZ), the area contains evidence of numerous past volcanic and sedimentary processes and products. Volcanism however forms the dominant control on regional development. Localised tectonic instability and climatic factors also influence geomorphic and geological development.

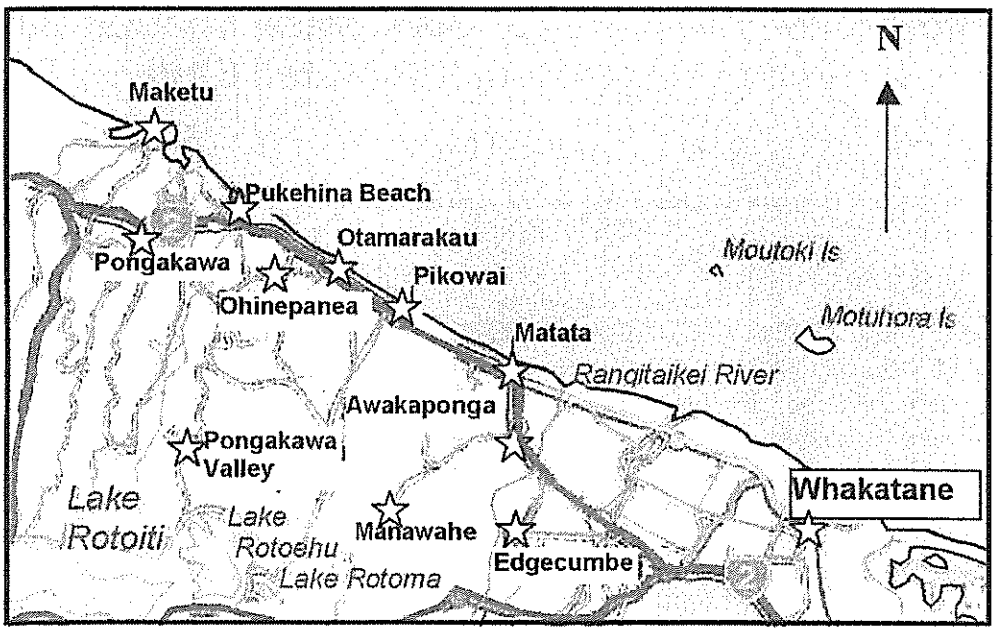

Figure 1. Location Map of Study Area.

The Okataina Volcanic Centre (OVC) is located directly south of the study area and forms the principal source of materials. Deposits are also found originating from several smaller vents located to the south-east of the study area (i.e. Manawahe, Putauaki/Mount Edgecumbe). These deposits are localised, of intermediate (dacitic and andesitic) composition, and where preserved, record early development prior to the increased dominance of Okataina volcanism, now evident across the field area. Uplift has also resulted in the exposure of various sedimentary materials and basement rock. Lithology is therefore variable with the majority of sections formed primarily of rhyolitic/silicic materials. Less silicic rock (i.e. andesite), basement and extensive, reworked deposits are also present.

Development can be summarised by the following:

- Erosion of basement and sedimentary deposition i.e. marine deposits. This stage is constructional and destructional.
- Initial and on-going eruption of local vents i.e. Manawahe Andesite extrusion. This stage is constructional.
- Caldera forming pyroclastic phase. Deposition of with large volume, welded and non-welded pyroclastic density current (PDC) materials i.e. Mamaku and Matahina Ignimbrites. This stage is constructional and destructional.
- Caldera alteration/ infilling events with smaller, lower volume PDC events i.e. Rotoiti Ignimbrite. This stage is constructional.
- Dome building phase with lava extrusion and eruption of, minor pyroclastics i.e. Rotorua Subgroup. This stage is constructional.

The study area is dissected by numerous NE-striking faults, closely mimicking structural trends that are consistent with its position in the northern Taupo Fault Belt. As a consequence the field area is tectonically active, with an extensive history of subsidence and uplift which began around 2 Ma with formation of the Whakatane Graben (eastern boundary of the study area). The Matata fault forms a prominent fault scarp dividing the Kaharoa Plateau from the Rangitaiki alluvial plains. Uplift along this fault has exposed greywacke gravels, evidence of past flooding events on the Rangitaiki Plains. Subsidence still occurs to the west, while uplift occurs in the east, resulting in a gradual tilting of the study area. Western subsidence has formed a distinct low-lying block faulted topography with local exposures of basement. Several large greywacke outliers are present, formed through the uplift of the Mesozoic basement, along a series of buried faults. Remnant greywacke is massive, extensively fractured, and shows signs alteration. Localised faulting has also resulted in the weakening of materials and provides a structural control for streams across the study area.

REGIONAL GEOMORPHOLOGY

The study area is a geographic rise between two lowlands. The eastern boundary of the study area is defined by the Rangitaiki Plains and Matata fault zone. The Pukehina Plains define the western extent. The Kaharoa Plateau dominates the central study area. The upper surface of this dissected ignimbrite plateau is comprised of moderately steep-low rolling hills (35-45°). Lithology is controlled by strongly welded ignimbrite and andesitic lava flows in the east and unconsolidated, non-welded flow and fall deposits in the west.

West of Matata, coastal sections show rapid termination of the upper surface of the Kaharoa Plateau and unconsolidated, non-welded materials form steep coastal cliffs (45-85°). Along this eastern section of study area the upper surface of the plateau is dissected by streams, forming narrow, convoluted escarpments that become deeper towards the coastline. Stream patterns follow the regional faulting trend where stream channels are narrow and steep, caused by water incising along fault scarps, cutting down through welded materials and consolidated deposits (Matata Cliffs). Stream channels are filled with coarse gravel and boulders (welded Matahina Ignimbrite and Manawahe Andesite) and small volumes of fine pumiceous silt. Groundwater is impeded in many areas, often caused by an impervious tephric, fine silty, clay surface that exists below the Matahina Ignimbrite. Along this contact zone seepage is heavy, and thick, altered, clayey layers may be found where seepage has weathered the underlying marine materials and surface colluvium.

Further south-east the Matahina Ignimbrite is down-faulted and only weak, unconsolidated pyroclastic deposits are exposed (Mangaone and Rotorua subgroups). Moderately thick loess deposits may also be found overlying the Matahina Ignimbrite. This material is soft, unconsolidated and subject to rilling.

The western side of the study area marks the termination of the Kaharoa Plateau and is characterised by lowland plains and broad alluvial valleys with low hills to the south. Figure 2. shows the Rotoehu valley which is typically bounded by a terrace of volcanic materials and infilled by gentling sloping alluvial fans (0-5°). The terraces are described as flat topped with moderately steep (26-35°), convex profile slopes. The Matahina Ignimbrite is absent from the western half of the study area, and stratigraphy is dominated by the non-welded Rotoiti Eruptives (e.g. Matahi Scoria, Rotoehu Tephra Rotoiti Ignimbrite, and reworked unit). The Rotoiti Ignimbrite is widespread, formed of several thick units, and provides a major geomorphic control. The ignimbrite overlies and mimics a gently dipping surface formed from older ignimbrites. The upper surface of this unit is truncated, showing evidence for post depositional erosion and stream channels are frequently infilled with reworked Rotoiti sourced pyroclastic materials.

Figure 2. Rotoehu Valley Morphology.

South of the coastal lowlands the western extent of the Kaharoa Plateau thins and terminates. The plateau surface (formed of Rotoiti Ignimbrite) is gently dipping, moderately elevated, and stream

incised. The ignimbrite surface has been eroded to form a stream-incised landscape with low rolling 'beehive' shaped hills. Tectonism has formed a terraced morphology. These terraces represent distinct periods within the geological development of the study area, where down-faulting and erosion have lowered the surface of the ignimbrite. Surface geology is permeable, consisting of a low density, highly vesicular, highly porous substrate, with low impedance therefore reducing surface flow and runoff and largely increasing groundwater recharge rates. Alluvial sediment is thick and extensive across the valley floors and subject to reworking during high intensity rainfall events. Hummocks are found at the base of steep sided terrace slopes and form through riverbank failure and aggradation. Streambeds have a clayey-fine sand base and contain dominantly fine-grained sediment with channels of low angles, bounded by a thick alluvial terrace, formed from reworked volcaniclastic deposits and representing a depositional regime.

Lithology and Failure Types

A number of failure types are seen across the field area; these are controlled by lithology, faulting and climatic conditions (i.e. frictional resistance, permeability, water volume and flow rate. There are two distinct trends:

- Rock fall and debris flow failures where welded and indurated materials are prone to large-scale mass movement processes. This is a dominant feature of stream valleys within the eastern study area, in the vicinity of Matata.
- Translational movement and soil failures are a dominant feature of the western study area.

The majority of reworked deposits across the field area can be described as soft, dominantly granular with a silty glass rich matrix. Deposits are both grain and clast supported. Tephric loess and sandy, fine-grained reworked deposits are common. Poorly sorted, frequently bedded deposits of indurated rock are also found to the east of the study area, indicative of numerous small debris flows. Debris flows are common within the eastern study area, where welded ignimbrite materials overlie impervious marine sands. The Matahina Ignimbrite displays thin, discontinuous jointing with a hexagonal and columnar pattern often common to welded ignimbrites. Slab failure is common along these joint planes, where joint propagation has occurred and is associated with high seepage and pore water pressure. Failure susceptibility is increased due to high intensity rain storms and the presence of a clay-rich drainage impeding surface beneath coherent ignimbrite materials.

Debris flows initiate in the headlands of local streams and exhibit run out distances of 2-3 km. Dispersal occurs as flows reach the cliff base and form wide depositional lobes. Such flows damage engineering structures (culverts, drains) and create a hazard to local roading systems (i.e. SH 2). These minor events occur frequently i.e. several times a year (based on field observations). Deposits described in the field suggest that the study area has in the past seen numerous erosional and mass movement events and been inherently unstable, particularly within zones defined by steep slopes and unconsolidated deposits. As Figure 3. shows, many stream beds, poorly sorted, poorly graded deposits are found, formed from reworked, welded ignimbrite and rhyolite lavas (e.g. upper Mimiha Rd, NZMS 260 V15 346 616). Debris deposits are also evident in geological history. Thick (2-6 m) layers are found within marine sands, where streams have now incised into the Matata cliffs (e.g. western Herepuru Rd, NZMS 260 V15 374 626). Paleo-flows form deposits similar to recent debris flow deposits, with coarse ignimbrite boulders and cobbles, dispersed with a fine sand and silt matrix. Recent failures (i.e. recent slips at Pikowai) also highlight this instability.

Smaller slumping events and subsurface failure (rills, gullying, sheet wash) features occur in low lying, rolling hill country, constructed of unconsolidated pyroclastic deposits to the west and south of the study areas, these events however, form low-risk events due to the unpopulated nature of the field area. Soil failures are common particularly in low angle, reworked volcaniclastic materials. Soil failure may occur due to increased load or pore water pressure and is common in clay rich soils. These clay rich layers have low frictional resistance and impeded drainage, resulting in high pore water pressure along the failure plane, and subsequent failure. Translational failures also occur frequently in low foothills, with low slope angles (5-30°), these are however of minor size (25 m length maximum). Recently deforested areas are prone to translational slides particularly during high rainfall events (e.g.

Manawahe Rd, NZMS 260 V15 378 563; Otamarakau Valley Rd, NZMS 260 V15 265 650). Failures occur easily within the soft granular substrate and include minor rills and gullying. Translational failure is common, particularly along alluvial flats and on interfluves where rich clay accumulation has occurred. Foot-slopes are particularly prone to gullying and slide failure. Roading systems are easily undermined as grain transport carries away sediment from beneath the surface.

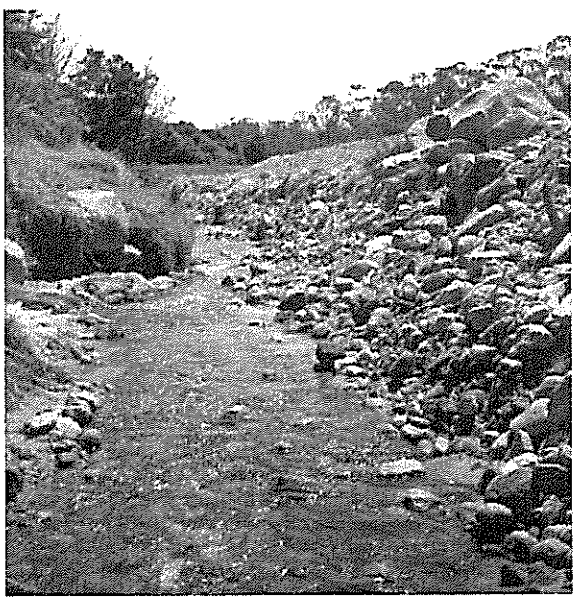

[Debris Alongside SH2, Ohinekoao]

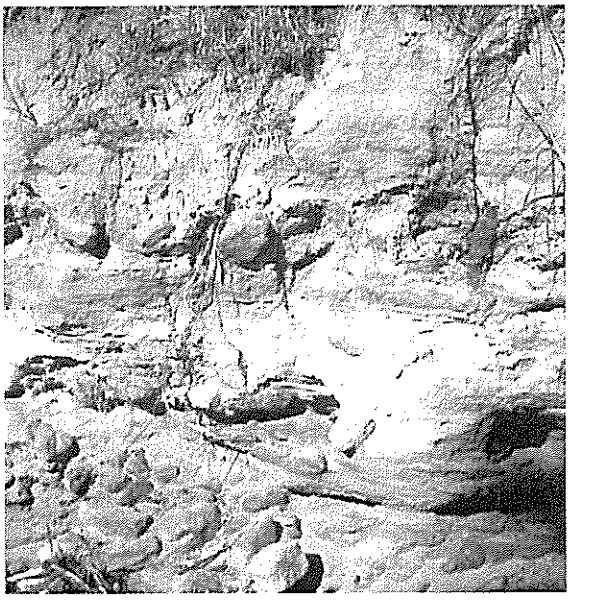

[Relict Debris Flow Upper Mimiha Road (NZMS 260 V15 346 616]

Figure 3. Reworked Volcaniclastic Deposits

In low lying areas (i.e. western section and south-eastern areas) high-volume surface water flows across soils and recently exposed unconsolidated substrate resulting in grain by grain transport. Slight depressions in topography result in concentration of flow and preferential incision into the ground surface i.e. formation of distinctive gullying along Manawahe Rd. Gullies exist on low angle slopes and range in size from 1-3 m diameter, and 5-7 m length. Rills are widespread across freshly exposed primary and reworked pyroclastic materials and form on low-steeply dipping slopes (3-60°). Size ranges between 5-20 cm. Sheet wash occurs across flat, low-sloped valley floors with low-density vegetation. Bedload transport is also unusually high considering low water volumes present within the streams and occurs as a direct result of preferential elutriation and transportation of fine, low density pumiceous materials. Coarse material is very rare, and larger clasts where present are pumiceous.

DEVELOPMENT

Initial investigation reveals that primary volcanic processes were vital in landscape modification in the area. In addition to this, field study shows that secondary processes have the potential to have a continued effect on the local environment, both disrupting infrastructure and creating a disturbance to human behaviour and developments, the most noticeable effect being on local waterways and road systems.

Landform development has been accentuated by erosional and depositional events throughout the Quaternary. Terrace formation is dominantly degradational, where reworking and erosion have changed the surface morphology of pyroclastic deposits (i.e. reworking of Rotoiti and Mangaone Tephra formations). Terrace construction also occurs where re-deposition has resulted in the formation of thick alluvial terraces (i.e. Pongakawa and Rotoehu valleys). Terraces are constructed with a flat upper surface and steep slopes, separated by alluvial valleys. At a closer scale, large gorges and fluvial reaches are often found within these valleys, with inner channels and low alluvial terraces. Migrating sand dunes are common towards the coast. Also minor north-south trending faults and jointing are common particularly along the coastline (Otamarakau Quarry) and are responsible for minor colluvium and talus deposits. Units are highly distorted around fault systems.

Primary Depositional Processes

Volcanism provides a large and instantaneous source of sediment and is responsible for the destruction of vegetation and hydrological systems. Primary volcanic deposits provide the principal source of detritus for resedimented volcaniclastics in the study area. Boundaries are defined through weathering and erosional contacts, i.e. paleosols, fluvial/aeolian deposits. Truncation and debris deposits provide evidence of erosion following the deposition of the Matahina and Rotoiti Ignimbrites. Volcanic deposition provides the foundation for morphological change. Geomorphic features relate directly with primary materials i.e. fine grained crystal rich deposits are prone to erosion. Thick non-welded pyroclastic fall deposits (i.e. Maketu and Hauparu Tephras) form the dominant lithology of low terraces to the west. These pumiceous deposits contain low density, coarse, highly vesicular clasts, which have extremely high friction values, enabling pumiceous deposits to form vertical faces as seen in Figure 4.

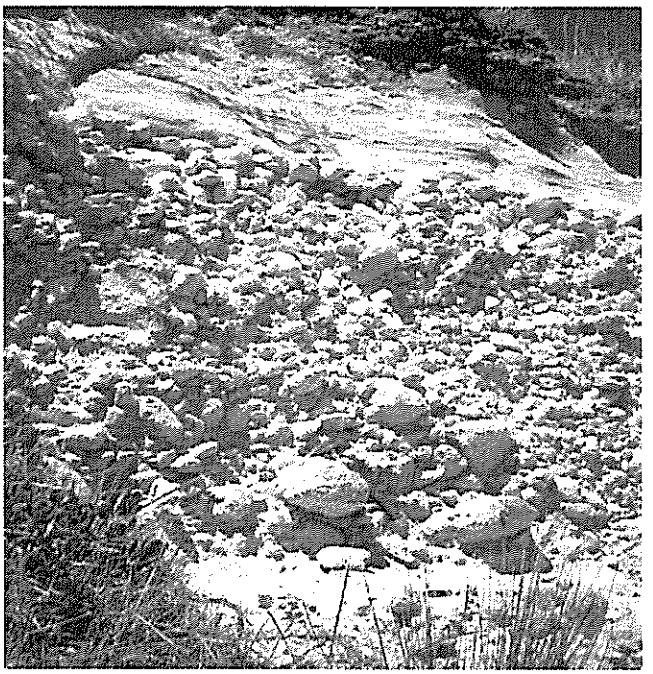

Figure 4. Hauparu Tephra as Seen at Otamarakau Marae (NZMS 260 V15 271 684).

Hydrological Processes

Large, gently sloping, low angle watersheds tend to have a large proportion of infiltration, with lower overland flow, compared to high angle, small catchments with quick surface runoff. Major floods will change stream bed geomorphology as the fluvial system adjusts to new conditions. Adjustment occurs when a stream exceeds the limiting threshold and new equilibrium conditions are required to account for increased bed load and water volume (Inbar, 2000). Gravel and boulders have a high shear threshold and require a higher flow regime to allow bed transport. Rivers with frequent flooding and riverbank failure events are found with a thin veneer of coarse alluvium over bedrock e.g. Ohinekoao Stream (NZMS 260 V15 375 627). Within the field area streams with a low flow regime (e.g. Hauone Stream) contain fine silts and sands and stream banks show fine sedimentary structures.

Dense vegetation along SH2 generally stabilises slopes, however with heavy rainfall events, load is increased on the substrate due to saturation and wet vegetation. A large section of vegetation was removed from the cliff face during a recent, localised failure event, and the exposed surface has been subject to extensive rilling. Within a recently felled forestry block (Manawahe Rd, NZMS 260 V15 387577) sheet wash and rill formation are clearly seen. Gullies with widths measuring up to 1 m and depths of 0.75 m, have formed rapidly in the newly exposed, silty, tephra rich substrate. The majority of damage in such an altered landscape is caused by concentrated flow erosion and winnowing of low density, porous materials.

Weathering and Alteration

The degree of alteration and weathering is also important. Devitrified pumice is soft, with low tensile strength, is easily deformed and is highly sensitive. Alteration weakens clasts (thermal oxidisation), however minor clay formation increases cohesion. Non-welded ignimbrites (i.e. lower Rotoiti Ignimbrite) and pyroclastic fall deposits essentially act as a large mass of individual grains.

Sea water reacts quickly with tephritic deposits, forming thick, well-indurated iron pans and lithified deposits resistant to erosion (Figure 5.).

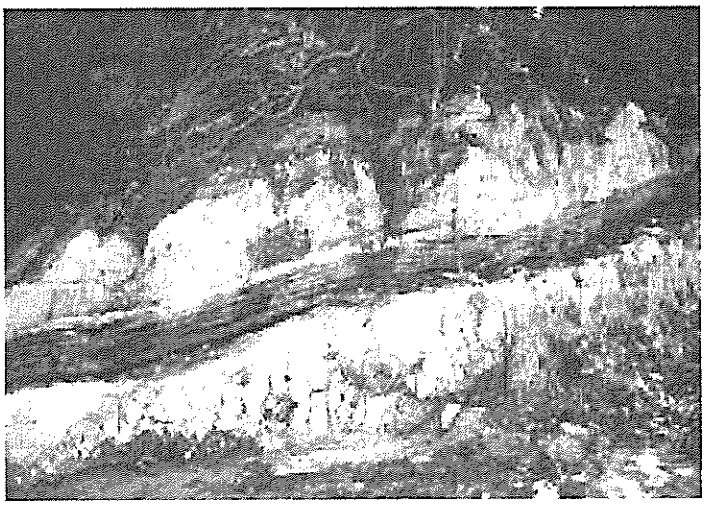

Figure 5. Well Indurated Iron Pan. Pukehina Beach (NZMS 260 V16 214 727).

Soil type also influences shear strength and hydraulic conductivity. Clay type is variable and dependant on climatic conditions. A temperate climate with frequent intense rainfall events has contributed to a variety of weathering and transportation processes responsible for the formation of extensive terraces, mass movement features and reworking processes and deposits. Limonite staining and leaching are also both common where there is impeded drainage and high rainfall. Thick (4-5 m) reworked deposits are found in the Pongakawa and Rotoehu valleys. Significant reworking occurred after the deposition of the Rotoiti Ignimbrite and Mangaone Subgroup tephras, due to a colder climate with intensified erosion. These reworked deposits are soft and prone to failure.

During phases where eruption rates are rapid, paleosols are poorly developed (i.e. few paleosols are seen occurring within the Mangaone Subgroup Tephras. Paleosols develop most readily during warmer climatic periods, therefore extensive paleosol development has occurred during the Holocene. Enhanced weathering and paleosols development is evident after the deposition of the Rerewhakaaitu Tephra, marking the end of the last glacial and the beginning of climatic warming. Deposits above this tephra bed indicate a significant reduction in fluvial aggradation, down-cutting processes, loess accumulation and increased paleosol development (Newnham *et al.*, 2001). Materials are more weathered and frequently reworked through pedogenic processes and incorporated within paleosol layers (e.g. Taupo and Kaharoa tephras).

Erosional Processes, Reworking, and Re-Deposition

Numerous stream deposits and relict debris flows indicate how a post-eruption surface can been subject to large scale reworking. Thick, poorly sorted, heterolithological (greywacke and volcaniclastic) reworked fluvial and debris deposits are found along stream beds (e.g. Taupo and Kaharoa Flood deposits) and have helped to construct the modern environment (Nairn and Beanland, 1989).

In the centre of the field area, laharic deposits are found. These deposits incorporate Matahina Ignimbrite and are overlain by Rotoiti Tephra, indicating that deposition occurred during the extensive

erosional break between units. Sections within the Herepuru and Ohinekoao Stream valleys display thick reworked fluvial and debris deposits, formed from weathered Matahina Ignimbrite. A number of sections also indicate large amounts of reworking, (i.e. Herepuru Valley, Mimiha Rd Pikowai Rd, and SH 2 Pikowai Pyroclastics sections) from a source outside the study area. These reworked deposits represent erosion and reworking of pyroclastic materials, no longer seen in their original state, within the field area. Faulting of these sediments has occurred since deposition and in the Pikowai Pyroclastics, is responsible for the formation of thick liquefaction structures within the deposit.

Deposits show a range of sorting classes, ranging from moderately well-sorted (moderately fine-grained traction current deposits, i.e. Mimiha Rd fluvial section) to very poorly sorted (fine to coarse-grained debris flow deposits, i.e. Pikowai Rd reworked section). A range of secondary transport processes is responsible for the formation of these deposits and these processes have resulted in significant alteration of primary source materials. In the western sector of the field area, preferential elutriation and transportation of fine pyroclastic materials, and high volumes of bedload within streams, has also caused major problems to drainage systems and land use (i.e. Hauone Stream). Gully and tunnel processes occur frequently causing slope failures and underslips, which undermine roads and fences (i.e. Pongakawa valley). Fine-grained reworked materials can be seen covering pastureland.

The Rotoiti eruptives have also been eroded and extensively reworked. The upper surface of the Rotoiti eruptives is truncated. In several sections a poorly sorted clay-rich unit overlies the eruptives and is interpreted to represent fluvially reworked welded Rotoiti Ignimbrite and incorporated Rotoehu Ash. Thick, coarse-grained loess deposits also overlie the Rotoehu Ash, i.e. at Cameron Quarry. Several sections along Manawahe Rd show truncation of both the Matahi Scoria and Rotoiti Ignimbrite caused through extensive erosion, most likely resulting from a cold climate and high rates of physical weathering and transport.

Colluvium and talus deposits are also common and susceptible to remobilisation due to low densities and high pore water pressures. Talus deposits can be rapidly destroyed by weathering, resulting in intensive surface erosion through rilling, gullying and sheet wash. Subsurface failure results in slumping. Erosion causes undermining at the base of the talus slope and results in shallow-seated slide failures.

A warmer wetter climate has also enhanced peat formation. Thick peat layers are found along the coastal plains in low lying areas, overlain and intercalated with Holocene tephras (Lowe *et al.,* 1992; Newnham *et al.,* 1995; Giles *et al.,* 1999). Scattered dune sands and blow-out dunes comprise areas of higher elevation (ridges and hummocks) and result from a migrating, prograding coastline and increased accretion (Nairn and Beanland, 1989). Voluminous tephra deposits have altered the coastline and been responsible for major progradational events.

Alluvial deposition and coastal progradation continues to occur along the Bay of Plenty coastline. Shoreline and longshore drift are influenced by northern storms and the predominant strong south-westerly winds. Frequent high intensity rain events and high rates of clay formation will cause the continued instability of coastal cliffs, therefore the probability of further debris flows along the coastal section is high. Aggradation is a common depositional processes, with streams displaying high bed load. Small debris flows and drainage channel infilling continue to occur along coastal sections. Impeded drainage and a clayey sub-surface also enhance mass movement processes (slumping and creep).

CONCLUSIONS

For simplification, landform development has been categorised into a series of stages based on major structural, depositional and erosional events, including:

- Deposition of Pre-Matahina materials (including reworked greywacke gravels, marine sands, intercalated tephras);

- Caldera formation south of the study area – with periodic ignimbrite deposition and reworking of post eruptive surfaces (Matahina Ignimbrite).
- Pre-Rotoiti erosion, reworking and transportation. (Upper Mimiha Rd Fluvial deposits, Pikowai Pyroclastics);
- Continuation of volcanic deposition (Rotoiti eruptives);
- Renewed erosion and reworking. Thick loess formation;
- Caldera modification and deposition of Mangaone and Rotorua Subgroup fall and flow deposits.
- Renewed erosion and reworking, with increased soil formation and alteration after the end of the last glacial period.

Study of geological history within the study area reveals periods of fluvial erosion, deposition of pyroclastic fall and flow materials, reworking and transportation, and this has resulted in a unique morphology. Landform development is summarised into cyclic phases of both constructive development (incorporating all depositional events), and destructive development (incorporating all erosional events).

Constructive (depositional) phases resulted in extensive terrace formation. This has occurred at several points in geological history (deposition of Matahina Ignimbrite, Rotoiti Eruptive and Mangaone Subgroup materials) and resulted in the formation of a stepped morphology. Erosional phases are responsible for truncation, surface alteration and failure events. Destructive phases have also caused formation of numerous heterolithological deposits (e.g. Pikowai Rd fluvial deposits, Pikowai Pyroclastics, assorted debris flow deposits and volcaniclastic fluviatile facies). A range of sedimentary facies is represented within these deposits, with a range of sorting and grainsize classes seen. These reworked deposits infill alluvial valleys and occur at several periods throughout the stratigraphic record. Erosion and reworking of the Rotoiti Ignimbrite also resulted in the deposition of extensive terraces. Reworked ignimbrite also forms low hummocks within alluvial valleys. Low (5 m thick) terraces are located in the north-west of the field area (Pukehina Plains) and are comprised of Mangaone Subgroup deposits.

Minor reworking and mass movement processes still operate within the study area. Debris flows are prevalent in the east (within jointed, hard rock substrate), while less prominent surfical erosion and subsurface failure (slumping, rill and gully formation, translational failure) occur in the west (soft, unconsolidated, granular pyroclastics). Such flows have a tendency to flow out over the road surface along the eastern, coastal cliff section causing minor damage to roadside structures and drainage systems.

ACKNOWLEDGEMENTS

The author would like to acknowledge the work of Associate Professor Roger Briggs, Associate Professor David Lowe and Dr Vicki Moon from the University of Waikato for assistance during field study and collation. Environment Bay of Plenty was responsible for funding this research.

REFERENCES

Giles, T.M.; Newnham, R.M.; Lowe, D.J. and Munro, A.J. (1999). "Impact of Tephra fall and environmental change: a 1000 yr record from Matakana Island, Bay of Plenty, North Island, New Zealand." *Volcanoes in the Quaternary.* Geological Society, London, Special Publications. Ed: Firth, C.R.; McGuire, W.J. 161, pp. 11-26.

Inbar, M. (2000). "Episodes of flash floods and boulder transport in the Upper Jordan River," In: *The Hydrology – Geomorphology Interface: Rainfall, Flooding, Sedimentation and Landuse.* Ed: Hassan, M.; Slaymaker, O. and Berkowicz, S. International Association of Hydrological Sciences. Publ. 261, pp. 185 – 200.

Lowe, D.J. and Hogg, A.G. (1992). "Application of new technology liquid scintillation spectrometry to radiocarbon dating of Tephra deposits, New Zealand." *Quaternary International.* 13/14, pp. 135-142.

Nairn, I.A. and Beanland, S. (1989). "Geological setting of the 1987 Edgecumbe earthquake, New Zealand." *New Zealand Journal of Geology and Geophysics.* 32, pp. 1-13.

Newnham, R.M. and Lowe, D.J. (2001). "The search for the Younger Dryas cooling in New Zealand." *Les Dossiers de l'Archeo-Logis.* 1, pp. 61-65.

Newnham, R.M.; Lowe, D.J. and Wigley, G.N.A. (1995). "Late Holocene palynology and paleovegetation of Tephra-bearing mires at Papamoa – Waihi Beach, western Bay of Plenty. North Island, New Zealand." *Journal of the Royal Society of New Zealand.* 25, pp. 283-300.

Stipp, J.J. (1968). "The geochronology and petrogenesis of the Cenozoic volcanics of the North Island, New Zealand." Unpublished PhD thesis, Australian National University. Lodged in the Australian Capital Territory Library, Canberra, Australia.

NZMS 260. V15 Edgecumbe. 1:50 000. Edition 1 1988, Limited Revision 1998. Land Information New Zealand.

Engineering Geological Characteristics of Andesite Rocks along the Proposed Favona Decline

T Adhikary
M.Sc., Pg Dipl, TIPENZ
Engineering Geologist, Sinclair Knight Merz

Abstract: Feasibility studies are underway for the design and construction of an exploration decline on the proposed Favona Underground Gold Mine at Waihi. The geology of the area has been investigated and it has been known that Andesite, as well as Hydrothermal Tuff and Breccia will be encountered in the proposed exploration decline.

These volcanic rocks are weathered and hydrothermally altered at the decline level. This paper presents the results of the engineering geological investigation from the ground surface to the decline invert level.

It is concluded that the weathering grade and type of alteration have considerable impact on the intact rock strength. Moisture Content, unconfined compressive strength, tensile strength, slake durability and CERCHAR Abrasivity have been obtained from laboratory testing and some discussion on the relationship with different rock properties are presented.

INTRODUCTION

Epithermal gold – silver bearing quartz veins of the Favona deposit are hosted in Late Miocene andesite lava flows and local dacite tuffs of Waipupu Formation. An exploration decline has been proposed 2km east of Waihi Township to further investigate the Favona and Moonlight lodes.

This paper describes the geology along the proposed length of the decline and the engineering geological characteristics of the andesite and associated rocks. It also summarises the mechanical behaviour and abrasivity of the volcanic rocks occurring along the decline. Finally, a comparison of unconfined compressive strength and Point Load Index values as well as that of unconfined compressive strength with moisture content, tensile strength and abrasivity index values are presented.

GEOMORPHOLOGY

The Favona deposit is located in the Waihi Basin within the Coromandel - Kaimai ranges of New Zealand. Figure 1 shows the study area with respect to the regional physiographic units. The Waihi Basin is an east-west (11km) elongated 8km wide depression infilled with 1.5km thick Early Pleistocene and Pliocene flat-lying ignimbrites and Lake Sediments.

The study area is situated on the eastern part of the basin with a gently undulating surface at an elevation of 100-160m above sea level. The area is to the east of Martha Mine at the edge of Waihi Township. It is bounded by the irregularly meandering Ohinemuri River on the east and south.

The Ohinemuri River runs through the basin towards west separating the ranges into two parts: Coromandel range to the north and the Kaimai range to the south. The ranges represent an uplifted block of Miocene and Pliocene volcanic rocks and is bordered with Hauraki Plains to the west and Tauranga Basin to the southeast.

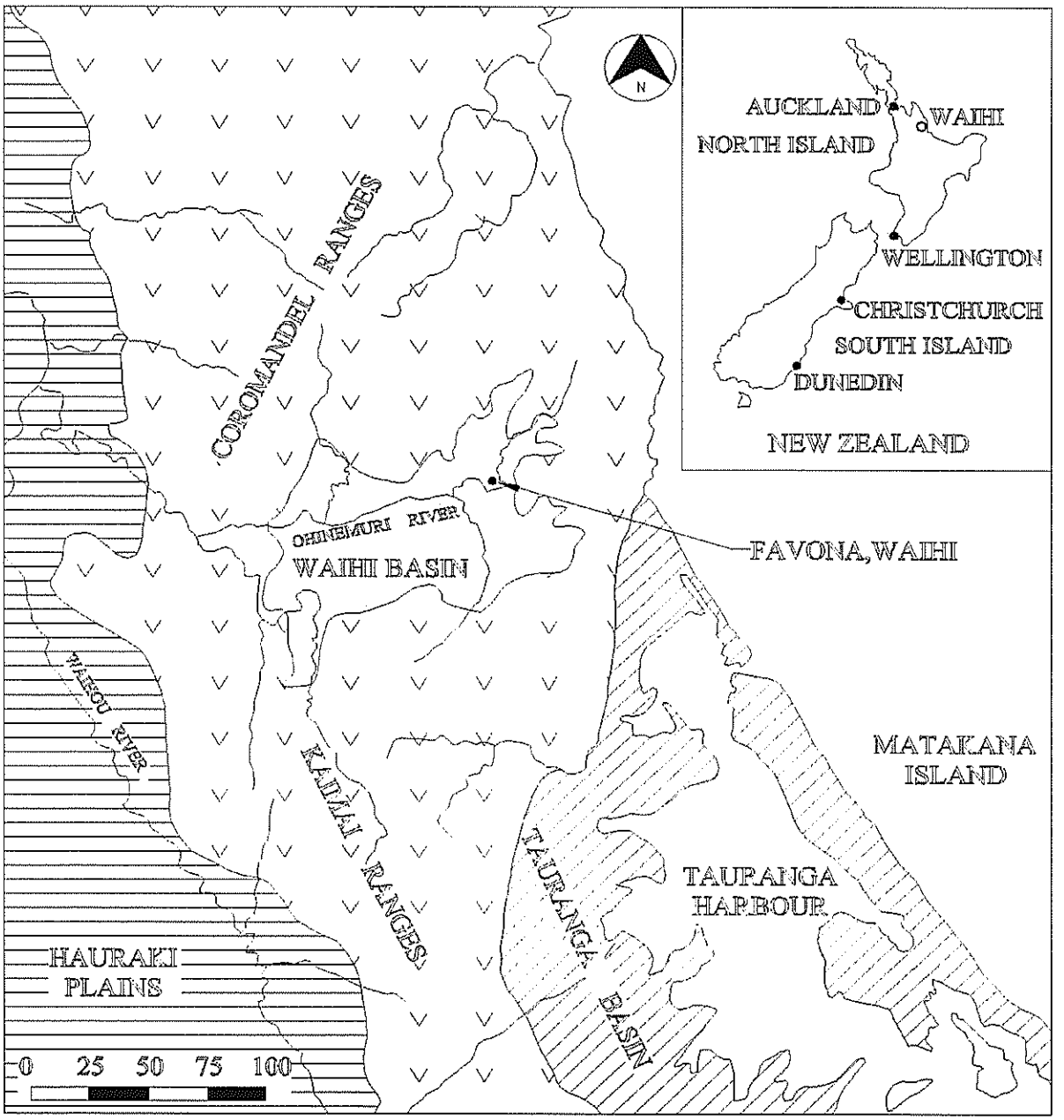

Figure 1. Location of Favona Area

GEOLOGICAL SETTING

Geologically, the Waihi Basin is located in the southern part of the Hauraki Goldfield. In the Waihi Basin, greywacke basement is considered to underlie the volcanic pile at depths of 2-3 km. The oldest rocks are Late Miocene andesites and dacites of Waipupu Formation, which are unconformably overlain by rhyolitic volcanics and volcaniclastics, and by late Miocene to Plio-Pleistocene post-mineral andesites, ignimbrites and sediments (Brathwaite and Christie, 1996). Figure 2 shows the geology of the Favona area.

Host rock andesites and associated tuffs and breccias have been highly weathered to depths of around 50m. Weathering has also influenced post-mineral lithologies like explosion breccias and pyroclastic sediments.

Andesite rocks underlying the Gladstone Hill and the surrounding area is characterised by intense argillic alteration, which overprint and grade laterally and at depth to propylitic alteration. Strong silicic alteration accompanied by kaolinitic clays is observed at shallow levels within wall rock andesites and hydrothermal tuffs/breccias (Simpson et al, 2002).

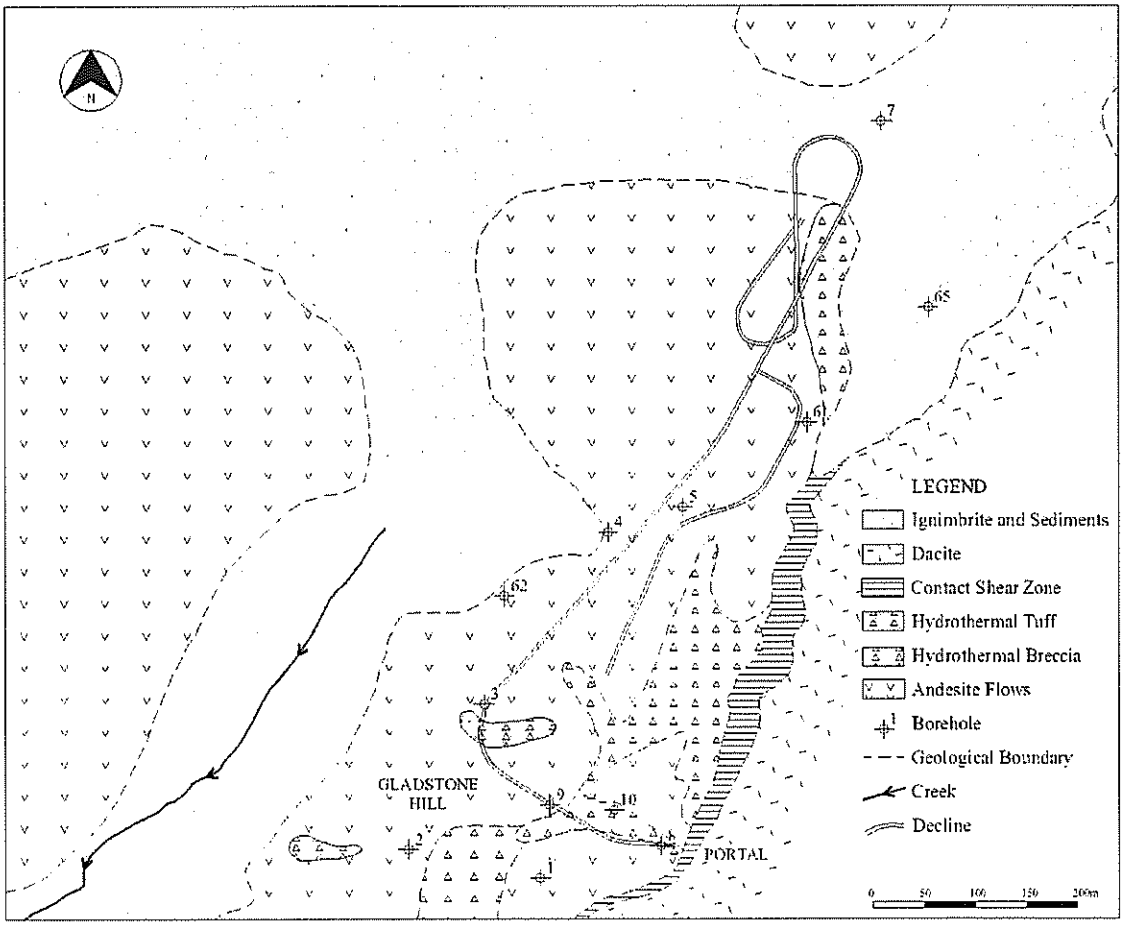

Figure 2. Geology of the Favona Area.
[This inset shows the location of the proposed Favona Decline and the location of the geotechnical boreholes.]

The NE-trending Waihi Fault and Golden Valley Fault are the major structural elements of the Waihi block, which is downthrown to the east in a series of step faults. Predominant quartz vein trends are northeasterly to east northeasterly at Gladstone and other small hills, where subsidiary northwest-dipping vein sets splay from principal steeply eastward-dipping veins such as the Martha (Brathwaite and Christie, 1996, and Simpson et al, 2002).

Gold has been mined since late 1800's and there are historic workings along the reefs Gladstone, Union, Amaranth, Silverton, Old Favona and Mascote as well as the Martha, Edward and Royal lodes from late 1800's to mid 1900's.

GROUND INVESTIGATION

Fieldwork was undertaken from June 2002 to September 2002 and comprised diamond drilling of ten HQ size holes along the proposed alignment of the decline ranging in depth from 16m to 140m. The length of the decline is approximately 1.6km at 1 in 7 gradient (Figure 2). The spacing between the boreholes varied between 50m and 100m. Five holes were vertical and five holes were inclined at different azimuths and dips to allow identification of rock structures. In-situ tests included water absorption packer testing in all holes at the decline elevation and standard penetration testing in one of the holes where the portal of the decline has been proposed. Additional information was obtained from two exploration boreholes located close to the alignment of the decline. Geological logging of the core samples was conducted to determine the soil/rock profile in the study area and estimate the rock type and conditions along the alignment of the decline.

Drilling conditions were highly variable with low high bit wear in the Gladstone hill area, but with good progress rates in the deeper low strength andesites.

Laboratory testing of the representative samples from decline elevation was conducted in geotechnical laboratories of New Zealand, Australia and Austria. Standard laboratory testing of samples for density, water content, uniaxial compressive strength, point load testing, triaxial compressive strength, splitting tensile strength and slake durability index were carried out to determine the intact rock parameters. Specialised non-standard laboratory testing to predict performance of roadheaders was undertaken which included abrasivity tests and compression tests. Petrographic analysis of a few-selected core samples from the decline zone were also carried out to obtain the petrographic description including mineralogy, textures and rock name.

GEOLOGICAL MODEL

Regional Geological Model

Volcanic eruption initiated in Miocene and continued until Early Pleistocene to form the Coromandel-Kaimai range. The upliftment and eastward tilting of the range led to the entrenchment of rivers like Ohinemuri in steep-sided, canyon-like antecedent gorges not only through the Coromandel-Kaimai range, but also in the Waihi Basin. In Late Miocene, the andesite and dacite lava flows, and associated hydrothermal tuffs and breccias formed isolated hills like Gladstone in the Waihi Basin. The lava flows and associated tuffs and breccias were later subjected to gold–silver mineralisation and hydrothermal alteration by rising hydrothermal fluids. Later in Pliocene to Early Pleistocene, the surrounding low lands were infilled with Lake Sediments and ignimbrites. The lava flows, tuffs and breccias from surface down to about 50m were strongly to moderately oxidised. In Late Pleistocene, eruptions of ash and pumice from Taupo volcanic zone and Mayor Island blanketed the area to a depth between 1 and 8m (Brathwaite & Christie, 1996).

Decline Geological Model

A schematic geological section drawn along the alignment of the decline provides an overview of the site geological conditions (Figure 3). Five geological units, as indicated below from older to younger, have been identified and described below. Quartz veins up to 2.5m thick were encountered in the rock mass. They have not been distinguished as a separate unit because of their limited and irregular occurrence within andesite.

- Andesite, Brecciated Andesite, and Hydrothermal Tuff (moderately weathered to unweathered)
- Highly Weathered Andesite, Brecciated Andesite and Tuff
- Residual Soil/Completely Weathered Material
- Post Mineral Ignimbrite and Lake Sediments
- Volcanic Ash

Andesite, Brecciated Andesite and Hydrothermal Tuff

Andesite, Hydrothermal Tuffs are the principal rock types through which the decline passes. The andesite flows have been intersected by hydrothermal vent tuffs. Minor hydrothermal breccia is also encountered. The interface between the tuff/breccia and the andesite is generally sharp and occasionally marked by the occurrence of stiff, white grey clay (up to 450mm) at the contact. The andesite is finely to coarsely porphyritic, weakly to strongly clay-altered, weakly to strongly silicified, and weakly to strongly brecciated.. Andesite is extremely weak to medium strong, very closely jointed, non-intact, broken to moderately widely jointed.

Hydrothermal tuff is generally matrix supported, extremely weak to very weak. Hydrothermal breccia is strongly to weakly silicified, strongly to moderately clay altered and extremely weak to moderately strong. It is clast supported and contains mainly andesite and quartz clasts. It includes up to 3m thick quartz veins and up to 4m thick, soft clay/silt horizons.

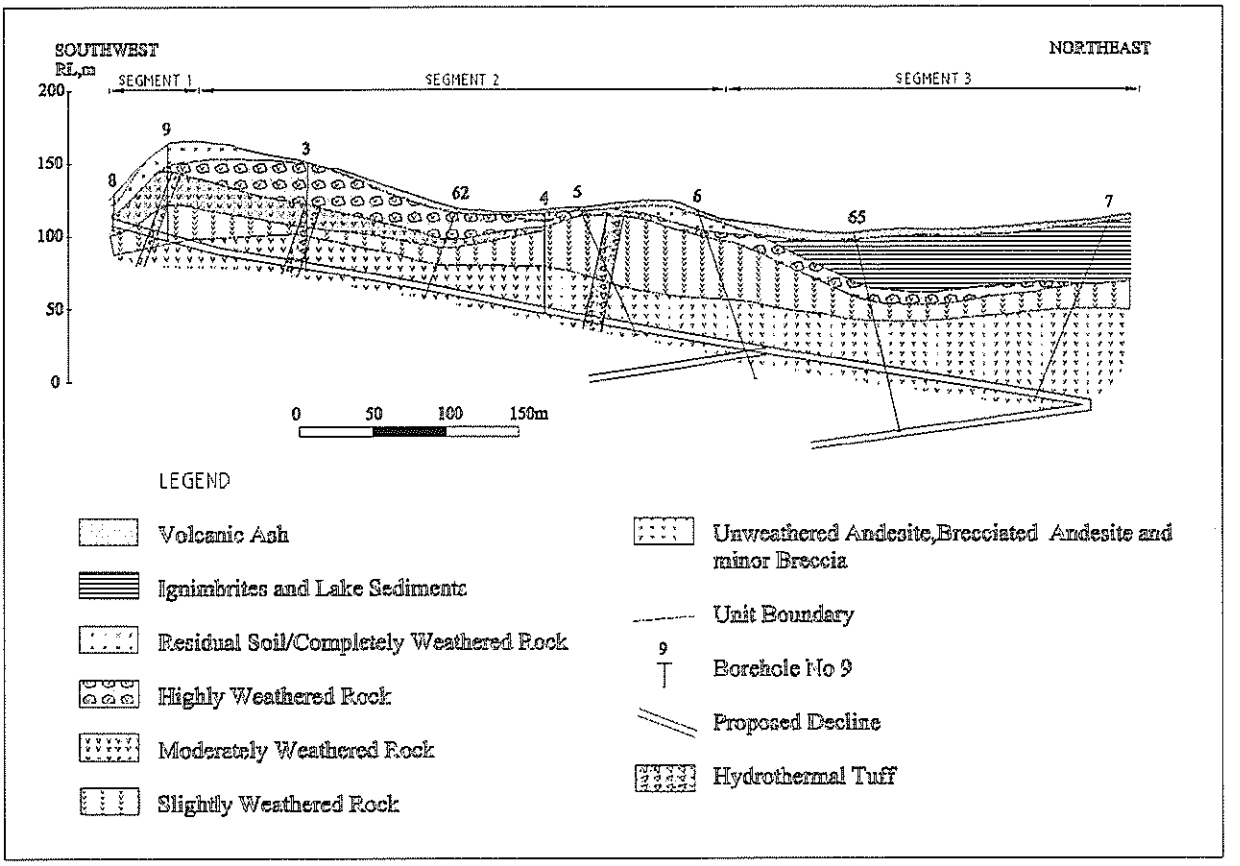

Figure 3. Geological Cross-Section Along the Decline.

Highly Weathered Andesite and Hydrothermal Tuff/Breccia

This unit is characterised by intense oxidation of clay-altered and silicified andesite, hydrothermal tuff and breccia. The rock is brown, orange brown, extremely weak to very weak. It is encountered from 3m to 50m below the ground surface.

Residual Soil/Completely Weathered Material

This unit is underlain by volcanic ash and extends down to maximum 16m below the ground surface. The thickness varies between 2m and 16m. This unit comprises sandy silt, silty sand, silty clay and fine to coarse gravel in silt/clay matrix. The gravel is represented by angular to sub-angular, weathered breccia and andesite fragments. Andesite boulders and cobbles are also present. The silt and clay are firm to very stiff. The coarse soil is medium dense to dense.

Post Mineral Ignimbrite and Lake Sediments

This unit is distributed in the lowland areas and is not intersected by the decline. It is underlain by Volcanic Ash. It shows lateral and vertical variation both in thickness and in composition. The thickness ranges from 25m to 40m. Sandstone and claystone occur at the base of the sequence, ignimbrites in the middle part and sandy silt/silty sand at the top of the sequence. Lateral variation result in absence of sandstone and claystone and predominance of ignimbrites.

Volcanic Ash

The Volcanic Ash provides a blanket over the entire site. It comprises brown, orange brown, firm to stiff, sandy clay, and clayey/sandy silt that extend from the ground surface to 3m. The thickness of the Volcanic Ash is spatially variable (1.5m-3m), reaching a maximum thickness on the lower slopes of the Gladstone Hill, but being absent at the top of the hill probably due to erosion.

Weathering and Alteration

Weathering has influenced the andesite and associated hydrothermal tuffs/breccias as well as post-mineral ignimbrites and sediments. There is a continuous weathering profile from residual soil/completely weathered material to unweathered rock from the ground surface to the decline level. The thickness of the different grades of weathering in the weathering profile is variable (Figure 3). The grades of weathering were generally identified by visual characteristics, rock strength and soil or rock-like behaviour of the material. Visual characteristics included basically oxidation (iron oxide staining), as well as textural and fabric changes. Highly weathered rocks consist of more than 50 percent of iron oxides, moderately weathered contain less than 50 percent of iron oxides, slightly weathered rocks display iron staining along the fractures. It was found that the higher the grade of weathering, the lower the strength of the rock material.

Hydrothermal alteration was observed in the drill core samples along the alignment of the decline. The andesite, brecciated andesite and hydrothermal tuffs/breccias have been influenced by argillic and silicic alteration. They are altered to the clay minerals, silica and pyrite. The intensity of alteration was evaluated in the moderately weathered to unweathered rock. Pyrite occurs with weak to moderate intensity at shallow level, but becomes very weak to strong at deeper levels. It is generally finely disseminated, but also occurs along fracture. The clay is mostly pervasive throughout the explored depth. It occurs with weak to moderately strong intensity. Silica alteration is weak, irregular at the upper part and becomes stronger and pervasive at deeper levels. Some holes indicated strong intensity of clay and silica alteration in the moderately weathered rocks, but becoming less intense in slightly weathered and unweathered rocks. Chloritic/carbonate alteration was not noted up to the decline level. It was found that the strongly clay-altered rocks were significantly weaker. Intensely silicified rocks were found to be moderately strong.

GEOLOGY OF THE PORTAL AREA AND THE DECLINE

The portal level of the decline is about 10m below the present ground surface to the east of the Gladstone Hill. It will be located in a box cut in brown, highly weathered, extremely weak hydrothermal tuff. The tuff is intensely clay-altered and sheared.

The decline along its length is divided into the three geotechnical segments (Figure 3). The first segment of the alignment passes through highly weathered, extremely to very weak hydrothermal vent tuff and andesite, which are intensely clay altered and highly fractured. Unweathered, weak to moderately strong andesite with minor hydrothermal tuff occur along the second segment of the decline. The strength of the rock is variable and ranges from very weak to moderately strong. Strongly clay-altered extremely weak andesites occur in places. Strong silicification is present and is marked by the occurrence of quartz veins and pervasive alteration of the rock mass by silica. Generally, the andesites are moderately to strongly clay-altered along the entire length of the second segment. Pyrite disseminations are pervasive. At the third segment of the decline, the less silicified brecciated andesites are very weak to extremely weak, very closely jointed and have very poor rock quality designation.

The petrographic analysis of andesite samples from the decline level revealed 46 to 50% of quartz, 46 to 50% of illite-smectite (clays), and about 4 to 6% of accessory minerals including adularia, titanite and opaques.

Discontinuities

The decline along its length will be intersected by steeply to very steeply inclined fractures, crushed rocks, and shear zones or faults. The fractures are infilled with iron oxides and oxidised clays in highly to completely weathered zones and are clay-infilled in moderately weathered to unweathered zones. Some fractures are healed by silica veins. Pyrite is disseminated throughout the rock. The fractures are generally rough planar with a dip angle generally greater than 40 degrees. Smooth planar and undulating rough fractures are also present. Occasional fractures are irregular and stepped. The shear

zones are represented by loose to well compacted clayey gravel. Strong clay and/or silica alterations are present in the faults/shear zones.

The results of the statistical structural analysis indicate five joint (dip/dip direction 23°/195°, 40°/292°, 55°/094, 84°/045° and 32°/346°) sets and a number of random joints.

Groundwater & Permeability

The discontinuities represented by joints, faults/shears and crush zones are the channels through which the groundwater flows within the host rock. The first segment of the decline is located within the oxidation zone, where staining is common in the fractures of the highly and moderately weathered zones indicating active groundwater movement in those areas. The other two segments of the decline are located below the oxidation zone in unweathered rocks. Some of the fractures at various depths are healed by silica and therefore, have lower permeability. The water absorption tests undertaken using single packer revealed laminar to turbulent flow resulting in highly variable permeability values along the decline. The measured values range between 1.4 x 10^{-6} m/sec and 8.6 x 10^{-8} m/sec.

ENGINEERING PROPERTIES

Rock Quality Designation (RQD)

The first segment of the decline indicates the rock quality designation ranging between 65 % and 100 %. The second segment shows 50 to 90 % RQD, but the rock quality deteriorates at the third segment (RQD 0 to 90%) of the decline.

Unconfined Compressive Strength (UCS)

Unconfined compressive strength and point load testing were performed on the samples from decline level and range from 2 MPa to 34 MPa. These values do not entirely depend upon the depth of the sample but on the degree and type of hydrothermal alteration. Oxidised and strongly clay altered samples show low strength values. Silicified rocks are stronger. The unconfined compressive strength generally decreases as the moisture content increases (Figure 4).

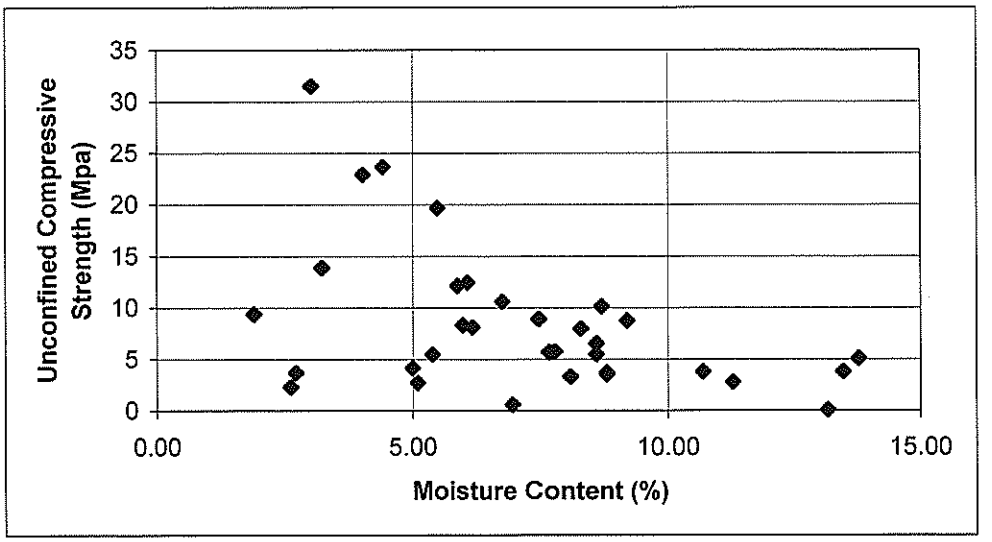

Figure 4. MC versus UCS

UCS and Point Load Strength Index [Is (50)] testing over a 0.4m sample interval show a direct relationship UCS = 9 x Is (50).

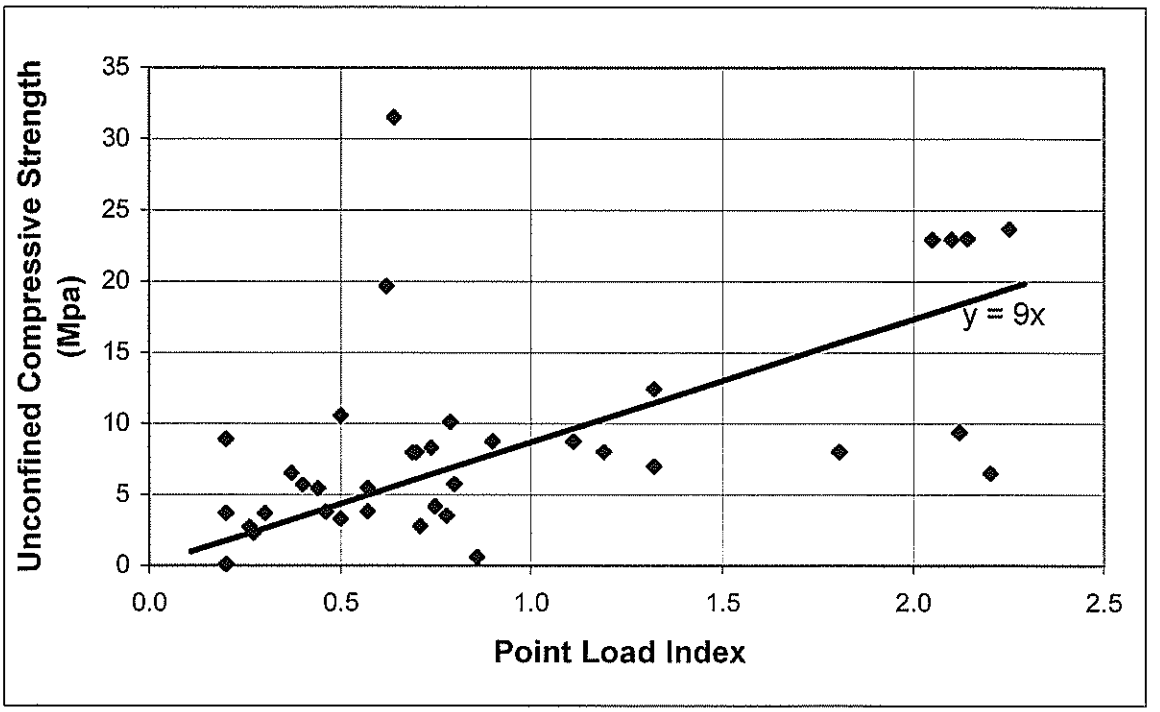

Figure 5. UCS Versus Is (50)

Mechanical Behaviour and Abrasivity

Selected samples taken from the decline level (depth ranging between 50m to 90m below the ground surface) were assessed for their mechanical behaviour and abrasivity. The rocks were little to moderately abrasive, tough to very tough, non-plastic. The rocks have low to average elasticity and low to moderate strength.

Figure 6 shows the relationship between the Unconfined Strength, Tensile Strength and CERCHAR Abrasivity.

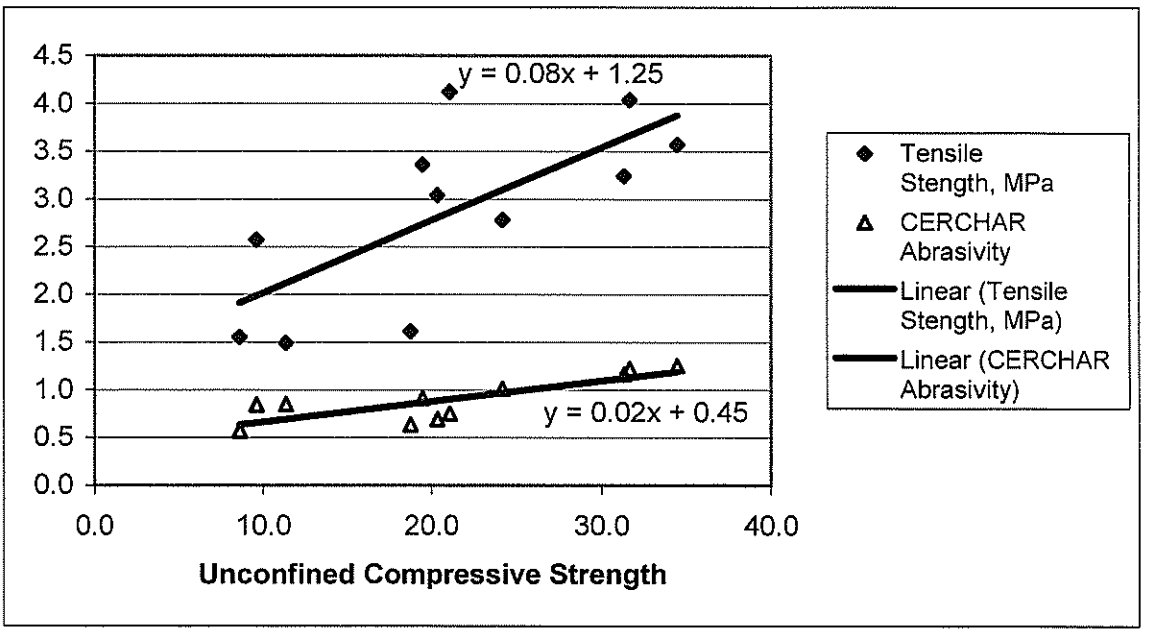

Figure 6. Relationship Between Unconfined Compressive Strength, Tensile Strength and Abrasivity

Slake Durability Index

Slake durability index of the andesite samples was found to be relatively high. The values generally ranged between 78 to 98%. The samples retained after the test were either virtually unchanged or the retained material consisted of large and small pieces. Low values ranging between 24 to 40% were occasionally encountered.

CONCLUSIONS

The andesite, brecciated andesite, and associated hydrothermal tuff and breccia of Miocene Waipupu Formation are widespread in the Favona Decline Project area. Pleistocene sediments comprising alternating claystones and sandstones and ignimbrites are locally observed in the low ground. The area is mantled by volcanic ash up to 3m in thickness.

The geology at the portal area is represented by extremely weak, highly weathered tuff breccia, which is intensely clay-altered and sheared.

The rock through which the decline is to be tunnelled comprises highly weathered to unweathered, and altered andesite flows and brecciated andesite with minor hydrothermal tuffs and breccias, and occasional quartz veinlets. They display five sets of discontinuities and a lot of random joints. The discontinuities are represented by joints, faults/shears and crush zones. The joints are generally clay infilled, but silica and pyrite infilling are also present. The rocks within the proposed decline zone are affected by weak to intense clay, pyrite alteration. Silicification is selective and is manifested in the intrusion of quartz veinlets and displacement of the parent material by silica.

The permeability of the andesite and breccia in the decline zone is highly variable. The measured values (1.4×10^{-7} and 8.6×10^{-8}) provide indicative permeability of the rock mass.

The rocks at the decline zone are generally very weak to moderately strong with unconfined compressive strengths ranging between 2Mpa and 34Mpa. Occasionally, they are extremely weak. With regard to mechanical behaviour, the rock is of low to moderate strength, tough to very tough, not plastic, low to average relative elasticity and requires a high to very high specific fracture energy. The rock in the decline zone is rated at low to moderately abrasive.

The following relationship has been established.

1. The weathering grade and rock strength increases with depth. However, there is no specific relationship of the clay alteration and silicification with depth
2. Fracture index and rock quality designation do not depend on depth below the ground surface.
3. The uniaxial compressive strength decreases with intense clay alteration and higher grade of oxidation, but increases with silicification.
4. The unconfined compressive strength is nine times the Point Load Index value.
5. The compressive strength decreases with the increase of moisture content.
6. The tensile strength and CERCHAR abrasivity increase with increased compressive strength.

ACKNOWLEDGEMENTS

The author would like to thank Newmont Waihi Operations for giving permission to publish this paper. I am grateful to Mr Grant Murray for going through the manuscript and providing suggestions. I express my appreciation to Mr Trevor Maton for reviewing the paper and providing valuable comments.

REFERENCES

Brathwaite, R. L. & Christie, A. B. (1996), Geology of the Waihi Area, scale 1:50,000. Institute of Geological and Nuclear Sciences geological map 21. 1 sheet + 64p. Lower Hutt, New Zealand: Institute of Geological & Nuclear Sciences Limited.

British Standard BS 5930:1999, Code of Practice for Site Investigations.

Houlsby A.C. (1976), Routine Interpretation of the Lugeon Water Test, Journal of Engineering Geology, Vol 9, pp 303-313, 2 Figs, 2 Tables.

Newmont Waihi Operations, (2002), Favona Pre-feasibility Study Report.

New Zealand Geomechanics Society, (1988), Guidelines for the Field Description of Soils and Rocks in Engineering Use, 43p.

Simpson M P and Hollinger E, (2002). The Favona Low Sulfidation Epithermal Au-Ag Deposit, Waihi, New Zealand.

Sinclair Knight Merz, (2002), Geotechnical Investigation Report, Favona Decline Project prepared for Newmont Waihi Operations.

Roading Geotechnics in Soft Soils: Correlation of Laboratory and Field Performance

T J Larkin,
PhD
Senior Lecturer, Department of Civil & Environmental Engineering, University of Auckland
B Ni
ME (Fuzhou), ME (Hons) (Auckland)
Research Fellow, Department of Civil & Environmental Engineering, University of Auckland
M J Pender
BE (Hons), PhD, FIPENZ, Life Member NZGS
Professor of Geotechnical Engineering, Department of Civil & Environmental Engineering, University of Auckland
S A Crawford
BE, MES (Sydney), MIPENZ, Registered Engineer
Geotechnical Principal, Tonkin and Taylor Ltd

Abstract: This paper presents part of the research work on the correlation between laboratory and field tests carried out at three sites of the Longswamp roading project, Waikato Region. The relationship between constrained modulus and cone resistance was explored and the value of the coefficient α for these sites was found to be in the range of 2 to 6. Based on laboratory and field tests, settlements of the embankment were calculated using both a one-dimensional empirical method and a 2D finite difference method. The 2D method used the FLAC code with the Cam-clay constitutive model and an elastic model. It has been found that results of the 1D method agree well with the measured settlements.

INTRODUCTION

The cone penetration test (CPT) is a simple and reliable field test for determination of cone resistance from which strength and stiffness can be estimated by using correlation. Considerable research work has been done on the correlation between cone resistance and laboratory tests. Various empirical relationships between the cone resistance, q_t, and the constrained modulus, M, have been provided by researchers. For cohesive soil Senneset et al (1989) suggested the following relationship:

$$M = \alpha(q_t - \sigma_{vo}) \qquad (1)$$

where:

M is the constrained modulus of soil,
q_t is the cone penetration resistance corrected for pore water pressure effects,
σ_{vo} is the total vertical stress at the depth corresponding to q_t,
α is a dimensionless coefficient, which varies from 5 to 15 for overconsolidated soil and between 4 and 8 for normally consolidated soil (Senneset (1989), Kulhawy and Mayne (1990) and others).

In New Zealand this relationship was explored by Pender et al (1999, 2001) through matching calculated settlements to observed settlements for several embankment sites. Settlements of fill were calculated using a one-dimensional method, and values of α were obtained using trial and error to give the closest overall agreement between calculated settlements and observed settlements. Values of α were found in the range of 2 to 8.

This paper presents part of the research work on the correlation of field tests with laboratory tests carried out on three sites of the Mercer to Longswamp Four Laning Project. Fourteen CPT tests were performed by the University of Auckland, 5 at Longswamp, 6 at Gully 2 and 3 at Orawiec. Values of α were explored both by directly correlating the constrained modulus obtained from oedometer tests to the cone

resistance and through matching estimated settlements to observed settlements. These two approaches gave similar values of α which varied from 2 to 6 for these three sites. Based on laboratory and field tests, settlements of the embankment at five locations of the Longswamp site were then estimated using both a one-dimensional empirical method and a 2D finite difference method in FLAC where the Cam-clay soil model was utilised.

SITE DESCRIPTION OF LONGSWAMP

Field and laboratory tests were performed on soils from three sites along the Mercer to Longswamp Four Laning Project. Figure 1 shows the records of cone penetration tests which were carried out in January 2001 at Location 28 of the Longswamp site. These results were obtained by the University of Auckland and Tonkin & Taylor Ltd respectively, prior to the construction of fill. The two records are generally in good agreement and show a substantial depth of low strength / stiffness material. A total of eleven specimens were obtained by using a 100 mm diameter thin-walled sampler (wall thickness of 3.3mm) from four boreholes at depths of up to 6 m. Laboratory tests showed that soils of the main compressible layer for these three sites were extremely compressible with the initial void ratio between 3.0 and 6.0 and bulk density from 1.2 to 1.5 t/m^3. Laboratory oedometer testing gave values for the coefficient of volume compressibility, m_v, in the range of 3.0 to 6.0 MPa^{-1} corresponding to a vertical pressure of 27 kPa. The natural water content varies from 90% to 230% and the plasticity index from 60% to 130%. The specific gravity of solids is about 2.45 and the organic content about 10%.

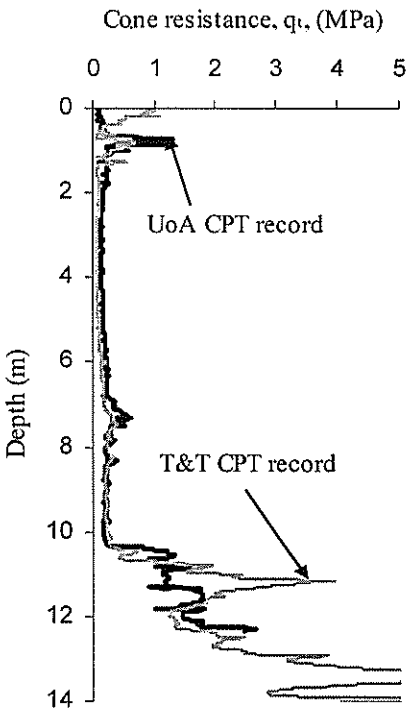

Figure 1. CPT Records at Longswamp
(Location 8, CH10160)

CORRELATION BETWEEN CONSTRAINED MODULUS AND CONE RESISTANCE

Figure 2 shows that the constrained modulus obtained from oedometer tests varies significantly with the vertical pressure. Therefore, constrained moduli corresponding to specific pressures were used for the

correlation with the cone resistance. Figure 3 shows the relationship of the oedometer constrained modulus, M, and the cone resistance, where M is assessed at the initial insitu effective vertical stress. It is seen that α varies from 1.1 to 2.7 with an average of about 1.6. Figure 4 shows the relationship where, for each borehole, the value of M is calculated as the average obtained from the oedometer test over the stress range imposed by the embankment at the depth of the sample. Accordingly α is found in the range of 2.0 to 6.0.

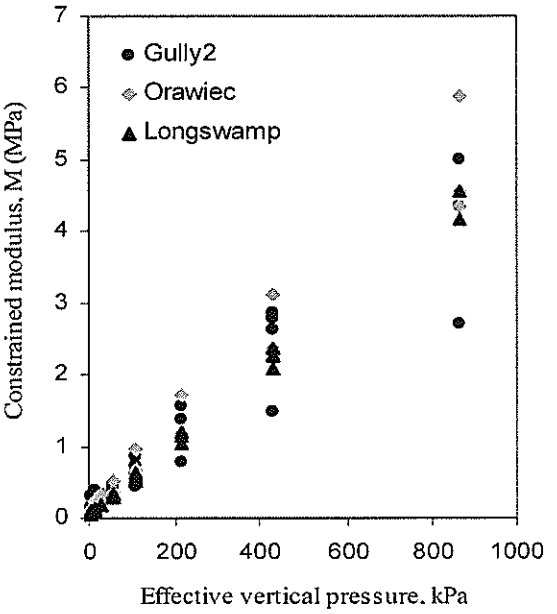

Figure 2. Oedometer Constrained Moduli for Three Sites

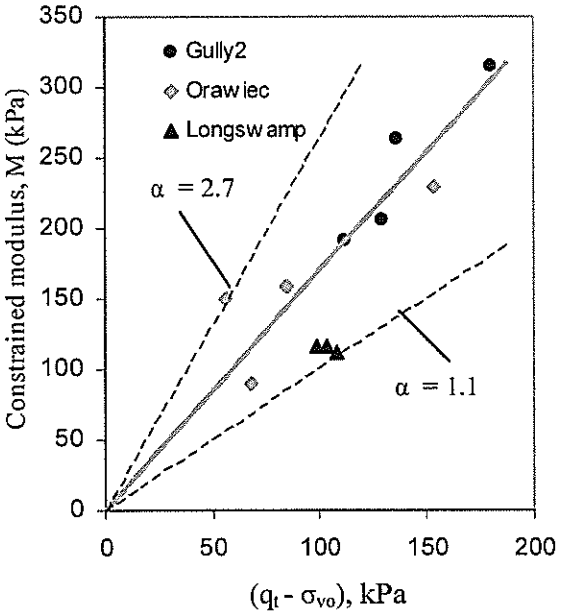

Figure 3. Correlation of M and $(q_t - \sigma_{vo})$ (M is assessed at the initial in-situ effective vertical stress)

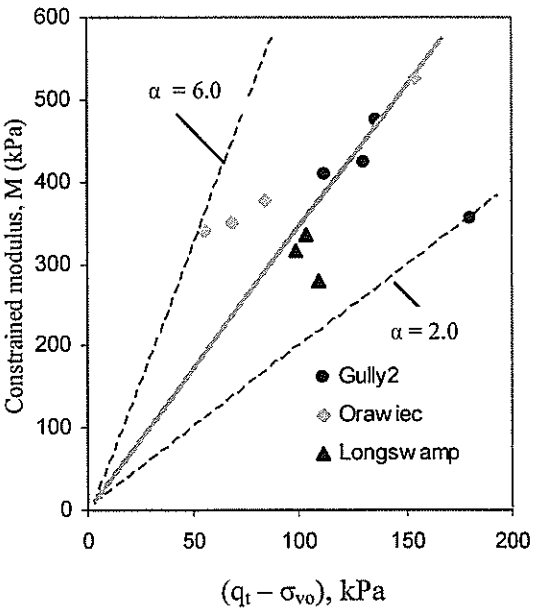

Figure 4. Correlation of M and $(q_t - \sigma_{vo})$ (M is averaged over the actual stress range of the soil under the embankment)

SETTLEMENT ANALYSIS OF THE LONGSWAMP SITE

Settlement at the site was measured using a profilometer developed by Tonkin and Taylor. This device is a pressure sensitive probe that is capable of measuring variations in elevation (±10mm). The probe is pulled through a tube (laid prior to construction), which is benchmarked at each side of the embankment.

The available settlement data up to June 2002 show a general trend of ongoing deformation of the soil for all the five locations at the Longswamp site. Therefore, the degree of consolidation of the soil associated with the last settlement records has to be assessed for each location.

Assessment of Degree of Consolidation of Soil

Data from Tonkin and Taylor covers the period from February 2001 to June 2002. Over this period of time two stages of filling were undertaken. Stage 2 started about six months after the completion of Stage 1 and the last settlement measurements were made shortly after the completion of Stage 2 filling. Therefore, the settlement data prior to Stage 2 were used for curve fitting to assess the degree of consolidation.

The procedure to assess the degree of consolidation involved curve fitting and the assumption of vertical flow, i.e. one dimensional consolidation:

- Estimate the ultimate settlement under Stage 1 fill by matching the settlement ~ time curve with a hyperbolic relationship
- Chose a given point in time and calculate the degree of consolidation at that point
- Calculate the average consolidation time under Stage 1 fill from the beginning to that point of time
- Calculate a notional value of c_v using one dimensional consolidation theory
- Work out the average consolidation time respectively for Stage 1 fill and Stage 2 fill from their individual start points to the last record point
- Calculate the average degree of consolidation respectively for Stage 1 fill and Stage 2 fill, i.e. U_1 and U_2 using one-dimensional method
- Estimate the overall degree of consolidation by the following equation,

$$U = \frac{\Delta H_1 \cdot U_1 + \Delta H_2 \cdot U_2}{\Delta H} \qquad (2)$$

Where: $\Delta H = \Delta H_1 + \Delta H_2$, ΔH_1 and ΔH_2 are the heights of Stage 1 fill and Stage 2 fill respectively. The fill heights are used in lieu of the consolidation settlement associated with each stage since these are not known.

The estimated degree of consolidation is summarised in Table 1 and a typical curve fitting is shown in Figure 5.

Chainage	10160	10240	10320	10560	10900
Embankment Location	28	29	30	33	35
U(%)	61	53	86	63	69

Table 1. Estimated Degree of Consolidation at the Last Settlement Measurements Made on the 24th of June 2002

The consolidation at Longswamp is not a one-dimensional situation since wick drains were installed at the site. The process described above is based on the classical one-dimensional solution which was used in the absence of quality pore water pressure data. A notional value of the one dimensional consolidation

coefficient for the site containing wick drains was estimated using the rate of settlement as described above.

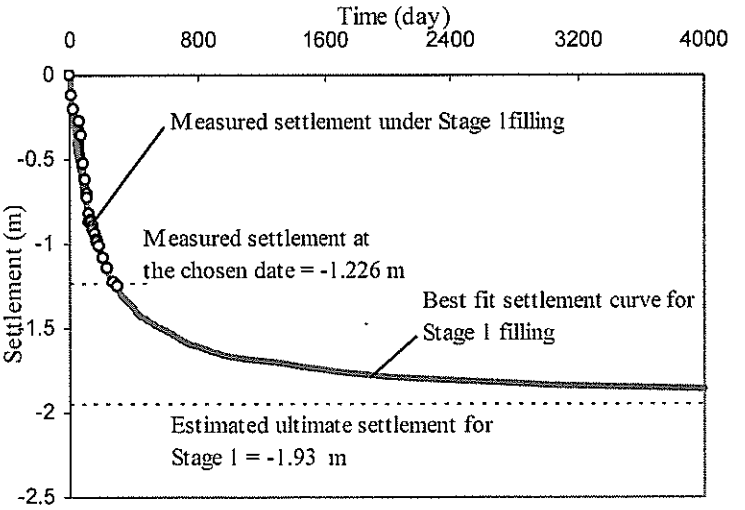

Figure 5. Curve Fitting for Assessment of Degree of Consolidation Under Stage 1 Filling at Location 28 (Settlements were measured at distance of 40 m from the set up pad pin)

One Dimensional Method of Settlement Calculation

The CPT records were used to obtain the constrained moduli by Eq.(1). To give "best fit" agreement with the recorded data, the value of α was chosen for each location. This was achieved by a trial and error method, but easily accomplished. The same value of α was used everywhere in the solution space. It was found that values of α obtained using trial and error were similar to those obtained from the previous correlation between oedometer tests and CPT tests. The soil profile is divided into a large number of thin layers and the thickness of the layers is consistent with the CPT recording interval, which in this case is 10 mm. The strain of each layer is evaluated:

$$(\varepsilon_v)_i = \frac{(\Delta\sigma_v)_i}{M_i} \tag{3}$$

The CPT tests sampled the main compressible layer and penetrated the less deformable layer. It is assumed that all significant settlement occurs within the depth of the CPT records. The surface settlement is then the summation of the settlement of each layer:

$$S = \sum_{i=1}^{N} (\varepsilon_v)_i \Delta z \tag{4}$$

where: i is the layer identifier,
N the number of soil layers,
$\Delta\sigma_v$ the vertical stress increment,
M the constrained modulus,
ε_v the vertical strain,
Δz the layer thickness (10 mm),
Δz and S the settlement at the ground surface.

To calculate the stress increment the fill is assumed flexible, with a unit weight of 17 kN/m^3, and the complex shape of the fill volume is divided into several sub-volumes with regular shapes. The vertical stress increments, $(\Delta\sigma_v)_i$, generated by these soil volumes can be obtained using formulae for a homogeneous isotropic elastic material. Details of the formulae are given by Poulos and Davis (1974).

Finite Difference Settlement Analysis with FLAC

The fill and soil were both modeled in a 2D finite difference approach using FLAC (Itasca (2000)). The model was three times as wide as the base of the fill and its height was the same as the length of CPT penetration. The modified Cam-clay model was used for the soil while the fill was considered elastic with an assumed shear modulus of 5 MPa and a bulk modulus of 20 MPa. The parameters of the Cam-clay model were derived from oedometer tests and CU triaxial tests, and are given in Table 2.

Layer	M	λ	κ	ν	p_I (kPa)	v_λ	γ (kN/m^3)
Main compressible layer	0.8	0.61	0.09	0.3	50	4.2	14
Underlying layer	1.0	0.1	0.03	0.25	50	3.0	16

Table 2 Cam-clay Model Parameters

Comparison of Calculated Settlements with Measured Settlements

It is found that the results of the 1D method compare well with the measured settlement. For the 2D analysis, the same Cam-clay soil parameters and elastic moduli of fill were used for all locations. Settlements obtained from the 2D analysis also agree well with measured settlements except at Locations 28 and 30. Comparisons are shown in Figures 6 to 10.

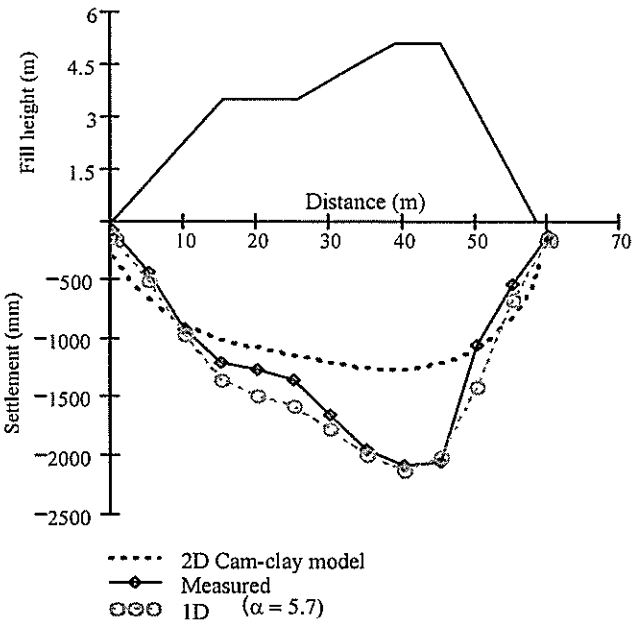

Figure 6. Settlement Profile at Location 28

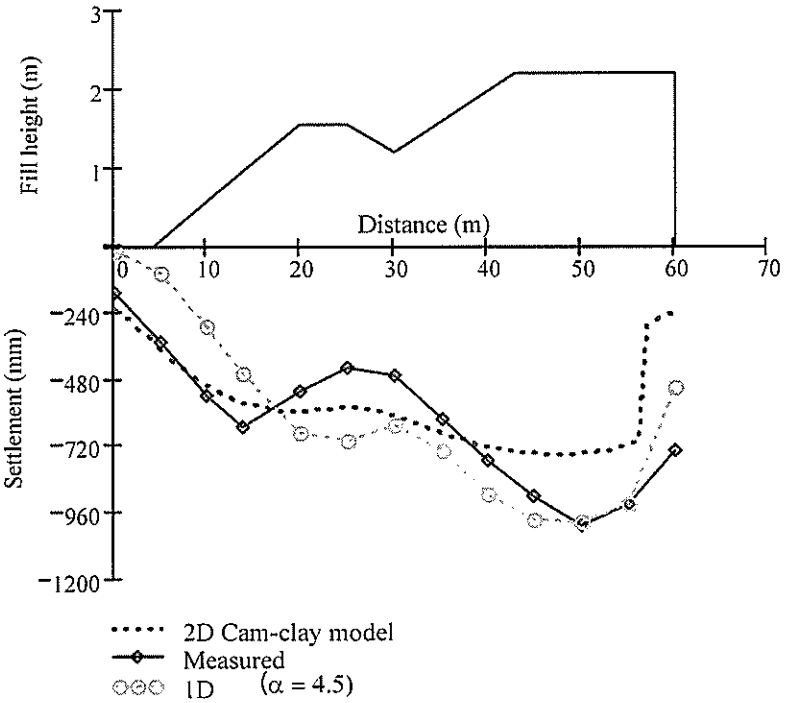

Figure 7. Settlement Profile at Location 29

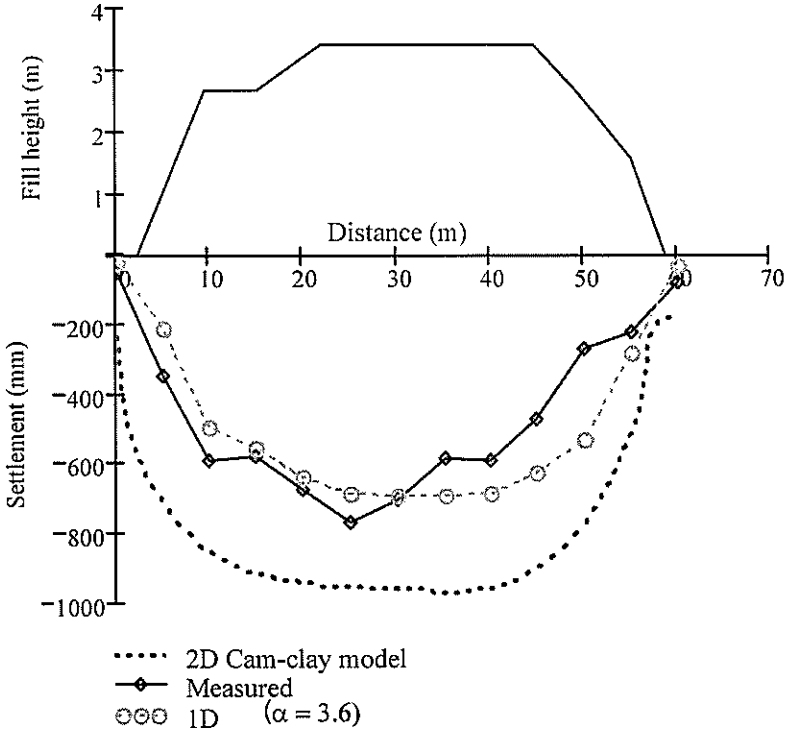

Figure 8. Settlement Profile at Location 30

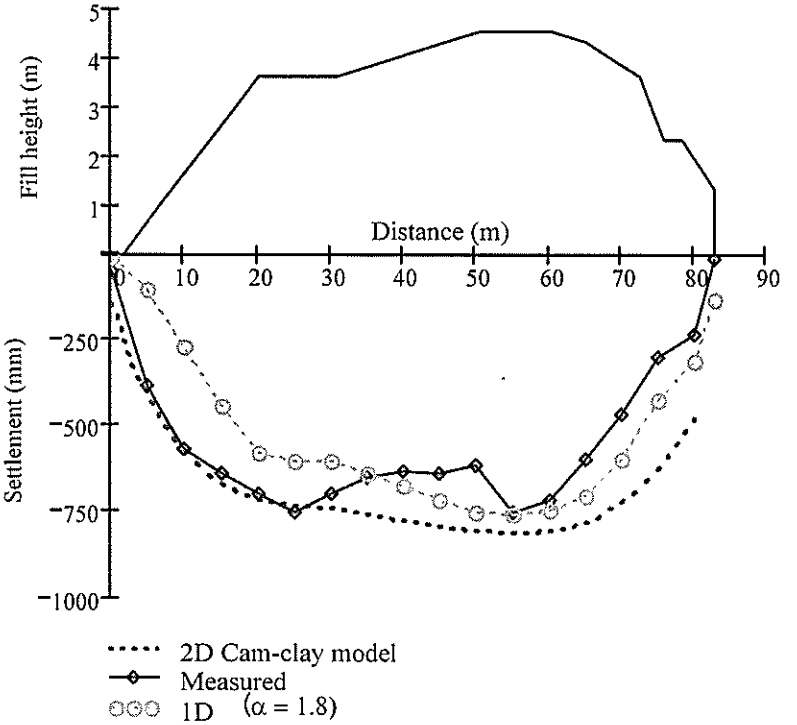

Figure 9. Settlement Profile at Location 33

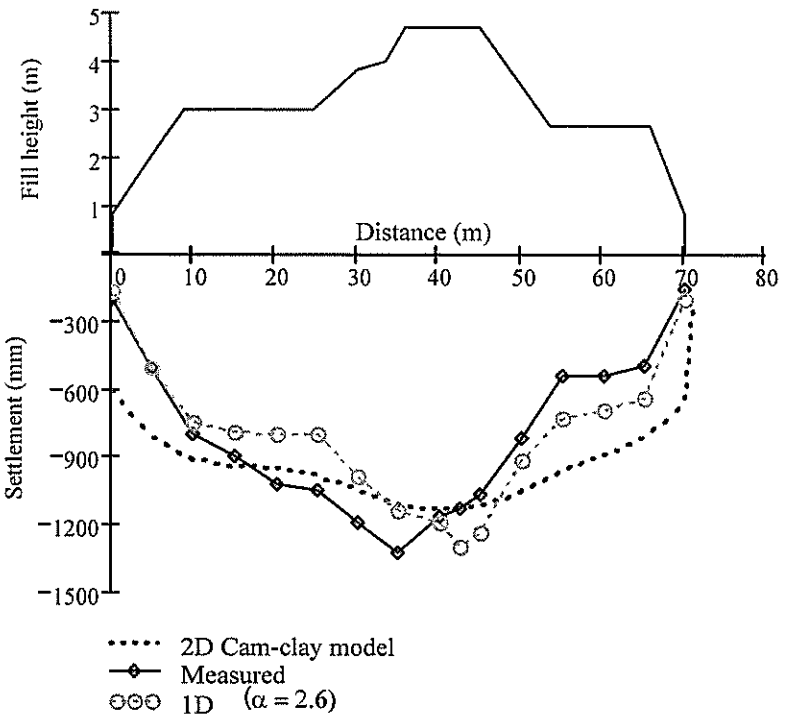

Figure 10. Settlement Profile at Location 35

To investigate the influence of the stiffness of fill on the settlement, 2D analyses were performed at Location 28 by varying the stiffness of fill. Figure 11 shows that the stiffness of fill has little effect on the overall settlement profile. Figure 12 shows a comparison of different methods of settlement calculation at Location 33. An additional method using a 2D elastic soil model in FLAC is included. The parameters used for this were derived from stress appropriate oedometer values of m_v (assuming Poisson's ratio as 0.4). A shear modulus of 55 kPa and a bulk modulus of 250 kPa were used for the main compressible layer. The *2D Cam-clay soil* method predicts larger settlement at the two sides of the embankment than the other methods. A possible explanation for this is that under the Cam-clay model the soil stiffness is dependent on the mean principal effective stress. The distribution of this stress in the FLAC model shows

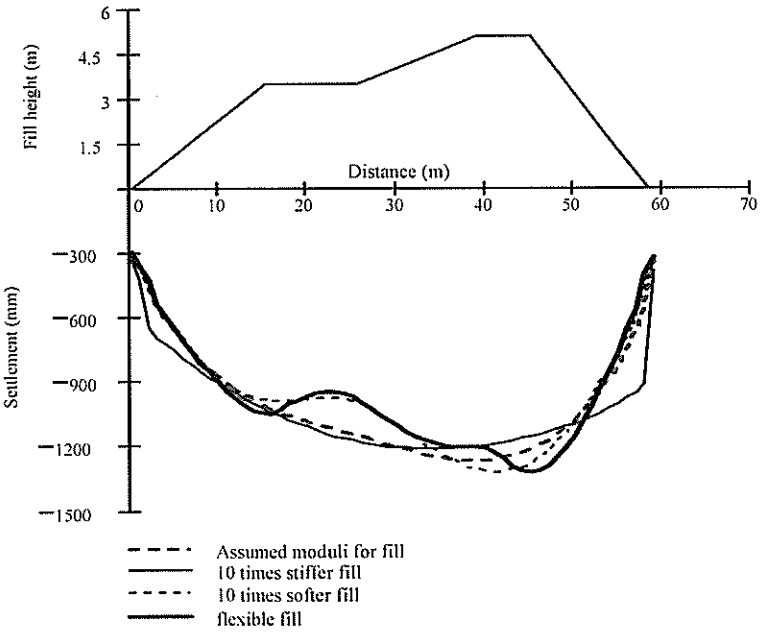

Figure 11. Influence of Fill Stiffness on Settlement at Location 28 (Cam-clay soil)

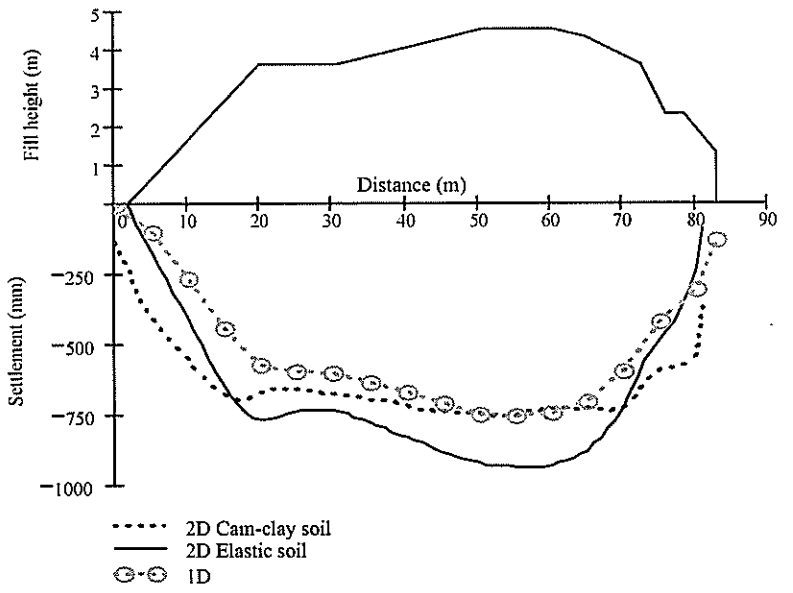

Figure 12. Comparison of Different Calculation Methods at Location 33 (Flexible fill)

that the mean principal stress is higher beneath the centre of the embankment and smaller beneath the edges. The lower stress gives a lower stiffness beneath the edges and hence more settlement.

CONCLUSIONS

The correlation of oedometer test results with CPT data was explored and the coefficient α was found to be in the range of 2 to 6 for soils at three sites within the Mercer to Longswamp Expressway project. Based on this range of α values, settlements of the embankment were calculated using a one-dimensional method and were found to be in good agreement with measured settlements.

For comparison with the 1D method, settlements were also analysed using a 2D finite difference method in which a Cam-clay soil model was implemented. Prediction of settlements was also found to be satisfactory except at two locations where the actual soil parameters of Cam-clay model might be significantly different from those obtained from the laboratory tests.

Comparing the various methods discussed in this paper, it is apparent that the simple one-dimensional method gives surprisingly good results. Thus for this type of work the use of sophisticated numerical methods seems unwarranted.

For these soft soils the use of laboratory tests appears to give satisfactory estimates of settlement. The settlements at Longswamp are very large and any sampling and laboratory effects may have a relatively small effect on the stiffness at large deformations.

ACKNOWLEDGEMENTS

The authors wish to acknowledge the financial support of the Foundation for Research in Science and Technology through contract UOAX007 "Essential Geotechnical Knowledge for NZ Infrastructure Development". The assistance of Transit New Zealand in allowing access to the site and field data is appreciated. The efforts of G Duske and J Melster during the field operations are much appreciated.

REFERENCES

Itasca Consulting Group (2000). *Theory and Background, FLAC version 4.0.*

Kulhawy, F.H. and Mayne, P.W. (1990). Manual on Estimating Soil Properties for Foundation Design, *Report EPRI EL-6800 Project 1493-6 Electric Power Research Institute Palo Alto.*

Lunne, T., Robertson, P.K. and Powell, J.J.M. (1997). Cone Penetration Testing in Geotechnical Practice, *Blackie Academic & Professional*, 45 - 145.

Poulos, H.G and Davis, E.H (1974). Elastic Solutions for Soil and Rock mechanics, *Wiley,* 36 – 91.

Pender, M.J, Jennings, D.N. and Crawford, S.A. (1999). Relation between Settlement & Cone Penetration Resistance at two sites, *Proc. 5th International Symposium on Field Measurements in Geomechanics* – FMGM99, Singapore, Balkema, 601-608.

Pender, M.J, Ni, B. and Cowbourne, A.J. (2002). Correlation Between Soil Stiffness and Cone Penetration Resistance at an Embankment Site, Proc. *3rd International Symposium on Lowland Technology*, Japan.

Senneset, K.R., Sandven R. and Janbu N. (1989). The Evaluation of Soil Parameters from Piezocone Tests, *Transportation Research Record No. 1235, pp24-37.*

Engineering Geological Influences on SH20 Mt Roskill Extension

D A Burns
MSc(Earth Sciences)
Manager Engineering Geology, Meritec Ltd
D C Davidson
ME
Geotechnical Engineer, Meritec Ltd
G B Farquhar
BE, BD, MSc(Lon), DIC, CEng, MICE, FIPENZ
Geotechnical Engineering Manager, Meritec Ltd

Abstract: The influences of engineering geology on the SH20 Mt Roskill Extension of the Auckland motorway network are discussed, including the extent and distribution of surface volcanic ashes and lava flows within a dammed valley environment and associated buried topography. A clearer understanding of the subsurface geology of the Mt Roskill area has been provided by geotechnical investigations along the route. The main influences on the design of the motorway and associated structures comprise embankment settlements due to soft sediments and a buried edge of a basalt flow; retention of a long cut face through the flank of a volcanic cone exposing a variety of materials; and bridge foundations on the buried edge of a basalt flow.

INTRODUCTION

Transit New Zealand is planning to extend State Highway 20 westward from its termination at Hillsborough Road, to near Richardson Road in Mt Roskill, Auckland. Associated with the extension are various works to connect to and upgrade existing roads. The proposed extension is approximately 5.3 km and is shown on Figure 1. Of particular note is the close proximity of the proposed motorway to the extinct Mt Roskill volcano (Searle 1981).

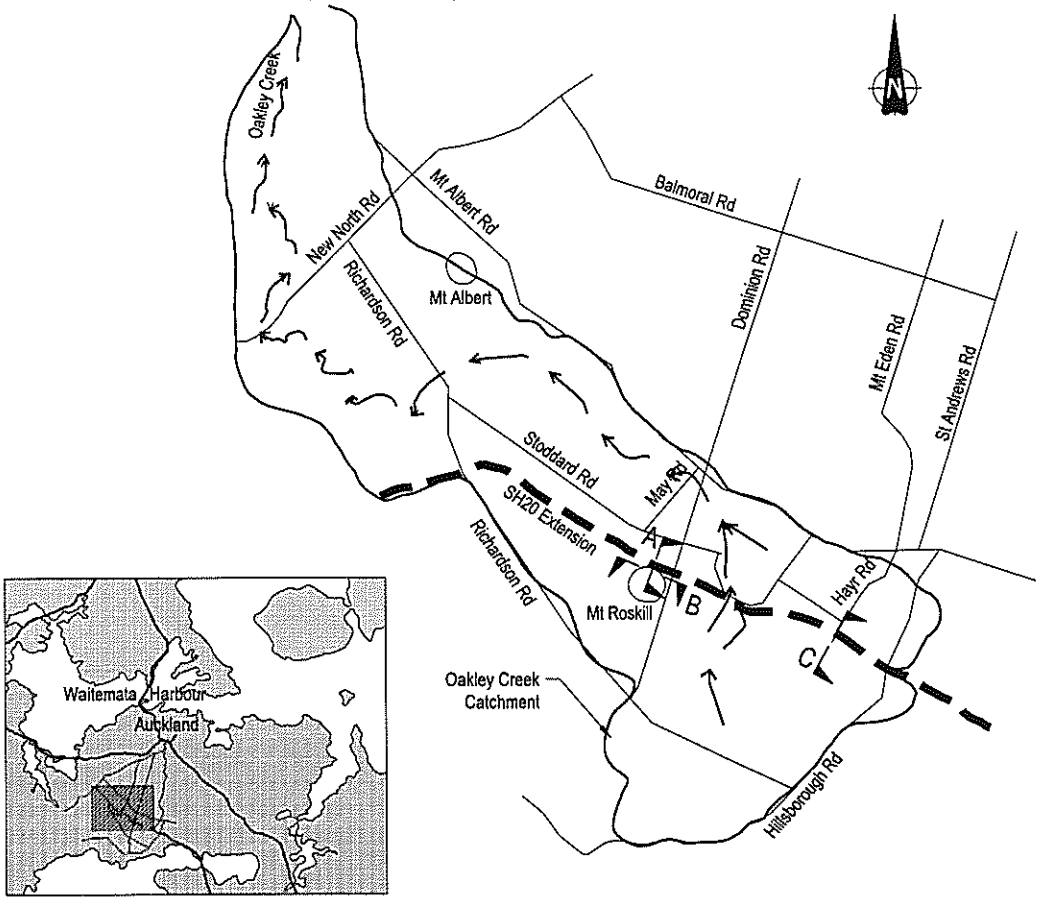

Figure 1. Site Plan

The complex geology along the route meant that an intensive programme of geotechnical investigations (Meritec, 2002) was required for design. This paper presents a geological history of the project area based on the results of the investigations, and discusses some of the influences of the geology on the engineering design of the project.

GEOLOGICAL HISTORY

An understanding of the engineering geology and, in particular, the geological history was important in interpreting the results of the geotechnical investigations and providing confidence for interpreting ground conditions between investigations. The geological events and processes that have resulted in the current ground conditions along the route are discussed in following sections, aided by a series of four figures illustrating the geological development of the project area (Figures 2, 3, 4 and 5).

Pre Mt Albert Eruption (Figure 2)

The route for the SH20 extension is predominantly in the upper part of the Oakley Creek catchment (Figure 1). The catchment is located towards the western side of the Auckland isthmus and drains northwest to Waitemata Harbour. The head of the catchment is the Hillsborough Road ridge.

The Oakley Creek valley was eroded in weak sandstone and siltstone rocks that form the geological 'basement' over most of the Auckland region. These bedded sediments (flysch) are part of a large grouping of marine rocks (Waitemata Group) that were deposited approximately 25 million years ago (Kermode, 1992). A long period of erosion followed uplift of the Waitemata Group rocks.

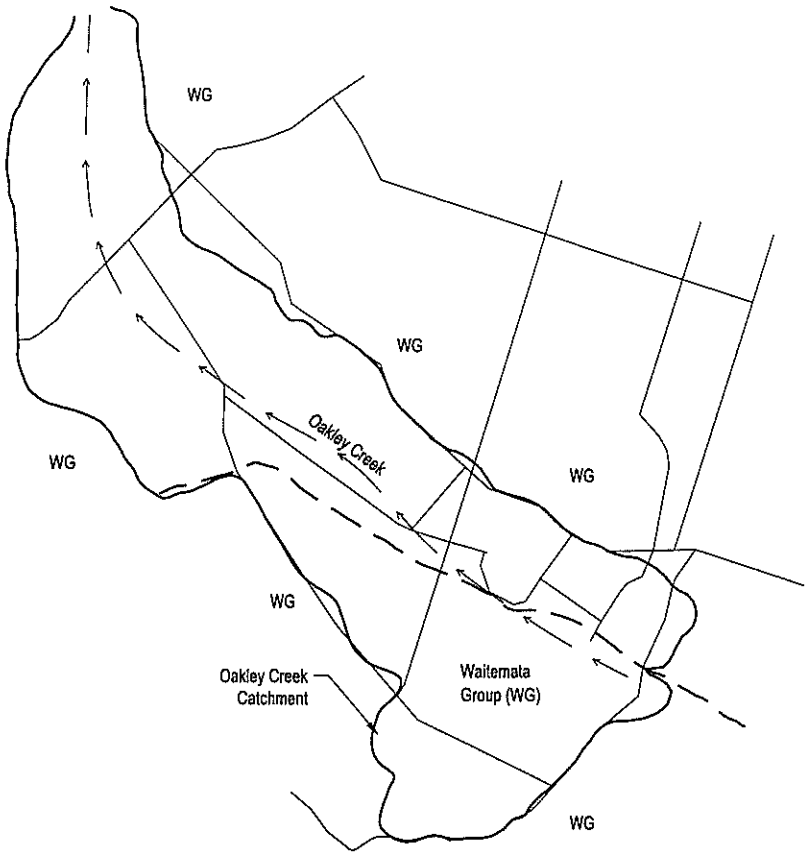

Figure 2. Pre Mt Albert Eruption

During the Pleistocene a series of broad terraces and ridges developed on the eroded Waitemata Group topography, including Oakley Creek valley. The terraces comprise fine-grained alluvial and estuarine sediments ('Terrace Alluvium'). Subsequent erosion within Oakley Creek valley removed most of the

'Terrace Alluvium' although remnants remain on some ridge crests and also as localised pockets and lenses on slopes.

Figure 2 shows the Oakley Creek Stream and catchment. The valley and the surrounding areas are shown as formed in Waitemata Group. 'Terrace Alluvium' is omitted for clarity.

Mt Albert Eruption (Figure 3)

About 30 thousand years ago Mt Albert erupted, constructing a scoria cone that blocked Oakley Creek valley. Alluvium and lake sediments were deposited behind the volcanic 'dam'. The sediments ('Mt Albert Alluvium') comprise sand, mud, silt and peat and extend upstream as far as Hillsborough Rd.

Oakley Creek subsequently cut down around the western edge of the Mt Albert lava dam, lowering base level of Oakley Creek and substantially eroding the 'Mt Albert Alluvium', which had the effect of partly exhuming the pre Mt-Albert valley upstream of Mt Albert.

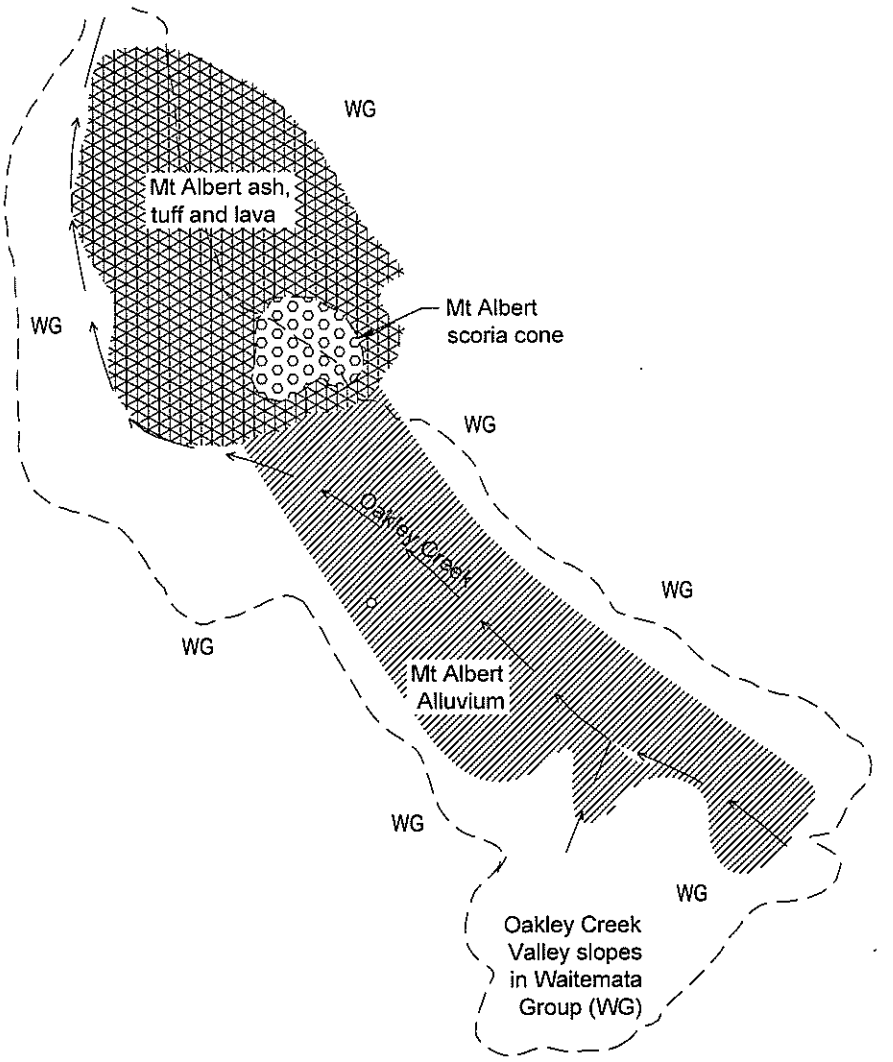

Figure 3. Mt Albert Eruption

Mt Roskill Eruption (Figure 4)

A relatively short time later Mt Roskill erupted in the valley, constructing a tuff ring and scoria cone and producing lava that flowed both upstream and downstream over the eroded 'Mt Albert Alluvium'. The lava filled the valley upstream of Mt Roskill to a depth of about 8m below present ground surface but did not overtop the highest remnants of 'Mt Albert Alluvium'. Downstream the lava filled the narrow valley around the southern and western flanks of Mt Albert.

Oakley Creek was forced eastwards to the edge of the lava flow in the upper and middle parts of the valley, eroding the remnants of the 'Mt Albert Alluvium'. The creek eroded weak valley slopes around the western flank of Mt Albert.

The Mt Roskill flows caused a second damming of Oakley Creek valley and further deposition of alluvium and lake sediments ('Mt Roskill Alluvium'), burying the lava flow upstream of the dam. The axis of the 'dam' is broadly along Dominion Rd. The large flat areas extending east from Dominion road to Hillsborough Rd near the head of the valley, represent the surface of the 'Mt Roskill Alluvium' (Figure 5).

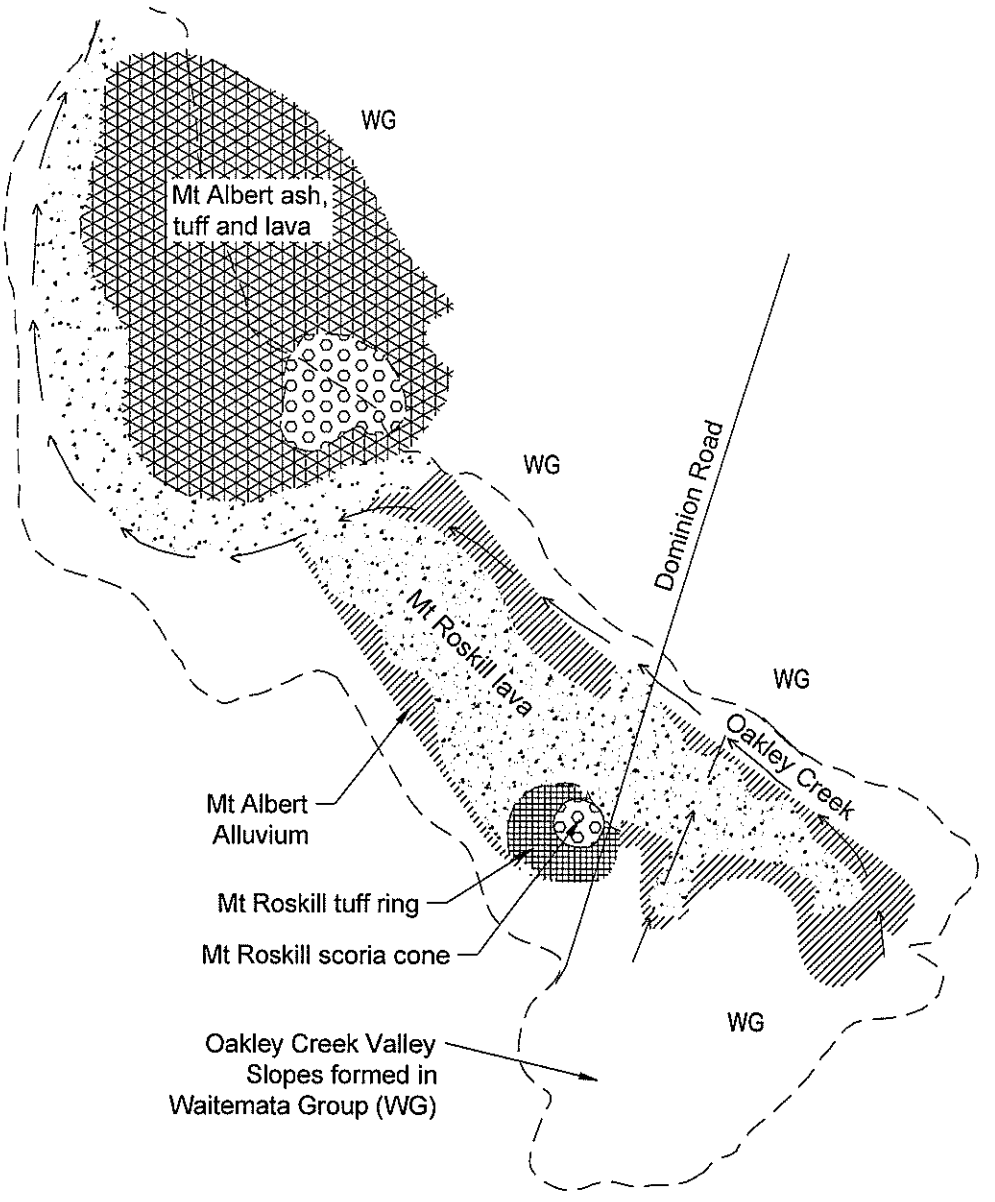

Figure 4. Mt Roskill Eruption

The lava also dammed the small Oakley Creek channel where the lava abuts the Mt Albert volcano resulting in deposition of 'Mt Roskill Alluvium' on the eastern side of the valley between Dominion Road and Mt Albert volcano.

Figure 5 illustrates the current geology in the vicinity of the Oakley Creek catchment. Modern Oakley Creek is only shallowly incised (1m to 3m).

In the period since the eruption of Mt Roskill other Auckland basalt volcanoes have been active (e.g. Three Kings and One Tree Hill) producing a thin (1m to 3m) cover of airfall tephra (Ash) over the area. For clarity, the extent of the ash cover is not shown on the Figure.

In addition, localised areas of Recent Alluvium associated with the modern channels of Oakley Creek tributaries, particularly those west of May Rd (i.e. 'downstream' of Mt Roskill) occur along the alignment. The alluvium is thin (generally less than 1m) and limited in area.

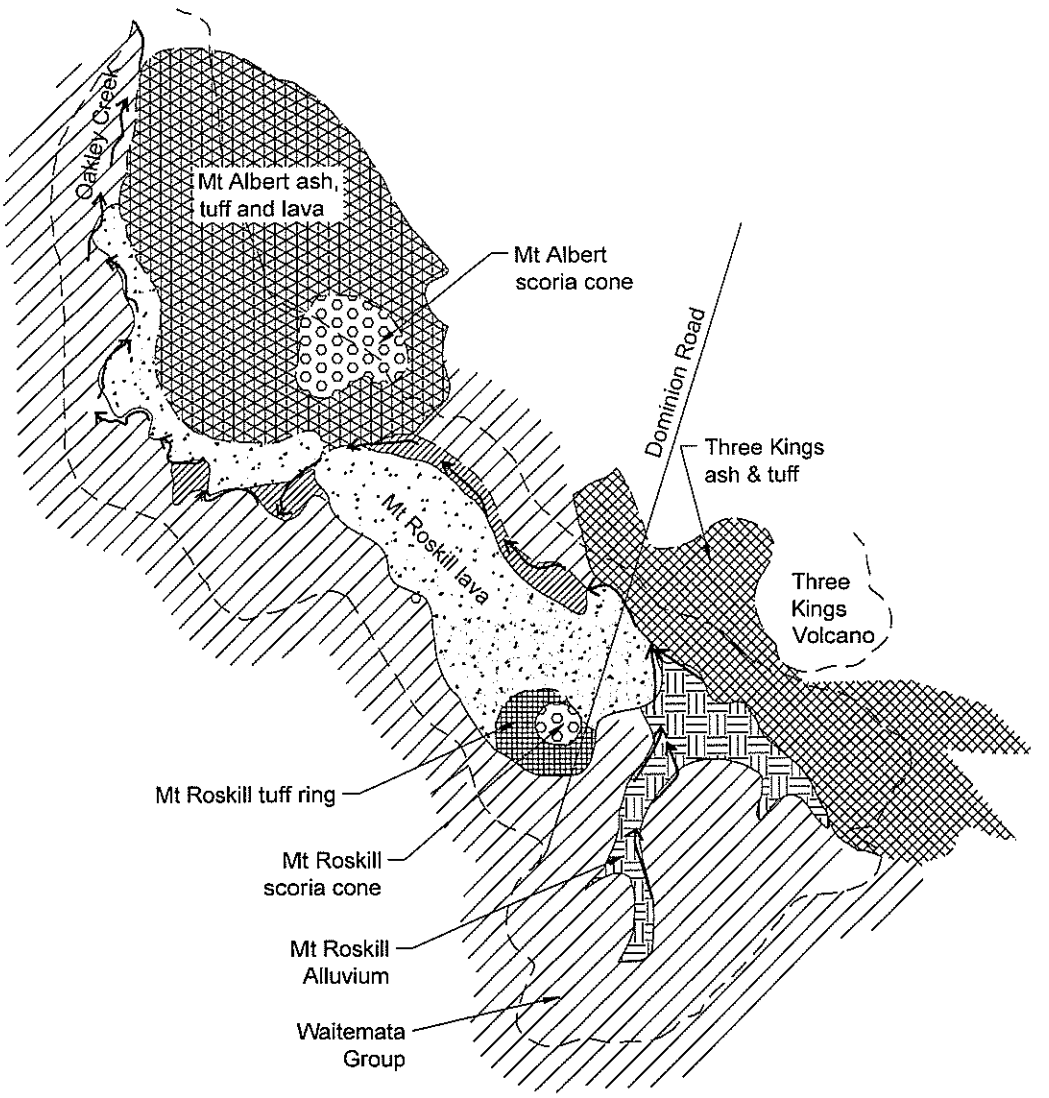

Figure 5. Present Day

GEOLOGICAL INFLUENCES ON DESIGN

Cut through Flank of Scoria Cone

The proposed motorway passes close to Mt Roskill and will form a deep cut through the lower flank of the scoria cone and adjacent lava field. The cut ranges in height to 10.5m and will be excavated in basalt and to a lesser extent in ash, scoria and tuff (Figures 6 and 7). Due to space constraints within the designation, the cut will be primarily sub-vertical and typically require retaining.

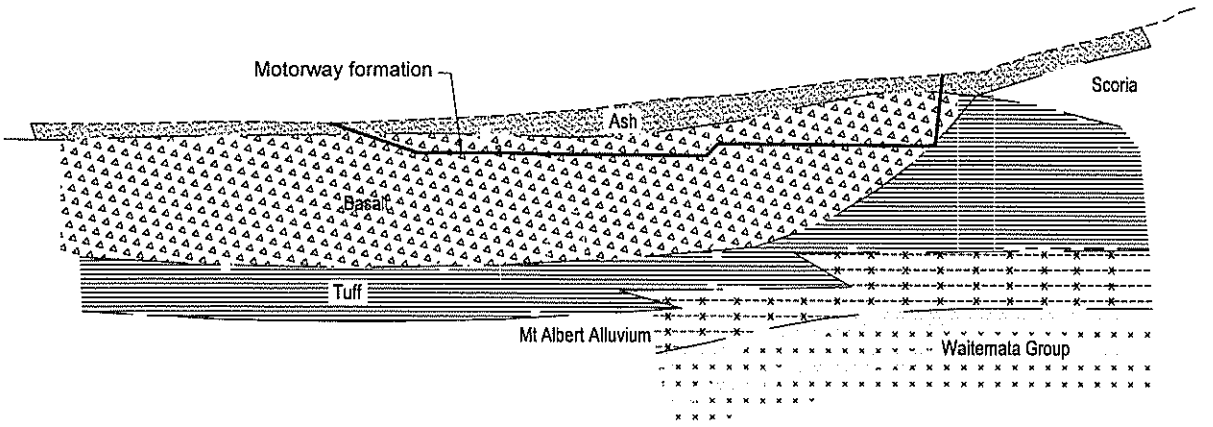

Figure 6. Geological Section A
(exaggerated vertical scale)

Issues for the cuts in basalt are excavability and support of cut faces. The main influence is the quality of the basalt rockmass, which is variable, ranging between highly vesicular (scoraceous), moderately weak rock and strong, moderately jointed rock. Typically the basalt is highly vesicular with moderate to closely spaced joints.

The southern side of the cut slope for the Dominion Rd westbound on ramp is closest to the scoria cone and will be in basalt, scoria and tuff. The distribution of materials in the cut face is illustrated on the geological long-section in Figure 7. Support of this cut face will be influenced by the variety of materials. Ash (stiff clayey silt and loose to medium dense silty sand), loose (lightly welded) scoria and dense sand/gravel tuff will be encountered where the excavation intersects the toe of the scoria cone and adjacent buried tuff ring.

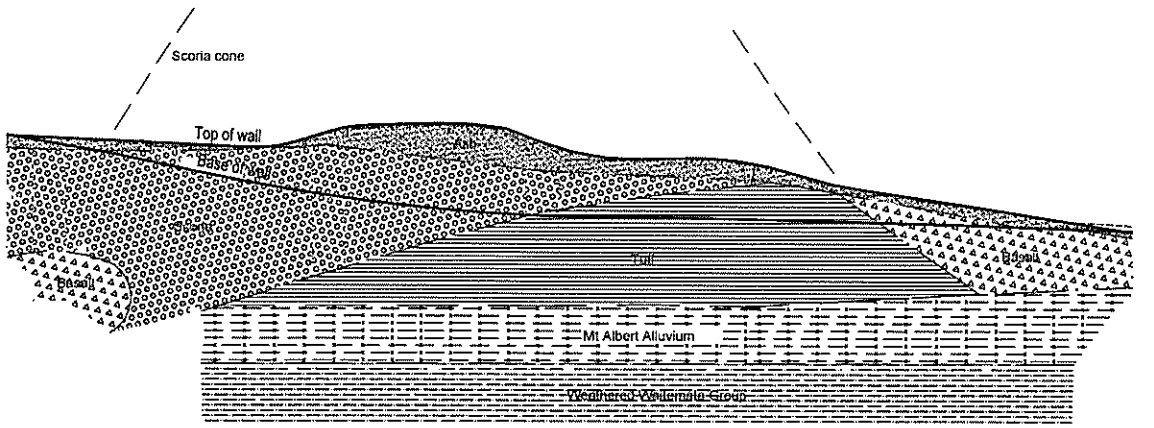

Figure 7. Geological Section B
(exaggerated vertical scale)

Soft Sediments and Edge of Basalt Flow

Approximately 1 km of the motorway, in the vicinity of Keith Hay Park and Hayr Rd, traverses the edge of the Mt Roskill lava flow. The motorway along this section is on embankment fill ranging in height up to 5 m. The geological section at the Hayr Rd overbridge presented in Figure 8 is typical of the geological profile along the 1 km portion of the route. Abutment fills are required for the overbridge.

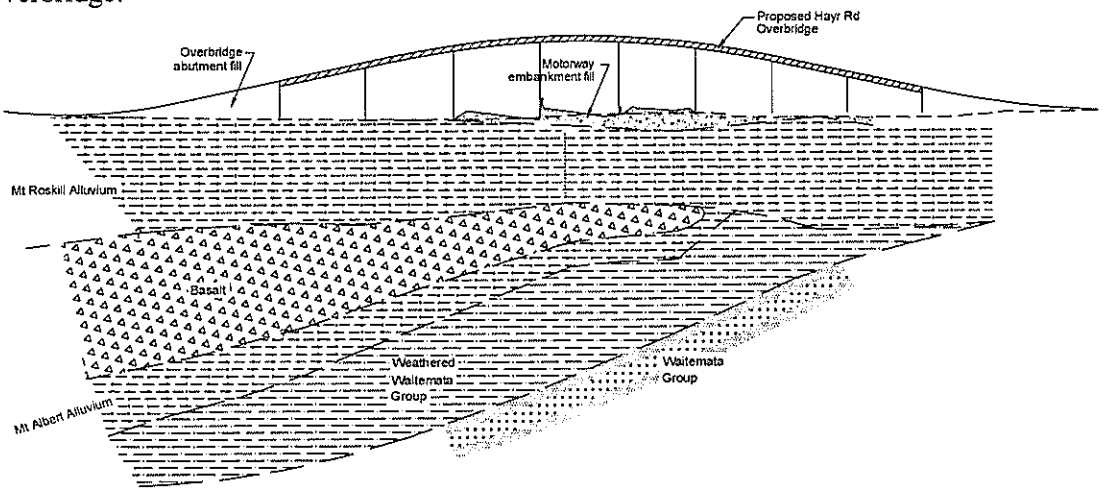

Figure 8. Geological Section C

Issues for design of the fill embankments are:

- Ground conditions are complex, comprising highly compressible materials of variable depth inter-fingered with incompressible basalt. The 'Mt Roskill Alluvium' (soft to firm silty clay and organic silt), ranges in thickness from 4m to 20m and overlies either basalt or weathered Waitemata Group rock. The basalt is underlain by 'Mt Albert Alluvium' and weathered Waitemata Group rock.
- The 'Mt Roskill Alluvium' is highly compressible and extremely slow draining. The 'Mt Albert Alluvium' underlying the Basalt is typically stiff to very stiff and of low compressibility.

Issues for design of deep foundations and approach embankments for bridges are:

- Piles are founded either on basalt layers at depth or Waitemata Group (basement rock).
- The thickness, quality and nature of the basalt at the edge of flow.
- Settlement of the 'Mt Roskill Alluvium'.

CONCLUSIONS

1. The geotechnical investigations along the route have provided a clearer understanding of the complex subsurface geology of the motorway route in the Oakley Creek catchment.
2. The project illustrates the importance of the engineering geological assessment, especially when working in complex geological environments.
3. The main influences on the design of the motorway and associated structures comprise embankment settlements due to soft sediments and a buried edge of a basalt flow; support of a long cut face through the flank of a volcanic cone exposing a variety of materials; and bridge foundations on the buried edge of a basalt flow.

ACKNOWLEDGEMENTS

Transit New Zealand is acknowledged for the use of information gained during the SH20 project investigations.

REFERENCES

Searle, E.J. (1981). "City of Volcanoes – A Geology of Auckland", Longman Paul.

Kermode, L.O. (1992). "Geology of the Auckland Urban Area", Scale 1:50,000, Institute of Geological & Nuclear Sciences.

Meritec Ltd (2002). "SH20 Mt Roskill Extension, PA2084, Geotechnical Factual and Interpretive Reports," Unpublished reports prepared for Transit NZ.

Design and Construction of a Large Cut Slope in Sensitive Volcanic Ash Soils

D L Dennison
BSc (Hons)
Principal Geotechnical Engineer, Opus International Consultants Ltd.
N J Edger
BE (Hons), MIPENZ, R Eng
Senior Geotechnical Engineer, Opus International Consultants Ltd.

Abstract: The PJK Expressways Project includes approximately eight kilometres of new roads, seven bridges and more than 1 million m^3 of earthworks. This paper describes the design and construction of one of the larger cut slopes in the project, the J3 Cut. This cut is up to about 20 m high and involves excavation of approximately 50,000 m^3.

Site investigations were carried out in several stages from 1989, including a full scale trial evacuation in 1992, and continued into the construction phase. Soils in the cut area are mainly sensitive fine grained volcanic ash soils.

Analysis demonstrated that control of pore pressures was critical in maintaining the stability of the slope. A variety of drainage measures were used including subsoil drains, bored horizontal drains and counterfort drains.

The excavation extends well below the original ground water table and encountered soils that were too soft or too slippery for standard earthworks equipment. The construction made use of a long reach excavator to dig most of the sensitive soils in a single large lift, working from a bench in the upper more friable soils. Most of the soil excavated was used in non-structural applications, such as stability berms for nearby embankments on soft ground.

A flexible observational approach to construction was successfully applied to deal with the variable soil and groundwater conditions encountered during construction of the J3 Cut.

INTRODUCTION

The PJK Expressways Project was the largest single roading contract in New Zealand when construction began in 1999. The project includes approximately eight kilometres of new roads, seven bridges and more than 1 million m^3 of earthworks.

Tauranga District Council and Transit New Zealand combined their separate projects into one construction contract to maximise flexibility for the contractor's programme. The single contract also simplified project management input from the consultant and clients.

The project comprises the following major components:

- Route K, approximately 4.5 km long, from SH29 to Interchange Area
- Route P, approximately 0.5 km long, from Route K to Takatimu Drive
- Route J, approximately 3.1 km long (including interchange), from SH2 to 15th Avenue.

The layout of the project is shown in Figure 1.

The project faced many challenging geotechnical issues including high embankments on soft compressible soils, placing moisture sensitive fill within a limited corridor, design of pile foundations for bridges, and large cut slopes in sensitive volcanic soils.

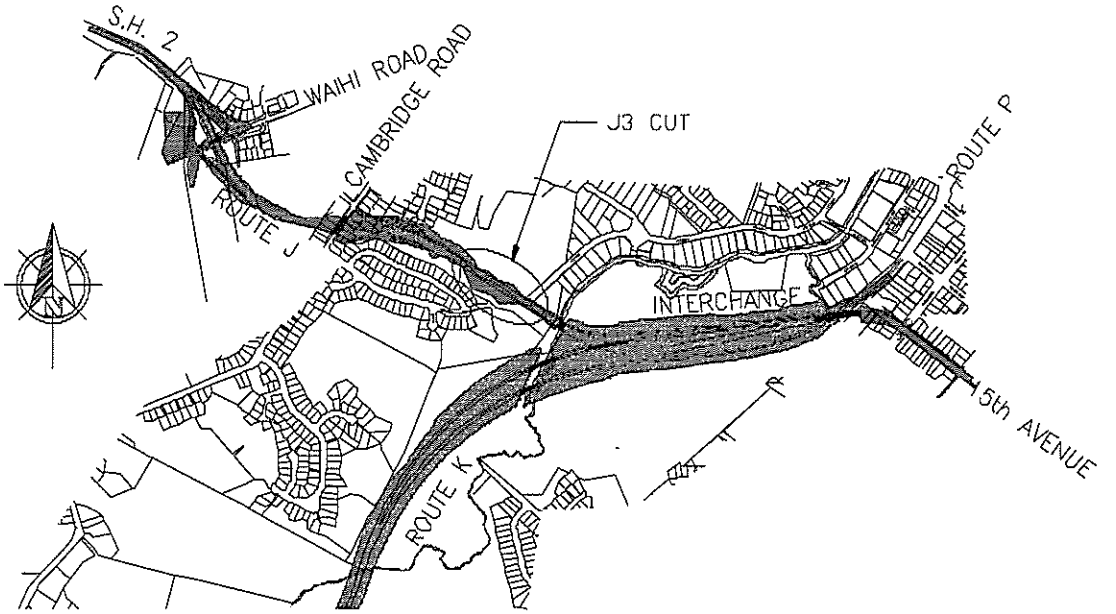

Figure 1. PJK Expressway Site Layout

This paper describes the design and construction of the J3 Cut. The location of the cut is shown on Figure 1. This cut is up to about 20 m high and involves excavation of approximately 50,000 m^3. A general overview of the cut during construction is shown in Figure 2.

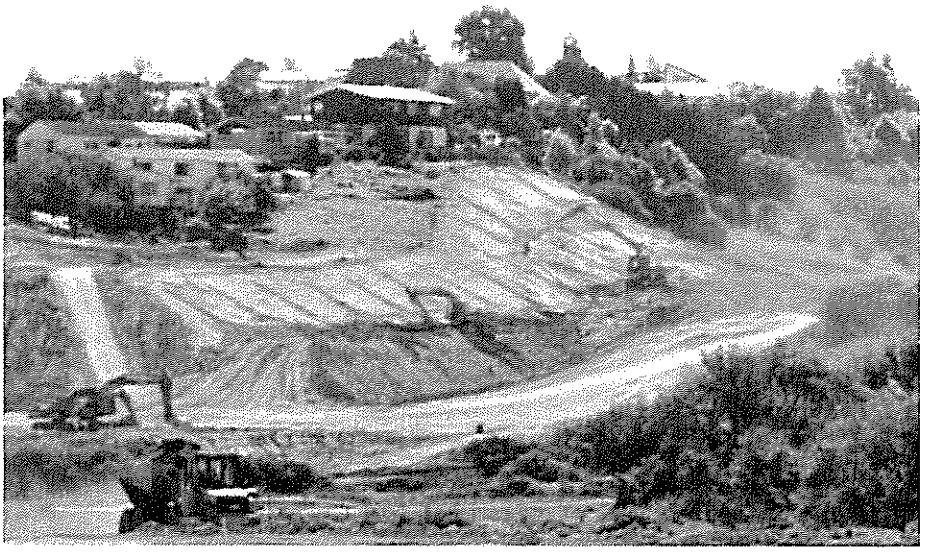

Figure 2. Overview of J3 Cut

SITE INVESTIGATION

Site investigation for the cut was carried out in several stages from September 1989, continuing into the construction phase. In the immediate area of the cut there were five cored boreholes, five cone penetration tests (CPTs) and three test pits. In addition, soil conditions were observed directly during the full scale trial excavation described below.

Extensive laboratory testing was carried out on soils from the J3 area including triaxial strength testing for cut slope design, CBR tests to determine pavement subgrade conditions and compaction testing to assess suitability of cut material as structural fill.

SUBSURFACE CONDITIONS

Soils in the cut area are mainly sensitive fine grained volcanic ashes. From the surface downward a typical geologic sequence consists of Younger Ashes, Rotoehu Ash, Hamilton Ash and Matua sub-group soils.

Younger Ashes are generally sandy and suitable for bulk earthworks provided moisture contents are well controlled. Some drying is often necessary to achieve adequate shear strength and workability. Rotoehu Ash is generally a white sandy soil and often has very high moisture content. Brown Hamilton Ash is more clayey, with high moisture contents that required conditioning before use as structural fill.

Underlying the Hamilton Ash is the Matua Sub-group that includes a large variety of soil types, ranging from pumice sands to clayey soils. A particularly sensitive soil, locally known as Pahoia Tephra, is included in the Matua Subgroup. Pahoia Tephra soils were expected to require extensive conditioning over a long period before using as bulk fill, or be cut to a soil disposal area. The Hamilton Ashes and Younger Ashes have an allophane mineral content of 5 to 7 %.

TRIAL EARTHWORKS

The initial investigations showed that the soils in the J3 area were likely to present significant construction difficulties and exhibit variable stability performance. A trial excavation and embankment constructed in 1992 had the following objectives:

- assess slope stability,
- assess suitability of the material from the cut for bulk and subgrade fill,
- determine the degree of construction difficulty associated with the excavation, hauling and placement of the cut soil in fill,
- assess the change in the characteristics of the excavated soil over time after placement in the embankment fill.

The trial excavation comprised a 1H:1V end slope up to 9.5 m high and 1.5H:1V side slopes up to 12 m high (Figure 3). Aside from erosion of some of the less cohesive materials exposed in the cut slopes in the first winter, there was no sign of instability in the trial cut.

Figure 3. Trial Excavation

Hauling and placement in the embankment became significantly more difficult when the more sensitive soils at and below the Hamilton Ash layer were reached in the excavation (Figure 4). Testing

indicated that a Pilcon vane strength of about 80 kPa was required to provide passage for trafficking of haul equipment.

Figure 4. Swamp Track Dozer Stuck in Sensitive Ash Fill

As part of the Route J trial fill, an experiment was carried out to assess drying of the soil using light agricultural discs. The equipment repeatedly became bogged down during the trial. A water content reduction of about 6% was achieved in eight days (Figure 5).

Soil sensitivity and moisture content increased with depth in the excavation, making plant movement and material handling increasingly difficult. Below about three to five metres depth the soil exposed in the cut was either too slippery or too soft to allow easy passage of haul traffic. Soils exposed near the base of the excavation remoulded to a viscous fluid consistency when disturbed by excavation and haul equipment.

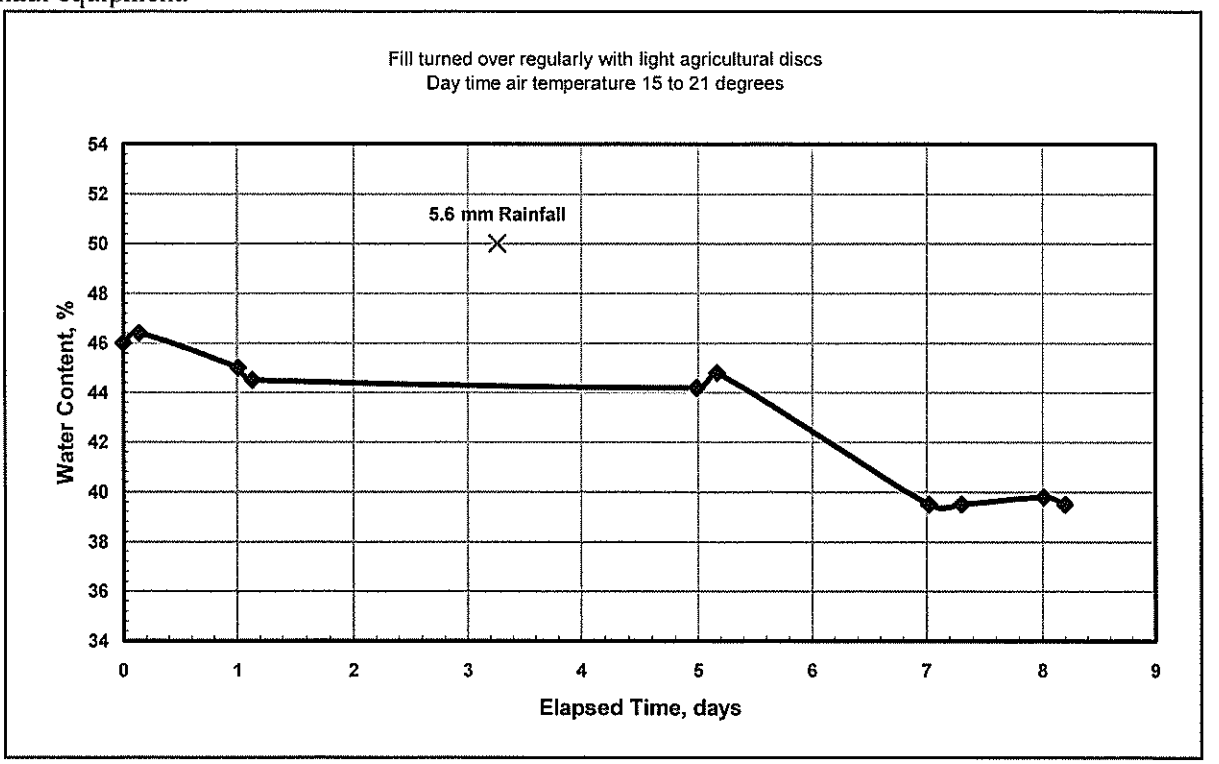

Figure 5. Results of Field Drying Trial

Additional testing was carried out in the trial fill approximately two years after initial placement. Pilcon vane strengths typically increased by about 20 kPa, to 80 kPa, over this time, although water contents were similar. The mechanism for the strength gain is not clear, but may be related to reformation of bonds within the soil.

SLOPE STABILITY

Previous landslips in the hillside to the northwest of the J3 Cut demonstrated the potential for stability problems at the site. Although the subsurface conditions are highly variable, the extensive investigation, lab testing and field trial provided a good indication of the range of soil properties that could be expected at the site. Shear strength properties of c'=15 kPa and ϕ'=25° were selected for stability analysis (Figure 6). Possible failure mechanisms include rotational slumping and possible sliding along a soil layer that is lower strength and/or is subject to high pore pressures from a perched water table.

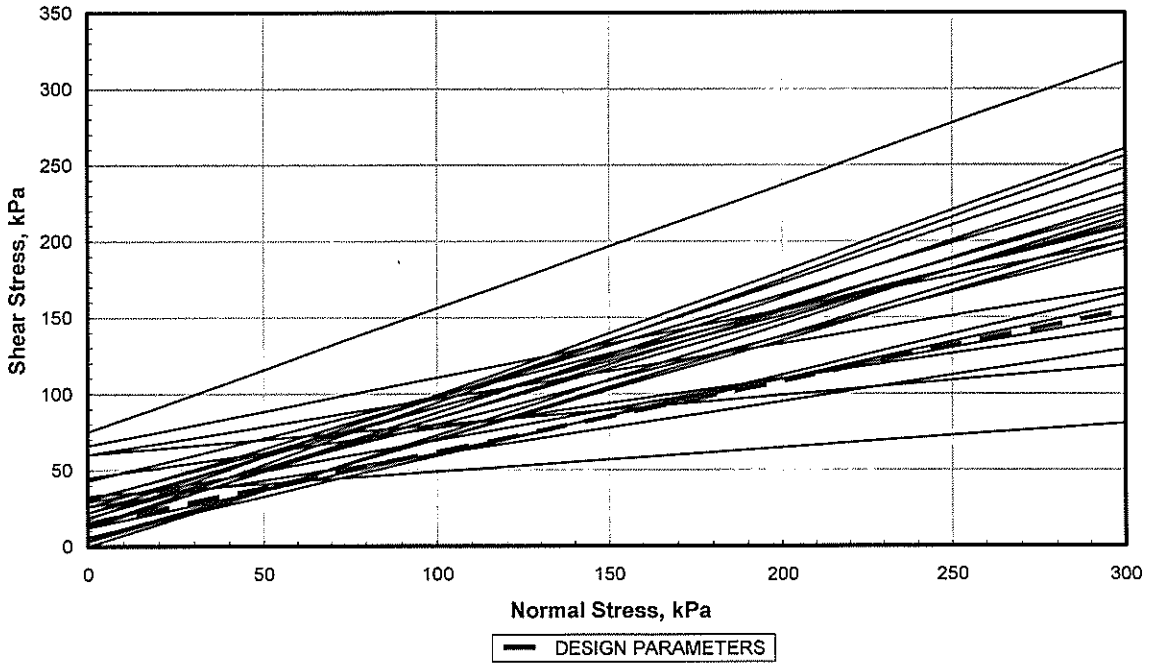

Figure 6. Summary of 24 Triaxial Test Results

The design batter angle is 1.5H: 1V on the left side of the cut and 2H: 1V on the right. The flatter slope on the right is due to the greater overall slope height, higher groundwater levels, and presence of houses at the top. In addition north facing slopes in the Bay of Plenty are often less stable due to increased infiltration caused by desiccation cracking.

Analysis demonstrated that control of pore pressures was critical in maintaining the stability of the slope. The bottom of the excavation was to be below the static groundwater levels measured in the initial investigations, so measures to draw the groundwater level permanently well below the level of the pavement were required. Drainage measures adopted at the site include:

- deep subsoil drains along both sides of the cut, comprising perforated subsoil pipes and clean rockfill,
- counterfort drains running down the slope at regular intervals,
- sub-horizontal drains drilled into the slope.

CONSTRUCTION CONSIDERATIONS

Maximum dry density in the standard compaction test ranges from about 0.95 to 1.20 tonnes/cu m for the soils encountered in J3 Cut. Optimum moisture content is about 40 to 60%. Moisture content of the ash soils is generally about 10% above the optimum moisture content measured in standard compaction tests.

Compaction tests indicate local ash soils are often sensitive to the moisture history of the sample. Samples from similar soils prepared by drying back from the natural moisture content give significantly different results than if they are wetted up from oven dried samples, as shown in Figure 7. Because of this, it can be difficult to control compaction using the standard moisture versus density laboratory test.

Curve	IWC* %	OWC %	$\rho_{d(max)}$ t/m^3
E	<5	45.5	1.07
F	64.5	57.5	0.98
G	75.3	64.0	0.93

*Initial Water Content

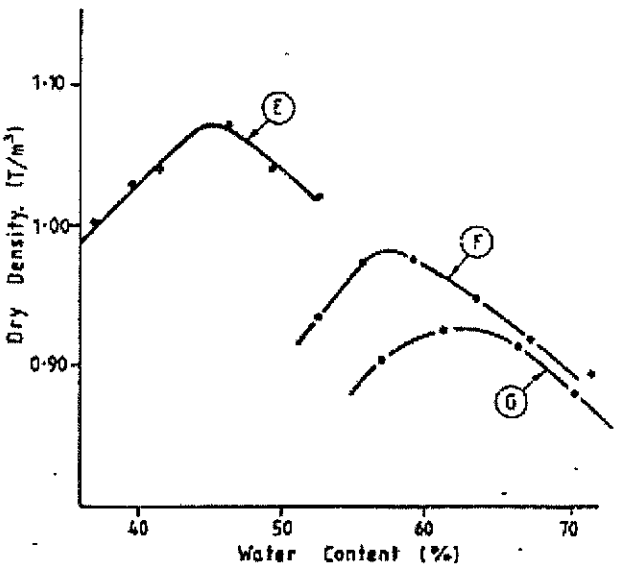

Figure 7. Compaction Curves at Different Initial Water Contents (after Parton & Olsen, 1980)

Moisture content readings by a nuclear densometer were poorly correlated to those measured in the laboratory, with no consistent difference between them. This required nuclear densometer readings to be frequently checked against oven dried moisture contents during construction.

The ash soils do not dry easily and it is generally not practicable to achieve compaction criteria based on optimum moisture contents determined in standard compaction tests. Attempts to dry the fill by disc harrowing may reduce the strength of the soil by remoulding rather than improve the soil by drying.

The compacted density of the ash fills was significantly greater than the original in-situ density. The amount of imported fill required depended partly on this difference in density. The compaction factor varies within the project area and with depth. Average dry densities measured in the trial excavation were not significantly different from dry densities measured in the trial fill. A large trench was excavated in similar soils at the Lakewood borrow area as part of the Route K enabling contract. The surveyed volume of the excavation was 14,750 cu m. The combined volume of the soil stockpiles and

fills made from this material was 11,600 cu m, giving a compaction factor of 79%. The soil stockpiles in the enabling contract were compacted only by construction traffic.

The J3 excavation extends well below the original ground water table and encountered soils that were too soft or slippery for standard earthworks equipment. Within the Route J trial excavation a long reach excavator was used to reduce the requirement for construction traffic because of the trafficability problems. The full scale construction also made use of a long reach excavator to dig most of the sensitive soils in a single large lift, working from a bench in the upper more friable soils (Figure 8). Most of the soil excavated was used in non-structural applications, such as stability berms for the embankments in the interchange area.

Figure 8. Single Large Excavation Lift

Because of the problems with water content and trafficability, temporary drainage measures in the cut were carefully maintained to minimise moisture within the excavations. Control of water was important for maintaining the trafficability of the cut surface and for maximising the use of cut materials in embankment fills. Temporary drainage measures in the cut were carefully maintained to maximise the use of cut materials in embankments and to reduce trafficability problems. Drains were needed to handle both surface run-off and groundwater inflows. As the base of the cut could not support even lightweight construction equipment, it was necessary to lay a filter cloth on top of the sensitive soils, and then use thick lifts of rockfill from the ends of the cut.

OBSERVATIONAL APPROACH

It was necessary to adopt a flexible observational approach to the construction because of the variable and difficult conditions. Activities during construction included additional investigation drilling, regular inspections of soil and groundwater conditions updating stability calculations, additional triaxial strength testing, and review of monitoring data (piezometer, inclinometer and survey data). Several changes were made to the design as a result of these activities, including the following:

- reticulated stormwater from the houses nearest to the top of the cut (previously using soakholes),
- additional bored drains, covered by filter fabric, extending deeper into the slope,
- increased number and depth of counterfort drains,
- additional instrumentation,
- changes to the hydro-seed mix,
- widened berm at base of the slope to provide more room for stormwater pipe installation,
- altered design of subsoil drains at the base of the slope,
- deeper subgrade improvement layer under the pavement at the base of the slope.

Flows from the bored drains ranged from nil to approximately 20 l/min. Some drains flowed for a while after installation and then stopped, while others are still flowing. Additional drains were installed in areas where springs were encountered and around initial drains showing significant flow.

An intensive rainstorm caused extensive damage in the Tauranga area in April 2000. Rainfall was estimated at more than 200 mm in a 25 hour period. The timing of the storm caught the J3 Cut at its most vulnerable stage, excavated to full depth but with vegetation not well established on the slope. Although there was some surface erosion at J3 (Figure 9), the drainage system worked well and no signs of serious instability were observed.

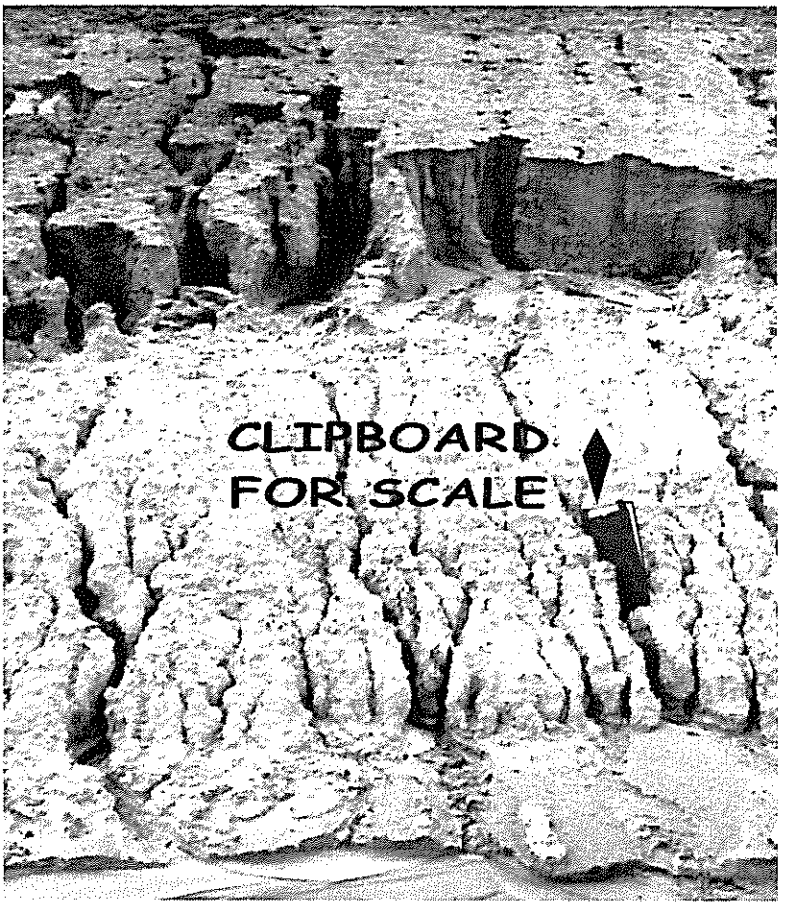

Figure 9. Storm Erosion

CONCLUSION

The sensitivity of the volcanic ash at the site, as well as the variability of soil and groundwater conditions, required extensive investigation work to provide information for cut slope design and earthwork management. The large scale trial excavation and embankment construction were particularly valuable to examine the ground conditions and identify appropriate construction techniques.

An observational approach to construction was required to adapt the design to the range of soil and groundwater conditions encountered. Key aspects to this flexible approach were:

- a reasonably conservative design,
- adequate contingencies in both programme and budget to handle changes,
- allowance in material balance for additional fill and/or waste soil disposal,
- a programme of monitoring, additional testing and design review during construction,
- communicating expected difficulties to other parties, especially those tendering for the work.

ACKNOWLEDGEMENT

We would like to thank Transit New Zealand for permission to publish this paper.

REFERENCES

Parton, I.M., Olsen, A.J., (1980), "Compaction Properties of Bay of Plenty Volcanic Soils, New Zealand", 3rd Australia-NZ Conference on Geomechanics. Vol.1, Wellington, NZ.

Design of a Pile Reinforced Embankment, PJK Expressways Project, Tauranga

A J Cowbourne
BE(Hons) BSc MSc(Hons) MIPENZ CPEng
Senior Geotechnical Engineer, Tonkin & Taylor Ltd, Tauranga

Abstract: The Route J alignment of the $90M PJK Expressways Project provides a new arterial road for State Highway 2 into Tauranga City from the north. Built over the last three construction seasons, the PJK Project has required significant geotechnical inputs, with observational techniques used to manage risk and allow optimisation of the alternative design-and-construct areas of the project.

Geotechnical aspects of the alternative design for one of the main fill areas, the 14 m high sidling fill at J2 Fill, are discussed. The complex foundation included highly weathered volcanic soils, landslide debris and recent sediments, with artesian groundwater pressure within the toe zone.

The alternative design for the J2 Fill successfully used a combination of revised road geometrics, shear pile reinforcement, lightweight filling, and an extensive underdrainage system to achieve the required design criteria.

INTRODUCTION

The PJK Expressways Project is jointly funded by Transit NZ, Tauranga District Council and Western Bays District Council. As shown on Figure 1, the project links expressways to the Tauranga City peninsula (Route P), to the north (Route J) and the west (Route K).

The J2 Fill section of Route J comprises a sidling fill embankment up to 14 m high constructed on the side of steeply sloping ground just to the east of Cambridge Road, extending partially into the Valley of Te Auetu (Figures 1 and 2). The fill provides for the five lane expressway as well as the on- and off- ramps for Cambridge Road. The conforming design for this area involved approximately 13,000 m^3 of polystyrene fill and geogrid reinforcement.

The J2 Fill area was one of several identified for value engineering initiatives by the Contractor, the Fulton Hogan Ltd – Smithbridge (NZ) Ltd Joint Venture and their design consultant, Tonkin & Taylor Ltd.

Upon award of the contract in late 1999, further geotechnical investigation was undertaken at the J2 Fill to enable development of an alternative design. The extra geotechnical information and other associated factors highlighted slope stability issues which affected the design of the route.

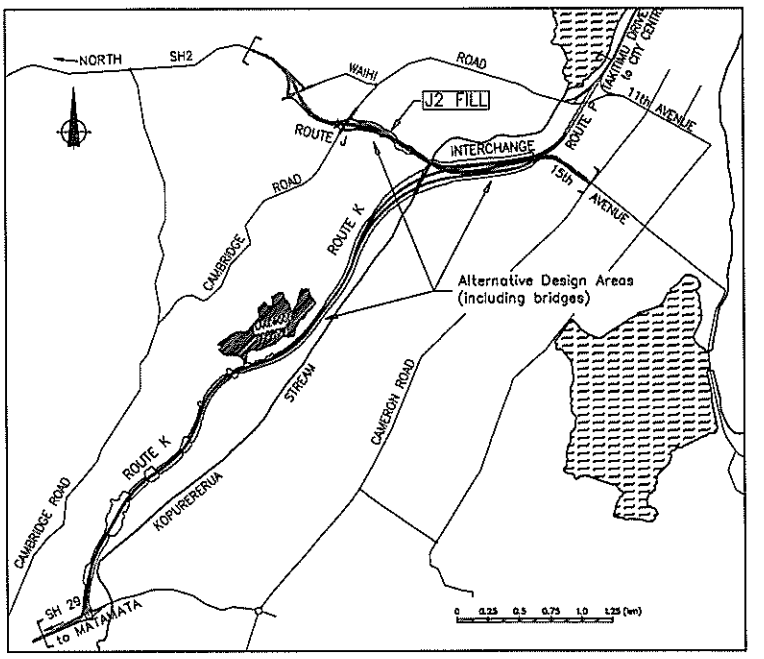

Figure 1 : PJK Project Location Plan

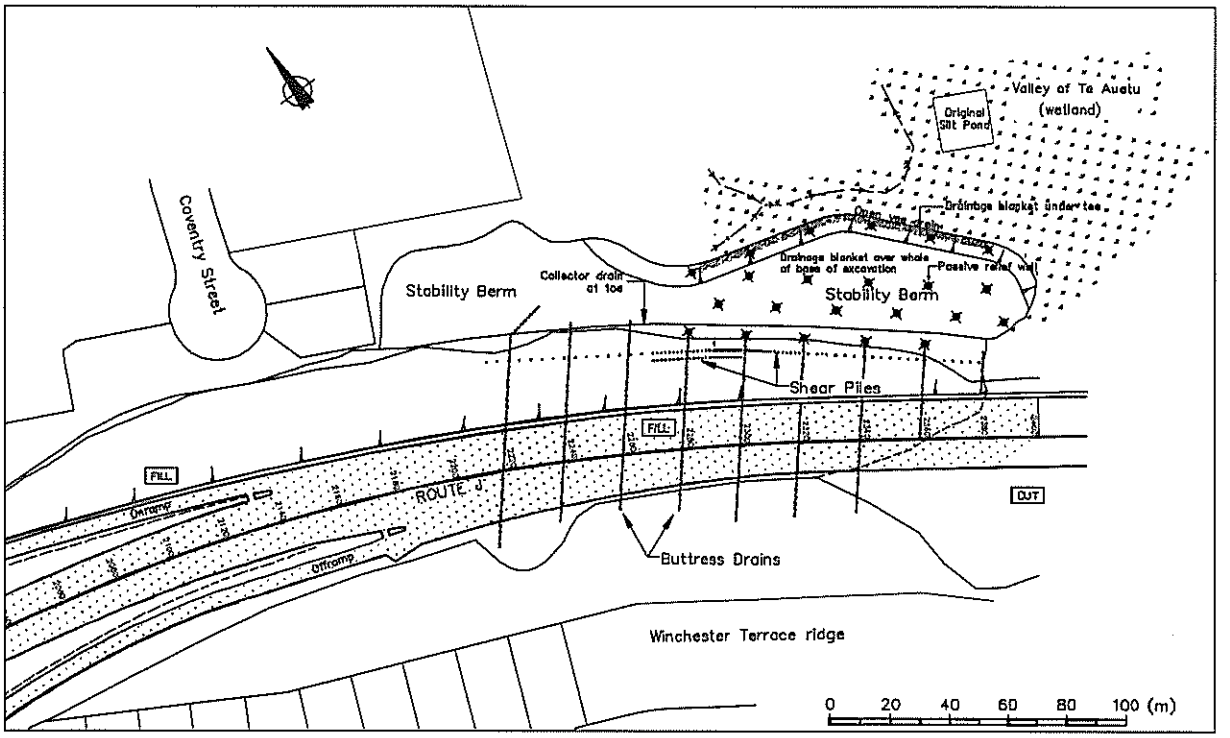

Figure 2 : J2 Fill Area

An alternative concept design was developed for the critical sections of the embankment to be constructed using lightweight pumice fill, a stability berm, foundation reinforcement piles, and revised road geometrics.

The alternative design also included the lowering of Cambridge Road, which allowed the overall height of the embankment to be reduced by up to 1.5 m and flatter batter slopes at the western end of the fill, thereby improving slope stability.

Design criteria had been set as part of the conforming design, and there was little or no change made to these during the alternative design process. Protocols were in place to limit the amount of disturbance of the natural ground and archaeological sites within the area, including an urupa (burial ground) on a small ridge directly in front of the embankment.

The J2 Fill was completed in early 2002 and the Route J Expressway was commissioned by April 2002. The total quantity of filling was approximately 130,000 m^3, comprising weathered brown volcanic ash, imported rockfill and pumice.

STRATIGRAPHY

The J2 Fill area comprises a complex series of primary volcanic deposits, lacustrine sediments and landslide materials, with several buried topographic surfaces. A brief summary of the main subsurface units is as follows, while a summary cross section is given in Figure 2.

Pumice Breccia

The local "basement" unit for the local area comprises a moderately to highly weathered dark yellow to light yellow pumice breccia (poorly welded ignimbrite). Borehole core showed it to be typically a dense fine to coarse sand with fine to medium sized pumice gravel, while the CPT cone resistance regularly exceeded 30 MPa.

Ash-Lapilli Deposits

Overlying the pumice breccia is a 3.5 - 7.5 m thick layer of moderately weathered light greyish brown loose to very loose ash-lapilli. This was generally recovered as very silty fine to very coarse sand. This is in turn overlain by a thick (up to 16m) unit of ash –lapilli. In the boreholes, this unit was recovered as very thin to thin (1 to 50mm) layers of fine to very coarse sand with minor fine gravel.

In the upper northern side of the valley the ash-lapilli materials are finer grained and were recovered as predominantly greyish white, clean, very fine to medium sand, directly overlying the pumice breccia. The materials are medium dense to dense, with CPT cone resistance in excess of 10 MPa.

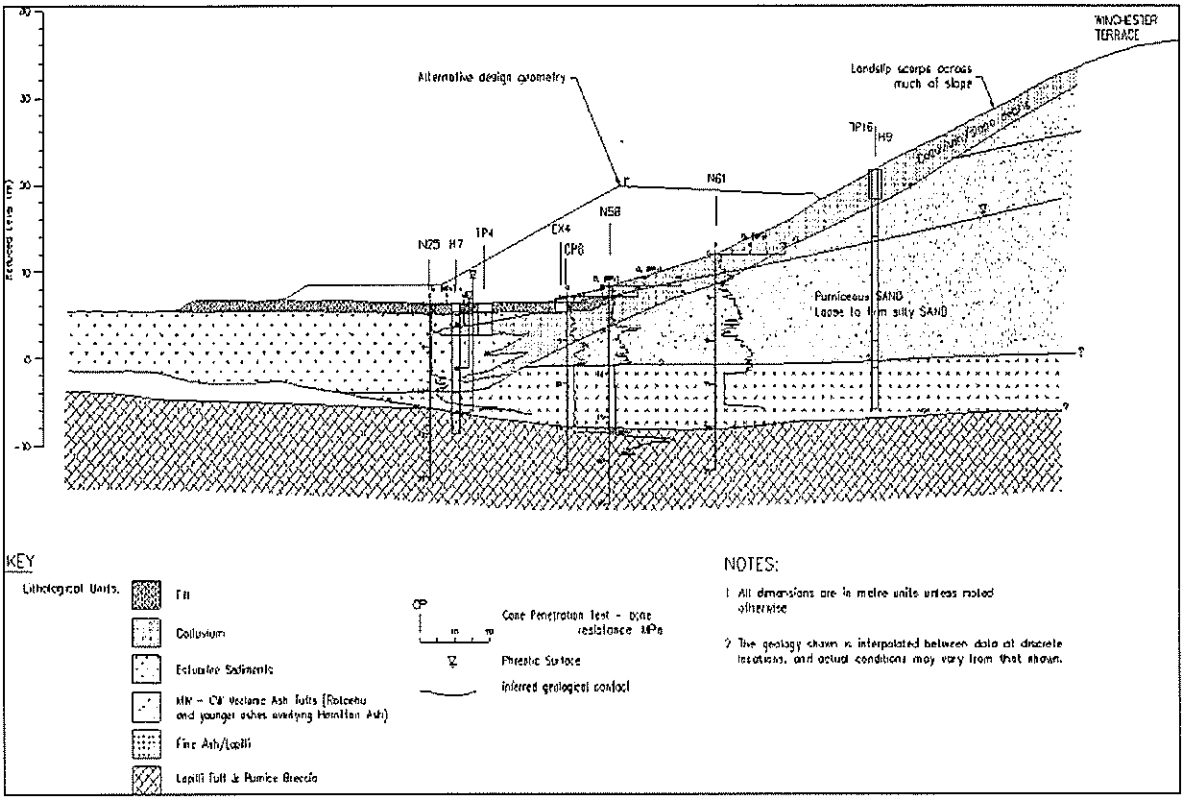

Figure 2(a) : Geological Cross Section, approx. Ch 2300 m

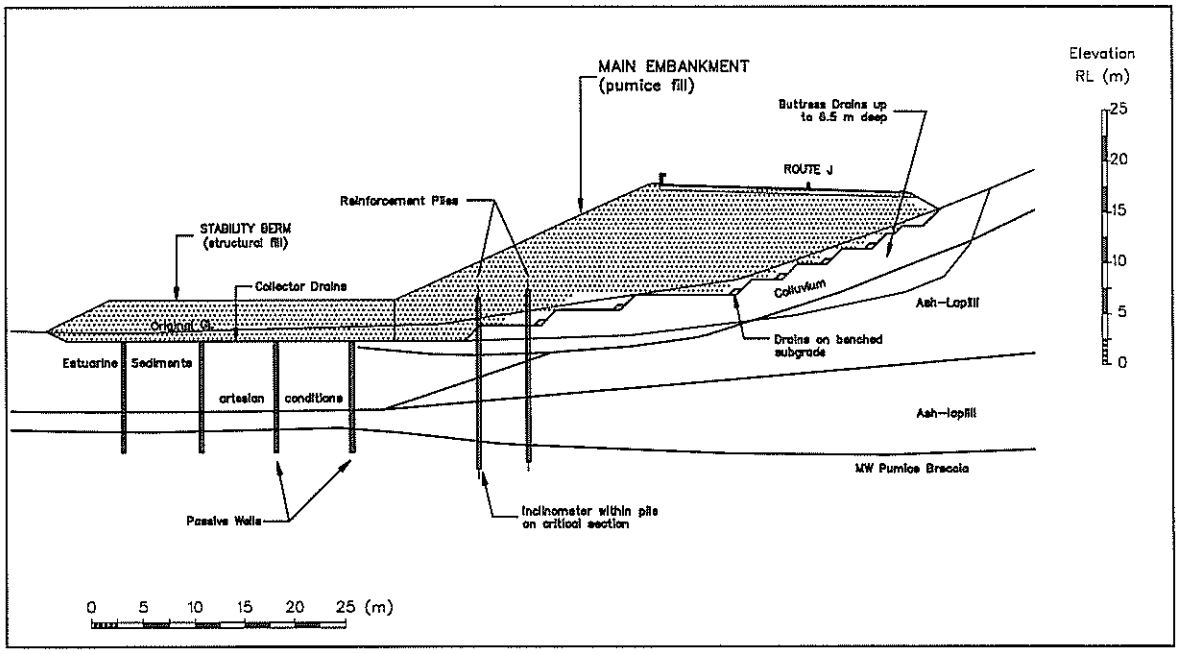

Figure 2(b) : Embankment Design Section, approx. Sta 2300 m

The upper layers comprise highly weathered fine grained volcanic ash layers, some of which may correlate to the Pahoia Tephra. These soils are generally stiff to very stiff, light brownish white clayey silt to clay. Measured water contents were typically in the range 45 – 100%, with a maximum of 143%. The material is typically very to extremely sensitive, deteriorating rapidly upon disturbance by excavation and/or trafficking to an extremely soft (<10 kPa) mud.

Estuarine Sediments
The estuarine sediments typically comprise very soft saturated grey clayey silt with some sandy silt beds containing shell fragments (up to 40mm size). Laboratory testing showed it to be normally consolidated, consistent with its young age (<10,000 years old).

Landslide Debris (Colluvium)
The lower slopes of the J2 Fill area contain a complex series of landslide debris lobes which interfinger with the estuarine sediments. The debris is typically a variable mixture of grey to light grey, very loose to soft, saturated silty sand and sandy silts. These materials also contain organic pockets, and wood (logs up to 0.5m thick were recovered in boreholes).

The colluvium is interpreted to be lobes of slope failure debris extending into the swamp/estuary, which were partially reworked with the estuarine sediments.

The main slope face is underlain by approximately 3 to 4m of stiff, cohesive, landslip debris. These materials typically comprise a variable mixture of stiff yellow brown silty clays and clayey silts with some local sandy zones. The colluvium appears to have been generally deposited in moderately thin to moderately thick (200 to 600mm) layers. It includes landslip debris from two large, mobile, landslips which occurred within the upper parts of the J2 Fill area in 1979, following heavy rainfall.

Ash mantle
The "typical" surficial ash sequence of Hamilton Ash, 60,000 yr BP Rotoehu Ash and post-Rotoehu ashes which mantles much of the topography in Tauranga is generally only present within the elevated areas of the Route J alignment. In the main part of the J2 Fill area, the ash sequence has generally been removed by past landslippage.

GROUNDWATER

Initial groundwater monitoring indicated a general groundwater table rising from the floor of the valley at approximately 1V:20H within the upper part of the valley, increasing to 1V:11H within the slope directly adjacent to the main fill zone (Stn. 2250 to 2380). The presence of thin (<50mm) clay layers within the thinly bedded ash-lapilli unit and instances of small seepage areas on the main slope indicated the presence of perched groundwater flows.

Additional site investigations showed artesian groundwater pressures within the foundation of the main embankment (that is, estuarine deposits, colluvium, and basal ignimbrite). For example, borehole H7 at the toe of the main slope showed a piezometric level +2m above ground level within the estuarine sediments, increasing to +4m above ground level within the underlying ignimbrite.

DESIGN APPROACH

The most significant risk to the embankment was shear failure through the estuarine sediments and colluvium in the valley floor, as shown on the typical cross section in Figure 2. Considerable effort was therefore spent in characterising strength, stiffness and extent of the soils. A summary of the undrained shear strength results is given in Figure 3, with information coming from:

- CPT tests carried out in the area of the proposed stability buttress. These indicated very low cone resistance (typically $q_c < 0.9$ MPa) and high strength friction ratio's, consistent with the very sensitive nature of the soils;

- Results from Geonor vane testing also indicated low strengths (Su <40 kPa) and high sensitivity (typically >20), although the peak strengths were somewhat higher than those based on the CPT results, averaging just over 30 kPa;

- During preparatory earthworks, there was a failure of the large silt pond within the Valley of Te Auetu. The mechanism of failure was clearly deep-seated rotational movement (Figure 4), a mechanism similar to one of the potential modes of failure being considered at the time for the main fill embankment. Back-analysis of the failure indicated the sediments had an undrained shear strength of 14 kPa. This was considered to be slightly conservative given some of the modelling assumptions.

Triaxial testing (CUP) carried out on samples of the estuarine deposits by Uniservices Ltd indicated a drained friction angle of 25° with no apparent cohesion.

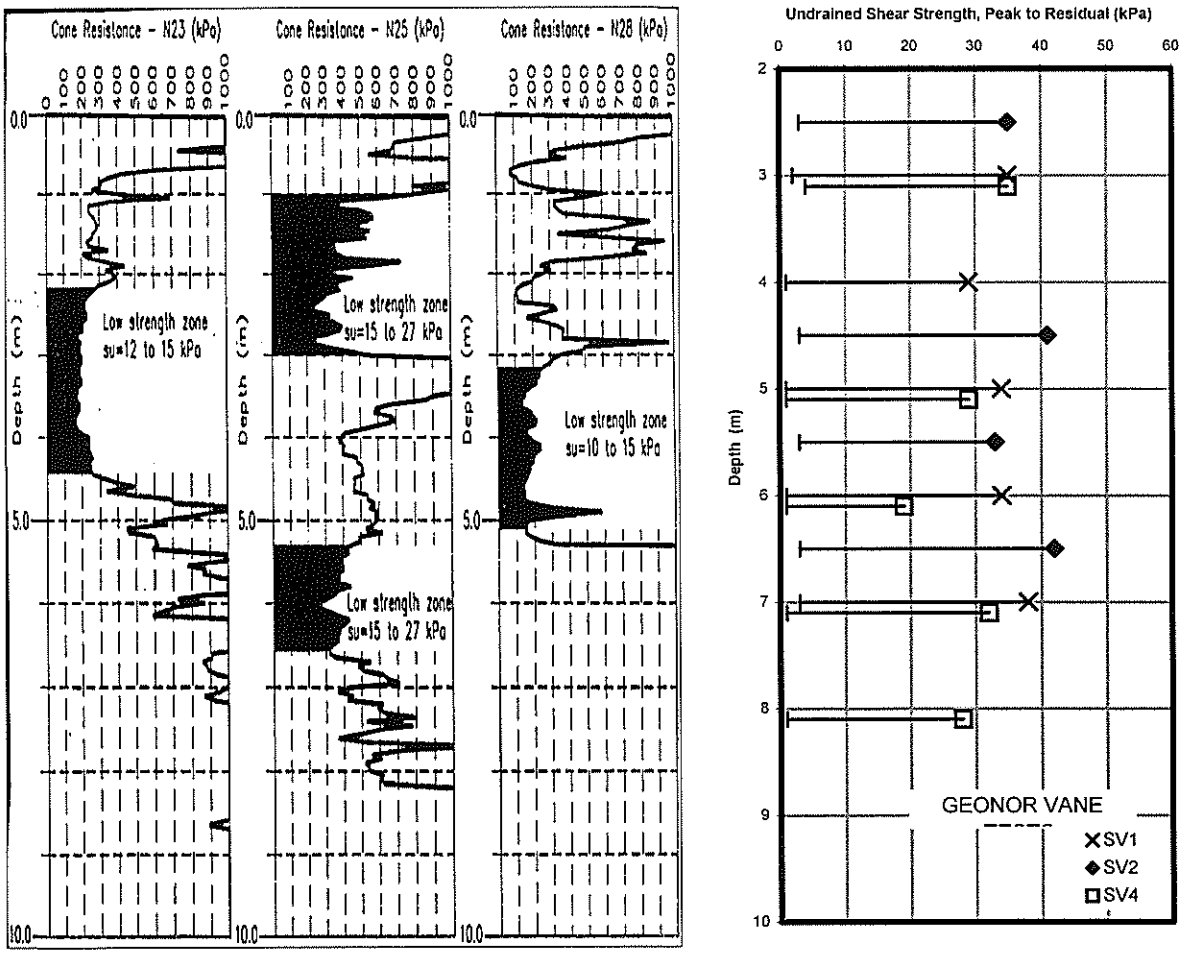

Figure 3 : Estimation of Undrained Shear Strength

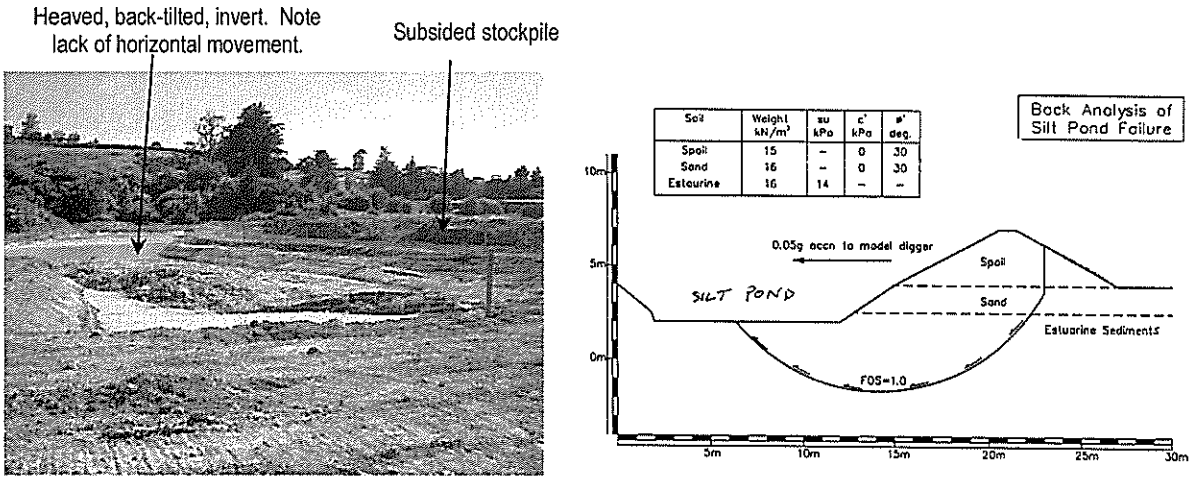

Figure 4 : Silt Pond Failure, Valley of Te Auetu

The parameters for other materials used for design of the embankment were determined from the recent site investigation results, previous design work by Opus International Consultants, historical data on similar materials, and full scale field trial embankments within the Interchange (another alternative design area of PJK). Extensive analyses were carried out to investigate the sensitivity to critical material parameters. Inferred values for key units are given in Table 1.

It was evident that the presence of very low strength estuarine deposits near the toe of the proposed embankment posed a significant risk for deep-seated shear failure. The design solution adopted was a combination of a large stability berm, shear key piles, and lightweight pumice filling.

Material	**Unit Weight (kN/m^3)**	**Su (kPa)**	**Cohesion (kPa)**	**Friction (°)**	**E (MPa)**	**ν**
Structural embankment fill	13 – 19	60	2	30	15	0.3
Stability berm	16	60	2	30	15	0.3
Estuarine deposits	17	14	0 - 2	25	1	0.3
Colluvium	16	50	2 - 5	30	5	0.3
Tephra	16	50 – 70	0 - 5	30	5	0.3

Table 1. Inferred Material Properties for Embankment Design

ANALYSIS

Analysis was largely undertaken as limit equilibrium stability analysis using SLOPE/W software. Some finite difference analysis was also undertaken using FLAC to consider deformation and strain softening characteristics. A Mohr-Coulomb (MC) model was adopted for the embankment, stability berm, colluvium and weathered ignimbrite, while a strain softening (SS) model was adopted for the estuarine deposits and tephra, with properties estimated on the basis of sensitivity and strain levels.

Seismic displacements were calculated using Makdisi & Seed (1979), with predicted displacements varying from 40 mm for the 150 year AEP event, up to 400 mm for the 1,000 year AEP event (0.26g and 0.48g respectively).

Settlement of the main embankment by up to 400mm was predicted using CPT correlation techniques similar to those used elsewhere on PJK and at other projects (Pender et al 2002, Pender et al 1999) and by FLAC analysis. The amount of settlement occurring during construction was assessed semi-qualitatively and then verified by settlement monitoring (actual range was 25% to >60%, depending on the construction programme). Allowance had been made in the design for the possibility of the stability berm settling over a longer time period.

SHEAR PILE REINFORCEMENT

The structural action of the piles is a complex relationship between pile stiffness and soil stiffness/strength. The problem was solved by considering it as two separate piles, one above and one below the failure surface, then solving each pile using finite difference methods (computer program EP6A), with a horizontal shear load applied equal to the required reinforcement loading. Rotation and moment compatibility at the head of the 'two' piles was achieved by varying the pile head restraint, thus providing a full deflection, bending moment and shear force profile for the pile. The variable shear force requirement could then be achieved by varying the pile spacing. P-y curves were calculated for the soils using the method developed by Reese and Matlock (1956).

The pile reinforcement capacity required to achieve a FOS of at least 1.5 for embankment stability was calculated. An economic analysis of steel and concrete piles at variable spacing indicated that 310-UC piles in one or two rows and variable spacing. were the best approach.

SUBSOIL DRAINAGE MEASURES

Monitoring of piezometric levels in the initial stages of the PJK Project showed artesian pore pressures within the estuarine sediments. This was interpreted to be the result of upward groundwater flow from the Cambridge Road ridge towards the valley area.

Calculations showed that adequate stability could not be achieved with the artesian pressures. A series of pressure relief wells were therefore installed within the toe zone (Figure 2) to achieve hydrostatic piezometric levels consistent with a groundwater table at swamp level. The wells consisted of bored shafts through the sediments, backfilled with a two-stage, filter compatible, drainage system. Filter compatibility with the surrounding ground was checked. Lateral collector drains (with some redundancy) were included.

Buttress drains up to 6.5m deep were constructed at 20m centres throughout the length of the fill. These were cut as deep as possible to maximise the interception of perched seepage horizons. Instability tended to occur when the trench encountered either saturated landslip debris or the top of the bedded tephra unit, which had sub-horizontal layers of particularly low strength silt. Backfill drainage material was selected to provide filter compatibility with the in-situ soil, removing the need for filter fabric, leading to simplified construction and cost savings.

Collector drains were included within the toe buttress to provide some redundancy of drainage outlet, and to avoid excavation through the urupa (burial ground) in the base of the valley. The collector drains were constructed in a similar manner to the buttress drains, with filter-compatible drainage material and a 100 mm dia slotted MDPE collector pipe.

Bench drains were included at the back of each bench cut into the in-situ ground. The drains consisted of a 0.5x0.5m gravel drain wrapped in filter fabric with a slotted MDPE pipe. The bench collector drains were 0.5m wide and of variable depth, and typically at 20m centres.

DISCUSSION

Other design changes to those described above included:

- Lowering of the vertical alignment of the main alignment (by optimisation of the geometrics);
- stormwater flowpaths were relocated away from the toe of the structural fill to allow the stability berm to be widened;
- the footprint of the stability berm at the toe of the critical embankment section was undercut by 0.75 m and backfilled with engineered fill.

At least three significant design iterations were undertaken during the construction phase of the embankment, to allow for adverse weather at critical times, as well as for refinement of the design of reinforcement piles and the pumice filling.

Construction monitoring included:

- Inclinometers, including one installed within a shear pile at the critical embankment section;
- Standpipe peizometers;
- Pneumatic peizometers;
- Settlement cells;
- Surface survey, including precise measurement of lateral displacements.

The measured deformations and piezometric levels remained within design tolerances, including lateral deformation of the shear key piles (Figure 5).

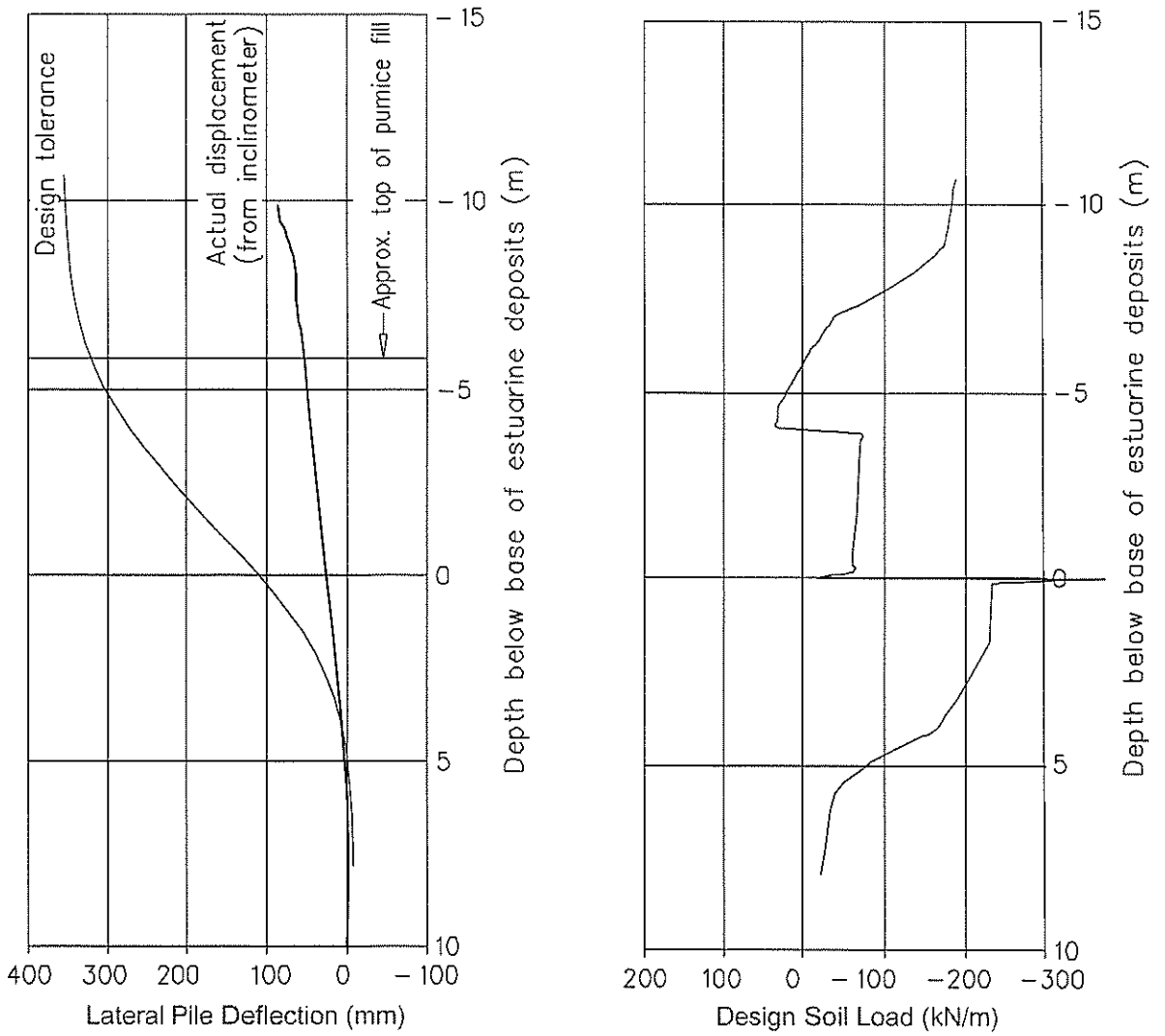

Figure 5. Pile Deflection Monitoring

CONCLUSIONS

The J2 Fill at the PJK Expressways Project in Tauranga involved construction of a 14 m high sidling embankment on a complex foundation of intercalated volcanic and sedimentary deposits.

Developed within the tight construction programme timeframe, the alternative design solution included reinforcement piles, lightweight filling, substantial underdrainage, a stability berm and revised geometrics. The unusual nature of the volcanic ash soils required special design provisions, with allowance made for low strengths, very high sensitivity, and the potential for internal erosion. Observational techniques were successfully used during construction to confirm design assumptions and to optimise the overall embankment design.

ACKNOWLEDGEMENTS

The permission of the project owners, Transit New Zealand and Tauranga District Council, and the Contractor, the Fulton Hogan Ltd – Smithbridge (NZ) Ltd Joint Venture, to use the monitoring data is gratefully acknowledged. The inputs of staff from the JV, subcontractors and T&T were vital to a successful outcome. Robin Dawson of T&T undertook the finite difference modelling. The inputs of the peer reviewer for the alternative design areas of the PJK Project, Professor M Pender, were much appreciated.

REFERENCES

Briggs RM, Hall GJ, Harmsworth GR, Hollis AG, Houghton BF, Hughes GR, Morgan MD, Whitbread-Edwards AR, 1996: Geology of the Tauranga Area, Sheet U14, 1:50,000. *Occasional Report No 22, Department of Earth Sciences, University of Waikato, NZ.*

FLAC . (1996) Fast Lagrangian Analysis of Continua. Users Manual.

Geosolve Ltd, 2000. SLOPE/W software.

Makdisi F, and Seed HB, 1979. Simplified Procedure for Evaluating Embankment Response. *Jnl Geotech. Div. ASCE 105 GT5 pp1427 – 1434.*

Reese, LC and Matlock H, 1956. Non-dimensional solutions for laterally-loaded piles with soil modulus assumed proportional to depth. *Proc. 8th Texas Conf. on Soil Mechanics and Foundation Eng, Austin, Texas.*

Pender, MJ, Jennings, DN and Crawford, SA, 1999. Relation between Settlement & Cone Penetration Resistance at Two Sites, *Proc. 5th International Symposium on Field Measurements in Geomechanics* – FMGM99, Singapore, Balkema, 601-608.

Pender, MJ, Ni, B and Cowbourne, AJ, 2002. Correlation Between Soil Stiffness and Cone Penetration Resistance at an Embankment Site. *Proceedings of the 3rd International Symposium on Lowland Technology*, Japan.

Tonkin & Taylor Ltd, 2000a. PJK Expressways Project, Tauranga - J2 Fill (Winchester Terrace) - Design Report. *Unpublished report prepared for the Fulton Hogan Ltd– McConnell Smith Ltd Joint Venture, March 2000, ref 17128.*

Tonkin & Taylor Ltd, 2000b. PJK Expressways Project, Tauranga - J2 Fill (Winchester Terrace) - Design Report Addendum. *Unpublished report prepared for the Fulton Hogan Ltd – McConnell Smith Ltd Joint Venture, Aug 2000, ref 17128.*

Piezometric Response in a Semi-Confined Aquifer to Pile Construction

C Y Chin
PhD, C Eng, Eur Ing, MICE
Senior Geotechnical Engineer, Beca Carter Hollings & Ferner Ltd
T McGuigan
BE (Hons), BA, GIPENZ
Geotechnical Engineer, Beca Carter Hollings & Ferner Ltd
D V Toan
BE (Hons), PhD, FIPENZ, MACENZ
Technical Director of Geotechnical Engineering, Beca Carter Hollings & Ferner Ltd

Abstract: The recent construction of the Britomart underground train station in Auckland has provided an opportunity to observe piezometric responses in soil due to piling and deep excavation construction. This paper presents piezometric monitoring data tracking the response of a semi-confined aquifer within the East Coast Bays Formation of the Waitemata Group rock to pile construction activities.

The data demonstrates that piezometric responses due to water extraction within the East Coast Bays Formation is not necessarily characteristic of responses expected of a semi-confined aquifer. From these observations, it is likely that other geological features such as jointing systems need to be considered when assessing piezometric responses.

INTRODUCTION

The Britomart Station project, situated on Auckland City's waterfront is a transport, urban renewal and heritage project for Auckland City. Valued at approximately $204 million, the major elements of the project are to develop a new 12m deep underground railway terminal, and bus interchange and to link Auckland's transport system as one.

As part of the Resource Consent conditions for this project, groundwater monitoring and measurements of lateral movement around the site were carried out. This paper describes groundwater drawdown effects as a result of pile construction activities at Britomart Station.

SITE LOCATION

The site is located in Auckland City bounded by Tyler Street on the north, Galway Street on the south, Britomart Place on the east and the previous Chief Post Office (CPO) on the west (Figure 1). Structures previously at this site, subsequently demolished in 2001, included the Britomart Bus Terminal and the Britomart Carpark building.

GEOLOGY

The Waitemata Harbour is a drowned river valley system (Searle, 1981). During periods of glaciation, the landform was eroded creating valleys in the semi-confined aquifer (Kruseman & de Ridder, 1994) of the East Coast Bays Formation (ECBF) rock comprising alternating layers of sandstone and siltstone. As sea levels rose the valleys were submerged and in-filled with alluvial and estuarine deposits of the Tauranga Group.

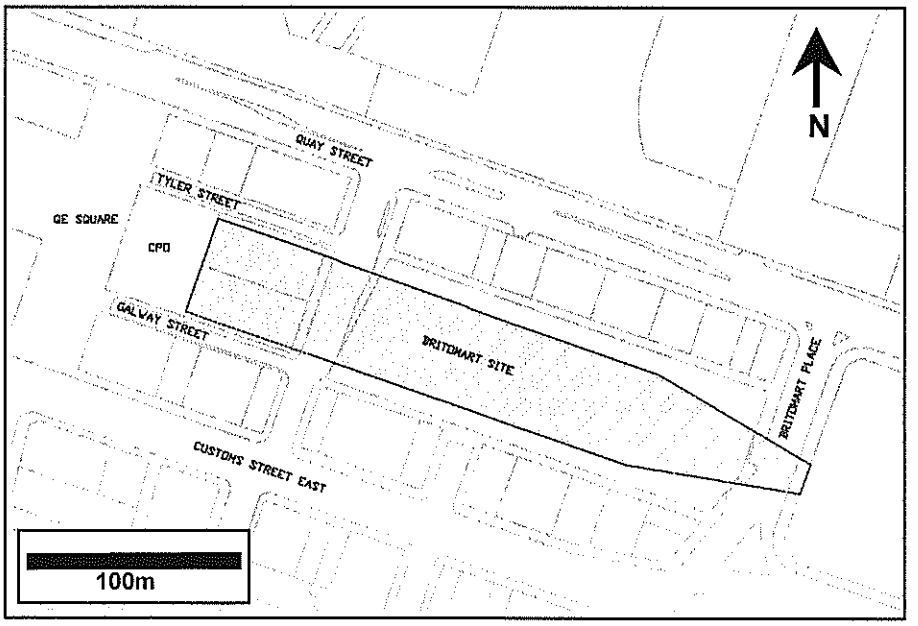

Figure 1. Site Location

The site is located on a series of harbour reclamations, which date back to the early 1900's. Reclamation fill at the site was variable comprising locally sourced and imported fill materials, dredged materials and hydraulic fill. A geological cross-section along the length of the site is shown in Figure 2.

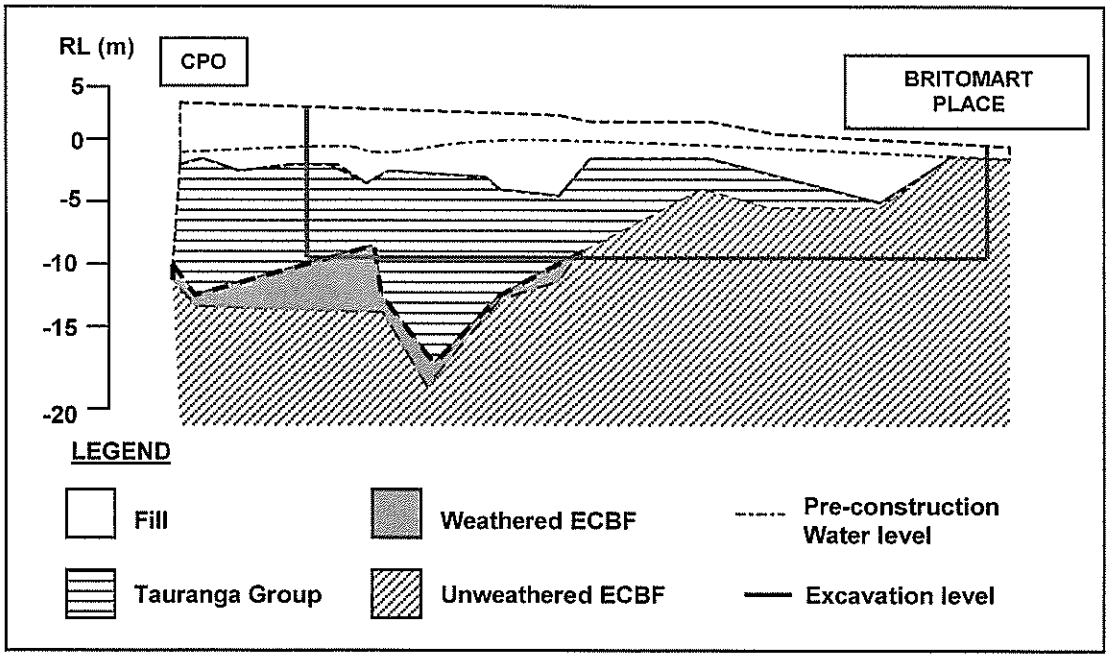

Figure 2. Site Geology

DESCRIPTION OF THE PROJECT

The construction of the Britomart station involved a 12m deep excavation over an area approximately 300m long by 45m wide. The basement excavation was retained by 880mm and 1200mm diameter secant pile walls over the western 130m of the site where founding ECBF rock levels were deeper, and with temporary sheet piles on the eastern end of the site with shallower ECBF rock levels.

The total perimeter length of the secant pile wall was 310m and that of the sheet pile wall was 340m. Stability and serviceability requirements resulted in the secant pile wall being bored a minimum of 4m into competent rock with single level props at ground level comprising transverse beams spanning the width of the station. Lengths of secant piles ranged from 17m to 24m Sheet pile walls were temporary works, constructed with multiple anchors and driven a minimum of 1m into the ECBF rock.

INSTRUMENTATION

Resource Consent conditions for the construction of the station require that groundwater monitoring and movement of ground & buildings around the site be closely monitored. In total 39 piezometers were installed at 13 locations around the site, shown in Figure 3. Each location had 3 piezometers to measure groundwater levels in defined stratigraphic layers, these being: - Fill, Tauranga Group and ECBF rock (referred to as Units 1, 2 and 3 respectively). In addition to daily monitoring of groundwater levels, six automatic piezometric transducers recording at 15-minute intervals were installed in Unit 3 at 6 of the 13 borehole locations.

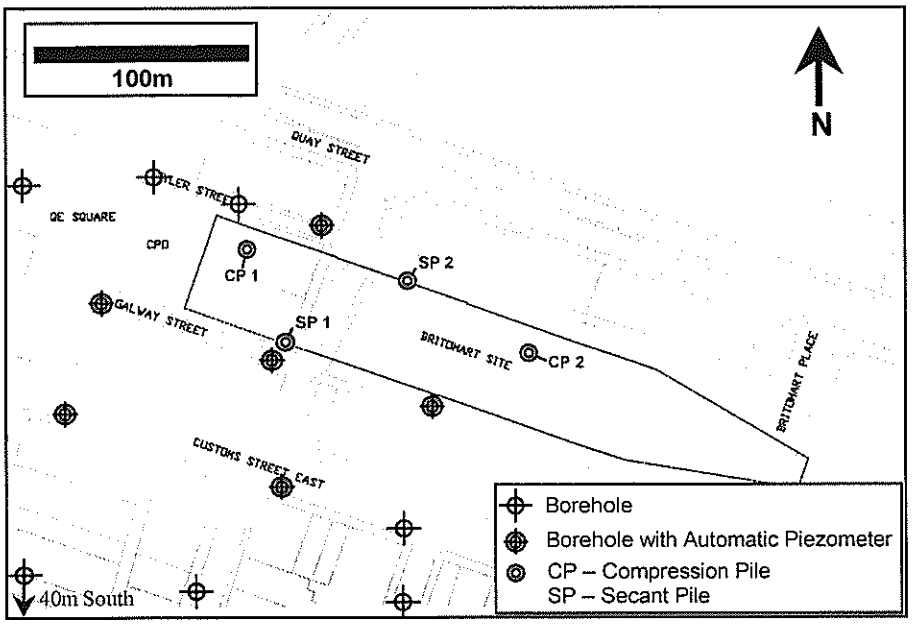

Figure 3. Borehole Locations

Maximum groundwater drawdown limits and trigger levels (set at 75% of maximum groundwater drawdown limits) were established in the Resource Consent for piezometric levels in Unit 3. Groundwater monitoring and the detection of trends in drawdown of groundwater levels provided an early warning to potential ground and building settlement. In addition to groundwater monitoring, settlement monitoring of pavement and building surveys were also undertaken at regular intervals.

PILE CONSTRUCTION

There were four types of piles constructed for the station. These are secant bored piles and sheet piles acting as both temporary and permanent retaining walls for the excavation, and bored compression & tension piles to the main station structure acting as founding and holding down piles respectively. As opportunities to record piezometric responses relating uniquely to either secant or compression bored piles were present, these construction details are described below.

Secant piles were either 880mm or 1200mm in diameter and were constructed on the western 130m of the site. Figure 4 shows a schematic of the secant pile construction sequence with one pile

typically constructed in 4 hours. Water extraction was typically restricted to water that would be mixed with the soil removed.

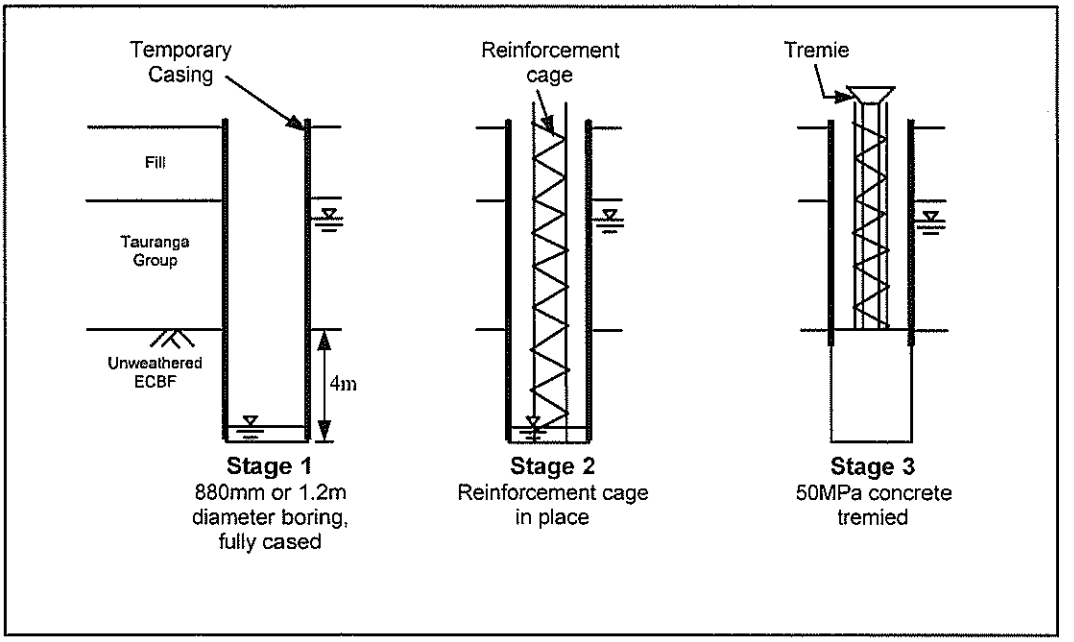

Figure 4. Schematic Secant Pile Construction

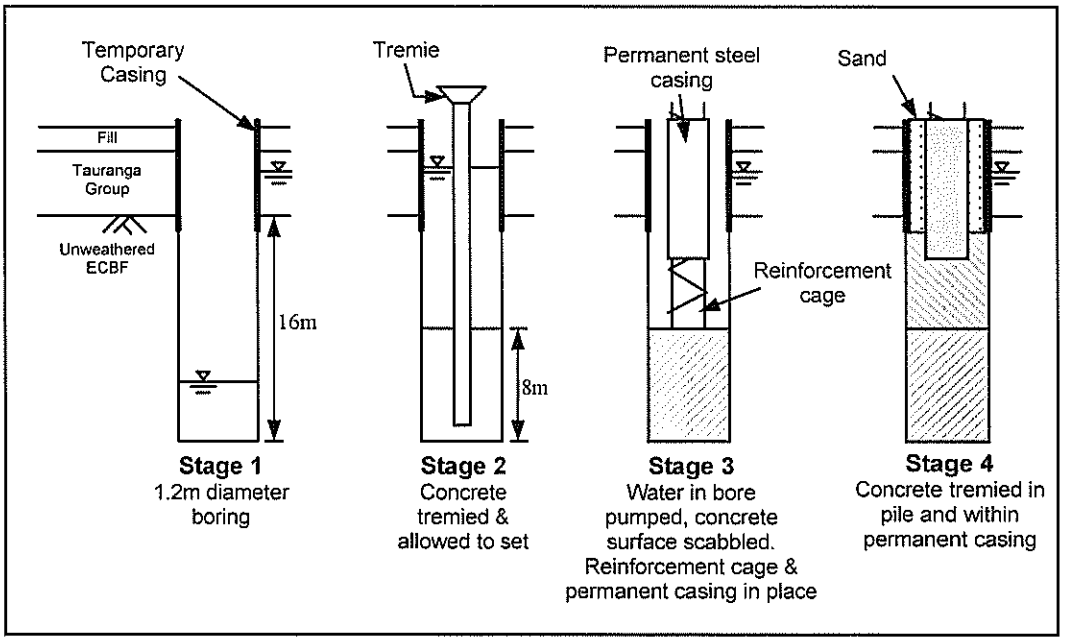

Figure 5. Schematic Compression Pile Construction

Figure 5 shows a schematic of a compression pile construction. These piles were bored 16m into the unweathered ECBF rock and typically took 4 days to construct and did involve full dewatering for short periods. In total, 32 compression piles were constructed.

Stage 3 of the construction required dewatering in order for the concrete laitance to be scabbled prior to the placement of reinforcement and a permanent steel casing. Concrete was subsequently tremied within the permanent steel casing while sand was used to fill the annulus between the temporary and permanent steel casing. This sand would be removed during excavation revealing the permanent steel casing, which formed columns within the station.

PIEZOMETRIC RESPONSES

Figure 3 shows the locations of compression piles CP1, CP2 and of secant piles SP1 & SP2. Piezometric records relating to the construction of piles CP1 and CP2 were selected as no other construction activity took place during their construction. Secant piles SP1 and SP2 were constructed simultaneously, during which there were no other construction activity.

Piezometric responses from automatic piezometers at 6 borehole locations are presented. These have been plotted as a function of the radial distance from the pile concerned to the piezometer.

Compression pile

Figure 6 shows the piezometric response for compression pile CP1. The start, duration and volumes of water pumping from the pile bore are indicated. It can be observed that piezometric drawdown coincides with water pumping and increased drawdowns at closer radial distances to the pile bore occurred, as can be expected for a semi-confined aquifer (eg., Walton, 1962).

Further east of the site during the construction of compression pile CP2, the piezometric response as shown in Figure 7 was very different.

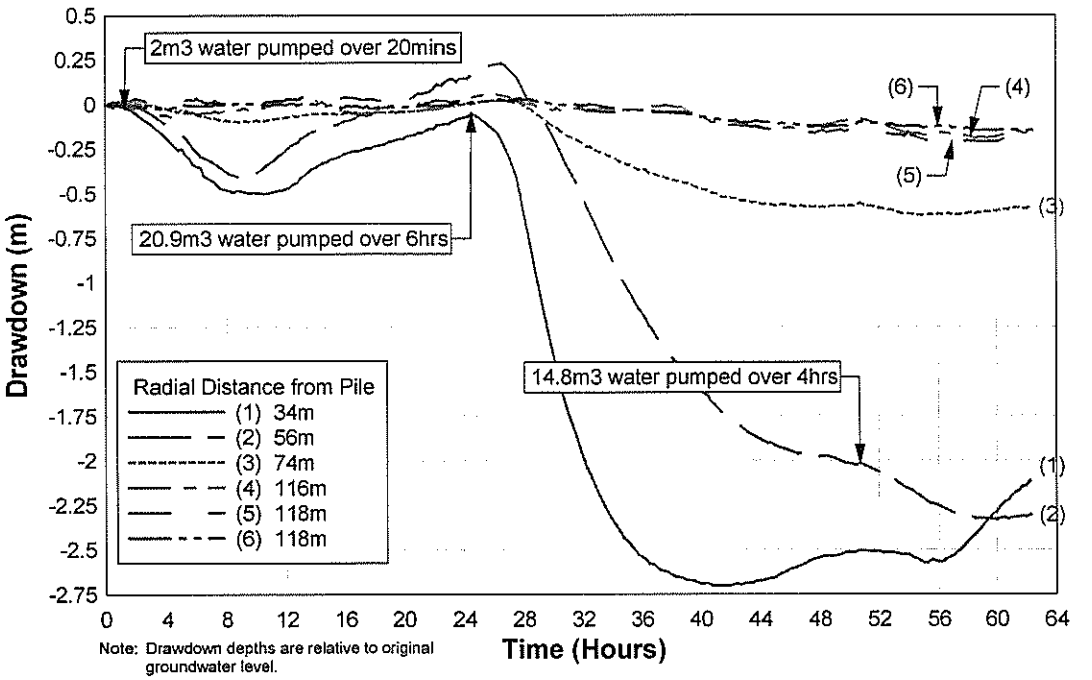

Figure 6. Piezometric Drawdown – Compression Pile CP1

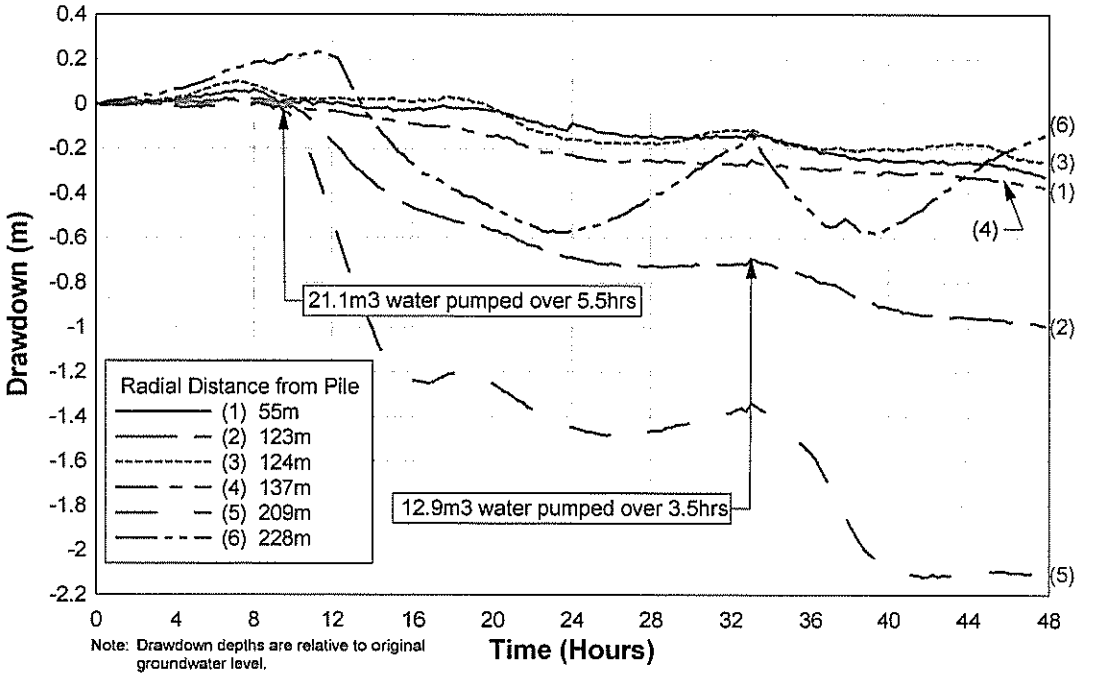

Figure 7. Piezometric Drawdown – Compression Pile CP2

As a result of pumping 21.1m^3 of water over 5.5 hours from pile bore CP2, 3 piezometers located radially further away from the bore than the nearest piezometer recorded greater drawdowns. Piezometers located 209m, 123m and 228m away from the pile bore recorded, in order of decreasing drawdown extents, drawdown responses in excess of the closest piezometer located 55m away from the bore.

These piezometric responses differ greatly from compression pile CP1 and are of interest.

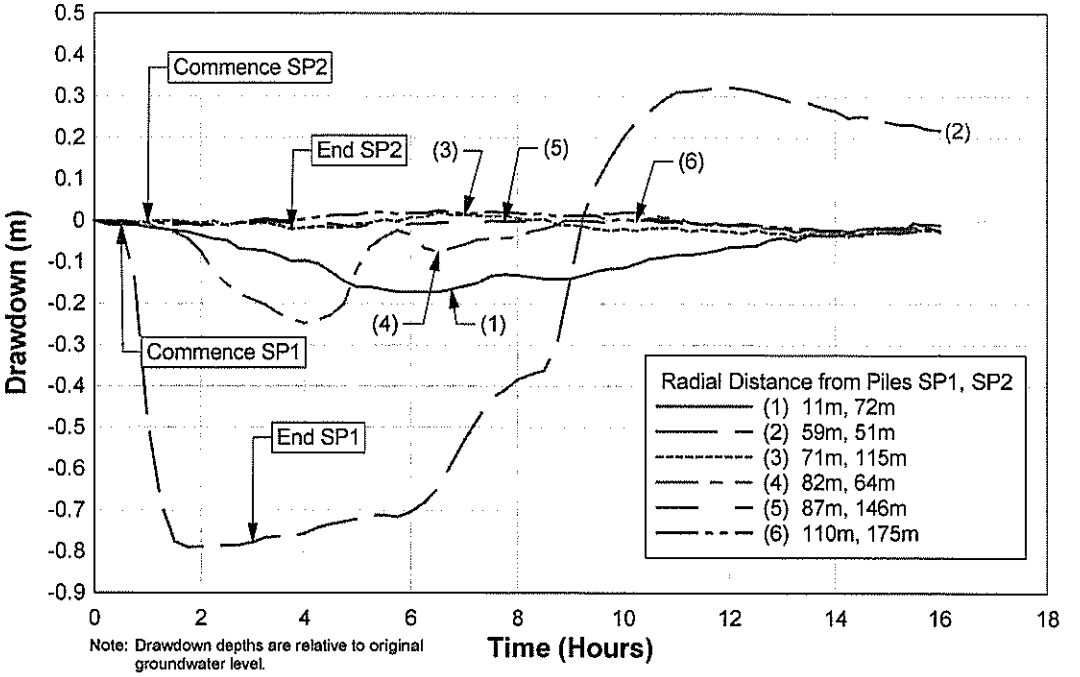

Figure 8. Piezometric Drawdown – Secant Piles SP1 and SP2

Secant piles

Figure 8 shows piezometric responses due to the construction of 2 secant piles – SP1 and SP2 on opposite sides of the site (Figure 3). Commencement and end times indicated in the figure refer to periods of pile boring. Water extraction occurred during boring, where both soil and water were removed simultaneously, and not as a result of direct water pumping.

It was observed here that when secant pile SP1 was being bored, prior to commencement of SP2, a piezometer located 59m away from SP1 reacted sharply as compared to a closer piezometer located 11m away from SP1 which had almost no response.

OBSERVATIONS

Clues that explained the reasons for observed piezometric responses seen in compression pile CP2 and secant pile SP1 were found during the excavation of the site. Excavation of the ECBF rock on the eastern part of the site revealed two distinct joint sets existing within the Unweathered ECBF rock.

One set of joints was observed to have a NE strike (032° to 050°), steeply dipping (80° to 90°), persistent through bedding, with apertures to 1mm and having spacings of between 300mm to 1m. An orthogonal joint set was also observed having a NW strike (275° to 310°), steeply dipping (80° to 90°) with similar apertures and having spacings of between 400mm to approximately 1m.

Water was observed to be flowing from these joints where these intersected with the interfaces of sandstone and mudstone. It is hypothesised that the presence of these interconnecting joints provides preferential paths that transmit piezometric pressures across the aquifer. This may provide an explanation as to how piezometers located further away from the point of water extraction would show piezometric drawdowns an order of magnitude higher than a piezometer located closer to the point of water extraction.

CONCLUSION

Piezometric monitoring data within the East Coast Bays Formation of the Waitemata Group rock were obtained during pile construction. These data demonstrate that piezometric responses due to water extraction within the East Coast Bays Formation are not necessarily characteristic of responses expected of a semi-confined aquifer.

A hypothesis, based on the observation of joint sets within the East Coast Bays Formation, that interconnected joints provide preferential paths which transmit piezometric pressures across the aquifer has been proposed to explain the piezometric responses observed.

ACKNOWLEDGEMENTS

The permission of Auckland City Council to publish this data is gratefully acknowledged. We also wish to acknowledge work done by Dr Barry O'Connor for his geological observations.

REFERENCES

Kruseman, G.P. and de Ridder, N.A. (1994). *Analysis and Evaluation of Pumping Test Data. 2nd Edition*, International Institute for Land Reclamation and Improvement, The Netherlands.

Searle, E.J. (1981). *City of Volcanoes. A Geology of Auckland.* Longman Paul.

Walton, W.C. (1962). "Selected analytical methods for well and aquifer evaluation." *Illinois State Water Survey Bull.* Vol 49.

The Construction of the Auckland Central Remand Prison on the Mt Eden Basalt Flow

G R W East
BSc, MNZRS, MGS
Geotechnical Principal, Opus International Consultants Ltd
A K George
BSc, MSc (Hons) (Geology), GIPENZ
Engineering Geologist, Opus International Consultants Ltd

Abstract: The central Auckland prison complex in Mt Eden is sited on the northwestern edge of the Mt Eden basalt flow abutting the Symonds Street Waitemata Group ridge. This condition and that of the modifications made to the site over the 140 years of the prison site's existence has resulted in an extremely complex site to construct the new prison. These complexities include a topographically hidden rubble in-filled quarry, and the boundary of the basalt flow and volcanic tuff crossing the site.

The Auckland Central Remand Prison at Mt Eden (ACRP) included the design and construction of a three floor level Accommodation Building and two floor level Administration Building within this complex geological setting. Opus International Consultants Ltd where commissioned to undertake the design and management for this project on behalf of the Department of Corrections. The prison was opened in 2000.

The structural/architectural layout of both buildings suited near surface footings with the preferred type and nominal dimensions finalised by consultation between the structural and geotechnical engineer(s) with respect to the likely performance. This paper reviews the subsurface conditions of the preferred foundations and the assessed performance.

This paper also outlines geotechnical investigations carried out from 1972 to 1998 to uncover geological features, and reviews historic and photogrammetry research that was included in the investigation.

Shown are the assessed outline and depth of the historic in filled quarry that required sub excavation. Also shown are the methods undertaken to numerically satisfy the differential settlement conditions of the wide strip foundations that spanned the insitu basalt, quarry backfill and the ash soils underlining the edge of the site. The result of settlement moduli obtained from triaxial, oedometer and insitu pressuremeter are compared.

INTRODUCTION

Opus International Consultants were commissioned by the Department of Corrections to undertake the geotechnical investigation for the Auckland Central Remand Prison (ACRP) constructed on a 1200m^2 site adjacent to Mt Eden Prison, off Lauder Road in Mt Eden.

The building covers some 5500m^2 and consists of two main buildings joined by an annex between. The eastern Accommodation Block has three stories and a basement, while the smaller western building is one to two stories high with a basement at the southern end including the annex. An access driveway and ramp with retaining wall runs from Lauder Road down between the western wing and the boundary to enter a service yard in the SW corner of the site and provides access to the basement of the annex. Vehicle exit is from the northern side of the annex basement via a driveway ramp up to Lauder Road (see Figure 1).

This paper describes the geological setting that the prison was constructed in and the geotechnical challenges faced to design and construct the building structure.

Figure 1. Auckland Central Remand Prison

BACKGROUND GEOLOGY

The geology of the area consists of underlying Miocene aged Waitemata Group sandstone and siltstone "bedrock", at a depth of some 30m below ground surface. This is overlain by some 4m-6m of Pleistocene alluvium that in turn has been overlain by a variable and largely indeterminate depth of volcanic lithic tuff and ash deposited during an early stage of volcanic activity.

At a later stage some 23,000 years ago Mt Eden began erupting a series of lava flows that spread out variously to cover the tuff/ash and alluvial deposits with thick basaltic lava flows interlain with air fall scoria layers. Initially these flows were relatively thin and extensive. Later flows were laid down on top of earlier flows and were much shorter in length and thicker. These flows built up a massive rubbly basalt "pedestal" at the base of the Mt Eden scoria cone. The northern edge of the basalt was located just to the south of Lauder Road.

The site as it was prior to construction of the ACRP was modified considerably over the previous 140 years with various quarrying and back filling operations. Intact basalt rock was overlain variously by 0.45m-7m of loose uncontrolled relatively clean basaltic rubble fill, which was in turn overlain over much of the site with an upper 2m thick layer of inorganic refuse, clay tiles, bricks, and lenses of silt.

A detailed account of the site history and quarry operations is presented below.

Site History And Quarry Operations

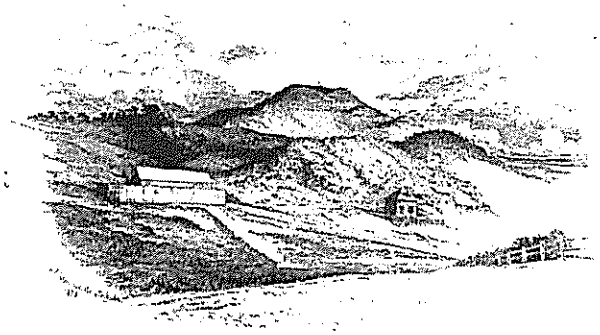

Figure 2. Mt Eden Stockade Mid 19th Century.

The Mt Eden stockade as it was previously known was established at the present prison site in Mt Eden in the middle of the 19th century.

An 1858 sketch of the site shows a rubbly basalt flow extending just to the north of the present Lauder Road but not as far as the railway line at the base of the valley that drains to the northeast of the site (see figure 2).

The top surface of the basalt flow rose moderately steeply to the south (15°-20°?) Reaching about 20m to 25m above the present level of the Auckland Grammar playing fields. The edge of the flow also

sloped eastwards such that the ground level at the present prison site was similar to the present day level. An 1876 photo of the prison taken from the new remand prison site again shows the rubbly nature of the basalt flow. The original ground surface appears to have been in the order of 10m higher than the present ground surface towards the southern part of the remand prison site, tapering down to several metres along the northern boundary with Lauder Road.

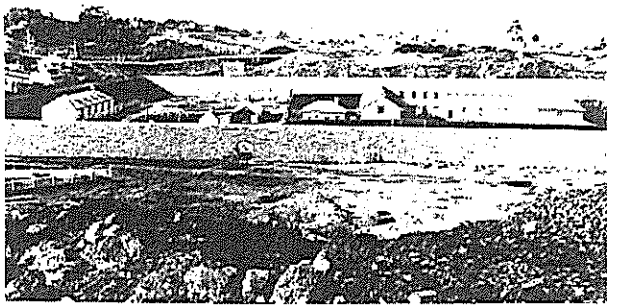

Figure 3. Photo of Mt Eden Prison 1876.

By 1876, the basalt stonewall had been constructed around the Mt Eden prison site, but the stone prison building was not constructed until shortly after this time. The basalt stones were won from a quarry adjacent to the prison, but no records of this early quarry operation could be procured. Some flat land between the western prison wall and the new remand prison site observed in the 1876 photo may be the result of this quarrying, but the 1858 sketch does indicate that most of this low lying area may in fact be the original ground surface.

Quarrying of the rock at and adjacent to the new remand prison site continued throughout the last two decades of the 19th century and into the 20th century. The first photographic evidence found of this activity is the series of NZAM aerial photos taken in 1940, followed by aerial photos flown in 1951, 1958, 1961 and 1972. The photographic evidence has been summarised on the plan below (see figure 4).

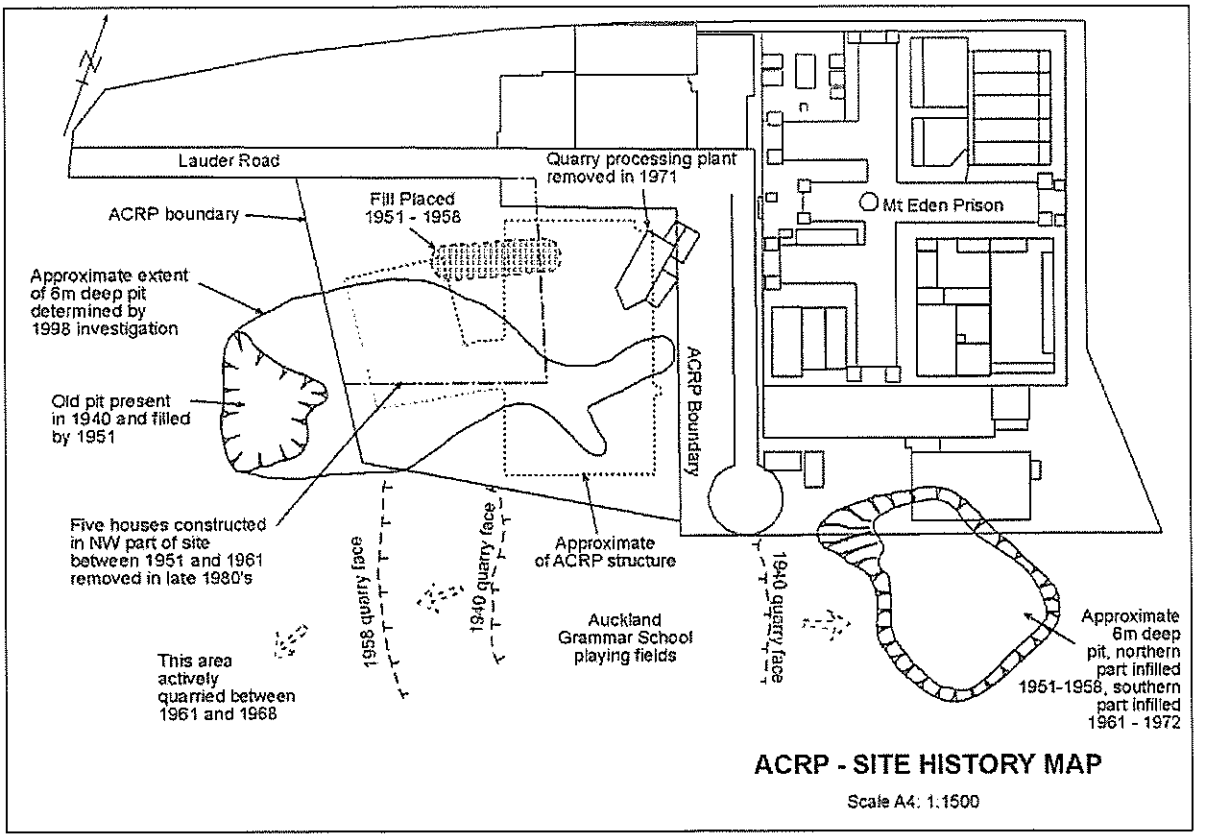

Figure 4. Summary of site history from photographic evidence.

The 1940 photo showed a 6m to 9m deep pit (below existing ground) immediately south of the prison that appeared to be recently quarried. It also showed an approximately 4m to 6m deep pit to the southwest of the remand prison site that was well vegetated and did not appear to have been worked for some time prior to 1940. In addition to this, the photo showed the main 20m high quarry face to the south of the remand prison site. The old pit to the southwest of the site is inferred to be part of a 6m deep in filled pit found during the geotechnical investigation of the remand prison site. The quarry processing plant was located at the northeastern corner of the remand prison site.

By 1951, the small pit to the southwest of the site had been filled in and quarrying continued in the main face to the south. The pit to the south of the prison was unchanged from 1940. The northern half of this pit had been in filled by 1961 with in filling in this area complete by 1972. Quarrying continued at a fast rate to the south-southwest of the remand prison site between 1958 and 1968. This area forms the main part of the lower Auckland Grammar School playing fields. Rock was transported to the processing plant at the northeastern corner of the remand prison site.

Whilst the quarrying activity continued, five houses for prison staff were built on the northwestern part of the site between about 1956 and 1961. A 1.0m to 1.5m high fill slope in this area was formed between 1951 and 1958. The houses were demolished in the late 1980's. Several sheds south of the houses were constructed at about the same time as the houses (1951 and 1958) and these were dismantled when a car park in the south west of the site was constructed in about 1970.

SITE INVESTIGATION

The site investigation for the ACRP utilised two phases of investigation:

1. An investigation between 1971-1972 undertaken for an earlier remand prison never built, which resulted in twenty boreholes drilled.

2. The second much later investigation was undertaken in 1998 for the ACRP, and involved drilling some twenty three boreholes to confirm ground conditions shown in the earlier 1971 boreholes, and to determine the ground conditions in areas where there had been no earlier drilling tests. The second phase of investigation also included seven test pits that were excavated to determine the nature of fill material and to take samples for the purposes of determining bulk earthworks properties.

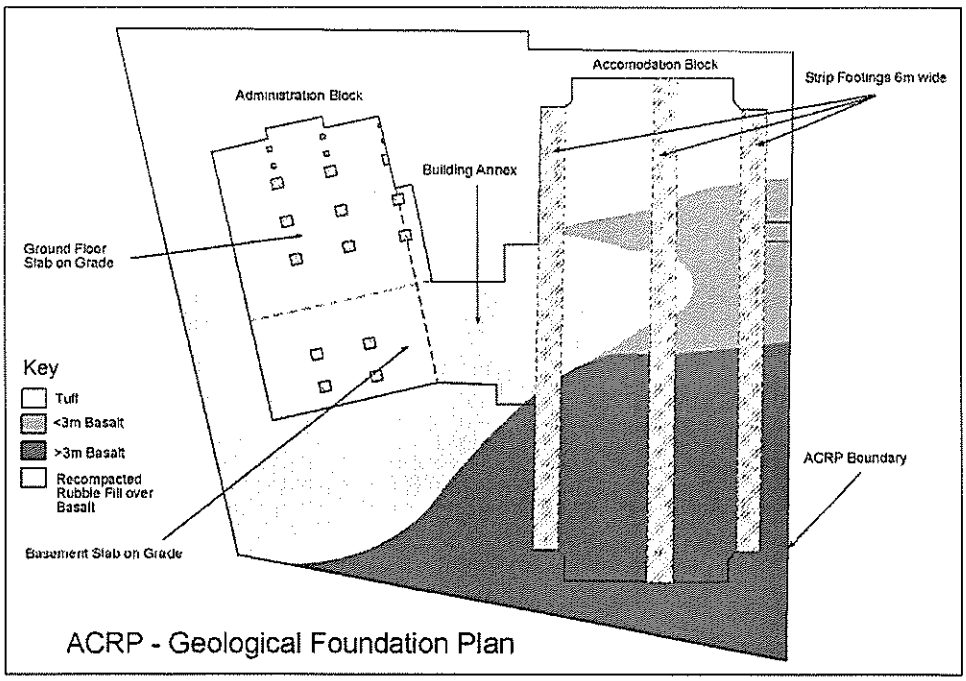

Figure 5. Geological Foundation Plan

The results of these investigations identified that the ACRP would be built across the edge of a basalt flow from Mt Eden with part of the prison requiring founding on volcanic tuff, another part on insitu basalt rock and the remainder on recompacted basalt rubble fill. Figure 5 above and Figure 6 below illustrate the foundation conditions of the ACRP identified in the geotechnical investigation and discussed in further detail for the remainder of this paper.

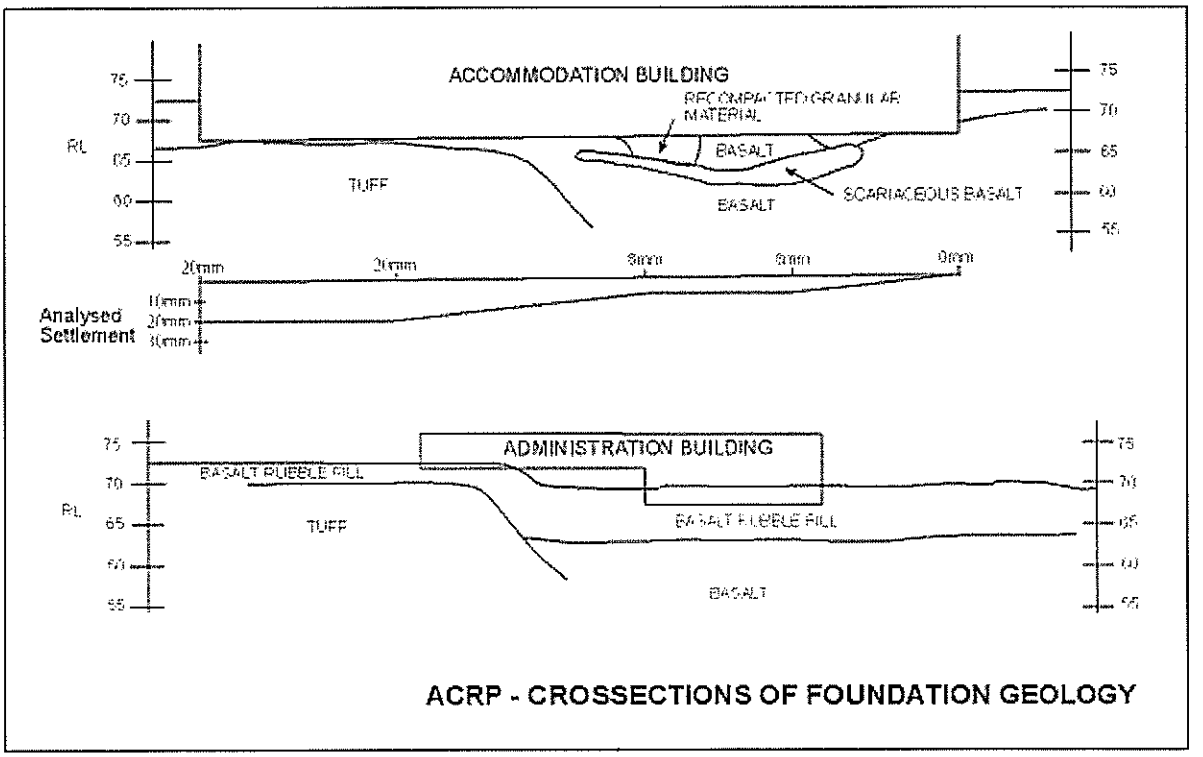

Figure 6. Foundation Crossections.

Figure 7 below, has a photograph showing the boundary of the tuff and basalt beneath the Accommodation Block. It also shows a buried tree uncovered within the tuff that allowed a carbon dating test to accurately determine the age of emplacement of the basalt as 23,480 ± 180 BP for geological interest.

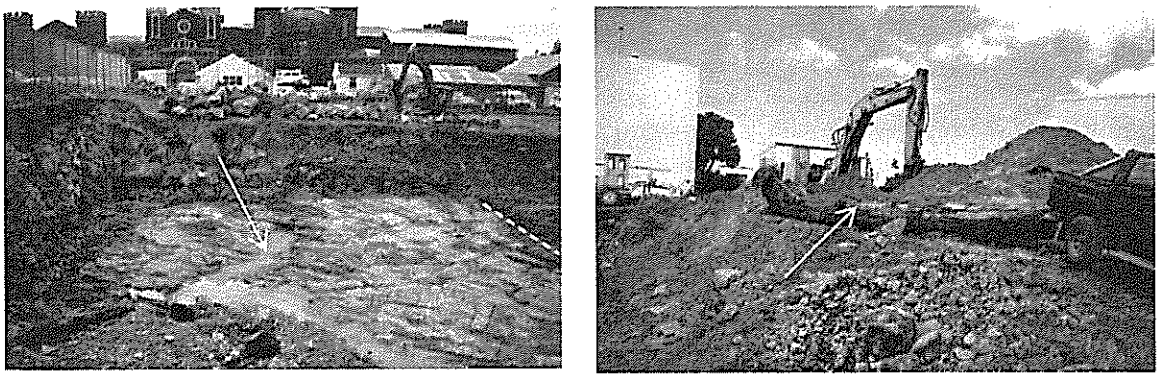

Figure 7. Photograph of the tuff and basalt boundary (dashed line) beneath the Accommodation block. The totara log removed from the tuff (arrow) was carbon dated at 23,480 ± 180 BP.

SITING OF THE BUILDINGS

The ACRP consists of two buildings, Accommodation and Administration, interconnected by an annex that contains a basement vehicle-loading bay. As outlined above the subsurface conditions are complex with both building footprints overlying the edge of the basalt rock flow and the adjoining

volcanic tuff (stiff silty clay) and hence spanning significantly different foundation materials. While the foundation bearing pressure for near surface footings could be compensated for by adequate pad or strip dimension sizing the settlement performance of the two materials is significantly different and differential settlement and angular distortion became the prime design criteria. A third foundation material, that of recompacted basalt fill infilling the remnant quarry also became part of the settlement criteria. The bearing capacity and settlement of the basalt rock under loading will be negligible and the compacted granular fill largely insignificant with adequate engineering. Only the tuff needs to be qualified.

The structural/architectural layout of both buildings required foundation support at 2 levels, near existing surface at RL 72 and a basement level at RL 68. The foundation investigation and assessment indicated that with the appropriate foundation and structural design preparation, near surface type footings could be accommodated at the 2 levels. The alternative option of piling through the tuff and the basalt edge to an adequate pile bearing (Waitemata Group "bedrock" at some 30m depth) was the costly fallback.

Apart from requiring the ULS ultimate bearing capacity not to be exceeded by the design loading a criteria for differential settlement was required. The angular distortion danger limits published by Bjerrum (1963) were considered appropriate and a conservative tolerance value of 1/600 was chosen as the limit for this project.

The ground water level was not detected during the investigations (lower than RL 52) but typically jointed/fractured basalt can have rapid dynamic responses to infiltration. Measurements were undertaken in periods that included one of the wettest winters in Auckland, as it was considered extremely unlikely that the ground water would ever rise to the basement level. Despite this a basement under drainage system was constructed for the buildings largely to alleviate local infiltration and to reduce the requirement for uplift in the floor slab design.

Administration Building

A 2 storey building with overall 30m x 50m footprint which spanned across firm tuff at the front and some 6m of infilled quarry rubble over the basalt quarry floor at the rear. The loose rubble was to be recycled and replaced and compacted as an engineered fill in a controlled manner. In section the rear 30m x 20m portion of the building is founded at basement level, while the remaining 30m x 30m was founded near existing ground level. Under these conditions the front portion of the building was founded largely on tuff and compacted granular fill in the centre. The basement level rear portion of the building was founded on some 2m of compacted granular fill over basalt rock.

The framed building is founded on 19 square foundation supporting columns on a variable grid that ranged from 5 to 13m spacing with a peripheral strip footings. Footing sizes and working foundation pressures varied from 1mx1m and 200kPa on the tuff to 3mx3m and 250kPa on the compacted granular fill.

Plate bearing tests were carried out to confirm the bearing of the recompacted basalt fill to assess the elastic modulus for settlement assessments (Figure 8). The relatively low moduli that resulted from the initial compaction trial using the recycled "dirty" basalt rubble fill (max size ≈ 200mm) was considered unsatisfactory, largely due to the high water content as a result of prolonged rain. The addition of quicklime (3%) to act as a stabiliser and drying agent resulted in satisfactory results although at a very slow placement rate. Ultimately the more reliable clean site excavated and crushed basalt was utilised (clean high strength AP65 basalt from a portable crusher) and the rubble fill was disposed of off site.

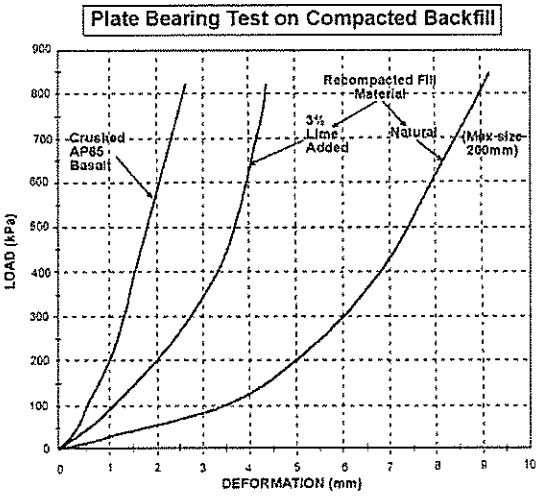

Figure 8. Plate Bearing Tests on Compacted Backfill.

Applying the parameters outlined in Appendix A the design bearing capacity was more than adequate and the differential settlement within tolerance. The high value of the Coefficient of Consolidation (Cv) in the tuff indicated fully drained conditions would prevail immediately on loading and the higher effective stress bearing capacity conditions will prevail immediately. The differential settlement required the use of the "clean" crushed basalt to be confident of attaining the angular distortion requirements.

Accommodation Building

This is a 14 metre high building with an overall 40m x 90m footprint that spans across firm tuff for some 30 metres length at the front and over basalt rock for the remaining 60 metres length commencing as a veneer and finishing at a full 20m thickness at the rear. The lateral interface between the tuff and basalt is considered to be an ill-defined zone of some 10 to 20 metres length. Some engineered granular fill was required over the basalt to infill a part of the old quarry that intruded into the footprint.

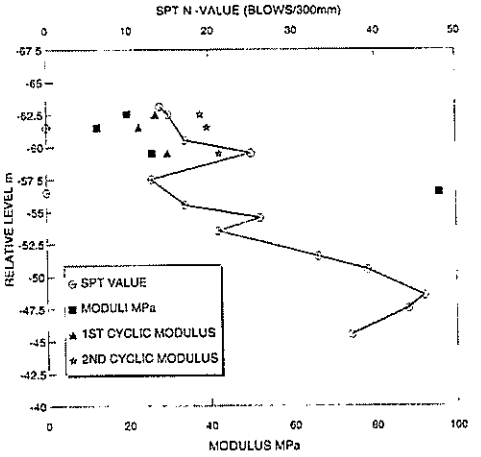

Figure 9. SPT Values and Pressuremeter Moduli.

The building is largely founded at a basement level of RL 68 although the outer edge is founded at the RL 72 higher level. To excavate to basement level at the front of the building a veneer of basalt was removed to expose the tuff. The framed building has loads that are concentrated at the sides and centre length wise, and the foundation system chosen was 3 strip footings of 6 metres width and 90 metres length with a working bearing pressure (under serviceability loading SLS) of some 110kPa. Equivalent strips footings adjoin these strips at the lesser dimension sides.

Applying the parameters outlined in Appendix A the design bearing capacity was more than adequate. A settlement of 20mm was calculated in the tuff but the differential settlement was within tolerance

(Figure 6). The high value of the coefficient of consolidation (Cv) in the tuff indicated fully drained conditions would prevail immediately on loading and the higher effective stress bearing capacity conditions will prevail immediately. The settlement assessment required specific verification in the tuff, including the use of a pressuremeter, as the wide footing generated a deep settlement inducing stress distribution (see figure 9 above). Design comments are given in Appendix B.

This building is sensitive to architectural cracking and although the theoretical differential settlement angular distortion was well within tolerance, there was some risk of more critical conditions existing especially over the ill-defined zone between the tuff and basalt. A structural break was designed in the building near the interface between the tuff and basalt some 25m from the front of the building.

CONSTRUCTION MONITORING

Civil works were begun in mid 1998 by Penrose Contractors to prepare the foundation platform for construction. At the conclusion of the civil works contract late in 1998, construction began with Mainzeal Construction in January 1999 through to completion of the project in May 2000.

To assess the differential distortion between the tuff and basalt in the Accommodation Building, the basement floor slab over the tuff foundation soils within the structural break was periodically surveyed for level. These indicated a gradual increase in settlement with construction but the values were significantly less than that predicted. At the time of abandoning the measurement some 4 months into construction the maximum settlement was only 3mm, some 15% of that predicted. While the structure was not completed at this time with one floor and the roof remaining plus the fit out including air conditioning it is unlikely that the settlement would have reached 30% of that predicted.

SUMMARY AND CONCLUSIONS

- The Auckland Central Remand Prison Accommodation Block was constructed partially on basalt and volcanic tuff erupted from Mt Eden approximately 23,000 years ago.
- Substantial quarrying operations over the previous 140 years had resulted in the removal of considerable basalt lava forming an irregular shaped quarry pit subsequently infilled with basalt rubble and some refuse fill. This material was undercut and recompacted to form the foundation for the Administration Block.
- The ultimate construction of the buildings without any detrimental effects from differential settlement on such a complex modified site was an indication that the foundation design criteria was suitable, and that the workmanship and supervision was more than adequate.
- The settlement in the tuff was significantly less than expected, which is difficult to quantify or qualify. It can be hypothesised that the predicted settlement constitutes a relatively low stain in the stressed soil mass ($\approx$ 0.1-0.2%). This, in conjunction with the low plasticity (PI $\approx$ 13) and high OCR ($\approx$ 10), may have resulted in the stressed soil mass having a significantly greater modulus than those obtained from the high strain testing, in a similar manner to dynamic shear modulus. An equivalent shear modulus (G) strain condition would indicate an increase in modulus by a factor in the order of 3 with a corresponding reduction in settlement (Sun J.I *et al.* 1988).

ACKNOWLEDGMENTS

The authors wish to thank The Department of Corrections for the permission to publish this paper.

REFERENCES

Bjerrum L, (1963). "Discussion on compressibility of soils", *Proc. Europ. Conf. Soil Mech. and Found. Eng.*, Weisebaden, 2 pp 16-17.

Harr M.E. (1966). "Foundations of Theoretical Soil Mechanics", McGraw-Hill, New York

Lee, White and Ingles (1983). "Geotechnical Engineering", Pitman publishing

Sun J. I., Golesorkhi R, Bolton Seed H. (1988). "Dynamic moduli and Damping Ratios for Cohesive Soils", *Earthquake Engineering Research Centre College of Engineering University of California* Report No UCB/EERC-88/15

Worth, C. P. (1975). "In-situ Measurements of Initial Stresses and deformation Characteristics", *Proc ASCE Specialty Conference on In-situ Measurements of Soil Properties*, Vol 2, Raleigh, pp 180-230

APPENDIX A: FOUNDATION DESIGN PARAMETERS

Tuff

SPT N Value Typical RL 72 to 58	Undrained Shear Strength (Triaxial) Cu kPa	Effective Stress Strength (Triaxial) c', ϕ '	Pressuremeter Limit Pressure (kPa)	LL, PL, PI	w%
10 – 17	100	24kPa, 30° 40kPa, 32° 18kPa, 33°	>900	60,47,13	49

Table 1. Bearing

Water Content w%	Preconsolidation (critical) Pressure pc (kPa)	Coeff of Compressibility mv (m2/kN	Coeff of Consolidation Cv (m2/yr)
35-49	700 - 800	0.7+04 to 1.0+04	>30
* Average of 3 tests			

Table 2. Settlement (Oedometer)

Oedometer E' MPa	Undrained Shear Strength (UU Triaxial) E_u MPa	Consolidated Undrained Shear (CU -Triaxial) E_u MPa	Insitu - Pressuremeter (1st Loading) E' MPa	Insitu - Pressuremeter (Cyclic) E' MPa	Seismic Shear Modulus G MPa**
16	13	17	20	27 to 40	700
* Average of 3 tests excluding outliers ** From $G_{max}/p_a = 120N^{0.77}$ -from Worth (1975)					

Table 3. Settlement (Modulus E)*

Compacted Granular Fill (Crushed Basalt AP65)

Ultimate Bearing (Plate Bearing Tests) q_{nf} kPa	Settlement Modulus (Plate Bearing Tests) E' MPa	Effective Stress Strength (Assumed) c', ϕ '	w%
>900kPa	>100	0kPa, 40°	3

Table 4. Compacted Granular Fill Properties.

APPENDIX B: COMMENTS ON METHODS USED FOR FOUNDATION ANALYSES

Bearing Capacity: The bearing capacity of the stiff silty clay tuff has been assessed using insitu pressuremeter testing in addition to conventional laboratory triaxial shear testing on undisturbed samples. Standard penetration testing (SPT) at 1.5m intervals down the boreholes also serves as a strength qualification and more significantly a qualification of the distribution of strength with depth.

The effective stress (c'=25, ϕ' = 30°) laboratory shear testing can be appropriately used in these rapidly consolidating soils to indicate that the geotechnical ultimate bearing capacity exceeds 1000 kPa, similar to that indicated by the pressuremeter testing (Pl > 900 kPa). Based on a conventional reduction factor of 0.5 the Ultimate Limit State (ULS) ultimate bearing capacity exceeds 500kPa, which is well in excess of the design loading. In addition the SPT testing undertaken beyond the shear testing depths indicated that the strength significantly increased beyond these values at a depth of some 10 metres below the footing level.

Settlement: Oedometer testing indicated that stiff silty clay tuff was highly preconsolidated (>800kPa) and rapid draining. Under these conditions the settlements can be analysed using an elastic approach. A conventional rigid foundation on an elastic soils approach has been used for the assessment.

Settlement $s = q B (1- \nu'2) I /E'$

Where
q = Stress on the footing
B = Width of the footing
ν' = Poisson's ratio of soil (Drained)
I_1 = Influence factor (Harr M.E., 1966 and Lee *et al*, 1983)
E' = Young's modulus of Elasticity (Drained).

The drained elastic moduli can be obtained from a number of sources (rebound oedometer, undrained triaxial, and the pressuremeter using the relationship $E'=E_u(1+\nu')/(1+\nu_u)$, $\nu_u = 0.5$, $\nu' \approx 0.3$

Administration Building: Settlement and differential distortion have been based on the recompacted granular material having a plate bearing test modulus of elasticity of 100MPa, which could be considered typical from literature (Lee *et al*, 1983) and value of 20 MPa for the tuff.

Under serviceability working foundation pressures the theoretical settlement under the 3mx3m footings founded on recompacted granular material should not exceed 6mm and that under the 1m x 1m pads, founded on tuff, is expected to be the order of 9mm. The peripheral strip footings, is expected to settle in the order of 3mm.

From these results differential settlements of some 3mm will occur between the compacted granular fill and the tuff with an angular distortion in the order of 1:1000. Such distortion should not be detrimental to the structure especially as it will take place during construction.

Accommodation Building: On assessing all these tests for the Accommodation Building, and giving weight to the insitu pressuremeter testing, a modulus of 20 MPa was chosen for virgin loading and 40 MPa for that part of the loading up to that removed by basement excavation (approx 80 kPa). These values are consistent with typical values shown in relevant literature. Because of the significant increase in strength some 10 metres below the strip footings settlement assessment was confined to above this depth. The spacing of the footing is sufficient not to consider stress overlap.

Using the serviceability working foundation pressures these moduli value resulted in theoretical settlements of the order of 20mm where the tuff soils are loaded. The settlement will occur almost instantly and certainly during construction. The value was considered to be conservative and is unlikely to be exceeded in practice.

From these results differential settlements of some 20mm will occur between the incompressible basalt rock and/or the compacted granular fill (assumed modulus of 100 MPa) and the tuff with an angular distortion in the order of 1:1000. Such distortion should not be detrimental to the structure especially as it will take place during construction.

Filtration and Slit-Film Geotextiles

K C Hudson
BE (Civil), MIPENZ, Regd Engr
Pavements Engineer, Duffill Watts & King Ltd

Abstract: Geotextiles may be divided into types by their method of manufacture. Each type of geotextile performs differently as a filter. Slit-film wovens tend to have a lower permeability, are more prone to clogging and tend to suffer more damage during installation than other types of geotextile. For soil retention ability non-wovens appear to be quite tolerant, whereas wovens are not so tolerant. These differences are difficult to specify against in a general geotextile specification.

For Transit New Zealand specification F/7 it is concluded that in general for filtration there are better geotextiles available than slit-film wovens.

INTRODUCTION

Transit New Zealand specification F/7 is for geotextiles for use in filtration and/or separation applications for state highway earthworks and pavements. Together with its Notes F/7 provides both a generic design tool and a geotextile materials and construction specification.

TNZ F/7 does not allow the use of slit-film woven geotextiles in filtration situations. This paper seeks to background this decision.

By definition geotextiles are a permeable textile material. (Koerner 1986). So permeability is a fundamental property for geotextiles.

Geotextiles can perform one or more functions. These functions may be (Lawson 1994); separation, filtration, reinforcement, drainage (within the plain of the geotextile), surficial erosion control and protection. This paper considers filtration, but recognises that to be a good filter a geotextile must retain its physical integrity.

Filtration may be defined as (Koerner 1986). "The equilibrium fabric-to-soil system which allows for free water flow (but not with soil loss), across the plane of the fabric over an indefinitely long period". Filtration thus requires both adequate permeability to allow the movement of water through the geotextile, and retention of soil particles. Also the soil-to-geotextile compatibility should not clog during the lifetime of the system. (Koerner 1986).

There are many published criteria for geotextile filters. Lawson (1994) makes the point that these are empirical relationships.

Bhatia and Smith (1996) recognise three criteria for the selection of a geotextile as a filter:

- A soil retention requirement to prevent piping,
- A permeability requirement to allow passage of water, and
- A non-clogging requirement.

The ability of a geotextile to fulfil these criteria and function as a filter relates to the largest pore sizes, the pore size distribution and the frequency or number of pores in the geotextile. (Bhatia and Smith 1996). The shape and complexity of the pores may well have an influence also.

EOS and permittivity requirements alone are insufficient to define a good geotextile filter.

The standard approach to evaluating the filtration ability of a geotextile is to measure its EOS and measure its across-plain permeability. This provides clear information on the larger pore sizes but provides only a limited indication of a geotextiles pore size distribution, frequency of pores and shape

of those pores. Hence the usual approach to determining the suitability of geotextile for filtration has limitations.

Geotextiles may be divided by their method of manufacture into woven, non-woven and knitted geotextiles. These types may be further subdivided by the type of fibre from which they are made, Eg wovens may be subdivided into circular monofilament, multifilament, and tape fibrillated and slit-film.

Slit-film wovens consist of slit-film tapes of continuous length, in both the warp and weft direction (Lawson 1986). Slit-film wovens may also be called split-film wovens or (non-fabrillated) tape wovens.

Woven geotextiles tend to be thinner than non-woven geotextiles. Heat-bonded tend to be the thinnest of non-woven geotextiles. Slit-film geotextiles tend to be the thinnest of all woven geotextiles. (Bhatia and Smith 1996).

Woven geotextiles generally consist of a single layer of intersecting fibres and the thickness of the geotextile is limited to the thickness of the fibre. Woven geotextiles thus tend to have short, near 2 dimensional pore structures. In contrast non-woven geotextiles have complex pore structures. (Bhatia and Smith 1996).

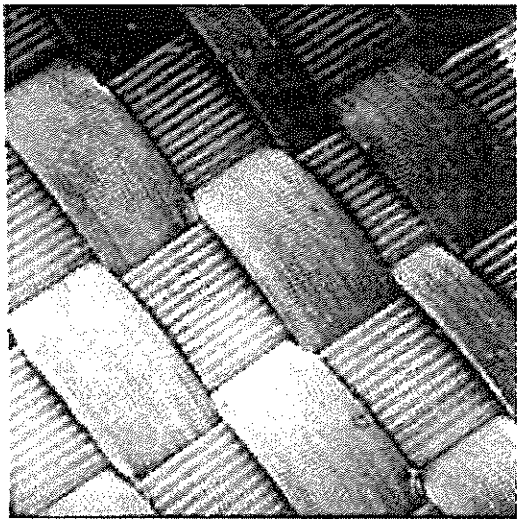

Figure 1. Slit-Film Geotextile (magnified 8 x)

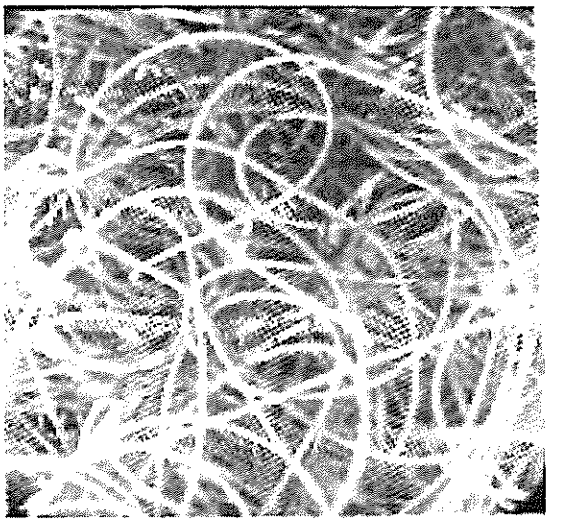

Figure 2. Non Woven Needle Punched Geotextile (magnified 40 x)

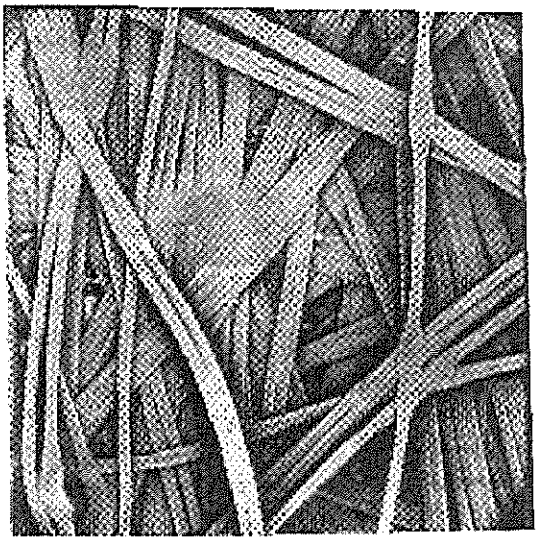

Figure 3. Non Woven Heat Bonded Geotextile (magnified 40 x)

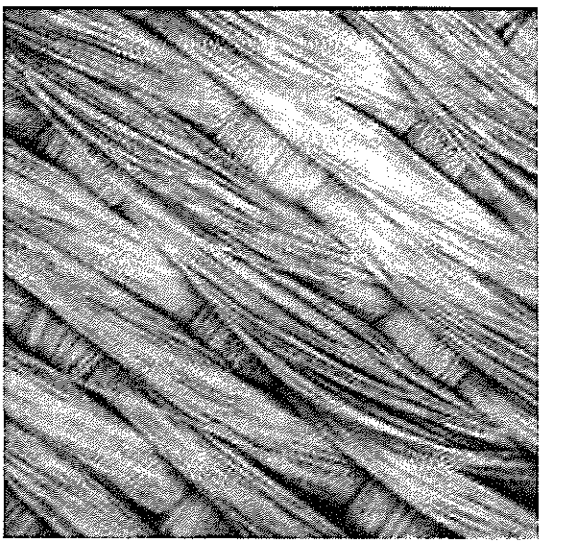

Figure 4. Multi Filament Fibre Geotextile (magnified 8 x)

Non-woven geotextiles tend to have a range of pore sizes. Conversely woven geotextiles have pore sizes within a relatively narrow band because of limitations in the manufacturing process (Bhatia and Smith 1996).

Each type of geotextiles performs differently as a filter, with some types of geotextile being better filters than others (Bhatia Smith 1996).

Within the woven group of geotextiles slit-film wovens will have a very different pore structure and thus different filtration performance to other types of wovens.

The above discussion suggests that some geotextile tend to be inherently better filters than others. Slit-film wovens with their lower frequency of pores, limited distribution of pores sizes and near two dimensional structure appear to be inherently less good filters than other types of geotextile.

PERMITTIVITY

Adequate permeability is one of the essential properties of a geotextile filter. Table 1 gives representative permeabilities for a range of types of geotextiles.

Geotextile Construction	**Permeability Flow Rate Q100** (litres/m^2/sec)
Non-Wovens	
Heat-Bonded	25 – 150
Needle punched	25 – 200
Resin-Bonded	20 – 100
Wovens	
Monofilament	25 – 2000
Multifilament	20 – 80
Tape	5 –15
Knitted	60 – 80

Table 1. Range of Representative Permeability Values (Refer Lawson 1992)

From Table 1 slit-film wovens tend to have a lower permeability than any other type of geotextiles. As permeability is an essential property for filtration, this suggests slit-film wovens are not good filters, particularly for granular materials, sands, or fissured cohesive soils. Indeed Lawson (1986) concludes that generally tape-woven geotextiles are not recommended for use in hydraulic structures where the easy passage of water is required.

PERCENT OPEN AREA

The low permeability of slit-film wovens shown in Table 1 indicates they have a relatively low number of pores in the geotextile (Lawson 1986). The flat shape of the tapes from which slit-film wovens are made results in relatively few pores and a low percentage of open area. For the easy passage of water a higher percentage open area (eg >40% in cohensionless soils) (Hudson and East 1991) is desirable.

SOIL RETENTION

Eichenauer et al (1994) investigated the soil retention ability of a number of geotextiles. Both woven geotextiles and non-woven geotextiles were capable of filtering out soil particles. However, in

filtration non-wovens retained a significantly greater percentage of soil particles than did woven slit-film or monofilament geotextiles with the same O/d ratio (opening size/soil size) for O/d ratios >1. While the wovens did retain a similar percentage of soil particles to non-wovens at O/d <1, there was a sharp break in the performance of the wovens at O/d = 1.

This suggests that if wovens are used for filtration they should be designed accurately such that the O/d ratio is <1 to guard against piping. However for fine grained cohesive soils (60μm >50%, PI ≥7 and/or 2μm ≥ 10%) that are intact or well compacted the water seepage velocities are likely to be insufficient to erode and/or transport soil particles under realistic hydraulic gradients. In such soils piping may not be an issue (East and Hudson 1990) so from the soil retention perspective slit-film wovens may be quite suitable.

CLOGGING

Eichenauer et al (1994) also tested clogging. The monofilament woven geotextile tested showed almost no clogging. The slit-film woven and the heat-bonded non-woven clogged very quickly. The needle punched non-wovens had good resistance to clogging, with their 3 dimensional structure helping to avoid blocking and encouraging soil arches to build up.

Clogging of slit-film wovens after years of use under highways has been difficult to measure as the soil particles blinding the bottom and caked on the geotextile tend to be lost during exhumation. However such tests suggested heat-bonded non-wovens may suffer more clogging than needle punched non-wovens. (Black and Holtz 1999).

Gradient ratio tests with mixtures of slit and sand showed that slit-film and heat-bonded geotextiles failed by clogging. Needle – punched and monofilament performed much better. (Koerner 1986).

From the above there is some evidence that heat bonded non-wovens and slit-film wovens are more prone to clogging than other types of geotextile. particularly needle punched. However this evidence is inconclusive, partly due to the problems with measuring clogging of in-service slit-film geotextiles.

SEPARATORS

Giroud recognised that separation geotextiles are only needed when the soil is wet. In these cases the geotextile must be permeable to prevent the build-up of water pressure. Under static loads (eg embankments) the separation geotextile should meet usual filter criteria. Under dynamic loads (eg within pavements) small pore sizes and high permeability criteria should be met by the geotextile.

Richardson (1997) notes that the M288-96 permittivity requirement of 0.02/sec is very low for a separator geotextile. This value should only be used if the subgrade is not wet. His practice is to require a minimum permittivity of 0.05/sec for a separator geotextile. This level of flow capacity is provided by all needle punched non-wovens and most monofilament or fibrillated woven geotextiles.

This permittivity of 0.05/sec may eliminate many slit-film woven geotextiles and some heat-bonded non-wovens, even if they have been used apparently successfully in separator applications.

INSTALLATION DAMAGE

Exhumation testing has shown that geosynthetics are damaged during installation then under subsequent service loads. Work by the FHWA has lead to the development of degradation damage reduction factors for reinforcement applications. The Industrial Fabrics Association International (IFAI) task force has also produced reduction factors. Table 3 gives these two sets of reduction factors.

Richardson (1998) gives general data on retained tensile strength after installation damage. This is shown in Table 2.

		% Retained Strength		
Geotextile	**Stone Size**	**100mm Depth Stone Overlay**	**250mm Depth Stone Overlay**	**350mm Depth Stone Overlay**
Non-Woven	78mm	62.3	63.6	75.3
Slit-film Woven	78mm	36.4	45.5	71.1

Table 2. Geotextile Degradation – Damage. % Retained Tensile Strength (Richardson 1998)

Geotextile	**Degradation – Reduction Factors**		
	FHWA Recommendation		**IFAI Recommendation**
	Backfill, Max Size 100mm, D_{50} about 30mm	**Backfill, Max Size 20mm,** D_{50} about 0.7mm	**Backfill, Max Size 20mm** 0.1mm $<D_{50}<$0.5mm
Non-Woven (PP and PET)	1.40 – 2.50	1.10 – 1.40	1.05 – 1.20
Woven (PP and PET)	1.40 – 2.20	1.10 – 1.40	1.05 – 1.20
Slit-film Woven (PP)	1.60 – 3.00	1.10 – 2.00	1.10 – 1.75

Table 3. Geotextile Degradation - Damage Reduction Factors (Richardson 1998).

The tests used to obtain the data in Tables 2 and 3 are stone on geotextile on stone tests, so are aggressive survivability tests.

Clearly the FHWA, the IFAI and Richardson (1998) indicate that slit-film woven geotextiles tend to suffer a greater amount of damage than non-woven geotextiles and also greater than for other types of woven geotextiles.

Drexel University in Philadelphia exhumed many geotextiles within hours of their installation. This showed degradation due to installation. These tests were from a wide range of types of construction, and levels of installation stress. The results showed that needle punched non-wovens were much better able to withstand installation stresses than were slit-film wovens. The non-wovens had little damage in almost all cases, whereas the slit-film wovens were damaged in 76% of the cases. (Polyfelt, 1998).

So slit-film wovens are prone to suffer more damage during installation than non-woven geotextiles, or other types of woven geotextiles. Also strength alone is not a sufficient criteria for the survivability of geotextiles

Drexel University also investigated the incidence of damage to geotextiles during installation. They concluded that the incidence of damage to light weight (eg $\leq$ 150qm/m^2) slit-film wovens was particularly high. As holes from such damage would affect the separation or filtration function of the geotextile, they concluded that light weight slit-film wovens should be avoided as separators in permanent construction works. (Polyfelt 1998).

STRAIN EFFECTS

Testing the Equivalent Opening Size (EOS) for geotextiles under strain showed that a woven geotextile tested increased its EOS under strains of 3%, 6% and 9%. In comparison the four needle punched non-woven geotextiles showed little change in EOS at these strains.

Filtration tests showed that the amount of suspended solids that passed through the woven geotextile increased as the strain of the geotextile increased. The four needle punched non-woven geotextiles exhibited little or no increase in the amount of suspended solids that passed through the geotextile (Moo–Young and Ochola, 1998).

These tests indicated that for geotextiles under strain in fine grained soils, needle punched non-wovens control piping better than slit-film wovens.

Fourie and Kuchena (1995) tested the flow rate through two different geotextiles under a hydraulic gradient (2.5), high flow, short – term conditions with a coarse sand soil. The geotextiles were unstressed, then stressed uniaxially and then stressed in both directions. A needle punched non-woven and a slit-film woven geotextile were used in the laboratory tests.

The tests showed that small changes in stress caused large changes in geotextile behaviour.

Under equal stress conditions the wovens showed the greatest percentage decrease, but still exhibited flow rates greater than those of the non-wovens. A comparison of geotextile performance under equal stress conditions is probably an unusual situation for filtration geotextiles.

The geotextiles were then tested on an equal strain basis. Under conditions of low but equal strain the slit-film wovens still exhibited a slightly greater flow rate than the needle punched.

These tests indicated that while stress and strain causes large changes in the permeability of both woven and non-woven geotextiles, slit-film wovens exhibited the greater percentage decrease in permeability but still exhibited a higher flow rate than the needle punched.

PRICE

From information provided by New Zealand suppliers of geotextiles in April 2002, slit film wovens are more expensive that non-wovens of the same F/7 (Pilot) strength and filtration class. The prices supplied are summarised in Table 4 below.

Measure	Price for Non-Woven Geotextiles	Price for Slit-film Woven Geotextiles
Lowest Price	$\$1.31/m^2$	$\$1.65/m^2$
Average Price	$\$1.65/m^2$	$\$2.33/m^2$
Median Price	$\$1.34/m^2$	$\$2.35/m^2$

Table 4. Summary of Prices of Non-Woven and Slit film Woven Geotextiles as provided by New Zealand Suppliers

From the pricing shown in Table 4 slit-film woven geotextiles are more expensive than non-woven geotextiles in terms of lowest price, average price and median price.

Examination of a recent Transit New Zealand project that included a significant quantity of geotextiles (Raumati Straights, SH1) showed that costs for the separation and filtration geotextiles were less than 4% of the project costs, and that even if slit films had been cheaper than non-wovens by the amount they were more expensive in Table 1 above, then the extra cost would be only some 1% of the project costs. This is less than the additional cost to the travelling public from prolonged 70kph speed

restrictions should a less good geotextile filter slow the job by say 1 month (eg 12 months to 13 months for the consolidation).

Thus there appears to be little or no financial incentive in New Zealand to accept any additional risk from the general use of slit-film wovens in filtration situations.

WICK DRAIN SITUATIONS

One of the uses of geotextiles is beneath embankments over weak foundation soils, where the geotextile is to protect a drainage layer from contamination. Consolidation of the foundation soils can be accelerated by the use of wick drains, which are usually punched down through the geotextile.

It is considered that wick drain situations are beyond the scope of the design and the strength criteria in F/7 and should be subjected to specific design.

CASE HISTORIES

There are many case histories where slit-film woven geotextiles have be used successfully in conjunction with wet soils. In terms of the function(s) fulfilled by the geotextile these cases included:

- Primary function reinforcing using a high strength woven.
- Primary function separation, used in conjunction with wick drains.
- Primary function separation.

There are many case histories where slit-film woven geotextiles have been used successfully over soft wet sub-grades. In the majority of the cases studied (Proper 2001, Fanelli 2002, Maccaferri 1996, Vicroads 1996, Stewart 2000) it appears that the dominant function was reinforcing and/or separation. Filtration appeared to be a secondary or tertiary function. Many of these cases appeared to have involved specific design for the geotextile. However the successful use of slit-film wovens in these cases suggests that they are able to successfully provide a filtration function.

SOIL GEOTEXTILE INTERACTION

For filtration of sands or fissured materials the flow rate of any water reaching the geotextile may be relatively high, so a geotextile with a relatively high permeability would be desirable. Slit-film geotextiles may not be desirable for these situations.

For filtration of fine grained soils with fissures or soils that have been disturbed and compacted the soil may result in low flow rates for any water reaching the geotextile (East and Hudson 1990), so a relatively less permeable geotextile may be adequate. Slit-film geotextiles may be adequate for these situations, but consideration needs to be given to piping, clogging and installation damage.

SUMMARY AND CONCLUSIONS

The ability of a geotextile to act as a filter relates to the largest pore sizes, the pore size distribution, the number of pores and the shape and complexity of these pores. The usual design approach of defining EOS and permittivity alone are insufficient to ensure a good filter. It does not necessarily ensure a good filter merely by specifying these two properties.

Each type of geotextile performs differently as a filter, so some geotextiles tend to be inherently better filters than others.

Slit-film wovens tend to have lower permeability than other types of geotextile, so are not recommended for filters where the easy passage of water is required. For separators many slit-film wovens have lower permeability than is desirable.

For soil retention ability non-wovens appear to be quite tolerant, whereas wovens need to be designed quite accurately and are not so tolerant.

There is some evidence to suggest both heat bounded wovens and slit-film non wovens are more prone to clogging than other types of geotextiles.

The trends from the effects of strain on the filtration performance of the various types of geotextiles are not clear.

Slit-film wovens tend to suffer more damage during installation than non-wovens, or other types of wovens.

These differences in filtration performance, clogging potential, change in pore size under strain and greater physical damage are difficult to specify against in a general geotextile specification.

Consideration of the above factors suggests that slit-film wovens tend not to be as good for filtration as other types of geotextile. In filtration situations the use of a less-good filter implies an increased risk relative to other better filters. This may only be a risk of an extended construction period, but some of the risk may be carried by Transit New Zealand or the road user.

A recent check indicates that slit-film wovens in New Zealand may be more expensive than non-woven geotextiles

It is thus concluded that in general for filtration, there are better geotextiles available than slit-film wovens.

ACKNOWLEDGEMENTS

The permission of Transit New Zealand to publish this paper is acknowledged.

REFERENCES

AASHTO (2000) "Geotextile Specification for Highway Applications". *AASHTO Designation M288-00.*

Amoco (1996). "Quantitative Proof of Improved Performance of Flexible Pavements". *Technical Bulletin. Virginia Polytechnic Institute and State University Research Study.* Amoco Fabrics and Fibres Company.

Austroads (1991). "Guide to Geotextiles". *Austroads Report.* Sydney.

Bhatia, S.K and Smith, J.L. (1996) "Geotextile Characterisation and Pore-size Distribution: Part 1. A Review of Manufacturing Processes". *Geosynthetics International. Volume 3.*

Black, P.J and Holtz, R.D (1999) "Performance of Geotextile Separators Five Years after Installation". *Journal of Geotechnical and Geo-environmental Engineering.* May 1999.

East, G.R.W. and Hudson, K.C. (1990). "Road Subsoil Drains: Fine Grained Soils. A Realistic Approach". *Forth International Conference on Geotextiles and Geomebranes.* The Hague.

Eichenauer, T, Faure, Y.H and Farkouh, B, (1994) "Filtration Behaviour of Geotextiles in Slurries". *Fifth International Conference on Geotextiles, Geomembranes and Related Products.* Singapore. 5 to 9 September 1994.

Fannelli, G. (2002). "Presentation to Transit NZ and Duffill Watts & Tse Ltd". *Amoco Australia, Part of the BP Group.* February 2002.

Fourie, A.B and Kuchena, S.M (1995) "The Influence of Tensile Stresses on the Filtration Characteristics of Geotextiles". *Geosynthetics International, 1995, Volume 2, Number 2.* St Paul, USA.

Gerke, R.J (1987). "Subsurface Drainage of Road Structures". *Australian Road Research Board. Special Report No 35.* April 1987.

Giroud, J.P: "Designing with Geotextiles". *Materials and Structures Issue.* RILEM.

Haliburton and Wood (1982) "Evaluation of the US Army Corp of Engineering Gradient Ratio Test for Geotextile Performance". *Proceeding of Second International Conference on Geotextiles:* Las Vegas USA.

Hudson, K.C and East, G.R.W. (1991) "Geotextiles". *Transit New Zealand Research Report No. 6.* Transit New Zealand. Wellington.

Koerner, R.M. (1986). "Designing with Geosythetics". *Prentice – Hall.* United States of America.

Koerner, R.M. (1997) "Designing with Geosythetics". *Forth Edition. Prentice – Hall.* United States of America.

Lawson, C. (1986) Various Papers. *Proceedings of Technical Sessions of Third Asian ICI Fibres Conference.* Thailand. October 1986.

Lawson, C. (1994) "Geosynthetics Course Programme". *Exxon Chemical Geopolymers.* UK.

Maccaferri, (1996). "Polyweave Woven Geotextile Performance Recognised at Lake George". *Maccaferri Newsletter.* Maccaferri Pty Ltd.

Moo – Young, H and Ochola, C. (1998). "Strain Effects on the Filtration Properties of Geotextiles". Circa 1998.

Pilarczyk, K.W and Breteler, M.K. (2000). "Geotextiles in Revertment Structures – a Dutch Approach". Balkema, Rotterdam.

Polyfelt (1988) "Investigations on the Installation Survivability of Geotextiles". *Polyfelt, T.S Geotextile Technical Note.* GRI Drexel University, Philadelphia.

Propex (2001) "Proper 4550 over Longswamp". *Propex News. Issue 8.* August 2001

Propex (2001) "Stabilisation of Extremely Soft Ground at Melbourne Port – Propex 2044". *Propex News. Issue 9.* November 2001.

Richardson, G.N and Christopher, B.R "Geotextiles in Transportation Applications: Course Outline".

Richardson, G.N (1997) "Designers Forum. Geotextiles in Roadway Separation Applications". *Geotechnical Fabrics Report.* June – July 1997.

Richardson, G.N (1998) "Field Evaluation of Geosynthetic Survivability in Aggregate Road Base". *Geotechnical Fabrics Report.* September 1998.

RTA (2001). "Geotextiles (Separation and Filtration). QA Specification R 63". *RTA. New South Wales, Australia.* September 2001.

Standards Australia (1990) "Geotextiles – Glossary of Terms". *Australian Standards AS 3704-1990.* Standards Australia.

Stewart, R. (2000) "Capping of Very Low Strength Tailings using Woven Geotextiles and a Geosynthetic Clay Liner". *Ancold 2000 Conference on Dams.*

Tan, H.H. Weimar, R.D. Chen, K.H. Demery, P.M. and Simons, D.B. (1982) "Hydraulic Function and Performance of Various Geotextiles in Drainage and Related Applications". *Second International Conference on Geotextiles.* Las Vegas. USA.

Tsai, W.S and Holtz, R.D (1997) "Laboratory Model Tests to Evaluate Geotextile Separators in Service". *Geosynthetics.* 1997.

Vicroads (Circa 2000) "Bass Highway Duplication". *Project Report.*

Wayne, M.H, Petrasic, K.W. Wilcosky, E. and Rafter, T.J. (1996) "Case History. An Innovative Use of a Non-Woven Geotextile". *Geotechnical Fabrics Report.* September 1996.

Health on the Volcano's Edge

C J Bauld
NZCE, BE (Hons), ME, MIPENZ, Regd Engr
Senior Geotechnical Engineer, Tonkin & Taylor Ltd

Abstract: Auckland Hospital's Grafton site is situated on the edge of the Domain Volcano in central Auckland. Continued pressure on the health infrastructure in Auckland has meant that expansion and upgrading of Auckland's hospital services became necessary. This has required a major construction programme at the Grafton site, including four new buildings and major refurbishment of existing structures. The most significant of these structures is the Acute Services Block (ASB) building, a 9 storey building covering nearly 1 hectare. Construction of this building within a tight budget was a significant technical challenge due to the variability of the underlying volcanic soils. The most significant being the basalt rock underlying only two thirds of the proposed building.

PROJECT OVERVIEW

The Project

The developments at Auckland Hospital are part of a wide-ranging strategy to rationalise the health services provided by Auckland Healthcare. These include the construction of four new buildings at the Auckland Hospital site, as well as further building at the Greenlane site.

The new buildings are a Pathology building, a mental heath unit, a Carpark building and major building to house acute services. In addition there are a number of additions and renovations to existing buildings including the Starship Childrens Hospital and the main hospital building.

After completion of the works, all of the in-patient services will be focused at the Auckland Hospital site. The Greenlane site will be devoted to out-patient services. At the time of writing the pathology, carpark and mental health buildings have been completed. The new Acute Services Block (ASB) building is nearing completion of the structure and fit-out of services is well under way. The total budgeted cost of the development is $423M, including $176M for the ASB building.

All of the structures constructed on the Auckland Hospital site presented unique challenges for the design of foundation systems. These ranged from uncontrolled fill to depths of up to 15m to sediments underlying welded tuff and basalt.

The ASB Building

The ASB building is by far the largest of the new structures and is the key to future health services in Auckland. A major portion of the in-patient services provided by the Auckland Health Board will be transferred to this building. The existing tower building will then be completely re-furbished to house administration, research, conference and teaching facilities.

The ASB building is a 9 level structure constructed around a central atrium to maximise natural light in the wards. Total floor area is over 70,000m^2, making the building twice the size of St Lukes Shopping centre and one of the largest buildings in the country. To assist with a flexible floor plan, the column centres are relatively wide at 7-8m spacing. Lateral load resisting systems are mostly braced frames rather than walls. The floor levels are matched to those of the existing tower block and Starship Childrens Hospital to allow free flow of traffic between the blocks.

Due to the sloping site, the building has a basement up to 13.5m below ground at one side, reducing to zero at the other side. Construction of the excavation and associated temporary retention was undertaken as a separate enabling contract.

DESIGN REQUIREMENTS

The Design Team

The design team appointed by Auckland Healthcare included Beca Carter Hollings & Ferner as structural and civil engineers and Jasmax as architectural designers under the guidance of an overall design manger. Carson Group undertook the management of the project with overview by a dedicated project team from Auckland Healthcare. Tonkin & Taylor (T&T) were engaged directly by Auckland Healthcare as geotechnical engineers for the project.

The final part of the design team was the main contractor, Fletcher Construction. They were selected in an attribute-based process before any consideration of pricing. Due to the unusual (for New Zealand) contract structure, Fletcher Construction was an integral part of the design team. Once selected as contractor, negotiations commenced with between the Contractor and the Principal to arrive at an agreed Guaranteed Maximum Price (GMP).

Clients Requirements

The project was, of course, driven by a set of functionality requirements that were arrived at by in depth studies and consultation within Auckland Healthcare. However an overriding driver behind the project was the requirement for strict cost control. As the regional health budget is very tight any over-run in costs was seen to be unacceptable.

Design/Pricing Process

A critical feature of the design process, which became the major driver for the extensive investigations, was the iterative pricing process. To ensure that the budget was adhered to the GMP was negotiated as the design was progressed. Any areas where the budget was exceeded were subject to redesign to allow the budget to be maintained.

This was particularly important for the foundation construction, as the Contractor was to take all geotechnical risk for the project. Given the variable nature of the volcanic soils there was a need to maximise the information available to the Contractor to reduce the risk portion of the price. This was true for both the foundation construction and the enabling works contract of basement excavation.

THE INVESTIGATION

Overview

As would be expected for such a major project the investigation was phased over a period of time to allow targeting of specific areas of uncertainty. In total there were 8 separate investigation phases, with the first started in 1998 and the final drilling completed in 2000. The scope of these ranged from desk studies of historical information, to major percussion and cored drilling investigations of 356 boreholes and a destructive test anchor program.

Cored boreholes were all HQ sized core, with some extended in solid basalt using down hole hammer equipment. Percussion boreholes were mostly drilled using specialist downhole hammer techniques as this provided the best spoil recover and definition for logging. Some percussion holes were completed using top drive percussion rigs when additional drilling rigs were required to meet programme constraints.

Historical Data

As part of initial preliminary investigations T&T researched historical information from our database of previous work. This provided 39 boreholes surrounding the site and including buildings such as the existing tower block, the Medical School and the Renal & Dialysis Unit. A further 8 boreholes were obtained from other records held by Auckland Healthcare.

Preliminary Investigation

A preliminary investigation was undertaken in 1998 in two phases. This included;

- 6 cored/percussion boreholes
- 3 percussion holes using a small top drive rig
- A small-scale seismic survey.

This initial investigation showed that basalt rock only underlies part of the proposed building platform. The boreholes extended to between 20 and 50 metres, demonstrating that basalt extended to a significant depth at some points on the site.

Design Investigation

The design phase of investigations was undertaken in the latter part of 1999 while the initial phases of design were underway. This investigation included;

- 6 cored boreholes
- 50 percussion boreholes using a down-hole hammer rig

The aims of this investigation were to provide additional information on the rock mass, provide better delineation of the edge of the basalt flow and provide information on the ground conditions along the lines of the proposed temporary retention system.

Supplementary information was also provided by a magnetic survey undertaken by Opus International Consultants as part of a water supply project.

The investigations did provide some further definition of the edge of the flow. However, the drilling that was intended to target the basalt edge instead showed the highly variable quality and profile of the flow edge.

Proof Drilling Investigation – Phase I

Phase 1 of the proof drilling investigation was undertaken in early 2000. This was the first phase of investigation specifically targeted at risk reduction and included;

- 5 cored boreholes to define depth to East Coast Bays Formation (ECBF) rock and fill gaps on the geological model
- 122 percussion boreholes using a down-hole hammer rig.

The major aims of the percussion drilling were to;

a) Provide definition of the likely founding level
b) Check for voids or weak areas immediately below foundation level

Proof Drilling Investigation – Phase II

Phase II of the proof drilling investigation was a continuation of Phase I and included 45 percussion holes drilled in locations that were previously inaccessible. A site plan showing the extent of investigations to this phase is given in Figure 1.

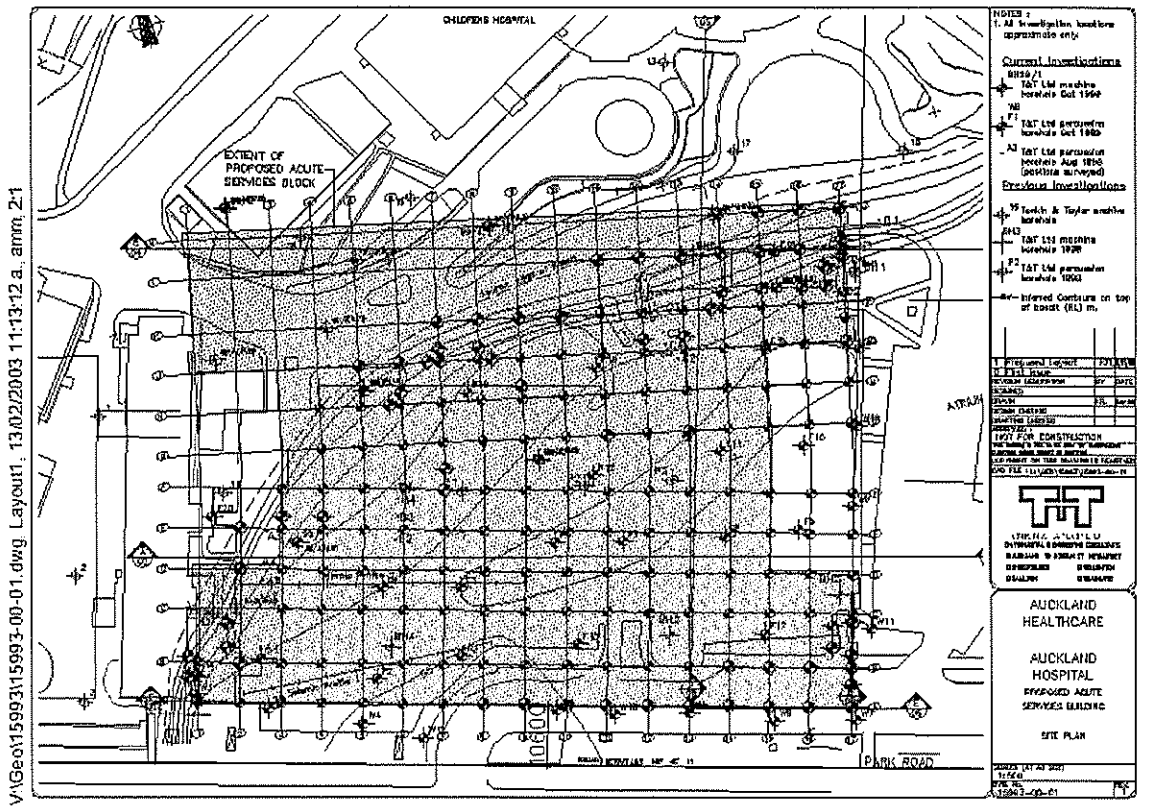

Figure 1. Site Plan

Proof Drilling Investigation – Phase III

Phase III of the proof drilling investigation was undertaken to assess specific foundation locations near the flow edge. This was to prove a sufficient extent of basalt around the foundation to provide the required bearing capacity and limit settlement. In addition a new foundation location was investigated as well as several foundation locations not previously accessible. A total of 24 percussion boreholes were drilled in this phase.

Proof Drilling Investigation – Phase IV

Phase IV of the proof drilling investigation was undertaken in September 2000 to provide confirmation that no obstructions or floating basalt boulders were present at locations of proposed bored piles.

GEOLOGY

Overview

The Grafton site of Auckland Hospital is located next to the Domain Volcanic cone. The eastern edge of the site is located on the historic tuff ring of the main vent. The site slopes north to north-east from the domain down into Grafton gully. The lower reaches of the site are at times relatively steep with extensive batter slopes and retention to create building platforms.

Published Geology

Published geology maps for the site (Kermode 1992) show the area to be underlain by lithic tuff and scoria ejected from the Domain Volcano complex. This is inferred to overlay the local "basement"

rock, which is the East Coast Bays Formation (ECBF), part of the Waitemata Group rocks. In addition, work by Searle (Searle 1980) shows the Domain volcano is in the order of 50,000 years old.

Kermode (Kermode 1992) described three applicable materials for this area in addition to the underlying ECBF soft rocks;

- Lithic Tuff, consisting of very thin beds of mud to sand sized particles of ejecta including native rock an basaltic materials. The unit may be very soft, compacted or welded.
- Scoria, consisting of vesicular, pebble to boulder sized ejecta of basaltic materials. These may weld together and form "rootless" lava masses.
- Lava, being dense to very dense, fine grained basaltic materials. Lava flows are commonly interbedded with scoria and further away may be mantled with scoria or tuff. Some flows also may include lava tubes or caves.

Recent studies (France et el 2002) indicate that at least two centres exist, the main one being the Domain centre as defined by the tuff ring surrounding the Domain. Recent geophysical surveys indicate another centre may also exist immediately to the south west of the domain, and underlying Outhwaite park. This centre appears to be the most likely source of the ash materials overlying the hospital site.

Historical Data

Historical information was available for buildings surrounding the ASB site. This indicated the buildings to the south (shallow foundations) and east (bored piles to basalt) of the site are founded on basalt rock. To the west (the site of the new Pathology building) the underlying soils are ash and tuff overlying Tauranga Group sediments, over ECBF rock. To the north the Starship Hospital is founded on bored piles through ash and sediments to the underlying ECBF rock.

These varied conditions hinted at a significant geological change across the ASB site.

GEOLOGICAL MODEL

Investigation Findings

The initial phases of the investigation defined a geological model that was confirmed and refined by the following phases of the investigations.

The model showed that the site was overlain by shallow layers for fill (approximately 1m maximum) that were generally associated with previous buildings on the site. Deeper areas of fill are found at the northern edge of the site where localised retention works have been constructed as part of the Starship development. Ash and tuff up to 15m deep then underlie the site.

Below the south-eastern corner of the site lies rubbly basalt/scoria at a depth of approximately 6-7m, which gradually increases in strength and density to a depth of approximately 10-12m, where it is a highly fractured basalt rock. This rock extends to a depth greater than 50m. A view of the highly fractured basalt rock is given in Figure 2. Upper surfaces of the rock mass tend to be very vesicular and scoriaceous. Significant amounts of mixing with ash soils have also occurred in the upper regions.

The basalt rock base rises toward the north-west, while the upper surface remains relatively level. The rock finally pinches out approximately two thirds of the way across the site. The basalt rock tends to become more fractured and vesicular toward the north-west. Mixing of the material with ash soils and scoria materials becomes more pronounced and extends deeper into the unit toward the north-west.

Figure 2. Fractured basalt

For engineering purposes the rocks and soils have been characterised as follows;

- Ash, being fine-grained clay and silt sized air fall materials. Generally the upper layers of the soils, but also including some of the soils intermixed with basalt.
- Lithic Tuff, silt to sand sized airfall material, often slightly to moderately welded.
- Granular Tuff, sand to gravel sized air fall material.
- Flow Breccia, Includes welded tuff materials, scoria and mixed basalt and ash materials.
- Basalt

As the basalt pinches out it rises over the top of weathered ECBF soils and Tauranga group sediments that underlay the ash soils. Underlying the north-western corner of the ASB building, and the link structure with the Starship hospital is approximately10-12m of ash/tuff over up to 10m of stiff sediments.

EXCAVATION

Overview

Bulk excavation for the ASB basement required excavation of approximately 40-50,000m^3 of material including basalt rock. This presented a significant area of cost risk for the project with the potential for hard basalt that would require blasting or other costly excavation methods. As the budget required a lump sum price for excavation an accurate assessment was required for pricing.

Part of construction required a temporary retention system along the east and south sides of the excavation. At the highest point this was up to 13.5m high. A number of temporary ground anchors were required to support this wall.

Excavation Assessment

A detailed check was undertaken to assess the likely excavation materials. This was required to assess whether ripping techniques would be usable, or if breaking or blasting would be required. Careful examination of the materials in boreholes indicated that the basalt rock was generally highly fractured, and often vesicular. Based on this we expected that all of the rock on site could be ripped using an excavator in the 35-45 tonne range with a single ripping hook. As part of pricing we estimated a credible worst case of 500m^3 for the volume of rock that may require breaker or similar equipment.

After completion of the excavation, including a localised deepening for the lift pits and access to the lowest level of the structure, the Contractor reported that all of the rock encountered had been ripped with a 45 tonne excavator. Although it was noted that one isolated area would normally have required breaking, but it was considered uneconomic to mobilise breaking plant for the small area (and a matter of pride).

Retention

Due to the difference in level of the ground across the site a basement excavation of up to 13.5m was required to provide a ground level access at the north-western corner. To achieve this a temporary retention system of steel piles cast in bored holes with a sand-cement mix was used. Timber lagging provided support between the piles. Temporary ground anchors were used to support the wall.

The bored holes for the piles were constructed using a combination of a 450mm down hole hammer and conventional piling equipment. The varied techniques were required because of the equally varied ground conditions. The down hole hammer equipment was very efficient in the hard rock materials. However the mixture of fine-grained materials overlying the clean rock proved difficult to flush with air driven equipment. Because of this a number of holes were drilled using a conventional piling rig and a rock auger.

Anchor Design

As for the other foundation systems on the site the Contractor was to take all geotechnical risk for the ground anchor systems. To minimise costs it was also proposed to found anchors in the ash and rubbly basalt soils rather than extending these to intact basalt. This also minimised the slope of the anchors, and hence the vertical loads applied to the structural elements of the wall.

To allow the Contractor certainty on the performance of the anchors, and hence minimise the cost to the client of this guarantee, a programme of anchor testing was undertaken. This included;

- 6 tests in total
- Use of post grouting
- Use of filter sock to reduce grout loss
- Creep testing

All tests were destructive tests with the anchors loaded to failure (unless the structural capacity of the anchor was reached). Based on the testing results the anchors were designed as;

- 200mm diameter hole
- Bonding in ash/scoria materials
- All anchor post grouted at high pressure

Monitoring of the anchors during construction showed performance was within the expected tolerences

FOUNDATION DESIGN

Overview

The changing ground conditions across the site provided complex conditions for foundation design. In addition, the foundation materials provided uncertainty for the location and capacity of individual foundations.

There were three main considerations for foundation design;

- Uncertainty of foundation conditions on the volcanic materials
- Low differential settlement tolerance (max 10mm over 8m), especially in areas around structural braced frames
- Changing foundation conditions across the site.

The most significant result of the complex changing ground conditions across the site was the need for changes in foundation type across the site. The changed from shallow foundations on basalt to deep bored piles socketed in ECBF rock. Normally mixing foundation types in this way is considered bad practice for both serviceability response and seismic performance. This potential was carefully considered during design of the foundations with total foundation settlements limited to a total of 10mm to ensure differential limits were complied with. In addition, lateral spring stiffness for both footings and piles were included in structural analysis to ensure that the building behaviour was acceptable under seismic conditions.

A major consideration was the variability of the volcanic materials, and the capacity of the materials at individual foundation locations. This was partially addressed by allowing for several standard designs depending on various possible ranges of conditions. These included piled foundations to ECBF and basalt as well as several sizes of shallow foundations. In addition a number of possible remedial options were specified.

The expected foundation type for each location was selected for every foundation on site including expected remedial actions such as undercut of unsuitable materials. During construction, a geotechnical engineer inspected every foundation location, to confirm the required foundation type.

Shallow Foundations

Shallow foundations were designed for all areas underlain by basalt rock. These allowed for three potential material types ranging from vesicular silty gravels to intact basalt. Bearing capacity and the related range of stiffness values was calculated for the lower strength materials using conventional bearing capacity theory. For the intact rock, values were limited to allow for localised defects and a minimum footing size was specified to allow bridging of potential defects. Several locations near the edge of the basalt flow required more intensive investigation during the proof drilling operation. This was to prove that a sufficient extent of basalt existed for appropriate load transfer into the basalt rock.

A further point noted during design was that reduction of footing size for the intact rock was not generally worth the cost saving in materials. This was due to a number of factors including the costs associated with having additional cage types on site and limitations of tolerances in the footings to provide space for reinforcing and column fixings.

During construction inspections were made of each foundation location and compared with proof drilling results. Some foundation locations were sub excavated by up to 3m and the excavation back filled with low strength concrete or flowable fill.

Construction and inspection of the foundation proved that initial assessments made from the proof drilling were generally accurate. All foundations constructed were the originally proposed type with only minor variation in sub-excavation depth required.

Piles to Basalt

Several areas of the structure were located outside the basement footprint and hence required pile foundations extending down to basalt rock. The piles were designed to socket into basalt rock using relatively low design strengths. This allowed for load spreading in the event of a localised area of weakness in the rock mass. The majority of piles were 900mm diameter to allow down hole inspections by a geotechnical engineer. Some 750mm diameter piles supporting the link structure to the existing tower block were used in a late phase of the project to provide cost savings.

These piles were constructed using conventional piling rigs and tungsten carbine tipped rock auger bits. This equipment allowed good production rates in the fractured basalt and produced a relatively economic solution with a high degree of reliability.

Inspections of the pile construction generally showed good agreement between proof drilling predictions and the actual installed pile penetration. However several pile locations did require extension of the socket to bridge past localised weaknesses in the rock. Another construction consideration of note was the location of the proof holes. A number of these holes were drilled slightly off the actual pile location. This caused some difficulties during pile boring as the piling equipment tended to wander and follow the line to the proof hole. This required some care on the part of the Contractor to ensure piles were within the required tolerance.

Piles to ECBF

The north-eastern corner of the site required pile foundations to the ECBF soft rock. Design checks were made to confirm the axial deformations of the piles were within the required serviceability limits of the structure. All pile locations were checked for obstructions such as volcanic boulders before construction. These piles were also 900mm diameter.

During construction a geotechnical engineer inspected all piles down hole. This proved valuable as the ECBF rock was relatively soft in this area making it relatively difficult for the Contractor's staff to pick the depth the unweathered rock based on drilling resistance and recovered material.

Driven Piles

Driven steel UC piles were designed for a link structure extending between the ASB building and the existing Starship Hospital. These were considered economic for this area due to the lower loading of the structure.

During construction, piles initially did not achieve design capacity at the desired level, despite location of the rock horizon with proof drilling. This was further investigated by testing of a number of piles using Pile Driving Anlayser (PDA) dynamic testing methods. This allowed the design team to confirm that the initial lower capacity was due to pore pressures induced by driving. Once the pile had been allowed to "set up" for a short period significantly increased capacities were measured on re-drive of the pile.

CONCLUSIONS

A number of important points may be taken from this project. Foremost among these was the importance of communication between client and all designers during the construction process. Technical problems generally have several feasible solutions, the important aspect of design is selecting one that provides the best solution for the client's needs rather than the elegant and strictly correct technical solution.

Geotechnical risk is often a major source of cost fluctuation in construction projects, more so in civil construction than in building projects such as the ASB building. The ASB building clearly demonstrates the effectiveness of achieving an acceptable solution through an interactive design and

pricing process. On the ASB project, geotechnical risk was managed by focussing on the areas with the greatest cost implications. Investigations and testing were targeted to resolve these, rather than to generate a complete understanding of the entire geology. For the ASB building this was the risk of variation in foundation type and depth rather than variations due to material properties. The eventual investigation managed to mitigate the cost implications of such variations in a way that fitted with the client's requirements.

REFERENCES

France, S. C., et al, (2002), "Geophysical and Geochemical Characterisation of Two Maars within the Auckland Volcanic Field", *Oral presentation to the Geological Society of New Zealand Annual Conference, 2-5 December 2002.*

Kermode, L.O., (1992), "Geology of the Auckland Urban Area", Institute of Geological & Nuclear Sciences Ltd.

Searle, E. J., (1980), "City of Volcanoes, A geology of Auckland", Longman Paul.

Ground Anchor Practice in New Zealand - A Review of Applications, Design and Execution

P A Wymer
BE (Hons), NZCE (Civil), M.IPENZ, Regd Eng
Managing Director, Construction Techniques Group Ltd
R A Robinson
Development Manager, Construction Techniques Ltd
D T Sharp
BE (Hons), M.IPENZ, Regd Eng
Construction Manager, Construction Techniques Ltd

Abstract: This is a discussion paper which considers the use of ground anchors in New Zealand, including design and execution in volcanic and seismically active environments. There are many international codes and guidelines used for ground anchorage design in New Zealand but there does not appear to be any particular practice adopted as the industry standard.

The paper will outline a variety of applications, design issues and construction aspects particular to the New Zealand market with a view to developing a more standardised approach to ground anchorage works. It makes particular reference to the issue of corrosion protection and how this can be rationalised in order for a unified approach for ground anchor design to be established. The material covered is not intended to establish specific design or installation procedures but to stimulate further development of appropriate guidelines relevant to New Zealand applications.

INTRODUCTION

Ground anchor practice in New Zealand has evolved in the same fashion as it has in any other country - it is based on the specific applications, design requirements and ground conditions prevalent. In this relatively small country, there exists a varied and challenging mix of considerations for ground anchor design and execution. Aside from all of the usual applications and load cases, the seismic environment requires additional consideration associated with seismic induced lateral loads on slopes and vertical restraint for instability or overturning of structures. Ground anchors have been utilised in New Zealand for some 30-40 years and during this time the materials, design and execution have developed and evolved consistent with international practice. As the number of installations increased, so too has the demand for more rational guidelines on the design, construction and testing of anchors. Since the early 1980's, ground anchor codes of practice and published guidelines have emerged throughout the world (CIRIA, 1980; DD81, 1982; FIP 1982; FIP 1987, DIN 4125, 1988; FIP 1996; PTI 1996; BS 8081, 1989; Geotechnical Engineering Circular No. 4, 1999; BS EN 1537, 2000). These documents reflect the wide variety of research and practical experience in ground anchors in these various nations with New Zealand electing to follow those most closely aligned with its engineering design and practice. In this regard, this paper primarily refers to the most recent and most commonly referenced publications in New Zealand, BS EN 1537, 2000 "Execution of special geotechnical work, Ground Anchors", FIP 1996, "Design and construction of prestressed ground anchorages" and BS 8081:1989 "British standard code of practice for ground anchorages." This paper considers some of the historical practices in ground anchor design and execution and focuses on the most recent developments in New Zealand.

DEFINITIONS

There are varying opinions on how ground anchors should be described. The English and French have their differences and one chooses to call them "anchors" and the other uses the term "ground anchorage." FIP 1996 uses the term "anchorage" and the latest BS EN 1537 uses the term "anchor." The difference in interpretation is very subtle and it is only highlighted to create awareness that both

terms will be seen from time to time. For the purposes of this paper, the term "anchor" has generally been adopted. From a New Zealand perspective, ground anchors can be found in the following situations:

- Stressed anchors in rock and soil
- Passive anchors in rock (non-stressed)
- Soil nails (network of passive anchors in soil)
- Deadman tiebacks (stressed or non-stressed)
- Lightly loaded anchor in rock and soil (non-stressed)

Associated with the above categories, anchors can also be categorised as temporary, permanent, restressable or detensionable. These are important considerations when selecting the type of tendon, configuration and anchorhead componentry to be used. It is extremely important to categorise the type of anchor at an early stage as it has a significant bearing on how it is to be designed, detailed and constructed. It will also assist in the selection of an appropriate specification and identify what parts of that specification will be relevant to the particular application.

Key international documents as referenced in this paper are as follows:

BS EN 1537 2000: Execution of special geotechnical work – Ground Anchors. This British Standard is the official English language version of EN 1537:1999. It supersedes those parts of BS 8081:1989 that deal with the construction ('execution') aspects of ground anchors.
BS 8081 1989: Code of practice for ground anchorages. This comprehensive code covers the full range of design, materials, corrosion protection, execution, testing and maintenance aspects associated with ground anchors. The execution sections have been superseded by BS EN 1537 and the other sections covering specific design are currently being harmonised into European Standard, EN 1997-1:1995 Eurocode 7: Geotechnical Design, Part 1 General Rules. Until EN 1997-1 is harmonised to cover ground anchors, the design parts of BS 8081 apply, whereafter BS 8081:1989 will be declared obsolescent in its entirety.
FIP 1996: Design and construction of prestressed ground anchorages. These recommendations were prepared by a Working Group of the FIP Commission of Practical Construction. They provide a guide to the planning, installation, testing and monitoring of permanent and temporary ground anchorages normally bonded to the ground by cement grout. The recommendations do not deal with the overall design of anchored structures or excavated faces.

The author's are of the opinion that these documents best represent acceptable practices which can be adopted for New Zealand ground anchor applications.

This paper assumes that the reader has some knowledge of the typical components of an anchor and further descriptions are not given. A basic anchor schematic and anchor nomenclature as defined in FIP 1996 is included in Appendix 1 for reference if required.

RESPONSIBILITIES

Ground anchors are usually specified for situations where their performance is critical to the overall design resistance of the structure. The accurate determination of the necessary anchor resistance loads is therefore a vital prerequisite to any ground anchor application. The determination of these design values needs to take into account the design demands of the overall structure in both the ultimate limit state (ULS) and serviceability limit state (SLS) conditions. Some examples of this design process for anchors are provided in Merrifield, Barley and Von Matt (1997). A more detailed analysis is provided in the informative Annex D of BS EN 1537: 2000.

In addition to this, there also needs to be due consideration of design life, level of corrosion protection, safety factors, testing, monitoring, etc. This importance of well defined responsibilities is well recognised in the various codes and recommendations and BS EN 1537: 2000 provides a table for an appropriate separation of design and execution activities. This table is as shown in Figure 1.

Overall Design Activities	Specialist Execution Services
1. Provision of site investigation data for construction of ground anchors	1. Assessment of site investigation data with respect to design assumptions.
2. Decision to use ground anchors, required trials and testing and provision of a specification	2. Selection of ground anchor components and details.
3. Acquisition of legal authorisation and entitlement to encroach on third party property	3. Determination of fixed anchor dimensions.
4. Overall design of anchored structure, calculations of anchor force required. Definition of safety factors to be employed.	4. Detailing of the corrosion protection system for the ground anchor.
5. Definition of ground anchor life (permanent/temporary) and requirement for corrosion protection.	5. Supply and installation of the ground anchor system.
6. Specification of anchor spacing and orientation, anchor loads and overall stability requirements.	6. Supply and installation of the ground anchor monitoring system.
7. Specification of minimum distance from the structure to mid fixed length to ensure stability of the structure.	7. Quality control of works.
8. Specification of load transfer mechanism from the anchor to the structure.	8. Execution and assessment of anchor tests.
9. Specification of any sequence of anchor loading required of the structure and the appropriate load levels.	9. Evaluation of on-site anchor tests.
10. Specification of systems for monitoring ground anchor behaviour and for interpretation of results.	10. Maintenance of ground anchor as directed.
11. Supervision of the works.	
12. Specification of maintenance for ground anchors.	
13. Instruction to all parties involved of key items in the design philosophy to which special attention should be directed.	

Figure 1. Design and Execution Duties

The overall design activities are usually best known by the Clients' consulting engineer and they are also in the best position to judge how the ground anchor will interact with the ground/structure system. They are also the most appropriate person for assessing the degree of risk involved. With this careful delineation of responsibilities and detailed description of requirements, the designer and Client can more accurately make a selection of the preferred anchoring option without having to consider vastly different systems and costs. There can be no doubt that the most successful projects are those where the design activities are well documented and the delineation of duties is clear from the outset.

PLANNING OF WORKS

It is vitally important to carefully plan all aspects of the ground anchor works from an early stage. All the best design, detailing and construction can be quickly undone if insufficient work has gone into the ground investigation, services inspection or boundary conditions. Work associated with ground anchors has a high level of unknown attached to it and hence a high level of risk. Risk can be greatly reduced if more details are available at an early stage. Anchoring activities are frequently linked to the critical path of projects and can cause significant time and cost overruns if unknowns are encountered. This can create large disruptions to activities which are to follow on. It will obviously be advantageous to the Client if measures are taken to minimise the risk of these problems at an early stage. There is

often a great deal of time (and money) spent sorting out problems and responsibilities during the course of the work when more careful planning could have greatly reduced the likelihood of this.

Anchors can be vertical, horizontal or inclined and frequently there is little geotechnical information available of the material to be anchored into. It is essential that any site investigation work contemplates the possibility of ground anchors and suitable boreholes planned to provide representative information. A common cause of anchor failure at the acceptance testing stage is the lack of accurate information on the ground conditions local to the anchor. To quote from BS EN 1537: 2000:

"Geotechnical investigation should be extended to site extremities so that the strata profile may be interpolated between the investigation locations rather than extrapolated outside the area investigated. Where possible, it should be extended to include ground formations outside the actual site if stresses induced by anchors are extended there."

It is well known that Clients are often reluctant to pay for more extensive geotechnical investigations. However, they should be reminded that they will likely be exposed to significant cost and time overruns which will probably dwarf the cost of more detailed investigation had it been carried out an early stage.

The advantage to a contractor having access to good geotechnical information at an early stage is that they are able to better qualify potential obstructions to drilling, the process of borehole drilling, borehole stability, flow of water into the borehole and loss of grout from the borehole. This will certainly assist in preparing a more detailed anchoring submission and help mitigate delays and additional costs during the course of the work.

ANCHORAGE DESIGN

This does not consider the structural design of a system (this was referred to previously in Section 3) but rather the mechanism of the anchorage obtained by virtue of the grout surrounding the tendon. There are various types of grout injection and these are shown in Figure 2.

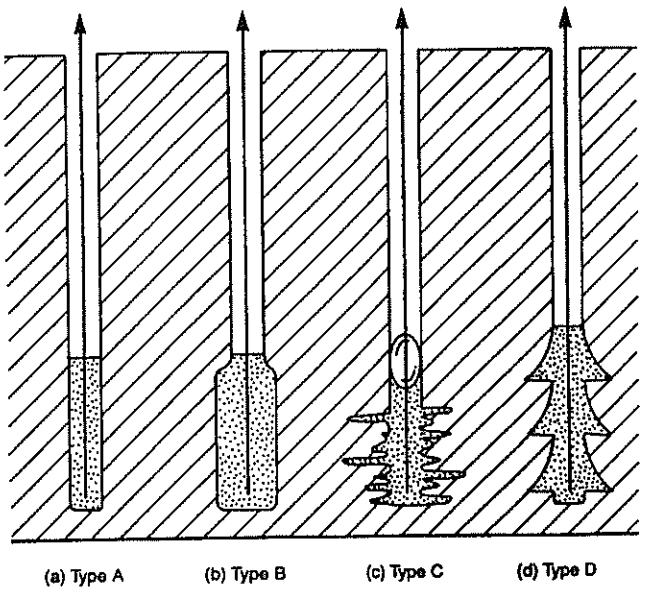

Type A
Gravity grouted shaft borehole, which may be lined or unlined depending on hole stability.

Type B
Low pressure (< 1000kPa) grouted borehole via a lining tube or insitu packer where the diameter of the fixed anchor is increased with minimal disturbance as the grout permeates through the pores or natural fissures in the ground.

Type C
High pressure (> 2000kPa) grouted borehole via lining tube or insitu packer, where the grouted fixed anchor is enlarged via hydrofracturing or compaction of the ground.

Type D
Gravity grouted borehole in which a series of enlargements (bells or underreams) have previously been mechanically formed.

Figure 2. Main Types of Cement Grout Injection Anchorage

It should be noted that other types of screwed or driven (non-grouted) anchorages are available and these include screw piles/screw anchors, duck-bill earth type and inflatable bag. These anchor types are typically used in low capacity, non-stressed, temporary applications and are not covered by ground anchor codes as discussed in this paper. The degree of corrosion protection offered by these types of

anchors needs to be carefully scrutinised as they do not comply with the requirements of BS EN 1537:2000.

It is important to get a clear idea of the applicable design loads as this can dictate the selection of the anchor tendon and type of anchorage. Currently, there does not appear to be any standard format for designating anchor design load requirements but BS 8081: 1989 does provide some useful guidance on appropriate safety factors to be used in conjunction with tendon and ground pullout capacity. In current practice, the load safety factor of an anchorage is the ratio of the ultimate load capacity to the working load. The proof load factor is the ratio of the proof load to the working load. For each potential failure mechanism, a safety factor should be chosen having regard to the accuracy with which the relevant characteristics are known, whether the system is temporary or permanent, and the consequence if failure does occur, such as danger to public safety and cost of structural damage. Figure 3 illustrates the key information included in BS 8081:1989 but reference should be made to the Standard for a more detailed description.

Anchorage Category	**Minimum Safety Factor**		
	Tendon	**Ground/Grout Interface**	**Proof Load Factor**
Temporary anchorages where a service life is less than six months and failure would have no serious consequences and would not endanger public safety, e.g. short term pile test loading using anchors as a reaction system	1.40	2.0	1.10
Temporary anchorages with a service life of say up to two years where, although the consequences of failure are quite serious, there is no danger to public safety without adequate warning e.g. retaining wall tie-back.	1.60	2.5	1.25
Permanent anchorages and temporary anchorages where the corrosion risk is high and/or the consequences of failure are serious, e.g. main cables of a suspension bridge or as a reaction for lifting heavy structural members.	2.00	3.0	1.50

Figure 3. Minimum Safety Factors for Design of Individual Anchorages

It is clear from the above factors, that the recommended safety margins are quite substantial and will have a significant influence on the design and selection of the tendon and anchorage mechanism. And if no factors are stipulated by the designer (or the loading descriptions are unclear), there could feasibly be some significant differences in anchoring proposals submitted for evaluation – with a risk that underperforming anchors could be installed.

MATERIALS

This section specifically deals with the base materials associated with an anchor and specific aspects relating to corrosion protection are dealt with in the following section. The numerous codes recommend that anchor systems shall be used for which successful experience with respect to performance and durability has been documented. All materials used shall be mutually compatible and material properties shall not change during the design life of the ground anchor in such a way that the anchor loses its serviceability. BS EN 1537: 2000 does not preclude the use of newly developed materials or methods of execution provided that the performance of the anchor and durability of the materials can be proven by system tests and approved such that the serviceability of the anchor system is maintained for the design life of the anchored structure.

Tendons

In New Zealand, there is a wide variety of anchoring situations each requiring different materials. It is common to tailor the anchor to the situation with the main difference being the selection of the tendon. The following tendon options are most common in New Zealand:

Reinforcement (Grade 500)
Typically, a fully threaded reinforcing grade bar is used (e.g. Reidbar). It is most common in low stress situations or passive anchors.

Stressbar (Grade 900/1030 or 1080/1230 – Yield/Ultimate MPa)
There is a great range of diameters (16-75mm) and UTS (190-4310kN) and selection is based on application, track record, thread configuration, availability and cost. Examples include Dywidag, VSL, Macalloy and Williams. These are all stressing grade bars and are typically found in high load applications.

High Tensile Seven Wire Strand
The most familiar strand types comprise 12.9mm (0.5″) and 15.7mm (0.6″) super grade low relaxation. This strand is manufactured in accordance with BS 5896 or AS1311. Although there are slight dimensional variations between the two manufacturing standards, the strand is virtually identical from each source. Strand is typically the most economical tendon and often the most versatile due to its flexibility. Some very high capacity tendons can be produced in a relatively small drillhole.

Proprietary System Anchors
There are a number of driven or screwed anchor systems and examples include Ischebeck (combined tendon/drillrod grouted in place), Screw piles (drillrod/tendon in flight auger configuration with no use of grout), Anchorloc (driven duck-bill earth anchor using threaded rebar as tendon), Soilex (driven tendon with inflatable bag). Each anchor type can provide a suitable anchorage for certain applications, but most have relatively low load carrying capacities, do not enable stressing and offer limited corrosion protection.

Couplers

Anchors are often required to be coupled and the basic requirement is that the coupling device should be able to transmit at least 100% of the tendon UTS and that the free extension should not be impaired. Corrosion protection is to be the same as in other sections of the tendon.

Grout

When cement grout is used, the aim is to keep the water/cement ratio as low as possible whilst still allowing the grout to be pumped. A ratio of 0.4 (by mass) is practical and sometimes a water reducer or plasticiser can be added to minimise the added water. At all times, the aim is to obtain a dense grout with minimal bleed. The use of aggregate filled grouts (block fill or concrete) should be avoided as it will be very difficult to introduce into the drillhole and it is unlikely that it will encapsulate the tendon adequately creating problems with bond and corrosion protection.

In most cases, a neat cement grout will perform as expected, although occasionally the designer will specify a special grout where an environment is found to be particularly aggressive or there is a requirement for early strength gain. Any special requirement should be clearly highlighted in the specification.

CORROSION PROTECTION

It is generally recognised that the severity of ground anchor proof testing, complimented by load and creep monitoring prior to acceptance of each anchor, has provided sound indemnity from an anchor failing due to interfacial bonding (Merrifield, Barley and Von Matt, 1997). Currently, there is no such observation mechanism to provide the same insurance against corrosion induced failure and as such, this matter has long received careful attention in published codes and recommendations. The results of a FIP working group published in 1987 collected 35 case histories of anchor failure by tendon

corrosion (Littlejohn, 1987) and their conclusions are extremely relevant when establishing the corrosion protection requirements to be incorporated into a standard:-

"While the mechanisms of corrosion are understood, the aggressivity of the ground and general environment are seldom quantified at the site investigation stage. In the absence of aggressivity data it is unlikely the case histories involving tendon corrosion will provide reliable information for the prediction of corrosion rates in service.
Case histories of tendon corrosion indicate that failure can occur after service of only a few weeks or many years. Invariably corrosion is localised and in such circumstances no tendon type (bar, wire or strand) appears to have special immunity.

Since there is no certain way of predicting localised corrosion rates, where aggressivity is recognised, albeit qualitatively, some degree of protection should be provided by the designer. In this regard, the anchor head is particularly susceptible to attack, and early protection of this component is recommended for both temporary and permanent anchorages.

Choice of degree of protection should be the responsibility of the designer (usually the Client's Engineer) and such choice depends on such factors as consequences of failure, aggressivity of environment, and cost of protection. In current practice the design solution normally ranges from double protection (implying two physical barriers) to simple grout cover.

Out of millions of prestressed ground anchorages which have been installed around the world, 35 case histories of failure by tendon corrosion have been recorded. With the passage of time, lessons have been learned and standards improved which augers well for the future. There is no room for complacency, however, and engineers must rigorously apply high standards both in design and construction in order to ensure satisfactory performance during service."

It is also noted that although the record of failure is limited, it is probable that in the next decade the frequency of anchor failures will increase as anchors installed prior to the implementation of rigorous protective requirements suffer from corrosion and the reduced load capacities fail to satisfy their intended role. With the knowledge that corrosion in certain environments may be mild, the FIP working group on this matter found that there was no certain way of identifying corrosion circumstance with sufficient precision to predict corrosion rates of steel in the ground and that all steel components which are stressed shall be protected against corrosion.

The following recommendation was made for permanent anchors and has been consistently maintained in documents since the FIP report was published in 1986:

"The minimum corrosion protection surrounding the tendon(s) of the anchor shall be a single continuous layer of corrosion preventative material which does not degrade during the lifetime of the anchor."

The fundamental requirements are that the tendon of a permanent ground anchor shall be provided with either:

a) a single protective barrier to corrosion, the integrity of which shall be proven by testing of the anchor insitu.
b) two protective barriers to corrosion such that if one barrier is damaged during installation or anchor loading, the second barrier remains intact.

In their simple form, the protective barriers may take the form of a combination of plastic ducts and cement grout injection. Corrugated duct encapsulation is a common method of corrosion protection in the fixed anchor length, whilst polyethylene sheathing is generally used in the free length. The corrugated encapsulations have been tested under various loading conditions and have high load transfer capabilities without sustaining damage.

BS EN 1537: 2000 stipulates the minimum requirements for wall thickness of external corrugated ducts ranging from 1.0mm for ducts less than 80mm diameter, 1.5mm for ducts 80-120mm diameter and 2.0mm for duct diameters greater than 120mm.

The adequacy of the cement grout to provide a protective barrier depends on the method of injection, cover between duct and tendon and crack width following application of service loading. For example, a single corrugated plastic duct containing a bar tendon and pregrouted with cement grout, comprises two layers of protection provided a minimum cover of 5mm between bar and duct and crack width does not exceed 0.1mm under service loading. It can be noted that the measurement of grout crack width and duct integrity could be difficult to undertake insitu. However, there are tests available and these are documented in the Standard.

While careful attention is usually devoted to the corrosion protection of the fixed anchor length, the same level of attention also needs to be given to the free length and anchorhead locations. The most common location for failure of anchors is at the anchorhead or immediately beneath the anchorhead. Hence, an equivalent level of corrosion protection should be provided at all locations in the anchor with special attention to detail at the anchorhead.

Detailed descriptions are contained in BS EN 1537: 2000 on the various protection systems for both permanent and temporary anchors, the key factor being the verification of the competence of the system. It is important to note that great care should be taken when using predictions of corrosion rates of steel and providing sacrificial steel cross-section as a means of protection against corrosion. This method is not recognised by BS EN 1537: 2000 and it has been found that accurate prediction of corrosion rates can be very difficult. Where doubt exists, the corrosion protection system should provide the tendon independent protection from the environment, thus negating the risk associated with variances in corrosion rates.

EXECUTION

This is a huge topic in its own right and it is not possible to cover this in any detail. However, there are some important considerations which are complimentary to many of the points highlighted previously and these are noted for general information.

Drilling

There are always a number of drilling options available for a project and the selection of technique and equipment is considered on a project by project basis. Suitable equipment will be selected based on access (or lack of), headroom for rig, type of ground to be drilled, presence of groundwater, sensitivity of the environment, requirement for casing through overburden, size of drillhole required to accommodate tendon and corrosion protection measures and potential for disturbance of the ground.

It must be recognised that "drilling necessarily disturbs the ground" (FIP, 1996) and there is nothing that can be done to prevent this. A drilling technique can be selected to minimise the disturbance but there should be careful consideration of the impact of any sensitivity or remoulding effects on the existing geotechnical formations.

The accuracy of drilling will vary depending on the ground conditions and recommended tolerances are noted in BS EN 1537: 2000. This allows an initial alignment deviation of ±2° from the specified axis of the borehole and a drilling deviation of 1/30 of the anchor length. Variations in the ground or obstructions can cause the hole to deviate greater than the nominated tolerances and some relaxation may be required. Careful attention will need to be given to the combination of these tolerances for anchors installed in close proximity to each other and in particular where the layout causes them to converge.

Tendon Manufacture and Installation

It should be recognised that each tendon type requires slightly different handling to take into account weight, flexibility and overall length. Manufacture should be carried out according to well laid out

fabrication sheets which form an important part of any QA system. It is critical that the tendon manufacture is right at this stage to minimise any problems further on. There is only a limited window of time to install the anchor and the tendon configuration must be accurate to ensure this process runs smoothly. The batch references and mill certificates of steel bar and strand need to be recorded for each anchor location to verify that appropriate materials have been used. It is imperative that any corrosion protection applied prior to installation is carefully handled and protected from any damage. Sometimes cranage will be required where a tendon is heavy or long. For pregrouted bar tendons, a rigid launching frame may be required to ensure the tendon is not bent or damaged during insertion into the hole. This controlled method of installation also assists in protecting the corrosion protection system.

Grouting

Grouting is typically carried out by injecting neat cement grout at low pressure into the anchor from the lowest point. To achieve this, provision has to be made for grouting tubes to be attached to the tendon. The presence of these grouting tubes does take up space within the tendon configuration and can sometimes influence the selection of duct diameter and overall drillhole size. The successful introduction of grout and complete encapsulation of the tendon is critical to anchor performance and requires careful consideration. In general, grouting should take place as soon as the anchor is installed to minimise any adverse effects on the freshly drilled hole.

In some circumstances, additional pressure grouting of the fixed anchor length is required to enhance anchor performance, particularly where weak ground conditions are expected. This technique can enhance anchor pull-out capacity significantly and is particularly useful when anchor creep is to be minimised. This procedure is carried out after initial anchor installation and primary grouting and is known as "post-grouting." Post-grouting can be carried out several times and grout take and grouting pressure are monitored to determine when the operation is deemed complete. Post-grouting will provide different results in different ground conditions and trial testing will quickly verify whether the post-grouting operation will provide acceptable results.

Stressing

The stressing of a ground anchor needs to be carried out using accurately calibrated jacking equipment. During application of the loading, the tendon elongation is measured and the anchor is monitored for overall movement (creep) out of the ground. In some situations, the applied forces are required to be measured to accuracies of 1-2% with tendon elongation and creep measured to ±0.2-0.5mm/hr. These accuracies are very fine and in practice, it may be very difficult to isolate measuring equipment from the influences of surrounding vibrations, ground movements, temperature effects and some relaxation of tolerances may be required. Careful note should also be made of the reaction mechanism for anchor testing. Anchors impart highly concentrated loads onto structures and a suitable reaction needs to be provided. This is particularly important where full-scale pull-out tests are conducted or proof load tests are stipulated. In these circumstances, the reaction structure or surrounding ground will almost certainly deform due the applied loads and hence influence any detailed monitoring of anchor elongation or creep.

Grout strength should be verified prior to any stressing. Grout strength is measured by way of cube testing and should be at least 20-30MPa prior to testing. This strength is usually achieved in 7-10 days but it may be possible to stress sooner. It should always be understood that an anchor will have to be abandoned if testing is carried out prior to attaining design strength and a failure occurs.

Safety

Drilling rigs, tendons, stressing and congested sites present a multitude of hazards which need to be worked through. There are some tremendous forces associated with drilling and stressing of anchors and these need particular attention to ensure the risk of any incident is minimised.

In some situations, the successful performance of deep basement excavations, propped walls or support to adjacent structures depends heavily on the performance of anchors. There should be no chances taken in these circumstances as the consequences of failure are severe and only well qualified anchor systems and installation procedures should be contemplated.

MONITORING

Load monitoring is an important consideration for permanent structures where the anchoring is critical to long term performance. It can also be important for temporary or staged construction where some interim loads/movement may influence the overall design philosophy.

Monitoring can be carried out by simple centrehole jacks (e.g. for bar tendons), specially designed anchorheads and lift-off jacks (for strand tendons) or by load cells. Experience and research has shown that whilst load cells are considered to be the most accurate, very convenient and can enable remote monitoring, they are also costly and unreliable. A combination of methods seems to be present practice internationally. Monitoring also involves inspection of anchorheads for early detection of failure due to corrosion. Typically, if a structure is to be observed, the monitoring is carried out at 6 month intervals to record the pattern of results, and then extended if results are favourable. Alternatively, a small number of anchors could be monitored on a regular basis to check for any adverse trends and then scaled up or down as appropriate.

CONCLUSIONS AND RECOMMENDATIONS

Ground anchors are usually installed as critical elements of a structural support system and are normally covered over and rendered inaccessible following completion of construction. It is for these reasons that it is imperative that anchors should be well designed from the outset and executed in a manner which will ensure that the performance expectations are satisfied. If there are any problems with the anchoring system at some time in the future, it is extremely difficult to carry out repairs or replace defective anchors.

The initial designation of design loadings requires careful consideration to ensure that the loading expectations are well understood by all parties including Client, geotechnical engineer, structural engineer and contractor. A clear delineation of responsibilities in line with those presented in Figure 1 will also ensure that all aspects of the anchoring system have been considered and allowed for. While this table of design and execution guidelines has existed in various international documents since 1996, it has not always been referred to as a priority in New Zealand practice. It is recommended that more attention to the information contained in BS EN 1537: 2000 will assist to standardise the design and execution approach for ground anchor use in New Zealand.

BS EN 1537: 2000 has now been adopted throughout Europe and it seems logical that New Zealand adopt a similar philosophy in its ground anchor practice. The guidelines are relatively generic and cross references to European loading codes could readily be substituted with New Zealand code equivalents. The standard also recognised the existence of varying practices across Europe in dealing with corrosion protection and presents some simple descriptive alternative courses of action that the designer may take in providing for a corrosion protection system.

The standard contains a good balance of reasonable prescription and sensible recommendation whilst underlining the responsibility of the industry to make decisions on performance and durability based on evidence currently available. In the form of a code of practice, there is the opportunity to adapt the information to suit specific New Zealand conditions, while always being mindful of achieving an anchoring system with an acceptably low level of risk of failure. It is now up to New Zealand engineers to apply high standards both in design and construction in an accepted and unified approach in order to ensure satisfactory performance in service.

REFERENCES

BS 8081:1989 British Standard code of practice for Ground Anchorages. BSI, 2 Park St, London.

BS EN 1537:2000 European Standard for Execution of special geotechnical work – Ground Anchors.

FIP: 1996 "Recommendations for the design and construction of prestressed ground anchorages".

FIP: 1986 "Corrosion and corrosion protection of prestressed ground anchorages". Thomas Telford Ltd, London EC1P 1JH, England.

Littlejohn, G.S. (1987). "Ground Anchorages: corrosion performance". Proceedings of the Institution of Civil Engineers. Part 1, 82, pp. 645-662.

Merrifield, C., Barley, A.D. and Von Matt, U. (1997). "The execution of ground anchor works: The European standard prEN 1537". International Conference on Ground Anchorages and Anchored Structures. Thomas Telford Ltd, London EC1P.

Weerasinghe, R.B. and Adams, D. (1997). "A Technical Review of Rock Anchorage Practice 1976-1996". International Conference on Ground Anchorages and Anchored Structures. Thomas Telford Ltd, London EC1P.

APPENDIX 1

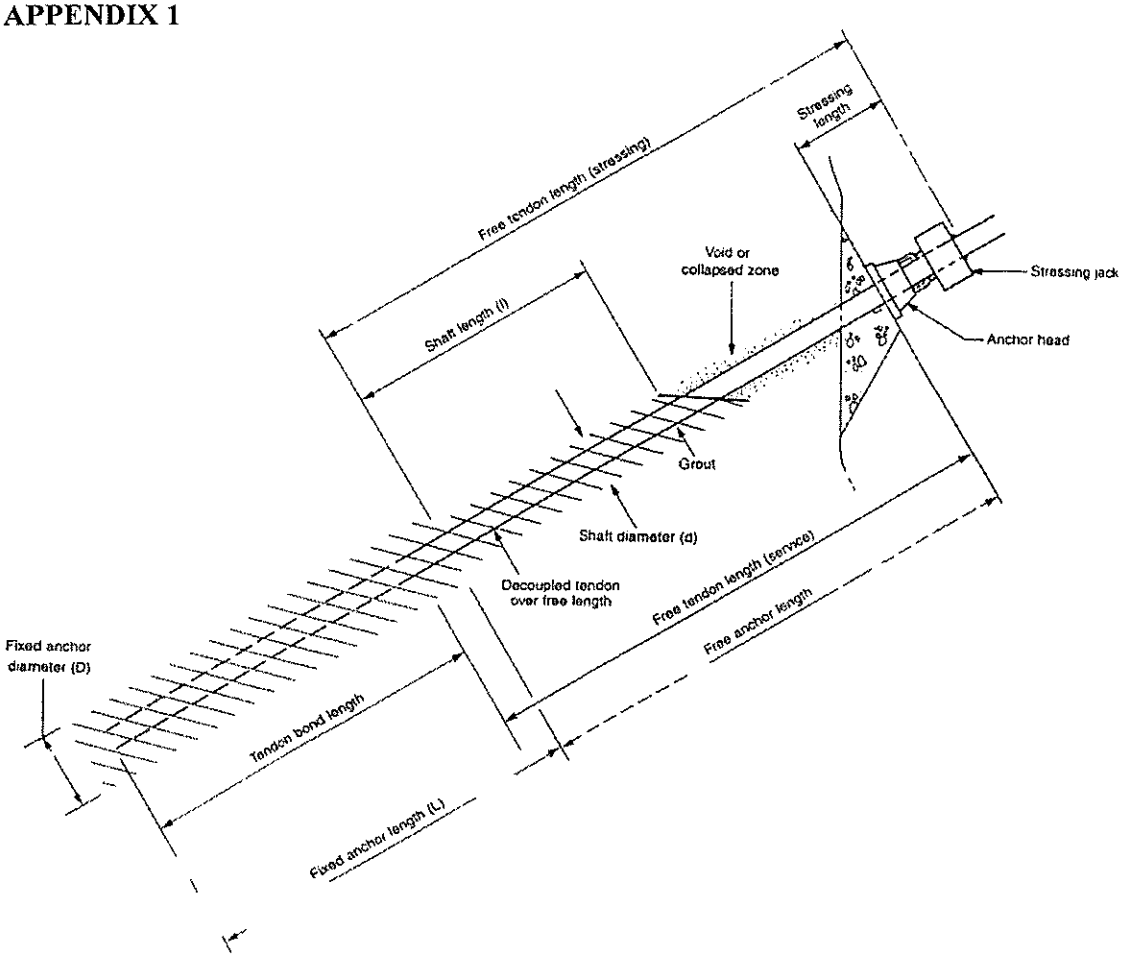

Ground Anchor Nomenclature

Geotechnical Design of a Deep Slot Excavation for the Waihi Gold Mine Crusher

E Giles
BSc (Eng) (Civil), MSAICE, PrEng
Principal, URS New Zealand Limited

Abstract: A slot of up to 20m depth was excavated at Waihi Gold Mine as part of an extension to the open pit mining operations. The slot was excavated to house a Stamler crusher and a jaw crusher that would break up ore from the pit for conveying to the extraction plant by conveyor. The subsurface location minimises operational noise. Excavation support was designed incorporating ad hoc inspections of each wall face immediately after each lift was removed. A succinct case history of the work is presented.

INTRODUCTION

As part of the Martha Mine expansion project at Waihi, a new facility was required to comminute ore brought from the pit to a grading suitable for conveyor transportation to the ore extraction facility located southeast of the township of Waihi. To satisfy resource consent conditions regarding noise, dust, vibration and other related environmental issues, the new Stamler crusher and Jaw crusher were required to be housed well below ground level. They are linked to a CVR1 conveyor.

The crusher slot required the removal of some 20.000 bcm of excavated material and was constructed in four blasting lifts from April to June 1999. Normal earthworks prior to rock blasting removed a blanketing layer of up to 10m of alluvial soils and completely weathered ignimbrite. The crusher slot has a design life of 10 years.

PSS LTD, on behalf of Waihi Gold Mining Co. Ltd undertook the project management and commissioned URS New Zealand (then Woodward Clyde) to provide design and construction support for the crusher slot. Blastronics Ltd undertook the blasting design for the slot and MacMahon Contractors Pty performed the construction.

SITE DESCRIPTION

The new facility (the Crusher Slot) is located in an area east of the planned pit extension called the Pit Facilities Area. It comprises the two areas for the crushers that are located either side of the CVR1 conveyor. The crusher slot walls were assigned the letter designation A to L, with letter I omitted. Figure 1 illustrates the crusher slot location, and wall notation.

The crusher slot was excavated in 4 main lifts. Initially, a pre-split blast was performed to the final depth of the slot to define the walls. Four blasting and excavation cycles followed to construct the slot to the final design level. The height of each lift within the main section of the slot was as follows:

Lift	Height m
1	3
2	3
3	6
4	2

Figure 1. Site Plan and Wall Numbering

PRE-EXCAVATION INVESTIGATIONS

Previous geotechnical investigations are reported by Engineering Geology Ltd., dated 19 August 1998. These investigations identified that most of the site is underlain low strength alluvium (Matua Subgroup) overlying strong welded ignimbrite (Waikino Ignimbrite). The alluvium is often overlain by both volcanic ash and mine waste. The alluvium and other softer deposits are mostly several metres in thickness, but were found the increase significantly towards the southern and western ends of the slot, where the depth to ignimbrite increased significantly. In these areas, the walls of the excavation were considered to be free of ignimbrite.

The previous investigations provided little information on discontinuity conditions and no data on the orientation of rock fractures within the ignimbrite. Core from some boreholes was available and the core was re-assembled to obtain data on recovery, RQD and joint data. These boreholes had been drilled near the deeper parts of the excavation. In addition, two shallow trenches were excavated to a maximum depth of about 2 m, primarily into the weathered surface of the Ignimbrite. In those trenches, measurements of fracture orientation, fracture persistence and parameters relevant to the fracture shear strength were obtained.

The preliminary investigations identified the dominant discontinuity sets to be continuous sub-vertical fractures and a poorly developed columnar jointing. The initial geological mapping indicated that two sub-vertical fracture sets were the most prominent, these striking NW to SE, and NE to SW.

ROCK MASS FEATURES

The high strength of the intact igmimbrite was considered sufficient to preclude failure through either the intact rock or the rock mass (a combination of rock fractures and intact rock). Accordingly, investigations and rock mass mapping focused on determining the orientation of the main fracture sets

and their shear strength. This would allow the dimensions of potentially unstable rock blocks to be determined and appropriate rock bolting patterns to be specified.

In between each excavation lift, the orientation and condition of the rock fractures exposed along each wall was recorded. The rock mass mapping allowed the rock fractures to be characterised into three main geomechanical classes, as shown in Table 1 below.

Class	Description
1	Sub-vertical fractures with extensive vertical and horizontal continuity, typically smooth and notably clay coated towards the northern end of the crusher slot.
2	A mid-angle (approx. 45 deg.) random fracture set of limited continuity (1-3 m).
3	Vertical, rough, cooling fractures of limited horizontal continuity.

Table 1: Main Geomechanical Rock Fracture Types.

The rock mass mapping data was input into the stereographic projection program DIPS for statistical determination of the main fracture set. The analysis and visual inspection of the excavation walls clearly showed that there are similar trends in the orientation of the main fracture sets across the slot.

The two Class 1 fracture sets typically strike North West to South East, and North East to South West, which was commensurate with our pre-excavation assessments. However, local variations in the attitude of these sets were apparent both with depth and laterally. In some cases these joint sets could be clearly distinguished from the hexagonal cooling joints. At others locations, these two sets could not be clearly identified and either were not present or merged with the columnar fractures defining the individual rock blocks.

Towards the southern and western sides of the slot, a more significant change in the jointing pattern was observed. Here, there was a tendency for the sub-vertical columnar joint sets to become significantly inclined.

To determine an appropriate shear strength value for use in our stability modelling, empirical criteria and published strength values were consulted. The condition of the rock fractures varied considerably. Towards the northern section of the slot, many fractures were clay coated and relatively smooth, whereas no clay coatings were observed along walls in the southern part of the slot. Where clay coatings were observed, these tended to be not continuous, and some wall to wall contact between the fracture could be seen. Accordingly, a conservative cohesion and friction value of 5 kPa and 30 degrees, respectively, were assigned to the rock fractures.

CRUSHER SLOT GEOTECHNICAL WALL DESIGN

The rock bolting and shotcrete design specified for each wall were based on the following:

- Stability of each wall after each excavation lift.
- Stability of individual rock blocks.
- Final wall stability due to static loads from trucks, retaining wall and crusher foundations.
- Final wall stability due to seismic loads of 0.2g

The support and reinforcement design was tailored to the geological conditions exposed on each wall and the likely geological conditions encountered on the next excavation lift. Accordingly, an optimal and pragmatic design methodology was obtained that also allowed rapid construction within planned budget.

The main design features of the main walls are presented at the end of the paper. However, during the slot construction, a number of design issues became more prevalent. These are discussed below.

First Lift Stabilisation

Excavation of the first 3m lift exposed very poor rock conditions along most walls, in particular the walls surrounding the Stamler Slot. Given the high truck and foundation loads to be applied at the crest of the Stamler walls, extensive ground treatment was required. Initially, an area 3m back from walls H, J and K was low pressure grouted on a 1m grid spacing. Rebar rods, 3m in length, were installed vertically into the grout holes to increase rigidity. All the excavated walls were cleaned with air and water flush to remove clay coatings from the fractures and loose debris, thus allowing improved adhesion of the shotcrete.

Given the relatively small rock block size of the poor quality ignimbrite, rock bolting alone would have been insufficient to capture all the blocks. Accordingly, it was decided to first shotcrete the walls and then bolt through the shotcrete to hold back any loose blocks. Initially, a layer of fibre reinforced shotcrete, 80mm thick, was sprayed over all the walls. Bolts ranging in length from 6m to 2.2m long split sets were installed in 3 consecutive rows. The first lift was completed with a final 80mm thick layer of fibre reinforced shotcrete. The shotcrete was also sprayed over the crest by about 1m.

Wall Stability Assessment

Observations of the fracture orientations and analysis of the rock mass mapping data showed that for most walls, the fracture orientations are favourable for stability. That is, the fractures do not form kinematically admissible rock blocks.

However, the analysis of data obtained from the first lift mapping identified several major fracture sets striking sub-parallel to walls F, H and the wall forming the corner of D-E. Accordingly, the rock bolting design was based on maintaining a sufficient margin of stability should these features daylight near the base of the wall on the final lift. This was considered to be the worst case scenario. Furthermore, consideration was given to the loads applied from trucks, retaining walls and earthquake events, on any kinematically admissible rock blocks, where they were appropriate.

In our preliminary stability assessment, the program UNWEDGE was used to identify and analyse the stability of rock blocks (wedges) defined by blocks siding on two planes. As the excavation proceeded, observations of the rock block geometries suggested that a simpler and more versatile analysis method was appropriate. A spreadsheet solution was developed for plane sliding, which allowed analysis of multiple bolts and external loads. The stability solution is based on that provided by Hoek 1999.

The stability assessment assumed the following:

- The shear plane is continuous, planar and daylights at the base of the wall.
- 3m and 6m long bolts have a maximum working capacity of 12 tonnes.
- Split sets do not improve the global stability of the slope.
- 3m and 6m long bolts have an ultimate capacity of 18 tonnes and this value is appropriate for seismic loading conditions.
- Truck loads and seismic loads are not applied concurrently.
- Bolts do not increase the cohesive strength of the shear surface.
- The shear surface is adequately drained by drain holes.

These spreadsheet figures have been calculated to show the loads on the bolts that give the required factor of safety. Both static and dynamic loading conditions were considered and the assumed working and ultimate capacity of the bolts were not exceeded. The design criteria for the walls are as follows:

- Normal static loads for critical walls: Factor of Safety =1.5
- Normal static loads for non-critical walls: Factor of safety = 1.2
- Seismic loads for critical and non critical walls: Factor of Safety = 1.2

All the walls of the Stamler slot are considered critical walls. During construction of the third lift, a significant overbreak occurred on the corner wall D-E. This damage required special support measures to be instituted. This included work undertaken by a separate contract to backfill voided space using a foam filler behind temporary shuttering. This was a preferred option to further blasting with the risk of additional damage.

The normal static loads are everyday working loads with one truck fully laden unloading into the Stamler slot.

For walls where the fracture sets do not allow kinematic admissibility of large scale blocks, bolting and shotcrete was applied to ensure local rock block stability.

Example sheets for the third lift of Walls F, G, J and K are given in Appendix A to illustrate the ad-hoc support specification made progressively during the excavation.

WEEP HOLES

The crusher slot excavation acts as a natural sump for local surface and groundwater flows. After heavy rainfall water, water flows from rock fractures were most prevalent on walls on the eastern side of the slot. To relieve the possible build up of water pressures behind shotcrete linings, weepholes were drilling at regular spacings (typically at 5 m centres horizontally on 3m vertical diamond staggered grid lines) around the slot. Some periods of significant flow from the holes have since been observed after heavy rainfall.

The weepholes adequately control the infiltration and pore pressure build-up is avoided.

CONSTRUCTION ASPECTS

Pre-Split over full depth

Civil design constraints regarding the unloading of ore into the Stamler crusher required tight tolerances to be met on the face of the excavation. Perimeter rock damage was limited by using smooth blasting techniques. In this instance, because rock support had to be installed as the depth progressed, a pre-split method was used.

Rock Clearing

Over parts of the excavation, the rockmass was quite blocky. Use of excavators or other mechanical plant had to be rigourously controlled so that scaling and barring down did not generate overbreak and local instability problems near the two main plant items. Split sets and thicker shotcrete applications were employed to assure the integrity of the rockmass and to keep the required tight vertical control. Away from the two crushers, the rock slopes could be battered back in some instances.

Rock Handling

Rockmass quality was variable. Generally, fragmentation was satisfactory and the large mechanical plant available could accommodate removal of large blocks. It was necessary to limit the blast energy to balance removal economies and rock wall quality as well as shotcrete integrity.

Shotcrete Application

A wet mix application was used. Emphasis was placed on the quality of the shotcrete materials supplied and on the application methods. Some early trial mix variations were required to address balling of the steel fibres. Repetitive washing of the walls was necessary in some locations to remove organic and other materials and create acceptable conditions for rock-shotcrete bonding. The extra

effort proved valuable as careful checking did not reveal any patches of unbound shotcrete and the difficult task of removal of steel fibre reinforced shotcrete and obtaining an integrated was avoided.

A concern on commencement of the work was the effect of subsequent blasts on shotcrete support immediately above the lift being prepared. Again, the rigourous control of the blast dynamics and of the shotcrete application appeared to be most beneficial as no integrity issues arose and no discernible damage was found.

CONCLUSIONS

The Crusher Slot was successfully excavated without any time loss incident. The use of very large mechanical plant for material removal and for charge hole and support drilling enabled a fast-track process to be achieved. This was balanced by the more measured production rate during careful blasting, scaling down of loose material and preparing surfaces for and applying shotcrete. The overall rate of progress was good.

The blend of a civil-mining contractual approach facilitated the refinement and optimisation of the design as the excavation progressed as outlined earlier. Each wall could be optimised based on exposed rock conditions and in this way, the limited required life of 8 years could be considered as work progressed without loss of overall safety assurance.

ACKNOWLEDGEMENTS

The approval of Newmont Waihi Operations to publish this paper is gratefully acknowledged.

APPENDIX A

WALL F: Strikes East-West

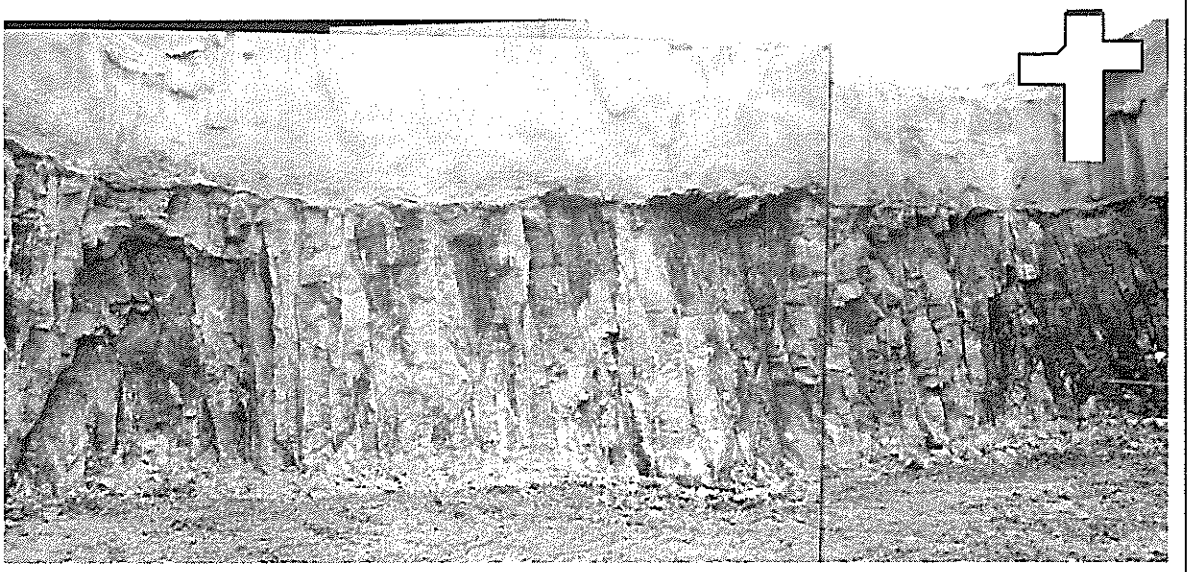

Wall F on third lift

Description

- Class 1 fractures daylighting and striking sub-parallel to wall.
- Fractures infilled with soft organic clay > 10mm in places.
- Paleao-gulley exposed on first lift.

Design Considerations

- Potential for steeply dipping wedges to cause significant overbreaks.
- Potential for significant wedge or planar type failure of entire wall.
- Stability of wall under seismic loads

Reinforcement & Support Specified

LIFT	Fibre Reinforced Shotcrete	Reinforcement
1	160 mm	1 row of 6m bolts @1.5m centres 1 row of 3m bolts @1.5m centres 1 row of split sets @1.5m centres Bolts orientated downwards at 5°.
2	100mm+	1 row of 6m bolts @ 1.5m centres 2 rows of 2m bolts @ 1.5m centres Bolts orientated upwards at 15°
3	50mm +	3 rows of 3m bolts @ 1m centres Bolts orientated upwards at 15°
4	50mm	2 rows of split sets @ 1.5m centres

WALL G: Strikes North-South

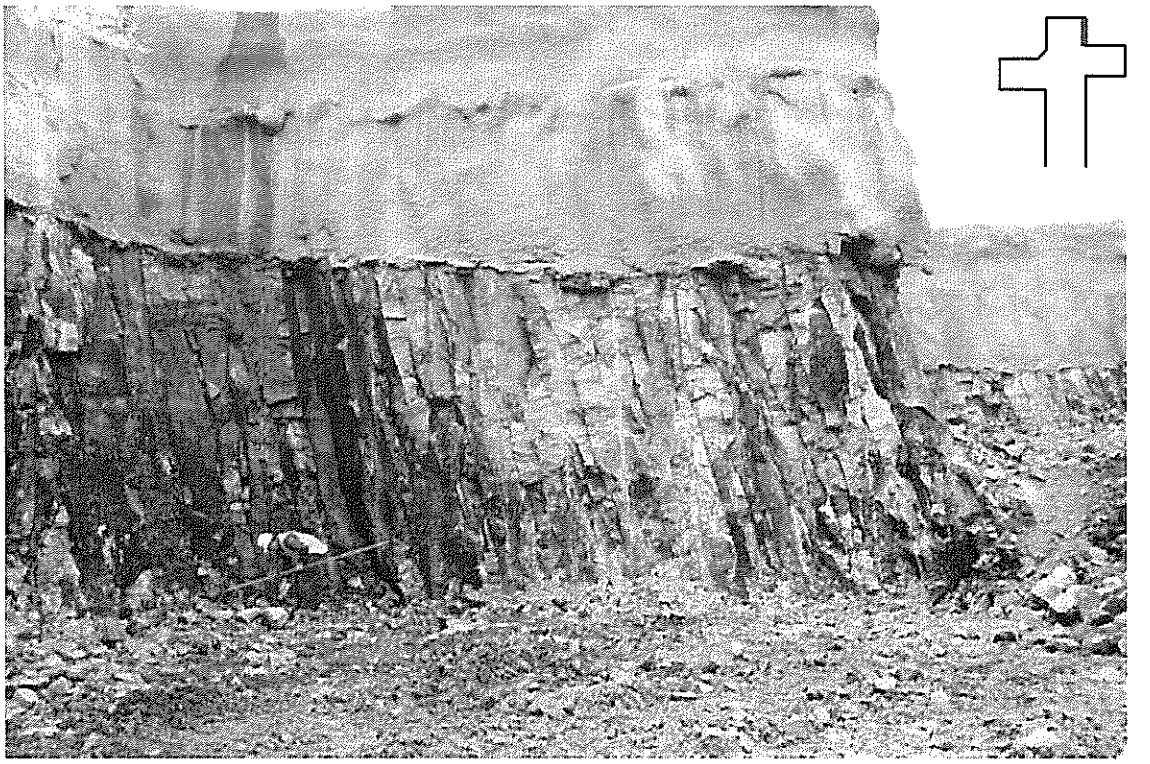

Wall G on third lift

Description

- Highly fracture rock mass on 1st lift
- Major fractures striking perpendicular to wall
- Fractures infilled with soft organic clay

Design Considerations

- Isolated rock block stability required
- No potential for major kinematically admissible instability.

Reinforcement & Support Specified

Lift	Fibre Reinforced Shotcrete	Reinforcement
1	160 mm.	1 row of 6m bolts @1.5m centres 1 row of 3m bolts @1.5m centres 1 row of split sets @1.5m centres Bolts orientated downwards at 5°.
2	100mm+	2 rows of Split Sets @ 2m centres Bolts orientated downwards at 5°.
3	50mm+	2 rows of 3m bolts @ 2m centres 1 row of split sets @ 2m centres Bolts orientated downwards at 5°.
4	50mm	None

WALL J: Strikes East-West

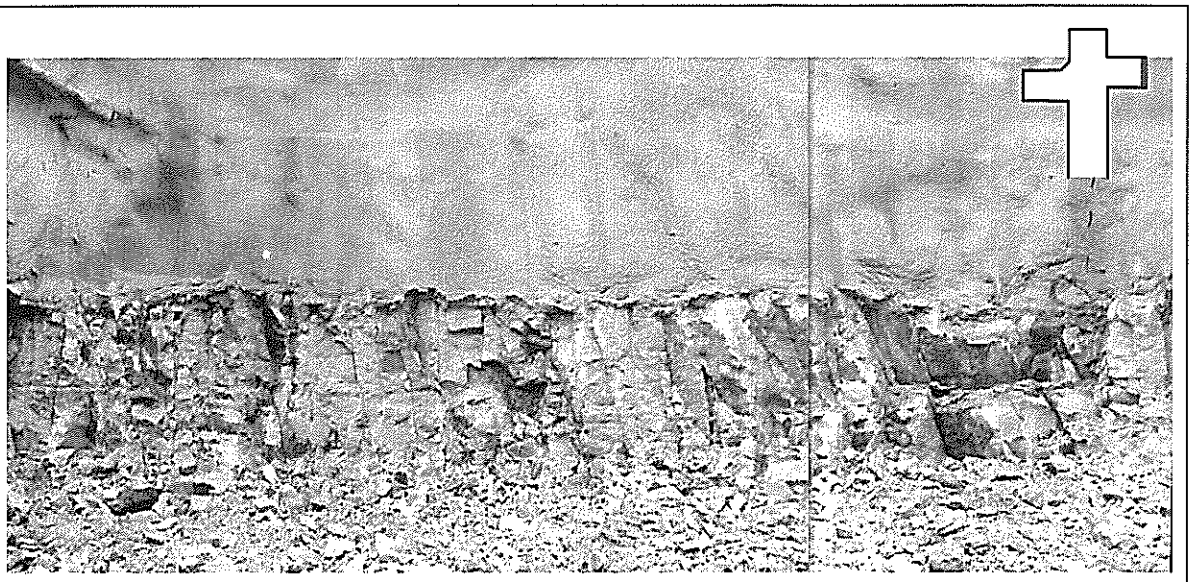

Wall J on 3rd lift

Description

- Highly fractured rock mass on 1st lift.
- No adverse fracture orientations observed.

Design Considerations

- Influence of truck loading on stability.

Construction Considerations

- Extensive grouting and reinforcement installed around crest of slope.

Reinforcement & Support Specified

Lift	Shotcrete	Reinforcement
1	Total of 160 mm applied in 2 layers pre and post bolting.	1 row of 6m bolts @1.5m centres 1 row of 3m bolts @1.5m centres 1 row of split sets @1.5m centres Bolts orientated downwards at 5°.
2	80mm + 50mm	3 rows of 3m bolts @ 1.5m centres Bolts orientated downwards at 5°.
3(i) (2m)	50mm+	2 rows of 3m bolts @ 1.5m centres Bolts orientated downwards at 5°.
3(ii) (2m)	50mm	1 row of 3m bolts @ 1.5m centres Bolts orientated downwards at 5°.

WALL K: Strikes North – South

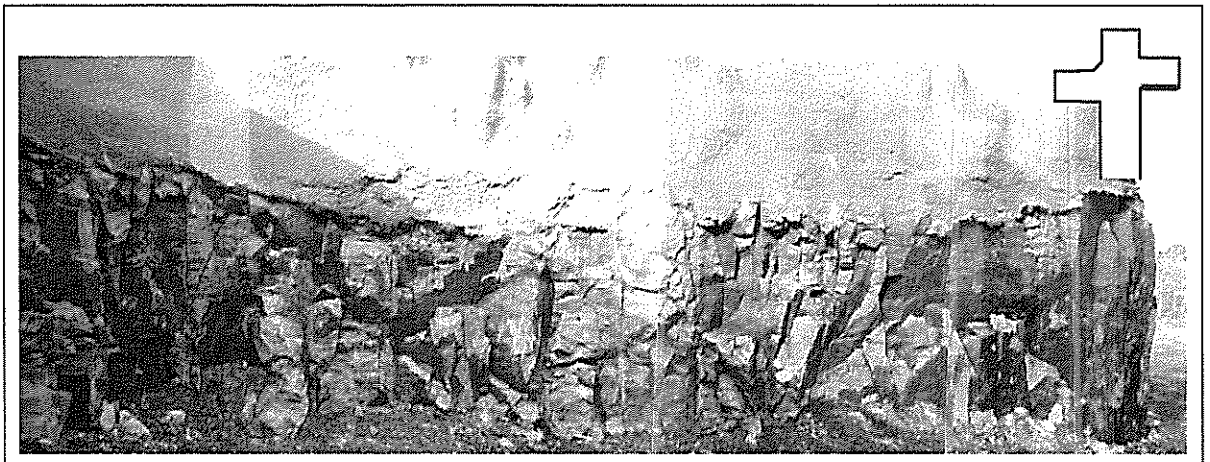

Wall K on 2nd lift

Description

- Highly fractured rock mass on 1st lift
- Major fractures dipping into slope

Design Considerations

- Influence of truck loading on stability

Construction Considerations

- Extensive grouting and reinforcement installed around crest of slope.

Reinforcement & Support Specified

Lift	Shotcrete	Reinforcement
1	Total of 160 mm applied in 2 layers pre and post bolting.	1 row of 6m bolts @1.5m centres 1 row of 3m bolts @1.5m centres 1 row of split sets @1.5m centres Bolts orientated downwards at 5°.
2	80mm + 50mm	3 rows of 3m bolts @ 1.5m centres Bolts orientated downwards at 5°.
3(i) (2m)	50mm+	2 rows of 3m bolts @ 1.5m centres Bolts orientated downwards at 5°.
3(ii) (2m)	50mm	1 row of 3m bolts @ 1.5m centres Bolts orientated downwards at 5°.

Settlement of Intake Structure, Meghnaghat Power Station

M Aravind
BE (Hons) MS CP Eng MIEAust
Senior Geotechnical Engineer, Sinclair Knight Merz, Auckland

Abstract: The design and construction of the Meghnaghat 450MW Combined Cycle Power Plant in Bangladesh is being undertaken by Hyundai Engineering and Construction Company Ltd (HDEC). The owners of the Power Plant are AES Meghnaghat Private Limited (AES).

This paper presents interesting design and construction geotechnical issues associated with the Cooling Water Intake Structure (CWIS).

The construction of the CWIS for the Power Plant commenced in early 2001. The CWIS was subjected to differential settlement due to adjacent construction activity and resulted in some cracking on the walls. In response to concerns over the long term settlement and serviceability of the structure, the construction sequence of the CWIS and its response to various loadings and groundwater conditions with respect to the subsurface profile was analysed using the latest version of the commercially available finite element program PLAXIS. The various components of the structure and the cooling water pipes were modelled as beam elements with defined elastic properties. The stresses in the structure and future settlement estimates were obtained from the finite element models.

The analysis demonstrated that further settlement will be negligible under normal operating conditions and therefore the proposed installation of an expensive expansion joint would not be required for the continued safe operation of the facility. The settlement monitoring data to date would seem to support the conclusions of the analyses presented in this paper

INTRODUCTION

A 450MW Combined Cycle Power Plant is being constructed by Hyundai Engineering and Construction Company Limited (HDEC) on an existing 28-hectare reclaimed platform located in Meghnaghat, 22 kilometres south of Dhaka, Bangladesh. HDEC have employed Sinclair Knight Merz (SKM) as their geotechnical sub-consultant to design foundations and address various construction related geotechnical issues on site.

This paper discusses the geotechnical works carried out by SKM for the above project which included an assessment of the settlement of the Cooling Water Intake Structure (CWIS). Finite element modelling was used to assess the settlement of the CWIS and the stresses on the Cooling Water pipes that formed an integral part of the CWIS. HDEC proposed the introduction of a coupler in the Cooling Water pipes to release any stress built up in the pipes as a result of differential settlement of the CWIS.

The CWIS is sited on the banks of the River Meghna at the edge of the reclaimed platform for the power plant and essentially comprises a reinforced concrete base slab some 14 m below ground level with reinforced concrete walls which support the pumps and other ancillary mechanical and electrical equipment. Two large diameter (2.1 m) concrete intake pipes are rigidly supported by the CWIS and transfer water from the CWIS to a larger diameter Cooling Water Pipe (CW3) which is located approximately less than 10 m away from the CWIS. Subsequent to the construction of the CWIS and the Cooling Water Pipes, additional site works in the area involved the driving of steel sheet piles to form the river inlet structure. The plant general arrangement is presented in Figure 1. Vibrations during installation of the sheet piles and the subsequent excavation activities resulted in differential settlement of the CWIS, inducing stresses in the transfer Pipes and resulting in minor structural cracks in the CWIS walls.

SITE DESCRIPTION

The Power Plant site is located on a 100 Ha reclaimed platform connected to the mainland by a causeway that is approximately 800 m long. The reclaimed platform is a hydraulic fill of silty sands and sandy silts, which were dredged from the riverbed. The final platform elevation of RL + 7.8 m PWD has been designed to be above a 1 in 200 year flood level with a freeboard of about 0.5 m. (Reference SKM Reports, 2002)

The area around the reclaimed platform was earlier used for agricultural purposes (paddy field) with an average of about one harvest per year before the monsoon season. The average river level during the non-monsoon season is about RL + 4 m PWD that rises to about RL + 5 m PWD during monsoon season. Extreme water level from a 1 in 100 year return flood event is about RL +6.5 m PWD.

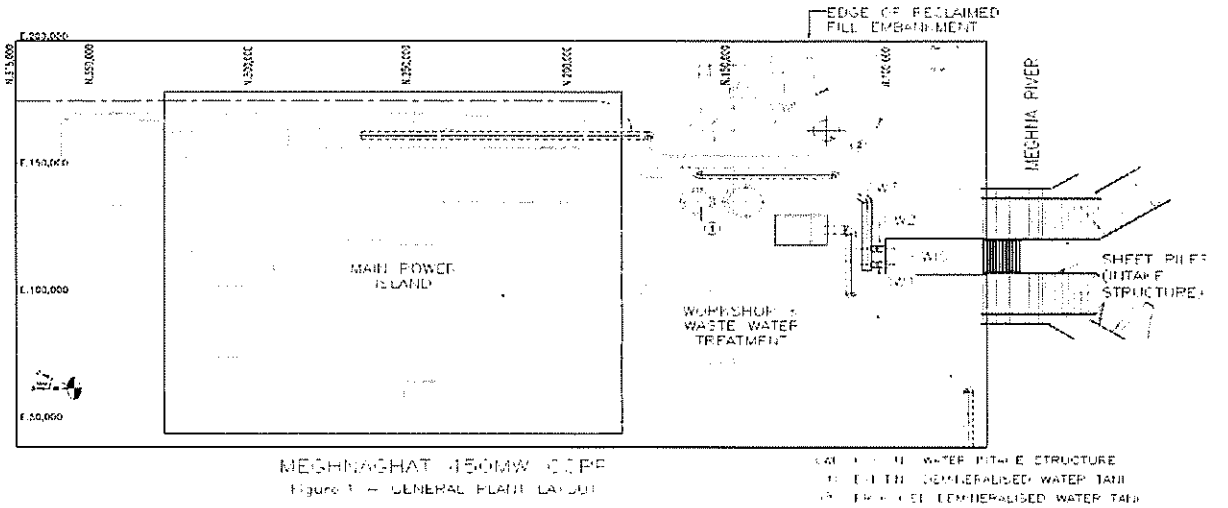

Figure 1. General Plant Layout

SITE GEOLOGY

Bangladesh is situated below the southeast foothills of the eastern Himalayas, where a number of major rivers (Ganges/Padma, Jamuna/Bhramaputra, Meghna) drain northern India, Nepal and Bhutan. During the monsoon months of June to October, the majority of Bangladesh is subjected to floods considered extreme by the standards of most other countries. During this period, huge volumes of sediment are eroded from the Himalayas and foothills, before being deposited in the lower energy alluvial environment of the Bangladesh lowlands. As a consequence, much of southeastern Bangladesh (including the Meghnaghat site) may be considered a giant river delta.

The geology of Bangladesh consists primarily of Pleistocene to Holocene aged deltaic alluvial sediments with an average thickness of about 180m in the northwest and thickening to the southeast where the Meghnaghat site is located. In eastern Bangladesh, the basement rocks are estimated to lie more than 3,000 m below mean sea level. The alluvial sediments consist of an alternating sequence of sands and silts, the recent sediments being predominantly flat bedded. Much of the sediments contain abundant quartz grains and a minor to moderate component of mica. The minerals owe their origin to the predominantly schistose and quartzose rocks of the Himalayas.

The upper sediments tend to be loose and normally consolidated. This combined with the common occurrence of high groundwater level present a potential for liquefaction during earthquake shaking. Large liquefaction events have occurred in the region in the recent past.

PROJECT BACKGROUND

The construction of the Cooling Water Intake Structure (CWIS) for the Power Plant commenced in early 2001. During installation of the CWIS equipment, it was observed that the CWIS had settled between 40 mm to 100 mm along the length of the structure. The differential settlement had resulted in the cracking of the CWIS walls. SKM assessed the geotechnical conditions at the CWIS and studied the causes, mechanism and implications of observed settlements on the structure. Figure 1 presents the general plant layout.

The Studies by SKM on the performance of the CWIS structure identified the various causes likely to have resulted in the settlement of the CWIS as being:

- Long term de-watering activity around the CWIS;
- Use of a vibro-hammer for the installation of sheet piles to the inlet structure;
- Construction and backfilling earthworks around the temporary excavation for the CWIS;
- Self weight of the CWIS and the dead weight from plant and equipment.

These studies concluded that the settlement was expected to reduce significantly upon completion of construction and dewatering activities and that no specific measure was recommended for reducing or mitigating long-term settlement of the CWIS.

In addition to this geotechnical assessment a structural analysis was carried out to:-

- Identify the primary cause of cracking to the North wall.
- Evaluate the integrity of the cracked wall and Cooling Water Pipes.
- Present recommendations for the repair and restoration of the North Wall and the Cooling Water Pipe.

The results of the structural analysis indicated that the cracking pattern on the North wall was a consequence of the tension developed in the cooling water transfer pipes when the CWIS settled.

SUBSURFACE CONDITION

In addition to the available geotechnical information, additional boreholes and Cone Penetration Testing (CPT) was carried out in the vicinity of the CWIS to assess the subsurface profile of the site. The CPTs indicated the presence of a very loose to loose zone of sands and silty sands on the southern side of the CWIS, where it abuts the sheetpile wall. The investigation revealed that the extent of loose soil was confined to the southern portion of the CWIS where the combination of sheet piling and earthworks may have resulted in some localised piping.

This loose zone comprised a very loose to loose sand and silt approximately 2 m thick fromelevation RL -8 m to RL –10 m. Typical SPT N values were in the range of 2 to 7 blows per 300 mm penetration and cone tip resistance, q_c, values between 0.6 to 2 MPa (this equates to a relative density range 10% to 30% - Reference Bowles, 1988).

The base of the CWIS is at RL –7.2 m PWD. The upper 3 m of Alluvium below the structure, Q_{al2} is assumed to be disturbed on the northern side of the CWIS and a naturally occurring weak / loose layer near the southern portion of the structure. The assumed ground conditions are summarised in Table 1.

Geological Unit		USCS	Depth m ± PWD	Description
Reclamation Fill	RF	SP/SM	+8.0 to +1.0	Medium dense, fine to medium poorly graded sand, minor silt
Alluvium	Qal_2	SM	+1.0 to –7.0	Loose to medium dense silty sand
Alluvium	Qal_2	SM	-7.0 to –10.0	Very loose to loose pocket (south)
Alluvium	Qal_2	SM	-7.0 to –10.0	Loose – Med dense silty sand (disturbed)
			-10.0 to –20.0	Medium dense silty sand (undisturbed)

Table 1 – Assumed Ground Conditions for CWIS

GEOTECHNICAL MODEL

Representative geotechnical parameters for the soil types are presented in Table 2.

Geological Unit		Bulk Density	Cohesion	Friction Angle	Modulus	Unload-Reload Modulus
		kN/m^3	kN/m^2	Degrees	MPa	MPa
Reclamation Fill	RF	20	5	40	16	48
Loose Alluvium	Qal_2	19	4	37	13	39
V Loose Alluvium (south)	Qal_2	18	2	30	4	12
Loose –Medium Dense Alluvium	Qal_2	19	4	38	7	81
		19	4	38	27	81

Table 2 – Geotechnical Parameters for the CWIS

The geotechnical parameters were selected based on available geotechnical data, previous laboratory test results and field observations. The groundwater levels were monitored from existing piezometers near the CWIS site and river levels were recorded by HDEC.

GEOTECHNICAL ASSESSMENT

General

The response of the CWIS and the underlying ground to the fluctuations in groundwater level and construction activity were analysed using a commercially available finite element program, PLAXIS.

The various components of the structure and the cooling water pipes were modelled as beam elements with defined elastic properties. The subsurface profile was modelled using the 'soil-hardening soil model' option in the program, which is an advanced model for simulating the elastic and plastic behaviour of soils to model variable stiffness and irreversible plastic strains under the defined loading conditions. The dynamic effects of sheet piling and other construction activities were not considered in the finite element model.

The finite element model was constructed to include the very loose to loose layer of sands and silts in the southern portion of the CWIS. A beam element was included to model the two cooling water pipes (CW1 and CW2). This finite element model was then modified with a hinge feature to assess the effect of cutting the existing pipe and incorporating a flexible coupling or expansion joint in the cooling water pipes.

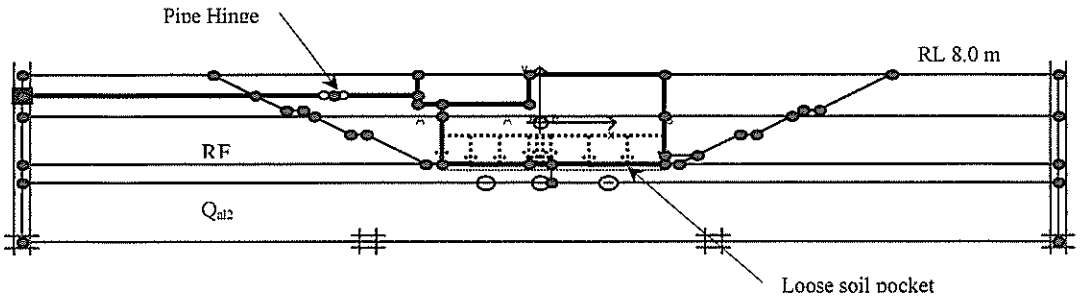

Figure 2: Finite Element Model with Cooling Water Pipe and Hinge (N-S)

Performance of the CWIS

The settlement from the finite element model predicted an approximate total settlement of 100mm of the CWIS base slab at the riverside of the structure and approximately 50mm on the plant side. This was in general agreement with the measured settlement values.

The PLAXIS model also indicates that in addition to the total settlement of the structure, some rotation and translation of the structure has occurred. The rotation and translation of the CWIS is attributed to the presence of the very loose to loose sands and silts on the southern side of the structure. The translation and rotation of the structure imposed additional stress on the Cooling Water transfer pipes, which were rigidly built with the walls of the CWIS.

The measured values of settlement were slightly greater than those assessed from the finite element model, which may be the result of the additional construction effects not modelled (vibrations from sheet piling). In addition to the vertical deformation, a horizontal translation of about **30 mm** was modelled on the northern side as a result of the differential settlement of the bottom slab. Therefore, the Cooling Water pipes CW1 and CW 2 are carrying some load from the CWIS.

In order to release the additional induced stresses in the Cooling Water pipes, HDEC proposed the construction of an expansion joint between the main Cooling Water Pipe, CW 3, and the CWIS. The finite element model was altered to include a hinge in the Cooling Water pipe to simulate the construction of an expansion joint in the pipe. The settlement of the CWIS base slab increased by less than 10 mm on the plant side of the structure and less than 5 mm on the river side of the structure. In addition to the vertical deformation, additional horizontal translation of about 10 mm was identified as a result of the increased differential settlement over the bottom slab.

Typical profile of the vertical deflection near the CWIS is presented in Figure 3.

Future Performance of the CWIS

The finite element model was modified to study the effect of long term settlement and creep deformations. The results of the analyses indicated that most of the settlement occured almost immediately after construction with insignificant long-term consolidation or secondary compression (creep) movements.

However, several factors would have an impact on settlement and performance of the CWIS, these include:

- Plant Vibration: The vibrations from plant and equipment in the CWIS, like the intake pumps, could induce some settlement of the saturated sands under the CWIS. This is hard to quantify without some measure of the vibration loading applied;

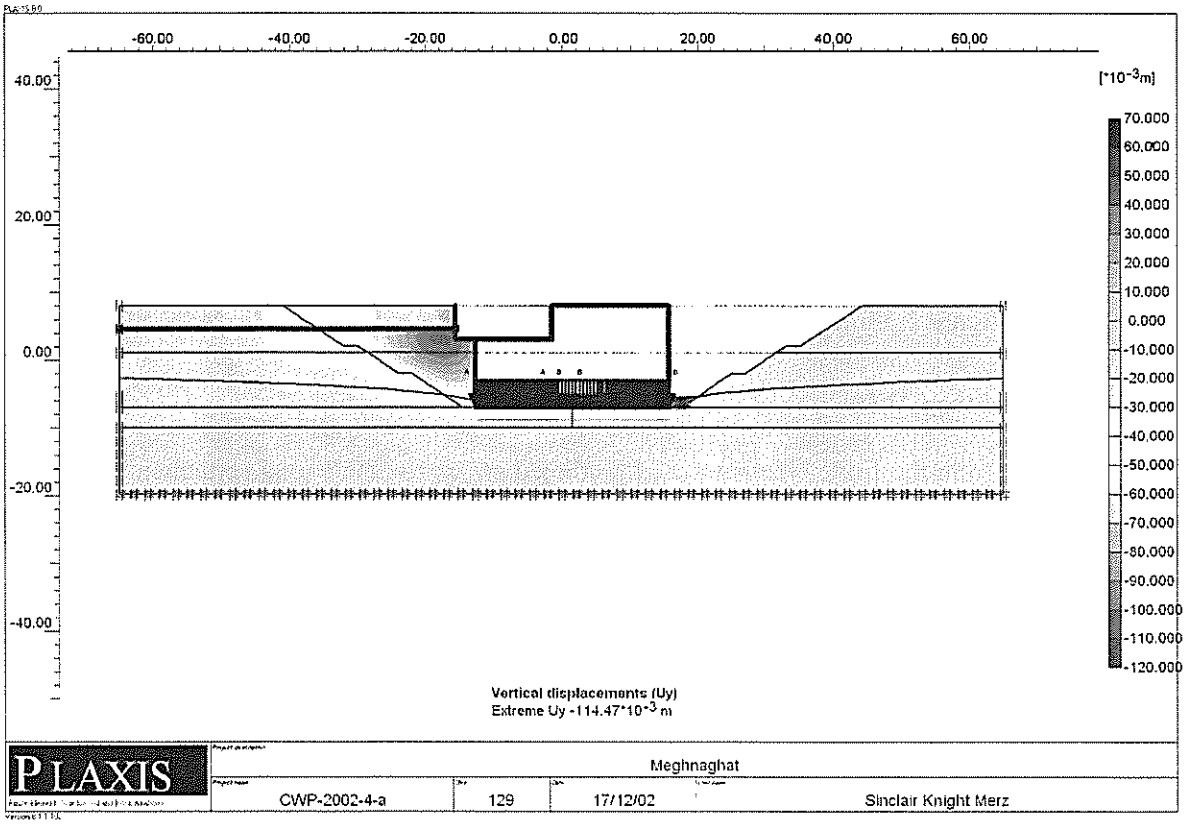

Figure 3: Typical Displacement Patterns near the CWIS

- Unusual change in ground water conditions: Extreme water levels affecting the structure were assumed at an elevation of RL 0.0 m (low) and RL 6.0 m (high). Groundwater level variations beyond this range are highly unlikely, but will have an impact on the settlement and performance of the CWIS;
- Seismic activity: Extreme seismic activity will have an adverse affect on the performance of the CWIS, such as liquefaction induced settlement, and has not been considered in the present analysis;
- De-watering in the vicinity of the CWIS: Construction of the sheet pile wall and dewatering had a significant impact on the settlement of the CWIS. Similar activities in the future could affect the CWIS;
- Cooling Water Leakage: This could create seepage paths and ground deformation as a consequence of ground support or material "wash-out" in a piping type of failure mechanism.

CONCLUSION

The stress state of the Cooling Water pipes assessed from the two dimensional finite element model is only our best approximation because of the three dimensional nature of the problem. However, the model does provide indicative stress levels for the given load conditions. The maximum bending moment in the Cooling Water pipe in its presently stressed condition is likely to be in the order of 3,000 to 6,000 kNm. These values are well within the structural capacity of the pipe. In any event, we are of the opinion that the stress developed will not be "locked-in" to the pipework since there will have been some release from the passive deformation of the pipe backfill and the cracking in the wall,

both of which have already occurred. Provided no further significant movement of the CWIS occurs, the stresses in the pipe are unlikely to increase.

As expected, the introduction of a hinge increased the settlement and rotation of the CWIS. Introducing an expansion joint would release whatever stresses in the Cooling Water pipe. Ignoring the disturbing effects of the construction procedures required to install the coupling, we estimate the settlement in the CWIS resulting from the introduction of the expansion joint is likely to be in the order of 5 mm to 10 mm.

The provision of an expansion joint or flexible coupling will limit the future development of stress in the Cooling Water pipes should additional settlement occur in the CWIS. However, it was demonstrated that further settlement will be negligible under normal operating conditions and therefore the expansion joint would not be required for the continued safe operation of the facility.

The settlement monitoring data to date supports the conclusions of the analyses presented in this paper. Subsequent to the completion of construction activity near the CWIS, the settlements over a period of six months were negligible (< 5 mm).

REFERENCES

Ansary M A and Rashid M A. "Generation of Liquefaction Potential Map for Dhaka, Bangladesh", Department of Civil Engineering, BUET, Dhaka-1000, Bangladesh, published on the University Webpages.

Bowles J E. (1988). "Foundation Analysis and Design", 4th Edition, Published by McGraw Hill.

Kumar J and Mohan Rao. (2002). "Seismic Bearing Capacity Factors for Spread Footings", In Geotechnique 52, No 2, pp.79-88.

NAVFAC Design Manual 7.02. (1986). "Foundation and Earth Structures", September 1986.

SKM Reports (2002). "Settlement of Cooling Water Intake Structure", Feb 2002; "Cracking of Cooling Water Intake Structure", March 2002.

Terzaghi K and Peck R B. (1967). "Soil Mechanics in Engineering Practice", 2nd Edition, Published by John Wiley and Sons.

Tomlinson M J. (1996). "Foundation Design and Construction", 6th Edition, ELBS Longman Publication.

Nonwoven Fabrics for Environmental Applications

M Bindra
MTech, MBA, MIPENZ, Regd Engr
General Manager, Permathene Ltd

Abstract: This paper presents a new technique of using Nonwoven Polypropylene Geotextile as opposed to the standard woven weed matting on the embankments for erosion and weed control applications. By incorporating nonwoven geotextile as an erosion and weed control material, soil erosion and vegetative detachment were greatly reduced. The geotextile provided an additional shear strength to the vegetative and soil structures, allowing large volumes of water to percolate into the ground, which resulted in the rapid growth of the vegetation.

At one site, some of the results were not acceptable due to the early break down of the geotextile. Tests were conducted to analyse the cause and concluded that the fabric must contain carbon black and sufficient UV inhibitor to perform well. The fabric can be engineered to last for a specific period say from 3 – 24 months.

INTRODUCTION

New Zealand is a very young country with few inhabitants. Since 1910 did it have over one million people, and today just less than 4 million. Although it does not have the pressures of overpopulation, it nonetheless suffers the ill effects of over exploitation. The country is world renowned for its "greenery" natural beauty and healthy agricultural products. Its economy is based largely on the energy from the soil. Due to treacherous terrain and previous exploitation, soil erosion of the land has become a major problem.

Thousands of hectares of land have vegetation removed or are laid bare each year around the main cities in New Zealand for construction purposes. Scientists estimate the loss of soil in New Zealand, through erosion and transport by rivers to the sea at 400 million tons per year. It arises mainly from the 22 million hectares of cultivated land, averaging 18 ton per hectare or 10-20 times the rate of natural soil formation. Without protection measures, the transformation of this land can result in accelerated on site erosion and greatly increased sedimentation of waterways, estuaries and harbours.

In addition to the soil erosion, a major objective of landscape maintenance programs is the suppression or elimination of weeds. Owing to Auckland's moist temperate climate, the city is often referred to as "the weed capital of the world". Weeds are controlled in landscapes using cultivation, hand weeding, organic and inorganic mulches, herbicides and physical barriers (black plastic and geotextiles) and various combinations of these methods. Each method has advantages and disadvantages.

Various techniques are used for erosion control applications from top soiling, revegetation, temporary & permanent erosion control blankets to runoff diversion channels, contour drains, hard and soft armor materials. The majority of the weed control fabrics used are heavy-duty woven polypropylene fabrics over 100 g/m^2 and they are superior to other ground covers available in the country.

In this paper a nonwoven polypropylene geotextile was used as a weed and erosion control fabric and was successful on most of the sites. The sites under consideration had mostly clay overlaying silty clay subsoil, which exacerbates the moisture problems. The fabric was laid and not covered with mulch but the predominantly smaller NZ native shrubs were planted at close intervals in order to cover the whole surface in 12 months time.

DESIGN

Based on the literature review and current applications, Permathene Ltd recommended Syntex 401 135 g/m² polypropylene nonwoven geotextile to be used for the erosion control and weed control application for the projects under review. Polypropylene is a very durable polymer commonly used in aggressive environments including automotive battery casings and fuel containers among other applications.

It was recommended to plant vegetation by making slits in the geotextile so that at a later stage it should provide the shade to the geotextile and reduce the UV light degradation. Due to the superior puncture and mullen burst strength, a 135 g/m² nonwoven geotextile is very resistant to the installation stresses.

Location

The two projects under review covered earthworks and some additional works for the following sites:

- New East Tamaki Arterial Route (ETCART) from Cavendish Dr. through to Orlando Dr. in Manukau City
- Slope Stabilization at Mayfair Retirement Village, Browns Bay, Auckland

Geotextile material

Syntex 401 polypropylene needle punched nonwoven geotextile manufactured by SI Corporation, USA

PROPERTY	TEST METHOD	TYPICAL[2] VALUES
Physical		
Mass per Unit Area	ASTM D5261 ISO9864	135g/m²
Thickness	ASTM D5199	1.2mm
Mechanical		
Wide Width Tensile Strength (Elongation @ Break)	ASTM D4595 BS 6906/1	9.0 kN/m (40%)
Grab Tensile Strength (Elongation @ Break)	ASTM D4632	555N (60%)
Mullen Burst	ASTM D3786	1650 kPa
Trapezoidal Tear	ASTM D4533	240 N
Hydraulic		
Pore Size (O_{95})	ASTM D4751 (Dry)	0.150mm
Permeability	ASTM D4491	190 l/m²/sec
Endurance		
UV Resistance (% retained @ 500 hours)	ASTM D4355	70%

[2] Values shown are in weaker principal direction. Typical indicates mean or average value of all test data.

INSTALLATION

The side slopes of the covered embankment were 2H:1V to 1H:1V. Initially all the existing unwanted plants were manually removed and vigorous weeds such as oxalis and couch were killed by spraying herbicide on the embankment prior to geotextile installation. All the rocks, clods and debris were also removed. The geotextile was laid over an area with existing plants. The fabric was arranged around plants and slits were cut for some of the plants to protrude. The fabric was placed in intimate contact with the base without wrinkles and folds. It was secured in place using 9 inch steel staples placed at approximately 0.5 m – 1.5 m intervals. Refer to Figure 1.

Figure 1. Installation of Geotextile on Embankments

The geotextile was placed with the machine direction parallel to the length of the slope. The adjacent geotextile sheets were joined by overlapping 300 mm in all instances. Extreme care was taken during installation so as to avoid any damage to the geotextile.

TESTING

"Perhaps the single most important property of a geotextile is its tensile strength. Invariably all geotextile applications rely on this property either as the primary function (as in reinforcement applications) or as a secondary function (as in separation, filtration or drainage)" Koerner, 1994.

The samples were tested in accordance to ASTM D 4632 – 91 for breaking load (grab strength) and elongation (grab elongation) of geotextiles using the grab method. The testing was done in dry conditions at Permathene's material laboratory. A continually increasing load was applied longitudinally to the specimen and the test was carried to rupture. Values for the breaking load and elongation of the test specimen were obtained from the machine electronic scales. It is a useful quality control or acceptance test, as it was desired to determine the "effective strength" of the fabric in use after the exposure to the UV radiation. Ten specimens each were taken in the machine and cross-machine direction respectively.

The ETCART project was installed in May - June 2000. The laboratory tests were conducted on samples retrieved from actual ETCART sites and recorded in Table 1. The results showed that about 37 % strength loss after 60 days of exposure, but the material was in tact and not broken down. The strength loss was seen and it was about 78 % in 13 months with no signage of breaking of the material. The area was partially covered with shrubs. This was quite convincing as New Zealand being a country prone to very strong UV, the results were satisfying. In summer, New Zealand typically receives around 50 % more UV than Southern Germany.

Samples	Time	Average Grab Tensile (Newton)		Apparent Elongation Breaking Point (%)	
		Machine Direction	Cross Machine Direction	Machine Direction	Cross Machine Direction
Virgin	Jun 2000	1015	535	83	87
1st	Aug 2000	543	387	72	61
2nd	Dec 2000	322	170	58	53
3rd	Mar 2001	265	130	49	49
4th	Jul 2001	220	116	45	48

Table 1. Grab Tensile Strength of the Geotextile at ETCART Site

As seen from the Figure 2, the strength decreases @ 37 % in 2 months, 68 % in 6 months, 75 % in 9 months and finally 78 % in 13 months. After 9 months of exposure, the strength loss was only 3 % in 4 months, which concludes that there will be not much further loss of strength before the geotextile fully breaks down.

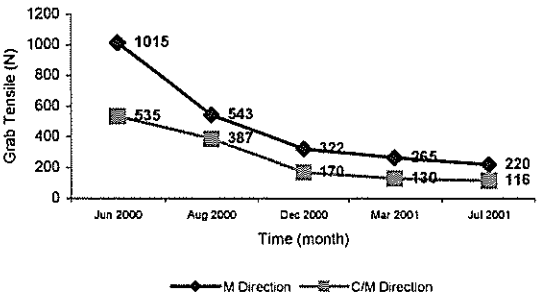

Figure 2. ETCART Site Grab Tensile Strength vs Time

The tests conducted on samples retrieved from the Mayfair Village project site were of concern as shown in the Table 2. These samples were taken from the areas badly damaged / broken down where the soil was exposed. The installation for Mayfair project was done in October 2000. As seen from the Figure 3, about 80 % strength loss after 60 days of exposure was observed and further 12 % strength loss in 90 days, thus a total loss of 92 % in 5 months and finally 93.5 % in 9 months. After 6 weeks of installation, it was noted that the material had broken down in most areas. The initial reasons discussed with the client's engineer were either the geotextile was tightly stretched in some areas or not being placed property on the ground or chemical attack. It was unusual for the 135 g/m² fabric to deteriorate in such a short span as compared with the ETCART project.

Samples	Time	Average Grab Tensile (Newton)		Apparent Elongation Breaking Point (%)	
		Machine Direction	Cross Machine Direction	Machine Direction	Cross Machine Direction
Virgin	Oct 2000	887	481	74	71
1st	Dec 2000	221	65	51	38
2nd	Mar 2001	114	12	45	25
3rd	Jul 2001	98	10	41	21

Table 2. Grab Tensile Strength of the Geotextile at Mayfair Site

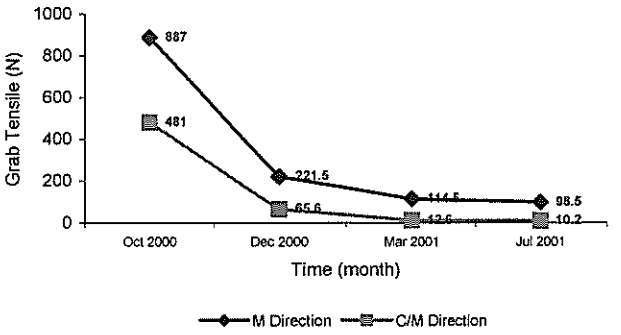

Figure 3. Mayfair Site Grab Tensile Strength vs. Time

In March 2001, we took the virgin sample of the geotextile and sprayed with isopropylamine liquid herbicide (Roundup) on the top. The tests were conducted on both the samples (Virgin and with roundup) and the results are shown in Table 3 and 4 respectively. As seen from the Figure 4 and 5 respectively, the strength loss was 20.5 % for virgin geotextile as compared to 23.5 % for chemically treated geotextile after 4 weeks of installation on an open levelled ground in fully exposed conditions.

Samples	Time	Average Grab Tensile (Newton)		Apparent Elongation Breaking Point (%)	
		Machine Direction	Cross Machine Direction	Machine Direction	Cross Machine Direction
Virgin	Mar 2001	930	498	81	79
1st	Apr 2001	651	443	69	58
2nd	Jul 2001	485	413	60	52

Table 3. Grab Tensile Strength of Geotextile Without Roundup Herbicide

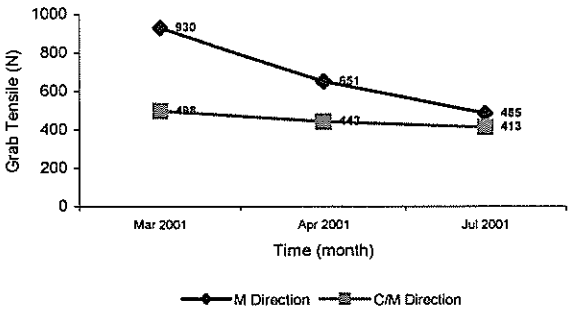

Figure 4. Grab Tensile Strength vs Time for Sample Sprayed without Roundup Herbicide

Samples	Time	Average Grab Tensile (Newton)		Apparent Elongation Breaking Point (%)	
		Machine Direction	Cross Machine Direction	Machine Direction	Cross Machine Direction
Virgin	Mar 2001	930	498	81	79
1st	Apr 2001	615	431	66	57
2nd	Jul 2001	463	379	62	51

Table 4. Grab Tensile Strength of Geotextile with Roundup Herbicide

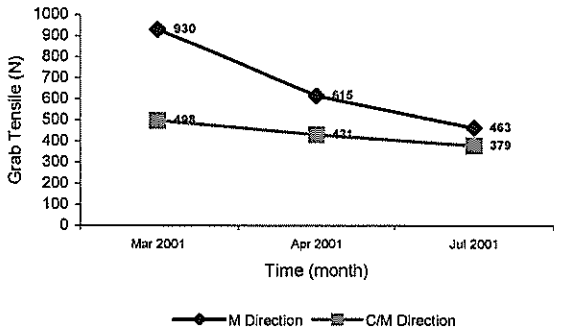

Figure 5. Grab Tensile Strength vs Time for Sample Sprayed with Roundup Herbicide

After 4 months, the tests were again conducted and the strength loss was 32.5 % for virgin geotextiles versus 37 % for chemically treated geotextile. Hence it was concluded that the herbicide spray has got no appreciable affect on the geotextile. The chemical may have been sprayed just prior to installation or even after the installation of the geotextile but will not affect the performance.

On the other hand, the degraded samples from the Mayfair job taken in April 2001 were sent to the manufacturer's laboratory for the carbon black content testing adopting ASTM D4218 standards. The results are reported as under in Table 5.

Degraded Samples	Carbon Black (%)
Virgin	0.64%
1st	2.80%
2nd	2.83%
3rd	1.20%
4th	0.78%

Table 5. Mayfair Site Samples Tested for Carbon Black Content

The test sample was divided into 4 small samples. Samples 1 and 2 respectively had visual signs of soil contamination and the high test results shown in Table 5 reflect soil contamination. This was also the thickest part of the field sample where the soil locks into the interlocking fibers of the geotextile. Sample 4 showed a high degradation and there were no visible signs of contamination due to fewer fibers for soil to lock into. The results for this sample came very close to the standard control results. This indicated that there was a minimal amount of carbon black in the sample. Is this 100% conclusive? No, a further step was taken to trace back the carbon black test results on the fibre used to make this particular geotextile. It was produced with standard 5-denier off-black fibre. Two different fibre batches were blended to make this nonwoven product, which is a standard manufacturing operation. The average carbon black test results from the last two years on the 5-denier off-black fibre was calculated as 0.57%. It was also confirmed that the manufacturer has made no changes to the additive package or suppliers of carbon black nor has their suppliers made any changes.

Based on the above test results, it was concluded by the manufacturer that there was no deviation from the norm in processing and testing of the material as related to the carbon black content in the fibre made to produce this particular product.

PERFORMANCE

- NW Geotextile specified in the ETCART project served the following purpose:

- It controlled the weed growth naturally without the continuous use of chemicals and sprays. Thus, water stagnation was prevented, soil was not soured. Roots were protected from the spread of fungus and bacteria and water evaporation were reduced.

- It provided an erosion resistant barrier until the vegetation was established. Seedlings were planted through a slit in the fabric and the fabric was laid around the existing plants by making a slit and protruding each plant through it.

- The soil, geotextile and vegetation worked together to provide a more stable embankment than vegetation alone. Non-reinforced vegetated areas were more likely to have individual plants dislodged due to soil erosion than reinforced vegetated slopes. The vegetation in conjunction with the geotextile function as a single unit instead of individual plants.

- The nonwoven geotextile has a high co coefficient of friction and hence acted as a non-slippery drainage medium for the water to seep through the fabric, rather than ponding over the fabric. It was permeable and able to absorb water.

- The vegetation was established very fast as compared with sites having standard woven matting.

Since it is known that polypropylene degrades during extended exposure to sunlight but this geotextile was produced with carbon black and other UV inhibitors to protect against degradation. These additives allow nonwoven polypropylene geotextiles to be exposed for a certain length of time.

On the Mayfair project, all the above objectives were achieved but in some areas, the soil was exposed within 6 – 8 weeks of the installation. In order to suppress the weeds in those particular areas, the herbicide was sprayed. The erosion problem was taken care of and the slopes were stabilized by using the geotextile.

It is becoming a standard practice to use nonwoven geotextile for weed and erosion control applications and extensive installations are going on along the motorways in this part of the world.

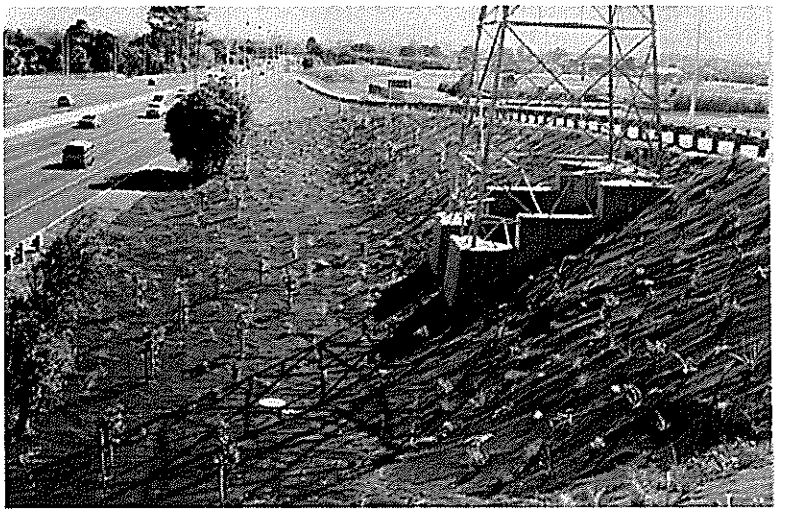

Figure 6. Stable Embankment without Vegetation – ETCART Project

Figure 7. Stable Embankment with Fully Grown Vegetation – ETCART Project

CONCLUSIONS

The ETCART project covered an area of approximately 22.000 m2 and the major advantages of using nonwoven geotextile were the low installation costs, easy handling of the fabric, aesthetically pleasing appearance and the ideal drainage performance. The native shrubs were planted making slits in the fabric in order to have a canopy faster. This was a new concept of using nonwoven geotextiles instead of standard woven ground cover fabrics and it was successful. The installation of the geotextile has prevented surface erosion during the shrubs establishment period and also assisted in the suppression of the weeds.

Upon final analysis of the Mayfair job we concluded that the problem here was of insufficient quantity of carbon black and uneven carbon dispersion in the fabric. For adequate UV protection of an exposed fabric, it is imperative that there should be sufficient dosage of carbon black and it is dispersed evenly through out the polymer. The Mayfair job had uneven carbon dispersion and this resulted in an early break down of the fabric in some areas. The exposed areas on this job were treated with herbicide, which have stopped the growth of the weeds in those areas.

In conclusion, 135 g/m^2 nonwoven geotextile specially produced with carbon black and other UV inhibitors can be used as a weed and erosion control blankets. It is more cost effective and easier to handle than the standard woven ground cover fabrics. It has an ideal drainage performance and enhances vegetation. The vegetated slope looks aesthetically pleasing and provides a good ground cover. Finally, Polypropylene is not harmful to soil and becomes a part of the soil as degradation progresses.

ACKNOWLEDGMENTS

The author would like to thank Marc S. Theisen from SI Corporation, USA for the peer review of the manuscript. The author is also grateful to Matthew Cossio, MD and the staff of Permathene Ltd and Ground Solutions Binco Ltd, New Zealand for their assistance with the laboratory and other site work.

The laboratory test reports and technical information of SI Corporation, USA is also gratefully recognized.

REFERENCES

AASHTO M288 (1997). Standard Specifications for Geotextile Specification for Highway Applications, Part 1 (18th Edition). USA: Materials and Tests Division of Texas Department of Transportation. Austin, Texas.

Appleton, B.L., & Derr, J.F. 1990. Growth and Root Penetration by large Crabgrass and Bermuda Grass through Mulch and Fabric Barriers. Journal Environ. Hort., 8(4):197-199.

Appleton, B.L., & Derr, J.F. 1991, March. Using Geotextiles for Landscape Weed Control. Geotechnical Fabrics Report, March 1991 20-22.

Cholmondeley-Smith, D.R. 1995, March. Erosion and Control Guidelines for Earthworks. New Zealand: Technical Publication No. 2, Auckland Regional Council.

Das, B.M. 1987. Advanced Soil Mechanics. (International Edition) USA: McGraw-Hill Book Company, London.

Gasper, F., & Burgdorf, D.W. 1997. "Geotextile Reinforced Vegetated Spillways." Geosynthetics ' 97 Conference Proceeding, Vol. 1. 563 –572.

Ivens, G., & Taylor, T. 1985. The New Zealand Garden Weed Book. New Zealand: Reed Methuen Publishers Ltd, Auckland.

Koerner, R.M. 1994. Designing with Geosynthetics. (3rd Edition). USA: Prentice-hall Inc. Englewood Cliff, New Jersey.

Seafriends - Soil in New Zealand : Seafriends Marine Conservation and Education Centre, 7 Goat Island Road, Leigh. Retrieved April 18, 2001 from the World Wide Web: http://www.seafriends.org.nz/enviro/soil/soilnz.htm.